

NOVEL METHOD FOR THE PREPARATION OF SILVER/CHITOSAN-O-METHOXY POLYETHYLENE GLYCOL CORE SHELL NANOPARTICLES

A.M. Abdel-Mohsen^{1,2*}, R. Hrdina¹, A.S. Aly²

¹*Institute of Organic Chemistry and Technology, Faculty of Chemical Technology,
University of Pardubice, Studentská 95, CZ-532 10, Pardubice, Czech Republic*

²*National Research Centre-Textile Research Division- El-Buhoth St., 12311 Cairo, Egypt*

*E-Mail: abdo_mohsennrc@yahoo.com

INTRODUCTION

Core/shell structured nanoparticles are now attracting investigation interest since these composite nanoparticles are constructed of cores and shells of different chemical compositions, which endow us with the possibility to combine the advantages or distinctive properties of varied materials together and, especially, to manipulate the surface functions to meet diverse application requirements (1-4).

In this communication, we describe an easy method for providing a novel core-shell nanostructure: chitosan-O-MPEG as shell and silver nanoparticles as a core. Formation of silver core is confirmed by TEM, UV/vis spectroscopy, XRD. The size of Ag nanoparticles can be controlled easily by varying the concentration of silver oxide. This method afforded a convenient platform for building novel core-shell nanostructures with specific properties.

MATERIAL AND EXPERIMENTAL

Chitosan DA 95% was obtained from Aldrich Chemical Company. Polyethylene glycol mono methyl ether (Mn 2000) was obtained from Fluka Chemical Company. Freshly silver oxide (Ag₂O) was laboratory prepared from silver nitrate and potassium hydroxide. Chitosan-O-methoxy polyethylene glycol was prepared in our previous work (5). All commercially available solvents and chemical reagents were used without further purification.

RESULTS AND DISCUSSION

Preparation of silver/chitosan -O-PEG core shell nanoparticles

Silver/chitosan-O-PEG core shell nanoparticles with different degree of substitution were prepared by the sequence of following reactions: reaction of chitosan amino group with 4-fold excess of phthalic anhydride (protection of amino group), then reaction of formed 2-N-phthaloyl chitosan with iodine modified methoxy polyethylene glycol (MPEG, where the terminal hydroxyl group was substituted by iodine) and then reduction (used hydrazine hydrate) of Ag⁺ to Ag⁰ and parallel deprotection of amino group together with the incorporation of Ag⁰ particles into formed grafted polymer (Scheme 1, Figure 1). The N-phthaloyl chitosan prepared in this study is soluble in several organic solvents such as DMSO, DMF, and dimethyl acetamide.

Therefore, the N-phthaloyl group is indispensable for both protection of amino functionalities of chitosan and solubilization of the product in an organic solvent, which is important for the next reaction with a halogenated derivative of MPEG. The intermediates and final products were separated from the reaction mixtures and their structure was confirmed.

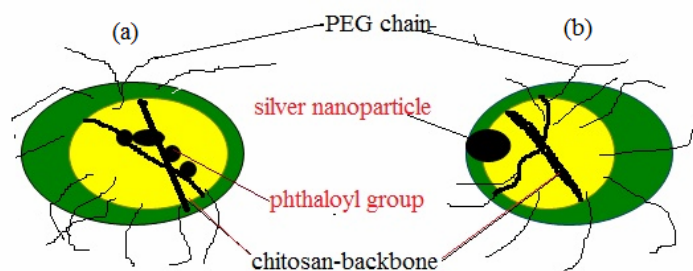
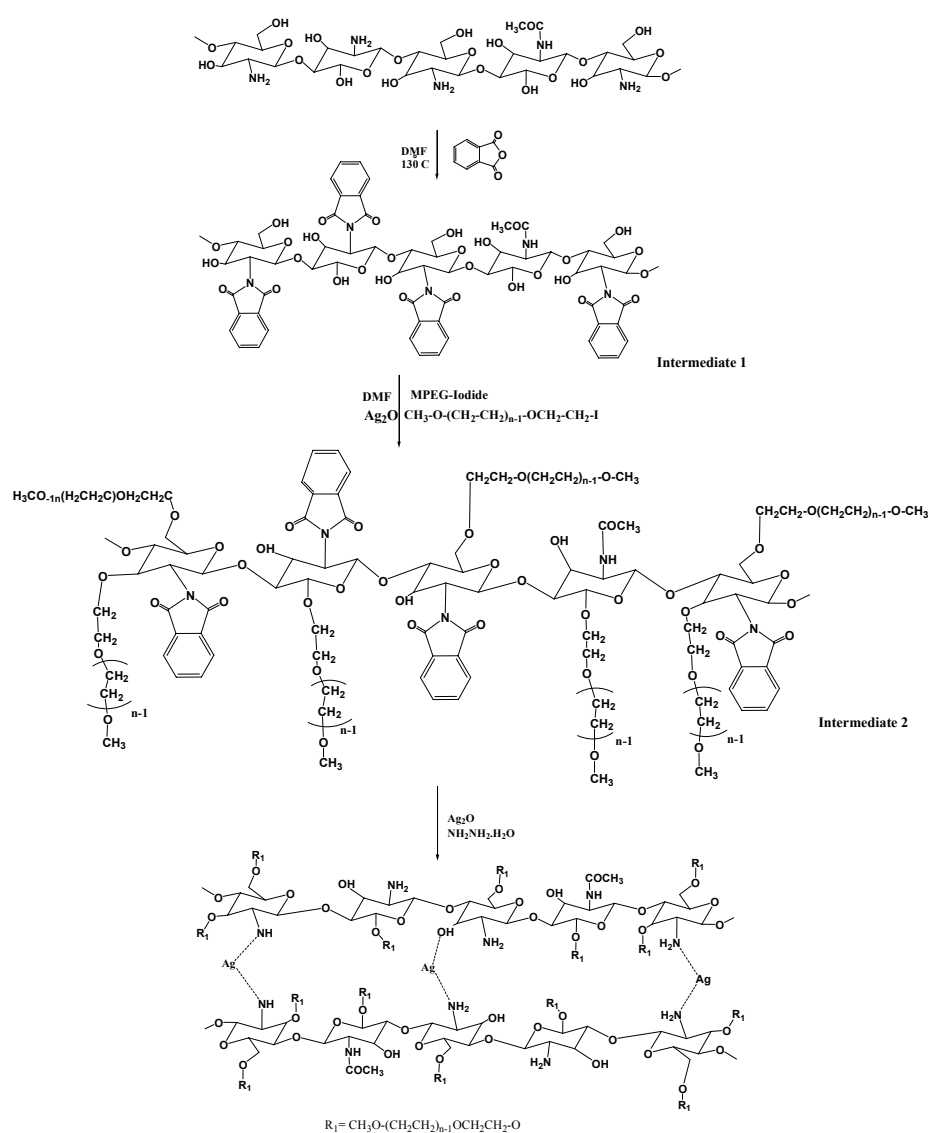


Figure 1. Schematic representations of
(a). Self- assembled of N- phthaloyl chitosan
(b). Interaction of silver nanoparticles with hydrophobic moieties of grafted chitosan within PEG chain



Scheme 1. Preparation of silver/chitosan–O-MPEG core-shell nanoparticles
Characterization of core shell nanoparticles

1. Transmission electron microscopy (TEM)

Figure 2a shows chitosan-O-MPEG nanosphere without silver nanoparticles. Figure 2b shows TEM images of chitosan-O-PEG nanosphere, which indicated the formation of hollow nanostructure, where the most of them were spherical shape while some were less regular. Figure 2b is TEM images of silver/chitosan-O-PEG core shell nanoparticles, synthesized using the above approach (degree of substitution DS 13, silver oxide concentration 8 mg). It can be seen that Ag nanoparticles are located in the interior of each chitosan-O-PEG sphere. The size silver nanoparticle is about 3 ± 2 nm and size of the shell particles is about 6 ± 2 nm. It was observed that the most of silver nanoparticles were not located in the centre of these hollow nanospheres. The Ag core tends to stick to the wall as result of the attractive force between their surfaces. Other investigation groups have reported similar phenomena (6, 7).

In Figure 2c can be seen, that the increasing of the degree of substitution (it means the increasing of PEG chains in chitosan) led to the increasing of the shell size (DS 99 %; Ag₂O 15 mg), where the size of silver core was 18 ± 3 nm and size of shell particles was 25 ± 5 nm. The next increasing of degree of substitution to 124 % caused the formation of nanorods with embedded silver nanoparticles (Figure 2d).

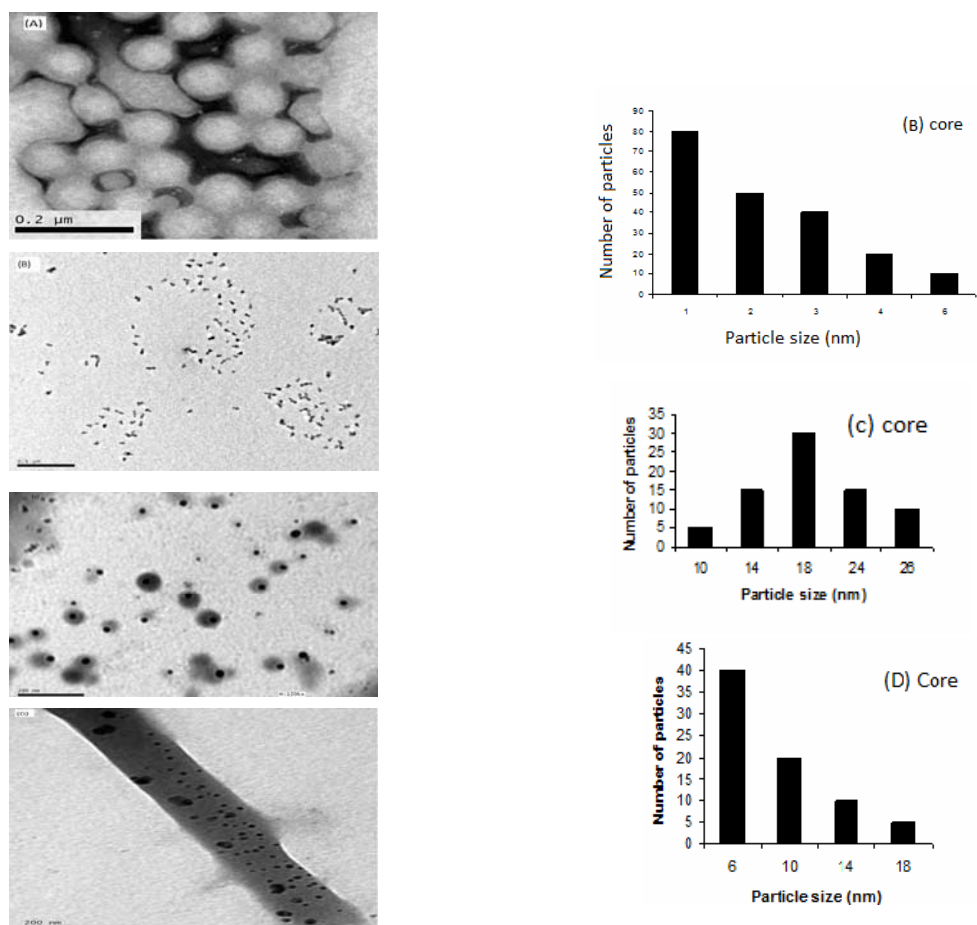


Figure 2. TEM images of silver-chitosan-O-MPEG core shell nanoparticles

- (a) Chitosan-O-PEG nanosphere nanosphere;
- (b) Silver-chitosan-O-PEG core shell nanoparticles (DS-13 %; Ag₂O concentration 8 mg);
- (c) Silver-chitosan-O-PEG core shell nanoparticles (DS-99 %; Ag₂O concentration 15 mg);
- (d) Silver-chitosan-O-PEG core shell nanoparticles (DS-124 %; Ag₂O concentration 20 mg).

2.2. X-ray diffraction of nanoparticles

Chitosan is semicrystalline polymer, whereas PEG is crystalline with defined crystal structure. Figure 3 shows the X-ray patterns of chitosan (Fig. 3a), N-phthaloyl chitosan (Fig. 3b), O-PEG-N-phthaloyl chitosan (Fig. 3c) and silver/chitosan-O-PEG core shell nanoparticles (Fig. 3d). From the presented figures can be seen that chitosan has reflection at $2\theta = 19.7^\circ$, and relative weak reflection at $2\theta = 10.2^\circ$, N- phthaloyl chitosan has one broad peak at $2\theta = 20^\circ$ suggesting the interruption of hydrogen bonds and for this reason this chitosan derivative appeared amorphous.

The diffraction diagram of N-phthaloyl chitosan-O-MPEG (Fig. 3c) shows three reflection at $2\theta = 23.24^\circ$, $2\theta = 19.14^\circ$ and broad peaks at $2\theta = 10.5^\circ$; this peaks are related to phthaloyl group which are shifted due to grafting of chitosan by PEG. The diagram of silver/chitosan-O-MPEG core shell nanoparticles (Fig. 3d) (after the treatment with hydrazine hydrate) shows five reflection peaks in addition to two sharp peaks related to PEG at $2\theta = 19.14^\circ$, $2\theta = 23.24^\circ$, and shows two sharp diffraction peaks in addition to the broad peak related to silver nanoparticles. The sharp peaks located at $2\theta = 38.2^\circ$ and 44.3° are assigned to (111) and (200) planes of the cubic structure of metallic Ag. No diffraction peaks that correspond to silver halide or silver oxide are observed, which confirms that component of the core is metallic Ag.

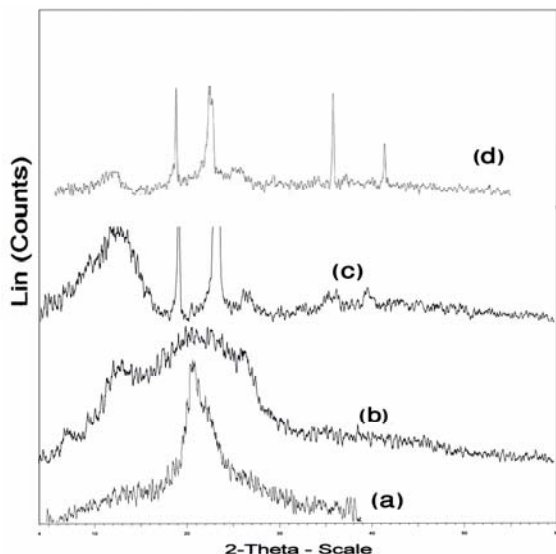


Figure 3. XRD patterns
(a) chitosan; (b) phthaloyl chitosan;
(c) 2-N-phthaloyl chitosan;
(d) silver/chitosan-O-MPEG core shell nanoparticles.

3.2.3. Scan electron microscopy (SEM) Figure 4 shows SEM of chitosan and silver/chitosan-O-MPEG core shell nanoparticles.

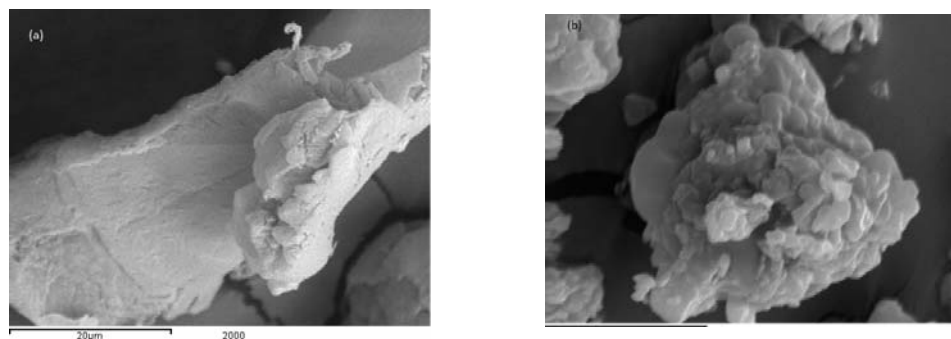


Figure 4. SEM of (a) chitosan; (b) silver/chitosan-O-MPEG core shell nanoparticle

CONCLUSION

Silver/chitosan-O-PEG core shell nanoparticles were prepared by the reaction of N-phthaloyl chitosan with methoxy polyethylene glycol iodide in the presence of silver oxide and hydrazine hydrate. These nanoparticles are stable in the time.

REFERENCES

- [1] Daniel, M. C. Astruc. (2004). D. Gold Nanoparticles: Assembly, Supramolecular Chemistry, Quantum-Size- Related Properties, and Applications toward Biology, Catalysis, and Nanotechnology. *Chem. Rev.*, 104, 293-346.
- [2] Caruso, F. (2001). Nanoengineering of Particle Surfaces. *Adv. Mater.*, 13, 11-22.
- [3] Xia, Y. N.; Gates, B.; Yin, Y. D.; Lu, Y. (2000). Monodispersed Colloidal Spheres Old Materials with New Applications. *Adv. Mater.*, 12, 693-713.
- [4] Liz-Marzan, L. M.; Giersig, M.; Mulvaney, P. (1996). Synthesis of Nanosized Gold Silica Core Shell Particles. *Langmuir*, 12, 4329-4335.
- [5] A.S. Aly, A.M. Abdel-Mohsen, A. Hebeish. (2010). Innovative Multi-finishing using Chitosan-O-PEG Graft Copolymer / Citric acid aqueous system for Preparation of Medical Textiles, *Journal of Textile Institute.* 101, No. 1, 76-90.
- [6] Kim, M.; Sohn, K.; Na, H. B; Hyeon, T. (2002). Synthesis of Nanorattles Composed of Gold Nanoparticles Encapsulated in Mesoporous Carbon and Polymer Shells *Nano Lett.*, 2, 1383-1387.
- [7] Kamata, K.; Lu, Y.; Xia, Y. (2003). A Facile Synthesis of Asymmetric Hybrid Colloidal Particles *J. Am. Chem. Soc.*, 125, 2384-2385.

APPLICATION EXPERIENCE OF CHITOSAN IN VETERINARY PRACTICE

Frolova M. A., Albulov A.I., Samujlenko A.J., Shinkarev S.M., Buhantsev O.V.

Russian research institute of technology and the biological industry, Russia

**E-mail: ynitibp@mail.ru*

INTRODUCTION

Natural biopolymer chitosan shows sorption, film-forming, radioprotecting, immunomodulating, and other properties. The analysis of the available scientific sources and the research data has shown that preparations of chitosan don't possess toxicity and ability to cumulate in an organism. This allowed planning research targeted to investigation of chitosan as treatment-and-prophylactic and immunostimulating preparation for young agricultural animals.

Application in veterinary science requires chitosan of certain physical and chemical characteristics and specific properties, which are substantially depend on molecular weight and degree of purification of a preparation [1, 2, 3]. For many years we have been developing new technologies of preparation of various forms and modifications of chitosan, and studied the efficiency of their application in various areas of economy, including veterinary.

It is known that in the first days and months of life the organism of newborn animals is most sensitive to the influence of environment and the activators of infectious diseases of the mixed etiology, which cause diseases of a gastrointestinal tract. Antibiotics, which besides antimicrobial effect, show immunosuppressive properties, are applied in treatment of diarrheas of calves and piglets, that with the laps of time lead to the resistance and loss of medical effect of antibiotics. We have carried out a complex of investigations on introduction of chitosan to veterinary practice as an enterosorbent and immunomodulator used in treatment of gastrointestinal diseases of young agricultural animals.

MATERIALS AND METHODS

Experiments on studying of efficiency of application of chitosan for treatment and prevention of gastrointestinal diseases of young agricultural animals were conducted on calves and piglets during periods of mass calving and farrows at farms of Moscow, Kursk and Tula regions. Medical and preventive (prophylaxis) doses and frequency of chitosan application were optimized. 2-3 % gel solution of chitosan with molecular weight 300-500 kDa, and 2 % gel solution of chitosan with molecular weight 80, 150 and 380kDa were used in the tests.

RESULTS AND DISCUSSION

The results of application chitosan in treatment and prevention of gastrointestinal diseases of young agricultural animals are presented in the table.

The calves with the diarrhea (1 group) received 50 ml of chitosan preparation (molecular weight 380kDa) 3 times per day 30 minutes before the feeding. On 3-4 day of treatment the condition of animals was normalized, the diarrheas syndrome persisted only for one calf, which however showed sufficient improvement of appetite and general health condition. The 2 group, which received a chitosan preparation with molecular weight 150 kDa, showed similar results, while effect of preparation with molecular weight 80 kDa (3 group) was substantially higher and reached 90% - 10 heads have recovered, 1 head had signs of deterioration and an insignificant diarrhea.

Chitosans with different molecular weight showed similar effect on piglets, although overall efficiency of preparation was somewhat lower than on calves.

The analysis of blood serum of animals during test has shown that the content of calcium and reserve alkali in serum of sick animals was 12-17 % lower than that of animals of prophylaxis and control groups; content of total protein, globulin fractions and hemograms corresponded to physiological norm.

Table. Results of application of chitosan at treatment and preventive maintenance of gastrointestinal diseases of calfs and pigs

Efficiency	Molecular weight chitosan, kDa	Quantity, head	Disease period, days	Weight gained during observation period (8 days), kg	Notes
Calves					
Medical treatment	380	29	3±1	4,6±1,2	1 head-diarrhea after treatment
	150	23	3±1	4,5±1,3	1 head-diarrhea after treatment
	80	19	3±1	4,6±1,1	1 head -diarrhea insignificant
Prophylaxis treatment	380	22	—	5,1±1,7	
	150	16	—	6,1±1,4	
	80	24	—	6,1±1,6	
Control	—	19	6±2	4,8±1,4	3 heads - ill 1 head -fallen
Piglets					
Medical treatment	380	13	4±1	2,9±0,8	1 head-diarrhea after treatment
	150	17	3±1	2,9±1,1	2 heads-diarrhea after treatment)
	80	11	3±1	3,0±1,0	
Prophylaxis treatment	380	19	—	3,1±0,9	
	150	10	—	3,2±1,0	
	80	18	—	3,2±1,1	
Control	—	16	7±2	3,0±1,2	4 heads - ill 2 heads -fallen

ACKNOWLEDGEMENTS

This work was conducted together with the experts of Kursk regional veterinary management in economy of Fatezhsky area, KSPH "Priupsky" the Tula region, SHPK «Moscow suburbs Dawn» Moscow region, and in the frames of creative scientific cooperation with chairs of chemistry, veterinary medicine and veterinary ecology of Bryansk state agricultural academy and All-Russia research institute of technology and the biological industry.

REFERENCES

- [8] Chitin and chitosan: Production, properties, application. Under the editorship of Skrjabin, K.G., Vihoreva, G.A., Varlamov, V.P. (2002) Izd. "Science", 368.
- [9] Gamzazade, A.I. (1999) Structural not uniformity as the factor of variability of properties of chitin and chitosan. Chemistry of polymers, 11, 48-31.
- [10] Chervinets, V.M., Bondarenko, V.M., Albulov, A.I., Komarov, B.A (2001) Antimicrobial activity chitosan with different molecular weight. Materials of VI International conference «New achievements in research of chitin and chitosan », M., VNIRO, 252-255.

VARIOUS APPROACHES TO METAL NANOPARTICLES STABILIZATION IN CARBOXYMETHYL CHITIN MATRIX

V.A. Alexandrova^{*}, L.N. Shirokova, A.S. Petrosyan

*A.V. Topchiev Institute of Petrochemical Synthesis, Russian Academy of Sciences,
Leninskii pr. 29, Moscow, 119991 Russia*

**E-mail address: alexandrova@ips.ac.ru*

INTRODUCTION

Currently, nanotechnologies and nanomaterials belong to research priorities. Metal nanoparticles are characterized by developed wall surfaces, higher atom availability and improved reactivity. However, in a solution they form clusters very quickly and require the use of stabilizers in the form of surfactants. Metal nanoparticles are also stabilized by various synthetic or natural polymers (polyvinyl pyrrolidone, starch, gelatin, chitosan and others).

Natural polysaccharides chitin and chitosan exhibit a unique combination of physico-chemical and biological characteristics namely biocompatibility, low toxicity, biodegradability, ability to form fibers and films, etc., which allow for their wide use in applied biochemistry and medicine [1, 2].

Polymer properties may be tuned by combining them with biologically active ingredients such as nanoparticulate metals (for example, silver nanoparticles known to display bactericidal activity). A number of studies are concentrated on the modification of polymers of chitin–chitosan series with metal nanoparticles. In work [3] chitin fibers modified with polyvinyl pyrrolidone and finely dispersed silver (Poviargol preparation) were shown to express increased antibacterial activity. Besides, the possibility to generate polymer systems of the kind by silver nanoparticles formation from silver salt solutions in a polymer matrix upon irradiation was shown in [4, 5]. However, the composition and purity of obtained materials were difficult to control.

We propose a method of polymer composition synthesis based on water-soluble chitin derivative where silver nanoparticles content may be easily controlled and regulated by UV spectroscopy.

Chitin and chitosan are known to be bactericidal biopolymers [6], which makes reasonable the choice of these polymers as starting materials for the preparation of biodegradable materials of biomedical applications, such as film wound coatings with silver nanoparticles to enhance the effect. Nanosized silver particles used in the present work were obtained by biochemical synthesis or generated by radiation-chemical way in reversed micelles of an anionic surface-active agent (SAA) in isooctane [7].

To realize the mechanism of metal nanoparticles stabilization in polymer carboxymethyl chitin matrix the nature of bonds formed in such system was studied in this investigation via FTIR spectroscopy. Besides, study of plant antioxidants ability to improve the aggregative stability of metal nanoparticles in carboxymethyl chitin water solutions was carried out.

MATERIALS and METHODS

A water-soluble carboxyalkylated chitin derivative, 6-O-Carboxymethyl Chitin (**CMC**), of 220 kDa with carboxymethylation degree of 1.0 was synthesized from chitin (ZAO Bioprogress) according to a procedure described in [8]. Sodium hydroxide (reagent grade), isopropyl alcohol (special purity grade), and monochloroacetic acid (reagent grade) were used as received. Silver nanoparticles (**AgNP**) were used in the form of reversed micellar solution (**RMS**) in isooctane or in the form of a water dispersion of silver (**WDS**) obtained from RMS [4].

AgNP were incorporated into the structure of polymer matrix (CMC) by the gradual addition of WDS into a polymer solution of a known concentration with continuous stirring. Then, the solution was stirred for 15 min at room temperature. In the case of RMS we used the ultrasonic treatment of heterophase system to transport AgNP from isooctane to the water polymer solution.

The quantitative determination of AgNP content and the evaluation of aggregative stability of nanoparticles in solutions with CMC were performed by measuring AgNP optical absorbance at 420 nm using a SPECORD M40 UV spectrophotometer (Karl Zeiss, Germany) in a quartz cuvette with an optical pass length of 1 mm in the range of 200–700 nm at 20°C.

AgNP size, as well as the size of polymer particles (both in the initial solution and in the composite with AgNP), was determined by photon correlation spectroscopy using a COULTER N4 MD laser autocorrelation spectrometer (Coulter Electronics, US).

All composites samples were investigated by IR Fourier spectroscopy (FTIR-spectrophotometer Bruker-113v, Germany) films method from 4000 to 400 cm⁻¹.

CMC films modified with AgNPs were produced from 4% (w/w) CMC water solutions poured onto Petri dishes and left for 24 h for the solvent to evaporate.

The bactericidal activity of CMC-based films with AgNPs were studied in the Gamaleya Institute of Epidemiology and Microbiology, Russian Academy of Medicinal Sciences, using international strains *Salmonella typhimurium* TMLR 65 and *Staphylococcus aureus* Wood-46 (collection of cultures of Legionella and Listeria genera) used as standards in legionellosis laboratory of the institute. The antibacterial effect was estimated as the number of colonies having appeared upon the incubation completion compared to the number in the control.

The size of AgNP in CMC-AgNP composites films was investigated by transmission electron microscopy (**TEM**) using Tesla BS-540 transmission electron microscope.

RESULTS AND DISCUSSION

One of the most perspective methods of stable metal nanoparticles formation is synthesis via the reduction of metal ions from an aqueous solution of their salts in an inverse – micelle system stabilized by the anionic surfactant – 1,4-bis[(2-ethylhexyl)oxyl]-1,4-dioxobutane-2-sulfonate (AOT). Even distribution of such metal nanoparticles in polymeric matrix results in an additive stabilization of them owing to steric hindrance of polymeric fragments.

Our preliminary studies have revealed those water-soluble derivatives of chitin and chitosan forming the most stable complexes with AgNPs. These were found to be anionic polyelectrolytes CMC and chitosan sulfate.

In case of polycations (chitosan, trimethyl chitosan, and others) aggregation-stable mixtures were hampered by the formation of AOT–polyelectrolyte complex destabilizing AgNP. Therefore, CMC was chosen as a polymer matrix as long as it lacked functional groups competing with the stabilizing shield around AgNP micelles.

An absorbance spectrum pattern of WDS, used in our experiments, is presented in Fig. 1. It is seen that AgNP in water dispersion exerted a characteristic absorbance band with λ_{\max} 420 nm.

The extinction coefficient of AgNP [7] and optical density in absorbance maximum were used to determine AgNP concentration in water dispersions or in CMC composites. It was shown using photon correlation spectroscopy that most of the metal particles in WDS, ~75 %, are small micelles of approximately 2-3 nm.

The stability of macromolecular systems towards aggregation was estimated from the comparison of absorbance spectra between solutions of individual components (water solutions of AgNPs and of polymer) and their mixtures (Fig. 1).

A typical TEM image that shows the dispersed WDS in the WDS-CMC system is represented in the Fig. 2. The particles diameters are in the range 2-4 nm. Most of AgNPs are separated from each other owing to the protection of CMC fragments.

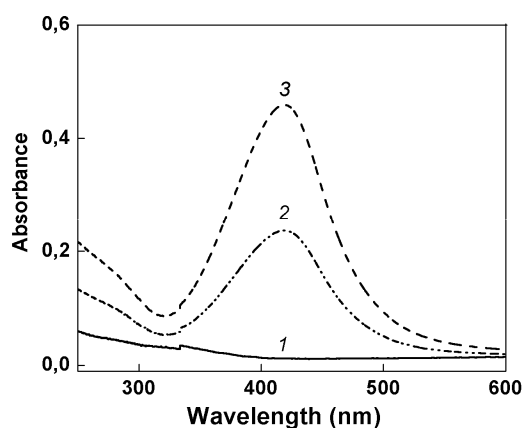


Figure 1. Optical absorbance spectra of the system with varying WDS content in CMC-WDS systems: 1 is 0,5% CMC water solution, 2 is CMC-WDS (10 : 1), and 3 is CMC-WDS (5 : 1)

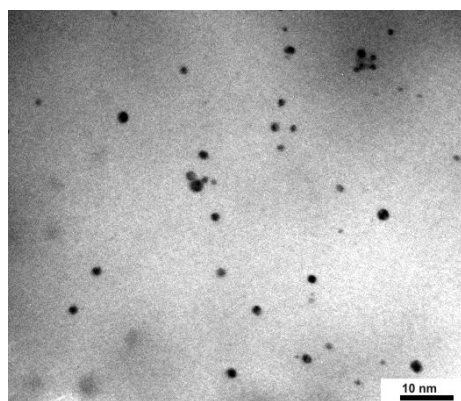
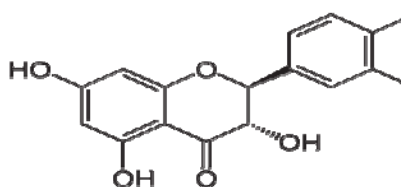


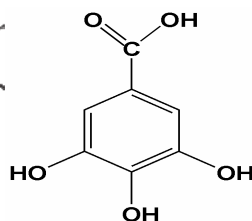
Figure 2. TEM image of SNP in AgNP- CMC composite film

So, metal nanoparticles can be introduced into a polymer aqueous solution via their aqueous dispersion which was obtained from the micellar solution of metal nanoparticles in isooctane.

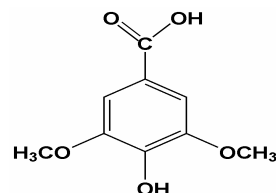
However, this process results in a certain loss of nanoparticles because of their oxidation and destabilization. Therefore, an attempt was made to obtain CMC-AgNP - composite system via the direct transfer of AgNP from their micellar solution in isooctane to an aqueous polymer solution with the use of ultrasonic treatment of the heterophase system. To improve the AgNP aggregative stability the plant antioxidants – dihydroquercetin (DHQ), gallic acid (GA) and syringic acid (SA) were added to CMC solution before sonification.



Dihydroquercetin



Gallic acid



Syringic acid

The most optical density of the characteristic absorbance band with λ_{\max} 420 nm was obtained at GA presence in the macromolecular system (Figure 3).

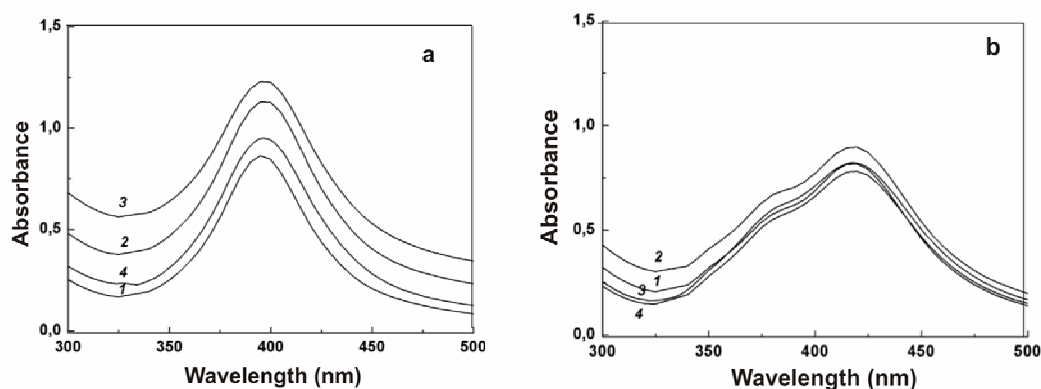


Figure 3. Electronic spectra of system containing 0,5% CMC, GA: a) 0,5% wt. (CMC mass.), b) 1,0% wt. (CMC mass.) and 0,12% AgNP, aged 1 (1), 4 (2), 7 (3), 14 (4) days

Increase in the concentration of AgNPs in CMC water solution at DHQ and SA presence in macromolecule system was less pronounced than that for GA. Such improvement in AgNP stability at GA presence in system may be due to not only an antioxidative activity of GA but a possible H-bonds formation in the resultant macromolecular system too. To confirm this assumption the nature of bonds in the AO-CMC system was studied via FTIR-spectroscopy.

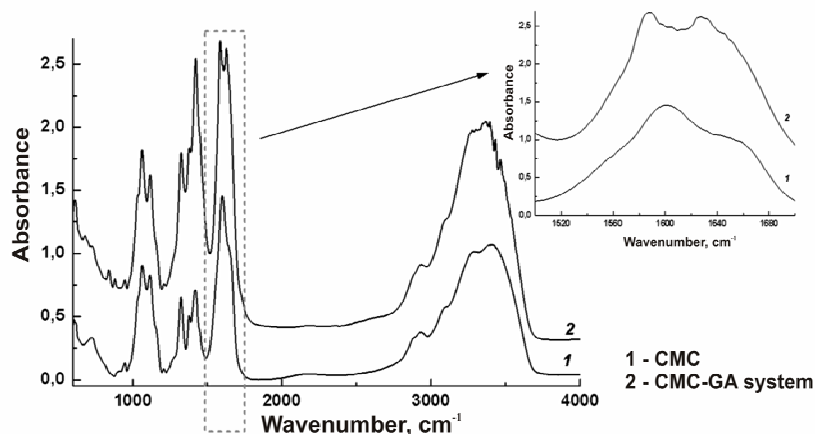


Figure 4. Comparison of FTIR-spectra of CMC and CMC-GA films from the aqueous solutions

Having analyzed the spectral data (Fig. 4) we concluded that considerable splitting of –OH and C=O absorption bands (amide and carboxylate groups $1660 - 1580 \text{ cm}^{-1}$) in CMC-GA complex was due to H-bonds formation between functional groups of antioxidant and macromolecule. Such interaction was accompanied by long wave shift of the characteristic bands. For the other AO investigated the spectral characteristics of such interaction were not as obvious as for GA.

Table 1. The dependence of the bactericidal effect of CMC–AgNP composites films on AgNP concentration (bacterial concentration 10^6 CFU/ml)

Strain, 10^6 CFU / ml	Sample	lg of living bacteria number in CMC and CMC-AgNP composites films into different time interval (h)			
		1,0	3,0	6,0	24,0
<i>Salmonella typhimurium</i> TMLR66	Initial culture	6,0	6,0	6,0	6,0
	CMC - I	6,0	5,8	5,5	3,0
	CMC - II	5,1	4,2	3,0	0
	CMC - III	0	0	0	0
<i>Staphylococcus aureus</i>	Initial culture	6,0	6,0	6,0	6,0
	CMC - I	6,0	5,7	5,3	3,5
	CMC - II	5,2	4,4	3,2	0
	CMC - III	0	0	0	0

CMC-I is initial CMC matrix, CMC-II is 0.03% w/w AgNP, and CMC-III is 0.06% w/w AgNP in CMC-AgNP composites films

The bactericidal effect of films, prepared from CMC solutions containing AgNPs in varying concentrations, towards *Salmonella typhimurium* and *Staphylococcus aureus* strains was studied. Samples represented films on a plexiglass support prepared by pouring the polymer solution onto the support. Control film was obtained from 4 wt % CMC solution, and films under investigation, from the same CMC solution containing 0.03 and 0.06 wt % of AgNP. The concentration of bacterial suspension applied to film was 10^6 CFU/ml. The data obtained is presented in Tab. 1. In experiments with bacterial dosage of 10^6 CFU/ml, polymer films containing 0.06% AgNP were found to inhibit cell growth completely in cultures of *Salmonella typhimurium* and *Staphylococcus aureus* after 1 h of incubation at 30°C . Meanwhile, films containing 0.03% AgNP exerted the same effect after 24 h of incubation with salmonellae and staphylococci strains. The application of control films made of CMC without AgNP resulted in the lowering of the number of colonies by three orders of magnitude during the incubation period.

CONCLUSIONS

Thus, the anionic polyelectrolyte CMC can be successfully used as a matrix for producing composites with metal nanoparticles. In such a system, the polymer serves not only as a film-forming material but also as a stabilizer of metal nanoparticles and a modifier changing the affinity of the surface of hydrophobic nanoparticle for water molecules. Interaction of AO and macromolecule with H-bonds formation resulted in improved stabilization of AgNP in CMC matrix. Film composites exhibited pronounced bactericidal activity towards strains *Salmonella typhimurium* and *Staphylococcus aureus* in a concentration-dependent manner.

ACKNOWLEDGEMENTS

We are grateful to G.N. Bondarenko and B.T. Dubinchuk for FTIR-spectroscopy and TEM researches, accordingly; B.I. Marakusha for the series of experiments on the determination of bactericidal activity.

REFERENCES

- [1] Rinaudo, M. (2006) Chitin and chitosan: properties and applications. *Prog. Polym. Sci.*, 7, 603-32.
- [2] Pillai, C.K.S., Paul, W., Sharma, C.P. (2009) Chitin and chitosan polymers: Chemistry, solubility and fiber formation. *Prog. Polym. Sci.*, 7, 641-78.
- [3] Mikhailov, G.M., Lebedeva, M.F. (2007) Sposobi polucheniya volokon na osnove khitina. *Zhurn. Prikl. Khim.*, 5, 705–15.
- [4] Revina, A.A., Dokuchaev, A.G., Khailova, E.B., Tedoradze, M.G. (2001) Optical and electrical characteristics of polymer films modified with nanostructured silver aggregates. *High Energy Chemistry*, 2, 74-8.
- [5] Chen, P., Song, L., Liu, Y., Fang, Y. (2007) Synthesis of silver nanoparticles by γ -ray irradiation in acetic water solution containing chitosan. *Radiation Physics and Chemistry*, 7, 1165-68.
- [6] Muzzarelli, R.A.A. (1986) Chitin in Nature and Technology. New York: Plenum.
- [7] Egorova, E.M., Revina, A.A. (2000) Synthesis of metallic nanoparticles in reverse micelles in the presence of quercetin. *Colloids and Surfaces A*, 1, 87–96.
- [8] Vikhoreva, G.A., Gladyshev, D.Y., Bazt, M.R. et al. (1992) Influence of activating additives on the structure and reactivity of chitin and chitosan, and synthesis of their carboxymethylated derivatives. *Cellulose Chem. Technol.*, 6, 663-74.

QUANTUM CHEMICAL VIBRONIC THEORY OF BIOLOGICAL ACTIVITY OF CHITOSAN AND ITS DERIVATIVES

B. Asqarov, B.L. Oksengendler, N.N. Turaeva, R.Yu. Milusheva, S. Sh. Rashidova

Institute of Polymer Chemistry and Physics ASRU, Uzbekistan

E-mail: dr.asqarov@mail.ru

INTRODUCTION

Development of new technologies of producing of valuable components out of natural high-molecular compounds presents an important task of the modern physics and chemistry of polymers. After obtaining chitin from wastes of silk warm pupae chitosan and a few of its derivatives have been synthesized. It turned out that chitosan and its derivatives have valuable physiological properties [1]. Presently in order to synthesis new important chemicals based on chitosan and its derivatives for medicine and agriculture a simple theoretical method of study of the reaction capability and biological activity of these amino-polysaccharides is necessary.

The object of modeling: monomer chain of chitin presents secondary amine – N acetyl glucoseamine, whose nitrogen is bounded C-2 by carbon of pyranose ring and acetyl group (see Fig.1). During the deacetylation process this secondary amine turns out the primary one and becomes glucose-amine. To study elementary act of the deacetylation process the following algorithms is proposed.

Research algorithm and the model: Model of reaction configuration (RC) will be presented in the form of tetrahedral molecule consisting out of central nitrogen atom and two multi atomic structure of the pyranosis ring and acetyl group and two hydrogen atoms(see Fig.1), i.e. we do not take into account internal oscillating freedom degrees of the pyranosis ring and acetyl group. Single-electron spectrum of RC has four energy levels with the following single-electron orbital's - $|1g\rangle, |2u\rangle, |3g\rangle, |4u\rangle$. In the basic state the bonding electrons are located on the first two orbitals. Hence the high occupied molecular orbital (HOMO) has odd symmetry and the lower un occupied molecular orbital (LUMO) has the even-g (see Fig.2). Thus the basic state of the RC has symmetry $uu=g$ and excited state has $ug=u$ symmetry. According to the Jahn-Teller [2] theory these states mixing and this leads to instability of the symmetrical nanostructure atomic cluster's. By this reason Q_u – oscillations of the nitrogen atom in the RC leads to the rupture of the chemical link of nitrogen either with the piranosis ring or with the acetyl Jan-Teller effect (see Fig.1). Coordinate of the reaction in this case depends on the value $\Delta Z = Z_p - Z_a$, where Z_p is effective charge C-2 of carbon of piranosis ring and Z_a acetyl group.

Thus in frames of the present of theoretical approach it was proved that a control of energetic parameters of the deacetylation and substitution process through Q_u and ΔZ values is necessary. To determine conditions for decrease of the energy barrier along the coordinate of the substitution reaction for the RC we will use vibration model of study of quasichemical reaction in non-metallic media [4]. Dependence of the electron energy on the Q_u and ΔZ for the basic state within frames of the chosen model can be expressed in the following form:

$$\varepsilon = \frac{\varepsilon_u + \varepsilon_g}{2} + \frac{1}{2} k Q_u^2 - \frac{1}{2} \sqrt{(\Delta + w_g)^2 + 4 |a Q_u + w_u|^2} \quad (1)$$

Here ε_g – the energy of the basic state of reactive configuration; not going beyond the approximation of the boundary Fukui orbitals [3], we can consider the energy gap Δ as the energy of excitement. It characterizes difference between electron energies of the initial and secondary amines and due to this reason its value will be proportional to the difference of the ionization potentials; a - vibron constant; k - force constant; w_g - even and w_u - odd components of the low-symmetrical distortion depending on ΔZ .

The first member in the formula (1) corresponds to full energy of electrons obtained in the Born-Oppenheimer approximation. The second member is the full energy of electrons along coordinate of reaction excluding immixture of electron states of the reactive configuration. The third member is stipulated by the Jahn-Teller effect.

For the potential relief along reaction coordinate in the area of the point

$Q_u = 0$ provided that

$\frac{4|aQ_u + w_u|^2}{(\Delta - w_g)^2} < 1$, from the relation (1) we find its approximate expression as following:

$$\tilde{\varepsilon} = \varepsilon_g - \frac{w_g}{2} + \frac{1}{2} \left[k - \frac{2a^2 + \frac{w_u^2}{Q_u^2}}{\varepsilon_g - \varepsilon_u + w_g} \right] Q_u^2 \quad (2)$$

Let us consider the case of absence of symmetrical and low-symmetrical distortions $w_g = w_u = 0$:

$$E = \varepsilon_g + \frac{1}{2} \left[k - \frac{2a^2}{\Delta} \right] Q_u^2 \quad (3)$$

The second member in the expression (3) reflects the barrier decrease due to the pseudo-effect of Jahn-Teller [3]. As one can see by this expression the steepness of increase of the energy barrier reduces due to the decrease of the force constant value of the chemical link. Effect of the vibron labilisation is the stronger the greater is the vibron constant and lesser is the ionization potential differences between the initial (Chitosan) and secondary (Chitin) amines. Replacement of the acetyl groups takes place quicker under impact of factors which increase the ionization potential of the secondary amine. From the expression (2) it follows that low-symmetrical distortions of the electron sub-system of the reactive configurations strengthen the process of vibron labilisation and can in this way to accelerate the deacetylation and substitution process.

Topologic modeling: more detail information regarding potential surface of the reactive configuration described by the equation (1) we can obtain on the basis of the Thom-Arnold [6] theory. According to the Thom's theorem the state of the single-parameter dynamic system is described by the potential

$$V = \frac{1}{3} X^3 + u_1 X; \text{ here } u_1 - \text{is ruling parameter.}$$

The stable state of the system is described by the critical variety

$$\frac{\partial V}{\partial X} = \tilde{X}^2 + u_1 = 0.$$

If $u_1 < 0$ than the system is in the stable state (see Fig.3) Under $u_1 > 0$ the system doesn't have stable state. Transition from the stable to the unstable state takes place in the point $u_1 = 0$ in form of "jump" of the parameter X that characterizes the system state. In the given case the elementary disaster of the A_2 type by Arnold and "jump" is called as an elementary catastrophe the "end" type [6]. If reaction of deacetylation is being considered in the form of the decay of reactive configuration along Q_u then all possible changes of the potential barrier of the reaction caused by the physical model parameters can be modeled by investigation of dependence of Q_u (coordinate of the stable configuration of RC) on the ruling parameter - u_1 . Using the methodic of topologic modeling [5] we obtain the Tom's potential for the coordinate of the stable configuration of RC: $V = \tilde{Q}_u^3 + u_1 \tilde{Q}_u$.

Dependence of the ruling reaction parameter on physical parameters of the model has the following form:

$$u_1 = -\frac{\Delta^2}{2a^2} \left[1 + \frac{\Delta^2 w_u}{24 w_g^3} \left(\frac{k\Delta}{2a^2} - 1 \right) \right].$$

Under $u_1 = 0$ transformation of the secondary amine into the primary amine takes place. Under $\frac{k\Delta}{2a^2} > 1$ (the case of vibronic labilisation) as symmetrical distortion grows the ruling

parameter works for the value $-\frac{\Delta^2}{2a^2}$; by this reason the lesser is Δ and the greater is a , the more

is the probability $\alpha \approx e^{-\Delta E / kT}$ of decay of the reactive configuration. Here ΔE – is the energy of activation reaction. Opposite, the growth of the low-symmetrical distortion stabilizes RC.

Under $\frac{k\Delta}{2a^2} < 1$ (case of the Jahn-Teller instability [3]) with growth of w_u jump-like transition of the secondary amine into the primary amine under condition

$$w_u = \frac{48 w_g^3 a^2}{\Delta^2 (2a^2 - k\Delta)} \quad (4)$$

Mechanism of biological activity chitosan: various chemical of chitosan with different acetylating degree were produced out of chitin and their possible effect upon physiological properties were studied [1]. Experimental researches on animals prove that these medicines differ by the degree of effect on immune reaction of an organism. The more deacetylation degree the stronger it activates immune response of organism on antigen. For example, quantity of nuclear-containing spleen cells in mice immunized by sheep erythrocytes increase symbatic with increase of the deacetylation degree of chitosan chemicals [1]. On the basis of effect of vibronic labilisation of the deacetylation reaction one can suppose that enforcement of the biologic activity of chitosan chemicals occurs under impact of low-symmetrical distortions of pyranose ring into its amine group. The formula (4) shows that the low-symmetrical distortion strengthen for amine centers with low excitation energy. Hence amine group of chitosan during interaction with lipid or protein structure of the biological object rebuilt electron structure in a such way that it reduces energy gap between the HOMO and LUMO of RC of amine center of chitosan. The amine group

is represented as a cluster with a tetrahedral bonds centered on a nitrogen atom. It has been found the conditions of vibronic instability realizations for this configuration, taking into account the Jahn-Teller effect (Fig.1) and pseudo Jahn-Teller (Fig.2) effect. It has been shown any substitution in pyranose ring by other atoms, leads to the stabilization by trigonal distortion of the atomic configuration of amines group (1). In the case of substitution of other ligands of nitrogen amine group its tetragonal distortion (2), which is accompanied by increased vibronic instability of the amines group.

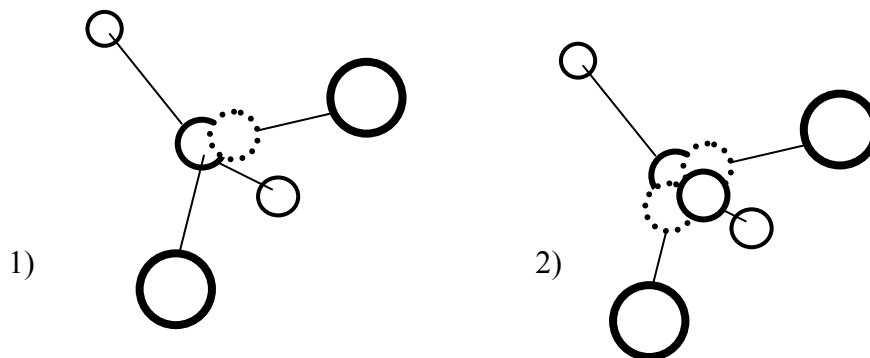


Fig.1 Trigonal distortions due to the Jahn-Teller effect in amine group.

Fig.2. Tetragonal distortions due to the pseudo Jahn-Teller effect in perturbed amine group.

The amine group is represented as a cluster with a tetrahedral bonds centered on a nitrogen atom. Based on this model, a comparative description of the biological activity of chitosan, chitosan sulfate and ascorbate have been fulfilled assuming that the Jahn-Teller effect significantly removes the steric restrictions.

CONCLUSIONS

Electron-vibronic theory of building the potential surface of chemical reactions combined with the method of topologic modeling gives important information about biological activity of some biopolymers. Planning of experimental researches based on ruling parameters of the topological modeling of physiology processes increases their efficiency and reliability.

REFERENCES

- [1] Rashidova, S.Sh., Milusheva, R.Yu. (2009) *Hitin i Hitozan Bombix Mori*. Sintez, svoystva i primeneniye, FAN AN RUz, Tashkent, 246 p.
- [2] Jahn, H.A., Teller, E. (1937) *Proc. Roy. Soc. London A*, 161, 220 -235.
- [3] Bersuker, I.B. (1984) *The Jahn – Teller effect and vibronic interactions in modern chemistry*. N.Y.: Plenum press, 320 p.
- [4] Askarov, B., Oksengendler, B.L., Yunusov, M.S. (1979) *Proceedings of International Conference on Radiation Physics of solids*. Nauka, Tbilisi, p.48.
- [5] Askarov, B., Oksengendler, B.L., Yunusov, M.S. (1981) *In Materials International Conference Defects in insulating crystals*, Riga, p.179-180.
- [6] Arnold, V.I. (1983) *Catastrophe Theory*, Moscow, Nauka, 80 p.

BIOPHYSICAL MODEL OF BACTERICIDAL ACTIVITY OF CHITOSAN

J.T.Azimov, N.N.Turaeva, B.L.Oksengendler, R.Yu.Milusheva, S.Sh.Rashidova

*Institute of polymers chemistry and physics,
100128 Tashkent, Kadiri str.7B, Uzbekistan*

E-mail: azimovjt@yandex.ru

Among various biological properties chitosan the special attention is deserved by its high bactericidal activity [1-4]. It does perspective its application in medicine. At the same time the researches has shown [2-4], that biological activity of chitosan is defined by its many characteristics: (its degree of deacetylation, charges along the chain, the molecular weight, the concentration of chitosan) and by the type of bacteria (gram-negative or gram-positive).

Analyzing the experiments on bactericidal properties chitosan it is possible to reveal the following conceptual facts:

1. The increase of the number of amine groups in chitosan and a positive charge of chitosan in solutions enhances its antimicrobial activity [3].
2. At moderated concentration of chitosan its antimicrobial activity increases with decreasing of its molecular weight, for gram-positive, and gram-negative bacteria. However, in a wide range of molecular weight there is unmonotonic dependence of bactericidal activity of chitosan (fig. 1) [3, 4].
3. Bactericidal activity of chitosan increases with the concentration of chitosan solution (fig. 1) [4].
4. Chitosan exhibits a stronger activity against gram-negative bacteria, than gram-positive bacteria [2, 3].

It is actual to work out a biophysical model of bactericidal activity chitosan, to cover these conceptual experimental facts and to reveal the condition of maximum bactericide activity of chitosan.

Analyzing the dependence of bactericidal activity of chitosan on molecular weight at its moderate concentration (fig. 1.) it is possible to conclude that at small and large molecular weights of chitosan the strong bactericidal activity takes place. From our opinion, it is connected with two different mechanisms of bactericidal activity:

- At shorter chitosan molecule it penetrates into the cell of bacterium from environment in which it formed complexes with DNA, inactivating the process of replication of DNA;
- At the large molecular weights the adhesion of a molecule chitosan on the cell wall is high, it penetrates into cell wall and corks its ionic channels, important for cell functioning. With the concentration of chitosan the number of corked ionic channels by chitosan increases.

In intermediate molecular weights of chitosan both these mechanisms appear to be not effective, that is the adhesion of chitosan is not high, and the molecules of chitosan don't penetrate into through the membrane.

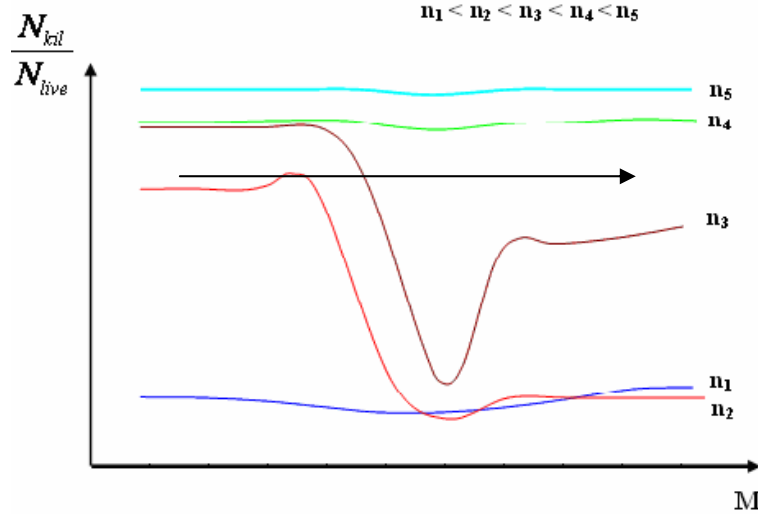


Fig. 1. Dependence of bactericidal activity chitosan upon its molecular weight (M) at its various concentration (N).

Let's consider conditions of realization of the first mechanism of bactericidal activity. Transition of the ion from the solution into the membrane can be considered as its transition from the medium with one dielectric permittivity to the medium with another dielectric permittivity energy of which can be estimated by Born's approach [5,6], account in the role of entropy.

Free energies of the charged macromolecule (i.e. chemical potential) in the water solution and in a membrane of cell can be defined as followings.

$$F_w = \frac{q^2}{2R_o} \left[-\left(1 - \frac{1}{\varepsilon_w}\right) \right] - TS_w \quad F_m = \frac{q^2}{2R_o} \left[-\left(1 - \frac{1}{\varepsilon_m}\right) \right] - TS_m - \frac{q \times q_m}{R}. \quad (1)$$

Here q – is the positive charge of chitosan, q_m – is the negative charge of membranes, S – is the conformational entropy of polymer coil, R_o – is the coil radius, R – is the distance between chitosan negative charged membrane. Assuming that each monomer of chitosan is positive charged, it is possible to express an ion charge in terms of chain length and the size of the coil. Considering a macromolecule coil as ideal it is possible to write the following expression

$$q = e \frac{L}{d_o} = e \frac{4R_o^2}{d_o l} = e \frac{Nl}{d_o} \quad (2)$$

Here L – is the length of the chain, d_o – is the size of a monomer, l – is the persistent length of the chain. Assuming that the coil has the same conformation in water, and in a membrane, it is possible to find free energy changing at transition of coil polymer from the water into the membrane

$$\Delta F \approx \frac{e^2 N^{3/2} l}{d_o^2} \left[\frac{1}{\varepsilon_m} - \frac{1}{\varepsilon_w} \right] - \frac{e N l q_m}{d_o R} \quad (3)$$

It has obvious from the formula (3) the change of free energies of the ion depends non-linearly on the number of segments in the coil (fig. 2).

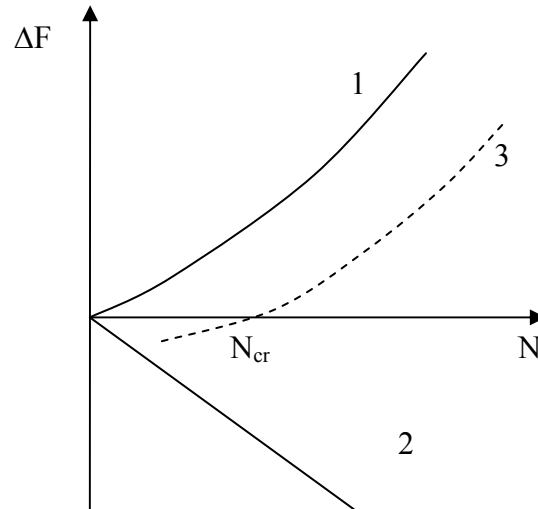


Fig. 2. Change of free energy of chitosan ion at its transition from water into the membrane : 1,2 – dependences of energy dehydration and energy of Coulomb interactions on the number of segments in the chain; 3 – the sum of curves 1,2.

At $\Delta F \leq 0$ chitosan coil spontaneously penetrates into the membrane. The conditions of spontaneous realization of this effect depending on number of chitosan segments are the following:

$$N^{1/2} \leq \frac{q_m d_o}{e R_{pore}} \left[\frac{\varepsilon_w \varepsilon_m}{\varepsilon_w - \varepsilon_m} \right] \equiv N_{cr} \quad (4)$$

Thus, at the lengths of macromolecules chitosan less than critical one, chitosan spontaneously penetrate through the membrane and into the cell, forms a complex with negatively charged DNA, thereby inhibits the process of its replication. As gram-negative bacteria have greater number of negative charges on the membrane compared gram-positive enhanced adhesion of polymer takes place.

Realization of the second mechanism occurs under the condition

$$\Delta F \approx \frac{e^2 N^{3/2} l}{d_o^2} \left[\frac{1}{\varepsilon_m} - \frac{1}{\varepsilon_w} \right] - \frac{e N l q_m}{d_o R} \leq 0 \quad (5)$$

Taking into account that the channel of membrane is of water medium we can define the following expression:

$$\Delta F \approx -\frac{e N l q_m}{d_o R} \leq 0. \quad (6)$$

Hence the adhesion of chitosan molecule on cell wall occurs spontaneously. Thus, the molecule of chitosan can cork ionic channels in the membrane, thereby disbalancing the ionic exchange between the cell and its environment. With the reduction of number of segments (i.e. molecular weight) adhesion of chitosan on cell wall of a bacterium decreases.

The concentration dependences of bactericidal activity can be explained on the base of its kinetics.

$$dN_{kill}/dt = k_1 N_{ch} + k_2 N_{chanal} \cdot N_{ch} - N/\tau, \quad (7)$$

where N_{kil} is the concentration of the killed bacteria, N_{ch} are the concentration of chitosan molecules, N_{chanal} is the number of ionic channels. $1/\tau$ is the probability of spontaneous destruction of bacterium, k_1 and k_2 are the constants of the chemical processes corresponding to the first and second mechanisms. The first term in the equation (7) corresponds to complexation of chitosan with DNA at realization of the first mechanism. The second term in the equation corresponds to the interaction of the chitosan molecules with ionic channels of membrane. It is possible to find the stationary solution of the equation (7) which is equal

$$N_{kill} = \tau[k_1 + k_2 N_{chanal}] \times N_{ch}.$$

The analysis of stationary value shows that at concentration increasing of chitosan the number of killed bacteria by chitosan (fig. 3) increases that is in agreement with the experimental results [4].

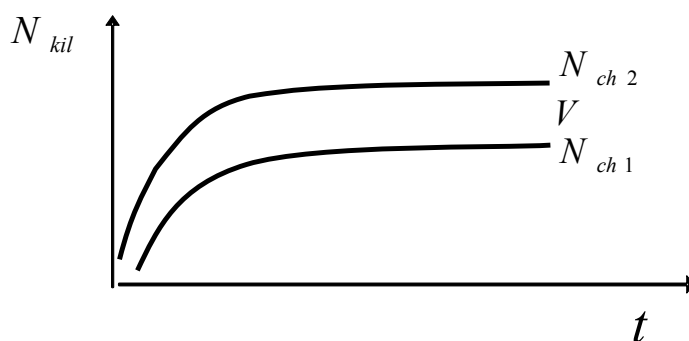


Fig. 3. Number of killed bacteria at two concentrations of chitosan ($N_{ch2} > N_{ch1}$)

Thus, on the basis of thermodynamic analysis based on calculations of change of free energy at transition of cation-polymer from water into the membrane taking into account the Born's energy, the conformation entropy and electric interaction of the cation with negative charges of cell wall, it is possible to conclude that two mechanisms of bactericidal activity of chitosan takes place. At small molecular weights chitosan penetrates through the membrane into the cell complexing with DNA with the subsequent inhibition of the process of RNA and proteins synthesis. At large molecular weights the positively charged chitosan interacted with negatively charged wall of bacterium cell, corks the ionic channels and interrupts normal functioning of the cell. From the kinetics of bactericidal activity chitosan it has been seen that with the concentration of chitosan the number of killed bacteria increases.

REFERENCES

- [1] Rashidova, S.Sh., Milusheva, R. Yu. (2009) Chitin and chitosan bombyx mori. Synthesis, properties and application. Tashkent: FAN, 246 p.
- [2] Rashidova, S.Sh., Milusheva, R. Yu. (2010) Nanostructured polysaccharides on the chitosan Bombyx mori base and possibility their using in medicine. 6th NANOFUN-POLY Conference, Madrid, p.92.
- [3] Mohy Eldin, M.S., Soliman, E.A. Hashem, A.I, Tamer ,T.M. (2008) Trends Biomater. Artif. Organs, 22 (3), 125-137.
- [4] Liu, N., Chen, X.-G., Park, H.-J. et al. (2006) Carbohydrate polymers, 64, 60-65.
- [5] Rubin, A.B. (2004) Biophysics, M: Nauka, 469 p.
- [6] Davydov, A.S. (1979) Biology and quantum mechanics. Kiev: Nauka Dumka, 297 p.

EFFECT OF CHITOLIGOSACCHARIDES IN MURINE ADIPOSE-SPECIFIC GENE REGULATION

**Soon-Sun Bak^{1*}, Byul-Nim Ahn², Jung-Ae Kim², Ratih Pangestuti², Chang-Suk Kong³,
Se-Kwon Kim^{1,2}**

¹ Marine Bioprocess Research Center, Pukyong National University, Busan 608-737, Republic of Korea

² Department of Chemistry, Pukyong National University, Busan 608-737, Republic of Korea

³ Department of Food and Nutrition, College of Medical and Life Science, Silla University, Busan 617-736, Republic of Korea

*E-mail address: nor-sun80@hotmail.com

INTRODUCTION

Obesity is mainly caused by a combination of excessive dietary calories, lack of exercise, unhealthy life style such as sedentary lifestyle, and genetic susceptibility. It may have an adverse effect on health, leading to reduced life expectancy [1]. Obesity increases the risk of many physical and mental conditions. These co-morbidities are reflected predominantly in metabolic syndrome such as dyslipidemia, fatty liver glucolipotoxicity, gluointolerance, hypertension, atherosclerosis, diabetes mellitus type 2 [2]. These health consequences can be categorized by the effects of increased fat mass (osteoarthritis, obstructive sleep apnea, social stigmatization) or by the increased number of fat cells. Therefore regulation of obesity by preventing the fat accumulation and stimulating the reduction of body fat is important in our body. Metabolism of the adipogenesis, lipogenesis and lipolysis are modulated by various kinds of transcription factors and obese gene. Several adipogenic transcription factors have been identified including peroxisome proliferator-activated receptor gamma (PPAR γ), CCAAT-enhancer-binding proteins alpha (C/EBP α) and adipocyte determination and differentiation-dependent factor 1/sterol regulatory element-binding protein (ADD1/SREBP1) [3,4], these three transcription factors play a regulatory role in the process of adipogenesis.

Chitooligosaccharides (COS) are hydrolyzed derivatives of chitin or chitosan which has shorter chain and free amino groups in D-glucosamine units. COS has been shown to exhibit a variety of biological activities including antimicrobial, antiviral, antitumor, antioxidant, free radical scavenging, immunostimulant, fat lowering and hypocholesteromic effects [5]. Moreover COS has been reported to protect pancreatic β -cells [6] and inhibit angiotensin converting enzyme (ACE) and coagulant [5]. Recently, it was reported that biological activities of COS are strongly correlated with their molecular weights of COS. Even though COS has been reported to have antiobesity activity [5,7-9], there has a little reported data of molecular signaling mechanism by COS with different molecular weights. Only Cho *et al.*, demonstrated that 1-3 kDa molecular weight of COS has the lowest TG concentration among the 1-10 kDa molecular weights of COS [7]. For that reason, in this study we designed the molecular weight of COS below 1 kDa to 5 kDa.

In our study, we investigated the inhibition activity of adipocyte differentiation and its signaling mechanism including adipogenic transcription factors by different molecular weights of COS in 3T3-L1 murine adipocyte cells.

MATERIALS and METHODS

Materials

Different molecular weights COS were kindly donated by Kitto Life Co. (Seoul, Korea): COS 1K (below 1 kDa), COS 3K (1 kDa to 3kDa), COS 5K (3 kDa to 5 kDa).

Cell culture and adipocyte differentiation

Mouse 3T3-L1 preadipocyte (ATCC, USA) were cultured in Dulbecco's modified Eagle medium (DMEM) containing 10% fetal bovine serum (FBS) and 1x penicillin-streptomycin at 37°C in a 5% CO₂ incubator. 3T3-L1 preadipocyte (2×10^5 cells/well) were seeded into 6-well plates, and cultured until become full. At day 0, cell differentiation was induced with a mixture of 0.5 mM methylisobutylxanthine, 0.25 μ M dexamethasone and 5 μ g/ml insulin in DMEM containing 10% FBS. After 48 h (day 2), the differentiation induce medium was removed and replaced with DMEM containing 10% FBS supplemented with 5 μ g/ml insulin. This medium was re-fed every 2 days and COS (1 mg/ml) was treated to the culture medium from day 0 to day 7. As adipocyte differentiation was fully at day 7 and the lipid dropft was no more formulate after 8 day, we qualified experiment for day 7.

Oil-red O staining

For Oil-Red O staining (Sigma-Aldrich Inc., St. Louis, MO, USA), cells were washed gently twice with PBS, fixed with 3.7% fresh formaldehyde in PBS for 1 h at room temperature, and stained with filtered Oil-red O solution (60% isopropanol and 40% water) for at least 1 h. After staining, the Oil-red O staining solution was removed and the plates were rinsed with water and dried. Dye retained in the cells was eluted with isopropanol and quantified by measuring optical absorbance at 500 nm using a microplate reader (Tecan Austria GmbH, Austria).

Measurement of triglyceride content

Cellular triglyceride contents were measured using a commercial triglyceride assay kit (Eiken Chemical, Triglyzyme-V, Tokyo, Japan). according to the manufacturer's instructions. Cells were treated with COS at concentrations of 1 mg/ml in 6-well plates during adipocyte differentiation for 7 days (from day 0 to day 7). The cells were washed twice with phosphate buffered saline (PBS), followed by the addition of 75 μ l of homogenizing solution (154 mM KCl, 1 mM EDTA, 50 mM Tris, pH 7.4) and sonication to homogenize the cell suspension. The residual cell lysate was centrifuged at 3000 \times g for 5 min at 4°C to remove the fat layer. The supernatants were assayed for triglyceride content and protein content. Triglyceride content was normalized to protein concentration using the BSA as a standard. Results were expressed as milligrams of triglyceride per milligram of cellular protein.

RNA extraction and reverse transcription-polymerase chain reaction (RT-PCR) analysis

Total cellular RNA was isolated from 3T3-L1 adipocytes using Trizol reagent (Invitrogen, Carlsbad, CA, USA). Total RNA (2 μ g) was added to RNase-free water and oligo (dT), followed by denaturation at 70°C for 5 min and immediately cooling. RNA was reverse transcribed in a master mix containing 1X RT buffer, 1 mM dNTPs, 500 ng oligo (dT), 140 U MMLV reserve transcriptase and 40 U RNase inhibitor at 42°C for 60 min and at 72°C for 5 min using an automatic Whatman thermocycler (Biometra, UK). The target cDNA was amplified using the following sense primer and antisense primers: forward 5'-TTT-TCA-AGG-GTG-CCA-GTT-TC-3' and reverse 5'-AAT-CCT-TGG-CCC-TCT-GAG-AT-3' for PPAR γ ; forward 5'-TTA-CAA-CAG-GCC-AGG-TTT-CC-3' and reverse 5'-GGC-TGG-CGA-CAT-ACA-GTA-CA-3' for C/EBP α ; forward 5'-TGT-TGG-CAT-CCT-GCT-ATC-TG-3' and reverse 5'-AGG-GAA-AGC-TTT-GGG-GTC-TA-3' for SREBP1; forward 5'-AGC-CAT-GTA-CGT-AGC-CAT-CC-3' and reverse 5'-TCC-CTC-TCA-GCT-GTG-GTG-GTG-AA-3' for β -actin. The amplification cycles were carried out at 95°C for 45 sec, 60°C for 1 min and 72°C for 45 sec. After 30 cycles, the PCR products were separated by electrophoresis on 1.5% agarose gel for 30 min at 100 V. Gels

were then stained with 1 mg/ml ethidium bromide and visualized by UV light using AlphaEase[®] gel image analysis software (Alpha innotech, CA, USA).

Western blot analysis

Western blotting was performed according to standard procedures. Briefly, cells were lysed in RIPA lysis buffer at 4°C for 30 min. Cell lysates (20 µg) were separated by 12% SDS-polyacrylamide gel electrophoresis, transferred onto a polyvinylidene fluoride membrane, blocked with 5% skim milk and hybridized with primary antibodies (diluted 1:1000). After incubation with horseradish-peroxidase-conjugated secondary antibody at room temperature, immunoreactive proteins were detected using a chemiluminescence ECL assay kit (Amersham Pharmacia Biosciences, England, UK) according to the manufacturer's instructions. Western blot bands were visualized using a LAS3000[®] Luminescent image analyzer (Fujifilm Life Science, Tokyo, Japan).

Statistical analysis

Data were expressed as mean \pm SEM (n=3). Differences between the means of individual groups were assessed by one-way ANOVA with Duncan's multiple range tests using the statistical software package, SAS v9.1 (SAS Institute Inc., Cary, NC, USA). Differences were considered significant at $p < 0.05$.

RESULTS and DISCUSSION

To investigate effects of COS on the lipid accumulation, 3T3-L1 cells were treated with different molecular weight of COS at 1 mg/ml concentrations for 7 days during differentiation periods (Fig. 1). Lipid accumulation was quantified by Oil-Red-O staining and TG measurement. Treatment of COS inhibited the formation of lipid droplet, especially, COS 1K significantly suppressed the number and size of lipid droplet compared to COS 3K and 5K (data not shown). For that reason, absorbance level of eluted Oil-Red-O stain was decreased significantly in COS 1K compared to COS 3K and 5K (Fig. 1A). Moreover, COS 1K and 3K significantly reduced TG concentration, main constituent of the fat droplet, compared to COS 5K (Fig. 1B). This result suggested that molecular weight of COS might associated with the adipocyte differentiation and low molecular weight of COS were the most effective in inhibiting the lipid accumulation. Therefore we estimated that low molecular weight of COS posses participate into signal transduction pathways via regulating adipocyte differentiation.

In order to determine whether COS inhibitory effect on lipid accumulation was associated with modulating of transcription factors in 3T3-L1 cells, Western blot and RT-PCR analysis were conducted. When the preadipocyte fully differentiated to adipocyte in 3T3-L1 at day 7, the expression level of the transcription factors including PPAR γ , C/EBP α and SREBP1c were high. Treatment of COS 1K significant reduced protein and mRNA expression levels of PPAR γ , C/EBP α and SREBP1c compared to COS 3K and 5K. It has been reported that these three main transcription factors directly influence adipocyte differentiation [10,11]. PPAR γ , one of the nuclear hormone receptor superfamily expressed in adipose tissue, appear as dominant activators of adipocyte differentiation [12]. C/EBP α induces adipose differentiation via PPAR γ activation both *in vitro* and *in vivo* and increased C/EBP α synthesis may needed for the adipocyte size increase and obesity advances [7,13]. SREBP1c induce during early adipocyte differentiation and correlated in cholesterol metabolism by regulates adipocyte specific gene expressions such as LPL and FAS [4,14,15]. Hence, the result of this study suggested that low molecular weight of COS suppress the adipocyte differentiation via PPAR γ , C/EBP α and SREBP1c mediated adipogenesis mechanisms.

It was still unclear why the different molecular weight of COS participate to different activities on adipocyte differentiation in 3T3-L1 cells. We suggested that the low molecular weight of COS might lead to high absorption activity into the cell and corresponds to the inhibition effects in adipocyte differentiation. In conclusion, our study revealed that COS elicits suppression in adipocyte differentiation on 3T3-L1 cells and activation of COS depending on the molecular weight. Data show that suppression in adipocyte differentiation on 3T3-L1 cells by COS was induced via modulating of adipocyte transcription factors, including PPAR γ , SREBP1c and C/EBP α . Based-on these findings, low molecular weight COS (below 1 kDa) may regulate the obesity through suppressing the adipogenesis in adipocytes.

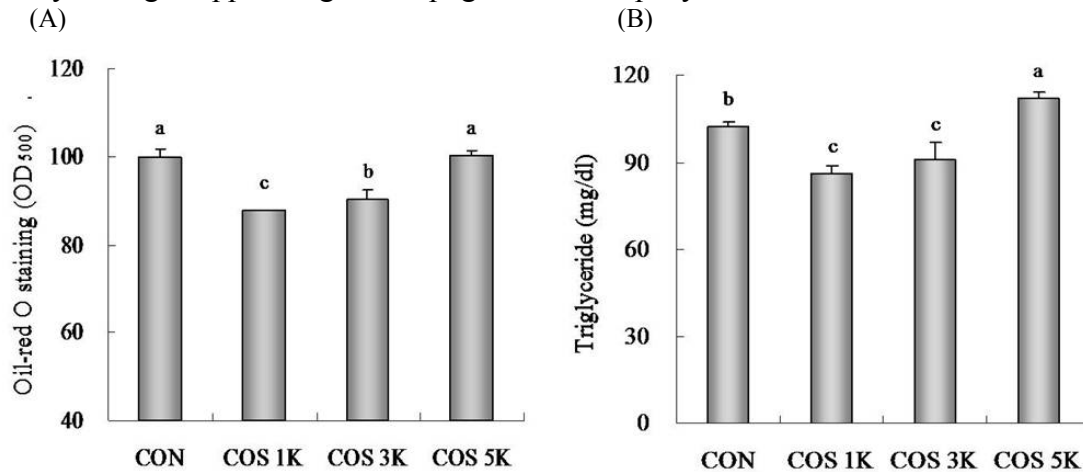


Figure 1. Low molecular weight of COS inhibit lipid accumulation using Oil-Red O staining (A) and triglyceride (B) 3T3-L1 cells were treated with different weight of COS (1 mg/ml) during the adipocyte differentiation for 7 days. The results (n=5) are indicated as a percentage of the control (without treated sample). Values are the mean \pm SEM. ^{a-c} Means with different letter are significantly different (p<0.05) by Duncan's multiple range test. CON: without treated sample, COS 1K: below 1 kDa molecular weight of COS, COS 3K: 1kDa to 3kDa molecular weight of COS, COS 5K: 3kDa to 5kDa molecular weight of COS

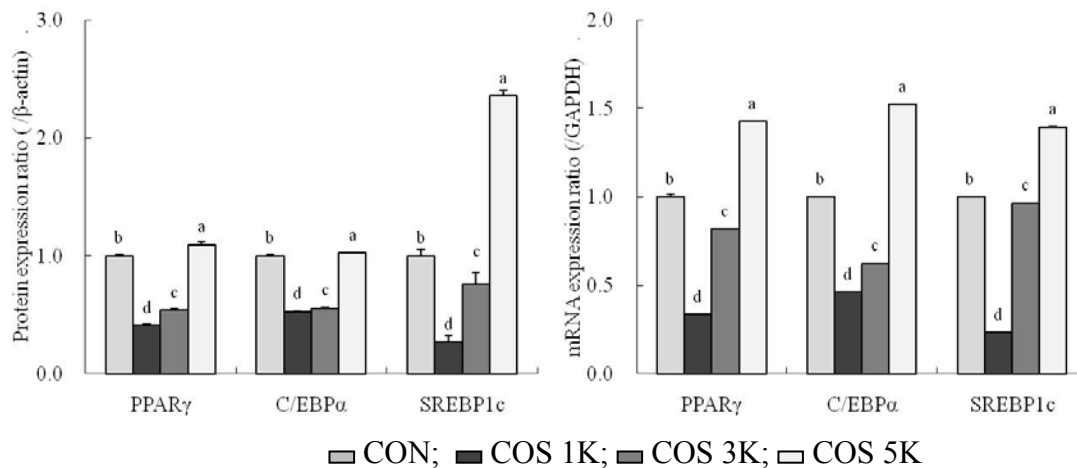


Figure 2. Low molecular weight of COS inhibit protein (A) and mRNA (B) expressions of PPAR γ , C/EBP α and SREBP1c

3T3-L1 cells were treated with different weight of COS (1 mg/ml) during the adipocyte differentiation for 7 days. The results (n=5) are indicated as a ratio of the control (without treated sample). Values are the mean \pm SEM. ^{a-d} Means with different letter are significantly different (p<0.05) by Duncan's multiple range test. CON: control (without treated sample), COS 1K: below 1 kDa molecular weight of COS, COS 3K: 1kDa to 3kDa molecular weight of COS, COS 5K: 3kDa to 5kDa molecular weight of COS

ACKNOWLEDGEMENTS

This research was supported by a grant from Marine Bioprocess Research Center of the Marine Biotechnology Program funded by the Ministry of Land, Transport and Maritime, Republic of Korea.

REFERENCES

- [1] Bower, J.F., Davis, J.M., Hao, E., Barakat, H.A. (2005) Differences in transport of fatty acids and expression of fatty acid transporting proteins in adipose tissue of obese black and white women. *Am. J. Physiol.* 290, 87-91.
- [2] Cao, G., Liang, Y., Broderick, C.L., Oldham, B.A., Beyer, T.P., Schmidt, R.J. et al. (2003) Antidiabetic action of a liver x receptor agonist mediated by inhibition of hepatic gluconeogenesis. *J. Biol. Chem.* 278, 1131-6.
- [3] Barak, Y., Nelson, M.C., Ong, E.S., Jones, Y.Z., Ruiz-Lozano, P., Chien, K.R., Koder, A., Evans, R.M. (1999) PPAR gamma is required for placental, cardiac, and adipose tissue development. *Mol. Cell.* 4, 585-95.
- [4] Brown, M.S., Goldstein, J.L. (1997) The SREBP pathway: regulation of cholesterol metabolism by proteolysis of a membrane-bound transcription factor. *Cell.* 89, 331-40.
- [5] Kim, S.K., Rajapakse, N. (2005) Enzymatic production and biological activities of chitosan oligosaccharides (COS): A review. *Carbohydr. Polym.* 62, 357-68.
- [6] Karadeniz F, Artan M, Kong CS, Kim SK. (2010) Chitooligosaccharides protect pancreatic β -cells from hydrogen peroxide-induced deterioration. *Carbohydr. Polym.* 82, 143-7.
- [7] Cho, E.J., Rahman, M.A., Kim, S.W., Baek, Y.M., Hwang, H.J., Oh, J.Y., Hwang, H.S., Lee, S.H., Yun, J.W. (2008) Chitosan oligosaccharides inhibit adipogenesis in 3T3-L1 adipocytes. *J. Microbiol. Biotechnol.* 18, 80-7.
- [8] Rahman, A., Kumar, S.G., Kim, S.W., Hwang, H.J., Baek, Y.M., Lee, S.H. et al. (2008) Proteomic analysis for inhibitory effect of chitosan oligosaccharides on 3T3-L1 adipocyte differentiation. *Proteomics.* 8, 569-81.
- [9] Kumar, S.G., Rahman, M.A., Lee, S.H., Hwang, H.S., Kim, H.A., Yun, J.W. (2009) Plasma proteome analysis for anti-obesity and anti-diabetic potentials of chitosan oligosaccharides in ob/ob mice. *Proteomics.* 9, 2149-62.
- [10] Rosen, E.D., Walkey, C.J., Puigserver, P., Spiegelman, B.M. (2000) Transcriptional regulation of adipogenesis. *Genes. & Dev.* 14, 1293-307.
- [11] Jeon, T., Hwang, S.G., Hirai, S., Matsui, T., Yano, H., Kawada, T., Lim, B.O., Park, D.K. (2004) Red yeast rice extracts suppress adipogenesis by down-regulating adipogenic transcription factors and gene expression in 3T3-L1 cells. *Life. Sci.* 75, 3195-203.
- [12] Cornelius, P., MacDougald, O.A., Lane, M.D. (1994) Regulation of adipocyte development. *Annu. Rev. Nutr.* 14, 99-129.
- [13] Rosen, E.D., Hsu, C.H., Wang, X., Sakai, S., Freeman, M.W., Gonzalez, F.J., Spiegelman, B.M. (2000) C/EBP α induces adipogenesis through PPAR γ : a unified pathway. *Genes. & Dev.* 16, 22-6.
- [14] Kim, J.B., Spiegelman, B.M. (1996) ADD1/SREBP1 promotes adipocyte differentiation and gene expression linked to fatty acid metabolism. *Gene. & Dev.* 10, 1096-107.
- [15] Tabor, D.E., Kim, J.B., Spiegelman, B.M., Edwards, P.A. (1999) Identification of Conserved cis-Elements and Transcription Factors Required for Sterol-regulated Transcription of Stearoyl-CoA Desaturase 1 and 2. *J. Biol. Chem.* 274, 20603-10.

PRODUCTION OF GLUCOSAMINE HYDROCHLORIDE FROM CRUSTACEAN SHELL

Martha Benavente^{1*}, Luis Moreno², Joaquín Martínez²

¹ National University of Engineering, Nicaragua

² Royal Institute of Technology, Sweden

*E-mail address: bena@kth.se

INTRODUCTION

Glucosamine (C₆H₁₃NO₅) or 2-Amino-2-deoxy-glucose chitosamine is an amino sugar naturally present in human body and crustacean shells. It is a precursor of biochemical synthesis of glycosilades proteins and lipids. Glucosamine in the form of glucosamine sulphate, glucosamine hydrochloride, or N-acetyl-glucosamine is extensively used as a dietary supplement in the treatment for osteoarthritis, knee pain, and back pain [1, 2], and a critical evaluation indicated that glucosamine is safe under current conditions of use and does not affect glucose metabolism [3].

Glucosamine can be prepared by acid hydrolysis [4, 5] using strong mineral acids or by enzymatic hydrolysis [6] using bacterial chitinase. Different methods for acid hydrolysis of chitin to produced glucosamine hydrochloride (G-HCl) have been studied. Leite et al. used the reflux technique to hydrolyze chitin with 37% hydrochloric acid (1:5 S/L ratios) at 100°C and under different reaction times [4]. Novikov carried out the acid hydrolysis of chitin and chitosan with 36.5% HCl at 50 and 70°C [5]. Li et al. increased the temperature from 60 to 90°C to optimize the preparation process of G-HCl [7].

Although glucosamine can be produced from different natural sources e.g. chitin and by fermentation of corn and wheat, the most effective one is derived from chitin of shellfish [8]. Chitin is a natural polysaccharide, no toxic, biodegradable and is part of the structural material of the fungal cell walls, insect exoskeletons and crustacean shells. Chitin and its derivative chitosan has a wide range of applications in different areas such as agriculture, drinking water and wastewater treatment, food and beverages, cosmetics and toiletries, biomedics and pharmaceuticals, fibres and textiles, and paper technology [9].

Nicaragua produces thousands of tons of crustaceans such as shrimps and prawns annually [10] and the waste shells, the raw material to produce chitin constitute approximately 40–50% of the total weight [11]. Currently, the wastes from seafood factory operations are available in large quantities. The use of these waste shells can be a low cost alternative to obtain valuable products such as chitin, chitosan and G-HCl.

The aim of this work is the use of crustacean shell as raw material to obtain glucosamine hydrochloride at laboratory level. For this purpose, chitin was extracted from shrimp shells using a chemical treatment, and glucosamine hydrochloride was produced by acid hydrolysis of chitin with 12 M hydrochloric acid using the reflux technique.

MATERIALS and METHODS

Materials

Shrimp waste (head, legs, shell, and tail) was provided by Camanica (PESCANOVA Group), a shrimp processing facility located in Chinandega, Nicaragua.

Chitin and D-Glucosamine HCl was purchased from Jining Green Group Co. Ltd, Shandong, China. D-Glucosamine HCl is a white crystalline free flowing powder with a 99.86% purity and -400 mesh particle size.

Chitin extraction

Chitin was extracted from shrimp waste by desproteinization, demineralization and depigmentation at laboratory level. The Figure 1 shows a block diagram of the overall process. The raw material was first submerged in 10 wt% NaOH solution for 2 h with constant agitation to remove proteins. The desproteinized material was then demineralized using 1.8 mol/L HCl solution for 12 h and subsequently, the product was submerged in 0.38 wt% NaClO solution for 1 h with agitation to remove pigments. Chitin was washed several times using distilled water until pH between 6 and 7 was achieved and dried at 50°C during 10 h. Finally, chitin was milled and screened to select the fraction of particles with a size lower than 0.22 mm.

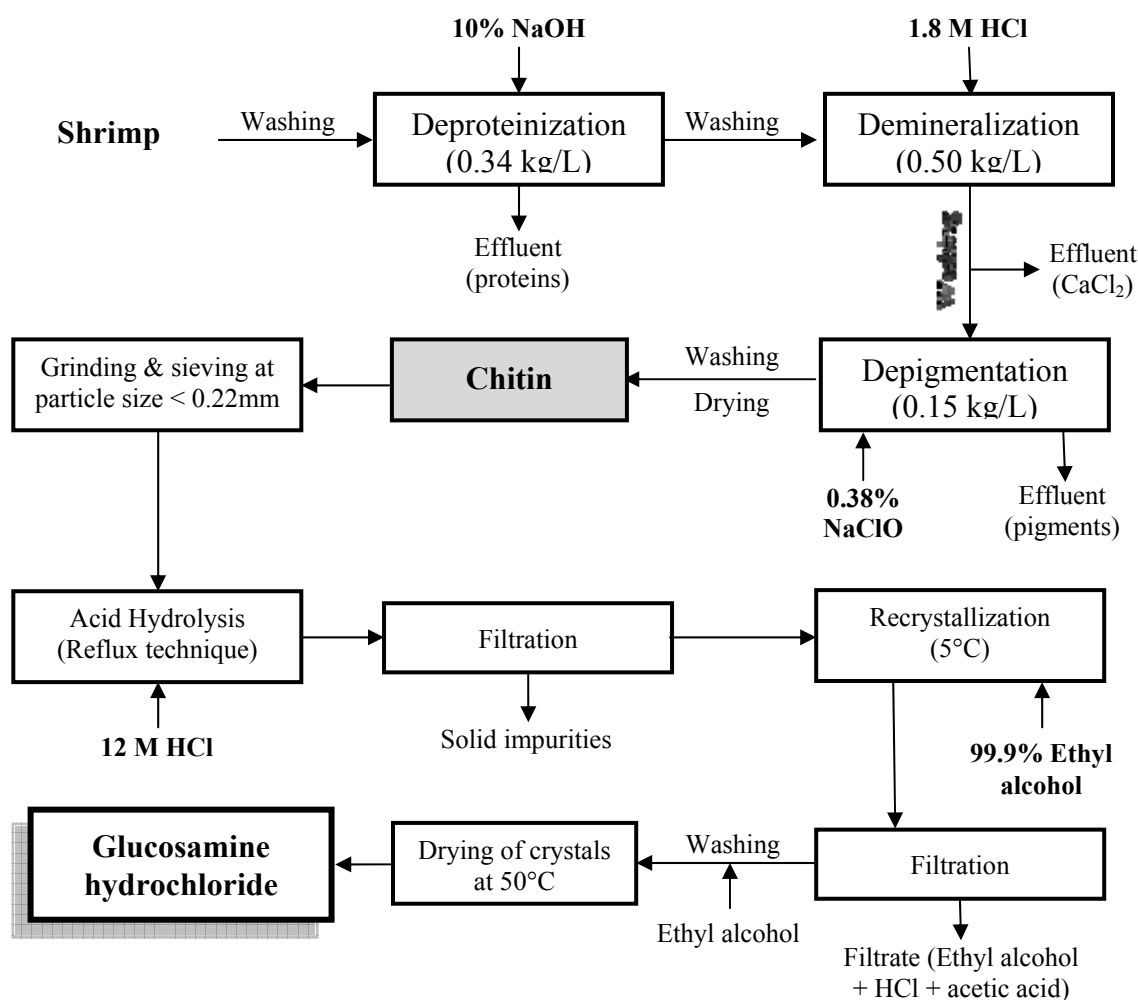


Figure 1. Block Diagram for the extraction of chitin from shrimp shells and production of glucosamine hydrochloride.

Glucosamine hydrochloride production

According to block diagram in Figure 1, the principal stages for G-HCl production from chitin were: (i) acid hydrolysis of polysaccharide, (ii) filtration of the solution, (iii) recrystallization of the product, and (iv) filtration, washing and drying of final product at 50°C.

The acid hydrolysis procedure was performed with 12 M hydrochloric acid using the reflux technique according to the procedure in [4]. However, in preliminary experiments under these conditions (hydrolysis for 1 h at 100°C) it was observed that the results were not satisfactory because HCl was consumed very rapidly in the first minutes of the reaction. Based in this experience, the acid hydrolysis was carried out in two experimental sets at different conditions (see Table 1): (1) Two different solid/liquid ratios, at different temperatures and agitation (with and without) and (2) different solid/liquid ratios, at temperatures range of 68–85 °C and with agitation. HCl was previously heated to 60°C before the addition of chitin, according to procedure in [7]. All experiments were carried out in duplicate.

Table 1 Work conditions in each experiment set for acid hydrolysis of chitin

Experiment set 1				Experiment set 2	
Exp No.	Solid/liquid ratio	Temperature (°C)	Agitation	Exp No.	Solid/liquid ratio
1.1	1:10	40	Without	2.1	1:10
1.2	1:10	68	With	2.2	1:20
1.3	1:20	58	Without	2.3	1:30
1.4	1:20	85	With	2.4	1:40

The process for G-HCl production was performed as follows: 1 g of chitin and an amount of 12 M HCl (depending on solid/liquid ratio) were introduced into a 150 mL reflux vessel. The mixture was kept at the given temperatures until the solid was completely dissolved. The resulting hydrolyzed was filtered by gravity through a VWR Grade 474 filter paper to remove the solid particles present in solution, and it was left to crystallize at room temperature (25±2°C) by 25 days. In order to increase the crystallization rate, ethyl alcohol (15 mL, $w = 97.9\%$) was added, and the resulting mixture was cooled to 5°C for 15 days. The mixture was once more filtered, and the solid crystals were washed with ethyl alcohol and drying at 50°C in an oven for 12 h.

Collection of FTIR Spectra

The spectra of chitin and G-HCl obtained in these experiments were compared with the commercial references. A Bruker Optics ALPHA FT-IR Spectrometer was used to determine their spectra. A spectral range between 400 and 4000 cm^{-1} was used.

RESULTS and DISCUSSION

Chitin characterization

The principal components of shrimp shells such as proteins, calcium minerals, and pigments were removed to get chitin as final product. The average content of chitin in the raw material (dry basis) was 25 %. The identification of chitin by comparing its FTIR spectrum with that of a reference sample showed a correlation coefficient of 95%.

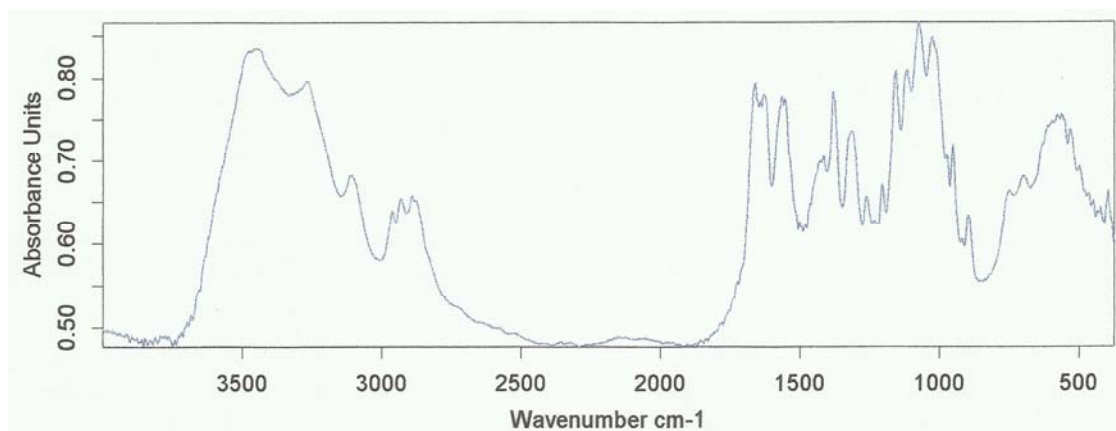


Figure 2 FTIR Spectra of α -chitin produced from shrimp waste (head, legs, shell, and tail).

Figure 2 shows FTIR spectrum of product in the $4000\text{--}400\text{ cm}^{-1}$ region where the different characteristic bands of the molecular structure of α -chitin can be identified. The fundamental vibrations are due to O–H and N–H stretching band (in the range $3700\text{--}3000\text{ cm}^{-1}$), C–H stretching band (in $3000\text{--}2850\text{ cm}^{-1}$) and carbonyl group (in $1830\text{--}1650\text{ cm}^{-1}$). In last range, two peaks are displayed: one which is attributed to the occurrence of intermolecular hydrogen bond $\text{CO}\cdots\text{HN}$ at 1660 cm^{-1} and another due to the intramolecular hydrogen bond $\text{CO}\cdots\text{HOCH}_2$ at 1625 cm^{-1} . The band split is used to distinguish between α -chitin and β -chitin since a single band is observed in case of the β -chitin at 1656 cm^{-1} [12].

Glucosamine production and characterization

The influence of temperature, solid/liquid ratio (g/mL), and agitation (with – without) on acid hydrolysis was studied. During the hydrolysis process, it was observed that chitin was completely dissolved in a period of 3 to 18 min, and immediately after that the solution darkens, becoming of a brown colour. The dissolution of chitin was influenced by temperature and agitation. The hydrolysis reaction was faster when the mixture was agitated and temperature was high. The change to brown colour in solutions can be caused by The Maillard reaction which involves amino groups reacting with an aldehyde and can lead to colour change associated with hydrolysis of chitin [13].

The hydrolysis process involves two acid-catalyzed hydrolysis reactions: the glycosidic linkage (depolymerisation) and the *N*-acetyl linkage (deacetylation). Hackman [14] observed that most of the degradation of the chitin chain occurred during the first few minutes, and that the products formed were oligosaccharides. Figure 3 illustrates the most accepted reaction mechanism for the acid catalyzed hydrolysis of a glycosidic linkage ($\text{S}_{\text{N}}1$) and the reaction mechanism for the acid-catalyzed hydrolysis of the *N*-acetyl linkage ($\text{S}_{\text{N}}2$ reaction) [15, 16].

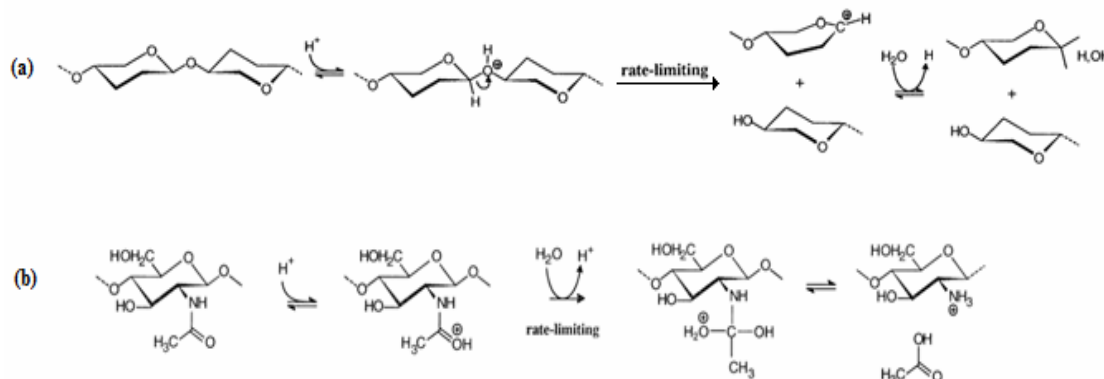


Figure 3 Schematic illustration of the proposed reaction mechanism for (a) the acid-catalyzed hydrolysis of the glycosidic linkage in chitosan [15] and (b) for the acid-catalyzed hydrolysis of the *N*-acetyl linkage [16].

It was observed that the recrystallization process was slow at room temperature ($25 \pm 2^\circ\text{C}$). Therefore, in order to increase the crystallization rate and to favour the crystal formation, the mixture was cooled to 5°C and 99.86% ethyl alcohol was added as solvent. The results showed that the crystallization time decreased and the crystals formed were thinner, clearer and brighter in these conditions. According to Myerson [17], the solvent can have a significant effect on the solubility of the solute, the structure and crystal size, as well as morphology and purity of the crystals. Temperature plays an important role in crystallization since it can influence nucleation and crystal growth via its effects on the solubility and supersaturation of the sample.

Table 2 shows the results of the yields of G-HCl and the correlation coefficient for the comparison between the product and the reference for the experiments of set 1. In general, the results showed that the yield of G-HCl can increase with temperature and with agitation of the sample can increase. The increase of temperature and the use of agitation lead to that chitin dissolves faster and this can contribute to a more effective hydrolysis.

Table 2 Results of the G-HCl production according to experimental conditions of set 1

Exp No.	Solid/liquid ratio	Yield (%)	FTIR spectrum Correlation* (%)
1.1	1:10	34.0	96.90
1.2	1:10	42.0	98.76
1.3	1:20	56.0	99.53
1.4	1:20	58.0	99.66

* With regard to the commercial reference.

Table 3 shows the results at different solid/liquid ratios, and in a temperatures range of 68 – 85°C and with agitation. We can observe that the yields of G-HCl with respect to chitin were 42, 58, 36 and 48% for solid/liquid ratios of 1:10, 1:20, 1:30, and 1:40 respectively. The best yield was obtained with at solid/liquid ratio of 1:20. The production of G-HCl is greatly influenced by the experimental conditions; however, it is not possibly to extract a conclusive tendency from the experiments.

The FTIR spectra were also compared and a coincidence between 98.76 and 99.66% was obtained. The highest correlation corresponds to the hydrolysis product obtained at solid/liquid ratio of 1:20.

Table 3 G-HCl production at different solid/liquid ratio at 68–85 °C and with agitation

Exp No.	Solid/liquid ratio	Yield (%)	FTIR spectrum Correlation* (%)
2.1	1:10	42	98.76
2.2	1:20	58	99.66
2.3	1:30	36	99.36
2.4	1:40	48	99.14

* With regard to the commercial reference.

FTIR analysis of Glucosamine hydrochloride (G-HCl)

The FTIR spectra provided by Bruker Optics ALPHA FT-IR Spectrometer, were used to identify the product and to determine the degree of similarity. The results of the comparison between the spectra of G-HCl products and the commercial reference revealed that a coincidence between 96.90 and 99.66% was obtained. The highest correlation corresponds to the hydrolysis product obtained at solid/liquid ratio of 1:20, temperature of 85°C, and with agitation (Exp 2.2). Lower values were obtained for lower temperature, larger solid/liquid ratio and without agitation. These results showed that in the range examined, G-HCl with high quality is produced with solid/liquid ratio of 1:20.

The FTIR spectra of G-HCl produced under the work conditions of Exp 2.2 (sample) and G-HCl commercial reference are displayed in Figure 3. The figure shows that the FTIR spectra of both materials are essentially identical with regard to the band-positions of G-HCl main groups. This fact is confirmed by the correlation coefficient of 99.66% which indicates a very high degree of similarity between sample spectrum and the reference spectrum.

The FTIR spectrum of G-HCl produced (Sample in Figure 3) exhibits an intense band at 3370–3300 cm^{-1} associated with the O–H and N–H stretching, a NH_2 scissoring band at 1615 cm^{-1} and at 1094 cm^{-1} due to secondary alcohol –OH.

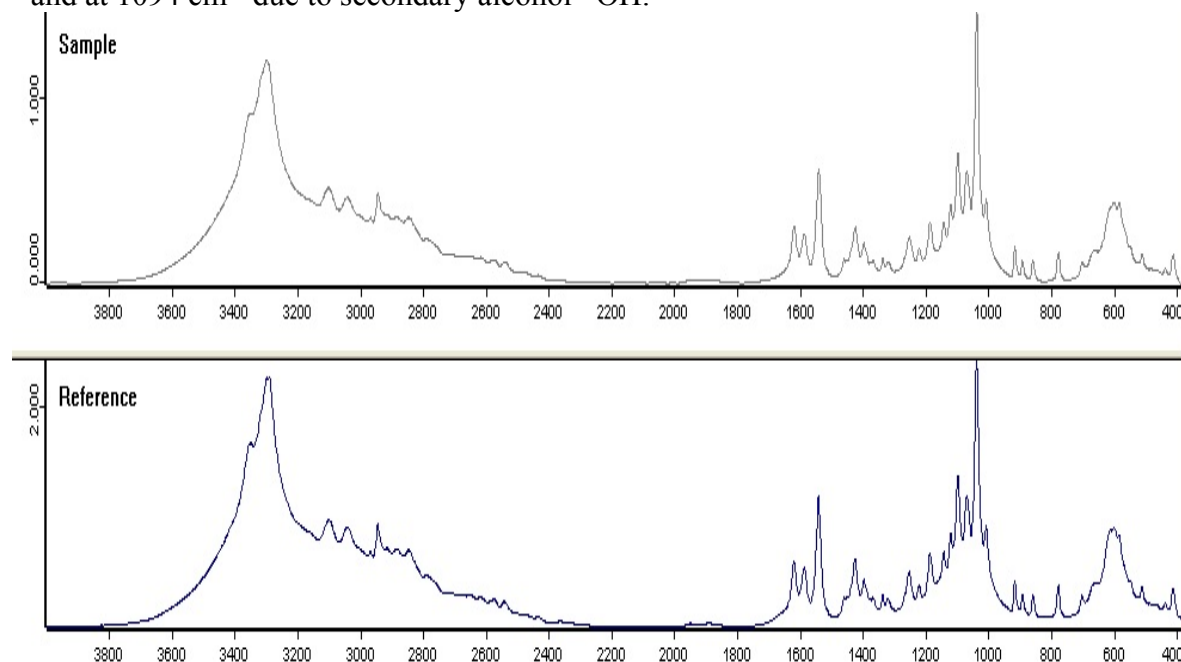


Figure 3 FTIR Spectra of Glucosamine hydrochloride produced under Exp 2.2 conditions (Sample) and D-Glucosamine HCl from Jining Green Group Co. Ltd (Reference)

These results showed that in the range examined, G-HCl with good quality is produced with solid/liquid ratio of 1:20, at high hydrolysis reaction temperature and with agitation. Additionally, the low temperature (5°C) and the use of ethyl alcohol support the formation of G-HCl crystals. These preliminary results show that it is possible to convert waste materials into valuable products such as glucosamine. However, more experimental work should be carried out to optimize the process. As well, additional information about biological and chemical behaviour should be necessary in order to assure if this product is suitable for dietary supplement.

ACKNOWLEDGEMENTS

The financial support of the Swedish International Developments Cooperation Agency (Sida) is gratefully acknowledged.

REFERENCES

- [1] Houpt J.B., McMillan R., Wein C. and Paget-Dellio S.D. (1999) Effect of glucosamine hydrochloride in the treatm. of pain of osteoarthr. of the knee. *J. Rheumatol.*, 26, 2423-30.
- [2] Luo, J., Hu, Y. S., Wu, Y. and Fan, W. K. (2005) Effect of glucosamine hydrochloride in ameliorating knee osteoarthritis. *Chin. J. Clini. Rehabil.*, 9, 70-72.
- [3] Anderson, J. W., Nicolosi, R. J. and Borzelleca, J. F. (2005) Glucosamine effects in humans: A review of effects on glucose metabolism, side effects, safety considerations and efficacy. *Food Chem. Toxicol.*, 43, 187-201.
- [4] Leite, A., Silveira, I., Matos, V., Matos, J., Monteiro-Moreira, A. and Mafezoli, J. (2002) In: VI Reunião Regional Nordeste SBBq, Fortaleza, Brasil.
- [5] Novikov, V. Y. (2004) Acid hydrolysis of chitin and chitosan. *Russ. J. Appli. Chem.*, 77, 484-87.
- [6] Pichyangkura, R., Kudan, S., Kuttiyawong, K., Sukwattanasinitt, M. and Aiba S. I. (2002) Quantitative production of 2-acetamido-2-deoxy-D-glucose from crystalline chitin by bacterial chitinase. *Carbohydr. Res.*, 337, 557-59.
- [7] Li, J.-l., Zhou, Y., Zhang, M. and Zhang, H.-b. (2007). Optimization of preparation process of glucosamine hydrochloride. *Anhui Med. Pharm. J.*, 2007-01.
- [8] Shahidi, F., Arachchi, J. K. V. and Jeon Y.-J. (1999) Food applications of chitin and chitosans. *Trends in Food Sci. Technol.*, 10, 37-51.
- [9] Ravi Kumar, M. N. V. (2000) A review of chitin and chitosan applications. *React. Funct. Polym.*, 46, 1-27.
- [10] CETREX (2010) Todos los productos de Exportación: Enero-Diciembre 2008-2009.
- [11] Xu, Y., Gallert, C. and Winter, J. (2008) Chitin purification from shrimp wastes by microbial deproteination and decalcification. *Appl. Microbiol. Biotechnol.*, 79, 687-97.
- [12] Sagheer, F. A. A., Al-Sughayer, M. A., Muslim, S. and Elsabee M. Z. (2009) *Carbohydr. Polym.*, 77, 410-19.
- [13] Pettersen H., Sannes A., Holme H. K., Kristensen Å. H., Dornish M. and Smidsrød O. (2000) Thermal depolymerization of chitosan salts. In: *Advances in Chitin Science 4* (Peter M.G., Domard A. & Muzzarelli R.A.A. eds.) University of Potsdam.
- [14] Hackman R. H. (1962) Studies on chitin V: Action of mineral acids on chitin. *Aust. J. Biol. Sci.*, 15, 526-32.
- [15] Edward J. T. (1955) Stability of glycosides to acid hydrolysis - A conformational analysis. *Chem. Ind.*, 36, 1102-4.
- [16] Stryer L. (1995) *Biochemistry* 4th ed. W.H. Freeman and Company, New York.
- [17] Myerson, A. S. (2001) *Handbook of Industrial Crystallization*. Elsevier Sci. Technol., 2nd Edition, ISBN 0750570126, pp.: 53-54, 93-94.

SELF-ASSEMBLY IN DILUTE SOLUTIONS OF SHORT CHAIN CHITOSANS OF LOW DEGREE OF ACETYLTATION

Inesa Blagodatskikh^{1*}, Evgeniya Bezrodnykh¹, Sergey Kulikov², Igor Yamskov¹, Sergey Abramchuk¹, Vladimir Tikhonov¹

¹*Nesmeyanov Institute of Organoelement Compounds of RAS, Moscow, Russia*

²*Kazan Scientific Research Institute of Epidemiology and Microbiology, Kazan, Russia.*

**E-mail address: blago@ineos.ac.ru*

INTRODUCTION

Chitosan represents a collective name for a group of polysaccharides consisting of glucosamine and N-acetylglucosamine or glucosamine only. As a result, the chemical structure of chitosan includes both cationic and hydrophobic sites. It is well-known from many papers that physicochemical and biological properties of chitosan depend on molecular weight (MW) and degree of acetylation (DA). Besides they may depend on molecular heterogeneity, namely molecular weight distribution (MWD), distribution of two kinds of repeating units along the chain, and variations in the nature of terminal groups. In fact, chitosan comes from a harsh treatment of chitin that affects the intrinsic parameters mentioned above. Consequently, there is a good reason to believe that molecular heterogeneity is one of the main reasons for an ambiguity in the experimental data on correlations between biocidal activity and physicochemical properties of chitosan. Physicochemical properties of chitosan in solution also may depend on the nature of counterions. In particular, it was shown in [1] that the nature of the counterion influences the microenvironment of polymer chains and the hydrochloride form of chitosan is more solvophobic than that of the acetate.

As most of the natural polymers, chitosan is well-known for its tendency to self-aggregate in aqueous solution. Thorough knowledge of self-aggregation of chitosan is highly significant for the accurate polymer characterization as well as for practical applications of physical hydrogels and chitosan-based materials in medicine. On the other hand, this phenomenon may affect the biological properties of chitosan. Therefore the self-aggregation of chitosan have attracted a lot of attention and been studied during last years. We can find in literature various experimental results concerning associating behaviour of chitosan in dilute solutions. Some authors revealed the effect of self-aggregation in dilute solutions by means of SEC coupled with a mass-sensitive light scattering detector [2, 3] and by static and dynamic light scattering (SLS-DLS) studies [4, 5, 6]. Others observed the transition from molecularly dispersed dilute solutions to associated systems in a semidilute regime [7].

It is commonly accepted to divide chitosans into high molecular weight (HMW) chitosans, low molecular weight (LMW) chitosans, and oligochitosan by their molecular weights. The boundaries between these groups are rather uncertain. It is known that LMW and oligochitosan have several advantages over HMW chitosan for some biomedical and industrial applications. In particular, due to a low viscosity and high compatibility with many additives their applications have no undesirable impact on the physicochemical properties of consumer goods. However, we can note that most structural studies of solutions were carried out using HMW chitosans [5, 7, 8], whereas associative behaviour in solutions of LMW and oligochitosan haven't been studied enough so far.

LMW chitosans and oligochitosans described in [9] have been prepared by means of depolymerization of HMW chitosan with the use of hydrochloric acid. The samples have a low DA, do not contain chemically active terminal groups and demonstrate a high stability during long-term storage. The advantage of these products is a high bactericidal activity against methicillin-resistant *S. aureus* [9]. Although the bactericidal properties of these products are very promising for biomedical applications, microscopic behaviour related to properties of oligochitosans in solution are far from being completely investigated.

The present paper describes our first results on self-assembling of these relatively short chain chitosans in aqueous media at various pH values as a function of chain length.

MATERIALS and METHODS

The samples of LMW chitosan and oligochitosan were prepared by depolymerization in hydrochloric acid as described in [9].

DA was determined by ^1H -NMR method [10]. MWD's were determined by HP-SEC on U-Styrigel columns with dextrans as calibration standards as described in [9, 11] and on PL-OH mix column using 0.2 M acetic acid/0.15 M ammonium acetate buffer (pH 4.5) as an eluent and pullulans as calibration standards.

Effective pK_a values of oligochitosan samples were determined by potentiometric titration of oligochitosan hydrochlorides in accordance with the modified method published in [12]. Briefly, 50 ml of oligochitosan hydrochloride was dissolved (1 mg/ml) in distilled water and pH was adjusted by HCl to pH 3.00-3.05. The solution was titrated with 0.5 M NaOH monitoring solution pH. The equivalent inflexion points of titration curves were taken as pK_a . All experiments were carried out in triplicate, and average values are shown in Table 1.

The characteristics of LMW chitosan and oligochitosan samples used in this study are shown in Table 1.

SLS and DLS measurements were performed using PhotoCor Complex spectrometer (PhotoCor Instruments, Russia) equipped with pseudo cross-correlation system of photon counting and He-Ne laser as a light source ($\lambda=633$ nm). The real-time correlator was employed in the logarithmic configuration. Measurements were performed in dilute solutions at 25°C within the range of scattering angles of 30°–140°. Zimm plot for a single concentration was used to determine the apparent M_w . Distributions over decay time and hydrodynamic radius were obtained by means of CONTIN program. Dn/dc was measured on Wyatt Optilab 903 refractometer. Solutions of sample 4 were dialysed against the solvent using Spectrapore membrane with 3.5 kDa cutoff.

Sample solutions for SLS-DLS study were prepared as follows: the chosen amount of the sample in the form of hydrochloric salt was dissolved in 0.1 M acetic acid, then the solution of 3 M tris(hydroxymethyl)aminomethan (TRIS) was added dropwise to adjust a desirable pH. Solutions were filtered through 0.22 μm pore size membranes (or through 0.8 μm membrane at critical pH values).

TEM micrographs were obtained with a LEO912 AB OMEGA electron microscope. 1% solution of uranyl acetate was used as a staining solution.

Table 1. Characteristics of chitosan samples

*Determined OH mix pullulans as standards. ** Determined Hydrogel dextrans as standards. *** Weight of calculated for form using $M_{unit}=198.5$	Sample number	$M_w^{* (**)}$	PI	DP ^{***}	DA (mol. %)	pK_a^{app}	
	1	2450 (2090)	1.45 (1.40)	12	2.6	6.6	by SEC on PL-column using calibration
	2	(9700)	(1.44)	48	2.7	6.4	by SEC on U-columns using calibration
	3	21500 (20000)	2.04 (1.66)	108	1.6	6.4	
	4	38100 (44000)	2.95 (2.25)	191	<0.5	6.4	average degree polymerization hydrochloric

RESULTS and DISCUSSION

Short chain chitosans shown in Table 1 were studied by static and dynamic light scattering (SLS and DLS) in dilute solutions ($c < 1/[\eta]$, $c = 0.003$ g/ml for samples 3 and 4, and 0.01 g/ml for samples 1 and 2) as a function of pH. It is obvious from DLS data that in the whole pH range up to the critical value, which approximately coincides with pK_a determined for these samples by titration, the main portion of scattered light is due to the diffusion motion of aggregates with hydrodynamic radii of about 40 nm (oligochitosan samples 1 and 2) and 70 nm (LMW chitosan samples 2 and 4). Hydrodynamic radii ($R_h^{(1)}$) of the fast diffusive mode agree rather well with those calculated from SEC data. On this evidence, we can believe that the observed aggregates are generated by rather weak bonds so that they are disrupted during dynamic experiments like SEC.

Figure 1 shows the distribution of hydrodynamic radii of chitosan 3 at various pH values. Figure 2 shows the variation of hydrodynamic radii of aggregates ($R_h^{(2)}$) as a function of pH depending on chain length. Figures 1 and 2 demonstrate also a coexistence of two aggregation modes at critical pH value: primary aggregates ($R_h^{(2)}$) and their clusters ($R_h^{(3)}$). Above the critical pH value we have observed macrophase separation with the formation of gel-like precipitate.

The characteristic feature of the solutions below critical pH is that the sizes of aggregates weakly depend on pH. Weak decrease of $R_h^{(2)}$ with pH increasing may be connected with a decrease of the extent of protonation simultaneously with an increase of ionic strength, which favours the screening of charges. The mean values of $R_h^{(2)}$ for each sample below critical pH are shown in Figure 3. We can see that there are two groups of samples with rather different R_h of aggregates. The apparent M_w values tend to segregate into the same two groups (about 20000 for samples 1 and 2 and about 100000 for samples 3 and 4).

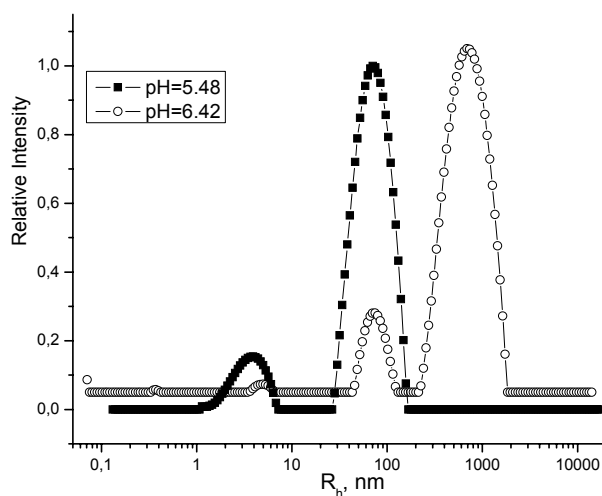


Figure 1. Distributions over hydrodynamic radius of chitosan 3 at pH below (5.48) and above the critical value (6.42).

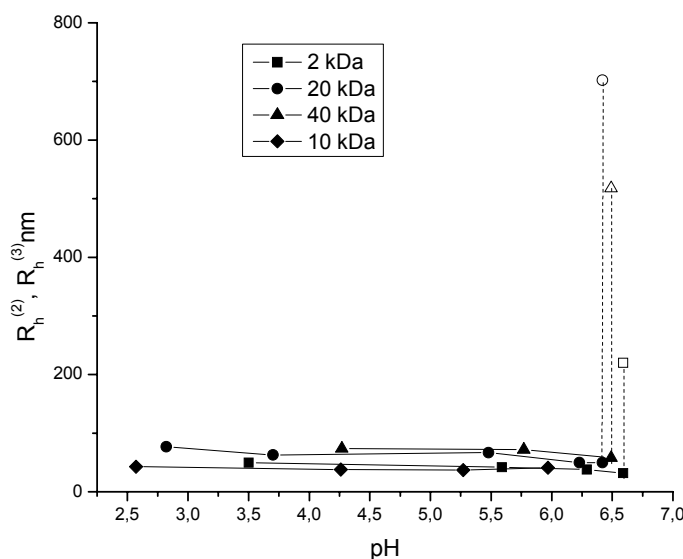


Figure 2. The variation of hydrodynamic radius of primary aggregates ($R_h^{(2)}$, dark symbols) as a function of pH for chitosans of various DP and the sizes of secondary clusters ($R_h^{(3)}$, open symbols).

To visualize the aggregation of oligochitosan, TEM image of sample 1 is shown in Figure 4, which confirms the formation of nearly spherical aggregates in aqueous solution.

In the theoretical work by Potemkin *et al* [13] the formation of optimal size clusters was predicted in dilute solutions of polyelectrolytes having many associating groups per chain. Multichain aggregates of chitosans keeping a constant size at the increase of chain length were recently observed in dilute solutions of HMW in [6]. The experimental data obtained in the present work can be discussed from the point of view of the abovementioned theory keeping in mind rather short chain lengths of the first group of oligochitosans, which are comparable with

the lowest values of intrinsic persistent length equal to 5 – 7 nm determined experimentally for chitosan [14 – 16]. We can suppose that the internal structure of aggregates formed by short chain chitosans which can't organize Gaussian coil must differ from that of long enough chains.

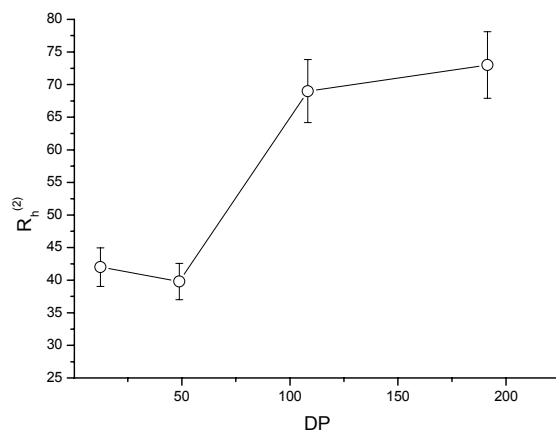


Figure 3. The variation of the mean R_h of aggregates below critical pH value as a function of DP. Error bars correspond to mean standard deviations.

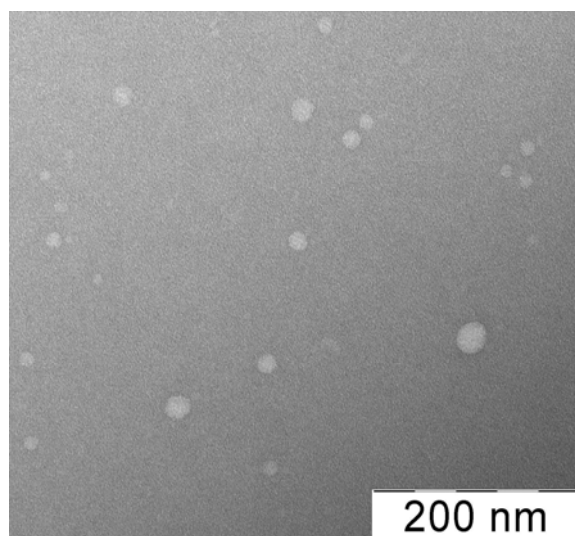


Figure 4. TEM images of aggregates in oligochitosan sample 1 stained with uranyl acetate.

REFERENCES

- [1] Boucard, N., David, L., Rochas, C., Montembault, A., Viton, C., Domard, A. (2007) Polyelectrolyte Microstructure in Chitosan Aqueous and Alcohol Solutions. *Biomacromolecules*, 8, 1209 – 1217.
- [2] Yanagisawa, M., Kato, Y., Yoshida, Y., Isogai, A. (2006) SEC-MALS study on aggregates of chitosan molecules in aqueous solvents: Influence of residual N-acetyl groups. *Carbohydrate Polymers*, 66, 192-198.

- [3] Ottoy, M. H., Varum, K., M., Christensen, B. E., Anthonsen, M. W., Smidsrod, O. (1996) Preparative and analytical size-exclusion chromatography of chitosans. *Carbohydrate Polymers*, 31, 253 – 261.
- [4] Sorlier, P., Rochas, C., Morfin, I., Viton, C., Domard, A. (2003) Light Scattering Studies of the Solution Properties of Chitosans of Varying Degrees of Acetylation. *Biomacromolecules* 4, 1034 – 1040.
- [5] Popa-Nita, S., Alcouffe, P., Rochas, C., David, L., Domard, A. (2010) Continuum of Structural Organization from Chitosan Solutions to Derived Physical Forms. *Biomacromolecules*, 11, 6 – 12.
- [6] Korchagina, E.V., Philippova, O.E. (2010) Multichain Aggregates in Dilute Solutions of Associating Polyelectrolyte Keeping a Constant Size at the Increase in the Chain Length of Individual Macromolecules. *Biomacromolecules*, 11, 3457 – 3466
- [7] Buhler, E., Rinaudo, M. (2000) Structural and Dynamical Properties of Semirigid Polyelectrolyte Solutions: A Light-Scattering Study. *Macromolecules*, 33, 2098 – 2106.
- [8] Lamarque, G., Lucas, J.-M., Viton, C., Domard, A. (2005) Physicochemical Behavior of Homogeneous Series of Acetylated Chitosans in Aqueous Solution: Role of Various Structural Parameters *Biomacromolecules*, 6, 131 – 142.
- [9] Kulikov, S.N., Bezrodnykh, E.A., Philippova, Yu.A., Lopatin, S.A., Blagodatskikh, I.V., Tikhonov, V.E. (2010) Antibacterial Activity of Oligochitosan Against Methicillin-resistant *Staphylococcus Aureus* (MRSA): Molecular Weight and pH Effects. This issue.
- [10] Hirai, A., Odani, H., Nakajima, A. (1991) Determination of degree of deacetylation of chitosan by ^1H NMR spectroscopy. *Polym. Bull.*, 26, 87 – 94.
- [11] Lopatin, S.A., Derbeneva, M.S., Kulikov, S.N., Varlamov, V.P., Shpigun, O.A. (2009) Fractionation of chitosan by ultrafiltration. *J. Anal. Chem.*, 64, 648 – 51.
- [12] Qin, C., Li, H., Xiao, Q., Liu, Y., Zhu, J., Du, Y. (2006) Water-solubility of chitosan and its antimicrobial activity. *Carbohydrate Polymers*, 63, 367 – 374.
- [13] Potemkin, I. I., Andreenko, S. A., Khokhlov, A., R. (2001) Associating polyelectrolyte solutions: Normal and anomalous reversible gelation. *J. Chem. Phys.*, 115, 4862 – 4872.
- [14] Buhler, E., Guetta, O., Rinaudo, M. (2000) Characterization of Semiflexible Polyelectrolyte Solutions in the Presence of Excess Salt: From Dilute to Semidilute Regime, *International Journal of Polymer Analysis and Characterization*, 6: 1, 155 – 175.
- [15] Rinaudo, M., Milas, M., LeDung, P. (1993) Characterization of Chitosan, Influence of Ionic Strength and degree of acetylation on chain expansion. *Int J. Biol. Macromol.*, 15, 281 – 285.
- [16] Schatz, C., Viton, C., Delair, T., Pichot, C., Domard, A. (2003) Typical Physicochemical Behaviors of Chitosan in Aqueous Solution. *Biomacromolecules*, 4, 641 – 648.

COMPOSITE MATRICES BASED ON CHITIN AND CHITOSAN FOR HUMAN SKIN CELL CULTIVATION

**A.M. Bochek¹, L.A. Noudga^{1*}, V.A. Petrova¹, E.F. Panarin¹, I.V. Gofman¹, Yu.G. Baklagina¹,
M.I. Blinova², N.M. Yuditseva², O.G. Spichkina², L.V. Kukhareva², I.A. Samusenko³, G.P. Pinaev²**

¹*Institute of Macromolecular Compounds RAS, Saint-Petersburg*

²*Institute of Cytology RAS, Saint-Petersburg*

³*Nikiforov All-Russian Center of Emergency and Radiation Medicine, EMERCOM of Russia, Saint-Petersburg*

**E-mail address: noudga@mail.macro.ru*

INTRODUCTION

The intensive development of cellular technologies which are used in the new area of medicine – regenerative medicine – requires the design of new materials serving as substrates for cultivated cells. The precondition for these materials is their ability to resorb after the implantation of corresponding cellular products into living organism.

Recently [1] we have shown that the materials obtained from partially deacetylated chitin and heat-treated chitosan films are able to provide adhesion, spreading and proliferation of fibroblasts and the formation of cell monolayer.

It is well known that in laboratory keratinocytes are being grown on collagen matrices. Transplantation of multilayer keratinocyte stratum (skin epidermis analogue) grown *in vitro* onto the wound requires several very complex procedures which damage this stratum to some extent. The possible solution of this problem consists in the growing keratinocyte stratum on the resorbable film; thus, the cell stratum can be transferred onto the wound together with this film and undergoes no damage. Since collagen substrate is necessary for normal keratinocyte functioning, suitable matrices can be obtained as two-layer chitosan-collagen films or after introduction of collagen into the film. Besides, the optimal conditions for the joint cultivation of both cell types (fibroblasts and keratinocytes) can be established in three-dimensional porous matrix. However, modification of matrix composition and structure may cause deceleration of its resorption in organism. This suggestion can be tested only *in vivo* using laboratory animals. The aim of this work is to solve the above-mentioned problems.

MATERIALS and METHODS

In the experiments the chitin obtained from crab shells (“Sonat”, Moscow) was used; it was additionally purified of calcium salts (treatment with 0.5 N HCl), lipids (acetone extraction) and proteins (extraction with 1.5 N NaOH), washed with water until neutral pH was achieved, rinsed with acetone and dried under vacuum at 40°C. The purified chitin had the following characteristics: ash content – 0%; protein – none; elemental analysis: C 46.40, H 5.86, N 6.19; $[\eta] = 8.4$ dl/g; $M = 137$ kDa (calculated using the following equation: $[\eta] = 2.4 \cdot 10^{-3} \cdot M^{0.69}$ [2]).

The partially deacetylated chitin (deacetylation degree 0.19) was used as described in [1].

Collagen was obtained in the Department of Cell Cultures of the Institute of Cytology RAS by acid extraction of rat tail tendons and purified by repeated precipitation [3,4].

Chitosan films were formed using dry method, heated at 120°C and stored dry in room atmosphere.

Composite film matrices were obtained from 3% chitosan solution in 2% acetic acid and collagen solution of the same concentration in the same solvent. The solutions were mixed in the following chitosan:collagen ratios: 97.5:2.5, 95:5 and 90:10. The films were obtained by dry molding. The porous materials were obtained by freeze drying of 0.5% chitosan solutions in 2% acetic acid; these solutions were subjected to dialysis in water until neutral pH was achieved.

Mechanical tests were performed using the universal instrument for mechanical tests UTS 10 (UTStestsysteme, Germany).

The suitability of film samples for cell cultivation was tested using the techniques described in [5]. The resorption of the matrices was additionally tested *in vitro* (keeping in nutrient medium in CO₂ incubator at 37°C for 35 days).

RESULTS AND DISCUSSION

For the purpose of improving adhesion and proliferation of dermal fibroblasts on chitosan matrix, collagen solution was introduced in molding solution (collagen content was 2.5, 5 and 10% of chitosan mass). The mechanical properties of films and their porosity were studied. The supramolecular organization was studied using X-ray structure analysis, their morphology was studied using scanning electron microscopy.

The results of mechanical tests (see Table 1) provide evidence of increasing rigidity of chitosan film after introduction of even small quantities of collagen; the increasing of collagen concentration leads to higher Young's modulus E , yield stress σ_y and ultimate strength σ_b without decreasing in ultimate deformation of material ϵ_b .

Table 1. Characteristics of composite films based on chitosan and collagen

Collagen content, %	Film properties				
	E , GPa	σ_y , MPa	σ_b , MPa	ϵ_b , %	Specific surface area, m ² /g
0	5.20 ± 0.21	107 ± 4	96 ± 4	13 ± 3	1.261
2.5	6.67 ± 0.25	142 ± 2	131 ± 1	11 ± 1	-
5	7.01 ± 0.23	150 ± 2	140 ± 1	14 ± 1	-
10	7.16 ± 0.29	152 ± 3	148 ± 3	14 ± 2	1.412
Two-layer film chitosan/collagen	4.72 ± 0.16	108 ± 5	120 ± 4	8 ± 1	2.688

The two-layer chitosan/collagen film is characterized by reduced Young's modulus as compared with the film made from pure chitosan. These results agree with SEM data showing that the basic mass of collagen spread on chitosan matrix, with the exception of thin surface layer ($\sim 0.4 \mu\text{m}$) consists of globular formations hardly able to take mechanical loads [5]. The specific surface area values of composite films (10% of collagen) and two-layer films (1.412 and 2.688 m²/g, respectively) are higher than that of pure chitosan film (1.261 m²/g), this indicating increasing porosity.

With the aim of providing better nutrition of cultivated cells and their spreading to the whole matrix volume, i.e., the formation of three-dimensional matrices, we have obtained sponge

matrices using chitosan solutions containing 10% of collagen in 2% acetic acid and in 2% glutamic acid. The characteristics of sponge matrix materials are given in Table 2. In the SEM image (Fig. 1A) the structure of sponge is shown; the sponge consists of through pores and cells. It was found that the best sponge for cell cultivation is the sample obtained from dialyzed chitosan solution containing 10% collagen in glutamic acid; on this sponge, cells form the multilayer stratum not only on the surface, but also in the bulk (see Fig. 1B).

Table 2. Characteristics of matrix materials for cell cultivation

The composition and type of the matrix	Characteristics of matrices			
	Porosity, %	Apparent density, kg/m ³	Specific surface area, m ² /g	Dehumidification, %
Chitosan + 10% of collagen sponge from 2% acetic acid	34.5	27.2	7.22	50.0
Chitosan + 10% of collagen sponge from 2% glutamic acid	36.1	28.4	-	91.6

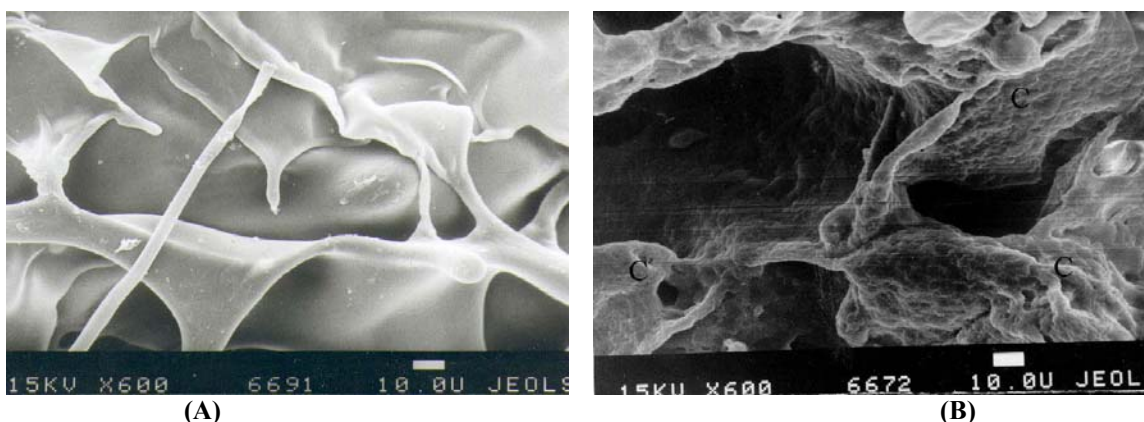


Fig. 1. SEM images of sponges obtained from the mixtures of chitosan solutions and 10% of collagen dissolved in 2% acetic acid. A – control sample: sponge without cells; B – sponge after cultivation of human skin fibroblasts for 10 days. Mark – 10 µm.

The influence of keratinocytes and fibroblasts cultivated on sponges and films on the inflammatory processes in the wound and on the efficiency of cell reproduction were estimated using the following three indicators: scab thickness, composition and intensity of wound inflammatory reaction and quantity of keratinocytes in wound.

The scab thickness serves as a criterion of activity of wound healing (Fig. 2). It was necessary to check the following:

- whether the matrix structure (sponge or film without cells) affects this process;
- whether the cells cultivated on the matrices and introduced into wound accelerate wound healing, and whether the matrix structure is of any importance for one or another cell type (keratinocytes and fibroblasts).

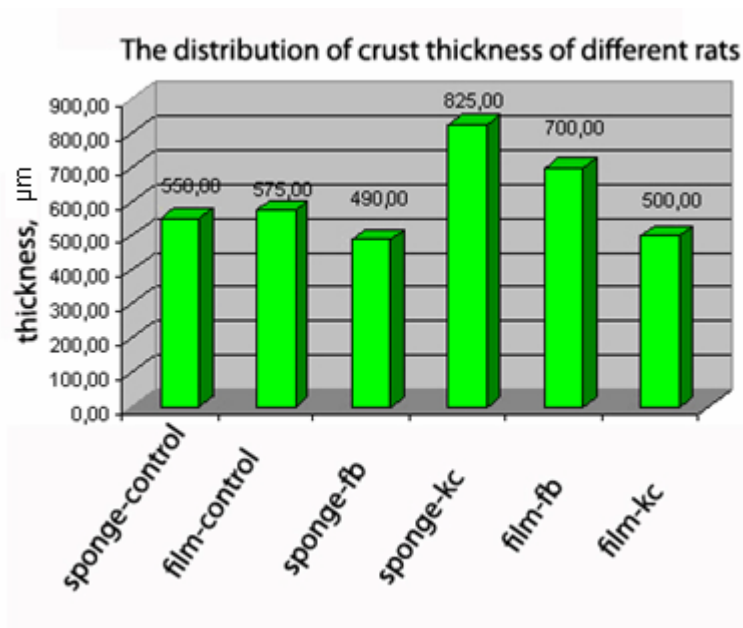


Fig. 2. Diagram of scab thickness distribution in the wound [5].

It was found that matrices without cells, fibroblasts on sponge and keratinocytes on film demonstrate approximately the same influence on healing activity. The most active healing took place in the experiments with keratinocytes on sponge and fibroblasts in film.

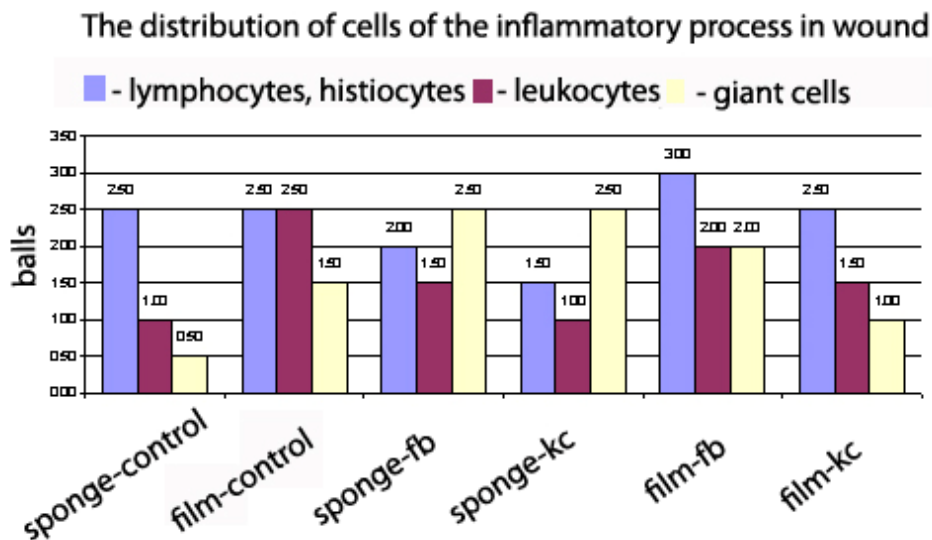


Fig. 3. The distribution of inflammatory cells in wound [5].

The resorption of material in the wound and the degree of inflammation caused by the matrix are important characteristics of resorbable matrices with cultivated cells (see Fig. 3).

The wound is an inflamed place, and the process of wound healing is accompanied by inflammatory reaction; thus, the presence of inflammatory cells generated in the organism and functioning actively in the process of healing indicates the inflammation degree and wound

condition. Lymphocytes, histiocytes, white blood cells, large multinucleated cells are specific cells, indicating inflammatory reaction in the organism.

The presence of large amount of gigantic cells (white rectangles on the diagram) in experiments with keratinocytes and fibroblasts on sponges may be caused by the fact that the sponge resorption is slower than that of the film. This suggestion is supported by the revealing of sponge remains in biopsy material of the tissue 12 days after transplantation, while in the experiments with films there were no remains by this time.

The quantity of keratinocytes in the section and their arrangement in the wound were also estimated (Fig. 4).

The large amount of keratinocytes in the wound after the introduction of sponge with cultivated cells indicates that active migration of keratinocytes takes place during healing process and, accordingly, wound epithelization proceeds faster, i.e. it closes faster. When keratinocytes are introduced on films, this process is slower (less active). It can be supposed that the structure of sponge matrix is more suitable for keratinocyte growth and subsequent wound healing, although sponge resorbs slower than film.

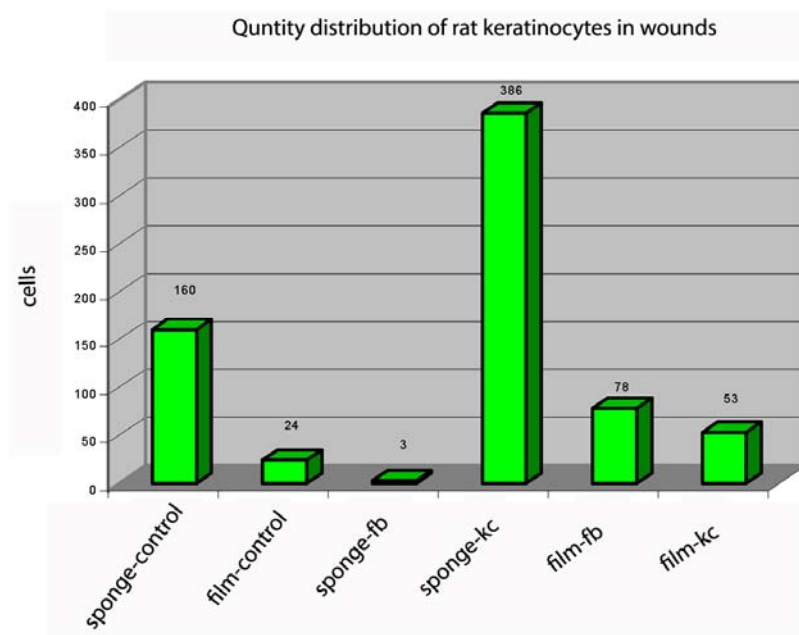


Fig. 4. Distribution of keratinocytes in the wound [5].

The obtained and characterized composite matrices based on chitosan and collagen in the form of sponges and films were tested as matrices for cell cultivation with the view to obtaining transplants for wound healing. The *in vitro* and *in vivo* tests have shown the absence of toxicity with respect to cultivated cells and living tissues. The cultivation of human skin fibroblasts *in vitro* on all samples for 35 days has not revealed biodegradation on any sample. In the wound healing experiments *in vivo* even 12 days after cell transplantation the complete film matrix resorption took place. There were no significant differences between the condition of regenerating tissue in biopsy material and between healing process characteristics in both matrix types (sponges and films).

The developed chitosan-collagen matrices are promising materials for wound healing. The sponge matrices are optimal for preparation of cell products in three-dimensional structures.

Our matrices are competitive in comparison with polymer-based synthetic materials used in medical practice. The application for patent concerning the method of obtaining these chitosan-based composite matrix materials [6] was made by authors (researchers of IMC RAS and INC RAS); it has undergone expert examination, and the patent will soon be issued.

REFERENCES

- [1] Panarin, E.F., Noudga, L.A., Petrova, V.A. et. al. (2009) Matrices for human skin cell cultivation based on natural polysaccharides – chitin and chitosan. *Cellular Transplantation and Tissue Engineering*, 5, 3, 42-46.
- [2] Terbojevich, M., Corrado, C., Cosani, A. et al. (1988) Solution studies of the chitin - lithium chloride - N,N-dimethylacetamide system. *Carbohydr. Res.*, 180, 73-86.
- [3] Chandrakasan, G., Torchia, D.A., Piez, K.H. (1976) Preparation of intact monomeric collagen from rat tail tendon and skin and the structure of the helical ends in solution. *J. Biol. Chem.*, 251, 19, 6062-6067.
- [4] Hilkin, A.M., Shechter, A.B., Istranov, L.P., Lemenev, V.L. (1976) Collagen and its use in medicine. Moscow: "Medicine".
- [5] Panarin, E.F., Noudga, L.A., Petrova, V.A. et. al. (2010) Composite matrices based on chitin and chitosan for human skin cell cultivation. *Cellular Transplantation and Tissue Engineering*, 5, 1, 65-73.
- [6] Patent application 2009140072; 29.10.2009. (51) Int. Cl³. C 08 B 37/00; C 08 L 5/00. Noudga, L.A., Petrova, V.A., Bochek, A.M., Panarin, E.F., Pinaev, G.P., Blinova, M.I., Yuditseva, N.M., Spichkina, O.G., Kukhareva, L.V. The method of obtaining composite resorbable matrices based on chitosan and collagen for human skin cell cultivation.

CHITOSAN AS AN OPTICAL WAVEGUIDE MATERIAL

Alexander Mironenko¹, Alexander Sergeev², Svetlana Bratskaya^{1*}, Alexander Nepomnyashchii²,
Valentin Avramenko¹, Sergey Voznesenskiy²

¹ Institute of Chemistry, Far Eastern Branch, Russian Academy of Sciences
159, prospekt 100-letiya Vladivostoka, Vladivostok 690022, Russia

² Institute of Automation and Control Processes, Far Eastern Branch, Russian Academy of Sciences,
5, Radio Street, Vladivostok 690041, Russia

*E-mail address: sbratska@ich.dvo.ru

INTRODUCTION

Silica has been widely used for many years as the main material for fabrication of optical fiber. There has always been an interest in the development of plastic optical fibers for both telecommunications and sensor uses, but this technology has tended to be somewhat 'in the shadow' of the silica-based approach.

Recently, polymers and polymer/inorganic hybrids have become of great interest for development of optical waveguides with tailored optical properties for telecommunications and sensor applications. Despite the fact that the polymer optics is based on synthetic polymers, whose functional composition can be controlled to provide materials with refractive indices ranging from ~ 1.3 to ~ 2.0 , some of the natural polymers can be considered as an alternative to synthetic polymers for optoelectronic applications due to their high availability, relatively low cost and good film-forming properties.

Aminopolysaccharide chitosan is one of the most promising biopolymer-candidates for development of optical waveguides and sensors. Advantages of chitosan are not limited to its easy processability, low cost and excellent film-forming properties. Chitosan is rather transparent material, whereas its refractive index can be tailored via metal ions binding, in-situ reduction and stabilization of metal nanoparticles or incorporation of optically active inorganic nanocrystals into the polymer thin film. This approach allows producing optical materials for various purposes with required mechanical and optical properties. Moreover, interactions of chitosan, as a hydrophilic polybase, with organic solvents, water vapor, mineral and organic acids change level of polymer hydration and/or protonation degree, and thus, optical properties of the film that is beneficial for sensing application.

MATERIALS and METHODS

Waveguide fabrication

The chitosan solution was prepared by dissolving 1-5% (w/v) chitosan (molecular weight 500kDa, deacetylation degree (DD) 80.5%) in aqueous solutions of acetic or citric acid at doubled molar ratio. The solution was allowed to stir overnight to ensure that the chitosan is dissolved completely in the acid solution. To remove dissolved gases the solution was evacuated and treated in an ultrasonic bath. Then the solution was filtered through the 1.2 μm , 0.8 μm and 0.45 μm membranes.

After preparation of chitosan stock solution, the Laurell WS-400B-6NPP-LITE spin coater was used to obtain thin polymer films. Films were spun onto glass and MgF_2 slides (square 50×10 mm), which were cleaned by sonication in boiling solution of $\text{NH}_4\text{OH}/\text{H}_2\text{O}_2/\text{H}_2\text{O}$ (1:1:1) for two hours and thoroughly rinsed with distilled water. To obtain the homogeneous film, the solution was evenly distributed on the slide surface and spun at 500-4000 RPM for 2 minutes.

Characterization methods

Ellipsometry. *In situ* ellipsometric measurement of swollen polymer films (phosphate buffer, pH = 7,4) refractive index were performed in a quartz cell at an angle of the laser beam exactly perpendicular to the cell wall (ellipsometer Sentech SE-402, Germany). Investigations of thickness changes were performed for films with a thickness of 20 nm. Increase of swollen film thickness was 15-20%.

Atomic force microscopy. To characterize the films surface topography atomic force microscope PNI Nano DST (USA) was used. Measurements were made in tapping mode, at a temperature of 22°C and humidity 25%. Rms value of surface roughness was calculated for a $2.36 \mu\text{m}^2$ area using the NanoRule+ software.

Measurement of optical losses. The scanning probe method was used to determine the waveguide propagation losses. The inventive method consists of registration of the emergent radiation from the surface of the waveguide track and measurement of the attenuation in the waveguide as a function of its length.

The scheme of the experiment is shown in Fig. 1. Focused light beam (wavelength 633 nm) was coupled into the waveguide via a flint glass prism. Radiation emerging from the waveguide was caught by the fiber probe and transmitted to a photodetector. Scanning probe was moved along the waveguide with a step of 1 mm perpendicular to its plane.

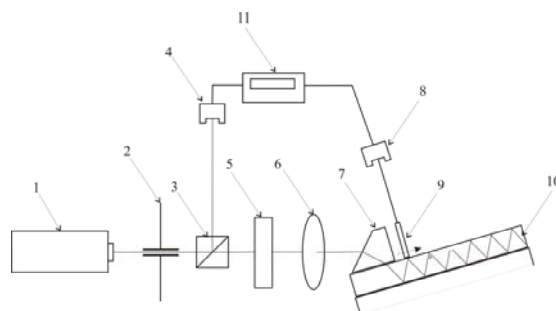


Figure 1. Schematic representation of apparatus for waveguide propagation losses measurement by the scanning probe method (arrow shows sensing direction): 1 - light source, 2 - diaphragm, 3 - beam-splitting cube (50:50), 4, 8 - photodetectors; 5 - polarizer, 6 - focusing lens ($f = 50\text{mm}$), 7 - input prism, 9 - scanning probe; 10 - waveguide, 11 - power meter.

Sensor properties investigation. Investigation of the influence of humidity on the optical characteristics of films was carried out in a special sealed chamber (Figure 2),

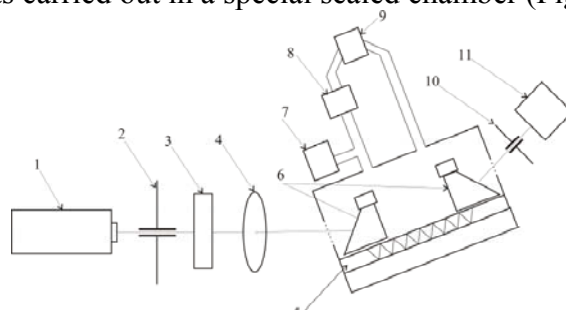


Figure 2. Schematic representation of apparatus for investigation of humidity influence on chitosan films optical properties (dotted line shows the quartz window for radiation input / output): 1 - light source, 2 - diaphragm, 3 - polarizer, 4 - focusing lens, 5 - waveguide, 6 - I/O prisms 7 - hygrometer, 8 - compressor, 9 - camera with an aqueous solution of sulfuric acid, 10 - diaphragm, 11 - photodetector.

where waveguide with a prism coupling element were placed. The chamber was mounted on a goniometric platform, allowing accurate calculation of the excitation angles of waveguide modes with an error of about 0.1°. Input and output prisms were made of flint glass with a refractive index at the working wavelength $n = 1.76412$. A semiconductor laser ($\lambda = 650$ nm), with an average output power of $I = 50$ mW was used as a radiation source.

Depending on the measured parameter, a power meter Newport 2935c or a profilometer Newport LBP were used as photodetector. Power meter was used to register the kinetic curves of the waveguide output intensity from the ambient humidity, while the profilometer was used to determine changes in the profile of the waveguide modes at different humidity values.

RESULTS AND DISCUSSION

Chitosan based waveguides were obtained by spin-coating process from two ionic forms of polycation - acetate and citrate. The concentration of chitosan solution ($\omega = 3\%$) corresponding to the conditions when the viscosity is high enough to produce films thicker than one micron, and at the same time, the fluidity of the solution is sufficient for the controlled coating process was chosen experimentally. Thus, films prepared from the 3% solution of chitosan acetate at rotation speeds 1500, 2000 and 3000 rpm had a thickness of 2020 ± 110 nm, 1545 ± 175 nm and 1300 ± 200 nm, respectively.

To improve the optical properties of the films, evacuation, ultrafiltration and centrifugation of chitosan solutions were used prior to spin-coating. The characteristics obtained by atomic force microscopy (Figure 3) indicate to high homogeneity of the films. Calculated mean-square roughness at $5.57 \mu\text{m}^2$ was 1.83 nm.

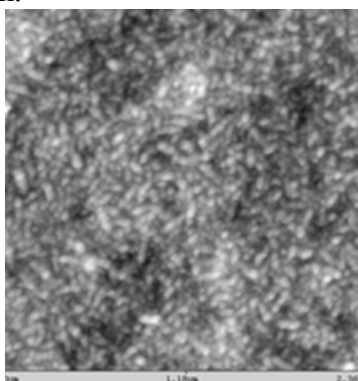


Figure 3. AFM image of the chitosan acetate film surface.

Many authors have previously noted the influence of anion nature on the physicochemical properties of chitosan [1], including the film-forming properties [2]. Differences in films structures formed from solutions of chitosan in different ionic forms, were also confirmed by wide angle X-ray diffraction. It was shown that the degree of crystallinity of chitosan acetate films was much higher than the films of citrate [3].

Optical loss is an important parameter that determines the suitability of the waveguide for optical communications and optical sensor systems. The technique used here allowed determination of the intensity of leaky modes during the propagation. This parameter indicates the possibility to use such waveguide for the sorption type sensor.

Figure 4 shows waveguide losses (wavelength 633 nm) for the chitosan films in different ionic forms on sodium-silicate glass slide measured by scanning probe method at relative humidity 25%.

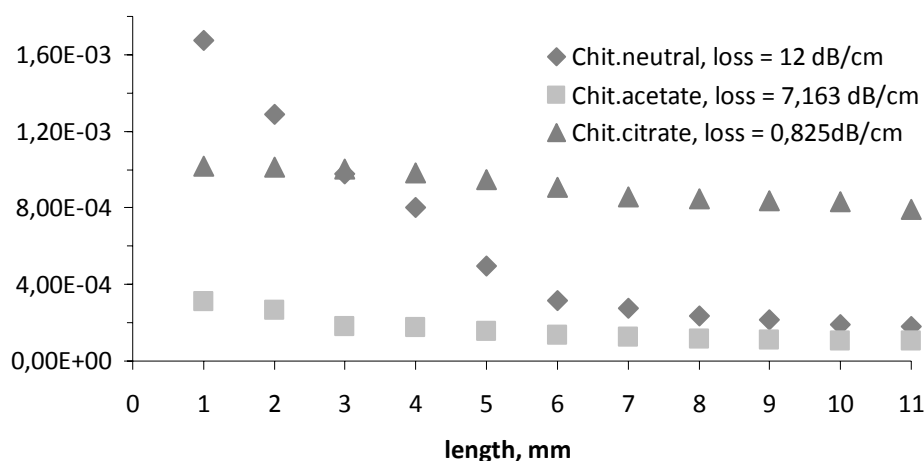


Figure 4. Relative values of scattered radiation.

The determined optical losses, depending on the salt form, were 0.8-12 dB/cm, and the effective refractive index - 1.53 ± 0.01 . Absolute refractive index of chitosan under the same environmental conditions determined by spectroscopic ellipsometry for the working wavelength (633 nm) was $n = 1.540$, which is in good agreement with literature data [4]. It was shown that the neutral form of chitosan had the worst waveguide properties with the largest optical losses.

The use of hydrophilic polymer materials for sensor applications is well known [5-7]. The changes in refractive index of synthetic and natural polymer hydrogels deposited on fiber (in dry and swollen state) allow detection of humidity in the range of 5-95%. The sensitivity and response time of optical sensor depends on the nature of polymer [6, 7] and the porosity of coating [7].

Figure 5 shows water sorption isotherm of free-standing chitosan acetate film, which is in good agreement with published data [8]. Obviously, a significant swelling of thin polymer film, leads to a change in its optical properties (refractive index and thickness). Changing the characteristics of the film as a result of the swelling was confirmed by *in situ* ellipsometry. For example, at a wavelength 633 nm, the refractive index of chitosan at humidity 20% was 1.540, while that of the maximum swollen film - 1.405.

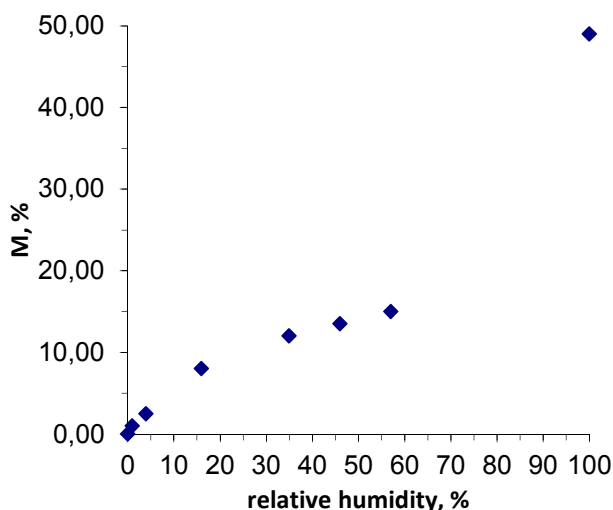


Figure 5. Chitosan water vapor sorption isotherm.

Figure 6 shows that the chitosan film begins to react to humidity changes almost immediately. Optical properties of the planar waveguide can be associated with a change in effective optical thickness and refractive index of the film due to swelling during the sorption of water [9] and changes in the polymer film structure.

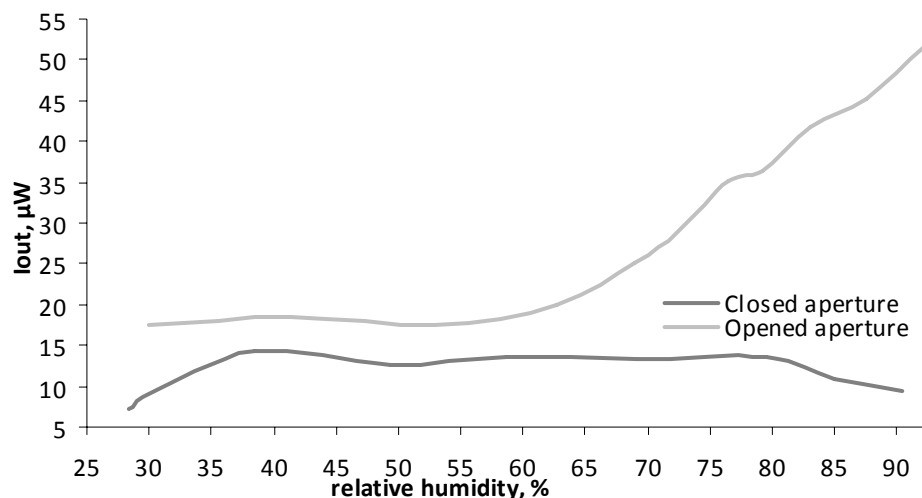


Figure 6. Output intensity of radiation with step increase (10%) of the ambient humidity (chitosan acetate on magnesium fluoride).

In the experiment with the ‘closed aperture’, when the signal change is recorded only in the axial part of output beam, no increase in output intensity was observed. At the same time, for the experiment with an ‘opened aperture’, increase of the output intensity starts at humidity about 65%. Decrease in the intensity of 80-90% for the experiment with the ‘closed aperture’ can be explained by redistribution of energy in the waveguide mode spectrum, which leads to reduction of intensity in the axial part (compared to the same value for the humidity of 25%).

Another approach to develop optical sensors is based on formation of multilayered polymer coatings containing responsive additives on the surface of commercial waveguides. The main advantage of this type of sensors is the possibility to obtain thin polymer films by electrostatic self-assembly at the surfaces of different nature and geometry with precise control of thickness and sensing additives content that provides high reproducibility of the sensors [9]. To obtain polymer coatings for ammonia detection, acid-base indicators were embedded to the chitosan-carrageenan multilayers obtained as reported in [10].

Figure 7. UV-vis spectra of chitosan-carrageenan multilayers with bromothymol blue (a) and bromocresol purple (b) in dependence of deposited double layers (DL)

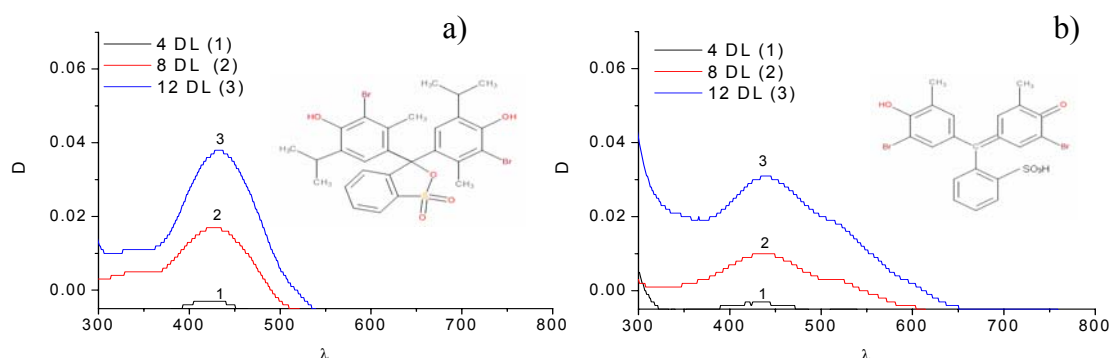


Fig.7 shows that the optical density of the coatings increases with DL number that corresponds to the increase of indicator content in the film. Chitosan-carrageenan films containing bromothymol blue are the most promising for sensing application, since the character of UV-vis spectra allows sensing of ammonia at wavelengths 605-615 nm (maximum of absorption of the indicator basic form), where acidic form does not absorb light and do not contribute to the optical losses. Thus 650 nm red laser can be used to monitor changes in the optical properties of the film in the presence of ammonia.

REFERENCES

- [1] Onsoyen, E., Skaugrud, O. (1990) Metal recovery using chitosan. *J. Chem. Tech. Biotech.*, 49(4), 395-404
- [2] Vihoreva, G.A., Galbraih, L.S. (2002) Films and fibers based on chitin and its derivatives. In *Chitin and Chitosan: Preparation, Properties, Applications* (K. G. Skryabin, G. A. Vihoreva, V. P. Varlamov ed.) pp. 254-79, Nauka.
- [3] Tanigawa, J., Miyoshi, N., Sakurai, K. (2008) Characterization of chitosan/citrate and chitosan/acetate films and applications for wound healing. *J. Appl. Polym. Sci.*, 110(1), 608-15.
- [4] Jiang, H., Su, W., Caracci, S. et al. (1996) Optical waveguiding and morphology of chitosan thin films. *J. Appl. Polym. Sci.* 61(7), 1163-71.
- [5] Yeo, T. L., Sun, T., Grattan, K.T.V. (2008) Fibre-optic sensor technologies for humidity and moisture measurement. *Sensors and Actuators A.*, 144, 280-95.
- [6] Muto, S., Suzuki, O., Amano, T., Morisawa, M. (2003) A plastic optical fiber sensor for real-time humidity monitoring. *Meas. Sci. Technol.*, 14, 746-50.
- [7] Arregui, F. J., Ciauurriz, Z., Oneca, M., Matias, I.R. (2003) An experimental study about hydrogels for the fabrication of optical fiber humidity sensors. *Sensors and Actuators B.*, 96(1-2), 165-72.
- [8] Despond, S., Espuche, E., Domard, A. (2001) Water Sorption and Permeation in Chitosan Films: Relation between Gas Permeability and Relative Humidity. *J. Polym. Sci: Part B.*, 39, 3114-27.
- [9] Corres, J. M., Arregui, F. J., Matias, I. R. (2007) IR Sensitivity optimization of tapered optical fiber humidity sensors by means of tuning the thickness of nanostructured sensitive coatings. *Sensors and Actuators B.*, 122(2), 442-9.
- [10] Bratskaya, S., Marinin, D., Simon, F., Synytska, A., Zschoche, S., Busscher, H.J., Jager, D., van der Mei, H.C. (2007) Adhesion and viability of two enterococcal strains on covalently grafted chitosan and chitosan/ κ -carrageenan multilayers. *Biomacromolecules*, 8 (9), 2960-2968.

EFFECTS OF THE BIOMASS NATURE AND GRINDING ON THE CHARACTERISTICS OF CHITIN

**Jorge Augusto de Moura Delezuk^{1,2*}, Jean-Michel Lucas², Stéphane Trombott²,
Laurent David², Sérgio Paulo Campana-Filho¹**

¹Universidade de São Paulo – Instituto de Química de São Carlos – BRAZIL

² Université Claude Bernard Lyon 1 - Ingénierie des Matériaux Polymères - FRANCE

*E-mail address: delezuk@gmail.com

INTRODUCTION

The studies on the structure/properties relationship and applications of chitosan in several fields, such as the food and cosmetic industries, pharmacy, dentistry and medicine, have produced a huge number of publications and patents in the last thirty years.¹⁻³ As a consequence, the importance of this biopolymer for practical applications has increased the interest of industries and entrepreneurs all over the world, resulting in new investments and efforts aiming the development of new technologies to produce chitosan possessing specific properties. Although chitosan occur in nature as a component of cell wall of some fungi, it is generally produced by carrying out the deacetylation of chitin. Chitin is an abundant polysaccharide whose primary structure consists of a disaccharide of 2-acetamido-2-deoxy- β -D-glucose units linked by a β (1 \rightarrow 4) glycosidic bond (Figure 01).

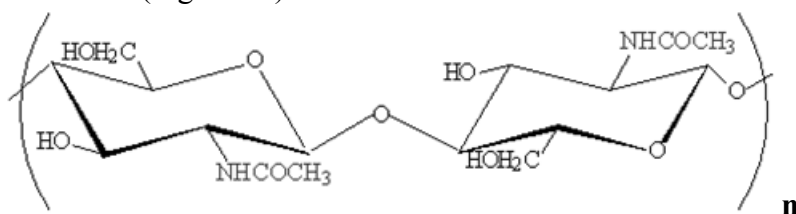


Figure 01 - Primary structure of chitin, where n is the degree of polymerization.

Chitin is a polysaccharide of high molecular weight, found in nature and responsible for giving support in the exoskeleton of crustaceans and insects, and in cell walls of fungi and other organisms. It is estimated that currently the worldwide industry of fishing, farming and processed shellfish (lobsters, shrimps, crabs and squid) produces more than one million of tons per year of solid waste rich in chitin. Taking into account the average content of chitin in such a biomass (20%-45%, depending on the biomass) and the average extraction yield (*c.a.* 15%), the availability of potentially extractable chitin significantly exceeds the current demand of chitosan, the main derivative of chitin.⁴

Due to the chemical composition presented by shrimp and crab shells, the procedure for obtaining chitin follows three steps⁵⁻⁶: demineralization, deproteinization and depigmentation, the execution of these steps being related to the removal of salts, proteins and pigments, respectively. The most used procedures for the extraction of chitin from the biomass generally comprise the use of acidic solutions (HCl or H₂SO₄) in the demineralization step and alkaline solutions (NaOH or KOH) in the deproteinization step. The elimination of pigments (mainly astaxanthin) occurs via extraction using organic solvents or by bleaching with oxidizing agents. However, it is important to note that all reaction conditions employed during the extraction steps should be mild, thus avoiding the occurrence side-reactions such as those leading to the depolymerization of chitin. In this study, alpha-chitin and beta-chitin extracted from squid pens (*Loligo sp.*) and shrimp shells (*Macrobrachium rosenbergii*), respectively, were subjected to grinding in a knives

mill and then to fractionation, resulting in three fractions (alpha-chitin) and four fractions (beta-chitin) classified according to the average particles size.

MATERIALS and METHODS

Extraction of Alpha-Chitin

The shells from *M. rosenbergii* were used as the raw material for the extraction of alpha-chitin. The method described by Percort et al.⁴ was used to remove proteins and the demineralization treatment was carried out with aqueous hydrochloric acid (1 M) under constant mechanical agitation for two hours at room temperature while the pigments were extracted with ethanol upon reflux for 24 hours.

Extraction of Beta-Chitin. For extracting beta-chitin the pens from *Loligo sp.* were used as the raw material. The method described by Chaussard, G. and Domard, A.⁷ was used to remove proteins from this biomass but the demineralization treatment was not carried out due to the low content of inorganic compounds in it. Both polysaccharides, alpha- and beta-chitin, were subjected to grinding in a knives mill (MA-048, Marconi), then sieved (using sieves with openings of 0.062, 0.075, 0.090, 0.125, 0.297, 0.425 mm) and classified according to the particles' size.

Characterizations. The average degree of acetylation (DA) of chitin was determined by nuclear magnetic resonance spectroscopy (¹H NMR) as described by Hirai et al.⁸. The intrinsic viscosities [η] were determined at 25,00 \pm 0,01°C by viscosity measurements of the chitin samples dissolved in N,N-dimethylacetamide/LiCl-5% as described by Terbojevich et al.⁹. The viscosity average molecular weight (Mv) was calculated by employing the values of K and a determined in the same solvent and temperature and according to the average degree of acetylation of the chitin sample. The thermal behavior, crystallinity and morphology of the samples were determined by thermogravimetric analysis (TGA), X-ray diffraction (XRD) and scanning electron microscopy (SEM), respectively. The solubility of chitin samples was tested in water, formic acid and aqueous hydrochloric acid 0.55 mol/L.

RESULTS and DISCUSSION

After grinding the beta and alpha-chitin samples were separated according to the particles size (Table 01). For beta and alpha-chitin we observed that the more abundant fractions corresponded to particles whose average size ranged in the interval 0.297 mm - 0.125 mm (fractions Beta-02 and Alpha-02). The different results showed between beta and alpha-chitin indicate that such chitins exhibit different behavior when subjected to grinding, this fact could be correlated with the crystallinity and morphology, alpha-chitin has a denser crystalline packing as compared to beta-chitin.

Table 01 – Fractions of chitin according to the particles' size and the corresponding mass

Fractions	Size (mm)	Mass (%)
Beta-01	0.425- 0.297	28.30
Beta-02	0.297- 0.125	57.90
Beta-03	0.125- 0.075	9.40
Beta-04	<0.075	4.50
Alpha-01	0.425- 0.297	26.00
Alpha-02	0.297- 0.125	62.00
Alpha-03	<0.090	12.00

The results obtained by viscometry ([η] and Mv) and nuclear magnetic resonance spectroscopy (GA) for the fractions of beta and alpha-chitin are shown in Table 02.

Table 02 – Values of intrinsic viscosity, viscosity average molecular weight and average degree acetylation of the fractions of beta and alpha-chitin

Fractions	$[\eta]$ mL/mg	Mv (g/mol) $\times 10^6$	DA (%)
Beta-01	4,858	1,74	85,0
Beta-02	4,827	1,73	69,0
Beta-03	4,153	1,39	68,5
Beta-04	2,745	0,76	59,9
Alpha-01	8,322	3,8	81,8
Alpha-02	5,197	1,9	62,9
Alpha-03	4,642	1,6	69,0

According to these data, it is observed that the fractions composed by larger particles presented higher Mv, in both cases. Indeed, comparing the values of Mv of the fractions composed by the largest (fractions Alfa01 and Beta01) and the smallest (fractions Alfa03 and Beta04) particles reveals that the Mv of the alpha-chitin and beta-chitin fractions decreased 42% and 44%, respectively. This fact is intrinsically linked to the polymer degradation provoked by shearing forces and heating due to grinding of the beta and alpha-chitin as the smaller particles were subjected to longer grinding time and thus experienced more severe degradation.

The variation of DA of the fractions of beta- and alpha-chitin as a function of the particles' size was similar to that observed in the variation of Mv, the decrease of particles' size resulting in the decrease of DA, probably due to heat-induced deacetylation. Correlating the variation of DA with Mv for beta-chitin it was observed the existence of three different situations: i-DA decreased with constant Mv (Beta01 to Beta02), ii-Mv decreased with DA constant (Beta02 to Beta03) and iii-DA and Mv decreased (Beta04 to Beta03). In the case of alpha-chitin two different situations were observed: i-DA and Mv decrease (Alfa01 to Alfa02) and ii-Mv decrease with DA increased (Alfa02 to Alfa03). Thus, it is apparent that the variation of DA and Mv does not have a trivial correlation in each case.

The values of crystallinity index (CI) and average crystallite size (Table 03) show that beta-chitin was more susceptible to morphological changes associated to grinding as both parameters decreased with decreasing particles' size while they remained approximately constant in the case of alpha-chitin.

Table 03 - Values of the crystallinity index (CI) and crystallite size (Lhkl) of beta and alpha-chitin

Samples	Crystallinity Index % (CI)	Crystallite Size $\text{\AA} (L_{hkl})$
Beta-01	89,0	29,9
Beta-02	89,0	29,9
Beta-03	84,0	26,3
Beta-04	78,0	19,9
Alpha-01	95,0	56,6
Alpha-02	95,0	57,7
Alpha-03	93,0	56,6

Through the micrographs (Fig. 01 and Fig. 02), obtained from SEM, we observed the variation of the particle size of beta and alpha-chitin fractions. The SEM analysis of beta-chitin (Fig. 01) reveals that, irrespective of the fraction, the morphology of the resulting particles have characteristics of the "fibrous", being longer and with smaller diameters. The micrographs of alpha-chitin (Fig. 02) showed a morphology similar to the "flakes", showing thinner and more rectangular shape.

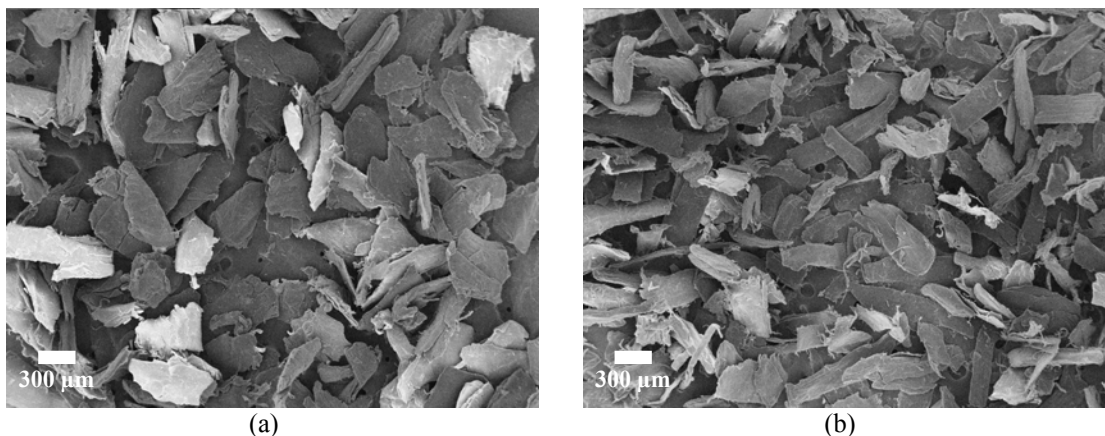


Figure 02 - Micrographs of the fractions of beta-chitin (a) 0.425 to 0.297 mm (Beta 01), (b) 0.297 to 0.125 mm (Beta 02).

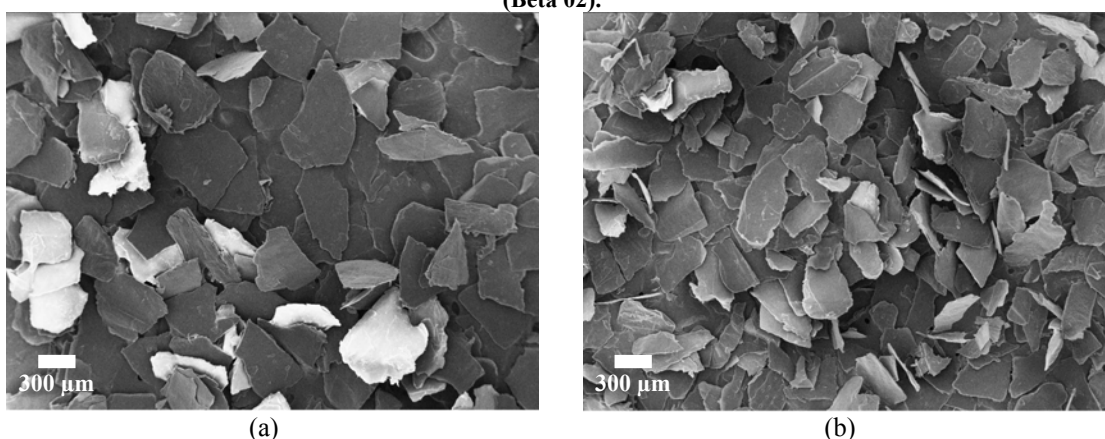


Figure 03 - Micrographs of the fractions of alpha-chitin (a) 0.425 to 0.297 mm (Alpha 01), (b) 0.297 to 0.125 mm (Alpha 02).

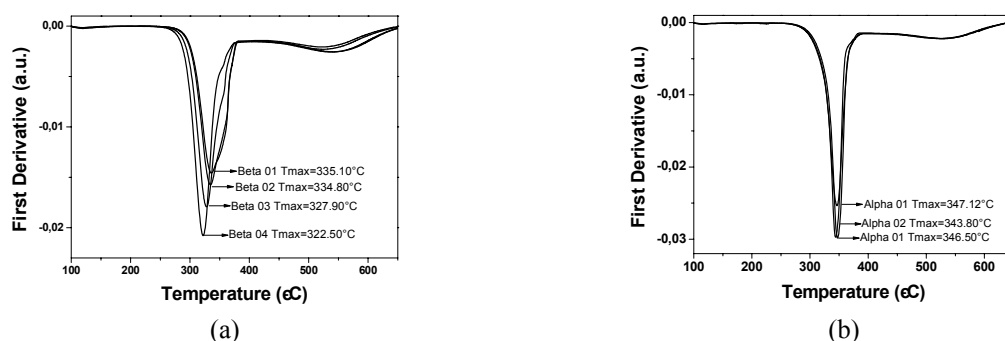


Figure 04 - Variation of the first derivative versus temperature (°C), for (a) beta and (b) alpha-chitins fractions with the degradation maximum temperature (Tmax) for each sample.

The thermal analyses of the beta-chitin fractions (Fig. 04 (a)) showed that the first two fractions (Beta-01 and Beta-02) and the last two fractions (Beta-03 and Beta-04) exhibited different thermal degradation behaviours. The thermal degradation of the samples is largely affected by the crystallinity, morphology and molecular weight, for the samples Beta-01 and Beta-02 these parameters were very similar. The thermal degradation presented by Beta-03 and Beta-04 were the same, but the maximum temperatures of degradation have some differences as noted in Fig. 04 (b), these variations being probably due to different values of crystallinity and Mw, and

morphological characteristics. The alpha-chitin samples showed almost the same values of the maximum temperature of degradation.

CONCLUSION

The study of production of different polymorphs of chitin (alpha and beta) showed that depending on the processing procedure samples with different characteristics are obtained. Currently the vast majority of studies related to chitin, and its main derivative chitosan, are focused primarily on the areas of applications of these polymers, and studies generally used as a basis for obtaining chitin and chitosan production are left in the background. The areas of applications of chitin and chitosan are numerous and range from the most trivial applications (for instance as a flocculating agent) to specific and sophisticated applications (such as the nanoparticles for drug delivery), all applications related to chitin and chitosan are closely related to the characteristics displayed by these polymers, such as molecular weight, polydispersity index and average degree of acetylation. The control of the main characteristics of both chitin and chitosan is one of the main challenges faced by researchers working in this area, because the reproducibility of these characteristics is considered essential for the properties' reproducibility. The main changes that occurred during the milling process are related to the average degree of acetylation and the viscosimetric molecular mass and from the experimental data we can conclude that the shearing forces and heat generated during the grinding of the samples caused the degradation and deacetylation of the chitin samples.

This work makes an important contribution to future exploration in production of chitosan, because through the various data obtained on the fractions of chitin (GA, Mv, crystallinity, etc.) studies aimed at the production of chitosan may use this in order to control the variables of the chitin used in deacetylation reaction.

REFERENCES

- [1] RINAUDO, M. (2006) Chitin and chitosan: Properties and applications. *Progress in Polymer Science*, 31, 603–632.
- [2] KURITA, K. (1998) Chemistry and application of chitin and chitosan. *Polymer Degradation and Stability*, 59, 117–120.
- [3] KUMAR, M. N. V. R. (2000) A review of chitin and chitosan applications. *Reactive & Functional Polymers*, 46, 1–27.
- [4] AGULLÓ, E.; PENICHE, C.; TAPIA, C.; HERAS, Á.; ROMÁN, J. S.; ARGÜLLES, W.; GOYCOOLEA, F.; MAYORGA, A.; NAKAMATSU, J.; ABRAM, A. P. (2004) *Quitina y Quitosano: obtención, caracterización y aplicaciones*. Perú: Pontificia Universidad Católica Del Perú/ Fondo Editorial, 312 p.
- [5] PERCOT, A.; VITON, C.; DOMARD, A. (2003) Characterization of shrimp shell deproteinization. *Biomacromolecules*, 4, 1380–1385.
- [6] ROBERTS, G. A. F. (1992) *Chitin chemistry*. London, MacMillan Press, 349p.
- [7] CHAUSSARD, G.; DOMARD, A. (2004) New Aspects of the Extraction of Chitin from Squid Pens. *Biomacromolecules*, 559–564.
- [8] HIRAI, A. ODANI, H.; NAKAJIMA, A. (1991) Determination of degree of deacetylation of chitosan by ¹H NMR spectroscopy. *Polymer Bulletin*, 26, 87–94.
- [9] TERBOJEVICH, M.; CARRARO, C.; COSANI, A. (1988) Solution studies of the chitin-lithium chloride-N,N-dimethylacetamide system. *Carbohydrate Research*, 180, 73–86.
- [10] LAVALL, R. L.; ASSIS, B. G. O.; CAMPANA FILHO S. P. (2007) β -Chitin from the pens of *Loligo* sp.: Extraction and characterization. *Bioresource Technology*, 98, 2465–2472.

CONDUCTING MATERIALS BASED ON CHITOSAN HYDROGELS: FROM 2D TO 3D MATERIALS

J. Desbrieres*, S. Reynaud, P. Marcasuzaa, F. Ehrenfeld

*Université de Pau et des Pays de l'Adour (UPPA) – IPREM/EPCP – UMR 5254 CNRS/UPPA –
Hélioparc Pau Pyrénées – 2 Avenue P. Angot – 64053 PAU cedex 09 – France*

INTRODUCTION

Chitosan (Chi) is biodegradable, biocompatible, non-irritant and exhibits good film-forming properties, high mechanical strength and adhesion [1,2]. All these characteristics make it suitable for a wide range of applications. Chitosan gel may be easily obtained by crosslinking reaction with glutaraldehyde [3]. These gels exhibit good swelling properties and efficient responses to external stimuli as pH, temperature which makes these materials eligible as artificial muscles [4]. However, in this domain of applications their developments are limited by the poor electrical conductivity resulting in a poor response time.

On the other hand, polyaniline (PANI) being most promising organic conducting polymer finds wide applications, such as in rechargeable batteries, corrosion protection of metals, gas separation membranes or molecular sensors [5-7]. It is easy to synthesize and it exhibits a wide range of conductivity, low operational voltage and a good environmental, thermal and chemical stability. PANI exhibits important advantages thanks to its unique and easy doping process [8,9]. It is a pH-responsive material exhibiting different chemical forms depending on acid/base treatment [10]. However PANI has limitations due to its poor solubility in common organic solvents, its infusibility and its poor mechanical properties [11,12]. To overcome these drawbacks, many studies have been done either by using additives, specific doping chemicals [13-15] or through the formation of polymer matrix/PANI composites. In the latter, the polymer matrix brings specific properties as better solvent solubility or mechanical properties while PANI provides conducting properties to the final composite. The obtained material will be stimulus-responsive and they may respond to various stimuli such as pH or electric stimuli. Moreover they may be used in controlled delivery systems if polymer matrix has hydrogel properties. Its swelling allows inclusion of active chemicals (among them drugs) and their release leading to be candidates for biomedical applications as recently studied [16].

In the present study, composites have been made by mixing chitosan and PANI to combine good processability of the matrix and electrical conductivity [12,17].

MATERIALS and METHODS

Materials:

Two samples (#1 and #2) of chitosan (Chi) samples were provided from Pronova (Norway) and respectively exhibit viscosity-average molar masses of 20,600 and 165,000 g.mol⁻¹ and degrees of acetylation of 18 and 21%. The average viscometric molecular weight was estimated from the intrinsic viscosity determined in the solvent 0.3 M CH₃COOH/0.2 M CH₃COONa using the Mark Houwink parameters $a=0.76$ and $K=0.076$ at 25 °C when the intrinsic viscosity is expressed [18] in mL.g⁻¹. The degree of acetylation was determined by ¹H NMR, generally considered the most sensitive technique [19].

Ammonium persulfate (APS) (Aldrich; 248614, >98%), aniline (ANI) (Acros Organics; 3,293-4, 99.8%), hydrochloric acid (Aldrich, 37%), ethyl alcohol (Atlantic labo, 96%) *N*-

methylpyrrolidone (NMP, Sigma Aldrich) and acetic acid (Prolabo, 90%) were used as received. Glutaraldehyde was used as a 25 wt% solution in water.

Composite films were prepared from 20 mL of solutions of chitosan or graft copolymer in 0.1 M HCl (polymer concentration of 1.5 mg.mL⁻¹). These solutions were deposited into a glass plate and dried at room temperature under air flow overnight.

Techniques :

UV-Visible spectroscopy

UV-visible spectra of deprotonated dedoped samples dissolved in *N*-methylpyrrolidone were recorded with a UV-VIS spectrophotometer UV2450 from Shimadzu corporation.

NMR spectroscopy

¹H NMR spectra were recorded at 25 °C on a Bruker Avance 400 NMR spectrometer in DMSO-*d*₆ in which a few drops of 1 M HCl were added. The chemical shifts were referred to the residual solvent peak. Polymer concentration was 20 mg.mL⁻¹.

Conductivity

The conductivity of PANI composites was measured on films using the four probe method.

Rheology

Rheological experiments were carried at 25 °C out on a DSR rheometer from Rheometrics using a plate-plate geometry. The frequency sweep was performed within the linear regime, checked before and at the end of each experiment.

Swelling

Swelling properties of hydrogels were evaluated by the thermogravimetric method from 25 to 130 °C and a rate of 10 °C.min⁻¹. The samples were kept at 130 °C for 60 min at the end of the experiment. The swelling properties at fixed relative humidity (RH) were performed in dessicators at 25°C containing a saturated solution of CaCl₂ (RH of 29%) and pure distilled water (RH of 100%).

Actuator test

To characterize the conducting hydrogel response, a Mecano-Electric Test-Stand (METS) system, previously developed in our lab was used [20,21]. It contains a VersaTest test stand to compress the hydrogels, an AFG load sensor to measure the applied compression by the VersaTest, a NI-DAQ device to measure the resulting voltage. A LabVIEW application was developed to register, view and analyse the data.

RESULTS and DISCUSSION

Synthesis and characterization of chitosan-graft-polyaniline copolymers

The synthesis of chitosan-graft-polyaniline was based on previous works reported by Tiwari *et al.* [22] (Figure 1). 220 mg of chitosan (1.3 10⁻³ monomol) and 100 mg of aniline (1.10⁻³ mol) were introduced in 200 mL of 0.1M HCl in a round bottom flask. After solubilisation, 244.6 mg of ammonium persulfate (1.10⁻³ mol) were added to the reactive medium and let under stirring at room temperature for 4h. The grafted copolymer was then neutralized by NaOH and precipitated with an excess of ethanol. The resulting precipitate was washed with NMP in order to remove free PANI. The latter was quantified by UV-Vis spectroscopy (molar adsorption coefficient of 1600 L.cm⁻¹.monomol⁻¹ at 328 nm). Finally, the copolymer was rinsed with HCl 0.1M and dried under soft conditions (room temperature and atmospheric pressure) to obtain doped copolymer.

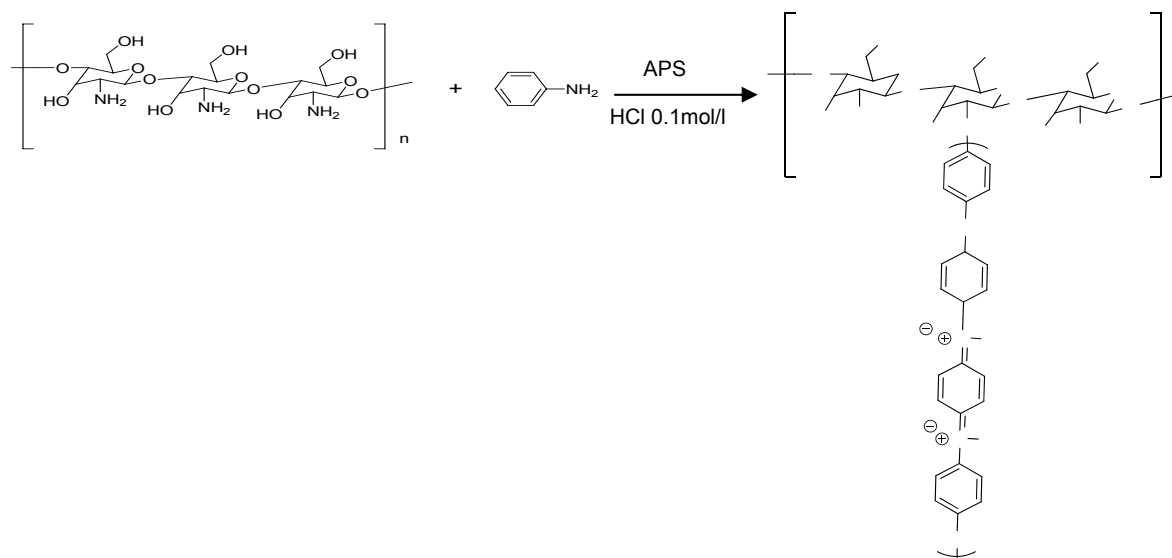


Figure 1. Synthesis of grafted copolymer

The experimental conditions and characterization of chitosan-*graft*-polyaniline (Chi-g-PANI) copolymers are given in Table 1.

Table 1. Compositions and characterization of chitosan-*graft*-polyaniline copolymers

Copolymer Sample name	# chitosan sample	$m_{\text{(Chi)}}/m_{\text{(ANI)}}$	$[\text{ANI}]/[\text{APS}]$	Grafting % of PANI on Chitosan	Conductivity ($\text{S} \cdot \text{cm}^{-1}$)	wt% PANI into the copolymer
PANI	/	0	1	/	10^{-2}	100
C1PANI_1a	1	1	1	95	10^{-1}	50
C1PANI_1b	1	1	0.5	89	10^{-2}	45
C1PANI_2	1	2	1	99	10^{-2}	33
C1PANI_4	1	4	1	99	10^{-5}	20
C2PANI_2	2	2	1	99	10^{-2}	33

Aniline is polymerized in the presence of chitosan. The reaction mechanism is of chain nature due to the formation of sulfate ion radicals, well-known ion chain carriers for graft copolymerization. Finally chitosan macroradicals and PANI cation radicals are combined to form Chi-*graft* -PANI graft copolymer [22]. The reaction of aniline on chitosan amino groups is favored compared to its homopolymerization.

NMR spectra of the copolymers demonstrate that no deacetylation occurs on chitosan during its chemical modification and that PANI is grafted onto chitosan chain. Moreover the degree of substitution of the chitosan amino group seems to be relatively small. From these considerations we assume that few long chains of PANI are grafted onto the chitosan backbone based on the small degree of substitution and the quantity of grafted PANI.

The conductivity of all the composites was measured above $10^{-2} \text{ S} \cdot \text{cm}^{-1}$ but the sample C1PANI_4 containing the lowest amount of PANI (Table 1). These aforementioned characteristics show that the objective was reached: the chitosan-*graft*-PANI composites exhibit both the intrinsic properties of chitosan and PANI. Indeed it is known that chitosan has film-forming properties, as all polysaccharides, and no detrimental effect of the PANI content was observed. In the same manner, chitosan-*graft*-PANI exhibits the conducting properties of pure PANI while pure chitosan is an insulating material ($<10^{-5} \text{ S} \cdot \text{cm}^{-1}$). The conductivity is better than

those reported by Tiwari [22] when compared at similar PANI content. In the same manner, the conductivity is much more higher (between 10 and 100 times at the same PANI content) than those obtained for semi-interpenetrating networks of chitosan and PANI [12,23]. The conductivity was enhanced by the H-bonding occurring between the chitosan backbone (H-acceptor amide group) and the PANI backbone (H-donor imino group) [24-26]. In order to highlight the advantages of the grafting route with respect to the blends method, a mixture of chitosan and PANI was prepared in the solvent phase. However, blends were not obtained because both polymers are not well soluble in a common solvent: 0.1 M HCl is a good solvent of chitosan but is not acidic enough to solubilize PANI, and chitosan is not soluble in 1 M HCl. NMP is a good PANI solvent but chitosan is not soluble. All these results demonstrate the interest and advantages of grafting PANI onto chitosan backbone compared with a mechanical mixture, which is generally accepted.

Optical microscopy observations were also carried out to follow the evolution of the film surface morphology. Due to the difference in hydrophily of chitosan and PANI, the conducting moieties are observed at the solid-air surface when the chitosan is preferably in the bulk. From the images it may be concluded that at 20 wt% PANI few connections are observed while at 33 wt% homogeneous dispersion was obtained.

Preparation of composite hydrogels

Hydrogels were prepared using glutaraldehyde as the crosslinking agent and chitosan sample # 1. First tests were carried out on different polyaniline-*graft*-chitosans described within Table 1. Using the insulating C1PANI_4, an insulating gel is obtained. On the other hand, no crosslinking reaction was obtained with C1PANI_2 as precursor. As a consequence, composite hydrogels exhibiting both conducting and mechanical properties have been obtained from a mixture of C1PANI_2 chitosan-*graft*-polyaniline and pure chitosan according to the following: 50 mg of graft copolymer and 50 mg of chitosan #1 were solubilized in 10 mL of 0.1 M acetic acid. After solubilization, the glutaraldehyde solution (crosslinking agent) was added to obtain the hydrogel at ambient temperature. The hydrogel was kept in a wet atmosphere to avoid any drying. Experimental conditions are given in Table 2.

Table 2. Experimental conditions of the synthesis of composite hydrogels.

m (chi) (mg)	m (C1PANI_2) (mg)	m _{cross agt} / m _(Chi+copo)	Hydrogel Name	Time for gelation
100	0	3.98	HG_4	few minutes
100	0	2.66	HG_5	few minutes
100	0	1.33	HG_6	4 hours
100	0	0.27	HG_7	No gel after 10 hours
50	50	2.66	HG_8	1 hour
50	50	3.32	HG_9	30 minutes
50	50	3.98	HG_10	10 minutes
50	50	4.65	HG_11	10 minutes
75	25	2.66	HG_12	10 minutes
25	75	3.98	HG_13	5 hours

The strategy we developed within this study led to a new kind of composite hydrogels where two cases may be considered : either (1) a semi-interpenetrating network in which linear graft copolymer was diluted in the chitosan matrix or (2) a mixed covalent network in which chitosan and graft copolymer were crosslinked together in the same network. The first assumption comes from above results showing that no gel is obtained from chitosan-*graft* -PANI alone when the chitosan/aniline ratio within the copolymer is equal to 2 (C1PANI_2), by contrast

with copolymer with a ratio of 4 (C1PANI_4) for which crosslinking was observed. Moreover, no loss of chitosan or copolymer was observed using specific solvents to extract polymers (NMP to extract PANI or derivatives and 0.1 M HCl to extract chitosan based copolymer). This may be the consequence either of the involvement of these chains within the crosslinked network or the existence of strong hydrogen bonds between chitosan and PANI under these conditions as already reported [27]. Whatever the nature of the network is, the presence of rigid and long PANI grafted chains decreases the ability of chitosan crosslinking reaction probably due to a decrease of the accessibility of amine groups. We may depict hydrogen bonding between chitosan and PANI chains leading to the formation of a zip-like architecture in which PANI side chains and chitosan backbone interact either from inter- or intramolecular hydrogen bonding. As a consequence amino groups are less accessible to aldehyde reactive functions. No scientific data can lead, at that time, to a definitive answer but we favor the covalent network assumption in relation with the complete absence of chitosan-graft-PANI removal, even at high swelling ratio of the hydrogel.

The gelation kinetics was followed with rheological measurements. It depends on the pH, the quantity of the crosslinking agent and the acetylation degree [28], hydrophobic interactions between acetyl groups being involved in the stabilization of highly acetylated chitosan gels.

Properties of hydrogels

Rheology:

The signature of the hydrogels was demonstrated from the evolution of G' and G'' moduli as a function of the frequency. The reached rheological moduli are of the same order of magnitude that already reported on such gels [3]. The hydrogel composition has a great influence on their strength. Increasing the copolymer content decreases the elastic modulus and makes the gel more brittle. This leads to consider that PANI is not a reinforcing charge (as observed within composite materials), which confirms that PANI is grafted onto the chitosan chain and not free within the hydrogel.

Swelling properties:

The swelling properties of these composite hydrogels were measured as a function of the relative humidity (RH) and are reported in Figure 2. The swelling properties may be considered reversible to a certain extent. This feature is due to the occurrence of numerous intermolecular hydrogen bonds between the components (chitosan and grafted PANI chains) when the hydrogel is exposed to lower RH. This leads to decrease further diffusion of water molecules when the gel is again exposed to higher RH.

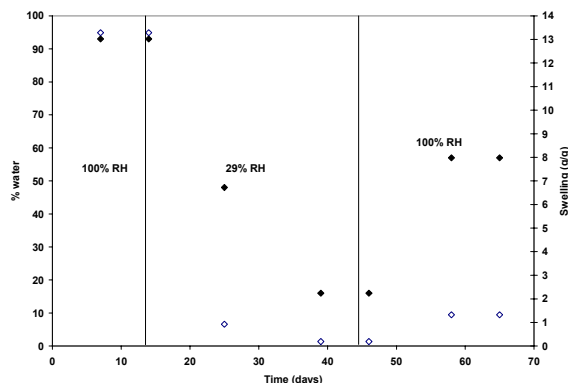


Figure 2. Swelling properties of chitosan/copolymer hydrogel (HG_10 hydrogel, C1PANI_2/chitosan 50/50) as a function of relative humidity (◆ in % water; ◇ in swelling ratio).

These properties make the composite hydrogel eligible for the development of applications as the inclusion and release of active matter as already demonstrated for semi-interpenetrating polyacrylamide-PANI hydrogels [15,29]. More specifically the presence of intrinsic conducting polymers within these hydrogels allows electrochemical control release of active matter [29].

Actuator tests

One of the primary requirements for designing advanced smart materials is a change in their properties in response to external stimuli. Recent literature shows an emerging interest in hydrogel-based actuating systems because of their stimuli responsive behavior [30-35]. Actuators are mechanical devices for moving or controlling a mechanism or system. Typically they take energy, normally created by air, electricity or liquid and convert that into kind of motion. Examples include mechanisms (hydraulic cylinders, motors, linear actuators...), human muscles, and in engineering systems to introduce motion or to cleanup an object so as to prevent motion... We studied the ability of the prepared composite hydrogel to convert mechanical work into electrical energy as referred to previous articles [21,36] similarly to "reverse actuators". Composite hydrogels were elaborated from mixtures of chitosan and graft copolymers. Composite hydrogel elaborated from a 75/25 chitosan/graft copolymer mixture (HG_12) presents an interesting behavior as compared to the 50/50 composite hydrogel (HG_10) which was too brittle. Indeed, this composite hydrogel was able to deliver a measurable tension acting thus as a mechano-electric device.

Figure 3 shows the electric response to a mechanic stimulus. For each cycle, an instantaneous response time is observed, and the delivered voltage under pressure reached 0.1 V on average. However, the relaxation rate is lower and it takes few minutes to record a constant voltage equal to the initial value to apply a new cycle. These data demonstrated the feasibility of a mechano-electric actuator using our new composite hydrogel as sensing material. Reproducibility of such a behavior was observed from series of tests.

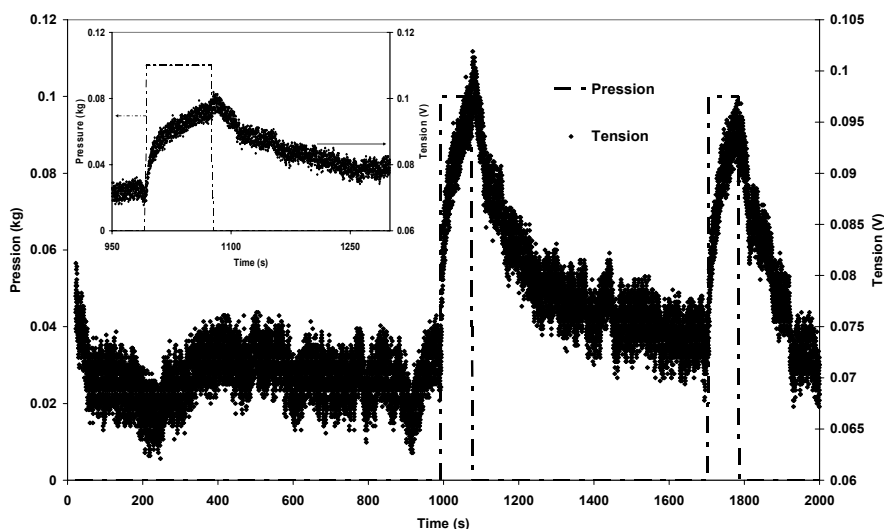


Figure 3. Pressure testing as actuator system (Chit1PANI_2/chitosan 1 HG_12 hydrogel). Insert is a zoom of the curve between 950 and 1300 seconds.

CONCLUSION

A new type of composite hydrogels was elaborated from chitosan-*graft*-polyaniline copolymers. These copolymers are intrinsic conducting polymers (conductivity larger than 10^{-2} S.cm⁻¹) and led to hydrogels exhibiting high and reversible swelling properties. Due to the total grafting of the conducting polymer (larger than 90% of aniline according to our reaction conditions) onto the polysaccharide backbone, no migration of the polyaniline occurs at the swollen state. This synthesis leads to the elaboration of stable materials in which the polyaniline is homogeneously incorporated. Chitosan enables to enhance the conducting properties thanks to hydrogen bond occurring between chitosan hydrogel network and polyaniline. In a last approach, the feasibility of actuator *i.e.* mechano-electric device using composite hydrogel as sensing material has been proven. However further works are still to be done to control and optimize the structure of the copolymers (length of PANI chains and the degree of substitution) and to determine the architecture of these hydrogels. This future work should allow the optimization of the actuator performances and allows development of new applications within the biomedical domain as an example.

ACKNOWLEDGMENTS

The authors are grateful for Dr Bruno Grassl for his help to measure actuator properties and helpful discussion.

REFERENCES

- [1] Mucha, M.; Wankowicz, K.; Balcerzak, J. (2007) *e-Polymers*, 16, 1-10
- [2] Wang, B.; Zhang, J.; Cheng, G.; Dong, S. (2000) *Analytica Chimica Acta*, 407, 111-118
- [3] Argüelles-Monál, W. ; Goycoolea, F.M. ; Peniche, C. ; Higuera-Ciapâra, I. (1998) *Polymer Gels and Networks*, 6, 429-440
- [4] Kim, S.J.; Shin, S.R.; Spinks, G.M.; Kim, I.Y.; Kim, S.I. (2005) *Journal of Applied Polymer Science*, 96, 867-873
- [5] Tan, C.K.; Blackwood, D.J. (2000) *Sensors and Actuators*, 71, 184-191
- [6] Karami, H.; Mousavi, M.F.; Shamsipur, M. (2003) *Journal of Power Sources*, 117, 255-259
- [7] Sengupta, P.P.S.; Barik, S.; Adhikari, B. (2006) *Materials and Manufacturing Processes*, 21, 263-270
- [8] Neoh, K. G.; Pun, M. Y.; Kang, E. T.; Tan, K. L. (1995) *Synthetic Metals*, 73, 209-215.
- [9] Stejskal, J.; Gilbert, R. G. (2002) *Pure and Applied Chemistry*, 74, 857-867.
- [10] Kohut-Svelko, N.; Reynaud, S.; François, J. (2005) *Synthetic Metals*, 150, 107-114
- [11] Tiwari, A. (2007) *Journal of Macromolecular Science Part A: Pure and Applied Chemistry*, 44, 735-745
- [12] Yavuz, A.G.; Uygun, A.; Bhethanabotla, V.R. (2009) *Carbohydrate Polymers*, 75, 448-453
- [13] Jayakannan, M.; Anilkumar, P.; Sanju, A. (2006) *European Polymer Journal*, 42, 2623-2631
- [14] Laska, J. (2002) *Synthetic Metals*, 129, 229-233
- [15] Tzou, K.; Gregory, R.V. (1993) *Synthetic Metals*, 53, 365-377
- [16] Xu, X.H.; Ren, G.L.; Cheng, J.; Liu, Q.; Li, D.G.; Chen, Q. (2006) *Journal of Materials Science*, 41, 4974-4977
- [17] Takahashi, K.; Nakamura, K.; Yamaguchi, T.; Komura, T.; Ito, S.; Aizawa, R.; Murata, K. (2002) *Synthetic Metals*, 128, 27-33
- [18] Rinaudo, M.; Milas, M.; Le Dung, P. (1993) *Int. J. Biol. Macromol.*, 15, 281-285

- [19] Rinaudo, M.; Le Dung, P.; Gey, C.; Milas, M. (1992) *Int. J. Biol. Macromol.*, 14, 122-128
- [20] Thévenot, C.; Khoukh, A.; Reynaud, S.; Desbrières, J.; Grassl, B. (2007) *Soft Matter*, 3, 437-447.
- [21] Xu, X.H.; Ren, G.L.; Cheng, J.; Liu, Q.; Li, D.G.; Chen, Q. (2006) *J. Mater. Sci.*, 41, 3147-3149
- [22] Tiwari, A.; Singh, V. (2007) *eXpress Polymer Letters*, 1, 308-317
- [23] Kim, S.J.; Kim, M.S.; Kim, S.I.; Spinks, G.M.; Kim, B.C.; Wallace, G.G. (2006) *Chem. Mater.*, 18, 5805-5809
- [24] Barthet, C.; Armes, S. P.; Chehimi, M. M.; Bilem, C.; Omastova, M. (1998) *Langmuir*, 14, 5032-5038
- [25] Ikkala, O. T.; Vikki, T.; Passiniemi, P.; Osterholm, H.; Osterholm, J.-E.; Pietila, L.-O.; Ahjopalo, L. (1997) *Synthetic Metals*, 84, 55-58.
- [26] Tang, Q.; Wu, J.; Sun, H.; Fan, S. ; Hu, D. ; Lin, J. (2008) *Carbohydrate Polymers*, 73, 473-481
- [27] Tao, Y.; Zhao, J.X.; Wu, C.X. (2005) *European Polymer Journal*, 41, 1342-1349
- [28] Draget, K.I. (1996) *Polymer Gels and Networks*, 4, 143-151
- [29] Lira, L.M. ; Cordoba de Torresi, S.I. (2005) *Electrochemistry Communications*, 7, 717-723
- [30] Cruz-Silva, R.; Escamilla, A.; Nicho, M.E.; Padron, G.; Ledezma-Perez, A.; Arias-Marin, E.; Moggio, I.; Romero-Garcia, J. (2007) *Europ. Polym. J.*, 43, 3471-3479
- [31] Sidorenko, A.; Krupenkin, T.; Taylor, A.; Fratzl, P.; Aizenberg, J. (2007) *Science*, 315, 487-490.
- [32] Kim, S. J.; Spinks, G. M.; Prosser, S.; Whitten, P. G.; Wallace, G. G.; Kim, S. I. (2006) *Nature materials*, 5, 48-51.
- [33] Beebe, D. J.; Moore, J. S.; Bauer, J. M.; Yu, Q.; Liu, R. H.; Devadoss, C.; Jo, B. H. (2000) *Nature*, 404, 588-590.
- [34] Osada, Y.; Matsuda, A. (1995) *Nature*, 376, 219.
- [35] Schreyer, H. B.; Gebhart, N.; Kim, K. J.; Shahinpoor, M. (2000) *Biomacromolecules*, 1, 642-647.
- [36] Sawahata, K.; Gong, J. P.; Osada, Y. (1995) *Macromolecular Rapid Communications*, 16, 713-716

THE STUDY OF LAWS OF N-ACETYL-D-GLUCOSAMINE ACID HYDROLYSIS

Natalia V. Dolgopyatova¹, Vitaly Yu. Novikov² and Nikolay M. Putintsev¹

¹*Murmansk State Technical University*

²*Knipovich Polar Research Institute of Marine Fisheries and Oceanography (PINRO),
Murmansk, Russia*

E-mail: iranion@yandex.ru

INTRODUCTION

One of directions of chitin use is its hydrolysis to monomers. Full depolymerisation of chitin is usually made in the acid solutions under the influence of hydrochloric acid at heating [2]. In these conditions, glucosidic bonds in polysaccharide decompose with formation of monomers - D-glucosamine and N-acetyl-D-glucosamine.

In the process of acid hydrolysis the monomers are generating in the form of salts of relevant acids in which hydrolysis is made.

There are two reactions during chitin's hydrolysis: depolymerization and deacetylation. Monomer D-glucosamine, formed as a result of deacetylation, is used in medicine for treatment of arthrosis.

Earlier it has been estimated, that reaction of deacetylation of chitin polysaccharide is described by the kinetic equation of 1st order. Dependence of this reaction rate on acid concentration has a maximum at concentration of hydrochloric acid 29.8 % [6]. Therefore research of features of monomer N-acetyl-D-glucosamine hydrolysis depending on temperature of process, concentration and the acid nature represents theoretical and practical interest.

In the presented work process of deacetylation N-acetyl-D-glucosamine for an estimation of a kinetic constant and critical increment of energy of these reactions in acids of the various nature is studied.

MATERIALS AND METHODS

Chitin produced from armours of the Kamchatka crab by well known technology[7].

Chitin hydrolysis for the purpose of D-glucosamine production made at constant mixing in concentrated hydrochloric acid at 98 °C during 2,5 hours. The ratio between chitin and acid was 1:20.

N-acetyl-D-glucosamine, received by acetylation of D-glucosamine has been used in research.

Hydrolysis of N-acetyl-D-glucosamine made in various acids (HCl, HClO₄, H₃PO₄) with concentration from 1.0 to 12.2 mol/dm³ at temperature 80 °C and at temperatures 40, 60, 70 and 80 °C for hydrochloric acid. The formed hydrolysates have neutralised by NaOH solution and filtered through the porous glass filter № 10. Contents of N-acetyl-D-glucosamine and D-glucosamine in mg/ml was defined in them. The formed hydrolysates have neutralised by NaOH solution and filtered through the porous glass filter № 10. Contents of N-acetyl-D-glucosamine and D-glucosamine in mg/ml was defined in them.

Contents of N-acetyl-D-glucosamine was defined by photometric method on reactions with N,N'-Dimethylbenzaldehyde by a technique [8]. Contents of the general sugar was defined by

photometric method on reactions with potassium ferrocyanide (III) by a technique [3]. Quantity of D-glucosamine was counted as difference between total quantity of N-acetyl-D-glucosamine + D-glucosamine and quantity of N-acetyl-D-glucosamine.

RESULTS and DISCUSSION

In figure 1, as an example, kinetic curves of hydrolysis N-acetyl-D-glucosamine and formations D-glucosamine in solutions HCl, HClO₄, H₃PO₄ are presented at equivalent concentration of acids 6 mol/l and temperature 80 °C. (For other studied concentrations similar laws are obtained).

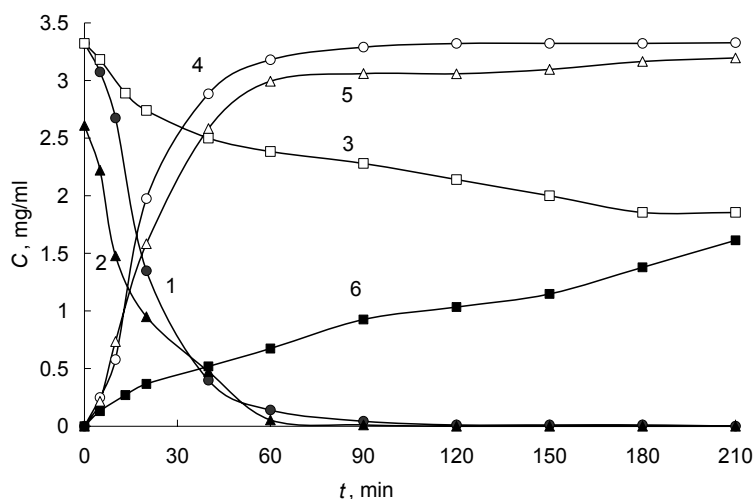


Figure 1 – Kinetic curves of hydrolysis N-acetyl-D-glucosamine in HCl (1), HClO₄ (2), H₃PO₄ (3) and kinetic curves D-glucosamine formation in HCl (4), HClO₄ (5), H₃PO₄ (6). Acid concentration = 6 mol/l.

In works [1], [6] it has been shown, that deacetylation reactions of chitin and N-acetyl-D-glucosamine rate depends on concentration of hydrochloric acid. Therefore the same dependence has been investigated at hydrolysis N-acetyl-D-glucosamine in HClO₄ and H₃PO₄. Rates constants of deacetylation N-acetyl-D-glucosamine reaction in various acids of different concentration have been calculated, using the equation (1) for the description of 1st order reaction [9]:

$$k_A = 1/t \ln (C_0/C) \quad (1)$$

where t - duration of reaction, s⁻¹; C - current concentration of substance by time moment t , mg/ml, C_0 – initial concentration of substance, mg/ml.

In figure 2 dependence of a specific reaction rate of N-acetyl-D-glucosamine deacetylation on concentration HCl, HClO₄ и H₃PO₄ is shown.

Analyzing the results shown in figure 2 in comparison with data, received in work [1], it is possible to tell, that kinetic constants of deacetylation N-acetyl-D-glucosamine in HCl and HClO₄ and chitin in HCl at 353 have identical order.

From figure 2 follows, that reaction rate of hydrolysis N-acetyl-D-glucosamine depends on nature of studied acids. In a case hydrochloric acids, the kinetic constant passes through a maximum at concentration 7,8 mol/dm³ and further, a little reducing, reaches constant values at concentration 10 mol/dm³. For perchloric acid the specific reaction rate is maximum at concentration nearby 6 mol/dm³. At the further increase in concentration k_A reduce in 2-5 times.

In a phosphoric acid speed of hydrolysis acetamidic bonds of N-acetyl-D-glucosamine more low, than in perchloric and hydrochloric acids. Evident increase in speed of hydrolysis in this case is observed at acid concentrations near 20-22 mol/dm³.

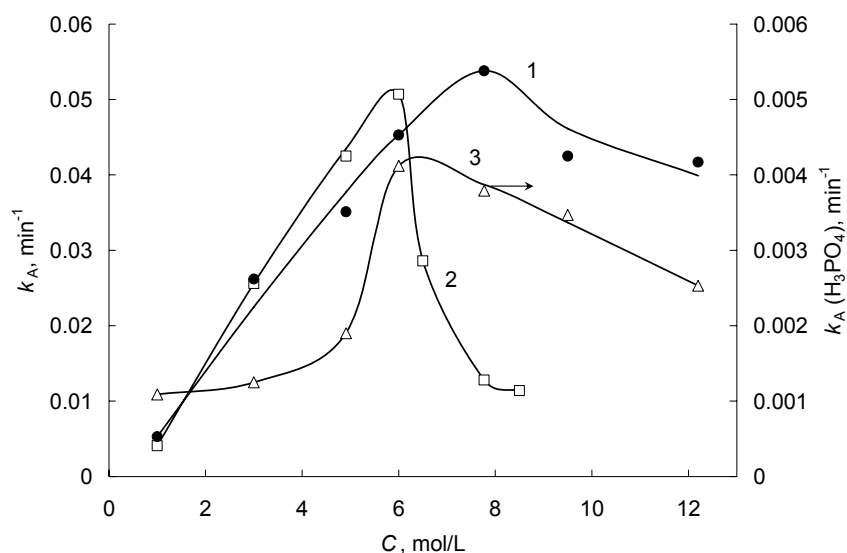


Figure 2 – Dependence of a reaction rate of deacetylation N-acetyl-D-glucosamine constant on HCl (1) and HClO₄ (2) concentrations at 80 °C.

Probably, speed of hydrolysis N-acetyl-D-glucosamine acetamidic bonds depends, first of all, on ion density of hydrogen, i.e. is defined by degree of acid ionisation. According to value pK_a acids (fig. 2) the maximum speed of hydrolysis decreases among: HClO₄ > HCl > H₃PO₄.

For strong acids HCl and HClO₄ it is possible to try to explain presence of extreme dependence of a kinetic constant of hydrolysis on concentration (fig. 2) from the point of view of the strong electrolytes Debye-Huckel theory. In solutions of strong electrolytes opposite charged ions between which there are electrostatic interactions are formed, round ions the solvate (hydrated) cover from polar molecules of solvent can be created. Besides, in solutions of strong electrolytes, at the raised concentration, there can be an ionic association, therefore instead of ion density it is necessary to use activity (activity coefficient). For strong electrolytes with concentration increase ionic strength of a solution grows. Values of ionic strength of the studied acids solutions, calculated on a known ratio

$$I = 0,5 \sum C_i \cdot Z_i^2 \quad (2)$$

for the concentration corresponding to the maximum values of speeds constants make 6-8.

It is known [5], that for solutions with $I = 0,005-0,1$ ionic activity coefficient of hydrogen changes within 0,975-0,83. With ionic strength increase of a solution change of an activity coefficient depending on concentration has difficult character. In the field of low and average values of ionic strength ($I < 2$) the electrolyte activity coefficient is usually less 1. For some electrolytes at enough large concentration, when owing to a lack of water ions partially or completely are deprived of hydrated cover, the activity coefficient can be more than 1, and, hence, activity is exceed concentration. [10].

After achievement of the maximum values k_A it is possible to explain reduction of hydrolysis speed to that in this area of concentration in a solution of strong electrolyte there can be a formation of ion pairs of electroneutral groupings of ions (+) (-) [4]. It can lead to reduction

of the general ion activity of hydrogen in a solution, and, as consequence, to decrease of hydrolysis speed. At the further increase in concentration HClO_4 it is possible to explain sharp reduction of hydrolysis speed by oxidation of monosaccharoses by perchloric acid and, as consequence, reduction of the maintenance of the general sugars and yield of D-glucosamine.

Using dependence of a specific reaction rate on temperature, activation energy (E_a) hydrolysis acetamidic bonds from the Arrhenius equation has been calculated [9]:

$$k_A = Ae^{-E_a/RT} \quad (3)$$

Activation energy is 82,2 kJ/mol.

As a result of work, specific reaction rates of N-acetyl-D-glucosamine hydrolysis in various acids have been calculated. Activation energy of reaction of N-acetyl-D-glucosamine hydrolysis in HCl is calculated. Dependence of rate constant of N-acetyl-D-glucosamine deacetylation on acids concentration has extreme character with maxima at acid concentration nearby with $(\text{HCl}) = 8 \text{ mole/dm}^3$, with $(\text{HClO}_4) = 6 \text{ mole/dm}^3$, with $(\text{H}_3\text{PO}_4) = 6 \text{ mole/dm}^3$. The maximum reaction rates at hydrolysis in HCl and in HClO_4 are almost identical.

ACKNOWLEDGEMENTS

The work was supported by the Federal Target Program «The scientific and scientific-pedagogical personnel of Innovative Russia», State Contract No. P744

REFERENCES

- [1] Gizatulina, G. A., Chebotok, E. N., et al. (2005) Kinetics of acid hydrolysis of acetylglucosamine. *Russ. J. Appl. Chem.*, 78 (5), 791-3.
- [2] Horowitz, S. T., Roseman, S. and Blumental, H. J. (1957) Preparation of glucosamine oligosaccharides. 1. Separation. *J. Amer. Chem. Soc.*, 79 (18), 5046-9.
- [3] Imoto, T. and Yagishita, K. (1971) A simple activity measurement of lisozyme. *Agric. Biol. Chem.*, 35 (7), 1154-6.
- [4] Krasnov, K. S. (2001) *Physical Chemistry. Vol. 1. Structure of matter. Higher School.*
- [5] Lourie, U. U. (1967) *Guide to Analytical Chemistry. Chemistry.*
- [6] Novikov, V. Yu. (1999) Kinetics of formation of D(+)-glucosamine by acid hydrolysis of chitin. *Russ. J. Appl. Chem.*, 72 (1), 156-61.
- [7] Nudga, L. A., Plisko E. A. and Danilov S. N. (1971) Produce of chitosan and study of its fractional composition. *Zhur. Obs. Khim. [(Russ. J. Gen. Chem.)]*, 41 (11), 2555-9.
- [8] Reissig, J. L., Strominger, J. L. and Leloir, L. F. (1955) A modified colorimetric method for the estimation of N-acetylamino sugars. *J. Biol. Chem.*, 217 (2), 959-66.
- [9] Semiochin, I. A., Strahov, B. V. and Osipov, A. I. (1986) Kinetics of homogeneous chemical reactions. Moscow.: Moscow University.
- [10] Zimon, A. D. (2006) *Physical Chemistry. Agar.*

FIBERS MADE OF BUTYRATE-ACETATE CHITIN COPOLYESTERS AS POTENTIAL MATERIALS FOR MEDICAL APPLICATIONS

Zbigniew Draczyński

*Department of Chemical Physics of Polymers, Technical University of Lodz, 116 Zeromskiego, 90-924
Lodz, Poland*

E-mail address: zbigniew.draczynski@p.lodz.pl

INTRODUCTION

Chitin is the second most abundant polysaccharide, next to cellulose. This naturally renewed polymer with excellent biological properties is composed of β -(1-4)-linked 2-acetamido-2-deoxy-D-glucopyranose units. Currently, main source of chitin production is focused on the chitin isolation from marine invertebrates like crab, krill, shrimp, lobster and others (79%) and fungi (21%), however some insects are also perspective source of chitin [1]. Chitin is insoluble in common organic solvents due to extensive hydrogen bonds and its highly crystalline structure. The existence in the chitin molecules of reactive hydroxyl groups offers possibility for obtaining of new perspective derivatives of chitin based materials. The substitution of its hydroxyl groups by hydrophobic bulky esters groups increases the solubility of ester derivatives of chitin in organic solvents. Butyryl-derivative of chitin with degree of substitution 2, known in literature as dibutyrylchitin (DBC), is well examined and widely described [3-5]. Excellent solubility of DBC allowed forming from it several products convenient for practical applications: transparent films, microspheres, fibers, non-wovens. It was found that non-woven materials made from DBC used as dressing materials in the cases of burns, postoperative and posttraumatic wounds and various entities leading to skin/epidermal loss promote fast wound healing and forming of the connective tissues without using of any other medicines. During healing processes dressing materials underwent of full enzymatic degradation and disappeared in the wound range [6]. However, manufacturing of non-woven dressing material from DBC fibers meets considerable loss of DBC due to rather weak mechanical properties of DBC fibers. It was supposed that introduction of two hydrophobic groups – bulky butyrylic and small acetylic – as the side groups into macromolecules of chitin might result in increasing of mechanical properties of fibers spun from chitin co-(butyryl/acetyl) copolymers without changing to the worse of their bioactive properties.

The aim of the works undertaken in this study was to determine the influence of the basic parameters of the fibers forming process on the sorption properties as well as strength of obtained fibers from butyric-acetic chitin copolyester. Due to role that such fibers comply in the polymer-fiber composite was pursued to obtain the fibers with the highest possible porosity. From the value of the total pores volume and nature of the porous structure, in the case of hydrophobic material, sorption properties of fibers which in turn conditioned by the absorption of physiological fluids and the subsequent component of the process of resorption of fibrous composite strictly depend.

MATERIALS AND METHODS

As a source for chitin copolyesters shrimp shell α -chitin, product of France Chitin has been used. Chitin was characterized by degree of N-acetylation of about 95%, intrinsic viscosity value in DMAc/5% LiCl, 25°C $[\eta] = 23.8$ dL/g. Acetic anhydride, (98%), POCh Gliwice, Poland;

Butyric anhydride, 98% and perchloric acid 70-72%, Aldrich Poland, were obtained from commercial sources and used as received. Organic solvents: acetone, ethanol of pure grade were also used as received. LiCl, 99%, A.C.S reagent, Aldrich Poland, was additionally vacuum dried overnight at 100°C before use.

Synthesis of chitin co-(acetate/butyrate) copolymers

Syntheses of the chitin co-(acetate/butyrate)s have been carried out under heterogeneous conditions in the presence of perchloric acid as a catalyst of reaction of esterification, following description given in previous paper [7]. In short the acylation mixtures consisted of the acetic (AA) and butyric (BA) anhydrides used in different proportion and of perchloric acid taken in the amount of 1 mole/mole of chitin have been prepared at low temperature of -10°C. The five-times excess ratio of anhydrides mixture to chitin molecule was used in the each reaction. A portion of dry chitin has been added to the acylation mixtures during mixing and cooling. After 3 hours of reaction raw product was immersed in cold water with ice cubes and washed several times with cold distilled water and with water containing ammonia liquor to pH=7 to remove any traces of acids, and next dried at 110°C. Final products – pure chitin co-(acetate/butyrate)s have been dissolved in ethanol and evolved in the processes of the solutions filtration and precipitation of the polymers from filtrates with distilled water. Dried final co-(acetate/butyrate)s were treated with acetone to find out eventual presence of pure DBC. Two types of copolyesters obtained with different ratio of butyrate to acetate side groups, first BAC 95/5 means copolymer with 95% of butyric side groups and 5% of acetic side groups and BAC 90/10 copolymer with 90% of butyric side groups and 10% of acetic side groups.

RESULTS AND DISCUSSION

The rheological properties of spinning solutions

Butyric-acetic chitin copolyesters with different ratio of butyrate to acetate side groups solutions in ethanol at similar values of intrinsic viscosity in range of 1.83-1.93 dL/g were the objects of the rheological tests. Proper solutions were obtained immediately after the stage of synthesis.

Concentration of obtained solutions were selected in such a way that they had a dynamic viscosity at a relatively low level, but still allow the fiber forming using wet processing method keeping the stability of the process. On the assumption of possible low concentration the rheological properties of spinning solutions play a particularly important role. Flow curves of copolyesters solutions (Figure1) shows that regardless of the chemical composition of the copolymer and its intrinsic viscosity, tested solutions are non-Newtonian solutions without a flow limit.

Table 1 Characteristic of the spinning solutions

Sample name	Intrinsic viscosity [dL/g]	Concentration [%]	Rheological parameter	
			„n”	„k”
BAC 95/5	1,83	12,82	0,88935	22,761
BAC 90/10	1,95	10,65	0,81922	26,53

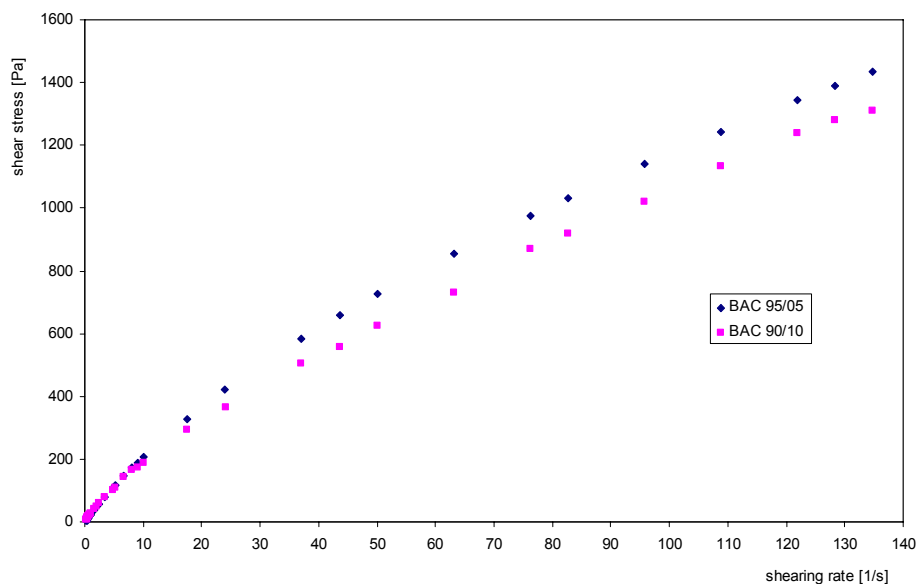


Figure 1 Dependence of shear stress to shearing rate for the solutions of butyric-acetic chitin copolyesters with different ratio of butyrate to acetate side groups

Shear stress increases less than proportionally with increasing shearing rate and flow curves pass through the origin. Closer to Newtonian fluids characteristics (higher values of the rheological parameter n) is the solution of the copolyester with the symbol BAC 95/5 obtained from the copolymer with a lower value of intrinsic viscosity and concentration of 12.8% (table 1). Rheological parameter " k " which is a measure of consistency of the solution, takes a slightly lower value 22.76, compared with solution of BAC90/10. Mentioned solution has more polymer nature which is consistent with the higher value of intrinsic viscosity of the copolymer. At the same time at a lower concentration of spinning solution rheological parameter " k " takes a higher value.

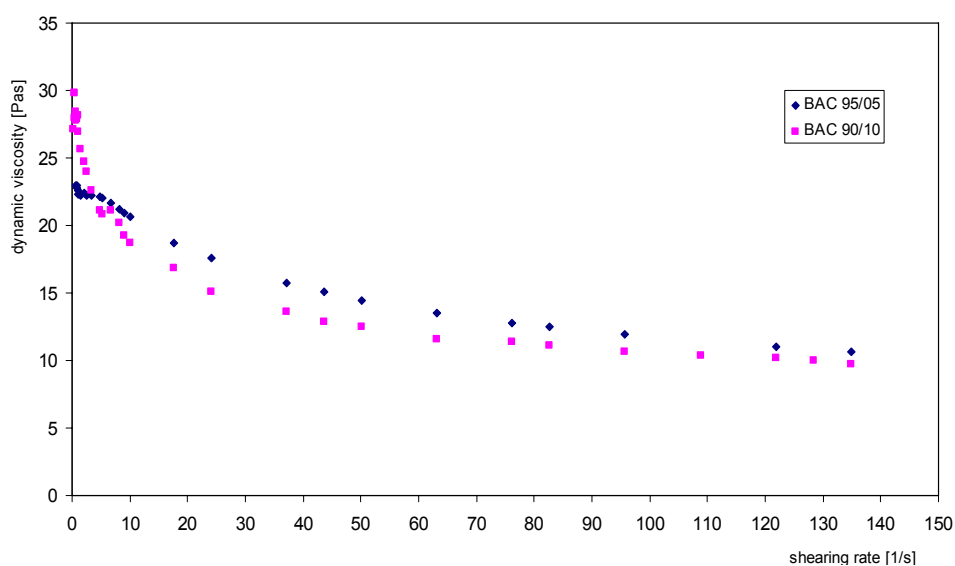


Figure 2. Dependence of apparent dynamic viscosity to shearing rate for the solutions of butyryl-acetyl chitin copolyester with different ratio of butyrate to acetate side groups

Changes in dynamic viscosity as a function of shearing rate are shown in figure 2. For both tested solutions it was observed reduction of dynamic viscosity with increasing of shearing rate which is typical for polymer solutions.

Effect of spun draw ratio and deformation during the stages of stretching on the structure and properties of fibers BAC.

The main parameter which fiber structure after solidification stage depends on, and fiber susceptibility to deformation processes in subsequent stretching stages is the value of the spun draw ratio. In the case of the rigid structure of macromolecules important role, as was found for the alginate fibers [8], plays the deformation of structural elements in the fluid stream. It is related to the value of elongated velocity gradient, varying along the road formation and dependent on the value of spun draw ratio.

Table 2. Butyric-acetic chitin fibers properties

Sample name	Spun draw ratio [%]	Total stretch [%]	Moisture sorption at 65% RH [%]	Moisture sorption at 100% RH [%]	Water retention value [%]	Strength [cN/tex]	Elongation at break [%]	Young's modulus, [N/tex]
95/5 a	-20	586,77	7,2	13,80	35,49	22,73	4,058	9,704
95/5 b	-10	503,63	7,05	13,49	32,42	23,37	4,512	9,408
95/5 c	+50	426,48	4,79	10,01	29,99	22,20	4,24	8,990
90/10 a	-20	800,75	6,08	10,10	49,90	21,02	3,676	9,729
90/10 b	-10	872,33	5,98	12,04	48,53	22,57	4,180	10,111

Using positive values of spun draw ratio leads to the achievement of fibers [9] with good strength. For the butyryl-acetyl chitin copolyester fibers with the symbol BAC 95/5 wide range of spun draw ratio from -20% to +50% were used, because of problems encountered during the process of fiber formation for BAC 90/10 only two spun draw ratios were used -10 and -20 (table 2). For all fibers samples, strengths value more than 21 cN/tex were achieved.

Table 3 Porosity data for samples BAC 95/5

Sample name	The total pore volume [cm ³ /g]	The total pore volume with diameter under 1000nm [cm ³ /g]	The total area of the inner pore [m ² /g]
95/5 a	0,913	0,197	9,581
95/5 b	2,132	0,415	37,413
95/5 c	0,490	0,184	17,871

For selected fiber samples porosity measurement was made (table 3). As it can be seen in the table 3 the highest volume of pores was achieved for sample BAC 95/5 b with spun draw ratio -10.

CONCLUSIONS

Used butyryl-acetyl chitin copolyesters soluble in ethanol are able to form suitable solutions for forming fibers using wet process. Regardless of the chemical structure of butyryl-acetic chitin copolyester and its intrinsic viscosity of the polymer, prepared spinning solutions are non-Newtonian fluids diluted with shear free boundary flow. Reducing the proportion of acetyl groups in the copolymer, received solutions are closer to character of Newtonian fluids. Fibers prepared from the BAC are characterized by high total pore volume, it allows to pass them to a group of fibers with high porosity. For BAC fibers were obtained for a unique combination of properties of high porosity with good tenacity above 24 cN / tex

ACKNOWLEDGEMENTS

The author is grateful to dr Lidia Szosland, dr Maciej Boguń for all advices and helpful discussions relating to this work and for help with experimental work.

The work was completed within the research project no. N R08 0017 06/2009, financed by the National Centre for Research and Development.

REFERENCES

- [1] Draczynski, Z. (2008) *J. Appl. Pol. Sci*, Vol 109, Issue 3, 1974.
- [2] Szosland, L. (1996) *J. Bioactive and Compatible Pol.*, 11, 61,
- [3] Szosland, L. (1997) in *Chitin Handbook: European Chitin Society*, 53.
- [4] Wrzyszczyński, A., Qu, Xia, Szosland, L., Adamczak, E., Linden, L., Rabek, J.F. (1995) *Polymer Bulletin*, 34, 493.
- [5] Szosland L., East G.C. (1995) *J. Appl. Pol. Sci*, 58, 2459.
- [6] Chilarski, A., Szosland, L., Krucinska, I., Blasinska, A., Cislo, R. (2005) in *Advances in Chitin Science*, vol. VIII, 185.
- [7] Draczynski, Z. (2011) *J. Appl. Pol. Sci* (accepted for publication)
- [8] Boguń, M. (2009) *Fibres & Textiles in Eastern Europe*, 17, 5(76), 17.
- [9] Mikołajczyk, T., Rabiej, S., Szparaga, G., Boguń, M., Fraczek-Szczypta, A., Błażewicz, S. (2009) *Fibres & Textiles in Eastern Europe*, 17, 6(77), 13.

CHITOSAN NEUTRALIZE AMYDOLYTIC ACTIVITY OF SULPHATE POLYSACCHARIDES

**N.N. Drozd^{1*}, V.A. Makarov¹, A.S. Tolstenkov¹, E.Iu. Savchik¹,
G.E. Bannikova², A.V. Il'ina², A.N. Levov², V.P. Varlamov², G.A. Vikhoreva³**

¹ Hematological Research Center RAMS, Moscow, ² Center "Bioengineering" RAS, Moscow,

³ Moscow state textile university of A.N.Kosygin

*E-mail: nndrozd@mail.ru

INTRODUCTION

Sulfate polysaccharide unfractionated heparin, a glycosaminoglycan (GAG) comprised of sulfated uronic acid (1→4)-D-glucosamine repeating disaccharide units, has been used clinically as an anticoagulant and antithrombotic agents since the 1940s [1]. The anticoagulant (A) activity of unfractionated (UFH) and low molecular weight (LMWH) heparins is mediated through its binding to the serine protease inhibitor antithrombin (AT); binding by heparin causes a conformational change in AT that enhances its binding to and inhibition of the coagulation cascade enzymes thrombin (FIIa) and factor Xa (FXa) [2].

The most important adverse effect of antithrombotic treatment is the occurrence of bleeding. In case of serious or even life-threatening bleeding in a patient who uses anticoagulant agents or when a patient on anticoagulants needs to undergo an urgent invasive procedure, anticoagulant treatment can be reversed by various specific strategies [3]. In some clinical situations, the anticoagulant activity of heparin must be neutralized. Polycation protamine sulfate (PS), a mixture of arginine-rich peptides used to neutralize heparin, binds to heparin causing dissociation of the heparin-AT complex [4]. Protamine sulfate, however, can induce adverse side effects, and thus, its use is generally limited to open heart surgery and emergencies [5]. Also, PS is less effective in neutralizing the anticoagulant activity of low-molecular weight heparin [6]. Thus, there is a need for alternative agents for neutralization of the anticoagulant activity of heparins and other new anticoagulants.

Research aim is an assessment of a precipitation of chitosan polycations with heparins/chitosan sulfate polyanions and of a neutralization of heparins/ chitosan sulfate inhibition of amidolytic activity FIIa and FXa.

key	deacetylation degree, %	molecular weight, kDa
Ch1	85	4,0
Ch 2	85	6,0
Ch 3	85	10,0
Ch 4	85	21,0
Ch 5	70	21,0
Ch 6	61	21,0
Ch 7	91	16,0
Ch 8	93	7,4

MATERIALS and METHODS

Samples of chitosan, chitosan sulfate and carboxymethyl chitosan sulfate (Ch, ChS, CMChS; were prepared from commercial crab shell chitosan Bioprogress, Russia) with an average molecular weight (MW) for Ch 4-21 kDa (tabl 1; desacetylation degree, DD: 61-93%) and for ChS – 9-56 kDa (table 2, table 5), low molecular weight heparin (LMWH; were prepared from unfractionated heparin – UFH D0110001 Changzhou Quianhong Bio-Pharm co. LTD, China, by depolymerization with enzyme complex "Proteasa C" [7] with MW 4,7 -7,0 kDa (table 2). The deacetylation degree (DD) of Ch samples was determined by potentiometric

titration [8], and MW was measured by a viscosymetric method [9]. A content of sulfur was defined using the automatic analyzer CHNS EA1108 'Carlo-Erba'. The anticoagulant activity of GAG derivatives was determined in vitro by two assays, which characterized their ability to accelerate the inhibition of FXa and of FIIa at the European Pharmacopoeia base [10,11]. The determination of polycation (protamine sulfate, PS (Sigma)/Ch) - polyanion (heparins or ChS) precipitates formation has made by means of biospecific electrophoresis in agarose gel [12]. For neutralization an amidolytic activity of GAG with Ch and PS we used the method based on inhibition of ability FIIa and FXa to hydrolyze chromogenic peptide substrates [13].

Table 2. Structure parameters and anticoagulant activity of chitosan sulfate and heparins

Anticoagulants	MW, kDa/ S, %	aXa activity, IU/mg	aIIa activity, IU/mg
UFH	13,8/	172±21	159±20
	6,1/	157±16	95±5
	5,7/	134±14	175±10
LMWH	5,4/	168±19	81±11
	4,7/	143±19	103±13
	3,4/	208±9	169±15
	40/16	3,5±1,3	57,0±12,1
ChS	30/16,8	2±0,3	92,1±18,0
	29/12	68±12	13,4±4,0
	9/14,6	131±19	13,0±4,2

RESULTS and DISCUSSION

Antithrombin activity of unfractionated heparin (MW 13,8 kDa) was 159±20 IU/mg, anti-factor Xa activity - 172±21 IU/mg (table 2); in some cases antithrombin activity of LMWH derivatives (obtained by hydrolysis UFH) was less, than UFH had, and aXa activity – reliability did not decrease. Formation of precipitates between anticoagulant and an antidote we analyzed carrying out horizontal electrophoresis in 1% agarose gel [12]. At motility's research in electric field of complexes LMWH derivatives / protamine sulfate (fig. 1) we noted increase of the peaks height of precipitation on the increasing of an

average molecular weight of LMWH derivatives (table 3). Correlation coefficients between the height of peaks of precipitation and average molecular weight has 0,90 - 0,92 ($p < 0,05$). With increased of activities ratio (aXa/aIIa) we observed the tendency to decreasing of the size of precipitation peaks ($r_{\text{aXa/aIIa} - \text{height}} = -0,49$ and $-0,46$; $r_{\text{aXa/aIIa} - \text{square}} = -0,43$ и $-0,54$) and also noted weak positive relationship ($r = 0,26$; $p < 0,05$) between aIIa activity and average molecular weight. That is, both UFH, and LMWH derivatives with smaller MW organises precipitates with PS. The size of precipitation peaks for UFH in 1,5 times more than for LMWH, that most likely, is relating to smaller MW [4,6]. Any appreciable interrelation between anticoagulant activity and the size of precipitation peaks is not revealed.

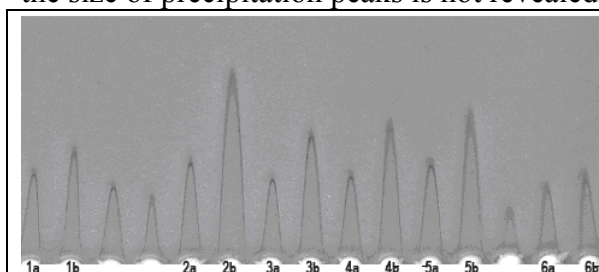


Figure 1. Peaks of a precipitation heparin - protamine sulfate in agarose gel at electrophoresis. Amount of heparin added in gel: a – 2,5 µg; b – 5 µg; 1- 4,0 kDa; 2 - 13,8 kDa; 3 – 4,7 kDa; 4 – 5,4 kDa; 5 – 5,7 kDa; 6 – 3,4 kDa

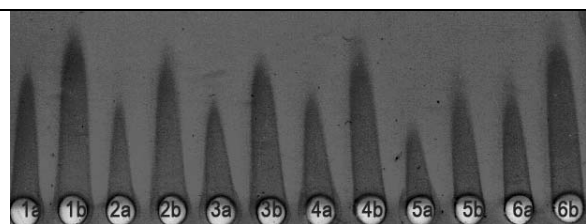


Figure 2. Peaks of a precipitation heparin – chitosan (MW= 21 kDa; DD= 61%) in agarose gel at electrophoresis. Amount of heparin added in gel: a – 1 µg; b- 2 µg; 1-13,8 kDa; 2- 5,4 kDa; 3- 5,4 kDa; 4- 6,1 kDa; 5 – 5,7 kDa; 6-4,7 kDa

We observed the same precipitation peaks carrying out electrophoresis of heparins (were added in the small cavities of agarose gel) with chitosans (were added in agarose gel) (table 3, fig. 2). Peaks precipitation with Ch 1 wasn't observed. The height of precipitation peaks with other chitosans those MM was more 4 kDa, compounded 2,7 - 25,2 mm (table 3). Moderate positive relation between MW of LMWH derivatives and height of precipitation peaks with chitosans was shown. Linear correlation coefficients compounded 0,6-0,93 ($p < 0,05$).

Because of great range of chitosan samples there is a need in rapid analysis of a possibility of complexes formation between heparins and chitosans as traditional methods of detection of complexes of heparins with antidote protamine sulfate are enough labour-consuming, demand a plenty of time, expensive instrumentation and reagents. The fast method of an assessment of complex formation allows with the minimum expenditures to eliminate chitosans which form no complexes with heparins or weak ones and consequently they are not capable to neutralize its anticoagulant activity. This method [12] allows to estimate quickly heparin about formation of complexes with prospective antidotes chitosans.

Table 3. Height of precipitation peaks (mm) in biospecific electrophoresis complexes of heparins with polycations (protamine sulfate and chitosans)

MW heparins, kDa	Chitosan								protamine sulfate
	DD 85%				DD 70%	DD 61%	DD 91%	DD 93%	
	MW 4 kDa	MW 6 kDa	MW 10 kDa	MW 21 kDa	MW 21 kDa	MW 21 kDa	MW 16,0 kDa	MW 7,4 kDa	
3,4	0	6,1±0,6	7,8±0,7	9,3±0,2	5,3±1,6	4,0±1,4	5,8±1,1	2,7±0,1	7,3±0,7
4,7	0	11,7±0,4	21,3±6,7	21,7±5,6	12,0±0,1	12,0±0,2	11,5±2,7	6,8±0,1	21,5±0,3
5,4	0	9,4±1,4	16,7±5,6	21,0±4,5	10,7±0,7	8,3±0,8	9,8±2,2	5,8±1,0	21,5±5,0
5,7	0	10,6±1,0	21,7±7,7	21,3±7,9	12,8±0,2	12,0±0,2	12,0±2,1	8,0±1,2	32,3±1,1
6,1	0	9,3±0,5	21,2±7,7	22,3±6,7	9,3±2,7	8,8±1,8	12,0±4,1	8,7±0,9	17,3±6,2
13,8	0	17,4±0,4	22,5±0,6	25,2±0,5	14,7±0,7	15,5±0,9	14,7±1,0	13,5±0,7	43,6±1,5

Table 4. Height of peaks precipitations (mm) at biospecific electrophoresis complexes of chitosan sulfate (ChS) with chitosans.

MW ChS, kDa	Chitosan							
	DD 85%				DD 70%	DD 61%	DD 91%	DD 93%
	MW 4 kDa	MW 6 kDa	MW 10 kDa	MW 21 kDa	MW 21 kDa	MW 21 kDa	MW 16,0 kDa	MW 7,4 kDa
9	0	5±2	4±1	2,5±0,5	4,5±1	8±2	4±0,3	4±1
29	0	5±1	6,5±3	3,8±1	6±2	8,3±2,2	6±1	6±1,3
40	0	4±1	6±2	5±1	5,3±1,5	6,7±1,7	5,5±0,7	7±0,6
30	0	5±2	5±1	3,8±0,6	6,8±1	7,3±2	6,1±0,5	5,5±0,4

Anticoagulants ChS with antithrombin activity 13-90 IU/mg form precipitates with protamine sulfate and chitosans (table 4, fig. 3). At motility analysis of complexes between ChS derivatives and protamine sulfate in electric field we noted increased of the sizes of precipitation

peaks with Xa activity of ChS derivatives increasing (fig. 3). The correlation coefficient between height of precipitation peaks and aXa activity of ChS derivatives compounded 0,89 ($p < 0,05$). We observed negative moderate relationship between height of precipitation peaks and antithrombin activity ($r = -0,5$; $p < 0,05$). With increased of MW and sulphur amount of ChS samples, the sizes of precipitation peaks decreasing ($r_{MM} = -0,65$; $p < 0,05$; $r_s = -0,7$; $p < 0,05$). No relation between MW of ChS and height of precipitation peaks is revealed (table 4).

Relationship between MW / DD polycations - chitosans and height of precipitation peaks and chitosan sulfate derivatives with different anticoagulant activity is shown on fig. 4 and fig. 5. Precipitation peaks with Ch1 wasn't observed. The height of precipitation peaks of other chitosans having MW more 4 kDa compounded 2,5 - 8,3 mm. Unlike relationship between MW of polycations - chitosans is most expressed and in height of peaks of a precipitation for anticoagulants of polyanions - ChS with an amount of sulfur 14,6 - 16,8 ($r = "0,45" - "0,6"$), relationship ($r = "-0,6" - "-0,75"$) between DD polycations - chitosans and height of peaks of a precipitation for anticoagulants of polyanions - ChS from MW 9-30 kDa

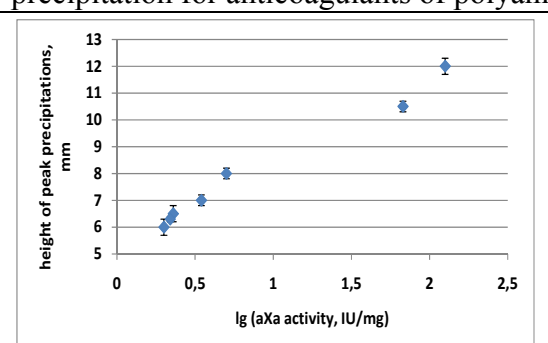


Figure 3. Relationship between anti-factor Xa activity and height of peak precipitations (mm) ChS (MW 9-40 kDa) with protamine sulfate

The height of precipitation peaks decreased with desacetylation degree of Ch derivatives increasing. Among Ch derivatives with DD 85% and MW 4 - 21 kDa precipitation peaks with the smallest size the sample with MW 21 kDa (Ch 4) has shown. Among Ch with MW 21 kDa and DD 61 - 85% precipitation peaks with the smallest size also same sample Ch 4 has shown. Thus, as optimal of precipitates should be chosen chitosans with MW nearby 10 kDa and desacetylation degree 60 - 70 %.

The sizes of precipitation peaks of carboxymethyl chitosan sulfate with protamine sulfate the more than those for chitosan sulfate with the same MW and smaller in 2-3 times (table 5). At

identical MW magnitude of peaks of a precipitation increased with anticoagulant activity increasing. With anticoagulant activity of carboxymethyl chitosan sulfate increase the intensity of a staining, a sharpness of borders and the sizes of peaks of a precipitation was enlarged. With increased of total negative charge of a molecule of polysaccharide ability to form complexes with polycation of protamine sulfate. It is known, that formation of polyelectrolytical complexes directly depends on degree of ionisation cation - and anion -polymers, density of charges and their allocation along polymeric chain, on concentration, an interrelation, duration of interaction and temperature [14].

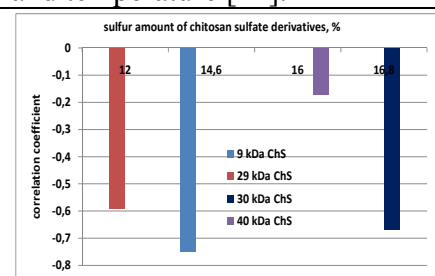


Figure 4. Connection between deacetylation degree of polycations - chitosans and height of precipitation peaks with anticoagulants chitosan sulfate derivatives ($p < 0,05$)

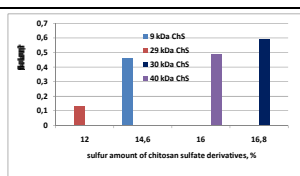


Figure 5. Connection between an average molecular weight of polycations - chitosans and height of precipitation peaks with anticoagulants chitosan sulfate derivatives ($p < 0,05$)

Table 5. Anticoagulant activity and scale of precipitation peaks of modified chitosan with protamin sulfate

derivatives	aXa activity, IU/mg	aIIa activity, IU/mg	height of precipitations peaks (pixel)			Square of precipitations peaks (pixel)		
			0,25 µg	0,50 µg	1,00 µg	0,25 µg	0,50 µg	1,00 µg
ChS, 10 kDa	1,3±0,9	0,021±0,01	15±3	25±4	52±5	112±8	348±16	621±27
ChS 56 kDa	4,4±1,6	0,12±0,08	22±5	34±4	74±5	334±21	785±40	2040±66
CMChS 56 kDa	40±9,8	0,71±0,43	25±6	48±5	123±15	939±29	1515±44	4870±85

Influence of protamine sulfate and chitosan Ch 6 (MW 21 kDa and DD 61 %) and Ch 7 (MW 16 kDa and DD 91 %) on neutralization of inhibition by anticoagulants (UFH, LMWH and ChS) amidolytic activity of thrombin and factor Xa in table 6 is shown. Protamine sulfate has neutralized influence of UFH, LMWH and ChS on amidolytic activity of thrombin by 93, 89 and 91 %; Ch 6 (MW 21 kDa and DD 61 %) - by 55, 57 and 81 %; Ch 7 (MW 16 kDa and DD 91 %) - by 94, 80 and 90 %. Protamine sulfate has neutralized influence of UFH, LMWH and ChS amidolytic activity of activated factor X by 58, 59 and 95 %; Ch 6 (MW 21 kDa and DD 61 %) - by 72, 58 and 71 %; Ch 7 (MW 16 kDa and DD 91 %) - by 95, 76 and 98 %.

Table 6. Effect of protamine sulfate (PS) and chitosans (Ch) on protease amidolytic activity in the presence of anticoagulants ($\Delta A_{405}/\text{min}$)

anticoagulant	Method	polycation	PS	Ch 6 (tabl. 1)	Ch 7 (tabl. 1)
		0 µg/ml	0,03 µg/ml	0,03 µg/ml	0,03 µg/ml
UFH, 13,8 kDa	1	0,042±0,009	0,140±0,021**	0,082±0,011*	0,141±0,018**
	2	0,058±0,014	0,115±0,017**	0,144±0,010**	0,191±0,014**
LMWH, 4,7 kDa	1	0,066±0,013	0,133±0,017**	0,086±0,013	0,120±0,014**
	2	0,028±0,011	0,118±0,025**	0,116±0,009**	0,152±0,010**
ChS, 9 kDa	1	0,075±0,015	0,137±0,011**	0,122±0,009**	0,135±0,015**
	2	0,039±0,012	0,190±0,021**	0,142±0,012**	0,195±0,021**

Notes: Concentration of anticoagulants 0.02 µg/mL; concentration of PS and Ch 0.03 µg/mL;

factor Xa (method 2) amidolytic activity and factor IIa (method 1) amidolytic activity without anticoagulants and antidotes: 0.120±0.003 $\Delta A_{405}/\text{min}$ and 0.135±0.004 $\Delta A_{405}/\text{min}$, respectively; * - $p < 0,05$ и ** - $p < 0,001$ significance level for comparison between samples without antidotes; n = 5.

Thus, anticoagulants sulphated polysaccharides - heparins with MW 3,4 - 13,8 kDa and sulfated chitosan derivatives with MW 9 - 56 kDa formed precipitates, both with classical antidotes protamine sulphate and with chitosans (from MW 6 - 21 kDa). On the basis of relationship between structure parameters of polycations chitosans and anticoagulant activity of polyanions (heparins/sulfate chitosans) we choose antidotes for neutralization amidolytic activity of key proteases blood coagulation system. Chitosan with MW 16 kDa and DD 91% is

better than protamine sulfate neutralize anti-factor Xa activity of UFH and LMWH; antithrombin activity of the investigated UFH, LMWH and ChS this chitosan neutralize's equally.

REFERENCES

- [1] Rodén, L. (1989) Highlights in the history of heparin, in: D.A. Lane, U. Lindahl (Eds.), Heparin: Chemical and Biological Properties, Clinical Applications, CRC Press, Boca Raton, FL.
- [2] Jin, L., Abrahams, J., Skinner, R., Petitou, M., Pike, R., Carrell, R. (1997) The anticoagulant activation of antithrombin by heparin, *Proc. Natl. Acad. Sci. U.S.A.*, 94, 14683–88.
- [3] Levi, M. (2009) Emergency reversal of antithrombotic treatment, *Intern. Emerg. Med.*, 4, 137-45.
- [4] Schulman, S. and Bijsterveld, N. (2007) Anticoagulants and their reversal, *Transfus. Med. Rev.*, 21, 37–48.
- [5] Welsby, I., Newman, M., Phillips-Bute, B., Messier, R., Kakkis, E., Stafford-Smith, M. (2005) Hemodynamic changes after protamine administration: association with mortality after coronary artery bypass surgery, *Anesthesiology*, 102, 308–14.
- [6] Gatt, A., van Veen, J., Woolley, A., Kitchen, S., Cooper, P., Makris, M. (2008) Thrombin generation assays are superior to traditional tests in assessing anticoagulation reversal in vitro, *Thromb. Haemost.*, 100, 350–55.
- [7] Bannikova, G., Stolbushkina, P., Drozd, N., Vikhoreva, G., Varlamov, V., Makarov, V. (2004) Hydrolysis of heparin by the immobilized enzymatic complex from *Streptomyces kurssanovii*, *Prikl Biokhim Mikrobiol.*, 40, 429-34.
- [8] Lim, S., Hattori, K., Hadson, S.M. (2000) Preparation of a fiber-reactive chitosan derivative with enhanced antimicrobial activity. In M. G. Peter, A. Domard, & R. A. A. Muzzarelli (Eds.), *Advantage chitin science* (pp. 454–459). Potsdam: University Potsdam.
- [9] Wang, W., Bo, S., Li, S., & Qin, W. (1991) Determination of the Mark–Hauwink equation for chitosans with different degrees of deacetylation. *International Journal of Biological Macromolecules*, 13, 281–285.
- [10] Teien, A. N., Lie, M., & Abildgaard, U. (1976) Assay of heparins in plasma using chromogenic substrate for activated factor Xa. *Thrombosis Research*, 8, 413–416
- [11] Hoppensteadt, D., Walenga, J., & Fareed, J. (1985) Validity of serine protease inhibition tests in the evaluation and monitoring of the effect of heparin and its fractions. *Seminars in Thrombosis and Haemostasis*, 11(2), 112–120.
- [12] Drozd, N., Tolstakov, A., Makarov, V., Bannikova, G., Varlamov, V., Skriabin, K. (2009) Patent Russian Federation 2370271.
- [13] Racanelli A, Hoppensteadt DA, Fareed J (1989) In vitro protamine neutralization profiles of heparins differing in source and molecular weight. *Semin Thromb Hemostasis*, 15, 386-389.
- [14] Il'ina, A., Varlamov, V. (2005) Chitosan-based polyelectrolyte complexes: a review. *Prikl Biokhim Mikrobiol.*, 41, 9-16.

ANTI-PROLIFERATIVE EFFECT OF PROTOCATECHUIC ACID CONJUGATED CHITOSAN OLIGOSACCHARIDE ON B16-F10 MOUSE MELANOMA CELLS

Tae-Kil Eom¹, Se-Kwon Kim^{1,2*}

¹Marine Bioprocess Research Center, Pukyong National University, Busan 608-737, Republic of Korea

²Department of Chemistry, Pukyong National University, Busan 608-737, Republic of Korea

*E-mail address: sknkim@pknu.ac.kr

INTRODUCTION

Skin cancer is the third most common human malignancy and its global incidence is rising at an alarming rate, with basal cell carcinoma, squamous cell carcinoma and melanoma being the most common forms. It is the most dangerous form, accounting for most skin cancer deaths. In addition, metastatic malignant melanoma is largely refractory to existing therapies and has a very poor prognosis, with a median survival rate of 6 months and 5-year survival rate of less than 5% [1], so new treatment strategies are urgently needed. Several literatures exist regarding the effects of antitumor activities of chitosan and chitosan oligosaccharide (COS) [2, 3]. However, little informative is available about the cytotoxic effect of chitosan and COS until now. Also, some research paper reported phenolic compounds anti cancer activity have melanoma cancer [4]. In the current study, we investigated the *in vitro* biochemical mechanism of protocatechuic acid conjugated COS (PTA-conj-COS) on mouse melanoma (B16-F10) cells proliferation. It was found that PTA-conj-COS significant reduced proliferation of B16-F10 cells in dose dependent manner.

MATERIALS and METHODS

Cell culture

B16-F10 mouse melanoma cells were cultured and maintained in DMEM supplemented with 100 U/ml penicillin G, 100 µg/ml streptomycin, 10% fetal bovine serum (FBS) and maintained at 37 °C under a humidified atmosphere with 5% CO₂.

Cytotoxicity assay

Cellular survival rate was measured with the PreMix WST-1 EZ-CyTox enhanced cell viability assay kit (Daeil Lab Service). Cells (1×10^4) were seeded into wells of a 96-well culture plate and after 24 h, various concentrations of PA-conj-COSs were treated and cytotoxicity was measured using WST-1 cell proliferation reagent was added directly to the supernatant (10 µl/100 µl growth medium), and incubated at 37 °C for 1 h. The absorbance of the solubilized dark red formazan product was then determined at 450 nm.

Morphological analysis

B16-F10 cells treated with various concentrations of PTA-conj-COSs for 72 h. After that, cells were washed twice with 1X PBS cold and fixed in 4% paraformaldehyde in 1X PBS for 30 min at room temperature. The fixed cells were washed with 1X PBS and stained with 1 µg/ml of the fluorescent DNA-binding dye, Hoechst 33342 at room temperature for 1 h. Cells were visualized and photographed under fluorescence microscope (CTR 6000; Leica, Wetzlar, Germany).

Western Blot analysis

Cells were seeded at a density of 1×10^4 cells/well in 10 cm dishes and incubated for 24 h. In the next day, cells were treated with different concentration of PTA-conj-COSs for 72 h. Cells

were lysis with RIPA buffer (Sigma-Aldrich, St. Louis) and supernatants were collected. Concentrations of total proteins were determined by using BCA protein assay kit (Thermo Science, Rockford, USA). Western blot was performed as previously described (Ta et al., 2006) with specific antibodies.

RESULTS and DISCUSSION

As shown in Fig. 1A, the cell proliferation was inversely correlated with the PTA-conj-COS concentration and treatment time. Cell growth was significantly inhibited in a dose- and time-dependent manner when B16-F10 cells were treated with PTA-conj-COS from 125 $\mu\text{g/ml}$ to 1000 $\mu\text{g/ml}$ for 72 h. In particular, when the cells were exposed to PTA-COS at 500 $\mu\text{g/ml}$, the cell proliferation was almost completely inhibited. In addition, Fig. 1B shows the morphological changes after 72 h exposure to various concentrations of PTA-conj-COS. The number of cells was remarkably reduced with increasing doses of PTA-conj-COS.

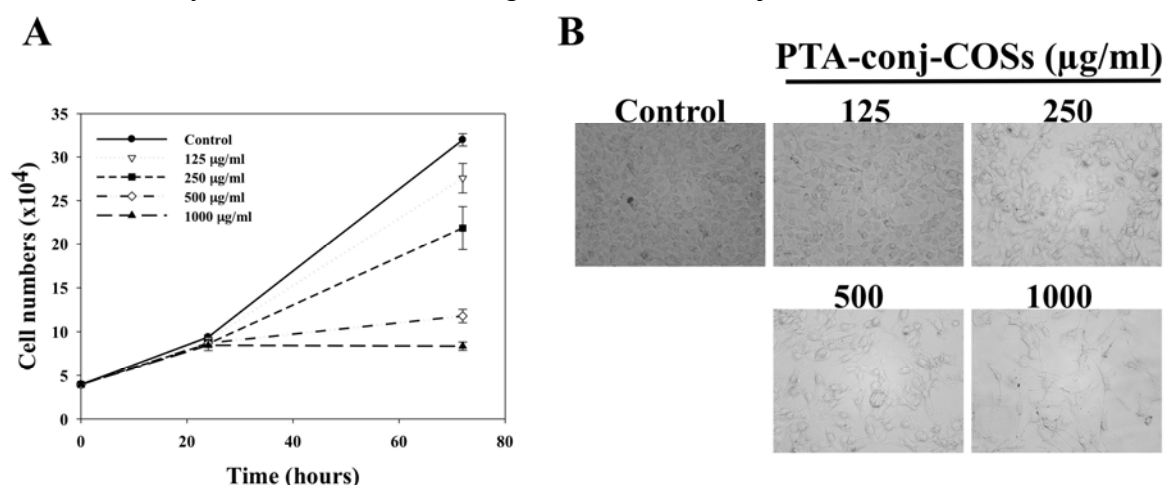


Figure 1. Effect of PTA-conj-COS on cell viability. A) Cell viability after PTA-conj-COS treatment; B) Cell morphology after PTA-conj-COS treatment for 72h.

To understand the molecular mechanism of growth inhibition by PTA-conj-COS in B16-F10 melanoma cell, the protein expression of cyclin and Cdks were examined, which are known to be operative in G1-S phase to investigate if their function is altered. Western blot analysis revealed that treatment of B16-F10 cells with PTA-conj-COS for 72 h resulted in a dose-dependant decrease in the protein expression of cyclin D1 and cyclin E. In addition, PTA-conj-COS affect the protein expression were decreased of these cyclin associated Cdks such as Cdk4 and Cdk2. (Fig. 2).

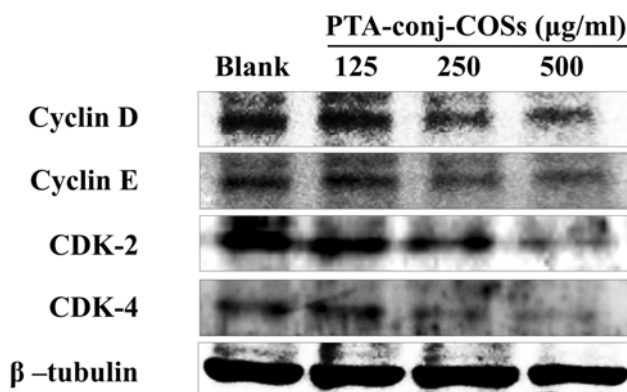


Figure 2. Effect of PTA-COS on the expression levels of cell cycle regulators

As shown in Fig. 3, PTA-COS treatment resulted in a dose dependent induction of p16, p21 and p27 expression levels in B16-F10 cells. p16, p21 and p27 play essential role in a regulating G1 progression, in relation with cyclin E, D, Cdk 2, 4. In addition, treatment of B16-F10 cells with PTA-conj-COS caused an initial down regulation in the levels of the phosphorylated form of GSK-3 in dose dependent manner. In contrast, the total GSK-3 increased dose dependent manner.

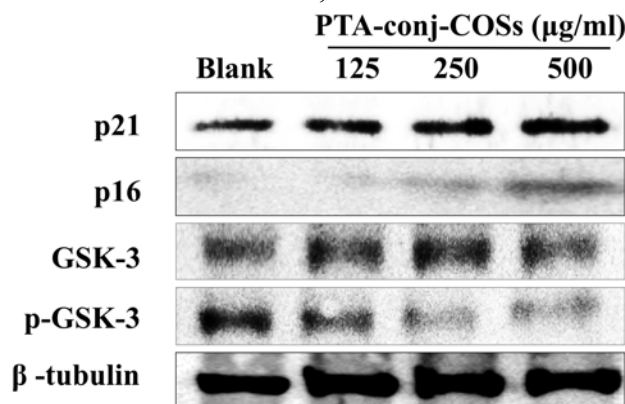


Figure 3. Effect of PTA-COS on the expression levels of cell cycle regulators inhibitors

As shown in Fig. 4, PTA-conj-COS decreased phosphorylation of ERK, p90RSK1, and CREB in dose dependent manner. In addition, MITF protein expression also decreased in PTA-conj-COS treatment groups. The result suggested that PTA-conj-COS inhibited B16-F10 cells proliferation through inactivation ERK pathway.

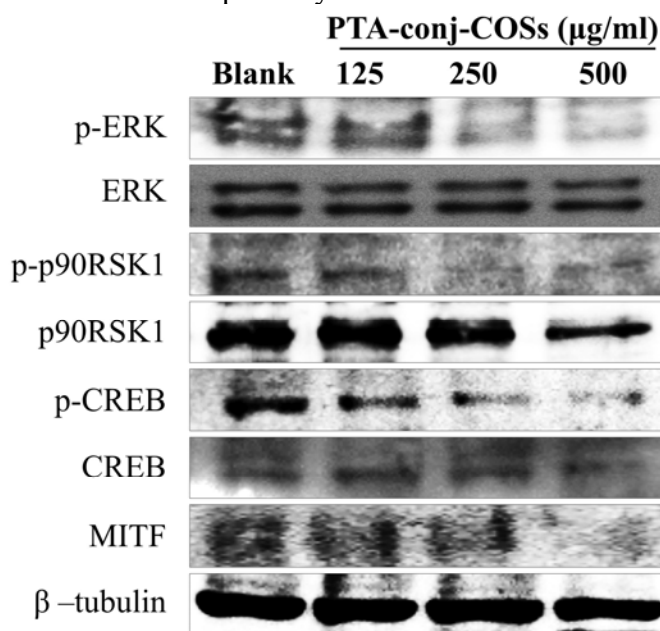


Figure 4. Effect of PTA-conj-COS on ERK induce proliferation pathways

As shown in Fig. 5A, protein expression of total p53 and phospho-p53 were increased in a dose-dependent manner after PTA-conj-COS treatment for 72h. These results indicated that a part of the anti-proliferative activity of PTA-COS is related to apoptosis through up-regulation of p53. In addition, treatment of B16-F10 cells with PTA-conj-COS caused an initial down regulation in the levels of the phosphorylated form of Akt in dose dependent manner. The total Akt had no

significant changed (Fig. 5). The results suggested that PTA-conj-COS induced apoptosis and cell cycle arrest appears to be accompanied ithe nhhibition of Akt activity.

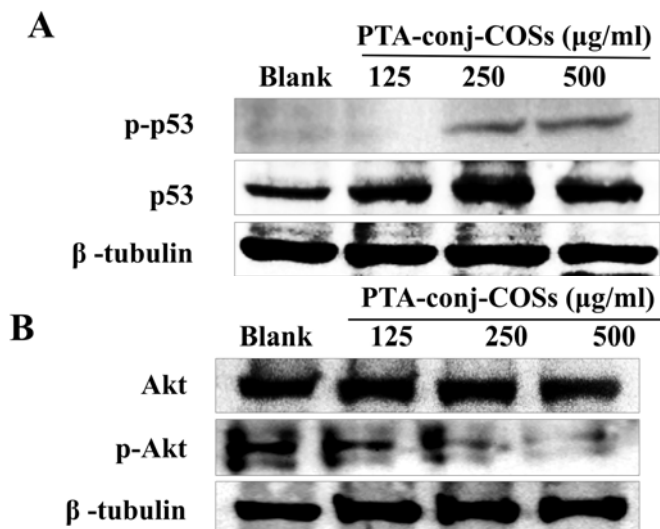


Figure 5. Effect of PTA-conj-COS on phosphorylation of p53 and Akt

In conclusion, PTA-conj-COS arrested cell cycle at the G1/S phase in B16-F10 cells and exhibited significant inhibition on the expressions of G1/S phase specific CDK, cyclin. In addition, PTA-conj-COS exhibited significant effect on up regulation of CDK inhibitors via down regulation of Akt and CREB pathways

ACKNOWLEDGEMENTS

The authors acknowledge Marine Bioprocess Research Center of Marine Bio 21 Project, funded by the Ministry of Land, Transport and Maritime Affairs, Republic of Korea.

REFERENCES

- [1] Cummins, D. L., Cummins, J. M., Pantle, H., Silverman, M. A., Leonard, Al. L and Chanmugam, A. (2006) Cutaneous malignant melanoma. Mayo. Clin. Proc., 81, 500-507.
- [2] Suzuki, K., Mikami, T., Okawa, Y., Tokoro, A., Suzuki, S. and Suzuki, M. (1986) Antitumor effect of hexa-N-acetylchitohexaose and chitohexaose. Carbohydr. Res., 151, 403-408.
- [3] Tokoro, A., Tatewaki, N., Suzuki, K., Mikami, T., Suzuki, S. and Suzuki, M. (1988) Growth-inhibitory effect of Hexa-N-actylchitohexaose and chitohexaose against Meth-A solid tumor. Chem Pharm. Bull., 36, 784-790.
- [4] Vad, N. M. Kandala, P. K., Srivastava, S. K. and Moridani, M. Y. (2010) Structure-toxicity relationship of phenolic analogs as anti-melanoma agent: An enzyme directed produg approach. Chem. Biol. Interact., 183, 462-471.

PROTocatechuic Acid Conjugated Chitosan-Oligosaccharide Induces Apoptosis in B16-F10 Cells Tyrosine Mediated Oxidative Stress Induced via p53 and NF- κ B Pathways

Tae-Kil Eom¹, Se-Kwon Kim^{1,2*}

¹Marine Bioprocess Research Center, Pukyong National University, Busan 608-737, Republic of Korea

²Department of Chemistry, Pukyong National University, Busan 608-737, Republic of Korea

*E-mail address: sknkim@pknu.ac.kr

INTRODUCTION

Chitosan oligosaccharides (COSs) lower viscosity and relatively small molecular size that make them water-soluble and readily absorbable in the *in vivo* systems. They also possess additional functional properties [1]. Phenolic acids are natural hydrophilic antioxidants, which occur ubiquitously in fruits, vegetables, spices, and aromatic herbs. They are of particular interest because of their potential biological properties [2]. Skin cancer is the third most common human malignancy and its global incidence is rising at an alarming rate, with basal cell carcinoma, squamous cell carcinoma and melanoma being the most common forms. It is the most dangerous form, accounting for most skin cancer deaths. In addition, metastatic malignant melanoma is largely refractory to existing therapies and has a very poor prognosis, with a median survival rate of 6 months and 5-year survival rate of less than 5% [3], so new treatment strategies are urgently needed. In the current study, we investigated the *in vitro* biochemical mechanism of protocatechuic acid conjugated COS (PTA-conj-COS) on mouse melanoma (B16-F10) cells. It was found that PTA-conj-COS significantly induced apoptosis in B16-F10 cells in a dose dependent manner.

MATERIALS and METHODS

Cell culture and Cytotoxicity assay

B16-F10 mouse melanoma cells were cultured and maintained in DMEM supplemented with 100 U/ml penicillin G, 100 μ g/ml streptomycin, 10% fetal bovine serum (FBS) and maintained at 37 °C under a humidified atmosphere with 5% CO₂. Cellular survival rate was measured with the PreMix WST-1 EZ-CyTox enhanced cell viability assay kit (Daeil Lab Service). Cells (1×10^4) were seeded into wells of a 96-well culture plate and after 24 h, various concentrations of PTA-conj-COSs were treated and cytotoxicity was measured using WST-1 cell proliferation reagent was added directly to the supernatant (10 μ l/100 μ l growth medium), and incubated at 37 °C for 1 h. The absorbance of the solubilized dark red formazan product was then determined at 450 nm.

Morphological analysis

B16-F10 cells treated with various concentrations of PTA-conj-COSs for 72 h. After that, cells were washed twice with 1X PBS cold and fixed in 4% paraformaldehyde in 1X PBS for 30 min at room temperature. The fixed cells were washed with 1X PBS and stained with 1 μ g/ml of the fluorescent DNA-binding dye, Hoechst 33342 at room temperature for 1 h. Cells were visualized and photographed under fluorescence microscope (CTR 6000; Leica, Wetzlar, Germany).

UV-Vis spectroscopy of enzyme mediated oxidation of PTA-COSs

A UV-Vis spectroscopy method was used to elucidate the progression of PTA-COS metabolism by tyrosinase/O₂ and HRP/H₂O₂. The spectra of a solution containing PTA-COS (100 µg/ml) and tyrosinase (100 U/ml) or HRP (20 U/ml)/H₂O₂ (100 µM) were recorded using a Carry UV-Visible spectral spectrophotometer (Varian, USA). Tyrosinase mediated *o*-quinone formation was determined spectrophotometrically by measuring the oxygen-dependent conversion of catechol substrate in the presence of an excess 3-methyl-2-benzothiazolinone hydrazine (MBTH). The spectra of a solution containing different concentration of PTA-COS, tyrosinase (100 U/ml) and MBTH (10 89mM) were recorded using a Carry UV-Visible spectral spectrophotometer (Varian, USA).

Cellular ROS Formation

Reactive oxygen species (ROS) formation was determined using 2',7'-dichlorofluorescein diacetate as described previously. B16-F10 melanoma cells were seeded at 1×10^5 cells per well in black 96-well microplates. The cells were incubated at 37 °C for 24 h to allow for cell adhesion and environmental adaptation. The media was removed followed by addition of 100 µL of 2',7'-dichlorofluorescein diacetate. The various concentrations of PTA-COS were added to the wells. Immediately upon addition, the plates were read at excitation 485 nm and emission 535 nm by a Genios Multifunctional microplate reader (Tecan, UK).

Cellular GSH measurement

In brief, the treated and control cells (1×10^6) were collected into 1.5 ml microcentrifuge tubes and centrifuged at 700 x g for 5 minutes to remove the supernatant. Then the cell pellets were lysed in 100 µl ice-cold cell lysis buffer. After that they were incubated on ice for 10 minutes, then centrifuged at top speed in an eppendorf centrifuge for 10 min and the cell lysate was transferred into new tubes for glutathione assay. Assay samples were diluted with cell lysis buffer to total volume of 100 µl. A 2 µl of the 50 U/ml GST reagent and 2 µl of orthophthaldehyde dye was added into each samples and incubated at 37 °C for 30 min. Then the fluorescence value was measured in a fluorescence plate reader at excitation/380 nm and emission 460 nm by a Genios Multifunctional microplate reader (Tecan, UK).

Western Blot analysis

Cells were seeded at a density of 1×10^4 cells/well in 10 cm dishes and incubated for 24 h. In the next day, cells were treated with different concentration of PTA-conj-COSs for 72 h. Cells were lysis with RIPA buffer (Sigma-Aldrich, St. Louis) and supernatants were collected. Concentrations of total proteins were determined by using BCA protein assay kit (Thermo Science, Rockford, USA). Western blot was performed as previous describe (Ta et al., 2006) with specific antibodies.

RESULTS and DISCUSSION

Cell growth was significantly inhibited in a dose- and time-dependent manner when B16-F10 cells were treated with PTA-conj-COS at 125-1000 µg/ml for 72 h (Fig. 1A). In addition, fig. 1B shows the morphological changes after 72 h exposure to various concentrations of PTA-conj-COS. The number of cells was remarkably reduced with increasing doses of PTA-conj-COS. As shown Fig. 2A, after reacting with tyrosinase for 1h, one peak appeared at 500nm in PTA and PTA-COSs, but COSs and blank groups did not show the same appearance. These results

indicated that the structural of catechol groups in the PTA-COS was changed to *o*-quinones by tyrosinase. ROS exhibits a strong apoptosis-inducing potential in different cancer cells. It contributes to the cellular injury during treatment with PTA-conj-COS. The group which treated with PTA-conj-COS produced a significantly high level of fluorescence than that of untreated group (Fig. 2B). In addition, PTA-conj-COS decreased the total GSH levels in dose- and time manner. The concentration of GSSG increased after PTA-conj-COS treatment (Fig. 2C).

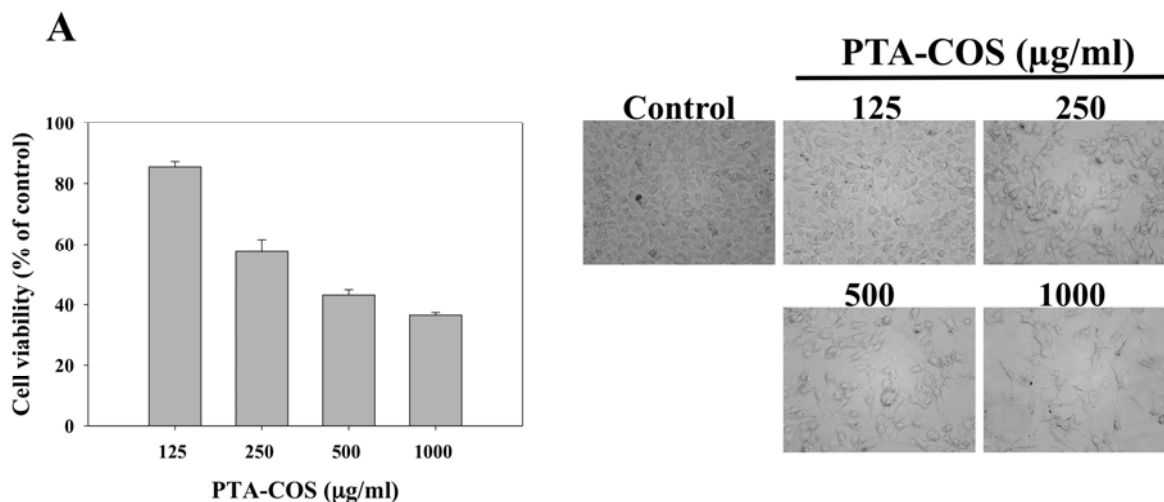


Figure 1. Effect of PTA-conj-COS on cell viability. A) Cell viability after PTA-conj-COS treatment for 72h, B) Cell morphology after PTA-conj-COS treatment for 72h.

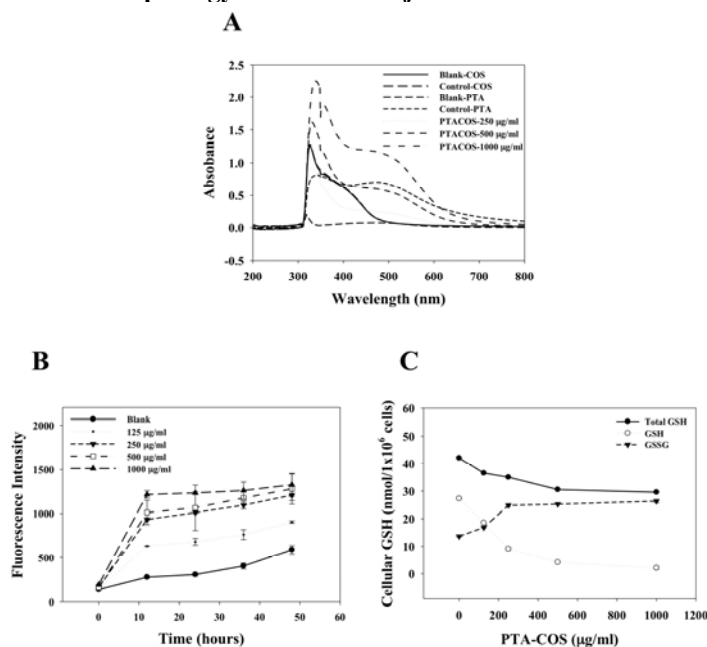


Figure 2. A) Tyrosinase mediated *o*-quinone formation in PTA-conj-COS ; B) Cellular ROS formation after PTA-conj-COS treatment; C) Cellular GSH level after PTA-conj-COS treatment for 72h.

PTA-conj-COS decreased Bcl-2, Bcl-xL and XIAP expression level. Further these proteins are associated with NF- κ B pathways inactivation, as well as decreased in phosphorylation of IKK, I κ B and protein expression level of p65 and p50 (Fig. 3).

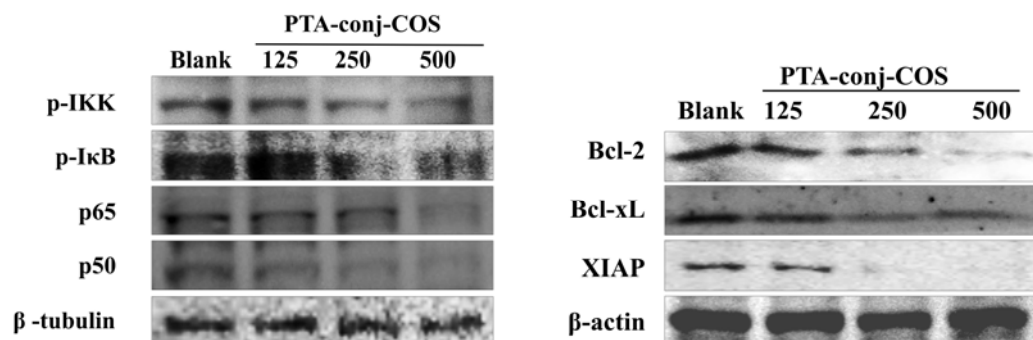


Figure 3. Effect of PTA-conj-COS on NF-κB pathways

Fig. 4 showed that PTA-COS increased p53 expression and activation. In addition, there was a dose-dependent increase in the levels of apoptotic related protein Apaf-1, Fas, Bax, and Bad.

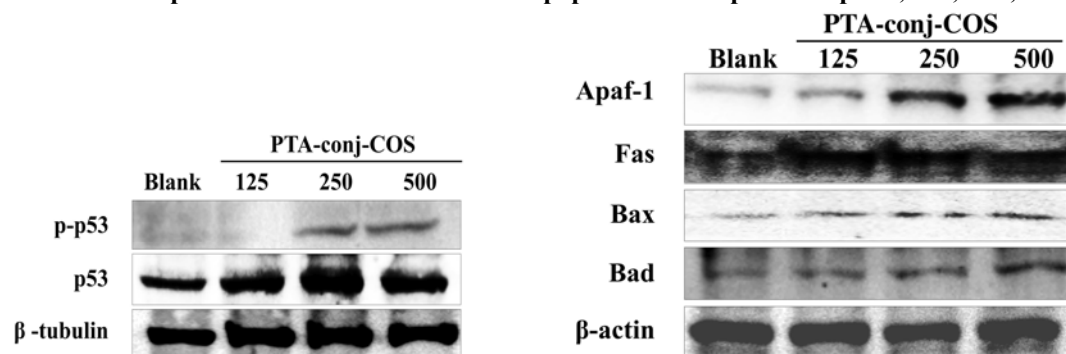


Figure 4. Effect of PTA-conj-COS on p53 pathway

These results suggested that PTA-COS induced apoptosis in B16-F10 cells through the suppression of the NF-κB pathway and activation of the p53 pathway. Moreover, PTA-COS was converted to quinone compounds by tyrosinase. Therefore, PTA-COS induced intracellular ROS and reduced intracellular GSH, triggering the apoptosis processes in B16-F10 mouse melanoma cells.

ACKNOWLEDGEMENTS

The authors acknowledge the Marine Bioprocess Research Center of the Marine Bio 21 Project, funded by the Ministry of Land, Transport and Maritime Affairs, Republic of Korea.

REFERENCES

- [1] Kim, S. K. and Rajapakse, N. (2005) Enzymatic production and biological activities of chitosan oligosaccharides (COS): A review. *Carbohydr. Res.*, 62, 357-368.
- [2] Kevlin, D. C. (1998) The chemistry and biological effects of flavonoids and phenolic acids. *Ann. N. Y. Acad. Sci.*, 854, 435-442.
- [3] Cummins, D. L., Cummins, J. M., Pantle, H., Silverman, M. A., Leonard, A. L. and Chanmugam, A. (2006) Cutaneous malignant melanoma. *Mayo. Clin. Proc.*, 81, 500-507.

HOMOGENEOUS N-ACETYLATION OF EXTENSIVELY DEACETYLATED CHITOSAN: PHYSICAL CHEMICAL CHARACTERISTICS AND DISTRIBUTION PATTERN

Sara C.P. Veiga, Sérgio P. Campana-Filho*

Universidade de São Paulo – Instituto de Química de São Carlos – BRAZIL

**E-mail: scampana@iqsc.usp.br*

INTRODUCTION

Chitosan is a copolymer of $\beta(1-4)$ linked 2-deoxy-2-amino-D-glucopyranose (GlcN) and 2-deoxy-2-acetamido-D-glucopyranose (GlcNAc) units whose properties are strongly dependent on its molecular weight and polydispersity, average degree of acetylation (DA), defined as the average number of GlcNAc units in its chains, and on the distribution pattern of GlcN and GlcNAc units in the polymeric chains [1]. However, as chitosan is generally produced by carrying out the heterogeneous deacetylation of chitin, the GlcN and GlcNAc units are not uniformly distributed in the polymer chains, a block-like distribution pattern being proposed in this case [2]. This work aims to evaluate the structural characteristics and properties of N-acetylated chitosan samples produced by carrying out the homogeneous acetylation of extensively deacetylated chitosan. Thus, beta-chitin extracted from squid pens was submitted to the ultrasound-assisted deacetylation process [3] and the resulting chitosan was employed in the N-acetylation experiments by reacting it with acetic anhydride at room temperature. The characteristics of the homogeneously N-acetylated chitosan samples, including DA and acetylation pattern, viscosity average molecular weight, morphological features and thermal behavior were determined and compared to those of beta-chitin and extensively deacetylated chitosan.

MATERIALS AND METHODS

Beta-chitin was extracted from squid pens (*Loligo sp.*), supplied by Miami Pescados (Cananéia, Brazil), by carrying out a mild deproteinization procedure as described in the literature [4]. Thus, the squid pens (200g) were thoroughly washed with tap water to eliminate impurities, dried at room temperature, ground and sieved. Following, the fraction of the particles with average dimensions in the range 250–425 μ m was suspended in 3.0 L of aqueous NaOH (1M) and the suspension was stirred for 18 hours at room temperature. The solid (beta-chitin) recovered by filtration was extensively washed with deionized water and dried at room temperature, being identified as sample CTo.

Extensively deacetylated chitosan was produced by submitting beta-chitin (sample CTo) to the ultrasound-assisted deacetylation process [3]. Thus, beta-chitin (4.4 g) was suspended in 50 mL of 14.1 M NaOH and the suspension was poured into a double-walled cylindrical glass reactor ($\theta_{int}=3.5$ cm) coupled to a circulating thermostat to allow the control of the reaction temperature at $65\pm 2^\circ\text{C}$. The beta-chitin suspension was submitted to the ultrasound irradiation by using a Branson Sonifier Model 450 ($\nu=20$ kHz) coupled to a $\frac{1}{2}$ ' stepped probe and the equipment was adjusted for intermittent irradiation to minimize the heat releasing due to the ultrasound irradiation. The irradiation amplitude was adjusted to low ($30\% < A_{max} < 50\%$) and the reaction proceeded for 50 min. The reaction was interrupted by cooling the glass reactor at -15°C ,

the pH was adjusted to 8-9 by adding dilute aqueous HCl, the solid was recovered by filtration and then it was extensively washed with 80% ethanol and dried at room temperature. The same procedure as described above was repeated twice to result in extensively deacetylated chitosan, named as sample CSo.

Homogeneous N-acetylation of Chitosan

The sample CSo (0.5 g) was suspended in 50 mL of 0.5% acetic acid, the suspension was stirred during 24 h at room temperature and then 40 mL of 1,2-propanediol were added to the resulting solution. Following, acetic anhydride was added to the reaction medium and the reaction was allowed to proceed homogeneously for 24 h at room temperature. The product was recovered upon addition of dilute NaOH for the adjustment of pH (≈ 8) and of absolute ethanol to provoke its precipitation. The solid (N-acetylated chitosan) was recovered by filtration and then it was extensively washed with aqueous ethanol and dried at room temperature. Five N-acetylated chitosans were produced according to the molar ratio acetic anhydride/amino groups of chitosan (MR) employed in the N-acetylation reaction: a) Sample RCSo1 (MR=0.3); b) Sample RCSo2 (MR=0.4), c) Sample RCSo3 (MR=0.5); d) Sample RCSo4 (MR=0.6); e) Sample RCSo5 (MR=0.7). All the N-acetylation reactions were duplicated and all resulting products were characterized as described in the following.

Characterizations

The beta-chitin (sample CTo), extensively deacetylated chitosan (sample CSo) and re-acetylated chitosans (samples RCSon) were characterized in terms of its chemical structure, average degree of acetylation (DA) and pattern of acetylation (PA), viscosity average molecular weight, morphological aspects and thermal behavior.

A BOMEM MB-102 FTIR spectrometer was used to acquire the infrared spectra of the beta-chitin (sample CTo), extensively deacetylated chitosan (sample CSo) and re-acetylated chitosan (samples RCSon). Thus, the sample was thoroughly mixed with KBr (1:100 sample/KBr), the mixture was dried at 80 °C and reduced pressure during 8h and then pressed to result in a homogeneous disc. The spectra were registered from 48 scanning at a resolution of 4 cm^{-1} , in the range 4000 cm^{-1} - 500 cm^{-1} .

The ^1H nuclear magnetic resonance spectroscopy was used to determine the average degree of acetylation (DA) and the corresponding pattern of acetylation (PA). The NMR spectrum of beta-chitin (sample CTo) was acquired from the solution resulting from the treatment of the polysaccharide (10 mg) with 1 mL of 35% DCl during 24 h at 40°C, and its DA and PA were determined as described in the literature [5]. The NMR spectra of extensively deacetylated chitosan (sample CSo) and homogeneously re-acetylated chitosan (samples RCSon) were acquired from the solutions of the samples (6 mg) in 1 mL of DCl/D₂O (1:100 v/v; pD=3-4), and the corresponding DAs were determined from the NMR spectra as described elsewhere [5]. To determine their patterns of acetylation (PA), the samples CSo and RCSon were treated with aqueous HCl/NaNO₂ followed by freeze-drying. The solid was redissolved in D₂O and then it was freeze-dried again. This procedure was repeated twice to promote the exchange of labile hydrogens by deuterium atoms. All NMR spectra were acquired at 90 °C by using a Bruker Avance DRX 500 MHz spectrometer, the acquisition parameters being those described in the literature [5].

The viscosity average molecular weight (Mv) of beta-chitin and chitosan were calculated from intrinsic viscosity values determined in the same solvent and temperature as the parameters "K" and "a" of the corresponding Mark-Houwink-Sakurada relationship. Beta-chitin was dissolved in N,N-dimethylacetamide/5% LiCl and the intrinsic viscosity determined at 25,00 \pm 0,01°C was used to calculate Mv [6]. Chitosan was dissolved in 0.3 M acetic acid/0.2 M sodium

acetate buffer (pH \approx 4.5) and intrinsic viscosity was determined at $25,00 \pm 0,01^\circ\text{C}$ as described elsewhere [3]. The corresponding M_v values were calculated by taking into account the DA of the chitosan sample [1,7].

The X-ray diffraction measurements were acquired by using a Rigaku diffractometer at continuous scanning ($1^\circ/\text{min}$) in the range $2\theta=3\text{-}50^\circ$, with an incident radiation $\text{CuK}\alpha(\lambda = 1,54\text{\AA})$.

The thermal behaviour of beta-chitin and chitosan was studied by thermogravimetric analysis (TGA). In a typical experiment, the sample (3-5mg) was heated at $10^\circ\text{C}/\text{min}$ in synthetic air atmosphere (20 mL/min) in the interval $20\text{-}700^\circ\text{C}/\text{min}$ in TGA-50 thermoanalyser (Shimadzu).

RESULTS and DISCUSSION

From the values of DA and M_v of samples CTo, CSo and RCSo_n (Table 1) it is observed that extensively deacetylated chitosan was produced by applying the ultrasound-assisted deacetylation (USAD) process to beta-chitin. However, as the USAD process was applied for three consecutive times a severe depolymerization was also observed. The homogeneously N-acetylated chitosan exhibited higher DA values the higher the molar ratio acetic anhydride/amino groups employed in the acetylation reaction, a linear relationship being observed (Figure 1A). No evidences of O-acetylation were found in the infrared spectra, the main peaks in the interval $1800 - 1000\text{ cm}^{-1}$ being similar regardless of the DA of the N-acetylated chitosans (Figure 1B). All chitosan were fully soluble in dilute acetic acid (pH \approx 4.5) while samples RCSo₄ (DA=48%) and RCSo₅ (DA=50%) were also soluble in aqueous solution of pH \approx 7.0.

Table 1: Values of DA and M_v of beta-chitin (sample CTo), extensively deacetylated chitosan (sample CSo) and reacylated chitosans (CSo_n)^a.

Sample	DA (%)	$[\eta]$ (mL/g)	M_v (g/mol) ^b	DP _v ^c
CTo	80	4008	1,320,000	7810
CSo	2	1353	354,000	2187
RCSo ₁	25	1100	182,000	1059
RCSo ₂	34	936	149,000	850
RCSo ₃	40	814	110,000	617
RCSo ₄	48	1068	151,000	833
RCSo ₅	50	1083	153,000	837

a)average values determined from two independent N-acetylation reactions.

b)average values determined from intrinsic viscosity values.

c)average values calculated from viscosity average molecular weight values.

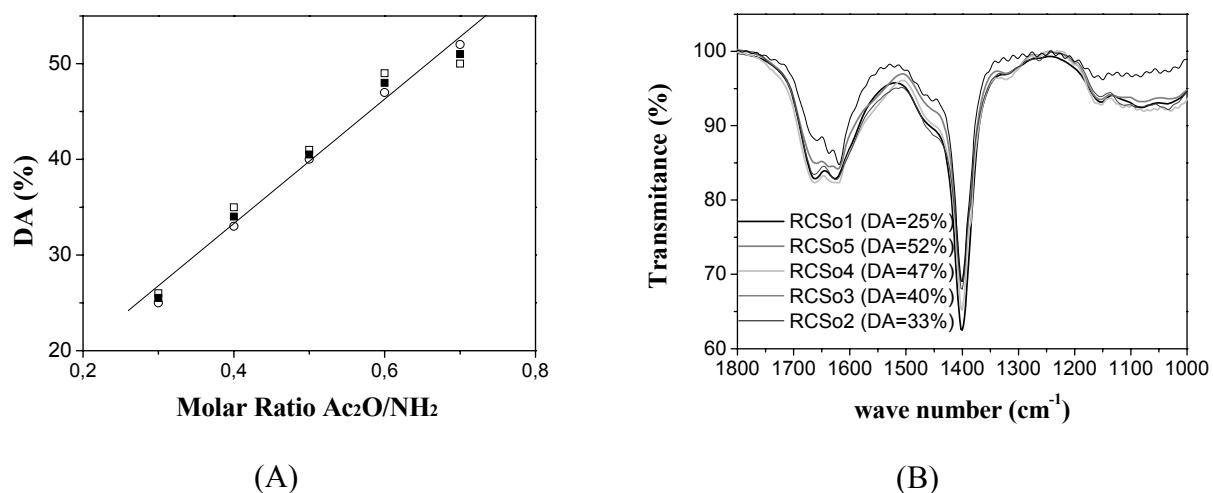


Figure 1: Dependence of DA with the molar ratio Ac₂O/NH₂, where the filled symbols correspond to DA values averaged from two independent N-acetylation reactions (A), and infrared spectra of N-acetylated chitosan in the region 1800 – 1000 cm⁻¹ (B).

The X rays diffraction analyses of N-acetylated chitosans resulted in similar patterns (Figure 2A) but the main peaks are broader and less intense than those observed in the case of beta-chitin (data not shown), revealing the loss of order. However, it seems that the more acetylated the chitosan sample the more defined and intense the peaks, confirming that DA, and probably the pattern of acetylation, has an important role in determining the arrangement of chitosan chains in the solid state.

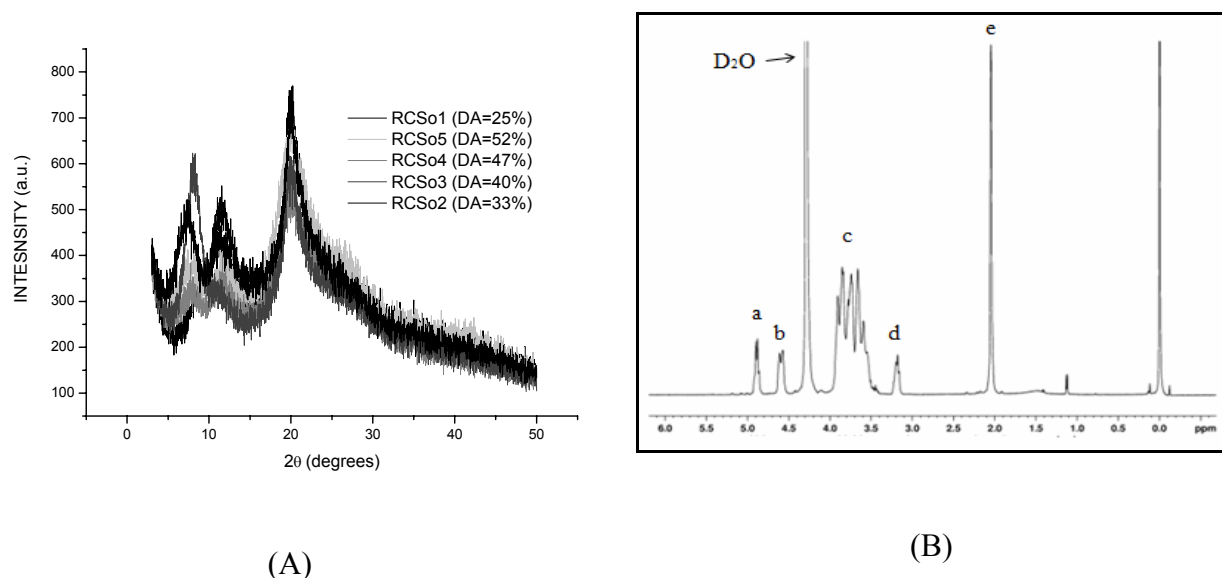


Figure 2: X rays diffraction pattern of N-acetylated chitosans (A) and ¹H NMR spectrum of sample RCS04 (DA=47%).

The ^1H NMR spectrum of sample RCSO4 (Figure 2B) is typical of chitosan with the presence of peaks attributed to hydrogen atoms bonded to carbon 1 of glucopyranose units (peaks a and b), hydrogens bonded to carbons 1, 3, 4, 5 and 6 of glucopyranose units (peak c), hydrogen bonded to carbon 2 of glucopyranose units (peak d) and methyl hydrogen of acetamido groups (peak e).

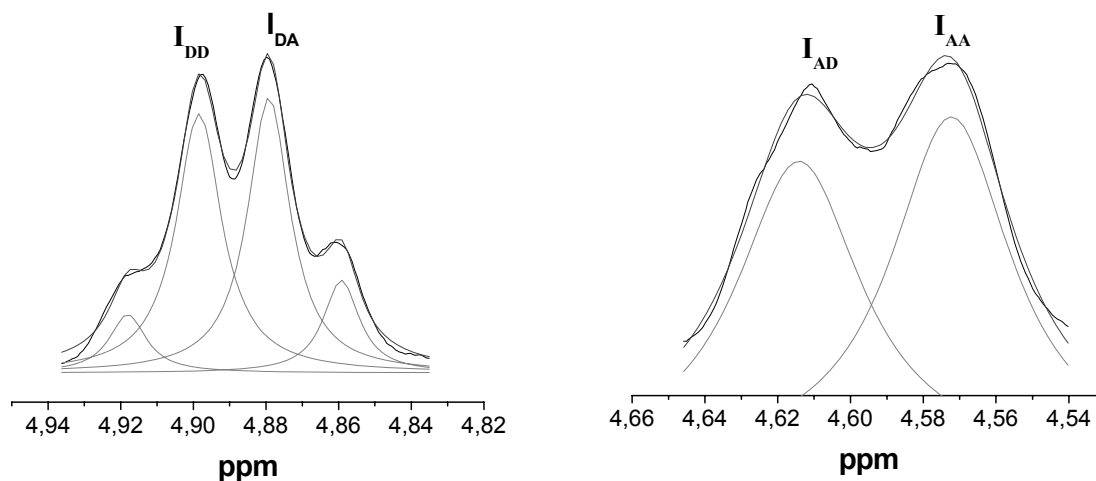


Figure 3: ^1H NMR spectrum of sample RCSO4 (DA=48%) in the region where the peaks due to the anomeric carbon atoms are observed showing the signals attributed to diads DD, DA, AD and AA, the deconvoluted curves (in gray) and the fitted curves (in dark gray).

The relative frequency of diads DD, DA, AD and AA, where D and A stand for GlcN and GlcNAc units, respectively, can be calculated from the intensity of the peaks due to anomeric carbons (Figure 3) and from them the acetylation pattern (PA) of N-acetylated chitosans can be determined. According to the literature [5], the perfect block, random and alternated patterns of acetylation are characterized by PA values of 0, 1 and 2, respectively. The PA values of the N-acetylated chitosan revealed that a random pattern of acetylation resulted for the samples possessing DA>30% while the PA of the less acetylated chitosan is closer to PA=1.5, indicating the occurrence of an alternated acetylation pattern (Figure 4A).

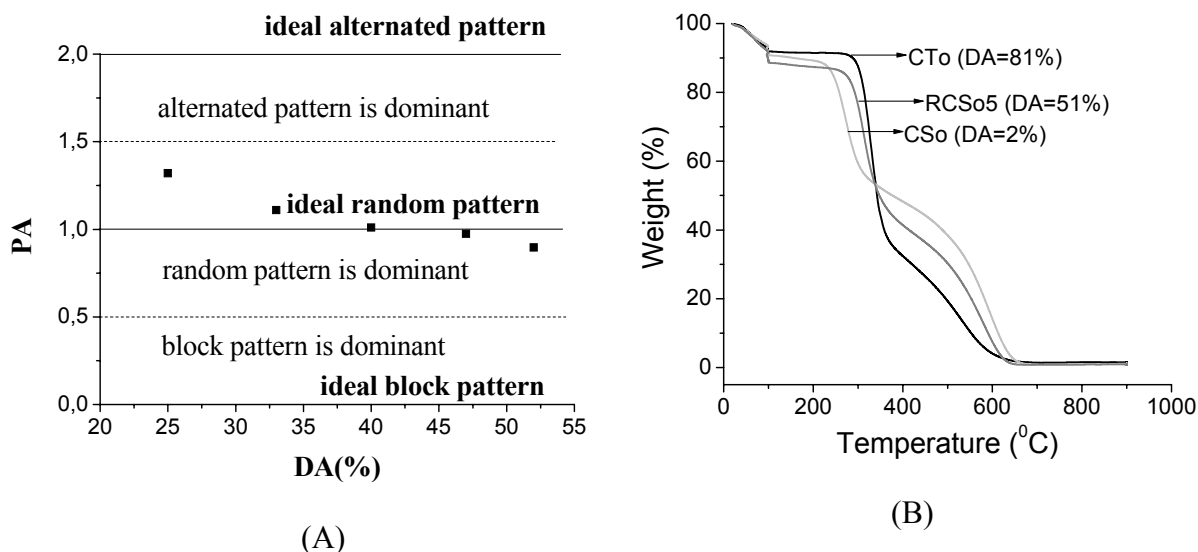


Figure 4: Dependence of the acetylation pattern (PA) on DA for N-acetylated chitosans (A) and comparison of thermogravimetric curves of beta-chitin, extensively deacetylated chitosan and N-acetylated chitosan (B).

The thermogravimetric analyses revealed that the extensively deacetylated chitosan sample was less stable than beta-chitin and N-acetylated chitosan, typical TGA curves being shown in Figure 4B. Indeed, from these curves it is observed that the thermal degradation of sample CSo (DA=2%) begins at a lower temperature, confirming its lower thermal stability as compared to samples CTo (DA=81%) and RCSO5 (DA=50%), the other N-acetylated chitosan samples exhibiting TGA curves similar to this latter. The whole set of data shown that homogeneously N-acetylated chitosan exhibited higher DA values the higher the molar ratio $\text{Ac}_2\text{O}/\text{NH}_2$ employed during the reaction and that a nearly ideal random acetylation pattern resulted when $\text{DA} > 30\%$. The N-acetylated chitosans presented similar infrared spectra and X rays diffraction patterns while the thermogravimetric analyses revealed that the higher the DA value the higher the thermal stability of the sample.

ACKNOWLEDGEMENTS

The authors thank to CAPES, CNPq and FAPESP for the scholarships and financial support.

REFERENCES

- [1] Rinaudo, M. (2006) CHITIN AND CHITOSAN: properties and applications. *Prog. Polym. Sci.*, 31, 603-632.
- [2] Lamarque, G.; Viton, C.; Domard, A. (2004) COMPARATIVE STUDY OF THE FIRST HETEROGENEOUS DEACETYLATION OF α - AND β -CHITINS in a multistep process. *Biomacromolecules*, 5, 992-1001.
- [3] Delezuk, J. A. M.; Cardoso, M. B.; Domard, A.; Campana-Filho, S. P. (2011) ULTRASOUND-ASSISTED DEACETYLATION OF β -CHITIN INFLUENCE OF THE PROCESSING parameters. *Polym. Int.*, in press.
- [4] Chaussard, G.; Domard, A. (2004) NEW ASPECTS OF THE EXTRACTION OF CHITIN FROM SQUID PENS. *Biomacromolecules*, 5, 559-564.
- [5] Kurmirska, J.; Weinhold, M. X.; Steudtee, S.; Thöming, J.; Brzozowski, K.; Stepnowski, P. (2009). *Int. J. Biol. Macromol.*, 45, 56-60.
- [6] Terbojevich, M.; Carraro, C.; Cosani, A. (1988) STUDIES OF THE CHITIN-LITHIUM CHLORIDE-N,N-DI-METHYLACETAMIDE SYSTEM. *Carbohydr. Res.*, 180, 73-86.
- [7] Brugnerotto, J.; Desbrières, J.; Roberts, G.; Rinaudo, M. CHARACTERIZATION OF CHITOSAN BY STERIC EXCLUSION CHROMATOGRAPHY. *Polymer*, 42, 9921-9927.

NANOPARTICLES AND FILMS FROM ULTRASOUND-PROCESSED CHITIN, CHITOSAN AND CELLULOSE

Érika V.R. Almeida, Mario S. Mariano, Sérgio P. Campana-Filho*

Universidade de São Paulo – Instituto de Química de São Carlos – BRAZIL

*E-mail: scampana@iqsc.usp.br

INTRODUCTION

Chitin, chitosan, a chitin derivative produced by carrying out the deacetylation reaction, and cellulose are abundant in nature and they also exhibit great potential for developing new biocompatible and biodegradable materials. However, chitin and cellulose are insoluble in common solvents while chitosan is soluble only in aqueous acid solutions, limiting the processing of these polymers via dissolution procedures. Recently, the ultrasound irradiation has been successfully applied as a top-down method for producing nanoparticles and nanofibers from polysaccharides, such as cellulose, chitin and chitosan, potentially applicable as components of biodevices and as scaffolds for tissue engineering [1]. The aim of this work was to produce ultrasound-processed stable aqueous suspensions of beta-chitin (from *Loligo sp.*) to investigate the effects of high intensity ultrasound irradiation on the particles dimensions. The properties of films casted from the ultrasound-processed suspensions of beta-chitin, in the presence or absence of mercerized cellulose or chitosan, were also determined.

MATERIALS AND METHODS

Beta-chitin was extracted from squid pens, which were supplied by Miami Pescados (Cananéia, Brazil), by carrying out a mild deproteinization procedure as described in the literature [2]. Thus, the squid pens (200g) were thoroughly washed with tap water to eliminate impurities, dried at room temperature, ground and sieved. Following, the fraction of the particles with average dimensions in the range 250–425 μm was suspended in 3.0 L of aqueous NaOH (1M) and the suspension was stirred for 18 hours at room temperature. The solid (beta-chitin) recovered by filtration was extensively washed with deionized water, dried at room temperature, ground and the fraction of the particles with average dimensions in the range 75 μm < ρ < 125 μm was recovered after sieving to be used in the subsequent experiments. Chitosan with DA=30%, from France Chitin (Marseille, France) was used as received. Cellulose from sisal, which was supplied by Lwarcell Ltda (Lençóis Paulista, Brazil), was mercerized by treating it with aqueous NaOH [3]. Thus, 10 g of sisal cellulose were suspended in 0.5 L of 20% sodium hydroxide and the suspension was stirred during 1h at 0 °C to minimize the occurrence of degradation of the cellulose chains. The solid recovered by filtration was extensively washed with distilled water to eliminate the excess of alkali and dried at 100 °C.

Sonication treatment

The beta-chitin suspension (0.4 g/L < Cp < 1.6 g/L) was poured into a double walled cylindrical glass reactor coupled to a circulating thermostat and then it was submitted to the high intensity ultrasound irradiation by using a Branson Sonifier Model 450 (ν =20 kHz) coupled to a 1/2" stepped probe. The irradiation amplitude (A) was adjusted to low (30% < A max < 50%), the duration of the ultrasound treatment ranged as 5min < t < 60min and the temperature was

maintained at 67 ± 2 °C. The resulting suspensions were cooled to room temperature and then they were analyzed by light scattering in an Appliance Zeta Trac to determine the average size and the conductivity of the suspended particles.

Aqueous suspensions containing beta-chitin and mercerized sisal cellulose (or chitosan) were also submitted to sonication and after ultrasound-processing as described above they were poured in Petri dishes. Following, the solvent was allowed to evaporate at room temperature to result in films which were detached and characterized. Four films were casted from the ultrasound-processed suspensions and their thickness (θ) were measured by using a caliper rule: a) Film B00660 ($\theta=0.04$ mm) was casted from a suspension of beta-chitin (0.06 g) in distilled water (25 mL) at pH=6 which has been sonicated during 60 min; b) Film B00630 ($\theta=0.03$ mm) was casted from a suspension of beta-chitin (0.06 g) in distilled water (25 mL) at pH=8 which has been sonicated during 30 min; c) Film BCh00830 ($\theta=0.02$ mm) was casted from a suspension containing beta-chitin (0.04 g) and chitosan (0.04 g) in distilled water (25 mL) at pH=5 which has been sonicated during 30 min; d) Film BCl00660 ($\theta=0.05$ mm) was casted from a suspension containing beta-chitin (0.045 g) and mercerized sisal cellulose (0.015 g) at pH=6 which has been sonicated during 60 min.

Characterization of the films

The films casted from the ultrasound-processed aqueous suspensions of beta-chitin were characterized in terms of morphological features, mechanical properties and thermal behavior by using scanning electron microscopy (SEM), dynamic mechanical thermal analysis (DMTA), differential scanning calorimetry (DSC) and thermogravimetric analysis (TGA) as described in the following.

The films were coated with gold and its morphological characteristics were investigated by SEM using a ZEISS EVO 50 microscopy.

The mechanical properties of the films (10.0 mm long and 5.3 mm wide) were determined by using a DMA 2980 (TA Instruments) using a tension-type clamp, frequency of 1 Hz, amplitude of 4 μm , preload of 0.15 N and a heating rate of 3 °C min^{-1} in the range 25 - 300 °C. The same equipment was employed for the determination of the tension strength as a function of the elongation of the films at room temperature, by using a force rate of 1.0 N. min^{-1} in the range 1.0 - 18 N and a force of 0.01 N as preload.

The differential scanning calorimetry of the films was carried out in a DSC50 (Shimadzu) by using a dynamic N₂ atmosphere ($\theta=20$ mL min^{-1}) and a heating rate of 20 °C. min^{-1} , in the range 25 - 450 °C. The thermogravimetric analysis was carried out in a TGA 50 (Shimadzu) under N₂ atmosphere ($\theta=20$ mL min^{-1}), a heating rate of 20 °C. min^{-1} , in the range 25 - 700 °C.

RESULTS AND DISCUSSION

Characteristics of the ultrasound-processed suspensions

The ultrasound-processed suspensions of beta-chitin were more stable the longer the treatment duration and the higher the concentration of chitin in the suspension, a representative example of such a behavior being shown in Figure 1. Indeed, the less concentrated suspensions ($C_p < 1.0$ g/L) and those which were submitted to short sonication time ($t < 20$ min) were not sufficiently stable while the more concentrated suspensions ($C_p > 1.0$ g/L) and those which were submitted to long sonication time ($t > 20$ min) were stable as the particles remained in suspension even after several days.

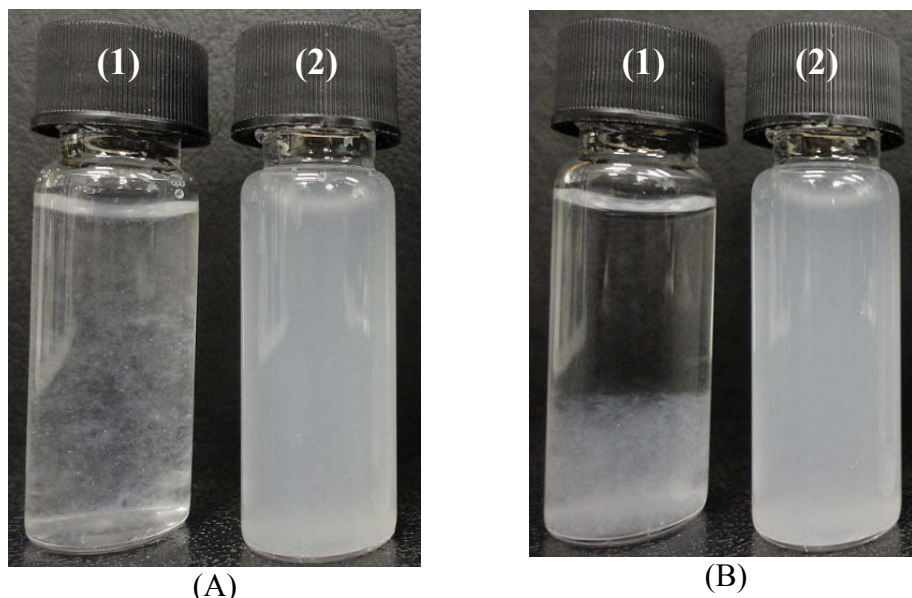


Figure 1: Ultrasound-processed aqueous suspensions of beta-chitin immediately after the ultrasound treatment (A) and one week later (B), where (1) stands for the beta-chitin suspension B0405 ($C_p=0.4$ g/L) sonicated during 5 min while (2) corresponds to the beta-chitin suspension B1630 ($C_p=1.6$ g/L) sonicated during 30 min.

Such a behavior of the ultrasound-processed suspensions of beta-chitin is attributed to the reduction of the particles size and the development of superficial charges due to the occurrence of cavitation during the ultrasound treatment. In fact, the measurements of zeta potential (data not shown) confirmed that the more concentrated the beta-chitin suspension and the longer the sonication time, the higher the particles superficial charge. The light scattering measurements also allowed the determination of the average diameter of the beta-chitin particles in the swollen state. Although there are no simple relationship between the sonication time and the average size of the beta-chitin particles (Figure 2), these data show a remarkable reduction of the particle dimensions since it ranged as $75\mu\text{m} < \rho < 125\mu\text{m}$ for the parent particles and it changed to $300\text{ nm} < \rho < 700\text{ nm}$ in the case of the ultrasound-processed particles. Actually, regardless of the concentration of the beta-chitin suspension a sonication time as short as 5 min already provoked the reduction of the particles size to $425\text{ nm} < \rho < 485\text{ nm}$ (Figure 2), the prolongation of the treatment leading to a complex pattern which seems to depend on the swelling capacity of the particles and on its tendency to aggregate.

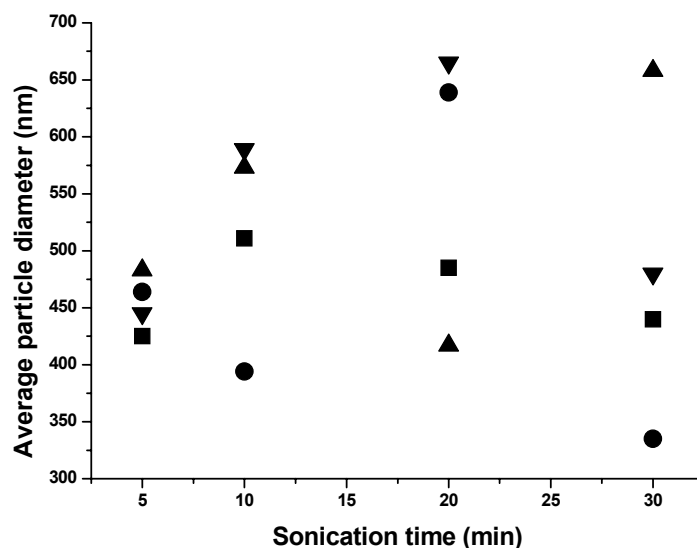


Figure 2: Dependence of the average diameter of the beta-chitin particles as a function of the sonication time, the ultrasound-processed suspensions being identified as: (■)B04 (Cp=0.4 g/L); (●)B08 (Cp=0.8 g/L); (▲) B12 (Cp=1.2 g/L); (▼)B16 (Cp=1.6 g/L).

Characteristics of the films casted from the ultrasound-processed suspensions

Initially it is important to remark that all attempts to cast films from untreated suspensions of beta-chitin, in the presence and in absence of cellulose or chitosan, were unsuccessful. However, all the ultrasound-processed suspensions allowed the casting of films whose surface morphology depended on the medium acidity and on the presence of other polysaccharides (mercerized cellulose or chitosan).

Comparing the surface morphology of film B00660, casted from an aqueous suspension of beta-chitin (Cp=0.06 g/L) previously sonicated during 60 min at pH=5, and that of film BCl00660, casted from an aqueous suspension of beta-chitin (Cp=0.045 g/L) and mercerized cellulose (Cp=0.015 g/L) at pH=6, reveals that the nanoparticles of beta-chitin strongly interact to form a relatively homogeneous matrix (Figure 3A) to which cellulose fibers are adhered (Figure 3B). In contrast, in the film BCh00830 chitosan is part of the film matrix, as it was soluble in the suspension medium at pH=5, while the nanoparticles of beta-chitin are homogeneously dispersed in it (Figure 3C e 3D).

From the infrared spectra and X ray diffraction patterns of these films (data not shown) it was observed that the chemical structure of beta-chitin, mercerized cellulose and chitosan were not affected by the ultrasound treatment and that amorphous materials were produced by casting films from the ultrasound-processed suspensions containing these polysaccharides.

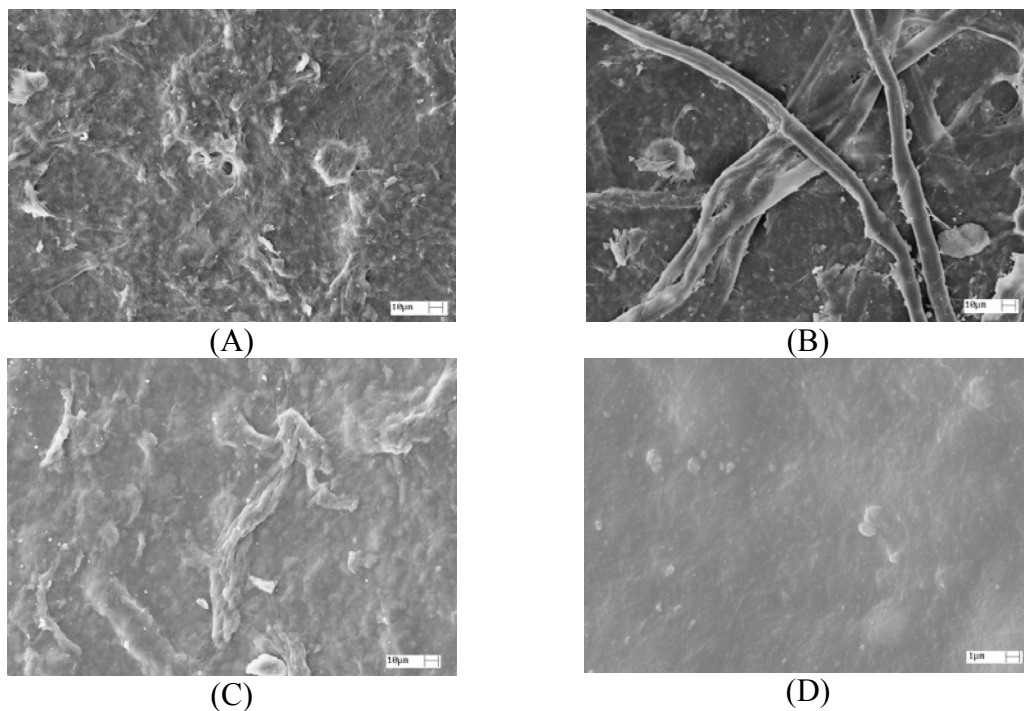


Figure 3: SEM analyses of the films casted from ultrasound-processed aqueous suspensions of beta-chitin (A), beta-chitin and mercerized cellulose (B), beta-chitin and chitosan (C and D). See text for more details on the suspensions.

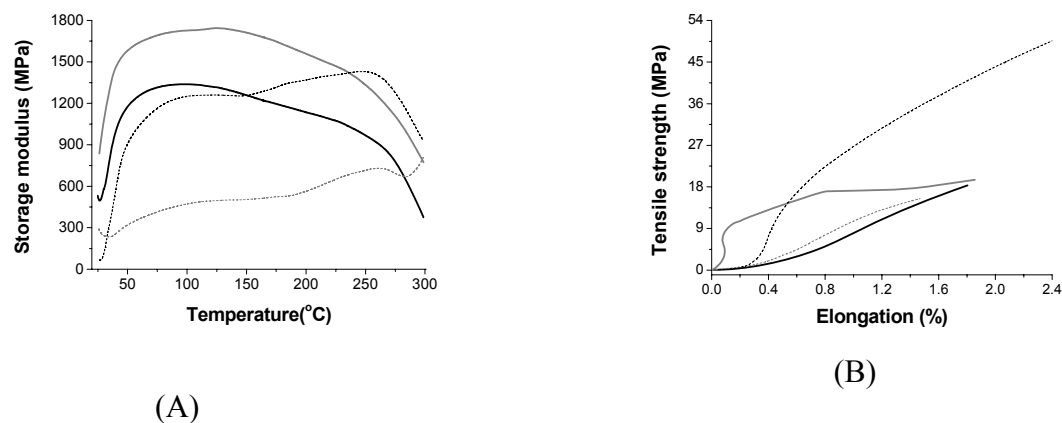


Figure 4: Storage modulus of the films casted from ultrasound-processed suspensions of beta-chitin as a function of temperature (A) and tensile strength as a function of elongation (B), with the films being identified as: B00660 (—); B00630 (.....), BC100660 (—), BCh00830 (.....).

The DMTA analyses revealed that all films casted from ultrasound-processed suspensions, except that one casted from a suspension containing beta-chitin and chitosan (film BCh00830), exhibited increasing storage modulus with heating up to a given temperature (which depends on the film composition and sonication time) followed by a sharp decrease (Figure 4A). The elongation of the films as a function of tensile strength was very small (<2%) in all cases (Figure

4B), but the mechanical behavior of the film casted from beta-chitin/chitosan suspension was different, indicating the occurrence of stronger interactions in this case.

According to the DSC and TGA analyses (Figures 5A and 5B) and from the comparison of the curves of the casted films with those of the individual polysaccharides (data not shown), it is concluded that the thermal behavior of beta-chitin, mercerized cellulose and chitosan were only slightly affected by the ultrasound treatment. Indeed, the same main thermal events, corresponding to water evaporation, polymer degradation and pyrolysis of polymer fragments, are observed in the DSC and TGA curves of the individual polysaccharides and of the casted films. However, it is observed that the corresponding temperature peaks are shifted toward slightly higher values in the curves of the casted films as compared to those of the individual polysaccharides, the stronger polymer/polymer and polymer/water interactions existing in the films being responsible for such a fact.

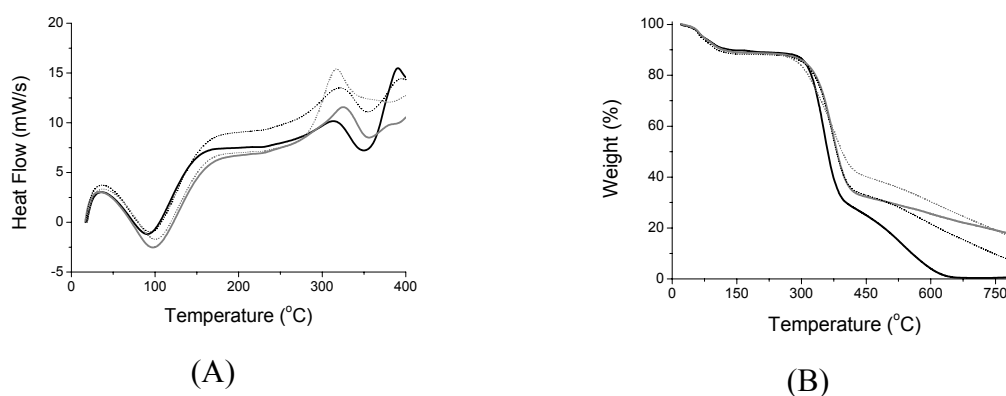


Figure 5: DSC curves (A) and TGA curves (B) of the films casted from ultrasound-processed suspensions of beta-chitin, with the films being identified as: B00660 (—); B00630 (.....), BC100660 (—), BCh00830 (-----).

ACKNOWLEDGEMENTS

The authors thank to CAPES, CNPq and FAPESP for the scholarships and financial support.

REFERENCES

- [1] Fan, Y., Saito, T., Isogai, A. (2008) PREPARATION OF CHITIN NANOFIBERS FROM SQUID PEN β -CHITIN BY SIMPLE MECHANICAL TREATMENT UNDER ACID CONDITIONS. *Biomacromolecules*, 9, 1919-1923.
- [2] Chaussard, G., Domard, A. (2004) NEW ASPECTS OF THE EXTRACTION OF CHITIN FROM SQUID PENS. *Biomacromolecules*, 5, 559-564.
- [3] Ciacco, G. T., Morgado, D. L., Frollini, E., *et al.* (2010) SOME ASPECTS OF ACETYLTATION OF UNTREATED AND MERCERIZED SISAL CELLULOSE. *Journal of Brazilian Chemical Society*, 21, 71-77.

HPLC FOR CHITO-OLIGOSACCHARIDES OBTAINED FROM ENZYMATIC HYDROLYSIS OF CHITOSAN

Talita L Honorato, Fernando R Frederico, Telma T Franco*

¹*School of Chemical Engineering – State University of Campinas, UNICAMP – SP, Brazil.*

**E-mail address: franco@feq.unicamp.br*

INTRODUCTION

Hetero-chitooligosaccharides (CHO's), which are composed of N-acetylglucosamine ((2-acetoamido-2-deoxy-D-glucose, GlcNAc or A for acetylated) and glucosamine (2-amino-2-deoxy-D-glucose, GlcN or D for deacetylated), have several potential applications in the food, agriculture and pharmaceutical industries [1, 2, 3, 4, 5] and consequently their utilisation would be particularly promising. These oligomers can be obtained by enzymatic hydrolysis of chitin and / or chitosan [6]. In order to develop reproducible methods to produce CHO, it is also needed to optimize the enzyme extract which will catalyze the hydrolysis, therefore selection of the microorganism strain, determination of pH and temperature for optimal activity of enzymes, among other factors [7, 8, 9] must be investigated. A suitable and easy analytical method to quantify the CHO produced in our laboratory was developed in order to follow their producing.

One of the most widely used techniques for separation, identification and quantification of oligomers is high performance liquid chromatography [10, 11]. High-performance liquid chromatography (HPLC) with pulsed amperometric detection (PAD) can provide efficient and accurate determinations of carbohydrate concentrations [12]. Previous HPLC–PAD methods able to separate amino sugars monomers from neutral sugars monomers [13] and analyze fructooligosaccharides [10] have been described. According to our best knowledge, this is the first HPLC–PAD method that simultaneously separates acetylated and desacetylated CHO with a single isocratic analysis.

Then, the objective of the work was to develop, with the aid of ion chromatography, an analytical methodology for separation, identification and quantification of chito-acetylated and non acetylated bioactivities oligosaccharides.

MATERIALS and METHODS

Reagents and solutions

The mobile phase consisting of a 50 mM NaOH and a solution of sodium acetate 50mM in 50 mM NaOH. Standards of 2-deoxy-2-acetoamido-D-glucose (N-acetyl-D-glucosamine, di-N-acetylchitobiose, tri-N-acetylchitotriose, tetra-N-acetylchitotetraose, penta-N-acetylchitopentaose) and 2-amino-2-deoxy-D-glucose (D-glucosamine, chitobiose, chitotriose, chitotetraose, chitopentaose and chitohexaose) from Seikagaku Corporation patterns were prepared in water solution at a concentration of 1 ppm and 10 ppm, isolated and mixed.

Procedure

A methodology was developed by using ion chromatograph consisting of a pump 850 Professional IC Anion MCS-LP-Gradient, a sampler with automatic gun Compact 863 Auto Sampler, a current sensing detector 871 Advanced Bioscan, a device interface 771 Compact IC, and two separation columns Metrosep Carb 1-150 (150x 4.0 mm 5µm particles of a copolymer of polystyrene / divinylbenzene) connected in series. The mobile phase by the chromatographic

system were equilibrated with 50 mM NaOH (Solution A) and eluted with a linear gradient of 500 mM NaAc in 50 mM NaOH according to the elution program (table 1).

Table 1. Experimental conditions - HPLC-PAD.

Time	% A	% B	Flow rate
Start	99	1	0.5 ml/min
20 min	90	10	0.5 ml/min
35 min	99	1	0.5 ml/min
45 min	99	1	1.0 ml/min

RESULTS AND DISCUSSION

Initially commercial standards of acetylated and non acetylated CHO (2-deoxy-2-acetoamido-D-glucose and 2-amino-2-deoxy-D-glucose) with varying DP, from 1 to 6, were injected into the chromatograph and eluted with 50 mM NaOH. However, with this procedure it was found that the retention time (R_t) of some acetylated CHO coincided with the R_t of some deacetylated CHO, impairing a suitable analysis of their mixtures.

We have studied an improvement on the performance of the HPLC conditions in order to better separate the CHO. A gradient mobile phase starting with 50 mM NaOH (Solution A) and linearly eluted with 500 mM NaAc in 50 mM NaOH was tested. Several other trials varying the composition and flow rate of mobile phase to obtain a good separation of CH, with different R_t , but only the conditions described by Table 1 were able to separate and quantify the five different acetylated and the five of the six non acetylated CHO. In our current study, HPLC-PAD conditions of analysis have been optimized to perform quantitative determinations of individual oligosaccharides present in the investigated hetero-CHO's products.

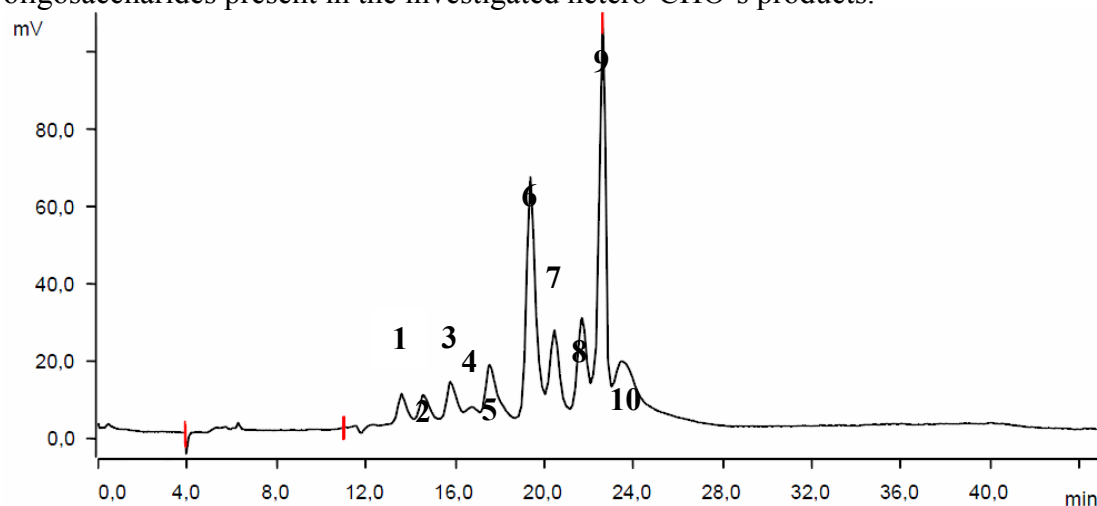


Figure 1. Chromatogram from the optimized method (10 ppm). Peak identification: (1) N-acetyl-D-glucosamine, (2) Di-N-acetylchitobiose, (3) Tri-N-acetylchitotriose, (4) Tetra-N-acetylchitotetraose, (5) Penta-N-acetylchitopentaose, (6) D-glucosamine, (7) Chitobiose, (8) Chitotriose, (9) Chitotetraose, (10) Chitopentaose.

Chitosans with different mol fraction of N-acetylglucosamine (F_A) were hydrolysed enzymatically by crude enzyme extract from *Trichoderma polysporum* and the composition of

the CHO was initially analysed by nanoESI-TOF-MS. Hetero CHO with degrees of polymerisation between 2 and 7 were identified. Currently we are injecting them into HPLC-PAD in order to compare with the previous ESI-TOF-MS results.

The CHO's used for biological studies are usually prepared by enzymatic hydrolysis of the chitosan, clearly yielding complex mixtures of oligomers. These oligomers differ in their degree of polymerization (DP; number of monomer units), as well as in the mole fraction of A residues (that is, homologues) and in the sequences of D and A residues (that is, isomers) [14].

Therefore, HPLC-PAD is a good tool to analyze CHO's and to determine the relative fractions of each individual aminoform. However, as commercially available standards of CHO with a large range of DP and F_A are not commercially available, it is difficult to determine and quantify a broad mixture of CHO, when new peaks are shown. Then, mass spectrometry (MS) would be a valuable tool to provide direct structural information about the CHO's population. It is not possible to directly integrate HPLC-PAD with MS, because the high salt concentration of mobile phase will interfere with the sample identification and overall sensitivity. Ideally, MS such as Nanoelectrospray quadrupole time-of-flight tandem mass spectrometry (nanoESI-Q-ToF-MS/MS), would be used to identify peaks of interest in HPLC-PAD after collecting and desalting the fractions. One way to directly analyze the HPLC-PAD mobile phase by MS would be with the use of an in-line membrane-desalting device. This would eliminate the need for collecting the fractions and desalting the sample, as a reverse phase HPLC coupled to a mass spectrometer [15].

CONCLUSION

The study consisted of varying the composition and flow rate of mobile phase to obtain the best separation patterns chito-acetylated and no acetylated oligosaccharides with degree of polymerization from 1 to 6. The developed analytical method by ion chromatography allowed the separation and quantification of a mixture of 10 chito-acetylated and deacetylated CHO.

ACKNOWLEDGMENTS

Financial support by the Brazilian funding agencies FAPESP, CAPES and CNPq is gratefully acknowledged.

REFERENCES

- [1] Aam, B. B., Heggset, E. B., Norberg, A. L. et al. (2010) Production of chitoooligosaccharides and their potential applications in medicine. *Marine Drugs*, 8, 1482–1517.
- [2] Deters, A., Petereit, F., Schmidgall, J. et al. (2008) N-Acetyl-D-glucosamine oligosaccharides induce mucin secretion from colonic tissue and induce differentiation of human keratinocytes. *Journal of Pharmacy and Pharmacology*, 60, 1-8.
- [3] Liang, T. W., Chen, Y. J., Yen, Y. H. et al. (2007) The antitumor activity of the hydrolysates of chitinous materials hydrolyzed by crude enzyme from *Bacillus amyloliquefaciens* V656. *Process Biochemistry*, 42, 527-534.
- [4] Wang, S. L., Lin, T. Y., Yen, Y. H. et al (2006) Bioconversion of shellfish chitin wastes for the production of *Bacillus subtilis* W-118 chitinase. *Carbohydrate Research*, 341, 2507-2515.
- [5] Dos Santos, A. L., El Gueddari, N. E. & Moerschbacher, B. M. (2008) Partially acetylated chitosan oligo- and polymers induce an oxidative burst in suspension cultured cells of the gymnosperm *Araucaria angustifolia*. *Biomacromolecules*, 9, 3411-3415.

- [6] Abd-Aziz, S., Sin, T. L., Alitheen, N. et al (2008) Microbial degradation of chitin materials by *Trichoderma virens* UKM1. Journal of Biological Sciences, 8, 52-59.
- [7] Silva, L. C. A., Honorato, T. L., Franco, T. T. et al (2010) Optimization of chitosanase production by *Trichoderma koningii* sp. under solid state fermentation. Food and Bioprocess Technology, article in press.
- [8] Binod, P., Sandhya, C., Suma, P. et al (2007) Fungal biosynthesis of endochitinase and chitobiase in solid state fermentation and their application for the production of N-acetyl-D-glucosamine from colloidal chitin. Bioresource Technology, 98, 2742- 2748.
- [9] Ramirez-Coutiño, L., Espinosa-Marquez, J., Peter, M. G. et al (2010) The effect of pH on the production of chitinolytic enzymes of *Verticillium fungicola* in submerged cultures. Bioresource Technology, 101 (23), 9236-9240.
- [10] Hernalsteens, S. & Maugeri, F. (2010) Partial Purification and Characterization of Extracellular Fructofuranosidase with Transfructosylating Activity from *Candida* sp. Food Bioprocess Technol, 3, 568–576.
- [11] Jardim, I. C. S. F., Collins, C. H. & Guimarães, L. F. L. (2006) Princípios básicos de cromatografia. In Fundamentos de cromatografia (Collins, C. H., Braga, G. L. & Bonato, P. S. Ed.) pp. 273-397, Editora Unicamp.
- [12] Rocklin, R. D. & Pohl, C. A. (1983) Determination of carbohydrates by anion exchange chromatography with pulsed amperometric detection. J. Liq. Chromatogr. 6: 1577–90.
- [13] Cheng, X. & Kaplan, L. A. (2003) Simultaneous Analyses of Neutral Carbohydrates and Amino Sugars in Freshwaters with HPLC–PAD. Journal of Chromatographic Science, 41, 434-438.
- [14] Cederkvist, F. H., Zamfir, A. D., Bahrke, S. et al (2006) Identification of a High-Affinity-Binding Oligosaccharide by (+) Nanoelectrospray Quadrupole Time-of-Flight Tandem Mass Spectrometry of a Noncovalent Enzyme–Ligand Complex. Angewandte Chemie Internacional, 45, 2429 –2434.
- [15] Adamo, M., Qiu, D., Dick Jr., L. W. et al (2009) Evaluation of oligosaccharide methods for carbohydrate analysis in a fully human monoclonal antibody and comparison of the results to the monosaccharide composition determination by a novel calculation. Journal of Pharmaceutical and Biomedical Analysis, 49, 181–192.

USE OF CHITOSAN AS COAGULANT IN THE REMOVAL OF NATURAL ORGANIC MATTER FROM FOUR DIFFERENT RAW WATERS

I. Garcia^{1,2*}, M. Benavente^{1,2}, L. Moreno²

¹*Faculty of Chemical Engineering, National University of Engineering (UNI), PO Box 5595, Managua, Nicaragua.*

E-mail: indianag@kth.se

²*Department of Chemical Engineering and Technology, Royal Institute of Technology (KTH), SE-100 44 Stockholm, Sweden.*

E-mail: lm@kth.se

INTRODUCTION

Nicaragua makes use of conventional treatment in the ten drinking water plants located in the central region of the country. The treatment plants use surface water as raw water sources and employ an inorganic salt such as aluminium sulphate for the coagulation process. Sources from surface waters in Nicaragua have low concentrations of natural organic matter in the dry season and the opposite in the rainy season; fulvic acid being predominant in the humic fraction [1]. However, due to the rainfall increment and anthropogenic activities, the NOM concentration has increased in recent years, reducing the performance of the drinking water plants working with conventional technology. The concern when removing more NOM in the drinking water plant of Nicaragua is to avoid the formation of disinfection by-products related to carcinogenic diseases [2].

Some studies have indicated that chitosan may be used in the production of drinking water [3, 4]; but, the majority of these studies have been done on a laboratory scale using synthetic water prepared with humic or fulvic acid or natural water. The aim of this study has been to assess the performance of chitosan as coagulant in the removal of NOM compared with that of aluminium sulphate using raw water sources from four Nicaragua drinking water plants.

MATERIALS and METHODS

Raw water

Raw water samples were taken from four drinking water plants, three of them from river sources (Boaco, Camoapa and Santo Tomas) and Juigalpa raw water from the Nicaragua Lake. Six samples were collected in the rainy season (May to August 2009), when the NOM concentration is high especially in the surface water.

Analytical determinations

Colour (HACH method 8025), dissolved organic carbon (DOC) (HACH method 10129), ultraviolet absorbance at 254 nm (UV₂₅₄) (HACH 10054), were determined in the laboratory. Specific ultraviolet absorbance (SUVA) and specific colour were calculated [5, 6]. All samples were treated according to the requirements for each analysis and the respective procedures as described in Standard Method (SM) and HACH analysis handbook [7, 8]. Each determination was carried out in duplicate.

Chitosan preparation for the coagulation experiments

Chitosan solution was prepared by adding chitosan powder to 100 mL of 0.1 M HCl. This solution was kept stirred overnight to ensure the total dissolution of the chitosan powder.

Deionized water was added to a volume of 1 L. 1 mL of this solution was equivalent to 1 mg of chitosan. A fresh solution was prepared daily.

Aluminium sulphate (AS) preparation

The type of aluminium sulphate ($\text{Al}_2(\text{SO}_4)_3 \cdot 18\text{H}_2\text{O}$) used at the drinking water plants was used. A stock solution was prepared where 1 mL of this solution was equivalent to 10 mg of aluminium sulphate.

Coagulation experiments

Coagulation experiments were performed using jar tests (Phipps and Bird[®]) at room temperature (22°C). The volume of raw water in each jar was 2 L. To compare the performances of aluminium sulphate and chitosan as coagulants, different dosages of aluminium sulphate (10, 20, 30, 40, 50, and 60 mg/L) and of chitosan (2, 4, 6, 8, 10 and 12 mg/L) were used. In preliminary experiments, it was found that a dose of aluminium sulphate greater than 60 mg/L did not significantly increase the NOM removal. In the coagulation experiments, a rapid mixing at 100 rpm for one minute was applied to disperse the coagulant, followed by flocculation with slow mixing at 30 rpm for 30 minutes, and settling for 1 hour. Aliquots of the supernatant liquid were taken from each jar to measure the different parameters and to carry out disinfection after the filtration step.

RESULTS and DISCUSSION

The values presented in this section are the averages for the whole sampling period (six runs). In each coagulation run, the jar selected was that with the higher UV_{254} removal. This parameter was chosen because it is widely used to characterize the aromatic content of NOM, since this fraction is more reactive with chlorine.

Raw water characteristics

Table 1 shows the average quality of the four raw water sources. Three of the waters were from river sources (Boaco, Camoapa and Santo Tomas) and Juigalpa was from a lake. The results show that the four raw waters have different values of the inorganic and organic parameters, presumably because the inputs of contaminant from urban, agricultural or geological areas to the catchments of these sources are very different.

NOM was determined indirectly by surrogate parameters such as colour, UV_{254} , DOC, SUVA and specific colour. These parameters characterize the complex mixture of organic matter present in the waters. The type of soil and vegetation in the surrounding catchment area and seasonal variations will influence the NOM present in river and lakes.

The aromaticity of the organic matter measured as UV_{254} varied widely from 0.076 to 0.355 1/cm depending on the raw water source. The lowest value was found in the lake water, and the higher values in the river water. Dissolved organic carbon (DOC) varied in the same way as UV_{254} . DOC has been commonly reported in a range from 2.0 to 15.0 mg/L [9]. The river sources showed high DOC values because the samples were taken during rainy season; indicating that organic matter present in the raw water is of the humic fraction type. Santo Tomas presented the highest UV_{254} and DOC values, which means that this water is more reactive with chlorine and therefore more THM formation can be expected than in the other sources.

The SUVA data for these sources denote a mixture of aquatic humic and other NOM, as well as a combination of hydrophobic and hydrophilic compounds of different molecular weights, since the SUVA values are in the range of 2-4 L/mg-m [5]. High SUVA values in these raw waters indicate that the DOC contained more aromatic compounds.

Colour is an indicator of a high degree of conjugation in the complex molecules of NOM having multiple bonds with highly substituted aromatic groups. It is linked to the higher molecular weight of NOM [6]. True colour concentrations are quite high in these sources, indicating an elevated content of organic matter. There is a strong relationship between the intensity of rainfall and NOM concentration, since the increased run-off leads to a higher NOM discharge from the upper parts of the soil profile. After heavy rainfall, highly coloured water can be observed in these sources because of the large amount of rich organic matter such as tannin.

Table 1. Raw water characteristics

Parameters	River Water			Lake Water
	Boaco	Camoapa	Santo Tomas	Juigalpa
UV ₂₅₄ (1/cm)	0.257±0.082	0.158±0.047	0.355±0.096	0.076±0.021
DOC (mg/L)	8.5±2.5	5.3±1.4	11.5±3.4	2.7±0.8
SUVA (L/mg-m)	3.0±0.6	3.0±0.7	3.1±0.3	2.8±0.7
Colour (mg/L Pt-Co)	240.0±80.4	132.3±55.5	269.3±86.1	44.8±11.8
Specific Colour (mg Pt-Co/mg C)	28.2±2.7	25.0±7.2	23.4±2.3	16.6±2.6

The Juigalpa raw water had the lowest degree of conjugation or aromatic group substitution, its specific colour value being 16.6 mg Pt-Co/mg C, which is lower than the value between 23.4 and 28.2 mg Pt-Co/mg C for the river water.

The highest NOM surrogate parameters values were found in the Santo Tomas and the lowest in the Juigalpa water sources. The difference found between rivers and lake water could be because lakes or reservoirs disperse the high organic content by mixing, while higher NOM concentration are found in free flowing river sources as a result of rainfall [10]. Another explanation may be that the internal NOM production in the Nicaragua Lake is low at the intake point because the nitrogen and phosphorus concentrations are low, since there is no pollution from domestic or industrial effluents.

NOM removal by coagulation with aluminium sulphate or chitosan

Table 2 presents the percentage removal of the surrogate NOM parameters after aluminium sulphate (AS) or chitosan (Ch) had been used as coagulant in the four raw waters.

Chitosan gave slightly higher UV₂₅₄ removal than aluminium sulphate for the river water, but the UV₂₅₄ removal in the Juigalpa water was higher with aluminium sulphate, although this removal was less than that from the river waters. The greater reduction of UV₂₅₄ with chitosan is because this compound acts as both coagulant and flocculant, so that the interaction with dissolved and particulate substances in the water is very efficient. Aluminium sulphate is less efficient because it acts only as a coagulant [11].

The greatest UV₂₅₄ reduction was observed in the Santo Tomas water, where 85.1% and 87.0 % of UV₂₅₄ removal were found with aluminium sulphate (50 mg/L) and chitosan (12 mg/L) respectively. In general, the UV₂₅₄ removal with aluminium sulphate was in the range 80-90% mentioned by Edzwald [12]. The UV₂₅₄ reduction using chitosan was in the interval 68.4-87.0 %, which is much higher than the values of 30-60% reported by Rizzo et al. [3]. Lower dosages of chitosan are necessary to destabilize NOM substances than aluminium sulphate due to the high charge density of the amino groups in the chitosan. The NOM still available in the water can indicate the amount of chlorination by-products to be formed in the disinfection step due to the aromaticity of this NOM fraction. The residual UV₂₅₄ after coagulation is mainly non-humic material but it is still quite reactive with chlorine.

The removal of dissolved organic carbon (DOC) was less than the removal of colour, and UV₂₅₄. The removal was 60.4% to 78.3% with aluminium sulphate, and 55.6% to 82.6% with

chitosan (Table 2). These values however exceeded those given by Edzwald and Tobiason [5] of about 25-50% when SUVA is between 2 and 4 and aluminium sulphate is used as coagulant. According to Sharp et al. [13], DOC removal is in the range of 10-90% when aluminium sulphate is used as coagulant. Most of the DOC removal occurs at dosages below 40 mg/L of aluminium sulphate, or 6 mg/L of chitosan. The percentage removal of DOC is slightly higher with chitosan than with aluminium sulphate for the river waters and the opposite for lake water. Machenbach [14] pointed out that chitosan is a poor coagulant for water with organic matter of low molecular weight like the Juigalpa water. The highest DOC removals were found in the river waters that had a high DOC concentration. The richer the water is in humic compounds, the greater is their removal due to their high molecular weight, lower solubility and size.

The colour removal for the river waters was greater than the range of 50-80% reported by Hakonsen et al. [4] with chitosan, and very close to the value of 90% using aluminium sulphate reported by Bratby [15]. In the Juigalpa lake water, the colour removal with aluminium sulphate was less than that reported by Bratby [15], but the reduction with chitosan agreed with the range reported by Hakonsen et al. [4]. The colour ranges obtained after coagulation treatment were 13.8-28.6 mg/L Pt-Co with AS and 15.2-19.4 mg/L Pt-Co with chitosan.

Table 2. NOM removal, in percentages

Parameters (Percentage Removal)	Boaco		Camoapa	
	AS	Chitosan	AS	Chitosan
UV ₂₅₄	82.9	86.8	77.8	79.7
DOC	77.6	82.4	60.4	66.0
SUVA	23.3	23.3	43.3	40.0
Colour	88.1	92.0	86.3	88.5
Specific Colour	46.5	54.3	65.6	66.4
	Santo Tomas		Juigalpa	
	AS	Chitosan	AS	Chitosan
UV ₂₅₄	85.1	87.0	71.1	68.4
DOC	78.3	82.6	63.0	55.6
SUVA	32.3	25.8	21.4	28.6
Colour	91.4	92.8	69.2	63.4
Specific Colour	60.3	58.5	16.9	17.5

AS: Aluminium Sulphate

SUVA decreased to values of about 2 L/mg-m in most of the treated waters. These values indicate that the treated water might be less reactive with chlorine because the NOM of humic type had been largely removed in the coagulation process. The formation of disinfection by-products such as trihalomethanes will therefore be lower, since most of the organic matter still present is non-humic having a low molecular weight. The lowest SUVA values were observed in the Camoapa river water, whereas high SUVA values were found in the Boaco river water regardless of the coagulant applied. The value of SUVA in the treated waters indicates that most of the NOM compounds of high molecular weight and high hydrophobicity have been removed; the remaining NOM in the coagulated waters is more difficult to remove.

Specific colour decreased greatly in almost all the river waters. The removal was 16.9-65.6% with aluminium sulphate and 17.5-66.4% with chitosan. This implies that the NOM of these treated waters has lower molecular weight and less aromaticity, which agrees with the SUVA results.

CONCLUSIONS

The use of chitosan as an alternative to aluminium sulphate was investigated in order to reduce the pollution in the Nicaragua waters. Four raw water sources used in the production of drinking water were used, three from rivers and one from a lake. The highest NOM removal measured as UV₂₅₄, colour, and DOC was found in the river waters when chitosan was applied instead of aluminium sulphate. Lower NOM removals were found in the lake raw water, where the aluminium sulphate performed better. The reason could be that the river waters have a higher NOM content than the lake water, and that the coagulation process is easier.

ACKNOWLEDGEMENT

The authors thank the Swedish International Development Cooperation Agency (SIDA) for financial support for this research.

REFERENCES

- [1] Garcia, I. and Moreno, L. (2009) Use of GAC after enhanced coagulation for the removal of natural organic matter from water for purification. *Water Science and Technology: Water Supply Journal*, 9(2), 173-180.
- [2] USEPA, National primary drinking water regulations: Disinfectant and disinfection by-products D/DBP, Final Rule, EPA 69389-9476 (1998), Office of Water, U.S. Environmental Protection Agency, Washington, DC.
- [3] Rizzo, L., Di Gennaro, A., Gallo, M., Belgiorno, V. (2008) Coagulation/chlorination of surface water: A comparison between chitosan and metal salts, *Separation Purification Technology Journal*, 62, 79-85.
- [4] Hakonsen, T., Ratnaweera, H., Lindholm, O. (2008) The use of chitosan in water treatment-An evaluation of practical application, *Natural Organic Matter: From source to tap*, Conference Proceedings. Bath, UK. 2-4th September, 123-134.
- [5] Edzwald, J., Tobiasson, J. (1999) Enhanced coagulation: US requirement and a broader view, *Water Science and Technology*, 40(9), 63-70.
- [6] Newcombe, G., Drikas, M., Assemi, S., Beckett, R. (1997) The influence of characterized natural organic material on activated carbon adsorption: I characterization of concentrated reservoir water, *Water Research*, 31(5), 963-972.
- [7] Clescery, L.S., Greenberg, A.E., Eaton, A.D. (1998) *Standard Methods for the Examination of Water and Wastewater*, APHA, 20th Edition, Washington, D.C, ISBN 0-87553-235-7.
- [8] HACH Handbook. www.hach.com
- [9] Hepplewhite, C., Newcombe, G., Knappe, D.R.U (2004) NOM and MIB, who wins in the competition for activated carbon adsorption sites? *Water Science and Technology*, 49(9), 257-265.
- [10] Aiken, G., Chin, Y., O'Loughlin, E. (1994) Molecular weight, polydispersity, and spectroscopic properties of aquatic humic substances, *Environ. Sci. Technol.*, 28, 1853-1858.
- [11] Renault, F., Sancey, B., Badot, P.M., Crini, G. (2009) Chitosan for coagulation/flocculation processes-An eco-friendly approach, *European Polymer Journal*, 45, 1337-1348.
- [12] Edzwald, J.K. (1993) Coagulation in drinking water treatment: Particles, organics, and coagulants. *Water Science and Technology*, 27(11), 27-35.
- [13] Sharp, E.M., Parsons, S.A., Jefferson, B. (2006) The impact of seasonal variation in DOC arising from moorland peat catchment on coagulation with iron and aluminium salts, *Environmental Pollution*, 140, 436-445.
- [14] Machenbach, I. (2007) *Drinking water production by coagulation and membrane filtration*, Doctoral thesis, Norwegian University of Science and Technology. ISBN 978-82-471-3831-1, 77-78.
- [15] Bratby, J. (2006) *Coagulation and flocculation in water and wastewater treatment*, 2nd Edition, IWA Publishing, ISBN: 18433911066, 87-113.

INDUSTRIAL CHITOSAN PRODUCTION – REQUIREMENTS ON PRODUCTION PROCESS, EQUIPMENT AND QUALITY CONTROL

Andreas Heppe, Anke Wunder

BioLog Biotechnologie und Logistik GmbH, Max-Planck-Ring 45, 06188 Landsberg, Germany.

E-mail address: chitosan@biolog-heppe.de

INTRODUCTION

BioLog and Heppe GmbH have developed several chitosan products and application technologies over the last 18 years. BioLog is also working in the development of production technology, production control and equipment development for chitin and chitosan production plants. After the reconstruction of a plant in China, new plants in Thailand and Saudi-Arabia followed. At present 2 new plants are in the planning stage with a capacity of 150 to 200 tons per year.

BioLog company is still focussing on the industrial use of chitosan for application in:

- waste water treatment (flocculants)
- paper and textil industry (coating, sizing agent)
- bioplastics
- chemical industry (paints and varnishes, adhesives)
- agriculture (feed additives, plant growth stimulator)

Main requirements for such applications are a constant quality and a constant price over a long time period. The quality stability is determined by the:

- raw material source
- production management
- automation of the production
- quality control with standard procedures at the producer, processor and customer

The price is mainly controlled by:

- raw material (shells) price
- costs for chemicals
- productivity of the plant
- market (competition of nutraceuticals and glucosamine)

RESULTS and DISCUSSION

Influences on Quality:

BioLog/Heppe GmbH has introduced a standardisation system for chitosan products with the target to describe the parameters of chitosan exactly enough, that the results of R&D work and production tests are traceable for the purchase departments of the companies, who want to

use chitosan for their applications. This system was already presented at the EUCHIS 1999 in Potsdam/Germany.

It seems to be a problem to introduce such a standardisation into the chitosan world, because then the quality and price can be compared between the competitors (platin, gold and silver quality, respectively high, middle and low viscose chitosans).

That would require

- equal measuring and analysing methods,
- equal sample preparation,
- equal equipped measuring devices
- equal maintenance

A lot of discussions between producer, trader and/or customer could be avoided, if the procedures for analysing and sample preparation are known. We have found deviations in test results caused by different procedures, for example:

- degree of deacetylation: sample preparation moisture subtracted or with moisture
- viscosity: influence of temperature, time and speed of stirring, spindle and torque
- ash content: temperature of muffle furnace – preheated oven, sample covered or not, measuring of sample after cooling down.

That's why BioLog supports the initiative of the EUCHIS to introduce a standardisation system for chitosan products.

The quality of the finished chitosan requires a continuous process control. This is especially assured with the automation of the production process and a data logging of the production parameters by a PLC (programmable logic controlling). The following data can be controlled, respectively logged and traced:

- date, time, operator
- raw material source, batch, harvest date
- concentration HCl, NaOH, reaction time, mixer speed, temperature, etc.

Arising quality deviations can be controlled and determined by the operator and production manager, and they can improve the process by changing the production parameters.

Influences on price:

It is difficult for traders and applicants of chitosan products to receive a long term quotation from e.g. Chinese suppliers, because most of them have to purchase the shells from different sources with varying prices. That's why most of the time the quotations are only valid for not more than 4 weeks. Sometimes the raw material amounts about 50% of the chitosan production costs. The fluctuation in the price is not a basis for long termed supplying contracts with industrial customers.

It means on the other hand, that a reliable production is only possible, if there is an own raw material source in sufficient quantity and quality available.

The solution for that is the cooperation with processing factories, which has the advantage, that they would solve their waste disposal problem and have additional to that a value creation. Because chitin and chitosan would be only a by-product for such processing factories and would

need a special marketing, it is advantageous to outsource the marketing to an already existing marketing organisation, which has the access to the chitosan market. Otherwise an own marketing needs to be organised and developed, which would take a lot of effort and time.

Facing all these problems regarding the industrial application of chitosan, BioLog has developed their own production technology with the following targets:

- constant quality
- competitive price
- reliability in contractual relationship
- service for application consultation and product optimisation

Therefore BioLog offers customised projects that take territorial and market conditions into consideration. With a specially developed matrix it is possible to make a projection about the efficiency of an investment, when provided with the data about raw material availability, salary costs, chemicals and other operating materials.

The chitin- and chitosan production, the PLC for the production and the quality control as the core of such production plants is planned, supplied and installed by BioLog. Other components like building, chemical storage, drying place, mill and packaging, supply and disposal lines could be delivered by the customer.

With this system it is possible to set up chitosan production facilities with capacities of 100 to 150 tons chitosan per year using the shells from 7000-10000 tons shrimps. The manual processes are minimised and the workers have mostly controlling functions. Using this system the production of 150 tons chitosan per year is possible with only 12 workers.

Of course the automated process requires a higher qualification level for the workers, especially in regards to understanding the complexity of the process and their actions.

This is why the qualification and training of the operators of the production plants are in special consideration in BioLog's work. For the optimisation of the production process and the process control a consulting contact between operator and technology supplier for at least 1-2 years after the start of production is advantageous.

As a result of this production technology it is possible to produce chitosan with a reliable price, because the high influence of the raw material costs is minimised.

BioLog offers the service of planning and set up of turnkey facilities as well as the technology transfer of several individual components:

- planning and engineering
- plant equipment
- quality control
- qualification and training
- marketing

The interaction of raw material source, production technology and marketing assures a long term economical production, especially suitable for industrial use of chitosan products.

CHITO-OLIGOSACCHARIDES PRODUCED BY CRUDE ENZYME EXTRACT OF *TRICHODERMA POLYSPORUM*

Talita L Honorato¹, Sueli Rodrigues², Bruno M Moerschbacher³ and Telma T Franco^{1*}

¹School of Chemical Engineering – State University of Campinas, UNICAMP – SP, Brazil.

²Departamento de Tecnologia de Alimentos – Universidade Federal do Ceará, Brazil.

³Institute of Plant Biology and Biotechnology – University of Muenster, Germany.

*E-mail address: franco@feq.unicamp.br

INTRODUCTION

Studies on chitin and chitosan have drawn interest due their possible conversion into oligosaccharides, which are water-soluble and could present attractive biological activities. Cost effective methods for the production of potentially bio-active chito-oligosaccharides (COS) are required [1]. *Trichoderma* species are among the most frequently isolated soil fungi and are found in plant root ecosystems [2]. These fungi are opportunistic, avirulent plant symbionts, and function as parasites and antagonists of many phytopathogenic fungi, protecting plants from disease. So far, *Trichoderma* species are among the most studied biocontrol agent fungal and they are commercially marketed as biopesticides and biofertilizers [3]. Their enthomopatogenicity is close related to their ability to synthesize hydrolytic enzymes. Several studies on the production of *Trichoderma* chitinase have been published [4, 5] and most studies are related to *T. harzianum*. To date, there are no reports on the production of chitosanase from *Trichoderma polysporum*. Here, solid state fermentation (SSF) of this strain was employed to produce a rich enzyme raw extract able to produce CHO.

MATERIALS and METHODS

Microorganisms

Trichoderma polysporum was selected between six strain (*Trichoderma harzianum*, *Trichoderma viride*, *Trichoderma koningii* and *Trichoderma polysporum*, *Aspergillus niger* NRRL 322, *Aspergillus niger* NRRL 2270 and *Aspergillus niger* NRRL 2001) isolated by Embrapa Semi-Arido (Petrolina - PE, Brazil) as a biocontrol agent and identified as producers of hydrolytic enzymes (chitinases and chitosanase) from a wide review and selection in CDA medium containing (g L⁻¹): 1.5 Na₂HPO₄, 3.0 KH₂PO₄, 0.5 NaCl, 1.0 NH₄Cl, 0.24 MgSO₄, 0.01 CaCl₂, 20 agar and 10g of chitosan (carbon source) dissolved in 1% acetic acid for detection of strains produced of chitinase and chitosanase under various conditions of pH (4.5, 5.5 and 6.5) at 30 ° C. Microbial growth was visually assessed daily for seven days. The subsequent proceedings were directed towards the solid state fermentation and using the strain that showed the best growth in diameter in cultivation in Petri dishes.

Optimization of chitosanase production

T. polysporum was cultivated in solid substrate containing wheat bran, commercial chitosan, and 2.5 mL of a mineral saline solution containing NaNO₃ (1.0 g/L); (NH₄)₂HPO₄ (1.0 g/L); MgSO₄·7H₂O (1.0 g/L); NaCl (1.0 g/L). The pH of the mineral solution was adjusted to 5.5 because the best microbial growth in CDA plates was observed at this pH value. The amount of wheat bran, chitosan and moistening water (pH 5.5) were changed according to a faced centered central composite experimental design (Table 1). The medium was autoclaved at 121°C for 15 min, cooled, inoculated with 1 mL of spore inoculums, incubated statically at 30°C for 72 h.

Samples were taken after 48 because after this time the medium of fermentation started to sporulate. Assays were carried out in 250 mL Erlenmeyer's flasks covered with cotton plugs.

Wheat bran was purchased from the local market (Mercado São Sebastião, Fortaleza-CE, Brazil). Commercial chitosan, from shrimp shell with 80 % of deacetylation degree, was purchased from Polymar (Fortaleza-CE, Brazil). Functional relationships (fitted regression models) between the responses and the factors were expressed by a second-degree polynomial function, obtained by multiple regressions, as presented in equation 1. The moisture content of the optimized culture medium was determined according to the AOAC method [6].

$$Y_i = \beta_0 + \sum \beta_i X_i + \sum \beta_{ii} X_i^2 + \sum \beta_{ij} X_i X_j \quad (1)$$

where: Y_i is the response variable; β_0 is a constant; β_i is the coefficient of the linear effect; β_{ii} is the coefficient of the quadratic effect; β_{ij} is the coefficient of the interaction effect, and X_i and X_j are the independent variables.

The best result found in the experimental design was set and chitosan was replaced for shrimp shell waste from commercial shrimp farming operations in Ceará, Brazil, as substrate. Prior to storage, the shells were washed with water and dried for 24 h at 60°C.

Preparation of enzyme extract

Enzymes were extracted from the fermented solid substrate by adding 20 mL of 200 mM, pH 5.5 acetate buffer to the flask and shaking at 27°C, 150 RPM, for 6 min. The enzyme extract was then separated by filtration through analytical filter paper (70 mm) and then through 0.2 μ m pore size Filtropur S (Sarstedt, Nümbrecht, Germany) syringe filters. The filtrate (enzyme extract) was concentrated in Vivaspin20 10,000 MWCO (Sartorius, Goettingen, Germany), desalted on prepacked Seph. G-25 columns (PD-10, Amersham Bioscience), equilibrated with ammonium acetate buffer 50 mM, pH 5.5, eluted with the same buffer and stored in vials at 4°C.

Enzyme activity assay

Chitosanase activity was measured in culture filtrates at the optimal assay conditions, previously determined (pH 5.5 and 50°C), using a solution containing 0.4% (w/v) of chitosan dissolved in sodium acetate buffer (200 mM, pH 5.5) as substrate. The assay was carried out mixing 100 μ L of the crude enzyme with 400 μ L of substrate and incubating for 60 minutes at 50°C. Enzyme activity was determined by measuring the released reducing sugar by the DNS method [7]. Results were expressed in IU per gram of dry substrate (IU/gds). One IU is the amount of enzyme that releases 1 μ mol of reducing sugar per minute at the assay conditions.

Detection of extracellular chitinase activity

SDS-PAGE of the proteins in the enzyme extract was performed according to Laemmli [8]. Protein bands with chitosanolytic activity were detected according to Trudel and Asselin [9] using polyacrylamide gels containing 0.01% (w/v) chitosan with a mol fraction of N-acetylglucosamine (F_A) value of 0.11 or chitosan F_A 0.56. After overnight incubation in 50 mM ammonium acetate buffer (pH 5.2) at 37 °C, overlay gels were incubated for 10 min in a solution containing 0.01% (w/v) calcofluor M2R (Sigma) in 500 mM Tris-HCl (pH 8.9). After 10 min, the calcofluor solution was removed, and the overlay gel was rinsed overnight in distilled water. Lytic zones were visualised by fluorescence under UV light.

Enzymatic hydrolysis assays

The enzyme extract was incubated overnight at 37°C with 2 g L⁻¹ chitosans with three different F_A (0.15, 0.27 and 0.56) in 50 mM, pH 5.5 ammonium acetate buffer. Each hydrolysate was mixed with a solution of ethanol/ammonia (7:3, v/v) in a 1:3 (v/v) proportion. The precipitated fraction was discarded and the supernatant was freeze-dried.

Mass Spectrometry

Nanoelectrospray quadrupole time-of-flight tandem mass spectrometry (nanoESI-Q-ToF-MS/MS) experiments were carried out with a quadrupole time-of-flight (Q-TOF) mass spectrometer (Micromass, Manchester, UK) in the positive ion mode. The QTOF mass spectrometer was interfaced to a personal computer running MassLynx software to control the instrument and to acquire and process the mass spectra. Gas-phase ions were generated from solutions containing approx. $7.5 \text{ pmol } \mu\text{L}^{-1}$ of the analyte material in water/methanol/formic acid (49/49/2, v/v/v) by nanoESI in the positive ion mode using a Z-spray source. Typical source parameters were as follows: source temperature 80°C , desolvation gas (N_2) flow rate of 75 L h^{-1} , capillary voltage potential of 1.1 kV and a cone voltage of 40 V.

RESULTS and DISCUSSION

Optimization of chitosanase production by response surface methodology

Table 1 presents the experimental design carried out to optimize the production of chitosanase by *T. polysporum* in solid-state fermentation. According to the results, the enzyme activity decreased after 48 hours of fermentation in all assays. Table 2 presents the effects of the independent variables on enzyme activity obtained at 48 hours of fermentation. The solid-state fermentation of *T. polysporum* (48 hours) yielded chitosanase activities ranging from 0.29 to 2.44 IU/gds in the experimental planning.

Table 1. Experimental design and chitosanase activity.

Assay	Wheat bran (g)	Chitosan (g)	H ₂ O (mL)	Enzyme activity (IU/gds) 48 h
1	3.0	0.5	3.5	0.84 ± 0.05
2	3.0	0.5	7.5	1.67 ± 0.07
3	3.0	1.5	3.5	1.06 ± 0.01
4	3.0	1.5	7.5	1.21 ± 0.12
5	7.0	0.5	3.5	0.29 ± 0.01
6	7.0	0.5	7.5	0.48 ± 0.10
7	7.0	1.5	3.5	0.30 ± 0.01
8	7.0	1.5	7.5	0.56 ± 0.06
9	1.6	1.0	5.5	2.44 ± 0.06
10	8.4	1.0	5.5	0.39 ± 0.03
11	5.0	0.2	5.5	0.74 ± 0.03
12	5.0	1.8	5.5	0.84 ± 0.18
13	5.0	1.0	2.5	0.42 ± 0.02
14	5.0	1.0	8.5	1.00 ± 0.07
15	5.0	1.0	5.5	0.77 ± 0.07
16	5.0	1.0	5.5	0.79 ± 0.01

The effects of wheat bran and water were statistically significant on enzyme activity where the effect of wheat bran effect was negative, while the effect of water was positive. This result indicates that an increase of water in the solid medium enhanced the production of enzyme, while an increase of wheat bran did not favor the production of enzyme. Chitosan acts as an enzyme inductor, while wheat bran was added to the culture medium because of its high ability to absorb water [10].

Table 2. Effects of the independent variables on chitosanase activity (48 hours of fermentation).

Factor	Effect	Standard Error
Mean/Interception	0.81*	0.16*
Wheat bran (L)	-0.96*	0.12*
Wheat bran (Q)	0.36*	0.15*
Chitosan (L)	0.00	0.12
Chitosan (Q)	-0.08	0.15
Water (L)	0.37*	0.13*
Water (Q)	-0.19	0.18
Wheat bran x Chitosan	0.08	0.16
Wheat bran x Water	-0.13	0.16
Chitosan x Water	-0.16	0.16

*statistically significant at 95 % of confidence interval.

The quadratic effect of wheat bran was positive and statistically significant, meaning that the addition of amounts of wheat bran increase the excretion of enzyme. The interactions between wheat bran and chitosan, wheat bran and water and the interaction between chitosan and water were not statistically significant. The interaction between wheat bran and water was negative and the interaction between wheat bran and chitosan was positive. The simultaneous increase of wheat bran and water and chitosan and water decreased the enzyme activity, while the simultaneous increase of wheat bran and chitosan enhanced the production of enzyme. The ANOVA and the F test showed that the model was statistically significant at confidence level of 95% because the calculated F-value ($F_{9,6} = 9.20$) was higher than the listed F-value ($F_{9,6} = 4.10$) with R^2 value of 0.93. Figure 1 present the response surface graphs built using the fitted model.

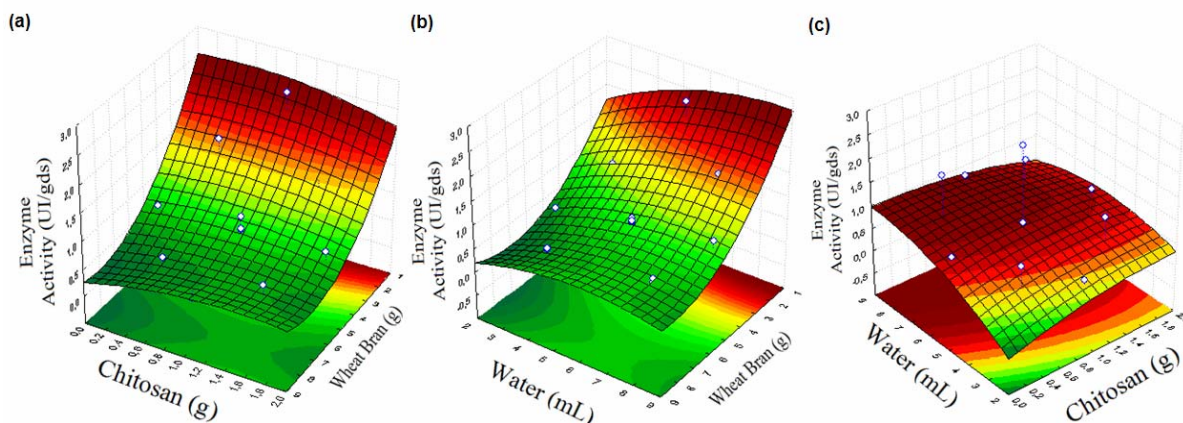


Figure 1. Enzyme activity obtained in the first experimental design after 48 hours of fermentation. (a) As function of wheat bran and chitosan (water = 2.5 mL). (b) As function of wheat bran and water (chitosan = 1.0 g). (c) As function of chitosan and water (wheat bran = 5.0 g).

The enzyme production was enhanced at low wheat bran levels. The enzyme activity was maximal at the surface graph edge (1.0 g of chitosan and 1.6 g of wheat bran) (Figure 1a). The addition of water to the solid medium maximized the activity of the enzyme, when low amounts of wheat bran (1.0 – 3.0 g) were applied (Figure 1b) because of the ability of wheat bran to absorb water [10]. The RSM confirmed that the highest enzyme production was obtained adding water in the range of 5.5 mL. The addition of moistening water directly affected the solid

moisture content, which is a key factor on solid-state microbial growth. The highest enzyme activity was obtained using the low amount of wheat bran (1.6 g) and the values were adjusted and validated to the solid medium containing 1.0 g of chitosan and 2.0 g of wheat bran, yielding 7.22 IU/gds. Moisture of the optimal solid state culture medium (containing 2.0 of wheat bran, 1.0 g of chitosan, 2.5 mL of described mineral solution and 4.0 mL of moistening water was 64.24% according to the AOAC methodology [6]. The optimization production yielded 4.84 IU/gds in a study about the optimization of the production of chitosanase in solid culture using a mixture of wheat bran and chitosan by *T. koningii* [5] indicating a increase of the activity in our optimization.

In the SDS-PAGE result (Figure 2a) is difficult to observe distinct bands but the overlaid native gels with chitosan (Figures 1b and c) showed that *T. polysporum* produces predominant chitinolytic activities for gel overlaid with chitosan F_A0.56 (26 and 77kDa) indicating the presence of chitinases rather than chitosanases. The gel overlaid with chitosan F_A0.11.

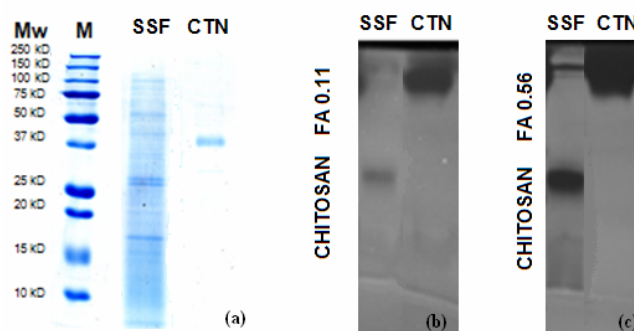


Figure 2. (a) SDS-PAGE analysis of the enzymatic extracts. (b) and (c) Evaluation of chitosanolytic enzyme production during SSF in overlay gel containing 0.01% (w/v), (b) chitosan F_A 0.11, (c) chitosan F_A 0.56. Legend: M – protein molecular marker; SSF – extract of SSF (filtration in paper filter and centrifugation); CTN – chitosanase standard.

The recalcitrant nutrient shrimp shells as sole carbon source. The complexity and cristalinity of the shells may have increased the selectivity of the culture media producing a reduced number of bands corresponding to chitinolytic enzymes which may also suggest that specific oligomers of different bioactivities may be obtained by those specific enzymes. Another work (Ramírez-Coutiño et al., 2006) showed that a close related fungus, *Lecanicillium fungicola*, was selected as a good chitinase producer, and it was used to obtain enzymes in submerged fermentation containing chitin in the medium. Four bands of proteins with molecular weights of 123.1, 85.5, 33.1 and 23 kDa were detected in crude extract by SDS-PAGE, and chitin hydrolysis with crude enzyme was carried out at 40°C and pH 5. Solid state fermentation using *Verticillium lecanii* on a mixture of shrimp waste silage and sugar cane pith bagasse showed the highest *N*-acetylhexosaminidase activity, however, the crude enzymatic extract exhibited a dark colour due to a high content of impurities affecting specific activities (Matsumoto et al., 2004). Important advantages of our present work with *T. polysporum* are the clear appearance not disturbing colorimetric assays and the presence of a reduced number of specific enzymes, more able to target tailor-made products. After 48 h fermentation, we obtained an enzymatic extract with strong activity, and only one-step overnight hydrolysis was necessary to produce CHO.

Three chitosan hydrolysates obtained by a concentrated and a clearer crude extract S4 and the composition of the oligosaccharides was analysed by ESI-TOF-MS (Table 3).

Table 3. Chitosan oligomer profile produced by hydrolysis of chitosan F_A 0.15, 0.27 and 0.56 by enzyme extract S4, identified by ESI TOF Mass Spectrometry.

Oligomers	Degree of polymerisation of chitooligosaccharides						
	DP1	DP2	DP3	DP4	DP5	DP6	DP7
Oligomers obtained by hydrolysis of chitosan F_A 0.15	D ₁ A ₁	D ₂	D ₃ D ₁ A ₂ D ₂ A ₁	D ₄ D ₁ A ₃ D ₂ A ₂ D ₃ A ₁	D ₅ D ₄ A ₁ D ₃ A ₂	D ₆ D ₅ A ₁ D ₄ A ₂	D ₅ A ₂
Oligomers obtained by hydrolysis of chitosan F_A 0.27		D ₂ D ₁ A ₁	D ₃ D ₁ A ₂ D ₂ A ₁	D ₄ D ₁ A ₃ D ₂ A ₂ D ₃ A ₁	D ₅ D ₄ A ₁ D ₃ A ₂ D ₂ A ₃	D ₅ A ₁ D ₄ A ₂ D ₃ A ₃	
Oligomers obtained by hydrolysis of chitosan F_A 0.56	A ₁	D ₂ D ₁ A ₁	D ₁ A ₂ D ₂ A ₁ A ₃	D ₁ A ₃ D ₂ A ₂ D ₃ A ₁ A ₄	D ₁ A ₄ D ₃ A ₂		

Trimers (D₂A₁, D₁A₂) were detected as the most abundant products in the hydrolysate derived from chitosan F_A 0.56, but dimer (D₁A₁) and tetramer (D₂A₂) were also present in considerable intensity. CHO of DP up to 5 were found and surprisingly no fully acetylated dimers were identified, even though these would be expected to be the major products of typical chitinases. The more hydrophobic and less soluble fraction of the hydrolysate may have been removed by centrifugation of the sample, as the solid phase was discharged. A trimer (D₂A₁), two tetramers (D₃A₁, D₂A₂) and two pentamers (D₄A₁, D₃A₂) were the most abundant in the hydrolysate from chitosan of F_A 0.27 in the hydrolysates from chitosan F_A 0.27. For chitosan F_A 0.15, the CHO found were of DP 6 (D₄A₂, D₃A₃) and DP 7 (D₅A₂) though at low intensity. The most abundant CHO in this material were two trimers (D₃, D₁A₂), a tetramer (D₄) and a pentamer (D₅). Most of these were deacetylated, probably due to the high degree of deacetylation of the chitosan used as a substrate. Interestingly, fully deacetylated products require the cleavage of a glycosidic bond between two glucosamine units and, thus, the presence of a chitosanase.

According to the literature, crude fungal enzyme extracts (*Trichoderma viride* and *Acremonium cellulolyticus*) hydrolysed chitin but as their main target was just to produce GlcNAc [11] there was no further detailed information. The results of the degradation of chitosans by bacterial chitinase from *Serratia marcescens* overexpressed in *Escherichia coli* [12] showed that the size distribution of the product mixtures shifts towards higher oligomer lengths for substrates with lower F_A values and, thus, longer and noncleavable stretches of consecutive D-units. A similar behaviour using chitosan with lower F_A was found here in our work, as shown by MS (Table 3) however we used non purified enzyme.

Fifteen fungal strains were evaluated for endochitinase and chitobiase production under solid-state fermentation using agro-industrial residues whereas *Trichoderma harzianum* TUBF 927 showed maximum chitobiase activity [13] but the highest efficiency was obtained when endochitinase and chitobiase were used in combination [14]. Here, *T. polysporum*, isolated and provided by Embrapa, was able to produce enzymes by solid state fermentation of shrimp shell was effective, and the produced enzymes degraded chitosan of different F_A . Higher DP oligosaccharide products were obtained when the substrate of the enzymatic hydrolyse had low F_A , indicating the presence of mainly chitinase activity. We decided to study the feasibility of using solid state fermentation (SSF) for the production of a suitable enzyme extract for the eventual obtention of CHO. We detected the presence of chitinase rather than chitosanase activity

and the production of hetero-oligomers with degrees of polymerisation between 2 and 7. The bio-activities of these oligomer mixtures are currently under investigation.

ACKNOWLEDGEMENTS

This research was supported by São Paulo Research Foundation – FAPESP, The National Council for Scientific and Technological Development (CNPq), Coordination for the Improvement of Higher Level Personnel (Capes) – German Academic Exchange Service (DAAD) and the European Union (EU) through its PolyModE project.

REFERENCES

- [1] Lin, S-B., Chen, S-H. & Peng, K-C. (2008) Preparation of antibacterial chito-oligosaccharide by altering the degree of deacetylation of β -chitosan in a *Trichoderma harzianum* chitinase-hydrolysing process. *Journal of the Science of Food and Agriculture*, 89, 238–244.
- [2] Harman, G. E., Howell, C. R., Viterbo, A. et al. (2004) *Trichoderma* species-opportunistic, avirulent plant symbionts. *Nature Reviews. Microbiology*, 2, 43–56.
- [3] Vinale, F., Sivasithamparamb, K., Ghisalbertic, E. L., et al. (2008) *Trichoderma*–plant–pathogen interactions. *Soil Biological Biochemistry*, 40, 1–10.
- [4] Binod, P., Sandhya, C., Suma, P. et al. (2007) Fungal biosynthesis of endochitinase and chitobiase in solid state fermentation and their application for the production of N-acetyl-D-glucosamine from colloidal chitin. *Bioresource Technology*, 98, 2742- 2748.
- [5] Silva, L. C. A., Honorato, T. L., Franco, T. T. et al. (2010) Optimization of chitosanase production by *Trichoderma koningii* sp. under solid state fermentation. *Food and Bioprocess Technology*, Article in Press.
- [6] AOAC—Association of Official Analytical Chemists (2010) In official methods of analysis (18th ed.). Washington: Association of Official Analytical Chemists.
- [7] Miller, G. L. (1959) Use of dinitrosalicylic acid reagent for determination of reducing sugar. *Analytical Chemistry*, 31, 426–428.
- [8] Laemmli, U. K. (1970) Cleavage of Structural Proteins during the Assembly of the Head of Bacteriophage T4. *Nature*, 227, 680-685.
- [9] Trudel, J. & Asselin, A. (1989) Detection of chitinase activity after polyacrylamide gel electrophoresis. *Analytical Biochemistry*, 178, 362-366.
- [10] Cavalcante, R. S., Lima, H. L. S., Pinto, G. A. S. et al. (2008) Effect of moisture on *Trichoderma* conidia production on corn and wheat bran by solid state fermentation. *Food and Bioprocess Technology*, 1, 100–104.
- [11] Sashiwa, H., Fujishima, S., Yamano, N. et al (2003) Enzymatic production of N-acetyl-D-glucosamine from chitin. Degradation study of N-acetylchitoooligosaccharide and the effect of mixing of crude enzymes. *Carbohydrate Polymers*, 51, 391–395.
- [12] Sørbotten, A., Horn, S. J., Eijssink, V. G. H. et al (2005) Degradation of chitosans with chitinase B from *Serratia marcescens* Production of chito-oligosaccharides and insight into enzyme processivity. *FEBS Journal*, 272, 538– 549.
- [13] Binod, P., Sandhya, C., Suma, P. et al. (2007) Fungal biosynthesis of endochitinase and chitobiase in solid state fermentation and their application for the production of N-acetyl-D-glucosamine from colloidal chitin. *Bioresource Technology*, 98, 2742- 2748.

OPTIMIZATION OF EXPRESSING RECOMBINANT CHITINASE, ASCHI61

Tsung-Han Lin¹, Chao-Lin Liu², Ruey-Shin Juang^{1*}

¹Department of Chemical Engineering and Materials Science, Yuan Ze University, Taiwan

²Department of Chemical Engineering and Graduate School of Biochemical Engineering, MingChi University of Technology, New Taipei City 24301, Taiwan

*E-mail address: rsjuang@saturn.yzu.edu.tw

INTRODUCTION

Chitin, a β -1,4-linked, insoluble linear polymer of *N*-acetylglucosamine (GlcNAc), is the second most abundant polysaccharide on the earth following cellulose. It is a major component of most fungal cell walls, insect exoskeletons and the shells of crustaceans [1]. This polysaccharide is found in fungi, algae, and especially in the exoskeletons of insects and crustaceans. The biodegradation of chitin is very slow. The turnover of chitin in the aquatic biosphere is enormous and mediated by chitinolytic bacteria [2]. Derivatives of chitin, inclusive of polysaccharides, oligosaccharides, and monosaccharides, have been shown to play a role in plant organogenesis and embryogenesis of invertebrates [3]. Recently, chitin oligosaccharides have been investigated to enhance the functions of immunological system in the host animal and they might display tumoricidal agents [4]. The physiology effects of chitin-oligosaccharides vary with the number of the oligomerization. Usually, the hexamers is the most significant [5]. A chitinase, ASCHI61, that produces hexameric chitin oligosaccharides has been identified and expressed in *Escherichia coli* system.

In recent years, numerous recombinant proteins used for industrial, agricultural or biomedical applications have increased dramatically. In the market, mass production of the recombinant proteins has a remarkable demand. *E. coli* is as a host for the rapid and economical production of recombinant proteins. These advantages, accompanied with a genetic and biochemical knowledge, have enabled the some economically applications of protein production, such as insulin and bovine growth hormone. These requirements have directed the development of a plenty of strategies for accomplishing recombinant proteins with high level expression. The efficiency of recombinant protein expression in *E. coli* is determined by various parameters [6]. Some are target protein specific (protein construct length and expression vector), while another is related to fermentation conditions (media type and fermentation time). In addition, another is protein induction conditions (inducer concentration and induction time). And the others are environmental factors related with the host growth and protein expression. Those are incubation temperature, oxygen-transfer rate, and pH [7].

In this study, the expression vectors were evaluated and then statistical design of experiments was performed for investigating the interactions between these parameters for the optimization of expressing recombinant chitinase, ASCHI61. The factors included inducer concentration, induction time, temperature, pH, and stirring rate. The interaction between temperature and stirring rate as well as inducer concentration and induction time plays crucial roles.

MATERIALS and METHODS

Chemicals

Chitin azure, chitinases from *Streptomyces griseus* as standard, and other chemicals, were purchased from the Sigma Chemical Co. (St. Louis, MO).

Bacteria culture medium

There are 10 g/L tryptone, 5 g/L yeast extract, and 10 g/L NaCl in Luria-Bertani (LB) medium.

Bacterial culture and protein measurements

The microorganism expressing recombinant ASCHI61, which is *E. coli* BL21 (DE3) expressing a secretory recombinant chitinase, was grown at 25°C in the medium with ampicillin and chitinase expression induced with isopropyl- β -D-thiogalactopyranoside (IPTG). The growth media were harvested for chitinase activity assays.

Protein concentration was determined by measuring the absorbance at 280 nm, and a Pierce BCA kit (Rockford, IL) using bovine serum albumin as a standard [8].

Bacteria growth curve

The *E. coli* growth curve was performed in LB medium with ampicillin. The overnight inoculation culture was diluted 50 times in fermentation. The optical density of culture reached was determined at 600 nm.

Measurements of chitinase activity

The chitin azure powder (4 g) was suspended in 40 mL of 37% (v/v) HCl for 50 min. Then, 1 L of distilled water was tardily added to the suspension. The pellet was collected and washed with distilled water. After suspension, the suspension was centrifuged with 8,000 x g for 20 min. Then colloid chitin azure was sterilized by autoclaving when the pH reached 3.5.

The samples were incubated with 3 mg/mL colloid chitin azure in 0.2 M potassium phosphate buffer at 25°C. The enzyme activity was terminated with boiling for 5 min. The absorbance of the supernatant was measured at 560 nm after the reaction mixture was centrifuged with 13,000 x g for 5 min. The enzyme activity was determined by using *S. griseus* chitinase as a standard [9].

RESULTS and DISCUSSION

Expression vector determination

Expression vector is the target protein specific factor for recombinant protein production. The ASCHI61 gene was subcloned into pET 15b, pET 22b, and pGEX-2T expression vector, respectively. The expression vectors with ASCHI61 gene were transformed into the *E. coli* DH5 α for pGEX expression system and BL21 (Δ DE3) for pET expression system. After induction with 1 mM IPTG, the culture was harvested every hour. The proteins of lysate were analyzed on SDS-PAGE. The recombinant ASCHI61 over-expressed in the pET 22b was observed (Fig. 1). But there were faint bands of recombinant ASCHI61 in the pET 15b and pGEX-2T (data not shown). Hence, the fermentation parameters of recombinant ASCHI61 were investigated in *E. coli* with pET 22b.

Basic factors of protein expression in E. coli with pET 22b-ASCHI61

For the basic knowledge of the *E. coli* BL21 (Δ DE3) with the ASCHI61 expression vector, the growth curve was measured (Fig. 2). The logarithmic phase was between 100 and 300 min. Also, the optimal onset for induction was 220 min.

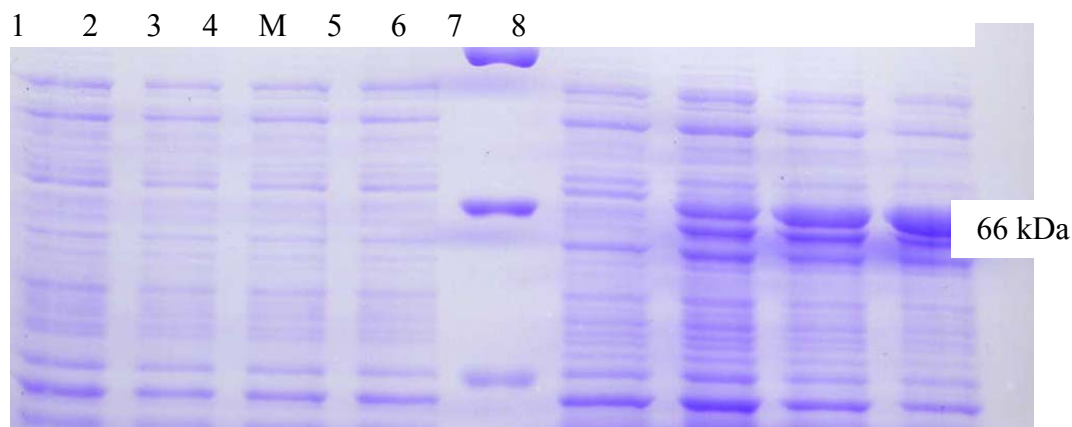


Figure 1. Recombinant ASCHI61 was over expression in *E. coli*. Lane, M, protein standard; Lanes 1-4, pET 22b only induction with IPTG for 0, 1, 2, and 3 h; Lanes 5-8, pET 22b-ASCHI61 induction with IPTG for 0, 1, 2, and 3 h

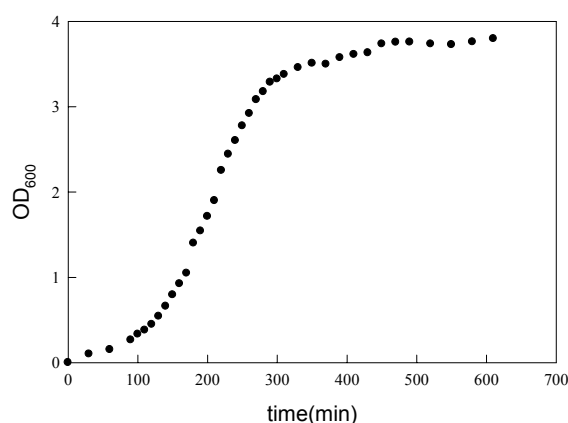


Figure 2. The growth curve of *E. coli* BL21 with pET 22b-ASCHI61

After induction, the total protein and enzyme activity were determined for 6 h (Figs. 3 and 4). The total protein only increased dramatically in 1 h after induction. However, the activity reach peak points around 3 h after induction. Those results indicated the optimal duration for investigation was around 8 h.

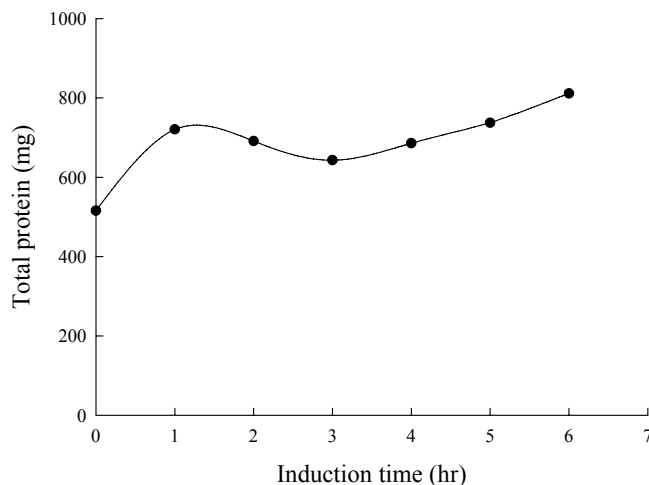


Figure 3. Total proteins of *E. coli* BL21 with pET 22b-ASCHI61 after IPTG induction

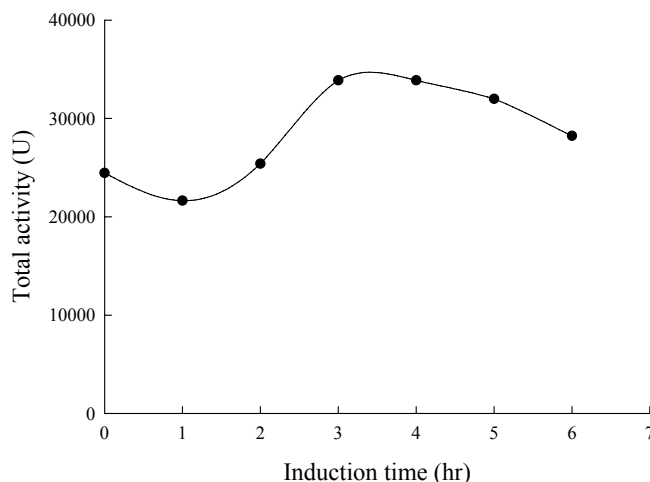


Figure 4. The chitinase activity of *E. coli* BL21 with pET 22b-ASCHI61 after IPTG induction

Screening experiments

The objective was to rapidly explore the effect of a wide range of factors on ASCHI61 activity. Some factors were sacrificed at this stage for identifying the main factors rapidly. The parameters were shown in Table 1. Fractional factors were designed by 2-level factors with Minitab. The total chitinase activity was determined as the response. The data from the experiments were collected and analyzed (Fig. 5). The present results have shown the interactions among temperature, stirring rate, inducer concentration, and induction time were significant.

Table 1. The factors and the level in the experiment design

Symbol	Factor	High level	Low level
A	pH	8	6
B	Temperature (°C)	35	25
C	Stirring rate (rpm)	400	200
D	Inducer concentration (mM)	3	0.1
E	Induction time (h)	10	2

In this work, the optima conditions for the recombinant ASCHI61 expression were investigated. The target protein specific factor, vector, was determined as pET 22b. In addition, the inductions time and duration were also evaluated as the factors related to protein induction condition. Finally, the complicated parameters, environment conditions interaction was simplified by experiment design. The interaction between temperature and stirring rate is one of the significant factors. The other is the interaction between inducer concentration and induction time. The optimal condition will be elucidated by response surface methods.

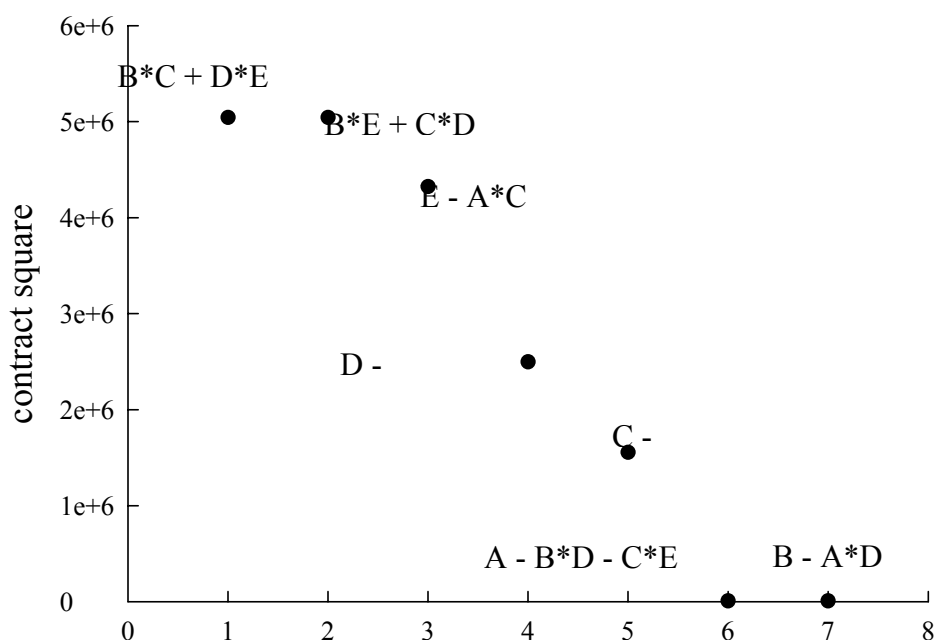


Figure 5. The screed plot for the parameter analysis on ASCHI61 expression in *E. coli* BL21

REFERENCES

- [1] Tanaka, T., Fukui, T., and Imanaka, T. (2001) Different cleavage specificities of the dual catalytic domains in chitinase from the Hyperthermophilic Archaeon *Thermococcus kodakaraensis* KOD1. *J. Biol. Chem.*, 276, 35629-35635.
- [2] Lonhienne, T., Mavromatis, K., Vorgias, C.E., Buchon, L., Gerday, C., and Bouriotis, V. (2001) Cloning, sequences, and characterization of two chitinase genes from the Antarctic *Arthrobacter* sp. Strain TAD20: Isolation and partial characterization of the enzymes. *J. Bacteriol.*, 183, 1773-1779.
- [3] Bakkers, J., Semino, C.J., Stroband, H., Kijne, J.W., Robbin, P.W. and Spaink, H.P. (1997) An important developmental role for oligosaccharides during early embryogenesis of cyprinid fish. *Proc. Natl. Acad. Sci. USA*, 94, 7982-7986.
- [4] Suzuki, K., Mikami, T., Okawa, Y., Tokoro, A., Suzuki, S., and Suzuki, M. (1986) Antitumor effect of hexa-*N*-acetylchitohexaose and chitohexaose. *Carbohydr. Res.*, 151, 403-408.
- [5] Shahidi, F., Arachchi, J.K.V., and Jeon, Y.J. (1999) Food applications of chitin and chitosans. *Trends Food Sci. Technol.*, 10, 37-51.
- [6] Jana, S., and Deb, J.K. (2005) Strategies for efficient production of heterologous proteins in *Escherichia coli*. *Appl. Microbiol. Biotechnol.*, 67, 289-298.
- [7] Islam, R.S., Tisi, D., Levy, M.S., and Lye, G.J. (2007) Framework for rapid optimization of soluble protein expression in *Escherichia coli* combining microscale experiments and statistical experimental design. *Biotechnol. Prog.*, 23, 785-793.
- [8] Yang, C.J., Liu, Y.K., Liu, C.L., Shen, C.N., Kuo, M.L., Su, C.C., Tseng, C.P., Yen, T.C., and Shen, C.R. (2009) Inhibition of acidic Mammalian chitinase by RNA interference suppresses OVA-sensitized allergic asthma. *Hum. Gene Ther.*, 20, 1597-1606.
- [9] Shen, C.R., Chen, Y.S., Yang, C.J., Chen, J.K. and Liu, C.L. (2010). *J. Biomol. Screen*, 15, 213-217.

MUTUAL INFLUENCE OF CHITOSAN AND POLYMETHYLACRYLATE ON THE PHYSICAL-CHEMICAL PROPERTIES OF BIODEGRADABLE COMPOSITIONS

**I.N. Kalashnikov*, V.F. Uryash, L.A. Smirnova, N.Yu. Kokurina, A.E. Mochalova,
V.F. Smirnov, O.N. Smirnova, V.N. Larina, N.E. Cverova**

*Research Institute of Chemistry, Nizhny Novgorod State Universit,
Nizhny Novgorod, Russia*

**E-mail: ltch@ichem.unn.ru*

INTRODUCTION

Recently, much attention is paid to the preparation of polymeric composites based on natural (chitin, chitosan, starch, cellulose) and synthetic polymers. The advantage of such hybrid polymer composites is their adjustable resistance to the action of microorganisms, which allows to obtain biological stability of the composition as well as on the contrary, is easily biodegradable. For purposeful design of such compositions need to know their physical and chemical properties, as well as the mutual influence of components on these characteristics. In this regard, we have synthesized block-copolymers of crab chitosan (ChTS) with methylacrylate (MA). The above compositions were exposed to fungi "*Aspergillus terreus*".

MATERIALS AND METHODS

By differential thermal analysis (DTA) in the $-190-350^{\circ}\text{C}$ studied the physical and chemical properties of hybrid polymer composites based on ChTS and PMA. The DTA was chosen as the method for investigating physical-chemical properties of the polymer compositions. The design of the device and the experimental technique are described in [1]. Quartz served as a reference. The charges of the specimen and the reference were 0.2–0.3 g. The specimen temperature and the temperature difference between the specimen and the reference were measured with a chromel-copel thermocouple with an error of 0.5 degrees. The thermocouple was calibrated using a reference platinum resistance sensor and reference substances within the entire temperature range. The experiment was carried out in the helium atmosphere. The heating rate in the experiments was 5 degrees/min. A deviation from linearity did not exceed 1%. Three heating and cooling cycles were accomplished for each specimen. After the first heating up to 150°C , the adsorbed water was removed from the specimen by vacuumization directly in the thermal chamber of the DTA setup and its concentration was determined by weighing. During the third heating cycle the specimen was subjected to destruction.

The investigations were carried out using chitosan (β -D-1,4-N-glucosamine, $(\text{C}_6\text{H}_{11}\text{O}_4\text{N})_n$) extracted from crab shells manufactured by "Shanghai AZ import & export Co., Ltd" (China). Its molecular mass was $1 \cdot 10^5$, the degree of deacetylation was 78%, the molar mass of the repeat CHS unit was 161 g/mol. Before using, the methyl acrylate was dried with CaH_2 and distilled in the setup with the complete condensation attachment collecting the fraction with $t_{\text{boil}}=80.2^{\circ}\text{C}$ and $\rho^{25}=0.950 \text{ g/cm}^3$. The films based on the CHS/MA block-copolymer were prepared by pouring of reaction mixtures on a lavesan substrate. For the salt form of chitosan to be converted into a protonation one, the films were treated with a 5% solution of NaOH (for 5 min) followed by rinsing in distilled water up to pH 7. Biodegradation was performed in the presence of strains of *Aspergillus terreus*. The investigations lasted 20 weeks. The micromycetes were offered by the

All-Russia Collection of Microorganisms (Pushino, Moscow Region). To reveal the effect of biodestruction on physical-chemical properties of polymer compositions, three series of experiments were carried out according to State Standard (GOST 9.049-91, method 1) to estimate the contribution of the direct action of micromycetes and the products of their vital activity. In series No.1, the films were placed under the solid completely agarized Chapek-Dox medium (the medium surface was seeded with the fungi), while in series No.2 the specimens were placed on a two-week-old lawn with fungi. The specimens of polymer compositions not subjected to the action of the fungi served as a reference.

RESULTS AND DISCUSSION

The obtained experimental results are presented in Figs. 1–4. The performed investigations showed that initial air-dry specimens contained 4.4–8.9 mass% of adsorption water which evaporated from them at 120–132°C (Figs. 1–5, curves 1). Several relaxation transitions (a β -transition and two devitrification ones) were observed in dehydrated CHS (Fig.1, curves 2 and 3). It is attributed to a complex molecular and supramolecular structure of the given polysaccharide. The β -transition in CHS is related to oscillations of pyranose rings around a glucoside bond. Chitin and other polysaccharides studied by us behave themselves in a similar manner [2–8]. Irrespective of the source of initial chitin, a distinctive feature of chitosan is two-stage destruction accompanied with the release of energy in the form of heat ($t_{\text{dest1}} = 302^\circ\text{C}$, $t_{\text{dest2}} = 328^\circ\text{C}$) (Fig.1, curve 3). The loss of mass in this case is 41%.

Devitrification in the PMA was observed at $t_c = 14.5^\circ\text{C}$. However, based on more reliable calorimetric data of B.V. Lebedev [9] $t_c(\text{PMA}) = 12^\circ\text{C}$. The PMA destruction is two-staged and it is accompanied by absorption of the energy in the form of heat. The first endothermic maximum is observed at $t_{\text{dest1}} = 326^\circ\text{C}$; the second one, at $t_{\text{dest2}} = 397^\circ\text{C}$.

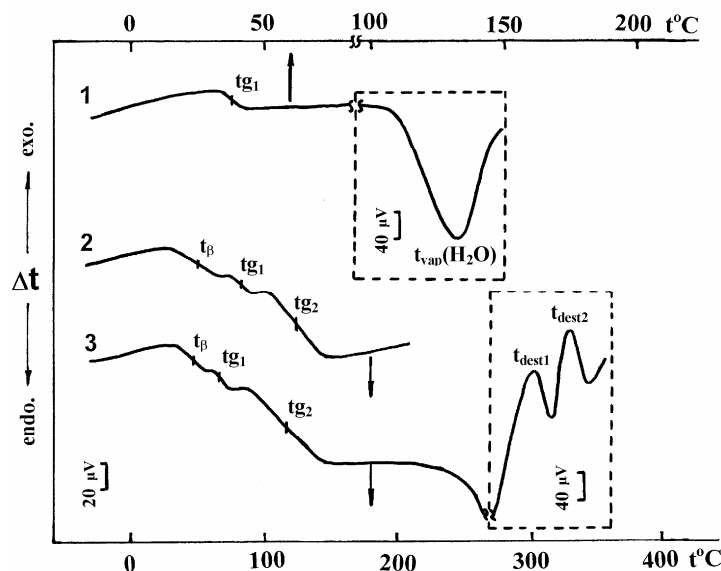


Figure 1. Thermograms of crab chitosan obtained at three repeated heating cycles: 1 - the first, 2 - the second, 3 - the third

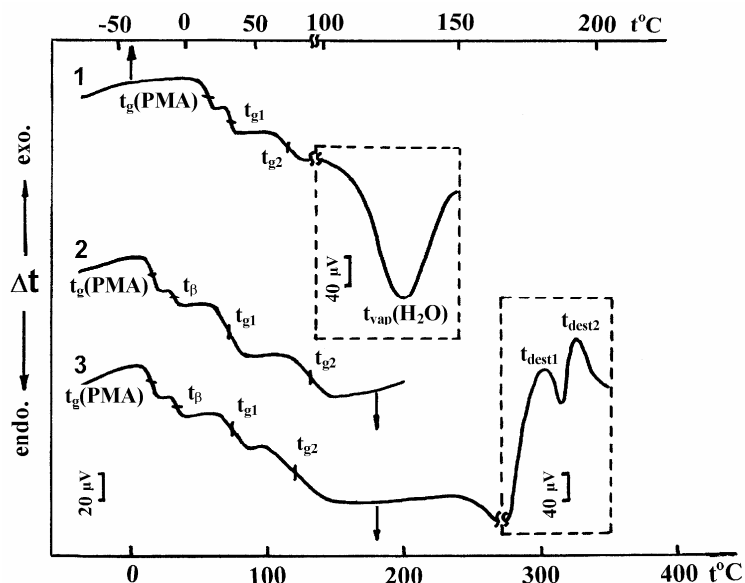


Figure 2. Thermograms of block-copolymer of chitosan with methyl acrylate obtained at three repeated heating cycles: 1 - the first, 2 - the second, 3 - the third

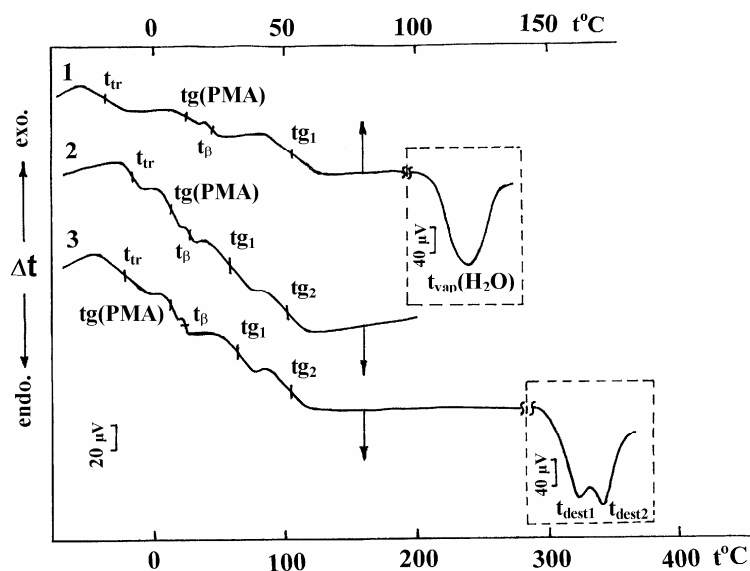


Figure 3. Thermograms of the specimen of block-copolymer of chitosan with MA after the action of *Aspergillus terreus* (series No.2) obtained at three repeated heating cycles: 1 - the first, 2 - the second, 3 - the third

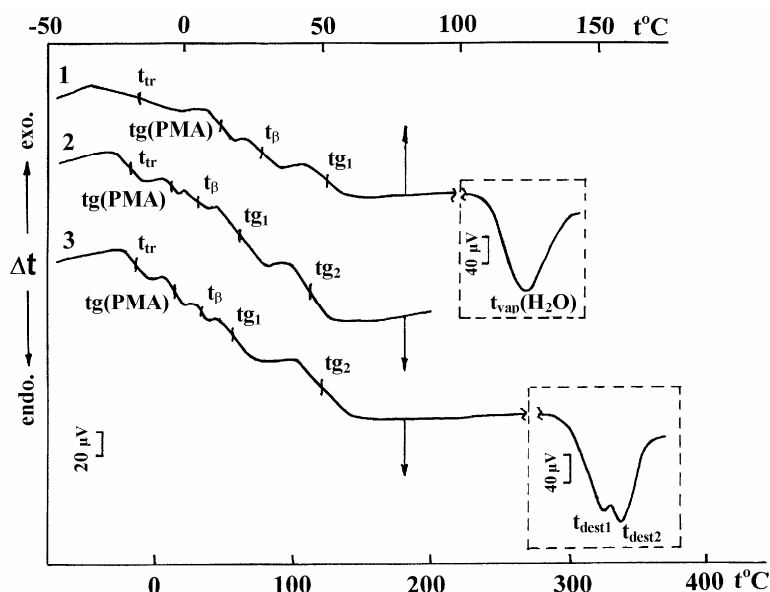


Figure 4. Thermograms of the specimen of block-copolymer of chitosan with MA after the action of *Aspergillus terreus* (series No.1) obtained at three repeated heating cycles: 1 - the first, 2 - the second, 3 - the third

A CHS/MA block-copolymer is characterized by the transitions typical for both polymers (Fig.2). Chitosan does not affect the PMA temperature t_c . In its turn, PMA slightly decreases t_β of CHS (up to 31°C), does not affect its t_{c1} (72°C), and increases t_{c2} (125°C). The PMA does not practically affect the chitosan destruction (Fig.2, curve 3). Only the loss of the specimen's mass decreases (by 2.5 times as compared to individual chitosan) since the concentration of polysaccharide in the copolymer is 25%.

We revealed variations in the temperature of CHS relaxation transition under the action of *Aspergillus terreus* on the CHS/MA block-copolymer. These variations are observed both under the direct action of micromycetes (series No.2) (Fig. 3) and in case of their indirect action taking the effect of the *Aspergillus terreus* vital life products into account (series No.1) (Fig.4). Under the action of the fungi, the specimens of the block-polymer demonstrated a relaxation transition at $t < 0^\circ\text{C}$ (Figs.3 and 4). It is likely to be related with minor (oligomer) residues of CHS macromolecules formed under the action of micromycetes. The fungi do not affect t_β of the chitosan in case of the indirect action of their vital life products, while at the direct action of micromycete floccs t_β of chitosan decreases by 5.5°C as compared to the initial copolymer. In both cases, a substantial decrease in its t_{c1} and t_{c2} , is observed, the vitrification of amorphous chitosan microregions taking place at the lower temperature if the film is placed under the nutrient medium seeded with *Aspergillus terreus* (series No.1), while highly-ordered microregions vitrify if the film is positions on a two-week-old fungi lawn (series No.2). This case can be related to both partial destruction of highly-ordered CHS microregions and the plastisizing effect on CHS from the side of low-molecular products of the fungi vital life. The temperature of PMA vitrification in this case does not practically change.

CONCLUSIONS

1. The comparison of physical-chemical properties of chitosan, its block-copolymer with methyl acrylate, and the CHS/PMA mixture showed that the polysaccharide does not practically affect the synthetic component, while PMA yields variations in the temperature of the chitosan

relaxation transitions. The MA blocks in the copolymer decrease the temperature of the β -transition and increase the temperature of vitrification of the ordered CHS microregions. As far as the mixture is concerned, PMA blocks the oscillations of pyranose rings of CHS and, thus, suppresses the β -transition of the latter.

2. The investigations performed using the DTA method revealed variations in physical-chemical properties of the CHS/MA block-copolymer under the action of *Aspergillus terreus*. In this case, chitosan is the first to be reprocessed by micromycetes, since it is the temperatures of the chitosan relaxation processes that change most substantially. The effect of *Aspergillus terreus* also manifests itself in the formation of a new relaxation process at $t < 0^\circ\text{C}$. It should be also noted that the effect of micromycetes on the CHS/MA block polymer yields a more substantial change in its physical-chemical properties in case of a direct action of micromycetes (series No.2) since both the flocculi of the fungi and the products of their vital life penetrate into the copolymer. An important sign of the micromycete action on chitosan is the disappearance of endothermic maxima of its destruction on the thermograms and the appearance of endothermic maxima of PMA destruction. A decrease in the temperature of the second endothermic maximum of the PMA destruction by $60\text{--}65^\circ\text{C}$ under the action of *Aspergillus terreus* on the block-copolymer allows assuming that PMA is also subjected to biodestruction.

ACKNOWLEDGMENTS

The work was performed with financial support of the Ministry of Education and Science of Russia in framework of the Analytical departmental goal program "Development of scientific potential of higher school (2009-2011)", (project No. 2.1.2/1056).

REFERENCES

- [1] Uryash, V.F., Mochalov, A.N., Pokrovsky, V.A. (1978) Device of the differential thermal analysis. Thermodynamics of Organic Compounds: Intercollege Bull., Gorky Univ. Publ., 7, 88-92.
- [2] Uryash, V.F., Rabinovich, I.B., Mochalov, A. N., Khlyustova, T.B. (1985) Thermal and calorimetric analysis of cellulose, its derivatives and mixtures with plasticizers. Thermochim. Acta, 93, 409-12.
- [3] Uryash, V.F., et al. (2010) Physical-chemical properties of natural polymers – potential carriers and delivery systems of biologically active substances for human applications. In Physical Organic Chemistry: New Developments (K.T. Burley, ed.) pp.183-265, Nova Sci. Publ., Inc.
- [4] Uryash, V.F., et al. (2005) Thermodynamic characteristics of pectin of different etherification degree in the 6-330 K range. Zh. Fiz. Khim., 79, 1383-89.
- [5] Uryash, V.F. (2002) Thermodynamics of chitin and chitosan. In Chitin and Chitosan. Fabrication, Properties, and Application (K.G.Skryabin, G.A.Vikhoreva, V.P.Varlamov, eds.) pp.119-29, Nauka.
- [6] Uryash, V.F., et al. (2004) Thermodynamic characteristics of amylase, amylopectin and starch within the 6—320 K range. Zhurn. Fiz. Khimii, 78, 796-804.
- [7] Uryash, V.F., Karyakin, N.V., and Gruzdeva, A.E. (2001) Optimization of the production process of biologically active substances based on calorimetric data, Perspektivnye Materialy, 6, 61-9
- [8] Uryash, V.F., Larina, V.N., Kokurina, N.Yu., Novoselova, N.V. (2010) The thermochemical characteristics of cellulose and its mixtures with water. Zh. Fiz. Khim., 84, 1023-29.
- [9] Lebedev, B.V., (1967) Thermodynamics of Monomers and Polymers of Vinyl Series, Candidate's Dissertation in Chemistry, 226 p. Gorki Univ. Publ.

SYNTHETIC STRATEGY OF CHITO-HETERO-OLIGOSACCHARIDES

Yuko Yoneda^{1,2}, Toshinari Kawada^{2*}

¹ Current affiliation: Dept. Applied Chemistry, Faculty of Engineering, University of Miyazaki,
1-1 Gekuen Kibanadai-nishi, Miyazaki, 889-2192, Japan

^{2*} Graduate School of Life and Environmental Sciences, Kyoto Prefectural University,
1-5 Hangi-cho, Shimogamo, Sakyo-Ku, Kyoto 606-8522, Japan

*Email: yyoneda@kpu.ac.jp, kawada@kpu.ac.jp

INTRODUCTION

Chito-hetero-oligosaccharide (CHOS) is a oligosaccharide consisted of *N*-acetyl-D-glucosamine (GlcNAc) and / or D-glucosamine (GlcN) linking with β -1,4-glucosidic bond. It has been revealing in these decades that CHOS exhibits numerous bio-activities, such as plant-microbe interactions, immune stimulation, chemotactic activities, antitumor effect, antimicrobial effect and so on [1 – 5]. Bio-activities and physico-chemical properties of CHOS are differed according to their (i) degree of polymerization (DP), (ii) mole ratio of GlcNAc / GlcN and (iii) sequence of GlcNAc / GlcN in the oligosaccharide chains, which becomes important information for utilizing CHOS. CHOS is obtained both by acid hydrolysis and by enzymatic hydrolysis of chitin and / or chitosan [6, 7], however the depolymerized products seem not to be easy to determine their exact chemical structure though there appeared some reports [8, 9]. Hence, the importance to prepare CHOS with well-defined chemical structure is growing in these days.

Depolymerization method is easy to produce chitoooligosaccharide mixture, but to purify the well-defined CHOS from the depolymerized mixture of chitin / chitosan is thought to be very difficult. On the other hand, although the chemical synthetic method for CHOS involves long-step reactions, it seems the most promising method to prepare each well-defined CHOS. In this report the synthetic strategy of CHOS starting from monosaccharide, D-glucosamine hydrochloride (GlcN-HCl), and some example of synthesis of di-, tri-, tetra- and polysaccharides of CHOS are described.

MATERIALS and METHODS

General methods

NMR spectra were recorded on JEOL GSX-270 or ARX-500 spectrometer, and measured with tetramethylsilane as an internal standard. The assignments of the signals were determined using ¹H-¹H correlated spectroscopy and / or ¹³C-¹H heteronuclear multiple-quantum correlation techniques. Coupling Constants (*J*) are given in Hz. ESI MS spectra were recorded with a Finnigan TSQ-7000 mass spectrometer. Flash column chromatography was performed on silica gel (Wakogel FC - 40). Preparative TLC was done on silica gel plates (Silica gel 60 F₂₅₄, Merck). Unless otherwise indicated, the usual workup for each reaction mixture consists of extraction with EtOAc, washing with distilled water and neutralizing with saturated solution of NaHCO₃, washing with brine, drying over sodium sulfate, and evaporation in *vacuo*.

4-O-Acetyl-3,6-di-O-benzyl-2-deoxy-2-phthalimido- β -D-glucopyranose (15)

To a solution of **11** (9.15 g, 14.2 mM) in THF (25 mL) were added acetic acid (0.40 mL, 0.5 eq) and TBAF (8.00 mL, 2.0 eq) at 0°C, and stirred for 1 h at 0°C. After workup, the residue

was purified by flash column chromatography using a solvent mixture of EtOAc / toluene (1/4, v/v), and recrystallized from EtOH to give crystals of **15** (5.98 g, 79.4 %); R_f = 0.59 (EtOAc / toluene = 1/1, v/v); $^1\text{H-NMR}$ (270 MHz, CDCl_3): δ = 1.94 (s, 3H, CH_3CO), 3.55 (dd, 1H, $J_{5,6b}$ = 3.79 Hz, $J_{6a,6b}$ = 10.72 Hz, H-6b), 3.56-3.65 (m, 1H, OH), 3.60 (dd, 1H, $J_{5,6a}$ = 5.11 Hz, $J_{6a,6b}$ = 10.72 Hz, H-6a), 3.79 (ddd, 1H, $J_{4,5}$ = 10.06 Hz, $J_{5,6a}$ = 5.11 Hz, $J_{5,6b}$ = 3.96 Hz, H-5), 4.17 (dd, 1H, $J_{1,2}$ = 8.41 Hz, $J_{2,3}$ = 10.72 Hz, H-2), 4.30-4.35, 4.54-4.62 (m, 4H, $2 \times \text{CH}_2\text{Ph}$), 4.50 (dd, 1H, $J_{2,3}$ = 10.72 Hz, $J_{3,4}$ = 8.90 Hz, H-3), 5.14 (dd, 1H, $J_{3,4}$ = 8.90 Hz, $J_{4,5}$ = 10.06 Hz, H-4), 5.36 (dd, 1H, $J_{1,2}$ = 8.24 Hz, $J_{1,\text{OH}}$ = 7.91 Hz, H-1), 6.87-7.01, 7.26-7.38 (m, 10H, $2 \times \text{Ph}$), 7.59-7.81 (m, 4H, Phthaloyl).

Trichloroacetimidoyl 4-O-Acetyl-3,6-di-O-benzyl-2-deoxy-2-phthalimido- α / β -D-glucopyranoside (16)

To a solution of dried **15** (1.01 g, 1.88 mM) in CHCl_3 (8 mL) were added DBU (56 μL , 0.2 eq) and CCl_3CN (0.56 mL, 3.0 eq) at room temperature. After stirring for 1 h at room temperature, the reaction mixture was purified by flash column chromatography using solvent mixture of EtOAc / hexane / Et_3N (1/4 / 0.01, v/v), and crystallized from EtOH / hexane to give crystals of **16** (0.803 g, 63.2 %); R_f = 0.57 (EtOAc / toluene / Et_3N = 1 / 3 / 0.01, v / v); $^1\text{H-NMR}$ (270 MHz, CDCl_3): δ = 1.95 (s, 3H, CH_3CO), 3.63 (dd, 1H, $J_{5,6a}$ = 4.95 Hz, $J_{6a,6b}$ = 11.05 Hz, H-6a), 3.67 (dd, 1H, $J_{5,6b}$ = 3.79 Hz, $J_{6a,6b}$ = 11.00 Hz, H-6b), 3.95 (ddd, 1H, $J_{4,5}$ = 10.06 Hz, $J_{5,6a}$ = 4.82 Hz, $J_{5,6b}$ = 3.83 Hz, H-5), 4.35 (d, 1H, CH_2Ph), 4.53-4.57 (m, 4H, CH_2Ph , H-2, H-3), 4.63 (d, 1H, CH_2Ph), 5.25 (m, 1H, $J_{3,4}$ = 8.78 Hz, $J_{4,5}$ = 10.06 Hz, H-4), 6.43 (m, 1H, $J_{1,2}$ = 8.74 Hz, H-1), 6.86-7.04, 7.24-7.35 (m, 10H, $2 \times \text{Ph}$), 7.64-7.76 (m, 4H, Phthaloyl), 8.57 (s, 1H, NH imidate).

tert-Butyldimethylsilyl 4-O-(4-O-acetyl-2-azido-3,6-di-O-benzyl-2-deoxy- α / β -D-glucopyranosyl)-3,6-di-O-benzyl-2-deoxy-2-phthalimido- α / β -D-glucopyranoside (19)

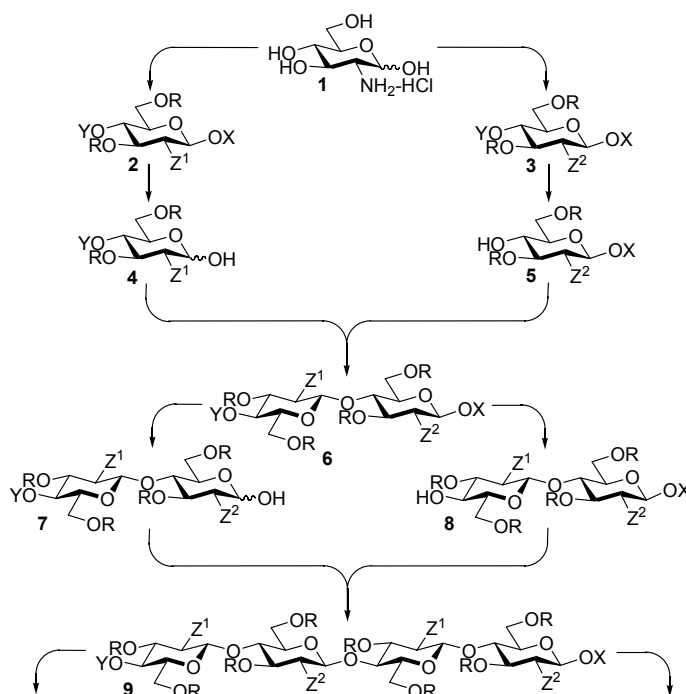
A solution of crystals of **16** (394 mg, 0.583 mM) and oily residue of **14** (323 mg, 1.1 eq) in anhydrous CHCl_3 (4 mL) was stirred with TMSOTf (2.11 μL , 0.02 eq) at -40°C for 2 h. After neutralization with Et_3N , the reaction mixture was worked up. The residue was purified by flash column chromatography using solvent mixture of EtOAc / toluene (1/9, v/v) to give **19** (495 mg, 83.8 %) as oil ; R_f = 0.55 (EtOAc / toluene = 1 / 6, v / v) ; ESI MS : m/z = 1035.42 $[\text{M} + \text{Na}]^+$.

RESULTS and DISCUSSION

Basic synthetic design

In the case the synthesis of complex and macromolecular compounds, the convergent synthetic method is generally preferred [10]. The basic synthetic design for CHOS is established based on the convergent method (Scheme 1).

Two kinds of the monosaccharide building blocks, derived from the starting material, GlcN-HCl, should be needed. Both monosaccharide building blocks should have X- and Y-group at 1-O and 4-O position, respectively, and R-group at 3- and 6-O positions, for the region-specifically control. At 2-C position, one kind of the monosaccharide building block should have Z^1 -group, and the other should have Z^2 -group. Here, X- and Y-groups are “temporary” protecting groups and R-groups is a “persistent” one. Z^1 - and Z^2 -group is converted into acetamido and / or free amino group, respectively.



Scheme 1. Basic synthetic design for CHOS.

Two kinds of the starting monosaccharide building blocks **2** and **3** were derived from GlcN-HCl (**1**). The removal of X-group from one of them and of Y-group from another one to prepare a glycosyl donor **4** and a glycosyl acceptor **5** (scheme 1 shows an example when compound **2** uses as a precursor of glycosyl donor). Subsequent β -glycosidation between the glycosyl donor **4** and the acceptor **5** by a proper manner (maybe the imidate method [11]) to the formation of a chitobiose derivative **6**, which also has the same protecting system as that of compound **2** and / or **3**. The chitobiose derivative **6** is further converted into a disaccharide glycosyl donor **7** and an acceptor **8**, reparatively. From these compounds **7** and **8**, a chito-tetraose derivative **9** is prepared. After repeating this set of two reactions, cleavage of X- and Y-groups and β -glycosidation, we will obtain CHOS derivative with any DP on demand. In the case of synthesis for CHOS with odd number DP, monosaccharide acceptor should be used. As Z^1 moiety **2** and Z^2 moiety **3** could be used both for a donor side and an acceptor side, the combination could be freely swapped according to an expecting sequence of target CHOS.

Selection of protecting groups

Hence the Z^1 - and Z^2 -group finally converted into an acetamido- and / or a free amino group, respectively, it is prerequisite to select Z^1 - and Z^2 -group which could remove independently. The acetamido group itself is a potential protecting group, but it easily forms an oxazoline under glycosidation conditions and leads to complex product mixtures [12]. After promising preliminary reactions and searching the literature [13] the azido and phthalimido groups were selected as Z^1 - and Z^2 -groups. The azido group is known to be stable under several conditions, while the phthalimido group is also stable under various conditions and can be easily introduced and cleaved [14]. Both, the azido and the phthalimido groups, can be converted into acetamido- and / or free amino groups [15].

The X- and Y-groups would be cleaved without any influence on Z^1 - and Z^2 -groups when the synthesized CHOS derivative converted into a donor moiety or an acceptor moiety. An

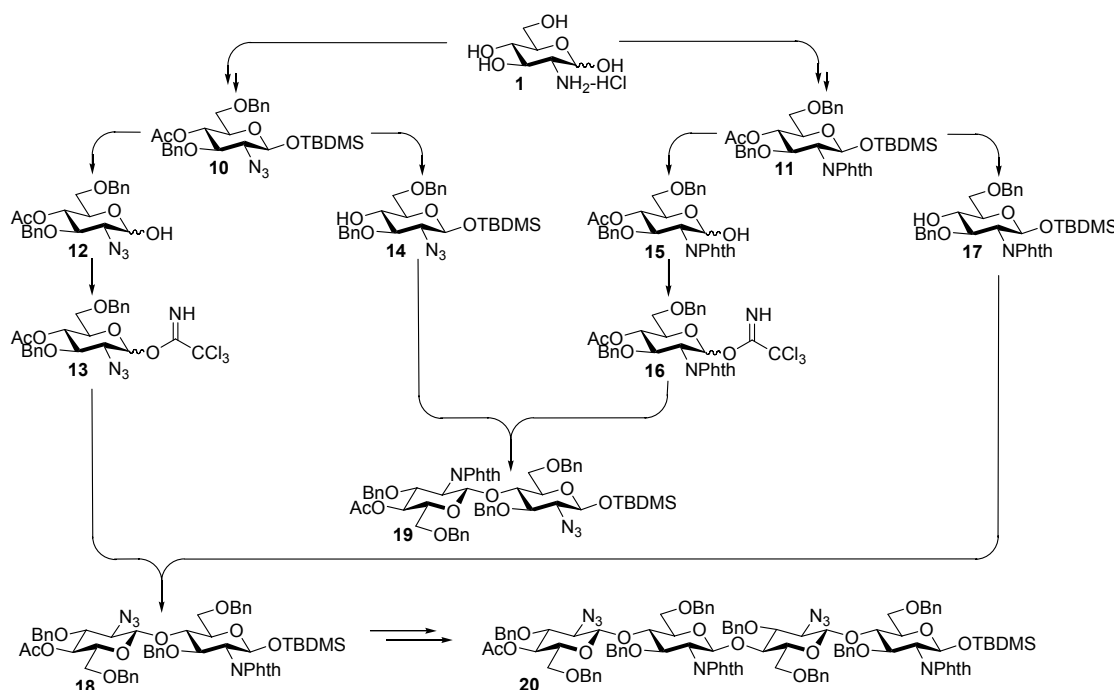
independent deprotection each other is also needed. To fulfill these requirements, the *t*-butyldimethylsilyl and acetyl groups were selected as X- and Y-group, respectively.

The R-group should equip large stability under various conditions, cleavage for Z¹-, Z²-, X- and Y-groups, introducing reaction of leaving group (trichloroacetimido group) glycosidation reaction. Benzyl group, well known protecting group in sugar chemistry, employed as R-group. As the results, two kinds of starting monosaccharide building blocks **2** and **3** are fixed as **10** and **11** as shown in Scheme 2 [16].

Synthesis of CHOS derivatives

The monosaccharide building blocks **10** and **11** were synthesized from GlcN-HCl (**1**) [16]. Cleavage of TBDMS group from **10** and **11** gave **12** and **15**, which lead to glycosyl donor **13** and **16** by trichloroacetimidoylation in good yield, respectively. In the meantime, **10** and **11** derived into glycosyl acceptor **14** and **17** by removal of acetyl group at 4-*O* position.

β -Glycosidation between **13** and **17**, **16** and **14** afforded CHOS disaccharide **18** and **19**, respectively. The phthalimido group at 2-*C* position performs neighboring group participation to ensure β -specific glycoside formation for gluco-type donor [17]. In the case of glycosidation reactions, using azido donors, the stereochemical outcome and yield highly depend on reaction conditions and reaction partners [18]. Actually, the **13** + **17** glydosidation, using azido donor, afforded disaccharide derivative **18** in 26 % yield, while the **16** + **14**, using phthalimido donor, gave **19** in 84 % yield.



Scheme 2. On demand synthetic scheme for CHOS.

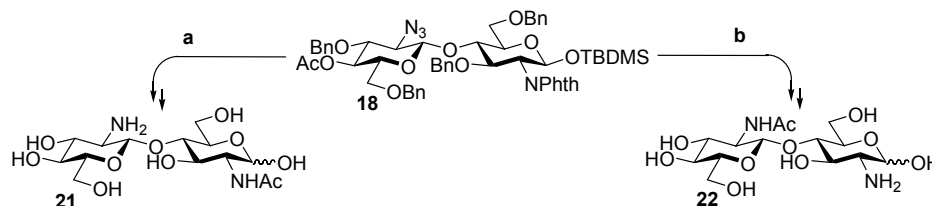
However, this advantage / disadvantage changes place of opposite side in the next glycosidation, chain elongation reaction. CHOS disaccharide derivative **18** was synthesized in 26 % yield, but CHOS tetrasaccharide derivative **20** was given in 84 % yield. That is, the disaccharide derivative **18** has already consumed disadvantage of the azido group as glycosyl

donor, and still keep the advantage of the phthalimido donor, β -specificity and high yield performance, for the next glycosidation reaction. The merit of the phthalimido donor worked well even for disaccharide donor + disaccharide acceptor glycosidation reaction.

Domard, Trombotto *et al.* reported a modification of our protecting system from view point of this low performance of the azido group [19]. They substituted the azido and phthalimido groups by *N*-trichloroacetyl and *N*-benzyloxycarbonyl groups, which contribute to increase yield of the glycosidation reactions. However, our protecting system has another advantage in deprotection steps as describing in the next section.

Deprotection

The advantage of our synthetic design is to permit two ways of deprotection manner to produce two kinds of CHOS's from one synthetic CHOS derivative; both the azido and / or phthalimido group could independently convert into both acetamido and / or free amino group, respectively. This would reduce your synthetic work into 50 %. For example, if all eight kinds of CHOS trisaccharides series (GlcNAc-GlcNAc-GlcNAc, GlcNAc-GlcNAc-GlcN, GlcNAc-GlcN-GlcNAc, GlcN-GlcNAc-GlcNAc, GlcNAc-GlcN-GlcN, GlcN-GlcNAc-GlcN, GlcN-GlcN-GlcNAc, GlcN-GlcN-GlcN) is to be synthesized, four kinds of CHOS derivatives should be constructed instead of synthesizing all eight CHOS derivatives.



Scheme 3. Two ways of deprotection manner.

The first choice is the phthalimido residue leads to GlcNAc, the azido residue to GlcN (Scheme 3. (a)). The phthalimido group in **18** was converted into free amino group using ethylenediamine in *n*-butanol [20, 21], while the azido groups did not suffered under the conditions. Subsequent acetylation gave an acetamido group. The acetyl and TBDMS groups were cleaved, and finally reduction reaction using 10 % palladium-carbon at normal pressure converted the azido and benzyl groups into free amino and free hydroxyl groups, respectively, to afford GlcN-GlcNAc (**21**)

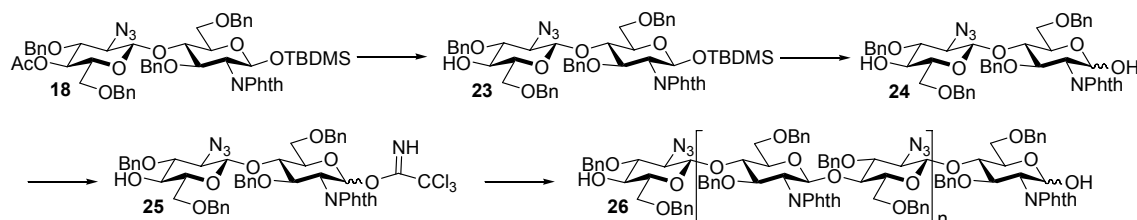
Another choice is the phthalimido residue leads to GlcN, the azido residue to GlcNAc (Scheme 3 (b)). The azido group in **18** was converted into free amino group using zinc / acetic acid, while the phthalimido group was stable under the conditions. Following reactions as same as the above finally produce GlcNAc-GlcN (**22**).

Synthesis of CHOS polymer

The β -specificity and high glycosidation performance of the phthalimido donor encourages a challenge using the phthalimido donor as a solo starting material for poly-condensation reaction. The essence of this poly-condensation applied is a poly-glycosidation reaction, which is based on a well known imidate method [11]. Normally, the glycosyl imidate (glycosyl donor) reacts with a suitable glycosyl acceptor, having a free hydroxyl group. However, if the glycosyl imidate itself contains a free hydroxyl group, it should act as both glycosyl donor as well as glycosyl acceptor. Consequently, the chain reaction would be expected to afford a polysaccharide.

The CHOS disaccharide **18** was converted into a solo starting disaccharide **25**, which possesses both characteristics, a glycosyl acceptor moiety (4'-OH) and a glycosyl donor moiety (1-*O*-trichloroacetimidoyl group) as shown in Scheme 4. The disaccharide **25** was poly-condensed using boron trifluoride diethyl etherate catalyst in anhydrous dichloromethane. After the reaction was finished, the reaction mixture was worked-up to gave poly-condensed product **26**, which was used for chemical analysis without any purification.

The stereochemistry of product **26** was determined by ^{13}C -NMR to find the poly-condensation reaction proceeded in a stereospecific manner and the product **26** is β -1,4-glucan. The molecular weight was determined by matrix-assisted laser desorption / ionization time-of-flight mass spectroscopy (MALDI-TOF MS). A series of CHOS derivatives up to dodecasaccharide (DP = 12) were clearly detected. GPC (Asahipak GSM-700H) analysis shows that the numerical average of DP is 4.5 and the degree of polydispersion (M_w/M_n) is 1.96.



Scheme 4. Synthesis of CHOS polymer.

ACKNOWLEDGEMENTS

This study was supported by KAKENHI (Grand-in-Aid for JSPS Fellows 20-11173). A part of this work is supported by Consortium Development Grant from The Senshu Ikeda Bank, Ltd.

REFERENCES

- [1] Hamel, L.-P. and Beaudoin, N. (2010) Chitooligosaccharide sensing and downstream signaling: contrasted outcomes in pathogenic and beneficial plant-microbe interactions. *Planta*, 232, 787 – 806.
- [2] Muzzarelli, R.A.A. (1993) Biochemical significance of exogenous chitins and chitosans in animals and patients. *Carbohydr. Polym.*, 20 (1), 7 – 16.
- [3] Usami, Y., Minami, S., Okamoto, Y., *et al.* (1997) Influence of chain length of *N*-acetyl-D-glucosamine and D-glucosamine residues on direct and complement-mediated chemotactic activities of canine polymorphonuclear cells. *Carbohydr. Res.*, 32 (2), 115 – 122.
- [4] Suzuki, K., Mikami, T., Okawada, Y., *et al.* (1986) Antitumor effect of hexa-*N*-acetylchitohexaose and chitohexaose. *Carbohydr. Res.*, 151, 403 – 408.
- [5] Jeon, Y.J., Park, P.J., Kim, S.K. (2001) Antimicrobial effect of chitooligosaccharides produced by bioreactor. *Carbohydr. Polym.*, 44, 71 – 76.
- [6] Kikkawa, Y., Kawada, T. (1990) Convenient preparation method of chito-oligosaccharides by acid hydrolysis. *Journal of the Faculty of Agriculture, Tottori University*, 26, 9 – 17.
- [7] Heggset, E.B., Dybvik, A.I., Hoell, I.A., *et al.* (2010) Degradation of chitosans with a family 46 chitosanase from *Streptomyces coelicolor* A3(2). *Biomacromol.* 11, 2487 – 2497.
- [8] Bahrke, S., Einarsson, J.M., Gislason, J., *et al.* (2002) Sequence analysis of chitooligosaccharides by matrix-assisted laser desorption ionization postsorce decay mass spectrometry. *ibid.*, 3, 696 – 704.

- [9] Vårum, K.M., Antohonsen, M.W., Grasdalen, H., Smidsrød. (1991) Determination of the degree of *N*-acetylation and the distribution of *N*-acetyl groups in partially *N*-deacetylated chitins (chitosans) by high-field n.m.r. spectroscopy. *Carbohydr. Res.*, 211, 17 – 23.
- [10] Vellus, L., Valls, J., Mathieu, J. (1967) Spatial arrangement and preparative organic synthesis. *Angew. Chem. Int. Ed. Engl.* 6, 778 – 789.
- [11] Schmidt, R.R., Michel, J. (1980) Facile synthesis of α - and β -*O*-glycosyl imidate; preparation of glycosides and disaccharides. *Angew. Chem. Int. Ed.*, 19 (9), 731 – 732.
- [12] Macmillan, D., Daines, A.M., Bayrhuber, M., Flitsch, S.L. (2002) Solid-phase synthesis of thioether-linked glycopeptides mimics for application to glycoprotein semisynthesis. *Org. Lett.*, 4, 1467 – 1470.
- [13] Green. T.W. (1981) Protective groups in organic synthesis. John Wiley & Sons.
- [14] Bamford, M.J., Pichel, J.C., Husman, W., et al. (1995) Synthesis of 6-, 7- and 8-carbon sugar analogues of potent anti-influenza 2,3-didehydro-2,3-dideoxy-*N*-acetylneuraminic acid derivatives. *J. Chem. Soc., Perkin Trans. 1*, 1995, 1181 – 1187.
- [15] Figueroa-Perez, S., Verez-Bencomo, V. (1998) Synthesis of dimeric Lewis X antigenic determinant with azido-type spacer arm by a sequence of regioselective glycosylation steps. 39, 9143 – 9146.
- [16] Kawada, T., Yoneda, Y. (2009) Selection of protecting groups and synthesis of a β -1,4-GlcNAc- β -GlcN unit. *MoChem.*, 140, 1245 – 1250.
- [17] Nanoub, J., Boullanger, P., Lafont, D. (1992) Synthesis of oligosaccharides of 2-amino-2-deoxy sugars. *Chem. Rev.*, 92 (2), 1167 – 1195.
- [18] Schmidt, R.R., Kinzy, W. (1994) Anomeric-oxygen activation for glycoside synthesis: The trichloroacetimidate method. *Adv. Carbohydr. Chem. Biochem.* 50, 21 – 71.
- [19] Barroca-Aubry, N., Pernet-Poil-Chevrier, A., Domard, A., Trombotto, S. (2010) Towards a modular synthesis of well-defined chitoooligosaccharides: synthesis of the four chitodisaccharides. *Carbohydr. Res.*, 345, 1685 – 1697.
- [20] DeMeo, C., Demchenko, A.V., Boons, G-J. (2001) A stereoselective approach for the synthesis of α -sialosides. *J. Org. Chem.*, 66 (16), 5490 – 5497.
- [21] Kawada, T., Yoneda, Y. (2009) Synthesis of a chito-tetrasaccharide β -1,4-GlcNAc- β -GlcN repeating unit. *MoChem.* 140, 1251 – 1256.

NEW MATERIALS ON THE BASIS OF THE CHITOSAN, MODIFIED WITH ALDEHYDES

N.R. Kildeeva^{1*}, I.E. Veleshko², L.V. Vladimirov¹, P.A. Perminov¹, L.M. Simanenkova³, V.I. Lozinsky³, S.N. Mikhailov⁴

¹*Department of Chemical Technology and Ecology, Kosygin Moscow State Textile University, M. Kaluzskaya 1, Moscow, 119071, Russia; National Research Centre "Kurchatov Institute", Kurchatov sq. 1, Moscow, 123182, Russia;* ³*Nesmeyanov Institute of Organoelement Compounds, Russian Academy of Sciences, 28, Vavilov str., Moscow, 119991 Russia;* ⁴*Engelhardt Institute of Molecular Biology, Russian Academy of Sciences, Vavilov str. 32, Moscow, 119991 Russia.*

**E-mail address: kildeeva @ mail.ru*

INTRODUCTION

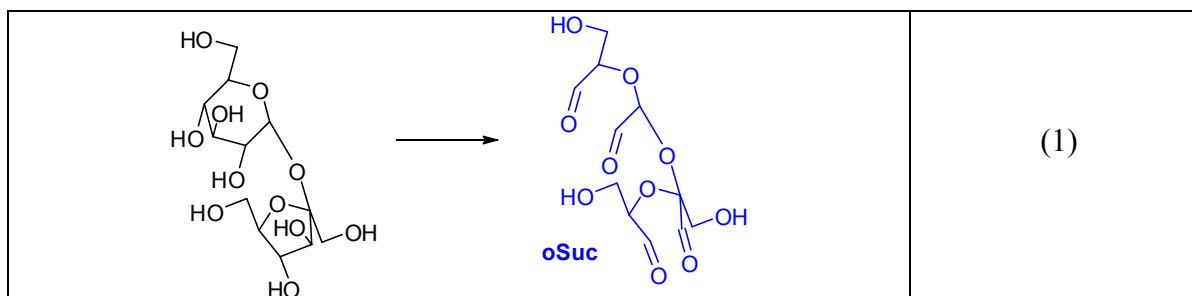
Modifications of chitosan with dialdehydes are widely used for the preparation films, microcapsules, granules, fibers, hydrogels and composite materials, and to fix in their structure biologically active compounds, drugs, enzymes and other proteins. To date, the most common crosslinkers are dialdehydes and the most effective and reliable is glutaraldehyde (GA). The main drawback of GA crosslinking is the formation of irregular products due to aldol condensation of GA [1,2]. This fact should be taken into consideration if the reaction of chitosan with GA is used to create materials for medical or pharmaceutical applications. To improve the characteristics of chitosan-based materials, we have proposed a series of novel and effective reagents which were prepared by periodate oxidation of nucleosides and 5'-nucleotides [3]. The use of these dialdehyde derivatives allow the effective crosslinking of macromolecular chitosan chains with simultaneous modification such as introduction of heterocyclic bases and leading to novel chitosan based biomaterials with low solubility in water over a wide range of pH.

In the present work the reaction of chitosan with GA and other aldehydes was used for obtaining some new materials: hydrogel films, capable of initiating the synthesis of the silver nanoparticles, and highly porous cryogels with high sorption capacity.

MATERIALS and METHODS

Chitosan (with a MW of about $2.0 \cdot 10^5$ and a degree of deacetylation of 87% was purchased from Roeper GmbH (Germany). All aqueous solutions were prepared with bidistilled water. A 2% solution of chitosan in 2% acetic acid had pH value equal to 4.1. To adjust pH of the chitosan solution to 5.6 (by 0.1 less than the turbidity point), the 0.5 N NaOH solution was added. Glutaraldehyde («Merck», Germany) was added to the solution in various amounts.

Oxidized derivative of D-sucrose was prepared by oxidation of D-sucrose of using excess of sodium periodate in water.



The values of elastic shear modulus for chitosan gels were found using the penetration method at a constant load. After completion of the crosslinking reaction, a weighed hydrogel sample was immersed in an excess of distilled water and kept until swelling equilibrium. Then the completely swollen samples were weighed after the removal of excessive surface water with a filter paper.

Carbonyl-containing chitosan films were obtained on the Petri dishes from the 1% solutions of chitosan in 1% AcOH, which contain the crosslinking reagents (CR): GA or oSuc. Molar ratio CR/NH₂ was 0.056 and 0.08 mole/mole. After drying at room temperature the films were incubated for 1 hour in the darkness in 0.02 M AgNO₃ (100 ml/g of film) and were irradiated for 3 minutes by UV light (mercury lamp).

Atomic force microscopy (AFM) images (5×5 μm) of the surfaces of chitosan films were measured by Tapping-mode image in air, using research complex «Integra» (Russia)

In the case of preparation of chitosan cryogels, the feed solutions of chitosan and GA mixtures were placed in 5-mL plastic syringes that, in turn, were transferred into the chamber of precision cryostat FP45-HP («Julabo», Germany) for 24 h, so the cryotropic gelation proceeded in the moderately-frozen systems at preset minus temperature. The cryogels thus formed were thawed out in the microwave oven M1712NR («Samsung», S.Korea) at 800 W for 1 min. Then the cryogels were washed with 1% acetic acid and distilled water.

The modification of chitosan cryogels with pyridoxal 5'-phosphate (PP) was accomplished after the completion of cryotropic gel formation and deprotonation of amino groups. For the deprotonation of the amino groups the cryogel were washed with diluted aqueous NaOH. The modification of cryogel with PP was carried out at room temperature by incubation in 0.05 M solution of PP during 1 hour. The content of PP in the sorbent was calculated from the change of absorbing of PP solution (λ=310 nm) after contact with the cryogel.

FTIR spectra were registered on a Bio-Rad FTS-40 spectrometer (Digilab) with a resolution of 4 cm⁻¹. The processing of spectra (normalization and base line correction) was carried out using the Win-IRv.4 software package (Bio-Rad, Digilab Division). Samples for spectrum recording were prepared as KBr pellets. For the convenience of comparison, the spectra were normalized using the 1153 cm⁻¹ band of valence vibrations of the C–O glycoside bond of the chitosan chain as an internal standard.

RESULTS and DISCUSSION

Two methods were used for the introduction of aldehyde groups into chitosan films: reaction with GA at the maximally possible pH at which the system remains single-phased and the use of the oxidized derivative of D-sucrose (oSuc), which contains 4 carbonyl groups (1). In spite of this the rate of gel formation in the solution of chitosan containing GA at pH 5.6 is considerably higher than in the case of oSuc (Figure 1). This fact is connected with the special features of the mechanism of interaction of chitosan with GA, which includes the aldol

condensation GA resulting in formation of conjugated $N=CHCH=C<$ and $O=CHCH=C<$ bonds, capable of further transformations [2].

The transition from a pseudoplastic liquid to the crosslinked structure of a gel corresponds to the gel point for each particular system, but not to the completion of the reaction between chitosan and aldehyde. We have studied the kinetics of variation of gel strength in time. It was found that shear module strongly depended on the CR/ NH_2 ratio and pH of the medium (Figure 2). The maximum value of the shear module was obtained in the case oSuc (curve 1, Figure 2). This may be due to the formation of the shorter intermolecular bridges with this CR.

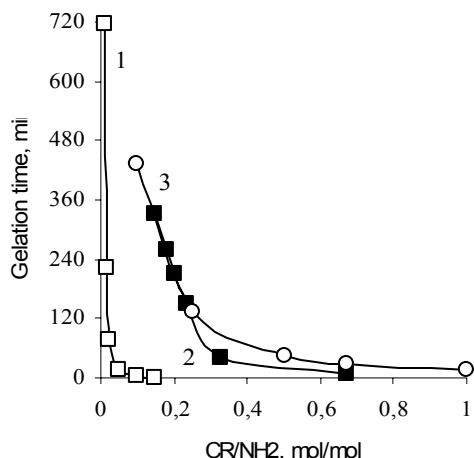


Figure 1. Dependence of the time of gel formation on CR/ NH_2 ratio in the presence of GA(1,2) and oSuc(3) at pH 5.6 (1,3) and pH 4.1 (2).

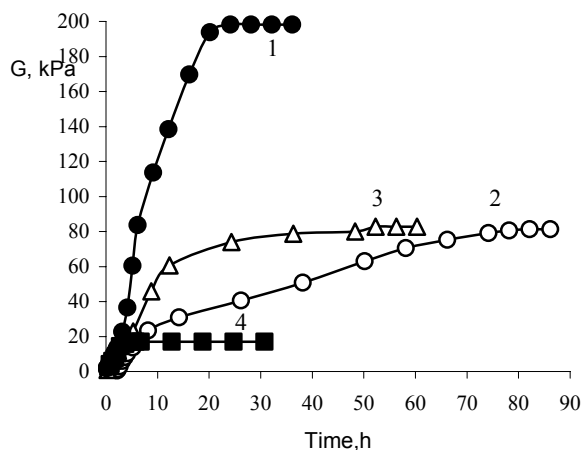


Figure 2. Kinetics of changes in the shear module for gels of chitosan crosslinked by oSuc (1-3) and GA (4) at pH 5.6 (1,3) and pH 4.1 (2,4). The ratio CR/ NH_2 0.67 mol/mol (1,2,4), 0.33 mol/mol (3).

The chitosan - GA and chitosan - oSuc films containing free carbonyl group were capable for photochemical reduction of $Ag(+1)$ ions. On Figure 3 AFM - images of the surfaces of chitosan films after incubation with 0.02 M $AgNO_3$ and irradiation with UV light are presented. On the images of surface films, are visible the particles, whose size changes, depending on type of CR and its concentration. It should be noted that under the same conditions on AFM - images of the film obtained from chitosan without any CR no particles are formed.

On film surface from the chitosan, modified with oSuc, a dense layer of small silver nanoparticles with size approximately 35 nm is formed. The use of GA leads to the formation of larger particles (50-70 nm) and this may be connected with the smaller content of carbonyl groups in this film, which are involved in the photochemical reduction of $Ag(+1)$ ions. An increase of the content GA result in a decrease of particle sizes and in increase in their surface concentration. The obtained results testify the direct participation of carbonyl groups in the formation of silver from the aqueous solutions of its salts.

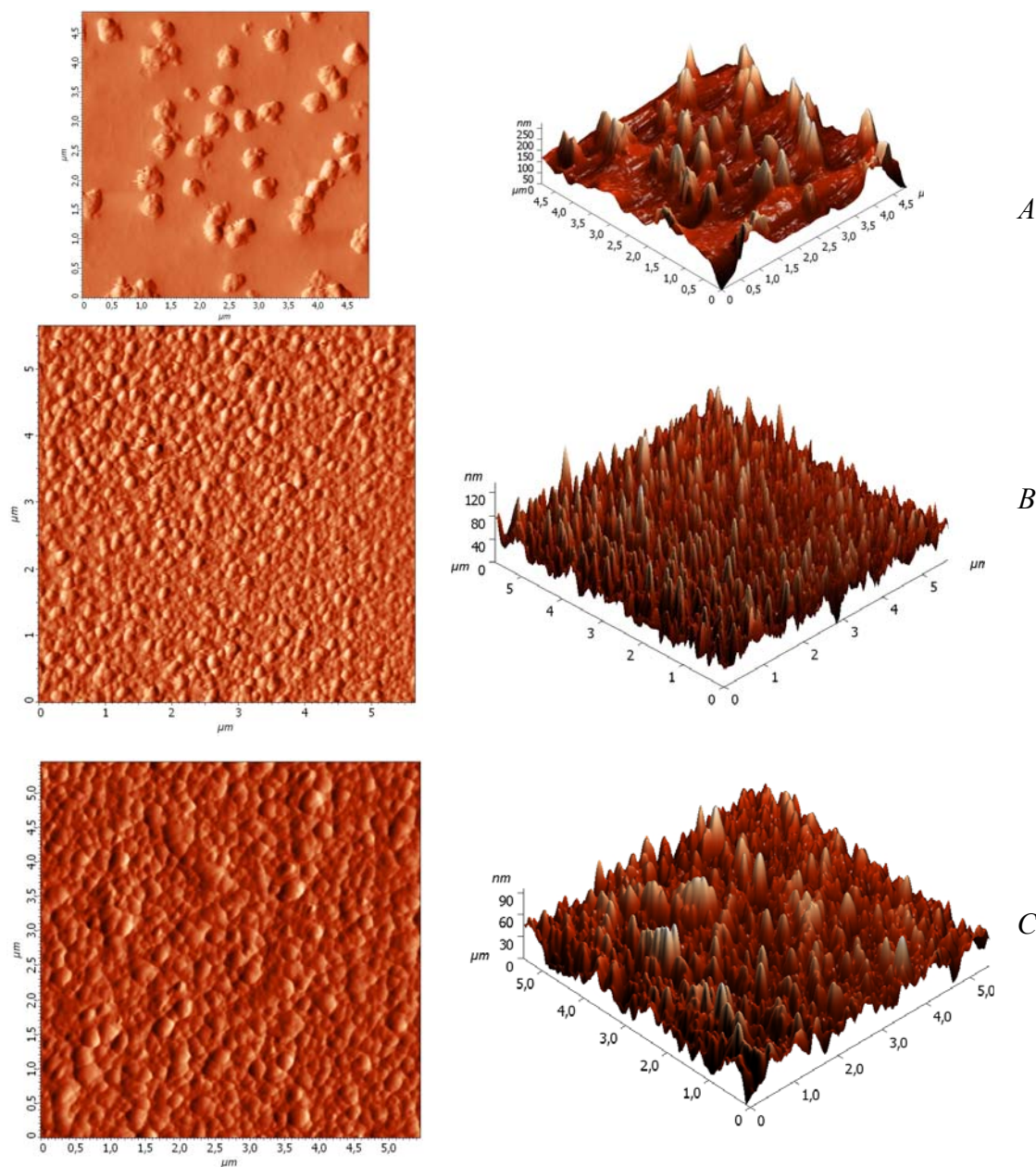


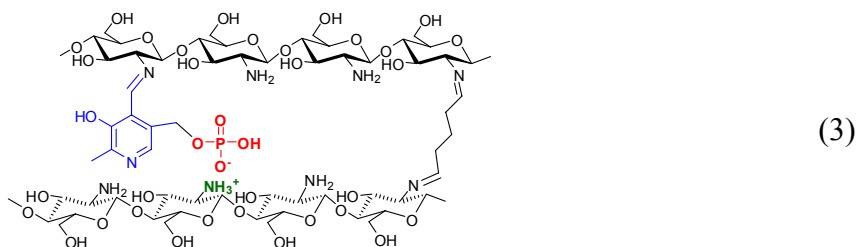
Figure 3. AFM - images ($5 \times 5 \mu\text{m}$) of the surfaces of chitosan films (top-view -left , 3d-view- right), containing silver nanoparticles. The films were obtained by crosslinking of chitosan with GA (A, C) and oSuc(B). The ratio CR/NH₂ was 0.056 (A,B) and 0.08 mole/mole (C).

Chitosan is the sorbent of copper, cobalt and other elements, which have vacant d- orbital. We have previously prepared highly porous cryogels by crosslinking of chitosan with GA at low temperatures [4] and have shown their use in the absorbing of the copper ions.

In order to increase the effectiveness of the absorption of the heavy metals and the radionuclides we decided to modify chitosan with pyridoxal 5'-phosphate (PP) (2), the cofactor of the PP- dependent enzymes, which contains, besides phosphate group, reactive carbonyl group capable to react with the primary amines.



The formation of the reaction product of chitosan with PP (3) was proven with the use of IR spectroscopy (Figure 4).



In order to decrease the spectroscopic contribution of the initial reagents the sequential subtraction method was used. The resulting difference spectrum is enriched by spectroscopic information about the reaction products. The elimination of the spectral contribution of chitosan made it possible to see on the difference spectrum of chitosan and product of its interaction with PP (spectrum 4, Figure 4) the absorption band of phosphate (1070 cm^{-1}). Furthermore the relative intensity of the peak of the bending vibrations of NH_2 - groups (1600 cm^{-1}), is reduced, and in the region $1680\text{--}1620\text{ cm}^{-1}$ appears the peak of the stretching vibrations of $\text{C}=\text{N}$ bond. These data indicate the formation of Schiff's bases as a result interactions of carbonyl group of PP with the amino groups of chitosan. The content of PP in the sorbent was estimated as 470 mg of PP to 1 g of chitosan or 0.32 mole/mole NH_2 group.

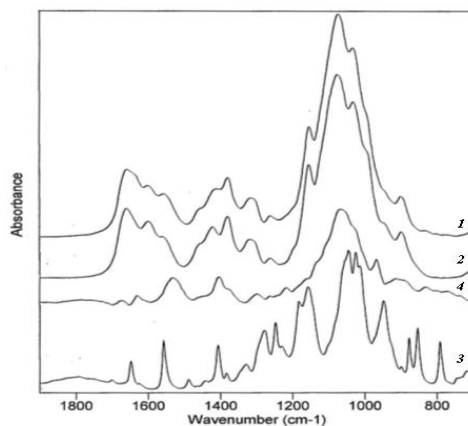


Figure 4. Fourier-transform IR spectra of samples of chitosan modified with PP (1), chitosan (2), PP (3) and the difference (4) spectrum obtained by subtraction of PP spectrum from spectrum 1.

Modifications with PP result in increasing of sorption capacity of the chitosan cryogels to the radionuclides. The sorption capacity for $^{152,154}\text{Eu}^{3+}$ was 0.47 mmol per 1 g of dried cryogel. Much higher sorption was observed in the case of $^{90}\text{Sr}^{2+}$ ions. It was shown that the developed materials may be used for effective extraction of radionuclides from their solutions.

ACKNOWLEDGEMENTS

The financial support of russian ministry of education and science (contract 16.740.11.0059) is gratefully acknowledged.

REFERENCES

- [1] Migneault, I., Dartiguenave, C., Bertrand, M.J., Waldron, K.C. (2004) Glutaraldehyde: behavior in aqueous solution, reaction with proteins, and application to enzyme crosslinking. *Biotechniques*, 37, 790–802.
- [2] Kildeeva, N.R., Perminov, P.A., Vladimirov, L.V., Novikov, V.V., Mikhailov, S.N. (2009) About Mechanism of Chitosan Cross-Linking with Glutaraldehyde. *Russian J. Bioorg. Chem.*, 35, 360-369.
- [3] Zakharova, A.N., Novikov, V.V., Donetskaya, A.I., Perminov, P.A., Kildeeva, N.R., Mikhailov, S.N. (2009) Dialdehyde derivatives of nucleosides and nucleotides: novel Effective crosslinking reagents. *Advances in chitin science*, Volume XI (Eds F.Rustichelli, C.Caramella, S.Senel, K.M.Vaarum) 469-474.
- [4] Nikonorov, I.V., Ivanov, R.V., Kildeeva, N. R., Bulatnikova, L.N., Lozinskii, V.I. (2010) Synthesis and characteristics of cryogels of chitosan crosslinked by glutaric aldehyde. *Polymer Science, Ser. A*, 52, 828-834.

A COMPARISON OF CHITOLIGOSACCHARIDES AND ITS DERIVATIVES IN RESPECT TO THEIR ANTIDIABETIC AND ANTIOBESITY EFFECTS

Fatih Karadeniz¹, Mustafa Zafer Karagozlu¹, Chang-Suk Kong², Se-Kwon Kim^{1,3} *

¹Department of Chemistry, Pukyong National University, Busan 608-737, Republic of Korea;

²Department of Food and Nutrition, College of Medical and Life Science, Silla University, Busan 617-736, Republic of Korea;

³Marine Bioprocess Research Center, Pukyong National University, Busan 608-737, Republic of Korea

*E-mail address: sknkim@pknu.ac.kr

INTRODUCTION

White adipose tissue is a major energy reserve in higher eukaryotes and storing triacylglycerol in intervals of energy excess, its mobilization during the energy requirement are its primary purposes. However, initiation and endurance of obesity occur pursuant to not only hypertrophy of adipose tissue but also differentiation of preadipocytes into adipocytes. This mechanism of adipogenesis is triggered by adipose tissue hypergenesis.[1] Obesity is closely correlated to the prevalence of diabetes, cardiovascular disease, hypertension and cancer.[2,3] Differentiated adipocytes secrete obesity-related factors called adipokines. Plasma leptin, tumor necrosis factor (TNF)- α and non-esterified fatty acid levels are all elevated in obesity and play a role in causing insulin resistance.[4] Therefore, suppression and regulation of obesity can be achieved by inhibiting adipocyte differentiation and forcing adipocytes to lipolysis to reduce accumulated white adipose tissue.[5] Thus, the increased control of the harmful effects on the accumulation of adipose tissue and its metabolism contribute to the search for a better understanding of the molecular mechanisms of obesity.

For in vitro adipocyte differentiation, function and adipose tissue accumulation studies, 3T3-L1 is a well-known and frequently used preadipocyte cell line. 3T3-L1 cells undergo an adipogenic differentiation when treated with a cocktail, including dexamethasone, methylisobutylxanthine and insulin. After acquisition of adipocyte function and morphology, 3T3-L1 cells accumulate microscopically detectable triglyceride droplets and express adipocyte-specific proteins. Adipocyte differentiation is coordinately regulated by several transcription factors. CCAAT element binding protein (C/EBP)- β and - γ , and acetyl-CoA and sterol response element binding protein 1 (ADD1/ SREBP1) are important transcription factors in lipid metabolism. These factors are active during the early differentiation process and induce the expression and/or activity of the peroxisome proliferator-activated receptor- γ (PPAR- γ) which is the essential coordinator of the adipocyte differentiation process. Differentiation into adipocytes and conserving adipocyte-like characteristics are controlled by these transcription factors, leading to elevation of adipocyte specific gene expression, secretion of adipokines as well as accelerated adipose and glucose metabolism.[6] Therefore, altered expression of these transcription factors might underlie the development of disorders characterized by increased adipose tissue.

Chitooligosaccharide (COS) are hydrolyzed derivatives of chitosan, which is a soluble form of chitin, cellulose-like polymer present in the exoskeleton of crustaceans, cuticle of the insects and cell wall of some microorganisms. Compared to chitin, COS has a lower viscosity, relatively small molecular size and is soluble in neutral aqueous solutions. With its high absorption rate in vivo systems, use of COS is expected to be more efficient than chitosan and chitin.[7] Moreover,

it has been reported that COS possesses a number of biological activities such as antitumor, antifungal, antimicrobial, antiviral, fat lowering and free radical scavenging activities.[8] This study was focused on the effect of COS on diabetic and obesity conditions. Furthermore, three derivatives of chitooligosaccharides (COS) which have already shown to have adipogenesis inhibitory effect, were synthesized through structural modification of –OH and –NH₂ residues. Furthermore, antiobesity and antidiabetic effects of synthesized COS derivatives were compared with COS. Beyond these, in this study with structural modification of COS, it is aimed to improve antidiabetic and antiobesity effects.

MATERIALS and METHODS

Materials

Chitooligosaccharides were kindly donated by Kitto Life Co. (Seoul, Korea). Cell culture medium, antibiotics, fetal bovine serum (FBS) were purchased from Gibco BRL, Life Technology (NY, USA). Primers and other RT-PCR chemicals were obtained from Bioneer Co. (Daejeon, Korea). Chemicals used in chemical compound synthesizing were purchased from Junsei Chemical Co. (Tokyo, Japan). All other chemicals were obtained from Sigma Chemical Co. (St. Louis, MO, USA)

Synthesizing of COS derivatives

a. Carboxylated COSs

Two types of carboxylated COSs were synthesized in this study. Synthesizing of carboxylated COS was made with a modified method adopted from Huang et. al. [9], using COS instead of glucosamine and changing succinic anhydride to maleic acid to synthesize a differently modified COS. Two types of chemicals were used as carboxyl group donor and the derivatives named after these chemicals (Figure 9).

b. Sulfated COS

10 g of COS was dispersed in 100ml of dimethylformamide (DMF) and put on a heating magnetic stirrer. Solution was heated up to 60°C while adding 8 ml of chlorosulfonic acid dropwise for 30 minutes. The resulting solution was stirred for 4 more hours at 60°C. After 4 hours of stirring, solution was cooled then dialyzed exhaustively against D.W. using an electro dialyzer (Micro Acilyzer G3, Asahi Chemical Industry Co., Tokyo, Japan) and lyophilized. Dialyzed samples were freeze-dried, gained as dark brown fluffy powder and named as SCOS.

Oil Red O staining

Measurement of lipid droplets accumulated in the cells was achieved by Oil Red O staining as previously described. Cells on day 6 of differentiation in 6-well plates were washed twice with phosphate buffer saline (PBS) prior to fixing with 3.7% (250 µl) formaldehyde (Junsei Co., Japan). Lipid droplets in the cytoplasm were stained with Oil Red O solution. After the staining process, Oil Red O solution was removed and wells were washed with water and dried. Images of stained cells were obtained by a fluorescent microscope (CTR 6000; Leica, Wetzlar, Germany). Later on, stain was eluted with isopropanol and quantified by measuring the absorbance at 500 nm. Triglyceride accumulation of the cells, which was calculated as stain amount, was evaluated as the relative percentage of untreated control cells.

Triglyceride assay

Cells were washed with PBS, and homogenized with buffer containing 154 mM KCl, 50 mM Tris and 1 mM EDTA. Triglyceride content of lysed cells was measured using a Triglyceride Assay Kit (Shinyang Chemical, Republic of Korea) according to manufacturer's instructions. Amount of intracellular triglyceride was standardized to the total protein amount of cells measured by protein assay kit (BioRad Laboratories, Hercules, CA).

Glycerol assay

Glycerol release into the medium of cultured and differentiated 3T3-L1 cells were measured. Foremost, glycerol reagent was prepared by dissolving free glycerol reagent (Sigma Chemical Co.) in 40 ml DW. Two hundred microliters of glycerol reagent was added to each well of 96-well plate. The culture medium of cells at differentiation day 6 was collected, centrifuged at 5000 rpm for 5 min. Supernatant was used as the sample for glycerol assay. Three microliters of sample was added to wells filled with 200 μ l glycerol reagent. Plate was incubated at 37°C for 15 min. Following the incubation, OD of the wells was determined at 540 nm using the microplate reader. Glycerol concentrations of the samples were measured by comparison of absorbance values of sample and standard glycerol concentrations.

Protein Glycation Assay

An assay made to check the effects of COS and its derivatives on glycation of bovine serum albumi proteins in the presence of sugar. Sample solution was prepared by dissolving different concentrations of compounds in 1ml reaction solution containing 7mg/ml bovine serum albumin, 25mM glucose, 25mM fructose, 0.02% sodium azide in phosphate buffer, pH 7.4. Reaction mixture was vortexed and incubated at 37°C for 4 weeks. During 4 weeks, each week fluorescence intensity of the reaction mixture was measured at 360nm/450nm of excitation/emission maxima to determine the AGE formation that indicates the protein glycation.

RESULTS and DISCUSSION

COS remarkably decreased lipid accumulation, an indicator for adipogenesis, in 3T3-L1 adipocyte cells, sulfation of COS increased adipogenesis inhibitory effect (Figure 1). Also mRNA expressions of adipogenic factors such as peroxisome proliferator-activated receptor (PPAR) gamma and sterol regulatory element-binding protein (SREBP) 1 were considerably decreased in comparison to COS and its derivatives. Protein levels of PPAR-gamma and CCAAT/enhancer-binding protein (C/EBP) alpha, the key adipogenic factors, downregulated with COS derivative treatment. Moreover, only sulfation of COS moderately inhibited alpha-glucosidase and alpha-amylase activity which are important enzymes for controlling blood glucose in diabetic conditions. However, COS and its carboxylation showed no effect. COS treatment decreased the stored triglyceride in the cells down to about 60% of untreated control groups at 1mg/ml concentration where SCOS decreased around 40% at same concentration (Figure 2). Related to triglyceride amount decrease, glycerol content of the medium was also increased by COS treatment, indicator for triglyceride hydrolyzation, relative to untreated control group. Carboxylation of COS did not change its effect significantly as CCOS and MCOS increased the glycerol content almost same amount with COS (Figure 3). But SCOS increased the glycerol amount of the medium almost double of COS did. Besides, it has been seen that modified COSs have a little effect on inhibiting protein glycation where COS have no effect (Figure 4).

In this study, COS was checked as an antidiabetic and antiobesity compound and by structural modification it was tried to improve COS's antidiabetic and antiobesity effect. Carboxylation and sulfation processes were carried out in order to modify COS side chains.

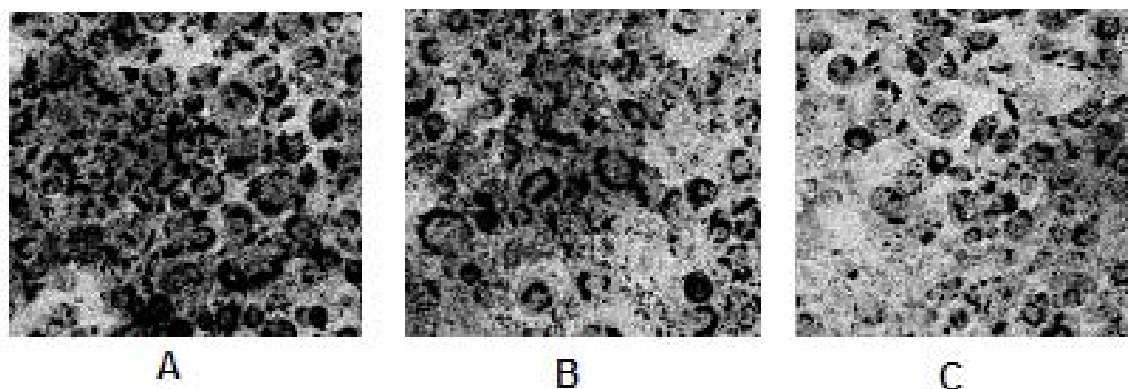


Figure 1. Images of Oil Red O stained cells that were untreated (A) or treated with COS (B) and SCOS (C)

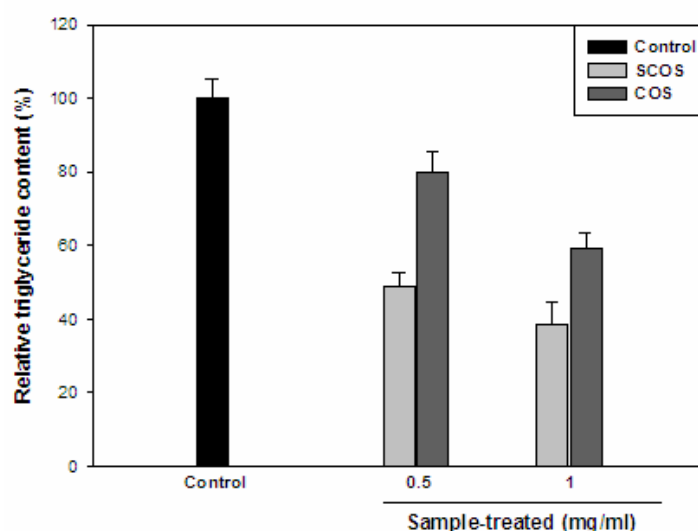


Figure 2. Triglyceride content of COS and SCOS treated cells relative to untreated (Control) cells.

To evaluate COS and its derivatives antiobesity effect, effect on 3T3-L1 cell differentiation was checked with lipid staining, triglyceride and glycerol content assays. These assay's results were clearly showed that COS inhibit adipogenesis in 3T3-L1 cell by decreasing lipid accumulation in the cells. CCOS and MCOS, carboxylated derivatives of COS, enhanced it's adipogenesis activity slightly where SCOS, sulfated derivative of COS, significantly improved COS's inhibitory effect on adipocyte differentiation. Same improvement results can be seen in triglyceride and glycerol content assays. Also proein glycation inhibitory effect of COS and its derivatives was checked to see the preventing effect against glycation because glycation is the major problem in diabetic microangiopathy and cardipvascular diseases. Protein glycation assay results indicate that COS did not inhibited protein glycation as it is expected. CCOS and MCOS slightly inhibited the protein glycation where SCOS significantly inhibited protein glycation which mean carboxylation and sulfation gave COS ability to inhibit protein glycation.

As a result, COS showed good antiobesity effect and structural modification by carboxylation and especially sulfation improved it's antiobesity effect. Where COS has no antidiabetic effect by mean of enzyme and protein inhibition, SCOS showed improved inhibitory activity against both enzyme and protein inhibition. Tha data indicates that COS and its

derivatives, especially SCOS can be used as antidiabetic and antiobesity additive compound in food industry and pharmaceuticals.

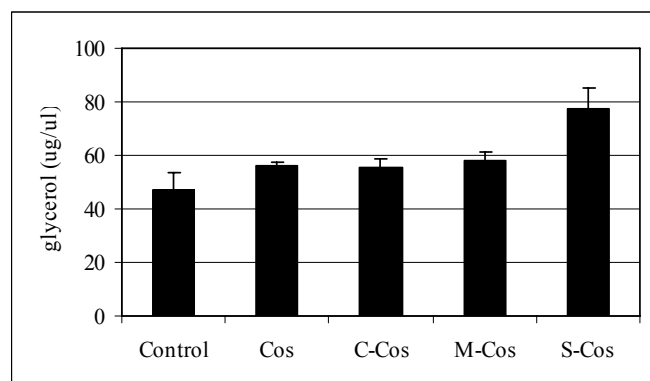


Figure 3. Glycerol content of COS, CCOS, MCOS and SCOS treated cell groups' medium at the treatment concentration of 1mg/ml.

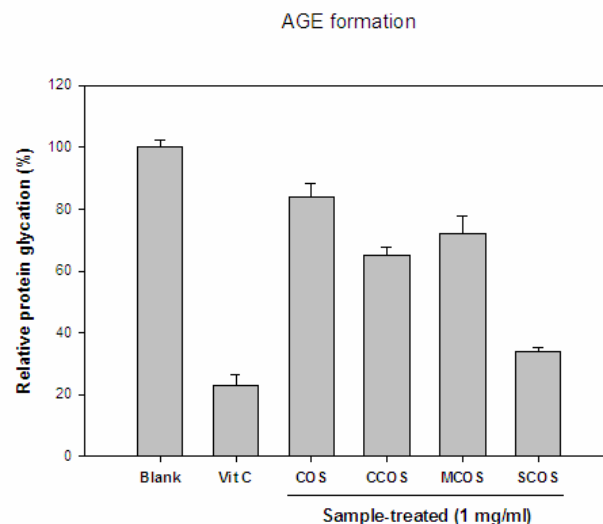


Figure 4. Effect of COS, CCOS, MCOS, SCOS and Vit. C on AGE formation

ACKNOWLEDGEMENTS

This research was supported by a grant from Marine Bioprocess Research Center of the Marine Biotechnology Program funded by the Ministry of Land, Transport and Maritime, Republic of Korea.

REFERENCES

- [1] Spiegelman, B. and Flier, J. (1996) Adipogenesis and obesity: rounding out the big picture. *Cell*, 87, 377–390.
- [2] Calle, E. and Kaaks, R. (2004) Overweight, obesity and cancer: epidemiological evidence and proposed mechanisms. *Nat. Rev. Canc.*, 4, 579–591.
- [3] Schwartz, M. and Porte Jr, D. (2005) Diabetes, obesity, and the brain. *Science*, 307, 375.
- [4] Leong, K. and Wilding, J. (1999) Obesity and diabetes. *Best Pract. Res. Cl. En.*, 13, 221–237.
- [5] Langin, D. (2006) Adipose tissue lipolysis as a metabolic pathway to define pharmacological strategies against obesity and the metabolic syndrome. *Pharmacol. Res.*, 53, 482–491.
- [6] Morrison, R. and Farmer, S. (1999) Insights into the transcriptional control of adipocyte differentiation. *J. Cell. Biochem.*, 75, 59–67.
- [7] Chae, S., Jang, M. and Nah, J. (2005) Influence of molecular weight on oral absorption of water soluble chitosans. *J. Contr. Rel.*, 102, 383–394.
- [8] Kim, S. and Rajapakse, N. (2005) Enzymatic production and biological activities of chitosan oligosaccharides (COS): A review. *Carbohydr. Polym.*, 62, 357–368.
- [9] Huang, R., Rajapakse, N. and Kim, S. (2006) Structural factors affecting radical scavenging activity of chitooligosaccharides (COS) and its derivatives, *Carbohydr. Polym.*, 63, 122–129.

ANTI-HIV-1 ACTIVITY OF PHOSPHORYLATED CHITOLIGOSACCHARIDES WITH DIFFERENT MOLECULAR WEIGHTS

Fatih Karadeniz¹, Mustafa Zafer Karagozlu¹, Chang-Suk Kong², Se-Kwon Kim^{1,3} *

¹Department of Chemistry, Pukyong National University, Busan 608-737, Republic of Korea;

²Department of Food and Nutrition, College of Medical and Life Science, Silla University, Busan 617-736, Republic of Korea;

³Marine Bioprocess Research Center, Pukyong National University, Busan 608-737, Republic of Korea

*E-mail address: sknkim@pknu.ac.kr

INTRODUCTION

Acquired immunodeficiency syndrome (AIDS) stands as one of the most important diseases worldwide with about 33.2 million people infected by human immunodeficiency virus type-1 (HIV-1) [1]. HIV-1 is identified as the causative agent of AIDS and up to now several drugs were tried to be promoted against HIV-1. However, HIV drug resistance, side effects and the need for long-term antiviral treatment urge the inevitable development of new anti-HIV agents, targets and therapies [2,3]. In this context, natural products offer excessive possibilities for discovering anti-HIV treatment as they possess a massive amount of potential of being a consistent source for successful drug discovery.

Polysaccharides have attracted much of attention as antiviral agents since the inhibitory activities of algal polysaccharides against mumps and influenza virus were firstly reported by Gerber et al. [4] Ehresmann et al. reported the inhibition of herpes simplex virus and other viruses by polysaccharide fractions from the extracts of ten red algae.[5] Sulfated polysaccharides from red alga, *Schyzimenia pacifica*, inhibited the HIV reverse transcriptase (RT) activity.

Chitosan oligosaccharides (COS) are hydrolyzed derivatives of chitosan composed of β -(1 \rightarrow 4) D-glucosamine units. They have better properties such as lower viscosity, relatively smaller molecular size in comparison to chitosan and short chain length with free amino groups which make COS highly soluble in aqueous solutions. COS are effective agents for lowering blood cholesterol and pressure, controlling arthritis, and enhancing antitumor properties.

Some chitosan derivatives are suggested to have antiviral effects. N-carboxymethylchitosan N,O-sulfate, which is derived from N-carboxymethyl chitosan by a random sulfation reaction, inhibited HIV-1 replication and binding to CD4 cell surface receptor.[6] Since chitosan oligosaccharides are biodegradable, water-soluble and nontoxic compounds, they might be beneficial biomaterials for the inhibition of HIV and the treatment of AIDS patients. In the present study, anti-HIV-1 properties of phosphorylated chitooligosaccharides (PCOS) and the effect of their molecular weight on the inhibition of HIV-1 was investigated.

MATERIALS and METHODS

Cell culture

H9 and H9/HIV-1_{IIIB} cell lines were obtained through American Type of Culture Collection (Manassas, VA, USA). CEM-SS cell line from Dr. P. Nara and C8166 cell line from Dr. G. Farrar were provided by the EU Programme EVA Centre for AIDS Reagents, NIBSC, UK.

Determination of syncytia formation

HIV-1 infection of CD4⁺ human T cell lines in culture results in significant cytopathic effects. Cell killing is characterized by initial formation of large, multinucleated giant cells and syncytia, followed later by destruction of single cells that swell and die.

1 x 10⁵ C8166 or CEM-SS cells in aliquots of 300 µl were seeded in triplicate to a 48-well plate containing 100 µl of serial dilutions of compound in complete medium. After 2 hours of incubation, the cells were infected with 100 µl of stock supernatant of HIV-1_{IIIB} diluted in complete medium at 200 CCID₅₀. The plates were incubated at 37°C for 72 hours and the number of syncytia was determined microscopically.

p24 antigen capture ELISA

H9 cells (3 x 10⁶ cells/ml) were incubated in the presence or absence of HIV-1_{IIIB} for 1 hour at 37°C. Cells were washed to remove unbound viruses and resuspended at 3 x 10⁵ cells/ml in culture medium. Aliquots of 1 ml were placed in a 24-well culture plate containing an equal volume of medium with/without sulfated COS. DS (Dextran sulfate) was treated as positive control. In order to determine the amount of virus released to the medium, HIV-1 p24 antigen capture ELISA was carried out with a commercial kit (Perkin-Elmer Life Sciences, Boston, MA) according to the manufacturer's instructions.

Western blot analysis

1 x 10⁶/ml H9 cells were cultured in 10 cm cell culture plates. Following sample treatment, plates were incubated for 2 hours and infected with HIV-1_{IIIB} at 200 CCID₅₀. After 96 hour of incubation at 37°C, cells were harvested for western blot analysis.

RESULTS and DISCUSSION

Primarily, PCOSs were evaluated for their anti-HIV properties according to its potential to inhibit syncytia formation on C8166 cells infected with syncytia inducing X4 tropic HIV-1_{RF} strain. Microscopic image of HIV-1_{RF} induced syncytia inhibitory activity of PCOS III (3~5 kDa) was shown on Figure 1. Syncytia formation on C8166 cells was observed and the number of syncytia was quantified 72 hours after the infection (Figure 2). PCOSs of all molecular weights treated exhibited a clear dose-dependent inhibitory activity on syncytia formation. Moreover, PCOS III appeared to be the most effective compound against syncytia formation. The EC₅₀ of PCOS III on inhibiting the giant cell formation was 3.58 µg/ml.

The protective activity of PCOSs on HIV-1 induced lytic effect was determined with MTT cell viability assay. Cells treated with PCOSs could maintain viability and the lytic effect of HIV-1 on C8166 cells was significantly suppressed. Among PCOSs, PCOS III also exhibited to be the most potent inhibitor of HIV-1 and protected the cells from lytic effect of HIV-1 with an EC₅₀ of 2.45 µg/ml. According to data obtained so far, further experiments were carried out using PCOS III only.

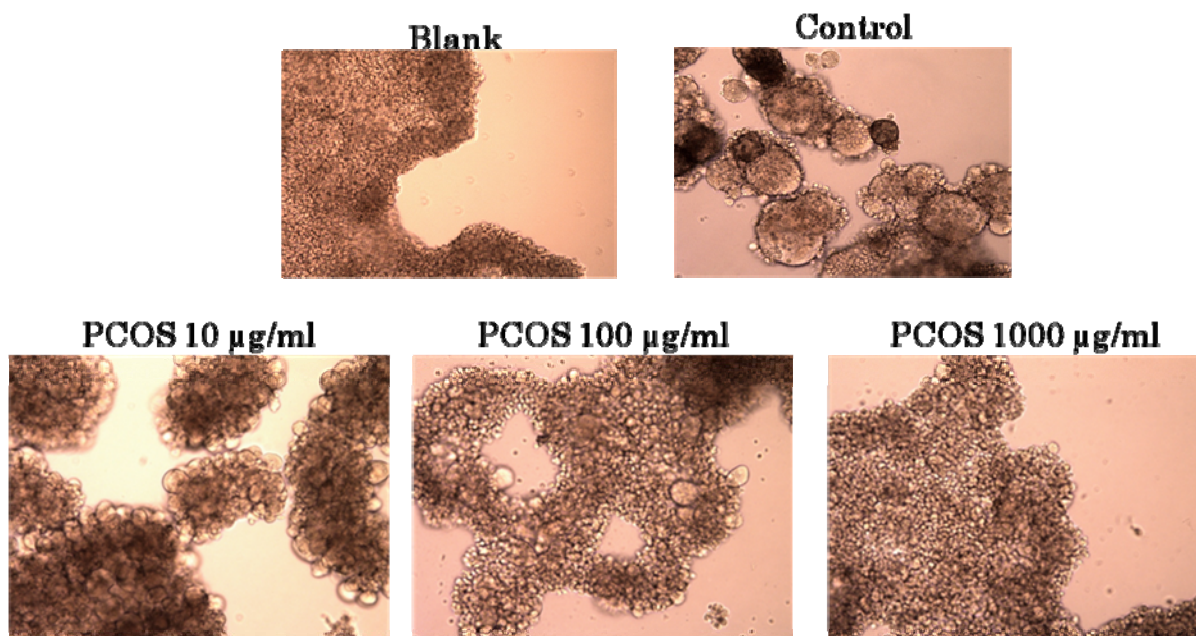


Figure 1. Cell images of HIV-1 infected cells in the presence of absence of PCOS at above-mentioned concentrations. (Blank: - HIV-1, - PCOS Control: + HIV-1, - PCOS)

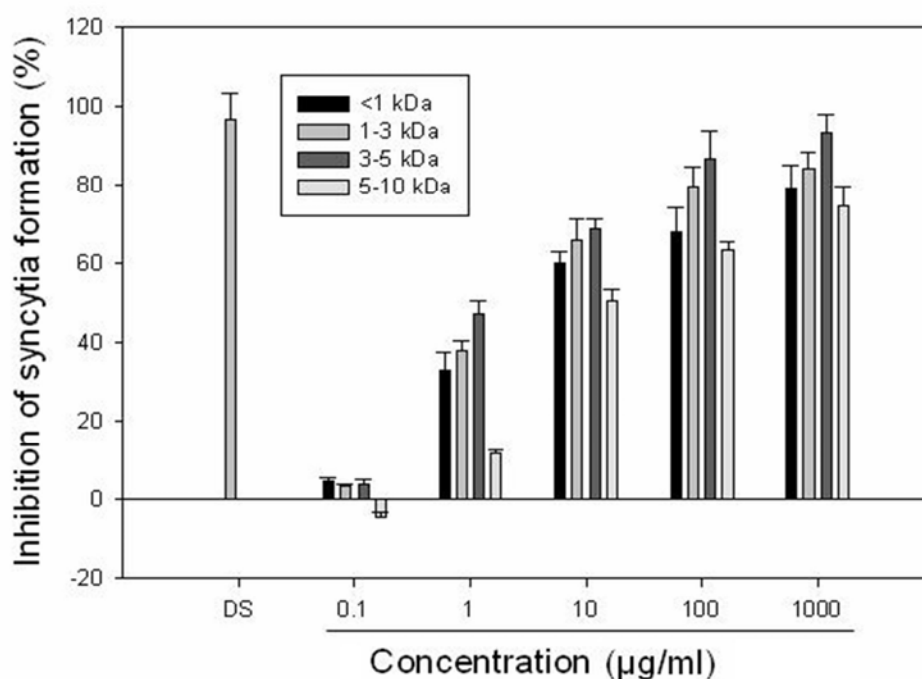


Figure 2. Inhibition of HIV-1_{IIIB} induced syncytia formation on C8166 cell line. Cells were treated with PCOS at the indicated concentrations 2 hours prior to infection. Dextran sulfate (100 µg/ml) was used as the positive control.

PCOSs were shown to be effective inhibitors of HIV-1 induced syncytia formation on C8166 cells as it was shown in microscopic images and protected infected cells from lytic effect of HIV-1. PCOS III appeared to be the most effective compound to protect cells from HIV-1

induced syncytia formation and lytic effect. Even though the protective effect of PCOS I on C8166 cells was higher than that of PCOS IV, PCOS I was the least effective compound on the inhibition of syncytia formation.

These results were consistent with the explanation given by Witvrouw and Declercq.[7] They reported that relatively low molecular weight (~1000 Da) polysaccharides (namely dextran sulfate) did not inhibit HIV-1 induced syncytia formation despite their other HIV-1 inhibitory properties. Therefore, the importance of molecular weight of sulfated polysaccharides on the inhibition of HIV-1 induced cytopathic effects was demonstrated.[7] They claimed that a significant increase was observed in anti-HIV-1 activity of dextran sulfate when molecular weight increased from 1 kDa to 10 kDa. At higher concentrations (10-500 kDa), however, HIV-1 inhibitory activity of dextran sulfate tended to decrease steadily. PCOSs protected cells from HIV-1 induced lytic effect at relatively lower concentrations when compared with the amount needed for the inhibition of syncytia formation which is consistent with the data explained before. This data indicates that PCOSs protect the cells from lysis once they are infected with HIV at some degree. However, the exact reason of this protection is not clear. Only PCOS III was used for subsequent experiments due to exhibiting better inhibitory activity on HIV-1 over other PCOSs.

Data obtained from syncytia formation and cryoprotective effect of PCOS III was consistent with the data obtained from ELISA and immunoblot analysis of p24 antigen. PCOS III effectively inhibited production of p24 antigen in cells infected with X4 or R5 tropic viruses (Figure 3). The EC_{50} for the inhibition of p24 antigen production was 5.63 $\mu\text{g/ml}$. In addition to p24 antigen capture ELISA data, inhibition of p24 protein production was further supported with data from immunoblot analysis. Immunoblot data indicated a dose-dependent inhibition of p24 protein produced by H9 cells acutely infected with HIV-1_{RF} (Figure 4).

In conclusion, the experiments pointed that PCOSs inhibited HIV-1 replication via blocking the interaction between HIV-1 glycoprotein gp120 and cell surface receptor CD4 and it was proved to be an effective inhibitor of HIV-1. Phosphorylated chitooligosaccharides (PCOSs) with different molecular weights were synthesized by a random phosphorylation reaction. In the present study, anti-HIV-1 properties of PCOSs were investigated in respect to their molecular weights. PCOS with the molecular weight of 3-5 kDa was found to be the most effective compound to inhibit HIV-1 replication and hinder HIV-1 infection. At non-toxic concentrations, 3-5 kDa PCOSs demonstrated significant inhibitory activities on HIV-1 induced syncytia formation (EC_{50} 3.58 $\mu\text{g/ml}$), lytic effect (EC_{50} 2.45 $\mu\text{g/ml}$) and p24 antigen production (EC_{50} 5.63 $\mu\text{g/ml}$). However, non-derivatized chitooligosaccharides did not show any activity against HIV-1 in all cases. It can be claimed that phosphorylated chitooligosaccharides could be potential HIV-1 inhibitors with their superior properties such as high absorption rate in the intestines which is a crucial feature for a drug candidate. Specific phosphorylation patterns and degree of phosphorylation of PCOSs could be a key factor in the inhibitory potential of PCOSs. Therefore, further experiments will be conducted to enhance the anti-HIV properties of PCOSs.

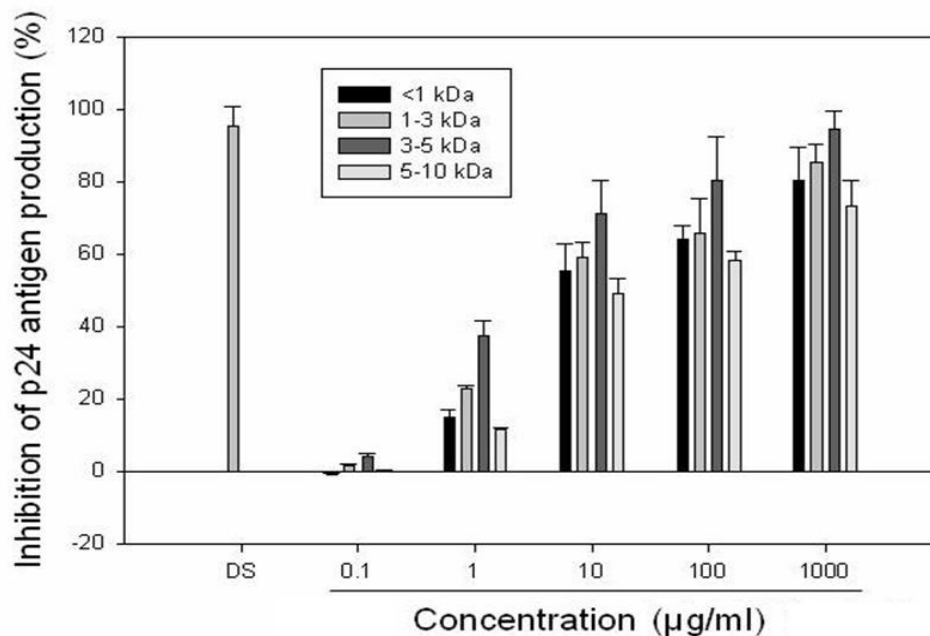


Figure 3. Inhibition of HIV-1_{IIB} p24 antigen production in the cell culture supernatant. Cells were treated with the indicated concentrations of PCOS and incubated for 72 hours. The p24 antigen amount was measured by p24 antigen capture ELISA.

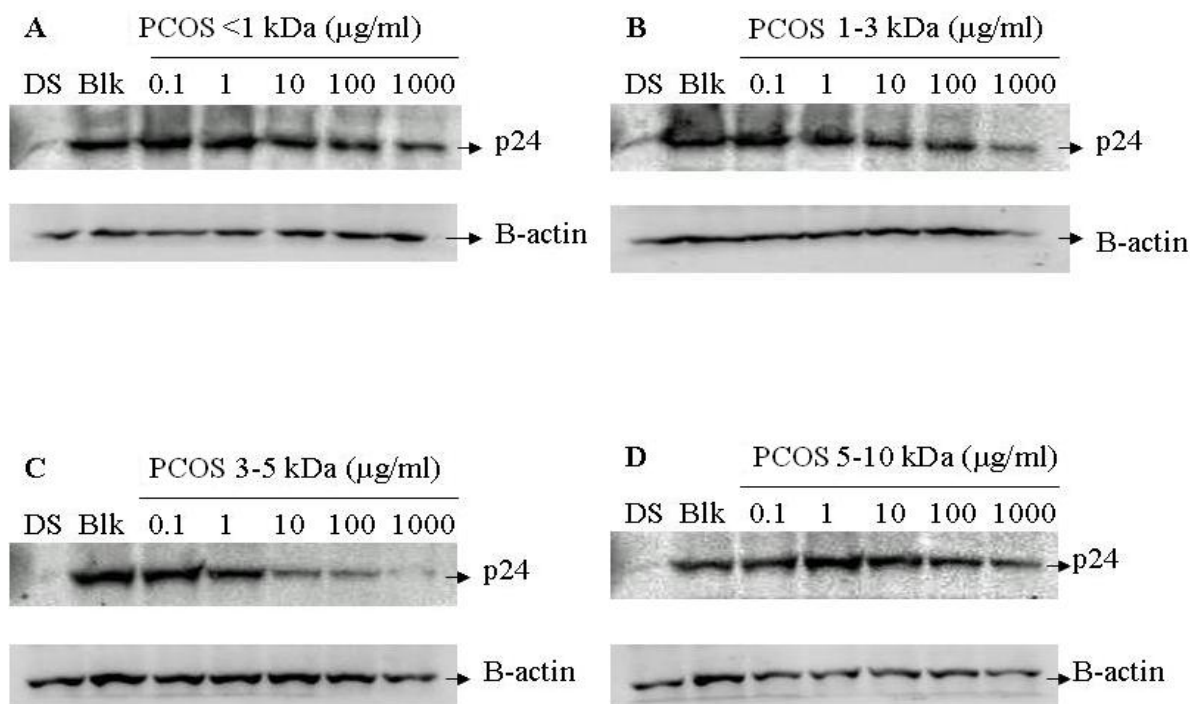


Figure 4. Western blot analysis of HIV-1_{IIB} 24 kDa p24 protein. Cells were treated with indicated concentrations of PCOS <1 kDa (A), 1-3 kDa (B), 3-5 kDa (C) and 5-10 kDa (D). H9 cells were infected with HIV-1_{IIB} and incubated for 96 hours. HIV-1 p24 core protein in the cell lysate was detected using mouse anti-p24 monoclonal antibody and horseradish peroxidase (HRP)-conjugated anti-mouse IgG secondary antibody.

ACKNOWLEDGEMENTS

This research was supported by a grant from Marine Bioprocess Research Center of the Marine Biotechnology Program funded by the Ministry of Land, Transport and Maritime, Republic of Korea.

REFERENCES

- [1] World Health Organization (2010) UNAIDS report on the global AIDS epidemic 2010. UNAIDS.
- [2] D'Aquila, R., Schapiro, J. and Brun-Vézinet, F. (2003) Drug resistance mutations in HIV-1. *Top. HIV Med.*, 11, 92-96.
- [3] Flexner, C. (2007) HIV drug development: the next 25 years. *Nat. Rev. Drug Discov.*, 6, 959-966.
- [4] Gerber, P., Dutcher, J. D., Adams, E.V. and Sherman, J. H. (1958) Protective effect of seaweed extracts for chicken embryos infected with influenza B and Mumps. *Proc. Soc. Exp. Biol. Med.*, 99, 590-593.
- [5] Ehresmann, D. W., Dieg, E. F., Hatch, M. T., Di Salvo, L. H. and Vedros, N. A. (1977) Antiviral substances from California marine algae. *J. Phycology.*, 13, 37-40.
- [6] Jayakumar, R., Nwe, N., Tokura, S. and Tamura, H. (2007) Sulfated chitin and chitosan as novel biomaterials. *Int. J. Biol. Macromol.*, 40, 175-181.
- [7] Witvrouw, M. and De Clercq, E. (1997) Sulfated polysaccharides extracted from sea algae as potential antiviral drugs. *Gen. Pharmac.*, 29, 497-511.

NANOFIBROUS MATERIAL BASED ON CHITOSAN-G-POLY(VINYL ALCOHOL) COPOLYMERS PREPARED BY SOLID-STATE SYNTHESIS

**L.V. Lesnyakova¹, A.O. Chernyshenko¹, T.A. Akopova², G.A.Vikhoreva¹, A.N. Zelenetsky²,
and L.S. Galbraikh¹**

¹*Kosygin Moscow State Textile University, Moscow, Russia 117091, Malaya Kaluzhskaya str.,1*

²*Enikolopov Institute of Synthetic Polymeric Materials of Russian Academy of Sciences, Moscow, Russia*

E-mail:kolaevalv@gmail.com

INTRODUCTION

Innovative way of development of world economy in many respects correlates with achievements and prospects of the nanotechnologies providing design of materials and systems with record quantitative or essentially new qualitative characteristics. One of such technologies is process of electrospinning (ES) that occupies a special place among all technological processes of fiber manufacturing employed in industry due to possibility to obtain superfine (nano) fibers. It knows as "dry" method of chemical fibers manufacturing because of its basic apparatus setup behavior. All process stages including: deformation of original polymer solution, solidification, fibers drift from nozzle to collector electrode and non-woven layer creation, are performed only by electric forces. The polymer spinning solution is fed, by gravity or excess gas pressure, at a preset volumetric flow rate from container to capillary injection nozzle. A metal electrode connected to regulated DC source that is placed in the container applies a high, usually negative potential difference to the free jet that is discharged from the nozzle. This causes the jet to steadily accelerate and thin out along an axis aligned with the general direction of the electric field. This is the first, relatively easy to regulate, stage of ES of fibrous materials, the stability and results of which control all its subsequent stages and, in the final analysis, the desired properties of the finished fiber [1]. This technique generates a material with developed surface that causes appropriateness of its usage to organize filtration and sorption processes, in particular, for the analytical purposes. Now nanofibers of polyvinylchloride, poly(vinyl alcohol) (PVA), polyethylene oxide, polycaprolactone, etc. are described [2-4]. In spite of the fact that throughout last several years the number of articles devoted to electroforming doubles every year, process yet hasn't found a sufficient theoretical and experimental justification for commercial development. It is necessary to conduct intense investigations, including chitosan-based materials promising for biomedical application.

Attempts to obtain by ES pure chitosan fibers using acetic acid polymer solutions have shown that only concentrated (80-90%) acid solutions possess the required values of electrical conductivity and surface tension to provide a success of molding. Of great interest to study the possibility of processing nanofibers of water-soluble chitosan derivatives having surface activity, in particular, its graft copolymers with poly(vinyl alcohol) (PVA), described in [5]. These products are obtained through innovation promising solid-state technology, which advantages are improved environmental and economic performance and high efficiency, especially for modification of natural polymers cellulose and chitin which is not soluble in common solvents. PVA is a hydrolysis product of poly-(vinyl acetate) (PVAc) and is a biocompatible water-soluble synthetic polymer. Besides, it is recognized as one of the few synthetic polymers particularly biodegradable under both aerobic and anaerobic conditions [6, 7]. PVA is used as a basic material for a variety of biomedical applications, including contact lens material, skin and artificial

cartilage replacement material, etc., because of its non-toxicity and desirable physical properties such as good ability to form films and fibers. Since chitosan is considered as fully biodegradable in human body polymer, its blends with PVA are attractive materials for numerous biomedical applications. These materials in a form of composite films, hydrogels, and scaffolds for cell attachments were prepared and characterized as biocompatible materials having desired properties for controlled drug delivery and tissue engineering [8–14]. The authors report a good compatibility of the components mainly due to hydrogen bonds which are formed between the functional groups of both polymers, results in an increase in mechanical properties of blend films. Among PVA/chitosan composites materials, temperature- and pH-responsive hydrogels and beads with porous cross-linked structure have been most widely studied. The physically crosslinked composites as well as those of materials prepared by using of different initiators and common cross-linking agents are essentially insoluble but good swelling in non-acidic aqueous solutions. At the same time, the main disadvantage of the commonly used "chitosan-based" method for many biomedical applications, in particular as a component of micro- and nanocapsules for encapsulation of sensitive to pH-value bioactive compounds, relates to chitosan poor solubility at physiological pH. Graft copolymerization is a known way to materials with new properties. The proposed synthetic scheme by employing as the precursors PVAc and chitin seem to be well efficient to prepare chitosan-g-PVA copolymers. To the best of our knowledge such systems were obtained first time. These systems that can be formed as films, microfibers and microcapsules were demonstrated to be very promising materials, in particular, as carriers of bioactive compounds and wound dressings [15, 16]. The developed stable polyelectrolyte microcapsules of the desired size and membrane thickness based on the chitosan-g-PVA copolymers were successfully used for a long term cultivation of animal cells [17, 18]. In addition, the obtained copolymers unlike those of their composite mixtures possess an excellent ability to stabilize the dispersions of inorganic particles, in particular TiO_2 nano-dispersions which play important role as photocatalytic sensibilizers of a multitude of biological processes [19, 20]. Thus, these copolymers could be successfully employed to prepare new hybrid polymeric systems with entrapped nanofillers both organic and inorganic origins.

The purpose of this work is to obtain water-soluble graft copolymers of chitosan and PVA using solid-state technique and to study their fiber forming ability by ES process.

MATERIALS and METHODS

Microgranulated PVAc with $\text{MM} = 500$ kDa (degree of polymerization of ~ 5800) was purchased from Sigma Aldrich (Germany), sodium hydroxide (98.5%, micropills with typical grain size distribution of $0.5 - 1.2 > 93\%$) was from Merck (Germany), chitin isolated from crab shells ($0.5 \pm 0.2\%$ ash, 5-6% moisture) was from Vostok-Bor (Russia). All solvents were purchased from Chimmed (Russia) as analytical grade and were used without further purification.

Water-soluble copolymers of chitosan and PVA containing 15 wt % of chitosan were obtained by solid-state synthesis as described earlier [21]. Briefly, PVAc and chitin solid mixtures in the presence of sodium hydroxide were processed with a semi-industrial co-rotating twin-screw extruder (ZE 40A×40D UTS, Berstorff, Germany) at elevated temperatures. The extruder has a variable set of processing elements providing a high shear strain and a powerful dispersive action. The power of this technique relies upon a variety of chemical (e.g.: polymeranalogous transformation and grafting) and physical transformations of solid polymers and monomers, occurring at conditions of joint action of high pressure and shear deformation. Intensive intermixing under shear deformation of solid reactive mixtures of chitin with sodium

hydroxide leads to formation of chitosan with high degree of deacetylation (more than 90%) at short duration of the process (5-10 min) at 180 °C. To prepare chitosan-g-PVA copolymer equal molar amount of PVAc (0.43 g per 1 g of chitin) and isopropyl alcohol (1 ml/g of reactive mix) were added and repeatedly co-extruded at 60 °C. To remove low molecular weight compounds, the prepared blends were exposed to water/organic mixture (ethanol/ethyl acetate/water) extraction for 48 hours followed by electrodialysis in an aqueous solution for 1-2 days. After filtration, the sample solutions were frozen and lyophilized at temperature $-10...+30$ °C up to moisture content of 2-3%. Formation of chitosan-g-PVA copolymers was confirmed by Fourier transform infrared spectroscopy (FTIR), gel penetration chromatography (GPC) and elemental analysis.

To analyze the samples by FTIR, thin films (5-10 μm thickness) were prepared by casting 2% (w/v) copolymer aqueous solutions onto glass substrates. The cast solutions were dried at 50 °C for 2 h. To estimate the chitosan content in the obtained products, a model blend film containing 20 wt% of chitosan was used. To prepare model blend film, a 10% water solution of PVA (Mowiol; 66-100; MW = 100 kDa; a content of vinylacetate units of 1%) and a 10% solution of chitosan (a content of N-acetylated units of 8 %, MW = 60 kDa) in 2% acetic acid were used. The film containing chitosan as acetate were held in 1 M NaOH for 1 h, carefully washed by deionized water, and dried. Glucosamine content was calculated from an intensity ratio of the bands assigned to chitosan $-\text{NH}_2$ bending at 1597 cm^{-1} , and $-\text{CH}_2-$ bending in PVA at 850 cm^{-1} . The IR-spectra were recorded in an absorbance mode at a resolution of 4 cm^{-1} and processed with Win-IR software v.4, Bio-Rad Digilab Division. All the spectra were normalized using the composite C–O band stretching vibrations of the pyranose ring at 1075 cm^{-1} as an internal standard. The data were kindly provided by Dr. L.V. Vladimirov.

The average MW of the samples was determined by GPC on Agilent 1200 (PLaque – OH 40 column, pre-calibrated with dextran standards, a flow rate of 1 mL/min, 25 °C). A 0.2% (w/v) sample solution in eluent ($\text{H}_2\text{O} + 0.02\%$ NaN_3) was used. Relative copolymer amounts were determined by means of an on-line refractive index detector. The data were kindly provided by Prof. A.V. Dushkin (ISSCM RAS, Novosibirsk).

Nanofibers were produced with nanospider NSLAB200S Elmarco Company. NS LAB 200 is designed for water and solvent ES, it can be configured to work with a wide variety of polymers and to produce a wide range of organic and biodegradable nanofibers. Fibers are obtained with linear speed of substrate 0.13 – 1.5 m/min, at 25-44 kV and concentration of a polymer solution of 6-15%. Electrical conductivity was measured with conductivity meter GS-117 (Russia) at voltage of 1V. Nanofiber images were received with SEM model JSM-5300LV (Jeol) at ISPM RAS (Moscow) by E.S. Obolonkova.

RESULTS and DISCUSSION

Fraction of the obtained products enriched with chitosan is dissolved in acidic aqueous media whereas a high content of grafted PVA-chains leads to solubility of the copolymers in water at neutral pH values (at 80-90 °C or 20-25 °C depending on length of grafted PVA fragments). Both water-soluble fractions were collected after dissolving (about 30% of entire blend) and used to prepare nanofibers. IR-spectroscopy was employed as the main method to analyze the copolymer structure. FTIR spectra of the samples after copolymer purification and precipitation from aqueous solutions contained characteristic absorption PVA and chitosan bands. The data showed that deacetylation degree of both polymers was almost complete (up to 95 – 98%). Figure 1 demonstrates FTIR spectra for chitosan-g-PVA sample (curve 2) compared

to a model mixture (curve 1). The calculations showed that the chitosan content in the obtained water-soluble copolymers were 15-20 wt%.

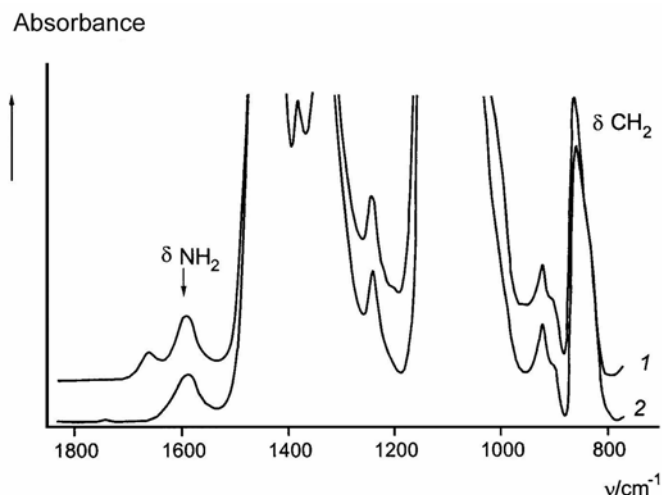


Figure 1- FTIR spectra of the chitosan/PVA (20/80 w/w) model mixture (curve 1) and chitosan-g-PVA copolymer (curve 2)

Glucosamine contents for chitosan and copolymers were also calculated from the results of elemental analysis using C/N ratio (5.29 in the case of initial chitosan). Elemental analysis data for both chitosan-g-PVA samples are (found/calculated, %): C, 52.96/53.05; N, 1.40/1.32; O, 36.91/36.87; H, 8.73/8.74. So, degree of PVA grafting onto chitosan was found about 450%.

The values of Mw of the copolymers determined by GPC method were 190 kDa for soluble at room temperature sample and 230 kDa for soluble at elevated temperature sample.

Conditions of ES process for copolymer samples are listed in Table 1. Successful molding was performed at concentration of a polymer solution of 9.5-14% and the applied voltage of 25-35 kV. It should be noted that if solution concentration was less than 9.5% the ES process has either defects or is not implemented.

Table 1- Conditions of ES process for chitosan-g-PVA samples

Solubility of chitosan-g-PVA copolymer	Solution concentration, w/v	Electric conductivity, $\times 10^{-3}$ (Ohm \times cm) $^{-1}$	Voltage, kV
at 80-90 °C	9.5	0.66	28-35
at 20-25 °C	14	0.37	28

Figure 2 shows SEM images of chitosan-g-PVA fibers of chitosan-g-PVA sample soluble in water at RT. It can be seen that an average diameter of fibers is \sim 50-100 nm.

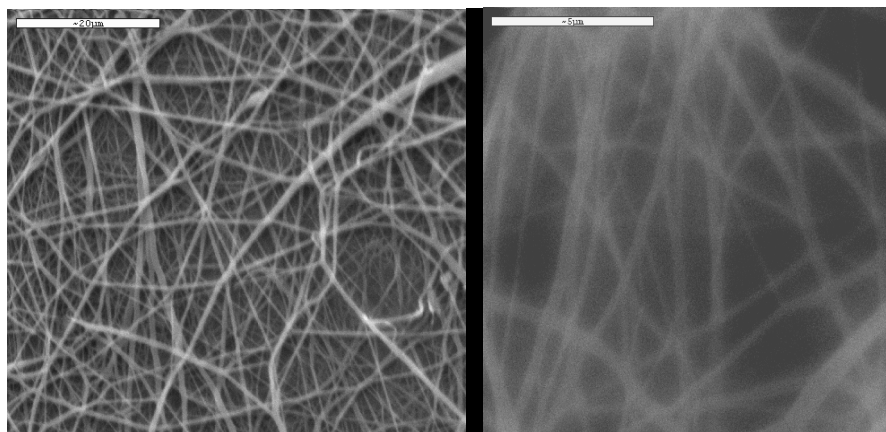


Figure 2 – Micrographs of nanofibers of chitosan-g-PVA sample

REFERENCES

- [1] Filatov, Y., Budyka, A., Kirichenko, V. (2007) *Electrospinning of Micro- and Nanofibers: Fundamentals in Separation and Filtration Processes*. New York, Begell House Inc.
- [2] Ignatova, M., Starbova, K., Markova, N., et al.(2006) Electrospun nano-fibre mats with antibacterial properties from quaternised chitosan and poly(vinyl alcohol). *Carbohydrate Research*, 12, 2098-2107.
- [3] Ojha, S., Stevens, D., Hoffman, T., Stano, K., et al.(2008) Fabrication and characterization of electrospun chitosan nanofibers formed via templating with polyethylene oxide. *Biomacromolecules*, 9, 2523-2529.
- [4] Hana, J., Zhanga, J., Yina, R., Maa, G., et al.(2011) Electrospinning of methoxypoly(ethylene glycol)-grafted chitosan and poly(ethylene oxide) blend aqueous solution. *Carbohydrate Polymers*, 83, 270–276.
- [5] Akopova, T., Zelenetskii, A., Ozerin, A. (2010) *Solid state synthesis and modification of chitosan. Manufacture, Properties, and Usage* (Ed. Samuel P. Davis), 16, Nova Science Publishers.
- [6] Matsumura, S., Tomizawa, N., Toki, A., et al. (1999) *Macromolecules*, 32, 7753–7761.
- [7] Corti, A., Solaro, R., Chiellini, E. (2002) *Polym. Degrad. Stab.*, 75 (3), 447–458.
- [8] Lee, S. Y., Pereira, B. P., Yusof, N., Selvaratnam, L., et al. (2009) *Acta Biomater.*, 5, 1919–1925.
- [9] Berger, J., Reist, M., Mayer, J. M., et al. (2004) *Eur. J. Pharm. Biopharm.*, 57, 19–34.
- [10] Mucha, M., Ludwiczak, S., Kawinska, M. (2005) *Carbohydr. Polym.*, 62, 42–49.
- [11] Kim, S., Park, S., Kim, S. (2003) *Reactive and Functional Polymers*, 55, 53–59.
- [12] Srinivasa, P., Ramesh, M., Kumar, K., Tharanathan, R. (2003) *Carbohydrate Polymers*, 53, 431–438.
- [13] Mangala, E., Kumar, T., Baskar, S., Rao, K. (2003) *Trends Biomat. Art. Organs.*, 17, 34-40.
- [14] Wang, T., Turhan, M., Gunasekaran, S. (2004) *Polym. Int.*, 53, 911-918.
- [15] Zelenetskii, A., Akopova, T., Kildeeva, N., et al.(2003) *Russ. Chem. Bull. Int. Ed.*, 53, 2073- 2077.
- [16] Akopova, T., Markvicheva, E., Vladimirov, L., et al. (2005) *Ext. Abst. Eur. Polym. Congress*, Moscow, Russia.
- [17] Markvicheva E., Zaitseva-Zotova D., Akopova T., Zelenetskii A.(2007) *Eur. J. Cell Biol.*, 86S1, 63.
- [18] Zaytseva-Zotova, D., Balysheva, V., Tsoy, A., Akopova, T., et al. *Macromol. Bio Sci.*, submitted.
- [19] Ozerin, A., Zelenetskii, A., Akopova, A. et al. (2006) *Polymer Science. Ser. A*, 48, 638-643.
- [20] Ozerin A., Perov N., Zelenetskii A., Akopova T. et al.(2009) *Nanotechnologies in Russia*,4, 331–339.
- [21] Ozerin, A., Zelenetskii, A., Akopova, T.,Vikhoreva,G., Chernyshenko, A. et al. (2007) Method of preparation of graft-copolymers of chitin and chitosan. RF Patent №. 2292354

CLONING FULL LENGTH GENE OF ASCHI61, A CHITINASE FROM *AEROMONAS SCHUBERTII*

Chao-Lin Liu^{*}, Kai-Ming Lin and Biing-Cheng Lim

Department of Chemical Engineering and Graduate School of Biochemical Engineering, MingChi University of Technology, New Taipei City 243, Taiwan

**E-mail: f2402002@ms16.hinet.net*

INTRODUCTION

Chitin, an insoluble linear (1→4)- β -linked homopolymer of N-acetyl-D-glucosamine (GlcNAc), is the much abundant polysaccharide on the earth second to cellulose. They are present in arachnids, most of higher fungal cell walls, insect exoskeletons, the shells of crustaceans, parts of invertebrates (1) and as an extracellular polymer of some bacteria (2). The formation rate and steady-state amount of chitin is about 10^{10} to 10^{11} tons every year. Most of the biological materials composed of chitin finally become biological solid waste if not degraded by the enzyme, chitinase. The chitinase could be obtained in numerous organisms, such as viruses, bacteria, higher plants and animals. (1). Chitinases produced by the organisms with chitin are presumably required for morphogenesis of cell walls and exoskeletons (1). And the control of chitinase digestion or deformation of the chitin should be effective. Others without chitin may produce chitinases primarily to provide carbon and nitrogen as a nutrient or other biological function (3, 4). Based on the catalytic mechanisms and products, chitinases are categorized three groups, endochitinase (EC 3.2.1.14), chitobiosidases (3.2.1.30), and exochitinase (EC 3.2.1.52) (5). But in prokaryotes and eukaryotes, the enzymatic degradation of chitin is similar. The first step, primary done by microbes and playing a key role in the solubilization and mineralization of chitin, is endochitinase randomly hydrolyze the glycosidic bonds between GlcNAc residues to oligomers. Then the exochitinase, β -N – acetylhexosaminidase, reduces the oligomer to monomer from the nonreducing end. In some organisms, chitobiosidases release GlcNAc dimers from the nonreducing end between the two steps to facilitate the degradation (1, 6).

Chitinases were applied for enzyme-immobilization and waste in the industry since 1970s. Chitin and its derivatives such as chitosan, deacetylation of chitin, inclusive of polysaccharides, oligosaccharides and monosaccharides of chitin are interested because they have apparently various biological functions and activities (7). They are biodegradable, histocompatible and nontoxic biomaterials and have been shown to play a role in plant organogenesis and embryogenesis of invertebrates (8). The addition of chitin to soil can reduce the populations of fungal plant pathogens and plant parasitic nematodes because of the populations of chitinolytic bacteria increase. Now, some of the biomedical materials are composed of chitin, such as artificial joint. Chitin oligosaccharides have also been investigated to enhance the functions of immunological system in the host animal and might display tumoricidal agents (9). In addition, the antimicrobial activities and cholesterol reduction were also demonstrated. While, the biological activity of chitin and its derivatives depends on the chain length and solubility. Recently, the hexamer with strong biomedical function has been described (Immune). Therefore, small chito-oligosaccharides are produced after chitin hydrolyzed by chitinases instead of chemical cleavage to obtain the more homogeneous oligomers. However, the stability and activity of chitinases are the key points on application.

We intended to obtain better chitinases producing hexamer of chitin derivatives and with rigid structure to be applied for mass production in the industry. In this study, microorganisms from the soil of the tropic Taiwan with chitinase activities are screened after induced with chitin. According to taxonomic rules, the organism was *Aeromonas schubertii*. Then two chitinases, ASCHI53 and ASCHI61 were purified with bioseparation techniques. After alignment of N-terminal amino acid sequences with database, the proteins were identified as novel ones. Impressively, those chitinases are SDS-resistant (SDSR) and the most biological activities chitin derivatives, hexamer, were obtained after their digestion of chitin. After genomic DNA extraction and restricted enzyme digestion, an adaptor obtained from plasmid treated with enzyme was ligated. Then the gene of ASCHI61 was cloned according the degenerated primer designed from the amino acid sequence.

MATERIALS AND METHODS

Chemicals

Chitin was purchased from in the local markets imported from Vietnam. Media for microorganism incubation were purchased from Difco Laboratories (Dentroit, MI). And other chemicals used were from Sigma Chemical Co. (St. Louis, MO).

Isolation of chitinase-secreting microorganisms by chitin inducing

The agar medium with 0.2% colloidal chitin was used as a selective plate for isolation of chitinase-secreting microorganisms in soil as described previously. The colonies with surrounding clear zones were selected to perform further experiments. The selected microorganisms were grown in 100 ml Luria-Bertani (LB) medium with or without 2% chitin powder at 28°C for 3 days, and the chitinase activity in growth medium was detected.

Culture and classification

A single colony of the selected microorganism with the chitinases from the plate with chitin was pre-inoculated in the BSH1 medium (0.07 % K₂HPO₄, 0.03 % KH₂PO₄, 0.05 % MgSO₄, 0.03 % Peptone and 0.03 % Yeast extract) with 2% glucose at 37°C overnight. Then the bacterium was transferred in chitin medium, BSH1 medium with 2 % chitin powder, at 28°C for chitinase induction. It was classified mainly according to the methods of Bergey's manual.

N-terminal amino acid sequence determination

The lysate of the isolated chitinases was detected by SDS-PAGE as described by Laemmli and visualized by staining with Coomassie brilliant blue R-250 (Laemmli, 1970).

The amino acid sequences of proteins were determined by protein techniques, as previously reported (10). The purified proteins were separated by means of SDS-PAGE and subsequently electroblotted onto a PVDF membrane with a semidry blotting system. The blot was stained with 0.1 % Coomassie brilliant blue in 50 % methanol 10% acetate and then destained. The protein bands were cut. The N-terminal amino acid sequences of purified proteins were then determined with the piece membrane subjected to a 476A sequencer (Applied Biosystems, Foster City, CA).

Protein measurement

The quantification of protein was performed by using Pierce BCA detecting kit with bovine serum albumin as a standard. The protein concentration was measured the absorbance at 280nm and calculated in the column chromatography.

RESULTS AND DISCUSSION

Isolation of inductive chitinase-secreting microorganisms from soil of the mangrove marsh

Chitin is a polymer of GlcNAc linked by β -glycosidic bond. Therefore, specific enzymes that hydrolyze β -glycosidic bonds are necessary to degrade native chitin. Chitin is degraded by

chitinase that is widespread in nature and distributed in many species. Its occurrence has been reported in several bacteria, for example *Serratia marcescens*, *Vibrio sp.*, *Altermonas sp.* and *Aeromonas sp.* etc. However, the applications of enzymes are limited due to neither thermal stable nor insensitive to chemical. Therefore, it is an important initial point to screen bacteria with unique chitinase that degrade chitin. At beginning, the microorganisms from the mangrove marsh soil of southern part of Taiwan were screening in the selective plate for one week in this investigation. Ten colonies of chitin-degrading microorganisms were obtained because of clear zone formation in the plates. Then, these were cultured with chitin powders and the mediums were collected for measurement of secretory chitinase activities directly by a novel substrate, colloidal chitin azure. Because the detection of the azure produced from chitinase hydrolysis would be free of disturbance with reducing sugars in the mediums. Strain E1 showed the strongest chitinolytic activity in the medium with detergent when it was inoculated at 28°C.

The strain formed large and clear halos at 28°C in the selective plate (Fig. 1). The phenotype of colony is round and white. It was shown that the bacteria is rod Gram-negative with the microscope examination. Taxonomic studies on the strain E1 was identified as *A.s schubertii*.

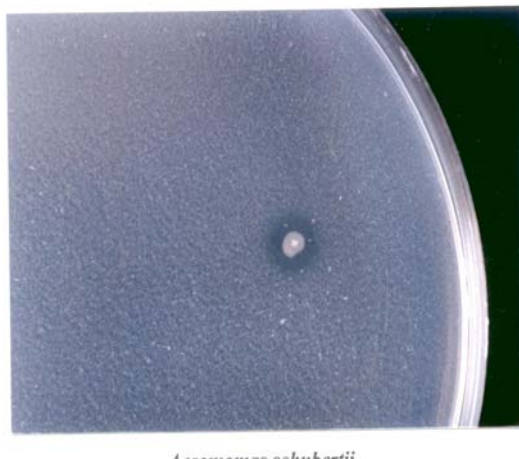


Fig.1. *Aeromonas schubertii* isolated from the soil of the southern part of Taiwan.

Microorganisms without chitin produce the chitinases to digest chitin as nutrient. In some of them, the chitinase only be expressed for supplement during poor nutrients. Single colony of *Aeromonas schubertii* was inoculated in LB medium overnight. Then the culture was transferred to two tubes of LB medium with or without the chitin powder. The chitinase activity was measured with the medium taken every 24 hours for four days. The strain secreted active chitinase only in the presence of chitin powder. It suggested that the chitinases secreted by *A. schubertii* were inducible enzymes.

Properties of ASCHI53 and ASCHI61

The molecular weights of these two proteins treated with 10 % β -mercaptoethanol (MSH) were the same as those without it. It suggested that both of them were pure monomeric proteins. The molecular weights calculated were 43 kDa and 55 kDa from the SDS-PAGE.

The accurate molecular weights were determined with MALDI-TOF. They were 53,527 Da and 61,202 Da respectively. They are designated ASCHI53 and ASCHI61 according to the molecular weight. By protein techniques with automatic amino acid sequencer, the N-terminal sequences were "VASTLP for ASCHI53" and "KEAWNGQEG" for ASCHI61. By BLAST, it was indicated two proteins are novel proteins with amino acid sequence analysis in the Database.

Rapid amplified gene end

An adaptor fragment was obtained from BMP plasmid treated with *Pvu* II. The genomic DNA and the adaptor fragment were digested with *Eco* R I, *Bam* H I or both of them. The genomic DNA and the adaptor treated with the same digestion condition were ligated (Fig. 2).

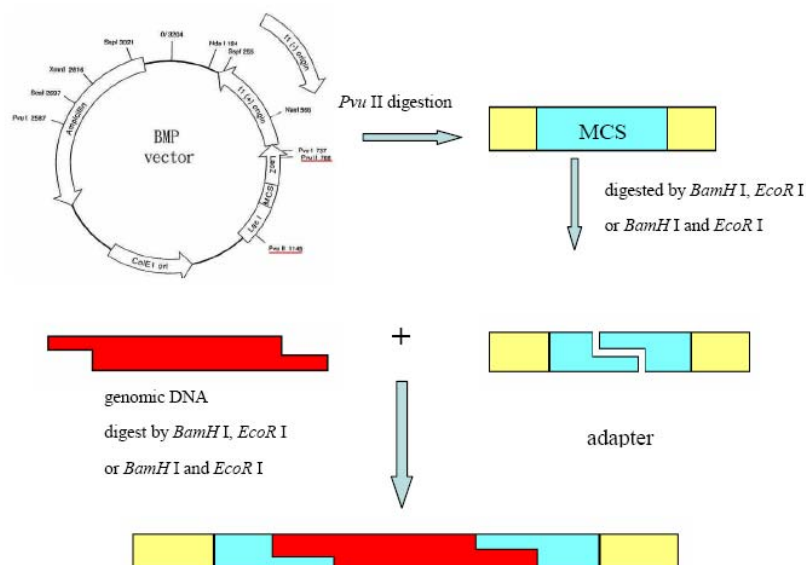


Figure 2. The strategy of genomic DNA library construction.

After the PCR with the degenerated primers designed on the amino acid sequences, ASCHI61 gene was cloned and sequencing. Sequence analysis showed that the ASCHI 61 gene contains 1,692 base pairs (Fig. 3), with an open reading frame encoding a preproprotein with 564 amino acid residue and predicted signal peptide for secretion.

1	ctggaggcct	ggaacgggca	ggagggggagc	gataccttcg	aggtcatctt	cgacagccag
61	gtgtggcaaa	acgcctggtg	ggtcggtgcc	agccattgtc	ccggcgaggc	tcagcccaat
121	gatcccaaca	acccatggcg	cgtggtacgt	gccgccacgg	cggccgaaat	gacccagtat
181	ggcaatccca	ccacctgtga	taccagtggg	ggcgggtggtg	agaccctgcc	tgatttcgat
241	gccagccagg	gttatcgga	aggggacaag	gtgactctca	atggggggcga	ctacctggcg
301	acggccgatg	tgctgtcta	cagcttcag	ccggcacaag	cctctcctg	ggctctctat
361	ctccccctgc	ccagctggca	gagcagtacc	gtttataaca	agggcgaccg	ggtgtctctg
421	gaggggcagg	gttatgaggc	cctgttctgg	accagggggg	atgatccttc	cgatcctgcc
481	aatcagaatc	cggagggaaa	taatggccgt	ccctggaagc	ctcttgggcc	gatgcacaac
541	tacacggacg	aggagtggc	ccaggctcca	cagctcgata	cgagcgtgct	ctatccggcc
601	gataccctgg	tgcaatttga	acaggggcat	cacgtatccc	gtcaacaggt	gcgcggggtc
661	cgtccggggg	atctatttc	ttggcagggc	tatgtggagt	ggggcaacgt	gaaagagcag
721	gtgggcacgc	ccaagcaccc	ctggccagcc	caggtctatg	ccccttatct	cgatgcgacc
781	ctcaacagtg	tgccgaacat	gggagagctg	gccagcaac	aggggggtcga	tcacttcacc
841	ctcgcccttg	tggtggccaa	ggatgccag	acctgtgtcc	cgacctgggg	gacctactac
901	aagatggggg	atttcccgtc	gtcttacagc	aacatcaagg	gattgcgcga	tcaaggtggg
961	gatgtgatgg	tctccatcgg	cggagcggcc	aatgcgccgc	tgccgcgcgc	ttgcgacaat
1021	atcgacgagc	tggcgcgtca	gtacatggat	atcgtcgaca	acctcaacct	gcaggtactc
1081	gactttgaca	tcgagggggac	ctgggtagcg	gatgcggtct	ccatcacccg	gcgcagccag
1141	gccctggtga	gggcccgaggc	ccagtgggct	gcgcaaggca	agcaggtggc	aatctggtat
1201	acctgcccc	ttctaccca	gggactcacc	gccgatggca	tcaaggtgct	gcagagtgcc
1261	cgggatcacg	gggtgaaact	gaccggcatc	aacgtcatga	ccatggacta	cggcgacagc

1321	gcctgcccgc	cgtcccaggg	tgagggagcc	aatattcagg	gccagtgcgg	ggtcgatgcc
1381	atcaacaacc	tgttccgcga	cgtcaaggcc	atcttcccgg	agaaggagga	tgccgccatc
1441	tgggcatgc	ttggcaccac	ccccatgac	ggcgtcaatg	acgtgcaaag	tgaggtgttc
1501	taccgctcgg	atcgggcgct	caccctgcaa	catgcgcagg	agcaagggat	cggcatgac
1561	ggcatctggt	ccatgccccg	cgatcagccg	ggcacggcgg	gtcaggtgtc	gcccagagcat
1621	agcggcctga	ccgaggctca	gtccccccgt	tacggcttca	gtgccctgtt	caaggcggtc
1681	accagcgct ga					

Figure 3. The nucleotide sequences encoding ASCHI61.

In this study, a novel SDS-resistant chitinase ASCHI61 was identified. In tradition, the gene usually cloned by primers designed from the similar enzyme of relative organism. A new technique was developed in the work. An N-terminal and internal amino acid sequence were obtained from protein technique. And the degenerated primers were designed from amino acid sequences accordingly. In the genomic library, adaptors and restriction enzymes were applied. Finally, the full-length gene was cloned by the novel method, rapid amplified gene ends (RAGE).

ACKNOWLEDGEMENTS

This study was financially supported by the grants of Nation Science Council 96-2221-E-131-008.

REFERENCES

- [10] Gooday, G.W. (1990) The ecology of chitin degradation. *Adv. Microb. Ecol.*, 11: 387-430.
- [11] Flach J., Pilet P.E. and Jolles, P. (1992) What's new in chitinase research? *Experientia*, 48:701-716.
- [12] Abeles, F. B., Bosshart, R. P., Forrence, L. E. and Habig, W. H. (1990) Preparation and purification of glucanase and chitinase from bean leaves. *Plant Physiol.* 47: 129-134.
- [13] Cohen-Kupiec, R. and Chet, I. (1998) The molecular biology of chitin digestion. *Curr. Opin. Biotechnol.* 9: 270-277.
- [14] Shen, C. R., Chen, Y. S., Yang, C. J., Chen, J. K. and Liu, C. L. Colloid chitin azure is a dispersible, low-cost, substrate for chitinase measurements in a sensitive fast reproducible assay. *J Biomol Screen* 2010, 15, 213- 217.
- [15] Wang, S. Y., Moyne, A. L., Thottappilly, G., Wu, S. J., Locy, R. D. and Singh, N. K. (2001) Purification and characterization of a *Bacillus cereus* exochitinases. *Enz. Microb. Technol.* 28:492-498.
- [16] Shahidi, F., Arachchi, J. K. V., and Jeon, Y. J. (1999) Food applications of chitin and chitosans. *Trends Food Sci. Technol.*, 10: 37-51.
- [17] Bakkers, J., Semino, C. J., Stroband, H., Kijne, J. W., Robbin, P. W. and Spaink, H. P. (1997) An important developmental role for oligosaccharides during early embryogenesis of cyprinid fish. *Proc. Natl. Acad. Sci. U.S.A.*, 94: 7982-7986.
- [18] Suzuki, K., Mikami, T., Okawa, Y., Tokoro, A., Suzuki, S. and Suzuki, M. (1986) Antitumor effect of hexa-N-acetylchitohexaose and chitohexaose. *Carbohydr. Res.* 151: 403-408
- [19] Liu, C. L., Shen, C. R., Hsu, F. F., Chen, J. K., Wu, P. T., Guo, G. S., Lee, W. C., Yu, F. W., Mackey, Z. B., Turk, J., and Gross, M. L. (2009) Isolation and Identification of Two Novel SDS-resistant Secreted Chitinases from *Aeromonas schubertii*. *Biotechnol. Prog.* 25:124-131.

ISOLATION OF CHITIN AND OTHER VALUE-ADDED PRODUCTS FROM DISCARDED DECAPOD CRUSTACEANS USING AN ENZYMATIC HYDROLYSIS-BASED PROCEDURE

M. García-López*, P. Ramos-Ariza, R. Gómez-Mariño, J.M. Vieites-Fernández, C. González-Sotelo, R.I. Pérez-Martín*

Instituto de Investigaciones Marinas-Consejo Superior de Investigaciones Científicas. 36208 Vigo. Spain

E-mail address: ricardo@iim.csic.es

INTRODUCTION

Fisheries discards and fishery wastes are a matter of concern due to their economic and environmental impact. With the aim of reducing these negatives impacts, the use and valorization of both discarded species and byproducts of fisheries is an active area of research.

The exoskeleton of crustaceans is a source of chitin, the second most abundant polysaccharide in nature. This biopolymer and its derivatives (e.g. chitosan) have multitude of applications in several areas such as: medicine, food preservation, wastewater treatment, etc [1].

In this work, four species of discarded decapod crustaceans caught on the Galician-Northern Portugal coast and/or the Grand Sole were considered for chitin isolation, namely: the galatheid *Munida spp* and the portunid crabs *Polybius henslowii*, *Liocarcinus depurator* and *Macropipus tuberculatus*. These organisms inhabit the Atlantic continental shelf and slope. Furthermore, three of them belong to the group of dominant decapod crustaceans on the Galician coast [2].

In crustaceans shells, chitin is associated to other components: proteins, minerals and pigments. As a consequence, its isolation involves three basic steps: demineralization, deproteinization and bleaching. The characteristics of each treatment and the order they are carried out are variable and conditioned by the raw material. Usually demineralization and deproteinization are accomplished with hydrochloric acid and sodium or potassium hydroxide solutions, respectively [1].

Notwithstanding, the enzymatic hydrolysis is a preferable alternative to the chemical alkali treatment since it is a less aggressive procedure; thus undesirable alterations of biomolecules such as lipids or proteins, which could be eventually of interest for commercial use, are minimized [3].

In this work, we aimed to take advantage of the whole potential of the aforementioned discarded crustaceans as a source of value-added products integrating in a single procedure the isolation of chitin as well as the production of pigment-containing, protein hydrolysates that might be used in aquaculture or animal feed.

Chitin recovery was assessed and its purity checked by infrared spectroscopy and proximate composition analysis.

MATERIALS and METHODS

Samples

Four species of discarded decapod crustaceans were considered, namely: the galatheid *Munida spp* and the portunid crabs *Polybius henslowii*, *Liocarcinus depurator* and *Macropipus tuberculatus*. These crustaceans were caught off the Galician-Northern Portugal coast and/or the Grand Sole and kindly provided to our laboratory by the local shipowner cooperative ARVI. Depending on the harvesting area, samples remained on board from a few hours up to three days

after having been caught. Crustaceans were preserved in ice until landing. Once received, species were biometrically characterized in terms of size, weight, genus and maturation state. Additionally, the proximate composition of a grinded pool of representative specimens was determined. After that, remaining specimens of each species were ground with a commercially available food grinder during a controlled time and finally blended to ensure sample homogeneity. Portions of 400 g were packed into plastic bags and frozen at -20 °C until use. Portions of the same material were used as control, in order to determine the proximate composition at the beginning of each experiment the same day it was conducted.

Reagents

Alcalase 2.4L food grade was donated by Novozyme (Bagsvaerd, Denmark). Commercial chitin from crab was purchased from Sigma-Aldrich (Steinheim, Germany). Sodium hydroxide was obtained from Vorquímica (Vigo, Spain). Chlorhydric acid 37% was provided by VWR (Briare, France) and sodium hypochlorite 10% (w/v) supplied by Panreac (Barcelona, Spain).

Chitin isolation

Chitin isolation involved three basic steps: deproteinization, demineralization and bleaching. Deproteinization was accomplished in two separated, non-consecutive stages consisting on an enzymatic hydrolysis and an alkaline treatment. The latter was included to ensure complete deproteinization of the final product.

The experiments were carried out in a water-thermostated 2 L-reactor, equipped with a temperature and pH probe. A burette containing a sodium hydroxide solution (1M) was electronically programmed and used to control the pH during the assays. Samples (400.0 g) were submerged in distilled hot water (ratio 1/5, w/v) and stirred for 10 minutes until 55°C were achieved. The pH of the mixture was adjusted to 8.0 with the sodium hydroxide solution before the addition of alcalase (ratio 0.5% v/w). Stirred samples were hydrolyzed for 2 hours at that constant pH and temperature, with the addition of sodium hydroxide when necessary. After that, the enzyme was deactivated by rising the temperature to 90 °C (maintained for 10 min). The mixture was allowed to cool and then consecutively sieved through 500 and 20 µm meshes. Recovered solids were combined and subjected to demineralization with chlorhydric acid (0.4 M; ratio 1/10, w/v) at room temperature, with continuous stirring, during 1 hour. The procedure was repeated 3 times. The filtered material ($\phi > 20 \mu\text{m}$) was washed with water (1/5, w/v) until neutrality and then further deproteinized with NaOH (1 M, 1/10 w/v) at 65 °C for 2 h. The obtained solid ($\phi > 20 \mu\text{m}$) was bleached with 1% NaClO in two steps of 30 min each. Finally, chitin was washed with water (1/5, w/v) and dried in an oven at 105 °C for 24 h.

Proximate composition and other analysis

Moisture, total nitrogen and ash contents were determined according to the AOAC methods [4]. In short, the moisture content was determined drying in oven at 105 °C until constant weight, the ash content by drying in a furnace at 525 °C for 24 h and the nitrogen percentage by the Kjeldahl method. Lipids were extracted following a modified Bligh and Dyer method [5] where chloroform was substituted by dichloromethane.

Residual protein in chitin was determined using a procedure described elsewhere [6]. Chitin was deproteinized with a 10% sodium hydroxide solution (ratio 1/10, w/v) for 2 hrs at 90 °C and the protein content determined in the supernatant with the bicinchoninic acid (BCA) assay [7].

Dried samples of crustaceans were digested with nitric acid in a microwave and their calcium, sodium, potassium and magnesium contents determined by inductively coupled plasma-optical emission spectroscopy (ICP-OES).

The purity of the final chitin product and the composition of the dried crustaceans were investigated by infrared spectroscopy.

RESULTS and DISCUSSION

The composition of crustacean shells was investigated by means of infrared spectroscopy. For that purpose, empty exoskeletons (free of viscera and muscle) of each species were dried, grinded and homogenized. In all cases, obtained IR spectra showed several bands, indicating that carapaces were a mixture of several compounds, of organic and inorganic nature, among them calcium carbonate (Figure 1). Thus, the isolation of chitin, requires a purification procedure to get rid of these other components.

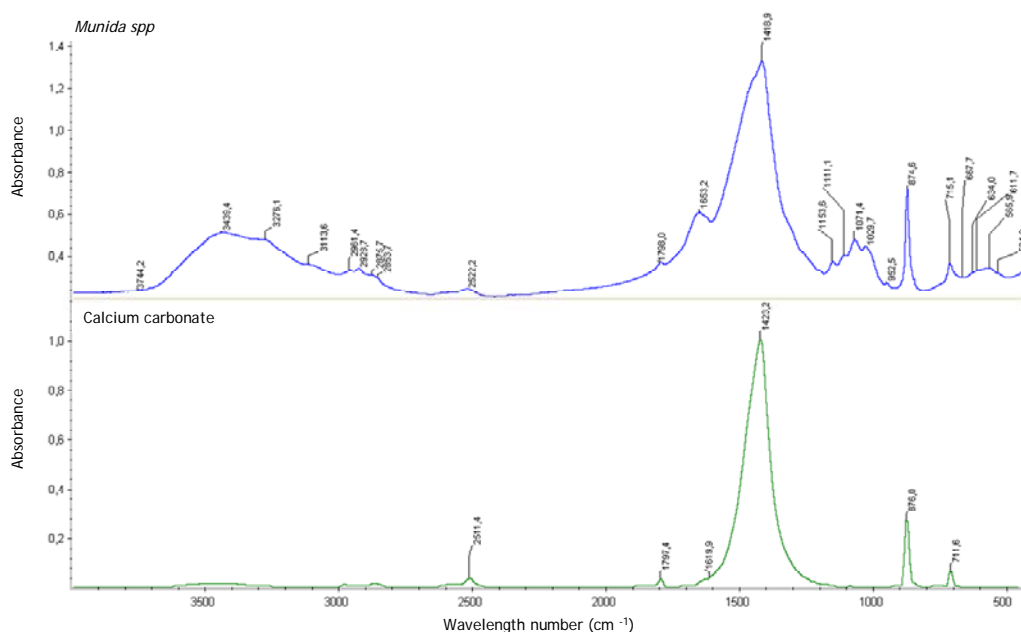


Figure 1. IR absorption spectra of *Munida spp* shell and CaCO_3 .

The proximate composition of the considered crustaceans was also determined. Table 1 shows the percentages of moisture, ashes, lipids and nitrogen of grinded samples employed as raw material in the experiments for chitin isolation.

Table 1. Proximate composition of grinded samples of crustaceans

	Moisture	Ash %	Lipids %	Nitrogen %
<i>Polybius henslowii</i>	67 ± 1	53.1 ± 0.2	1.6 ± 0.3	5.4 ± 0.5
<i>Liocarcinus depurator</i>	73.2 ± 0.4	52 ± 3	1.85 ± 0.05	6.2 ± 0.2
<i>Macropipus</i>	74.0 ± 0.1	48.90 ± 0.01	0.46 ± 0.09	5.90 ± 0.09
<i>Munida spp</i>	67.7 ± 0.3	54.8 ± 0.7	0.40 ± 0.04	5.0 ± 0.7

Mean ± standard deviation. Ashes, lipids and nitrogen percentages are referred to dry weight.

According to these data, crustaceans had high water and ash contents, with values above 67% and 48%, respectively. The ash percentage is directly correlated with the mineral content of the sample. For these crustaceans, calcium represents around the 14-16% of the dry weight while sodium, potassium and magnesium together account for about 4%.

Assays for chitin isolation were conducted in triplicate and the recoveries, expressed as the mass percentage of the initial dried material subjected to the experimental procedure, ranged from 3.9 ± 0.5 and 7.0 ± 0.4 % (Table 2).

Table 2. Chitin recoveries for the four crustaceans

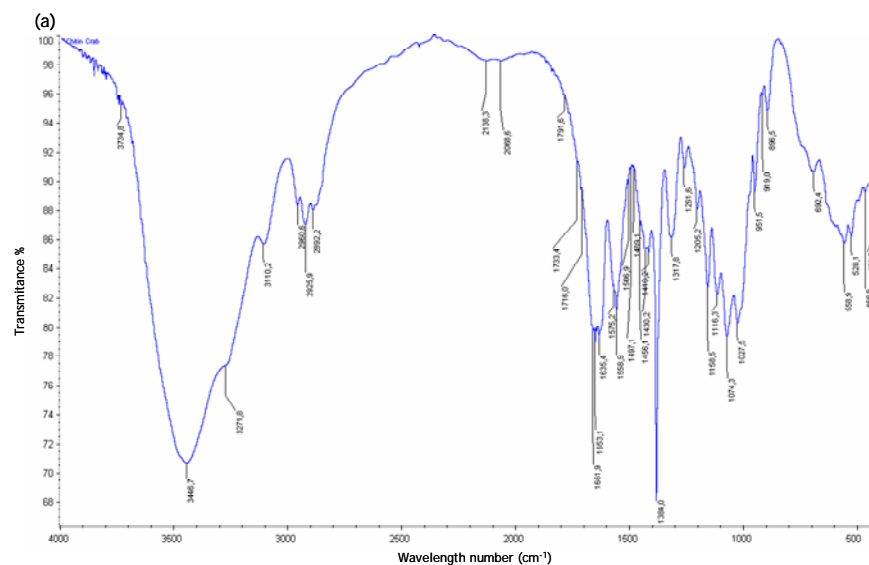
	R %
<i>Polybius henslowii</i>	7.0 ± 0.4
<i>Liocarcinus depurator</i>	5.2 ± 0.4
<i>Macropipus tuberculatus</i>	3.9 ± 0.5
<i>Munida spp</i>	5.0 ± 0.3

Mean \pm standard deviation

These values are lower than other found in the literature [8, 9], however it is worth noting that in this work not only the shell but the whole crustacean was employed.

The proximate composition of the final product was also assessed. Bearing in mind that the mineral content of these species was about the 50% of the dry weight, the ashes percentage of the final chitin is a parameter to be concerned about. The proposed demineralization procedure, consisting on three acidic washing steps, kept the ash content of chitin below 11%. It is important to point out that the efficacy of this treatment strongly depends on the raw material. For instance, in the case of shrimp two steps of the same treatment sufficed to obtain a final product almost free of ashes, with values below 1%. The protein residue and the lipid content in the final chitin were below 1.6% and 0.6 %, respectively.

Figure 2 shows the high purity of the chitin obtained from *Polybius henslowii* which matches the IR spectrum of a commercial chitin from crab.



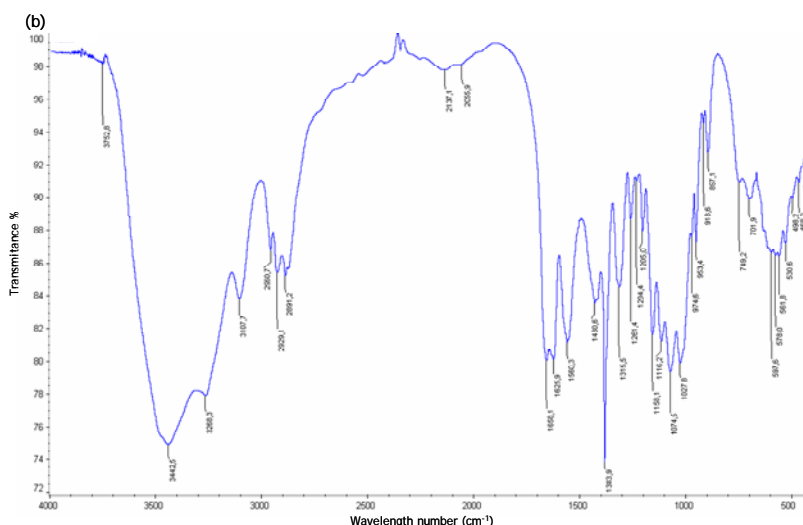


Figure 2. (a) IR spectra of commercial chitin from crab and (b) chitin obtained through the presented procedure from *Polybius henslowii*.

ACKNOWLEDGEMENTS

Financial support from projects MMA033E (Xunta de Galicia) and Interreg POCTEP 0330-IBEROMARE-1-P (European Union) is acknowledged. The authors also thank the services from the C.A.C.T.I. (University of Vigo) for their instrumental support.

REFERENCES

- [1] Synowiecki, J. and Al-Khateeb, N.A. (2003) Production, properties, and some new applications of chitin and its derivatives. *Crit. Rev. Food Sci. Nutr.*, 43, 145-171.
- [2] Fariña, A.C., Freire, J. and González-Gurriarán, E. (1997) Megabenthic decapod crustacean assemblages on the Galician continental shelf and upper slope (north-west Spain). *Mar. Biol.*, 127, 419-434.
- [3] Duarte de Holanda, H. and Netto, F.M. (2006) Recovery of components from shrimp (*Litopenaeus setiferus*) processing waste by enzymatic hydrolysis. *J. Food Sci.*, 71, C298-C303.
- [4] A.O.A.C. (1990) Official methods of analysis. Washington D.C.: Association of Official Analytical Chemists.
- [5] Bligh, E.G. and Dyer, W.J. (1959) A rapid method of total lipid extraction and purification. *Can. J. Biochem. Physiol.*, 37, 911-917.
- [6] Synowiecki, J. and Al-Khateeb, N.A.A.Q. (2000) The recovery of protein hydrolysate during enzymatic isolation of chitin from shrimp *Crangon crangon* processing discards. *Food Chem.*, 68, 147-152.
- [7] Smith, P.K., Krohn, R.I., Hermanson, G.T., Mallia, A.K., Gartner, F.H., Provenzano, M.D., Fujimoto, E.K., Goeke, N.M., Olson, B.J., Klenk, D.C. (1985) Measurement of protein using bicinchoninic acid. *Anal. Biochem.*, 150, 76-85.
- [8] Al Sagheer, F.A., Al-Sughayer, M.A., Muslim, S., Elsabee, M.Z. (2009) Extraction and characterization of chitin and chitosan from marine sources in Arabian Gulf. *Carbohydr. Polym.*, 77, 410-419.
- [9] Naczki, M., Williams, J., Brennan, K., Liyanapathirana, C., Shahidi, F. (2004) Compositional characteristics of green crab (*Carcinus maenas*). *Food Chem.*, 88, 429-434.

TERMOADSORPTION SEPARATION DNA OF FRAGMENTS BY CHITOSAN

M. Marasulov*, J. Azimov, N.N. Turaeva, B.L. Oksengendler, R.Y. Milusheva, S.S. Rashidova

*Institute of polymer chemistry and physics, Tashkent, 100128, Kadiri str., 7B, Uzbekistan
E-mail: mbm1005@mail.ru*

In the problem of increasing the adsorption by solid adsorbents, there are two ways:

1) increasing the specific surface area of adsorbent, 2) strengthening of interaction between adsorbate and adsorbent. Depending on the physical and chemical nature of sorbate and sorbent the realization of the ways of enhanced sorption can be solved differently. So increasing the surface of adsorbent may be implemented in two ways: either decreasing the size of sorbent particles (for example transition to nano scale) or increasing the porosity. The specific surface of sorbents depends on the size of spherical particles according to the formula:

$$S_{\text{sp}}(d) = \frac{6 \times 10^3}{\rho d} \quad (1)$$

where d is the diameter of spherical particles, ρ is the density of the particles [1]. It has been seen from this formula that decreasing the particle size increases the specific surface and the sorption capacity.

According to the well-known concept of fractals [2], the sorption capacity is associated with the surface of an adsorbate molecule (σ) at its size of δ and the fractal dimension (D), which characterizes the porosity of sorbent according to the formula

$$n \propto \delta^{-D} = \sigma^{-D/2} \quad (2)$$

However, the adsorption process depends not only on the geometric characteristics of the adsorbent. It is of great scientific interest to determine the nature of physical interactions between adsorbate and adsorbent. In this paper we will discuss the nature of physical interaction at the adsorption and desorption processes of single-stranded DNA fragments on porous chitosan containing the polar groups as $-\text{NH}_2$.

Consider the interaction of the charged adsorbate (DNA) with the dipoles of the polar groups of $-\text{NH}_2$ of chitosan. According to the Gauss's theorem [3], the electric field of negative charges on DNA chain locating in pores of chitosan can be regarded as a electric field of total charges located in the center of the pore. In this case, the ion-dipole interaction is responsible for the retention of charged molecule on dipoles in nonpolar media (Fig. 1).

The potential energy of attraction between the charged adsorbate and the dipole of the polar group is described by the following expression [4]:

$$U = -\frac{pq \cos \theta}{4\pi\epsilon_0 \epsilon r^2}, \quad (3)$$

where p is the dipole moment, q is the ion charge, θ is the angle between the electric field and the dipole, ϵ is the dielectric constant of the medium, ϵ_0 is the permittivity of vacuum, r is the distance between the ion and the dipole. The total energy of the ion interaction with all dipoles of chitosan is the sum of energies of its interaction with each dipole. Then the expression for total energy is the following:

$$U_t = -N \frac{pq}{4\pi\epsilon_0 \epsilon r^2} \langle \cos \theta \rangle, \quad (4)$$

where N is the number of polar groups in the pore, $\langle \cos \theta \rangle$ is the average cosine of the angle at some spatial distribution of dipoles in thermal equilibrium and equals to

$$\langle \cos \theta \rangle = \frac{\int \rho(\theta) \cos \theta d\Omega}{\int \rho(\theta) d\Omega} = \frac{\int_0^\pi 2\pi \sin \theta \cos \theta \rho(\theta) d\theta}{\int_0^\pi 2\pi \sin \theta \rho(\theta) d\theta}, \quad (5)$$

where $\rho(\theta)$ is the distribution function. The distribution function can be chosen in several different ways, depending on specific systems. The systems of dipoles can be classified by three types: 1) the fixed dipoles on the sorbent have a constant direction relative to its axis ($\rho_1(\theta)$), 2) the fixed dipoles are distributed randomly about the axis of the macromolecule ($\rho_2(\theta)$) 3) the dipoles are distributed in accordance with the Boltzmann law. In the first case, we have

$$\langle \cos \theta \rangle = \frac{\int_0^\pi 2\pi \sin \theta \cos \theta \delta(\theta - \theta_o) d\theta}{\int_0^\pi 2\pi \sin \theta \delta(\theta - \theta_o) d\theta} = \cos \theta_o. \quad (6)$$

In this case, the potential energy of interaction will be

$$U_t = -N \frac{pq}{4\pi\epsilon_o\epsilon r^2} \cos \theta_o. \quad (7)$$

In the second case, due to the random nature of the distribution of the dipoles relative to the chain the total interaction energy equals to zero. In the third case, the Boltzmann law of distribution is valid, that is $\rho_3(\theta) = e^{-pE \cos \theta / kT}$. For this case $\langle \cos \theta \rangle = L(pE / kT)$ [4], where $L(x)$ is the Langevin function.

In the case of $pE \ll kT$, we obtain

$$U_t \approx -N \frac{p^2 q^2}{(4\pi\epsilon_o\epsilon)^2 r^4} \frac{1}{3kT} \quad (8)$$

The number of polar groups on the inner surface of a spherical pore of radius R_0 can be defined as $N = n_o \delta 4\pi R_o^2$ where n_o is the number of dipoles per unit volume of chitosan, δ is the cross size of chitosan macromolecule.

Let's consider two different situations: 1) the pore size is comparable to the persistence length of a chain ($2R_o \approx l$) and 2) the pore size is much greater than the persistence length ($2R_o \gg l$).

Note that $q = e \frac{2R_o}{d_o}$, where d_o is the distance between neighbour the charges on DNA.

Then for the energy of interaction of DNA with chitosan dipoles in the pore we can write the expression

$$U_t^{(1)} \approx -n_o \delta \frac{p^2 e^2}{3\pi(\epsilon_o\epsilon)^2 d_o^2} \frac{1}{kT} \quad (9)$$

Hence it has been seen from this expression, the energy of interaction of DNA with chitosan dipoles does not depend on the pore radius. This nontrivial result is suitable for the case when the pore diameter is comparable with the persistence length of DNA [5]. Let's estimate the parameters of the expression (9). The average size of pores in the chitosan is 4 nm and the cross size of chitosan $\delta=1\text{nm}$. The number of dipoles per unit volume of chitosan can be determined by the formula $\eta_0 = \frac{N_{at}}{V} \alpha$ where the N_{at} is the number of atoms of chitosan in the unit cell of the

volume V . And α is the fraction of dipoles in the unit cell. The estimations show that $\eta_0 \delta \approx 1.5 \times 10^{18} \frac{1}{m^2}$. We can calculate the dipole moment of the polar group-NH₂ (Fig. 2) by

$p = q_H \vec{r}_1 + q_H \vec{r}_2 + q_N \vec{r}_3 \approx q_N \vec{R}$, where $\vec{r}_1, \vec{r}_2, \vec{r}_3$ – are the coordinates of hydrogen and nitrogen atoms q_H and q_N are their charges, \square is the distance from the nitrogen to the mass center of two atoms of hydrogen. The nitrogen atom of the polar group has approximately a charge of $-0.9e$. The estimations show that the dipole moment at $R = 0.4 \text{ nm}$ equals $p = 1.44 \times 10^{-29} \text{ C} \cdot \text{m} \approx 4D$. The distance between the charges (d_0) on DNA chain can be equated to the size of DNA nucleotide (0.34 nm).

The second case. The pore size of chitosan is much greater than the persistence length of DNA chain ($R_o \gg l$). Suppose that the conformation of DNA fragment is of ideal coil form. In this case, the ideal coil size is given by $4R_o^2 = Ll$. Hence the charge of the fragment of DNA is:

$q = e \frac{4R_o^2}{d_0 l}$. Then the energy of interaction of DNA with chitosan dipoles has the form:

$$U_i^{(2)} \approx -U_i^{(1)} \left(\frac{2R_o}{l} \right)^2$$

Thus, in the second case the energy of interaction of DNA with chitosan dipoles can be compared with the first case and depends on the size of the coil, which fills the entire pore. We can evaluate the critical temperature of deadsorption of DNA from the pores of chitosan. The condition that the fragment of DNA in pores of chitosan, will be retained in it till the critical temperature at T^* , is the following: $U_i = kT^*$. From this expression we obtain the formula for

$$T^* \text{ taking into account the general expression (8): } T^* = \frac{pq}{4\pi\epsilon_o\epsilon R_o^2 k} \sqrt{\frac{N}{3}}$$

For the considered two cases, we have

$$T_1^* = \frac{pe}{d_o\epsilon_o\epsilon k} \sqrt{\frac{n_o\delta}{3\pi}} \approx 4 \times 10^{14} \frac{p\sqrt{n_o\delta}}{d_o\epsilon} \text{ (K)} \quad (10)$$

$$T_2^* = T_1^* \frac{2R_o}{l} = \frac{2peR_o}{d_o\epsilon_o\epsilon kl} \sqrt{\frac{n_o\delta}{3\pi}} \approx 8 \times 10^{14} \frac{pR_o\sqrt{n_o\delta}}{d_o\epsilon l} \text{ (K)} \quad (11)$$

It is obvious, that the critical temperature of DNA fragment deadsorption from chitosan depends on the properties of adsorbent (p, n_o, δ, R_o), adsorbate (d_o, l) and medium (ϵ). And for the first case no dependence on the pore size is there, whereas in the case of big pores, the critical temperature depends on the size of pores, which means that deadsorption temperature of DNA increases with the pore size of chitosan.

The estimation of T_1^* taking into account all calculated magnitudes of parameters of expression (10) gives $T_1^* \approx 288K$. Thus, on the basis of the above theoretical analysis we can propose a method of termoadsorption spectroscopy of different DNA fragments.

The algorithm of the method is as follows:

1-st step. Adsorption of DNA molecule in the pores of chitosan with a certain size distribution at low temperatures (below T_1^*).

2-nd step. As the temperature increases eventually to T_1^* the desorption of DNA fragments with the length comparable with the length of DNA segment.

3-rd step. At further increase of temperature to T_2^* desorption DNA fragments with the length of R_o^2/l occurs. It means gradually allocation of initially small fragments of DNA, then large DNA fragments, according to the following expression and taking into account $4R_o^2 = Ll$ and the expression (11)

$$L \approx l \frac{T_2^{*2}}{T_1^{*2}} \quad (12)$$

Expressing the length of the chain (L) in terms of the number of nucleotides pairs (b) ($L = b \cdot d_o$) the temperature dependence of desorption on the number of nucleotides pairs has the following form:

$$T_2 = \sqrt{\frac{bd_o}{l}} T_1. \quad (13)$$

Accounting the values at $d_o=0.34nm$, $l=4nm$, we obtain $T_2 \approx 0.3T_1\sqrt{b}$.

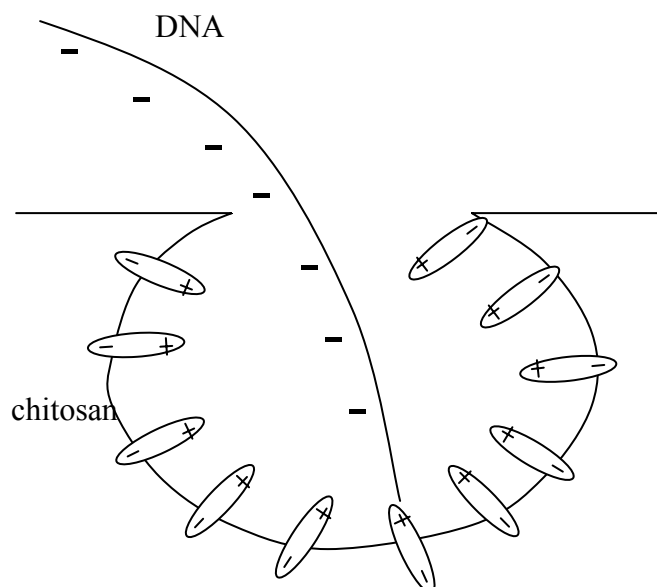


Fig1. Adsorption of DNA with negative charged groups on the chitosan pore, with polar groups of - NH₂

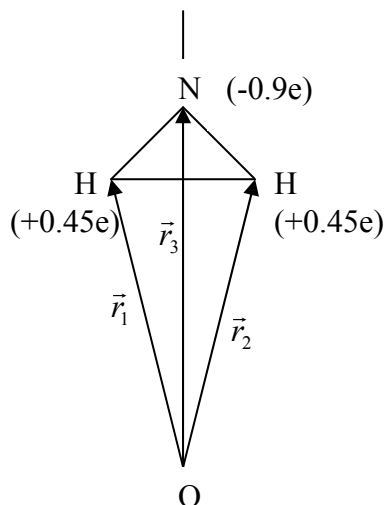


Fig2. Dipole moment of polar group of -NH_2

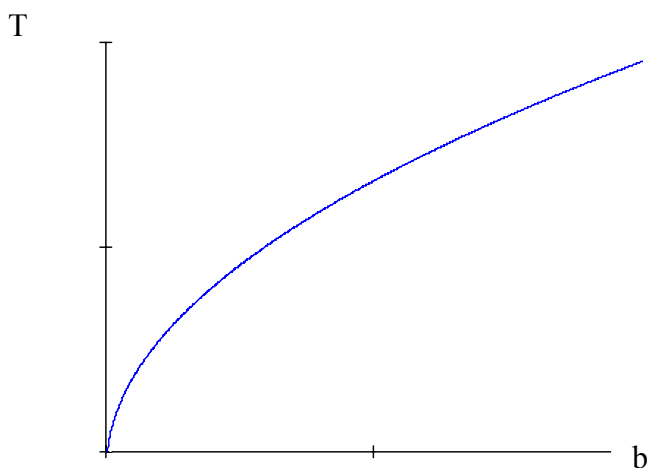


Fig3. The dependence of temperature of DNA deadsorption from the chitosan pore on DNA length.

CONCLUSIONS

Thus, in this work we consider the theoretical aspects of thermoadsorptive separation of different DNA fragments from the surface of chitosan by the controlling parameter of temperature.

REFERENCES

- [1] Charles Poole, M.L., Owens, F.N. Nanotechnology, MA: Cam-2007, 376 p.
- [2] Feder, E. Fractals, Moscow: Mir, 1991, 260 p.
- [3] Tamm, I.E. Fundamentals of Electricity, Moscow: Nauka, 1989.
- [4] Kittel, C. Introduction to Solid State Physics, Moscow: Nauka, 1978, 791 p.
- [5] Wolkenstein, M.V. Biophysics, Moscow: Nauka, 1981.

CHEMICAL, PHYSICAL AND MICROBIOLOGICAL PARAMETERS OF CHITIN AND CHITOSAN FOOD AND INDUSTRIAL PURPOSES

G.V. Maslova^{1*}, LA Nudga², G.M. Mikhailov², S.V. Nemtsev³, A.I. Albulov⁴

¹ GYPRORYBFLOT Research and Design Institute for Development and Operating of Fleet, St. Petersburg.

² Institute of Macromolecular Compounds, ICS, RAS, St. Petersburg.

³ All-Russia Research Institute of Fisheries and Oceanography, Federal State Unitary Enterprise VNIRO, Moscow.

⁴ Joint Stock Company "Bioprogress", Moscow

The most abundant and biologically renewable raw material for obtaining chitin and chitosan can be found in the shells of crab, shrimp, krill, crayfish, fresh water shrimp Gammarus and other crustaceans.

An average content of chitin in crustacean waste, depending on the type of raw material, totals Chemical, Physical and Microbiological Parameters of Chitin and Chitosan Used for 20-30%. The use of crustacean wastes left after production of such traditional products as canned, frozen, cooked-and-frozen, minced and pasted crab meat is very important for the fishing industry as it results in comprehensive non-waste production, improves environmental situation, helps to produce valuable medications the cost of which exceeds to a great extent the price of the above mentioned food products and, consequently, increases the profit gained by fishing fleet and fish processing enterprises.

The properties of chitin and chitosan depend on the methods used for the harvesting and preservation of raw material, its storage temperature, conditions and methods of obtaining, degree of proteins, lipids and mineral salts removal, methods of deacetylation. Biopolymers of non-uniform quality can be obtained from one and the same raw material. The chemical, physical and microbiological parameters of chitin and chitosan are determined both by their producers and consumers in medicine, veterinary, cosmetology and many other (food, paper, textile and agriculture) industries.

However, until now in Russia and internationally no uniform requirements for the parameters of chitin and chitosan have been developed, moreover, still there is no international or national standard specifying any requirements to such parameters and methods for their determination. Physical and chemical properties of biopolymers are often determined by different methods, with the use of non-standardized instruments. Sometimes they are expressed in different units and are calculated in different ways.

Hence, the determination of criteria for chitin and chitosan parameters and prospects for their use in a particular sector of economy is a very important issue for the development of further production and sales.

The need to unify and standardize the parameters of chitin and chitosan, methods of their determination has been discussed at international European and Asia-Pacific congresses, conferences of Russian Chitin Society.

Basing upon the analysis of papers published by Russian researchers, recently developed regulatory documents, proceedings of international conferences, results of patent searches and other data, the authors have developed a draft national standard (Code of Practice) specifying the key parameters of biopolymers that need to be determined with the view that they will be used in manufacturing of edible and non-food products. Chitin is mostly used as a raw material for the industrial production of chitosan and is very rarely used by itself.

Chitosan with its wide scope of basic characteristics is successfully used in agriculture, sewage treatment, paper industry. However, the application of chitosan in medicine, veterinary and food industry implies the use of this natural polymer with well-defined characteristics. Hence the gradation of normalized parameters should meet the requirements of individual industries. In food industry chitosan is used to increase the shelf life of products both as a food ingredient and as a protective film coating. The use of chitosan improves functional properties of bakery products, helps to stabilize the structural characteristics of food. For instance, in dairy industry chitosan is used as a biologically active additive to dairy produce.

Parameters of chitosan applicable for food industry are listed in Table 1.

Table 1

Parameter	Characteristics and standard
Appearance	Scales, flakes or grits
Colour	From white to cream or pink with mother of pearl shine or without it. Greyish or yellowish tint is possible.
Flavour	Chitosan typical flavour, odorless.
Moisture content, %, not more than	10
Mass fraction of mineral substances, %, not more than	0,7
Mass fraction of proteins, %, not more than	1,0
pH 1 %-solution of chitosan in 2 % acetic acid, not more than	6,5
Mass fraction of insoluble substances, %, not more than	0,2
Degree of deacetylation, %	85-95
Molecular weight, kDa	50-250
Mesophilic aerobic and facultative anaerobic microorganisms, KOE in 1 g of chitin, not more than	2×10^4
Kinematic viscosity of 1 % solution in 1% acetic acid solution, cps, at least	50

In agriculture, chitosan is used to improve plant resistance to various diseases. Since the biocidal activity of chitosan increases in line with its molecular weight extra treatment of chitosan is vital. The rest of the requirements for agriculture are less strict than those applied to chitosan used for food and medical purposes (Table 2).

Table 2

Parameter	Characteristics and standard
Appearance	Scales, flakes or grits
Size of scales, mm, not more than:	
- scales and flakes	10
- grits	5
Colour	From white to cream, grayish or yellowish
Moisture content, %, not more than	10
Mass fraction of mineral substances, %, not more than	2
Mass fraction of proteins, %, not more than	0,5
Degree of deacetylation, %	80 – 88
Solubility in 2% acetic acid, %, at least	80
Viscosity of 2 % solution in 2 % acetic acid, cps	100-500

In veterinary chitosan is used to improve nonspecific resistance of animals to infectious diseases and for increasing the weight gain in calves. In the first case, this requires intramuscular

injections of chitosan solution, in the second chitosan is added to animal feed. Accordingly, in the first case, the requirements applied to chitosan are similar to the medical purpose, in the second - similar to food chitosan (Table 3).

Table 3

Parameters	Characteristics and standards		Testing methods
	Acid-soluble chitosan	Water-soluble chitosan	
Appearance	Fine powder or scales ranging in color from light-yellow to pink cream	Fine powder or scales ranging in color from light-yellow to pink cream	4.1
Activity index of hydrogen ions (pH)	4,5-6,5	7,0-9,0	4.2
Residual moisture, %, not more than	10,0 (spray dried); 4,0 (freeze dried)	10,0 (spray dried); 4,0 (freeze dried)	4.3
Base material content, %, at least	85,0	85,0	4.4
Relative viscosity of 2% solution, at least	1,5	1,5	4.5
Degree of deacetylation, at least, %	75,0		4.6
Degree of substitution, %		50,0	4.7
Adsorption activity of copper ions, mg / g, not less than	50,0	50,0	4.8
Microbiological purity in 1g: the total number of aerobic bacteria, not more than Total number of fungi, not more than Escherichia coli Staphylococcus aureus Salmonella в 10 g	10 ⁷ 10 ² Not allowed Not allowed Not allowed	10 ⁷ 10 ² Not allowed Not allowed Not allowed	4.9

Chitosan is also used in the form of thin film materials for various purposes: coatings, packaging materials, sprays, as a part of membranes for the purification of matrix materials in cell cultivation. In these cases, the requirements applied to edible chitosan shall be more strict in terms of molecular weight, degree of deacetylation and microbial contamination (Table 4).

Table 4

Parameter	Characteristics and standard
Appearance	Scales or powder
Colour	From white to yellowish
Moisture content, %, not more than	10
Mass fraction of mineral substances, %, not more than	0,2
Mass fraction of proteins, %, not more than	None
pH 1 % chitosan solution in 2 % acetic acid, not more than	6,5
Mass fraction of insoluble substances, %, not more than	0,1
Degree of deacetylation, %	90-98
Molecular weight, kDa	200-400
Mesophilic aerobic and facultative anaerobic microorganisms, KOE in 1 gram of chitin, not more than	None

In the paper industry chitosan is used for the surface treatment of special types of paper in order to improve its strain-and-strength properties. In this case, chitosan shall form a continuous film on the surface of paper that will ensure cellulose fibers bonding, which requires high

viscosity of the solution, i.e. sufficient molecular weight of chitosan. Ash content parameter in chitosan in this case is not significant, since paper contains mineral fillers.

In the textile industry chitosan is used for durable anti-bacteric finishing of fabrics and for improving fabric dyeability. Requirements for chitosan in this case are close to the requirements applied in the paper industry. Parameters of chitin for the pulp and paper and textile industries are shown in Table 5.

Table 5

Parameters	Characteristics and standard
Appearance	Scales, flakes or grits
Size of particles, mm, not more than:	
- scales and flakes	10
- grits	5
Colour	From white to cream, grayish, yellowish
Moisture content, %, not more than	10
Mass fraction of mineral substances, %, not more than	2
Mass fraction of proteins, %, not more than	0,5
Degree of deacetylation, %	90 – 95
Solubility in 2% acetic acid, %, at least	98
Viscosity of 2 % solution in 2 % acetic acid, sps	200-400

Chitosan is a multipurpose adsorbent and can be successfully used in many applications: sewage treatment agents, enterosorbents for lipids and heavy metal ions excretion and radioprotectors. In these cases, requirements applied to the quality of chitosan vary greatly. For example, purification of wastewater from heavy metal ions requires chitosan with high ash content the molecular weight of which is not very important, while radioprotectors demand low ash content and low molecular weight (10 - 30 kDa). Hence, each type of sorbent needs its own standard of quality.

In the cosmetic industry chitosan and its derivatives are used as gelling agents, moisturizers and anti-inflammatory agents. Chitosan has no allergenicity, efficiently penetrates through the skin, is compatible with other components of cosmetic formulations, has no color and smell. Parameters of chitosan used for perfume and cosmetic industries are shown in Table 6.

Table 6

Parameters	Characteristics and standard
Appearance, colour	Scales or mother of pearl cream powder
Activity index of hydrogen ions (pH) in 1-% water solution	7,0-9,0
Residual moisture, %, not more than	5,0
Solubility	Water soluble, 1 g of substance in 40-50 ml
Dynamic viscosity of 2% solution, 20°C, mPa	1500-2500
Degree of substitution, %	75-90
Mesophilic aerobic and facultative anaerobic microorganisms, KOE in 1 gram of chitin, not more than	1×10^3
Spore-forming bacteria, coliforms, staphylococci, actinomycetes, microscopic fungi	None

The use of chitosan is not limited by the applications enlisted in the present paper. For some other purposes it might be recommended to use the above mentioned parameters of chitosan the values of which are mostly close to the requirements specified by its application in the industry.

REFERENCES

- [1] Chitin and Chitosan: Production, Properties and Usage / Edited By Academician of the Russian Academy of Agricultural Sciences K.G. Skryabin, G.A. Vikhoreva, Dr. Sc. (Chem.), V.P. Varlamov, Dr. Sc. (Chem.)/ - M.: Science, 2002. – 368 p.
- [2] Hirano S.// Chitin and Chitosan. Sources, chemistry, biochemistry, physical properties and applications/Ed. G.SkjAK-Br/EK, T.Anthonsen, P.Sandford.L., N.Y.:Elsevier Applied Science. 1990. p. 37-43.
- [3] Peter M.G., Domard A., Muzzazelly R.A.A. (Ed.)//Advances in Chitin Science. V. IV. Proc. of the Jnt. Conf. of European Chitin Soc., Potsdam: Potsdam Universitaet. 2000. 650 p.

HEPATOPROTECTIVE, ANTICOAGULANT AND IMMUNO-STIMULATING PROPERTIES OF CHITOSAN BOMBYX MORI DERIVATIVES

R.Yu. Milusheva^{1*}, F.H. Inoyatova², A.A. Batyrbekov³, S.Sh. Rashidova¹

¹*Institute of Polymer Chemistry and Physics, Academy of Sciences, Uzbekistan, Tashkent*

²*Tashkent Medical Academy, Tashkent*

³*The Institute of Immunology, Academy of Sciences, Uzbekistan, Tashkent*

*E-mail: carbon@uzsci.net, milur@rambler.ru; immuno@uzsci.net

INTRODUCTION

Wide application of chitosan and its derivatives in medicine is determined by a combination of valuable biochemical properties: bactericidal, biocompatibility and biodegradability of this polymers. These allow to assign them to a group parapharmaceutics - natural substances with pronounced pharmacological activity. Chitin derivatives are biocompatible and bio-destroyed to normal substances for a body of (N-acetylglucosamine or glucosamine) and possess immunomodulatory, antimicrobial, antitumor, radioprotective, anti-inflammatory and hypolipidemic activity [1-3].

MATERIALS and METHODS

We used chitin Bombyx mori, isolated from silk production waste; the synthesis of chitosan (Ch) and its derivatives: polymermetalocomplexes (PMC) of chitosan with Co^{2+} (Ch-Co^{2+}) chitosan sulfate (ChS) and chitosan ascorbate (ChA) were realized. Deacetylation of chitin was carried out in heterogeneous conditions. Chitosan samples were obtained at an elevated temperature at different time of reaction. Depending on the conditions of producing, the molecular weight chitosan from Bombyx mori was varied from 25000 to 200000.

A test of action of the synthesized products on different types of microorganisms: Staphylococcus, Enterococcus, Streptococcus, Pseudomonas, Escherichia, Proteus, Salmonella, Shigella, Candida was carried out.

The effect of chitosan polymermetalocomplexes on state of the structure of the gastric mucosa and intestine under the development of chronic heliotrine hepatitis and effect of chitosan sulfate under experimental hypercholesterolemia was studied.

In the study of polymers were used infrared spectroscopy, X-ray diffraction, absorption studies and electron microscopy. Determination of immunological and hematological parameters were carried out by a direct method of local hemolysis by Jerne and Nordin. Content determination of insoluble glycoproteins was performed by the method of Gottschalk A. with Ehrlich's reagent. Platelet aggregation, thrombin time and fibrinogen were measured on the Human analyzer (Germany)

RESULTS and DISCUSSION

The clinical and preventive medicine widely used medications on the basis of polysaccharides of animal and vegetable origin (chitins) - crab, mushrooms, bees, etc. Uzbekistan

have unique sources of raw materials for such drugs creation - waste of pupae of the silkworm *Bombyx mori*, it is about 10 - 15 thousand tons per year.

At the Institute of Polymer Chemistry and Physics of Uzbekistan Academy of Sciences (Laboratory "Synthesis of perspective polymers") in first time was derived of environmentally safe natural polymer chitin and its derivatives from the pupae of the silkworm *Bombyx mori*. Chitosan is synthesized from chitin by deacetylation reaction using concentrated alkali of 40-50% NaOH. Flowsheet of chitosan synthesis, developed and implemented in an IPCP mini-workshop, consists of a series of successive stages: - the oil extraction, deproteinization, demineralization, bleaching, washing after each stage and the drying of the product. The IR- (Fig. 1) and -NMR spectra (Fig. 2) contains all bands corresponding to the synthesized products.

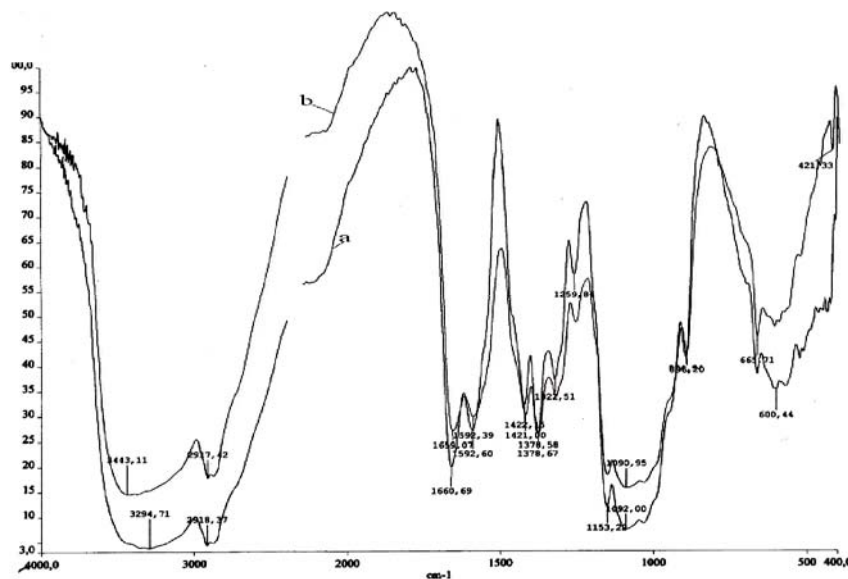


Fig.1. The IR- spectra of chitosan *Bombyx mori*

On the IR spectra of the Ch could be seen an intense broad absorption band with a peak at 3460 cm^{-1} (valent vibrations of OH- groups included in the hydrogen bonds and the absorption bands at $2900 - 3120\text{ cm}^{-1}$, which correspond to valent vibrations of CH- and CH₂ - groups). On the right side of the peak of OH - groups is visible the superposition of the absorption band of NH - groups at 3220 cm^{-1} . The Ch is also characterized by absorption bands of Amide - I (1665 cm^{-1}) and Amide - II (1600 cm^{-1}), due to the valent vibrations of C=O and NH - groups, as well as several bands associated mainly with the deformation vibrations of CH-, =CO-, -COC - и C=C - groups in the range of $1300-1450\text{ cm}^{-1}$ and $1000-1260\text{ cm}^{-1}$.

¹³CP/MAS C-NMR spectra (Fig. 2) were recorded on a UNITY 400 (100 MHz) - NMR spectrometer at room temperature. Compare the ¹³C-NMR spectra of chitin and chitosan shows that there was a strong decrease the intensity of the peak of methyl (CH-) and carbonyl (C=O) of chitosan sample. Almost complete absence of the relaxing characteristic for signal of methylcarbonyl (at 23 ppm) as well as carbonylcarbon signal (at 174 ppm) confirms the high degree of chitosan deacetylation.

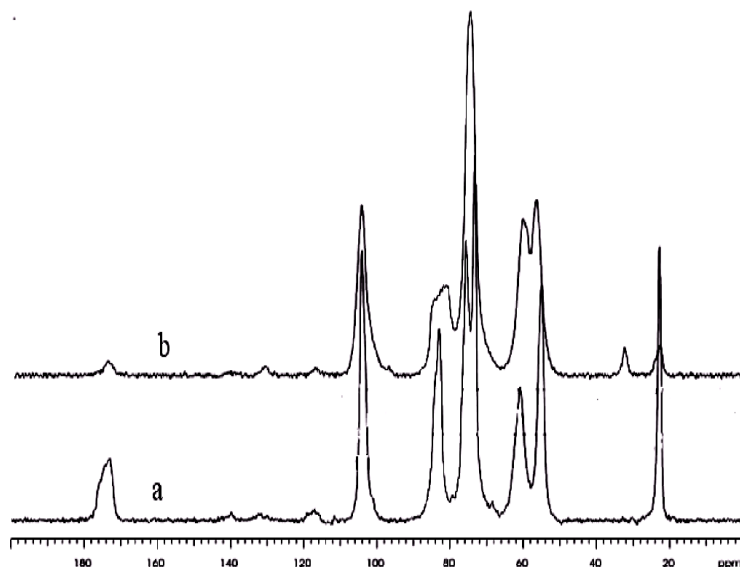


Fig.2 ^{13}C - NMR spectrum of chitin (a), chitosan (b) *Bombyx mori*

On the base of the derived samples there were synthesized complexes of chitosan with metal ions of d-transition series to create a biologically active polymer systems. Cobalt chloride used as the metal salt, as it is well known of its exceptional role in vital processes of living organisms [4].

Hepatoprotective properties polymetallocomplexes of chitosan with Co^{2+} were studied in comparison with a known drug “Zinariks”.

Assessment of the structure state of the gastric mucosa and intestine at the development of chronic heliotrin hepatitis and exploration ways to correct the identified changes under chitosan effect was conducted. At the same time the content of phospholipids, cholesterol, nitrogen oxide, the activity of phospholipase A_2 and enzyme activity in the mucosa and the chitosan effect on these processes in comparison with “Zinariks” were studied.

The experiments were conducted on white rats, which for 60, 90 and 120 days were studied the development of chronic heliotrin hepatitis. Chronic heliotrin hepatitis caused by hepatropic heliotrin poison. The animals were divided into 3 groups (1-control- untreated, 2 - treated with chitosan and 3 – treated by drug comparison – “Zinariks”).

It was found that the phospholipid content in the mucosa of the stomach and intestine is reduced during all periods of the study in compare with intact animals, which is especially distinct on 90-day of experiment 1,21 - (control 1.89); 2.02 (control 3,53). Reduction in phospholipid content is explained by increased activity of phospholipase A_2 , which is also most expressed at 90 day of the experiment

The correcting effect of chitosan on the content of phospholipids and cholesterol indicates a more pronounced regenerative chitosan action compared with “Zinariks”. During all periods of the study of compare chitosan with “Zinariks”, chitosan more pronounced decreases of cholesterol in compare with untreated group.

In the pathogenetic mechanisms of mucosal injury in gastroduodenal zone special role presents a disorder of organ blood flow, tissue hypoxia. One of the systems, regulating the microcirculation and blood flow of whole organ is nitric oxide. Nitric oxide is considered one of the most important factors in protecting of the gastric mucosa. Now it is proved the participation of nitric oxide in providing of the motor function of the gastrointestinal tract. Therefore, the

studying of the state of these systems plays an important role in understanding the mechanisms of disorder of protective barrier synthesis.

It has been studied changes of the content of nitric oxide in the gastric mucosa and intestine. It was established that the content of nitric oxide in chronic heliotrin hepatitis in the gastric mucosa (as compared with the control group decreased by 60, 90, 120 day studies in 2.85, 2.93, 2.41 times respectively)

Thus, chronic heliotrin hepatitis is characterized by impaired structure of the gastric mucosa and intestine, which is accompanied by a decrease in the content of the main components of membranes - phospholipids and cholesterol, as well as nitric oxide. Investigated Ch-Co²⁺ used in much lower doses (~ 6 times) in compare with "Zinariks" and has more pronounced effect on the structure of the regenerating mucosa of the stomach and intestines.

Effect of chitosan on the protective barrier of gastric mucosa and intestine caused by stimulation of the synthesis and improving of the quality of the insoluble glycoproteins. This will allow further to recommend products based on chitosan for the treatment of changes in the gastric mucosa and intestine at the development of chronic heliotrin hepatitis.

Immunological and some hematological parameters ChS and ChA were studied in the experiment: the number of AFT (antibody- forming cells); the common quantify of nuclei-containing spleen cells (NCSC); the total number of cells in the thymus, the total number of cells in the bone marrow, red blood cells and peripheral blood leukocytes . It was shown that chitosan sulfate and ascorbate have the ability to increase the number of cells in the central (thymus, bone marrow) and peripheral organs of immunity, and influent on hematological (leukocytes) blood parameters.

The effect of chitosan sulfate on hemostasis indexes in experimental hypercholesterolemia was studied, the effectiveness of hypolipidemic effect on experimental models of atherosclerosis was estimated. For evaluation of the effect of chitosan sulfate (ChS) on lipid metabolism was used Heparin- a anticoagulant widely used in the clinic as a control, and hypolipid drug - Gemfibrazil related to fibrates and used in clinical practice for the treatment of hypercholesterolemia and atherosclerosis. Studies have shown that when applying (ChS), a decline of high values of triglycerides occurs, phospholipids and total cholesterol, respectively, relatively to the levels of untreated animals. The effectiveness of chitosan sulfate was higher than Gemfibrazil. Along with the hypolipidemic action ChS also possess anticoagulant properties. Introduction ChS during one month contributes to decreasing of platelet aggregation values to 1.96-fold (P <0.001), thrombin time to 1,1 times and soluble monomer-fibrin complexes- SMFC - to 1.34-fold (P <0.05).

Hypoaggregation properties of chitosan sulfate exceeds Gemfibrazil and no different from Heparin. It was revealed that - anticoagulant properties of chitosan sulfate increases with increasing concentration of the drug.

Action of sulfate and ascorbate chitosan and their nanostructured forms on the model of metabolic syndrome were studied. It was shown that chitosan sulfate and ascorbate reduce high levels of total cholesterol in serum of blood (Fig. 3). This manifested more pronounced in the application of chitosan sulphate, especially nanostructured form.

A test to detect the influence of synthesized drugs on 12 kinds of microorganisms - causative agents of various diseases; Staphylococcus, Enterococcus, Streptococcus, Pseudomonas, Escherichia, Proteus, Salmonella, Shigella, Candida. It was revealed that the drugs based on chitin and its derivatives have a fairly marked effect on microbial culture, such as Streptococcus, Pseudomonas aeruginosa and Escherichia. With increasing concentration of polymer products the antibacterial activity was significantly increased. Studies of polymeric

drugs based on chitosan and its derivatives were revealed that the synthesized polymer systems are the drugs of wide action because effected the microorganisms of various types.

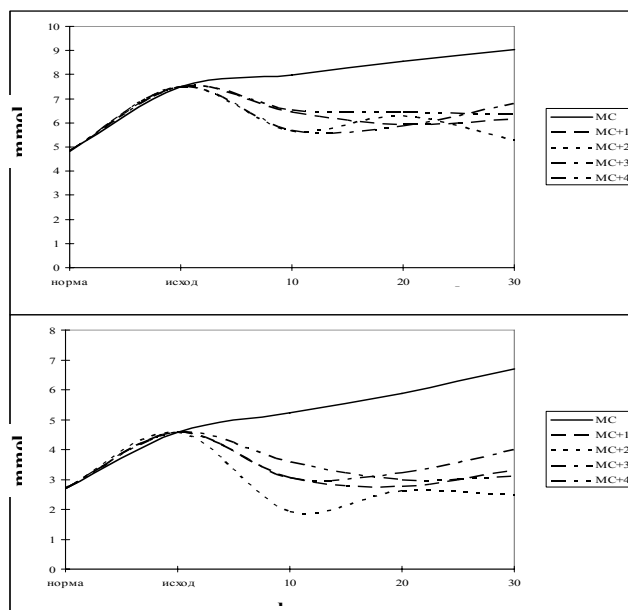


Fig.3 Influence of various derivatives of chitosan on total cholesterol (top) and low density lipoprotein (bottom) in the serum of blood of rabbits with metabolic syndrome

Thus, using of drugs based on chitosan for treatment of diseases of various etiologies will allow to identify the most active modification of chitosan, to establish a relationship the chemical structure with their biological activity and to create effective chitosan preparations for application in clinical practice.

ACKNOWLEDGEMENT

This work was supported by a grant GSTP FA-A-14-T-043

REFERENCES

- [1] Muzzarelli, R.A.A., Muzzarelli, C. (2002) Chitosan in Pharmacy and Chemistry, Atec, Italy.
- [2] Rinaudo, M.(2006) Chitin and chitosan: properties and applications. Prog Polym Sci, 31, 603–32
- [3] Jayakumar, R., New, N., Tokura, S., Tamura, H.(2007) Sulfated chitin and chitosan as novel biomaterials. Int J Biol Macromol, 40, 175–81.
- [4] Muzzarelli, R.A.A., Muzzarelli, C. (2005) Chitosan chemistry: relevance to the biomedical sciences. Adv Polym Sci ,186,151–209.

ENZYMATIC / MASS SPECTROMETRIC FINGERPRINTING OF PARTIALLY ACETYLATED CHITOSANS

Bruno M. Moerschbacher^{*}, Frank Bernard, Nour Eddine El Gueddari

Institute of Plant Biology and Biotechnology, University of Münster, Hindenburgplatz 55, 48143 Münster

^{}E-mail address: moersch@uni-muenster.de*

INTRODUCTION

Chitosans are a family of versatile polysaccharides with many potential uses in material, food, and life sciences. However, life science applications - e.g. in plant disease protection or in wound dressings promoting scar-free healing - are hampered by poor reproducibility of most of the many biological activities described for partially acetylated chitosans. We have argued that this is due at least in part to the widespread use of poorly characterised chitosans, with significant batch-to-batch variations [1].

Over the past ten years, we and others have, therefore, performed detailed structure / function analyses of partially acetylated chitosans, concerning both their physico-chemical properties and their biological functionalities [2]. We were able to show that these are strongly influenced by both the degree of polymerisation (DP) and the degree of acetylation (DA) of the chitosans used. Thus, chitosan polymers of intermediate DP and very low DA exhibited highest anti-microbial activities, while plant strengthening activities were most pronounced with chitosans of high DP and intermediate DA. Based on this knowledge, we have greatly improved the efficacy and reliability of chitosan as an active ingredient in plant protectants. In contrast, the wound healing and immuno-modulatory activities of chitosans towards human cells and tissues proved to be more complex, and we have hypothesised that this is because the patterns of acetylation (PA) are crucially involved in determining the biological functionalities in a target tissue containing sequence-specific chitosan hydrolases [3]. We have shown that human chitotriosidase is such an enzyme which is now thought to be centrally involved in the turn-over of chitosans applied to human tissues and, thus, in determining their biomedical and pharmacological properties [4].

Due to the chemical de-acetylation or re-acetylation processes involved in the production of partially acetylated chitosans, they are invariably characterised by random PAs [5-7]. We believe that enzymatic production strategies might be able to supply chitosan oligomers and polymers with other-than-random, e.g. blockwise PA [3]. We have, therefore, embarked on an extensive discovery programme to identify novel chitosan modifying enzymes. We are mainly interested in chitin deacetylases and chitosan hydrolases. To identify such enzymes or their genes, we are pursuing two parallel approaches, one knowledge-based and one metagenomic. The metagenomic approach is still in its infancies; we are currently screening high quality metagenomic libraries we established from environmental samples with a long history of chitin or chitosan exposure. On the other hand, the knowledge-based approach has already yielded interesting, novel chitosan modifying enzymes.

This approach is based on our finding that biotrophic plant pathogenic fungi appear to modify their surface properties upon penetration into their host plants' tissues, by replacing chitin through chitosan on the surfaces of their cell walls [8,9]. We have concluded that such fungi should contain chitin deacetylases, and we have in fact found a surprisingly high number of genes

containing polysaccharide deacetylase domains or of isoenzymes capable of deacetylating the soluble chitin derivative glycol-chitin in the genomes or culture supernatants of such fungi. We have cloned a number of such genes and heterologously expressed them to obtain recombinant enzyme, or purified the enzymes using conventional chromatography steps, and we are in the process of characterising them. We are especially interested in their substrate specificities and modes of action, as processive chitin deacetylases would lead to chitosans with blocks of deacetylated, GlcN units and, thus, a non-random PA. As an example, we have heterologously expressed a polysaccharide deacetylase gene from the obligately biotrophic wheat pathogen *Puccinia graminis* f. sp. *tritici*, the wheat stem rust fungus, in a fission yeast, *Schizosaccharomyces pombe*, and obtained good quantities of recombinant protein which showed deacetylase activity towards a range of chitinous substrates. Chemically produced, partially acetylated chitosan polymers were further deacetylated using this enzyme, and the resulting chitosans with a lower DA were shown by NMR to possess a non-random, more blockwise PA. Fully acetylated GlcNAc oligomers of DP 3 to 6 were deacetylated by the enzyme, invariably leading to products with two acetylated units left at their non-reducing end. Again, thus, the products of this enzymatic deacetylation had a non-random, blockwise PA. Other polysaccharide deacetylases from bacterial, fungal, and plant origin are currently under investigation.

The observation of chitosan in the cell walls of the endophytic infection structures of plant pathogenic fungi raised the question of how plants have reacted to this disguise strategy of their microbial pathogens. As there are no confirmed reports of plant chitosanases, we turned our attention to endophytic fungi living inside plant tissues, without being pathogenic and without any visible mutualistic effect on their host plants. We argued that such fungi may supplement the plant's own repertoire of defensive enzymes by providing chitosanases and, thus, protecting plants from pathogenic fungi. While this hypothesis is still unproven, we did find a surprising diversity of chitin deacetylase, chitinase, and chitosanase isoenzymes in the culture medium of many such fungi [10]. The little studied and mostly unknown plant endophytic fungi might, thus, represent a rich source for novel chitin or chitosan modifying enzymes. The first such enzymes have now been purified or their genes cloned and heterologously expressed, to be characterised concerning their substrate specificities, modes of action, and product patterns.

Another knowledge-based approach makes use of the observation that not all fungi are equally sensitive to the antimicrobial activities of chitosans [11]. We found that fungi highly tolerant to chitosan in their medium, such as *Alternaria alternata* or *Penicillium expansum*, degraded the chitosans into small oligomers and, as expected, we found rather high chitosanolytic activities in their spent growth media. Again, the first enzymes from this approach have been purified or their genes cloned and heterologously expressed, and we are currently characterising the substrate specificities, modes of action, and product patterns of these enzymes.

We are especially interested in chitosan hydrolases with distinct substrate specificities. It is known that chitinases belonging to glycosyl hydrolase family GH18, due to their substrate assisted mode of action, absolutely require a GlcNAc (A) residue at their -1 subsite, i.e. at the newly formed reducing end, while the requirement for an A residue at the +1 subsite, i.e. at the newly formed non-reducing end, can be less strict [12]. All GH18 chitinases, thus, can cleave the AA-linkage, while only some can also cleave the AD linkage. Chitinases belonging to GH19, in contrast, have a different mode of action and appear to have a higher specificity for an A unit at the +1 than on the -1 subsite, so that they can either cleave the AA-linkage only, or the AA and the DA linkages [13,14]. The common identifier for all chitinases, thus, appears to be their ability to cleave the AA-linkage. This is also true for chitinolytic enzymes such as lysozyme belonging to GH22 which appear to typically require three A units at the -2, -1, and +1 positions [15]. On

the other hand, chitosanases have been classified into three different groups, cleaving the DD-linkage only, the DD- and the DA-linkage, or the DD- and the AD-linkage [16]. Again, thus, the common identifier for chitosanases is their ability to cleave the DD-linkage. From the knowledge-based approach, we have recently identified a novel chitosan hydrolase with an absolute specificity for an A-unit at the -1 and for a D-unit at the +1-site, thus cleaving exclusively the AD-linkage [17]. This enzyme, thus, is neither a chitinase, as it does not cleave the AA-linkage, nor a chitosanase, as it does not cleave the DD-linkage. We have, therefore, named it chitinosanase.

Clearly, thus, chitinases, chitosanases, and the new chitinosanase are sequence-specific hydrolases, though their specificity is rather limited, apparently extending to not more than two glycosidic units upstream and downstream of the cleavage site. Still, such enzymes can be used for the development of an enzymatic / mass spectrometric fingerprinting analysis of partially acetylated chitosan polymers (Fig. 1). Sequence specific chitosan hydrolases can degrade partially acetylated chitosan polymers into tell-tale oligomers which can be analysed in molecular detail using state-of-the-art mass spectrometry. The bouquets of oligomers produced by chitosan hydrolases with given, known cleavage specificities then allow to draw conclusions concerning the PA of the chitosan polymer used as a substrate. The strategy is similar to one described for partially methyl-esterified homogalacturonan pectins which also are linear polysaccharides consisting of two different building blocks only, galacturonic acid (GalA, G) and methyl-esterified galacturonic acid (GalAMe, M) [18,19]. In an extension of a chemical / chromatographic fingerprinting method [20], an enzymatic / mass spectrometric analysis for the pattern of methyl-esterification (PM) of pectins was developed, making use of pectin hydrolases and/or lyases with a specificity for the GG- or MM-linkages [21]. We have applied this method to chitosans, using some of our well characterised chitosanolytic enzymes coupled with HPTLC-MALDI-TOF- or LC-ESI-MS/MS analyses of the products to determine their DP and DA. If a chitosan with known and defined DP and DA is degraded by a chitosan hydrolase with a known sequence specificity, the product bouquet for a random PA can be predicted accurately. If the products found differ from the products expected, we can conclude that the polymer used as a substrate did not have a random PA. Reversely, finding the expected product pattern does not necessarily prove a random PA of the substrate, though it makes it highly likely.

Using chemically reacylated chitosans with a presumed random PA - made likely also by showing the expected diad distributions in the NMR - and enzymes with strict substrate specificities for the AA-, DD, or AD-linkage, we were able to verify the fingerprinting method. Also, this method corroborated the non-random PA of the chitosans enzymatically deacetylated using the fungal chitin deacetylase from *P. graminis* described above.

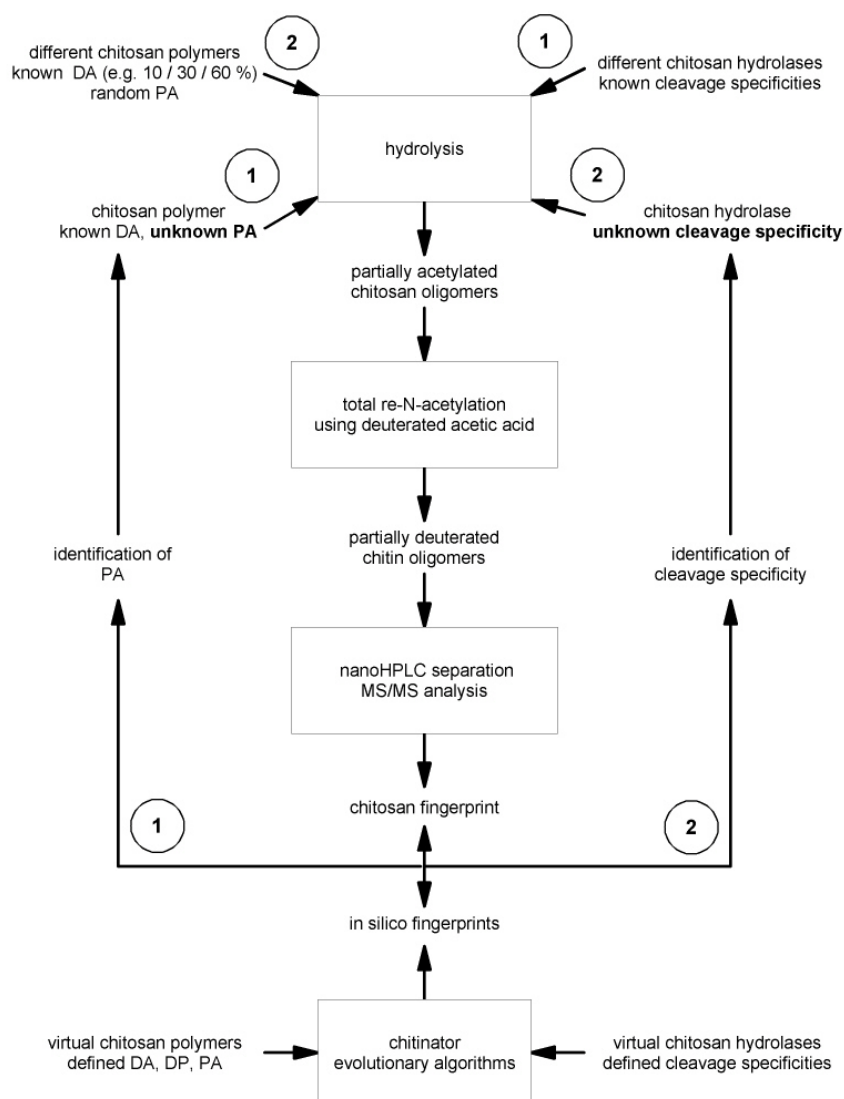


Figure 1: Fingerprinting (1) and reverse fingerprinting (2) to analyse the pattern of acetylation of an unknown chitosan using chitosan hydrolases with known cleavage specificities, or to analyse the cleavage specificity of an unknown chitosan hydrolase using chitosans with known random PA.

In an extension of this fingerprinting method, we are now combining it with a bioinformatic approach, simulating a chitosanolytic enzyme in silico (Fig. 2). This approach is based on previous attempts to define the subsite specificities of a bacterial chitinase using HPLC and NMR analyses of the products obtained upon hydrolysing partially acetylated chitosans with a presumed random PA. Mass spectrometry gives a wealth of highly accurate information on the DP and DA of the products of an enzymatic hydrolysis - with the notable drawback of not giving precise quantitative results. We have overcome this limitation by refining a method for the quantitative re-N-acetylation of partially acetylated chitosan oligomers using deuterated acetic anhydride [22]. This step allows us to quantify the oligomers detected, as fully acetylated chitin oligomers can be used as standards. Moreover, it also allows sequencing the oligomers by MS/MS analyses as it eliminates the different fragmentation frequencies of the four different glycosidic linkages found in a partially acetylated chitosan oligomer - AA, DA, AD, and DD - as

they are all converted to AA. The combination and standardisation of these techniques yields a very powerful tool for the fingerprinting analysis of PA, the power of which we are only beginning to exploit.

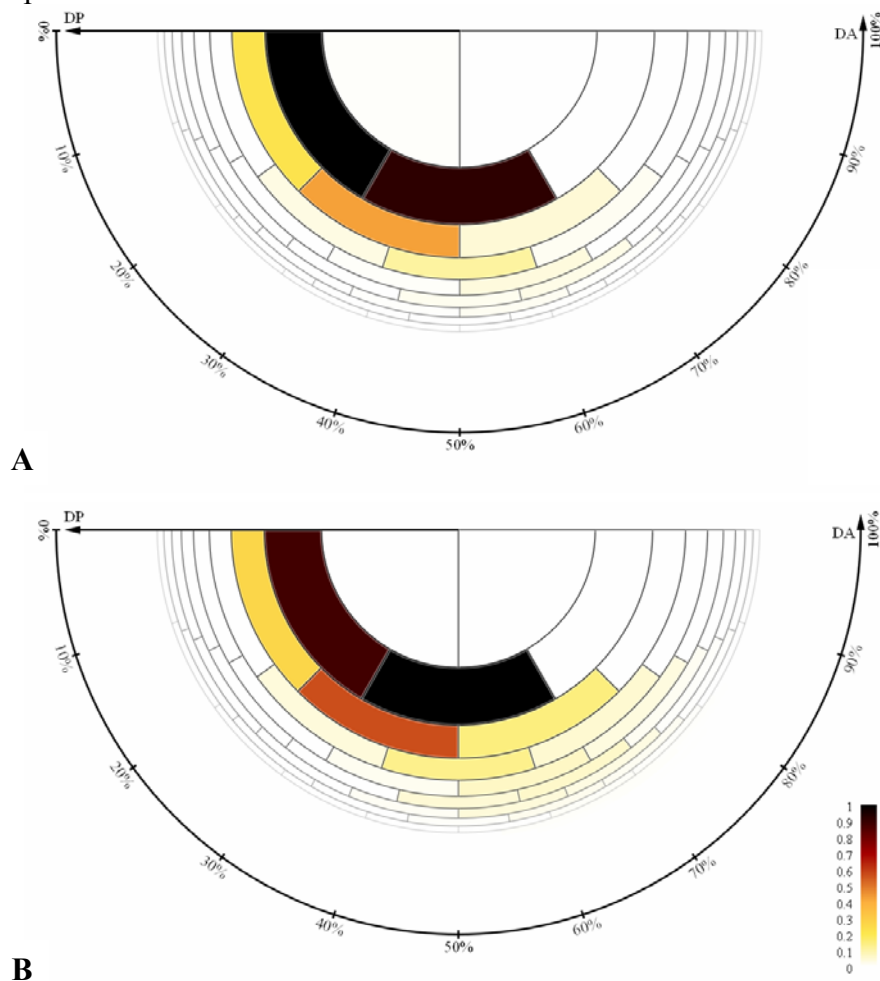


Figure 2: In vitro (A) and in silico (B) fingerprint for the degradation of a polymeric chitosan (DA 40%) by a chitosanase from *Streptomyces* spec.

Of course, this same technique can also be used to determine the substrate specificities of chitosanolytic enzymes with a much higher precision than hitherto possible, again in analogy to what has been done previously for pectin degrading enzymes [23]. In the fingerprinting analysis, we use enzymes with known substrate specificities to analyse the PA of an unknown chitosan. But if we use a chitosan with a known random PA, we can analyse the substrate specificity of an unknown enzyme. Using this reverse fingerprinting approach (Fig. 1), we have begun to analyse the subsite affinities of a range of chitinases and chitosanases, with surprising, though still preliminary results.

We are convinced that chitosan modifying enzymes provide the key for both the generation and analysis of novel chitosans with non-random PA. Once such chitosans will be available, they can be tested for their physico-chemical properties and their biological functionalities. As mentioned above, we have hypothesised that the PA of chitosans crucially determines their biological activities in a target tissue containing a sequence specific chitosan hydrolase such as

human chitotriosidase [4]. This holds true irrespective of whether it is the polymers applied or the oligomers generated enzymatically *in situ* that are responsible for the biological activity. The PA of the chitosan in combination with the substrate specificity of the chitosan hydrolase will determine the half life of the polymer in the tissue, and the quantity and quality of products produced, as well as the kinetics of their generation and degradation. Hopefully, thus, the availability of well defined chitosans with confirmed non-random PAs will in future allow the development of more effective and more reliable biomedical applications of chitosans, e.g. in drug, gene, or vaccine delivery, cell and tissue engineering, wound healing, etc.

REFERENCES

- [1] El Gueddari, N. E. and Moerschbacher, B. M. (2004) A bioactivity matrix for chitosans as elicitors of disease resistance reactions in wheat. In *Adv. Chitin Sci.* 7 (I. Boucher, K. Jamieson & A. Retnakaran, eds.), pp. 56-59.
- [2] Moerschbacher, B. M. (2005) Bio-activity matrices of chitosans in plant protection. In *Emerging Trends in Plant-Microbe Interactions* (S. S. Gnanamanickam, R. Balasubramanian, N. Anand, eds.) pp. 186-190, University of Madras, Chennai
- [3] El Gueddari, N. E., Schaaf, A., Kohlhoff M. et al. (2007) Substrates and products of chitin- and chitosan-modifying enzymes. In *Adv. Chitin Sci.* 10 (S. Senel, K.M. Vårum, M.M. Sumnu, A.A. Hincal, eds.) pp. 119-126.
- [4] Gorzelanny, C., Pöppelmann, B., Pappelbaum, K. et al. (2010) Human macrophage activation triggered by chitotriosidase-mediated chitin and chitosan degradation, *Biomaterials*, 31 (33), 8556-8563.
- [5] Kurita, K., Sannan, T. and Iwakura, Y. (1977) Studies on chitin, 4. Evidence for formation of block and random copolymers of N-acetyl-D-glucosamine and D-glucosamine by hetero- and homogeneous hydrolyses. *Die Makromolekulare Chemie*, 178 (12), 3197-3202.
- [6] Vårum, K.M., Anthonsen, M.W., Grasdalen H. et al. (1991) ¹³C-N.m.r. studies of the acetylation sequences in partially N-deacetylated chitins (chitosans). *Carbohydrate Research*, 217, 19-27.
- [7] Bahrke, S., Einarsson, J.M., Gislason, J. et al. (2002) Sequence Analysis of Chitooligosaccharides by Matrix-Assisted Laser Desorption Ionization Postsource Decay Mass Spectrometry, *Biomacromolecules*, 3 (4), 696-704.
- [8] El Gueddari, N.E., Rauchhaus, U., Moerschbacher, B.M. et al. (2002) Developmentally regulated conversion of surface-exposed chitin to chitosan in cell walls of plant pathogenic fungi, *New Phytologist*, 156 (1), 103-112.
- [9] Tucker, S.L., Besi, M.I., Galhano, R. et al. (2010) Common Genetic Pathways Regulate Organ-Specific Infection-Related Development in the Rice Blast Fungus, *Plant Cell*, 22 (3), 953-972.
- [10] Govinda Rajulu, M.B., Thirunavukkarasu, N., Suryanarayanan T.S. et al. (2010) Chitinolytic enzymes from endophytic fungi, *Fungal Diversity*, 47 (1), 43-53.
- [11] Oliveira, E.N., El Gueddari, N.E., Moerschbacher, B.M. et al. (2008) Growth of Phytopathogenic Fungi in the Presence of Partially Acetylated Chitooligosaccharides, *Mycopathologia*, 166 (3), 163-174.
- [12] Horn, S.J., Sorbotten, A., Synstad, B. et al. (2006) Endo/exo mechanism and processivity of family 18 chitinases produced by *Serratia marcescens*, *FEBS Journal*, 273 (3), 491-503.
- [13] Heggset, E.B., Hoell, I.A., Kristoffersen, M. et al. (2009) Degradation of Chitosans with Chitinase G from *Streptomyces coelicolor* A3(2): Production of Chito-oligosaccharides and Insight into Subsite Specificities, *Biomacromolecules*, 10 (4), 892-899.
- [14] Sasaki, C., Vårum, K.M., Itoh, Y. et al. (2006) Rice chitinases: sugar recognition specificities of the individual subsites, *Glycobiology*, 16 (12), 1242 -1250.

- [15] Vårum, K.M., Kristiansen Holme, H., Izume, M. et al. (1996) Determination of enzymatic hydrolysis specificity of partially N-acetylated chitosans, *Biochimica et Biophysica Acta (BBA) - General Subjects*, 1291 (1), 5-15.
- [16] Fukamizo, T., Ohkawa, T., Ikeda, Y. et al. (1994) Specificity of chitosanase from *Bacillus pumilus*, *Biochimica et Biophysica Acta (BBA) - Protein Structure and Molecular Enzymology*, 1205 (2), 183-188.
- [17] Kohlhoff, M., El Gueddari, N.E., Gorzelanny, C. et al. (2009) Bio-engineering of chitosans with non-random patterns of acetylation - a novel sequence-specific chitosan hydrolase generating oligomers with block-PA. In *Adv. Chitin Sci.* 11 (F. Rustichelli, C. Caramella, S. Senel, K.M. Varum, eds.) pp. 463-468.
- [18] Albersheim, P., Darvill, A.G., O'Neill, M.A. et al. (1996) An hypothesis: The same six polysaccharides are components of the primary cell walls of all higher plants, *Pectins and Pectinases*, 14, 47-55.
- [19] Voragen, A.G.J., Coenen, G.J., Verhoef, R.P. et al. (2009) Pectin, a versatile polysaccharide present in plant cell walls, *Structural chemistry*, 20 (2), 263-275
- [20] Mort, A.J., Qiu, F. and Maness, N.O. (1993) Determination of the pattern of methyl esterification in pectin – distribution of contiguous nonesterified residues, *Carbohydrate Research*, 247, 21-35.
- [21] Daas, P.J.H., Meyer-Hansen, K., Schols, H.A. et al. (1999) Investigation of the non-esterified galacturonic acid distribution in pectin with endopolygalacturonase. *Carbohydrate Research*, 318 (1-4), 135-145.
- [22] Haebel, S., Bahrke, S. and Peter, M.G., (2007) Quantitative Sequencing of Complex Mixtures of Heterochitooligosaccharides by vMALDI-Linear Ion Trap Mass Spectrometry, *Analytical Chemistry*, 79 (15), 5557-5566.
- [23] Chen, E.M.W. and Mort, A.J. (1996) Nature of sites hydrolyzable by endopolygalacturonase in partially-esterified homogalacturonans, *Carbohydrate Polymers*, 29(2), 129-136.

CHITOSAN SCAFFOLDS WITH ACTIVE NANOFILLERS PREPARED BY ELECTROLYTIC METHOD

Maria Mucha*, Michał Tylman

*Technical University of Łódź, Faculty of Process and Environmental Engineering,
Łódź, Poland*

**E-mail address: muchama@wipos.p.lodz.pl*

INTRODUCTION

Chitosan is a biocompatible (non negative reaction of the organism) and biodegradable material, which may find wide application in bone tissue engineering [1-3]. Biodegradable implants are a support for reconstructing tissue and after total reconstruction are metabolized by the organism and excreted in the form of non-toxic products. Additive of hydroxyapatite provides to osteoblasts appropriate amount of phosphorus and calcium for the regeneration of damaged mineral bone. Application of this type of implants significantly reduces the time of rehabilitation, while eliminating the risk of the implant rejection.

There are several methods of producing chitosan implants for bone tissue engineering. The most popular methods are: freeze-drying method and electrospinning. The freeze-drying method involves on sublimated evaporation of solvent from the pre-frozen chitosan solution. Places containing solvent in the polymer matrix after evaporation of frozen solvent remain as pores [4-5].

However such scaffolds, require etching in ethanol or in low concentrated NaOH solution to remove acetate groups or cross-linking. Chitosan acetate is soluble in water, and it prevents its direct application in a internal environment of organism.

The electrospinning method involves on dispersal of polymer fiber from a chitosan solution in the electric field. Subsequent layer of chitosan fibers formed a porous structure. This method requires the use of high-voltage generator and a precision infusion pump giving the appropriate amount of polymer into the nozzle for dispersal fibre.

The paper presents a electrolytic method of scaffolds producing [6-8]. The process involves on the electrolysis of a chitosan solution in acetic acid. In aqueous solution of acetic acid chitosan is a polycation. Under the influence of current flow it is reduced together with hydrogen ion at the cathode. Material is deposited in the form of a porous structure. Additional amount of ions in the electrolyte derived from the partial dissociation of hydroxyapatite significantly enhances the process. Obtained on the electrode scaffold is subjected to lyophilization to remove residual electrolyte in its pores. Obtained product contains chitosan, which does not dissolve in water.

In order to obtain an additional protective barrier against pathogens (a very important factor in a perspective implantology) nanosilver is introduced to the surface of the scaffold. Silver in a form of nanoparticles damage in bacteria mechanisms of activity of the cell membrane, mitochondria and nucleus. Due to the broad effects of silver on various cellular organelles any strains of immune bacteria to nanosilver are known.

MATERIALS and METHODS

In the experiment chitosan (CS) with a degree of deacetylation of 85% and the viscosity of 120mPas produced by BioLog GmbH was used. In order to improve the osteoconductivity properties of scaffolds a hydroxyapatite (HAp) $\text{Ca}_5(\text{PO}_4)_3\text{OH}$ Sigma – Aldrich was applied. To the manufacture of nano-silver's particles a silver nitrate AgNO_3 produced by Chempur and as a reducing agent L(+)-ascorbic acid $\text{C}_6\text{H}_8\text{O}_6$ produced by POCh were used.

Electrolyte preparation

1% chitosan solution in 1% aqueous acetic acid was prepared. Then to the solution appropriate amount of hydroxyapatite usually at 10% by weight fraction of chitosan was added. The solution was stirred on a magnetic stirrer for 20 minutes and then subjected to the influence of ultrasound (20min) to obtain a good dispersion of HAp in the solution. The processes of magnetic stirring and ultrasound was repeated twice.

Nanosilver preparation

Nanosilver used in the process has been produced by chemical reduction. Reducer of the system was ascorbic acid, and silver ions was derived from the dissociation of silver nitrate. The reaction proceeded according to schedule:



For that purpose 0.2 molar solution of AgNO_3 and 0.1 molar solution of ascorbic acid in deionized water was prepared. Then silver nitrate solution by drop wise into the beaker with ascorbic acid was added subjecting them to intensive stirring on a magnetic stirrer. Obtained solution of free silver was stirred by ultrasound in order to separate the agglomerates.

Preparation of chitosan scaffold

Previously prepared a chitosan solution in acetic acid containing hydroxyapatite was introduced into the electrolytic cell. In the electrolysis a rotating electrode system was used (Fig. 1). Rotational movement of the cathode induced detachment of hydrogen gas bubbles from the cathode surface, which what influenced to the reduction of pore size of scaffolds. The system was powered by a laboratory stabilized power feeder. The voltage applied to the electrodes was $U = 20\text{V}$, value of current flowing through the system was dependent on the instantaneous conductivity of the system. Process taking place on the electrode occurred until scaffold reached the intended size. Figure 1 shows a diagram of the cell with a rotating electrode and the with specified reaction scheme running on the cathode.

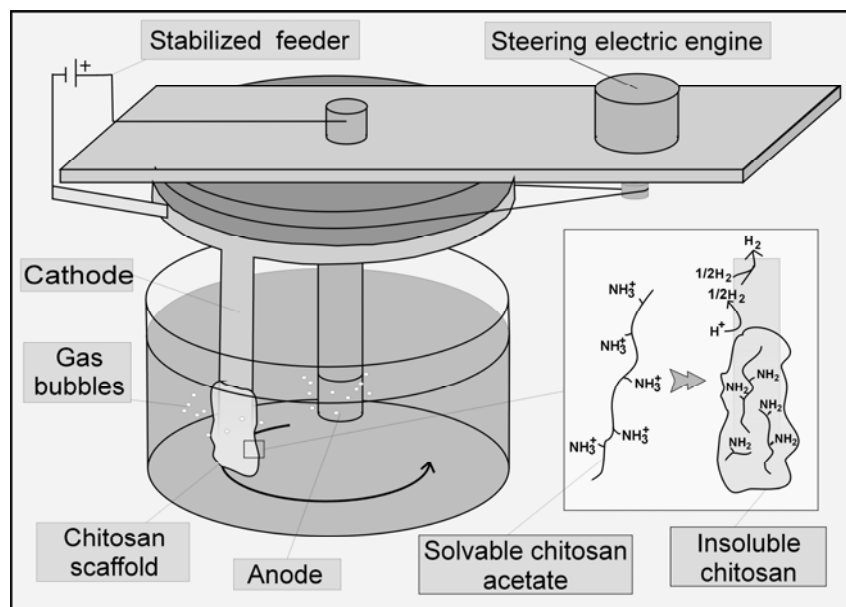


Fig.1 Diagram of the cell with a rotating electrode.

A minute before the end of the process to the electrolyte the solution containing nanosilver was introduced. This resulted in a deposition of silver nanoparticles only onto the surface part of in scaffolds.

The thickness of the nanosilver layer was around 0.2 mm.

Obtained structure was removed and subjected to preliminary freezing in -37°C for the time 12h. Then the freeze-drying was carried out. The resulting structure was subjected to further testing.

RESULTS and DISCUSSION

Average porosity of the scaffolds was determined by following way (1).

$$P[\%] = \frac{V_s - V_c}{V_s} \cdot 100 = \frac{V_s - (m_c / \rho_c)}{V_s} \cdot 100 \quad (1)$$

where: V_s - volume of scaffolds [cm³], V_c - volume of chitosan in scaffold, m_c - weight of scaffold, ρ_c - density of chitosan (~1,342 g/cm³).

The value of the porosity of scaffolds depends on the content of hydroxyapatite and it changes in the range 92-96%.

The greater concentration of hydroxyapatite in the electrolyte solution, the lower the residual porosity of obtained scaffolds. Simultaneously increasing amount of hydroxyapatite in the system allowed for intensification of the electrolysis process. The mass of the scaffolds depends in a linear way on the amount of hydroxyapatite in the electrolyte (Fig. 2).

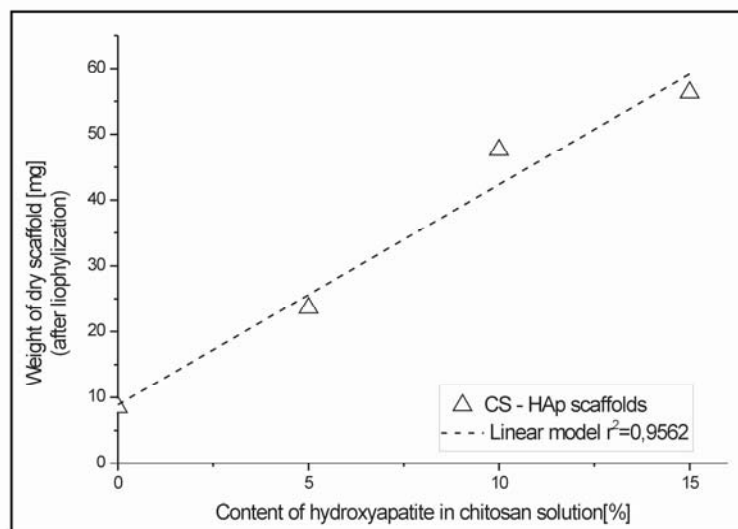


Fig.2 Dependence of dry weight of scaffolds (obtained during the five minutes of electrolysis) from the concentration of hydroxyapatite in solution.

In the order to investigate the morphology of the obtained scaffolds images by polarizing optical microscope were performed.

Microscopic analysis of obtained scaffolds allowed to determine the average pore size of 0,07-0,2 mm. In the polymer structure can also see a few pores of a size much larger than the average size (1-2mm).

Figure 3 shows the photomicrograph of chitosan scaffolds structure containing HAp (after lyophilization) made with using polarizing optical microscope.

Optical micrographs from the polarizing microscope shows existing a crystalline order in the obtained structures. Further analysis of the scaffold properties is in course.

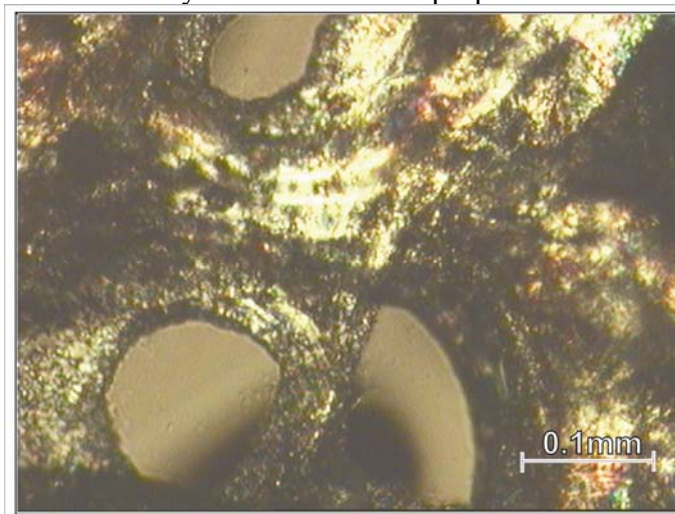


Fig.3 Photomicrograph of chitosan scaffolds structure containing 15% HAp from the optical polarizing microscope.

CONCLUSIONS

Implants based on biopolymers (bioactive, biocompatible) such as chitosan can be a future for bone tissue engineering. Biodegradable implants after the time of a fulfillment of their supporting role in relation to the regeneration bone would be biodegraded and its non-toxic products metabolised or excreted from the body. Chitosan scaffold systems prepared by electrolytic method have adequate porosity to the implants. The implants are insoluble in water, which allows for direct application in an environment of bone tissue (in-vivo). The method of preparation allows to control of pore size, thickness of the layer of nano-silver, and within certain limits, the level of porosity of the scaffolds. Bioactive additives such as nanosilver would help protect a patient against a infection by pathogens and hydroxyapatite accelerates the osteoconductivity properties of implant significantly reducing the duration of treatment and rehabilitation.

REFERENCES

- [1] Xia, W., Liu, P., Zhang, J., Chen, J. (2011) Biological activities of chitosan and chitooligosaccharides. *Food Hydrocolloids*, 25, 170-179.
- [2] Mucha, M. (2010) Chitozan - wszechstronny polimer ze źródeł odnawialnych (Chitosan - universal polymer from renewable sources) WNT, Warszawa.
- [3] Muzzarelli, R.A.A. (2011) Chitosan composites with inorganics, morphogenetic proteins and stem cells, for bone regeneration, *Carbohydrate Polym.*, 83, 1433–1445.
- [4] Tylman, M., Mucha, M. (2010) Porous chitosan structures for medical application. *Progress on Chemistry and Application of Chitin and Its Derivatives*, XV, 97-105.
- [5] Mucha, M., Balcerzak, J., Michalak, I., Tylman, M., (2011) Biopolymeric matrices based on chitosan for medical applications. *e-Polymers*, 3, 1-8.
- [6] Twu, Y.K., Chang, I.T., Ping, Ch. (2005) Preparation of novel chitosan scaffolds by electrochemical process. *Carbohydrate Polymers*, 62, 113–119.
- [7] Yi, H., Wu, L.Q., Bentley, W.E., Ghodssi, R., Rubloff, G.F., Culver, J.N. , Payne, G.F. (2005) Biofabrication with Chitosan. *Biomacromolecules*, 6, 2881-2894.
- [8] Tylman, M., Mucha, M. (2011) Electrolytic method for obtaining porous chitosan structures with hydroxyapatite. *Progress on Chemistry and Application of Chitin and Its Derivatives*, XVI, (in press).

IN VITRO ANTI-OXIDATIVE ACTIVITY OF GALLATE CHITOOLIGOSACCHARIDES

Dai-Hung Ngo¹, BoMi Ryu¹, Se-Kwon Kim^{1,2,*}

¹*Department of Chemistry, Pukyong National University, Busan 608-737, Republic of Korea*

²*Marine Bioprocess Research Center, Pukyong National University, Busan 608-737, Republic of Korea*

**E-mail address: sknkim@pknu.ac.kr*

INTRODUCTION

Osteoarthritis is a common chronic disease of joints including the cartilage in bone tissues. The metabolic and structural changes in the articular cartilage are considered to play a significant role in the commencement and the progression of the disease process [1].

The generation of highly reactive oxygen species (ROS) plays an important role in the modulation of inflammatory reactions. Major ROS are produced during oxidative processes within living cells and tissues. As a defensive system against oxidative stress, cells possess many antioxidant molecules such as superoxide dismutase (SOD) and glutathione (GSH) to scavenge superoxide radical and hydrogen peroxide. If ROS are not scavenged, these species may lead to impaired physiological function through widespread DNA, protein and lipid damage, cartilage damage and induction of bone resorption as well as signal transduction [2].

Nuclear factor kappa B (NF- κ B) is found in almost all animal cell types and is concerned in cellular responses to stimuli stress, cytokines, free radicals and oxidized low-density lipoprotein. The NF- κ B signaling pathways may contribute to the pathogenesis of various rheumatic diseases, in particular, rheumatoid arthritis and osteoarthritis [3].

Chitoooligosaccharides (COS) are chitosan derivatives (polycationic polymers comprised principally of glucosamine units) and can be generated via either chemical or enzymatic hydrolysis of chitosan. It has been reported that COS possess many biological activities, such as anti-inflammatory [4] and antioxidant [5] properties.

Recently, the combination of COS and phenolic compounds have been gained a great deal of interest in the pharmaceutical and medicinal areas. In this study, gallic acid (3,4,5-trihydroxybenzoic acid), which possesses high antioxidant property [6], is attractive for grafted onto COS for a novel bio-functional material.

The purpose of this study is to examine if gallic acid conjugated COS (G-COS) are capable to inhibit intracellular free radicals generated through oxidation. Furthermore, the oxidative inhibition effects of G-COS on major cellular biomolecules such as DNA, proteins and lipids were investigated. In addition, the expression of antioxidant enzymes (SOD and GSH) and NF- κ B in the presence of G-COS with stimulation of hydrogen peroxide are determined.

MATERIALS and METHODS

Synthesis of G-COS

COS (molecular weight 3.0-5.0 kDa, 2.4814 g) was dissolved in 20 ml distilled water (DW), 40 ml methanol and adjusted to the pH 6.8 with triethylamine to obtain a solution A. Gallic acid (0.9404 g) was dissolved in methanol (10 ml) and combined with 10 ml of dicyclohexylcarbodiimide (DCC)-methanol mixture (1.0315 g DCC in 10 ml methanol) to obtain

a solution B. The solution B was gradually added to the solution A while stirring at 30 °C and 150 rpm for 5 h, thereafter, it was filtered to remove dicyclohexyl urea. The reaction mixture obtained was kept at 2 °C overnight and diethyl ether (90ml) was added. Subsequently, the solution was filtered using a filter paper to obtain a precipitate. The precipitate was dissolved in 20 ml DW and dialyzed against DW for 48 h using dialysis membranes molecular weight cut off below 1 kDa in order to remove un-reacted gallic acid. The product was freeze dried to give G-COS (1.4882 g).

Electron spin resonance (ESR) spectrometer

1,1-diphenyl-2-picrylhydrazyl (DPPH) radical scavenging activity was measured using the method described by [7] with slight modifications.

Hydroxyl radicals were generated by Fenton reaction and trapped using a 5,5-dimethyl-1-pyrroline N-oxide (DMPO) nitron spin trap [13] with slight modifications.

Superoxide radical anions were caused by UV irradiated riboflavin/ethylenediaminetetraacetic acid (EDTA) system.

Carbon-centered radicals were generated by 2,2'-azobis(2-amidinopropane) dihydrochloride (AAPH) [8].

Cell cytotoxicity, membrane lipid, protein, DNA oxidation and reactive oxygen species (ROS) determination

Cytotoxicity levels of samples on cells were measured using the 3-(4,5-dimethylthiazol-2-yl)-2,5-diphenyl tetrazolium bromide (MTT) method as described by [9].

Cells were analyzed for the generation of lipid peroxidation products by modification of the thiobarbituric acid reactive substances (TBARS) and 2,4-dinitrophenyl hydrazine, diphenyl-1-pyrenylphosphine (DPPP) methods [10].

The degree of oxidation of the cell membrane proteins was assessed by determining the content of protein by carbonyl groups [11].

Genomic DNA was extracted from cells using standard phenol/proteinase K procedure with slight modifications. Hydrogen peroxide mediated DNA oxidation was determined according to [19].

Intracellular formation of ROS was assessed according to a method described by employing oxidation sensitive dye 2',7'-dichlorofluorescein diacetate (DCFH-DA), as the substrate [13].

RNA isolation and reverse transcription polymerase chain reaction (RT-PCR) & Western blot analysis

Total cellular RNA was extracted from treated cells using TRIzol[®] reagent (Invitrogen Corporation, Faraday Avenue, USA) according to the manufacturer's protocol. Changes in the steady-state concentration of antioxidant enzyme expression were assessed by RT-PCR.

For separate extraction of nuclear and cytoplasm proteins, CellLytic[™] NuCLEAR[™] Extraction kit (Sigma-Aldrich Co., St. Louis, MO, USA) was used following manufacturer's instructions. Cells were lysed and cell lysates were resolved on electrophoresis gel, electrotransferred onto a nitrocellulose membrane, and primary monoclonal antibodies were used to detect target protein using chemiluminescent ECL assay kit.

RESULTS and DISCUSSION

Structural characterization of G-COS

In the Fourier transformed infrared (FT-IR) spectra, G-COS show significant peaks in 1955 and 1520 cm^{-1} , implying the ester and amide linkages between COS and gallic acid (Fig. 1A). From these results, it can be concluded that the gallyl group of gallic acid was successfully introduced into COS via amide and ester linkages. Furthermore, the proton nuclear magnetic resonance (^1H NMR) spectra, G-COS show a new peak at 6.98 ppm belonging to the phenyl protons as compared with COS (Fig. 1B). This confirms the successful conjugation with gallic acid. From ^{13}C Carbon (^{13}C) NMR spectra, G-COS show the aromatic carbon of the gallyl group at 109.54, 128.01, 135.84, and 144.45 ppm (C=C) and 174.8 ppm (C=O) implying successful conjugation of gallic acid onto COS (Fig. 1C).

Radical scavenging potency in non-cellular systems

Free radical scavenging activities were assessed in non-cellular systems using ESR spectroscopy followed by a similar scavenging trend observed in cellular system. ESR spectra obtained with control groups confirmed that DPPH, DMPO and α -(4-pyridyl-1-oxide)-N-tert-butyl nitron (POBN) trapping chemistry is functioning properly resulting in a clear spin adducts DPPH-H, DMPO/ $^{\bullet}\text{OH}$, DMPO/ $\text{O}_2^{\bullet-}$ and POBN/ R^{\bullet} radicals [14]. As shown in Table 1, the IC_{50} values of COS and G-COS (concentration to scavenge 50% radical activity) on scavenging hydroxyl and superoxide radicals were more efficient than carbon-centered and DPPH radicals. The IC_{50} value on scavenging the DPPH $^{\bullet}$ of G-COS (31.50 ± 0.050 $\mu\text{g/ml}$) is almost six-fold lower than COS (184.00 ± 0.020 $\mu\text{g/ml}$). The IC_{50} values of COS and G-COS on scavenging $^{\bullet}\text{OH}$ are 66.00 ± 0.048 $\mu\text{g/ml}$ and 16.00 ± 0.050 $\mu\text{g/ml}$, respectively. The IC_{50} value in scavenging $\text{O}_2^{\bullet-}$ of G-COS is 25.00 ± 0.050 $\mu\text{g/ml}$ while the COS is 78.00 ± 0.050 $\mu\text{g/ml}$. Based on this result, $\text{O}_2^{\bullet-}$ scavenging activity of G-COS is three-fold more effective than COS. The IC_{50} values in scavenging carbon-centered radicals of G-COS is 36.25 ± 0.012 $\mu\text{g/ml}$ and COS is 355.00 ± 0.032 $\mu\text{g/ml}$. These results clearly demonstrate that G-COS is fairly an effective radical scavenger based on the substitution of the gallyl groups.

Table 1. The IC_{50} values of COS and G-COS to scavenge DPPH, hydroxyl, superoxide and carbon-centered radicals.

	Radical	$\text{IC}_{50}^a \pm \text{SD} (\mu\text{g/ml})$	
		COS	G-COS
1	DPPH	184.00 ± 0.020	31.50 ± 0.050
2	Hydroxyl	66.00 ± 0.048	16.00 ± 0.050
3	Superoxide	78.00 ± 0.050	25.00 ± 0.050
4	Carbon-centered	355.00 ± 0.032	36.25 ± 0.012

Radical scavenging activities in cellular systems

Cytotoxic effects of COS and G-COS were determined by the MTT assay. The results showed that no significant toxic effect was observed in human chondrosarcoma (SW1353 cells) under the tested concentrations (Fig. 2A). Therefore, based on the above results, those concentrations of COS and G-COS were used for all experiments.

SW1353 cells are commonly used to determine ROS-induced cellular issues as they are able to produce high amounts of ROS following stimulation. Intracellular ROS was measured

using the fluorescence probe DCFH-DA. During labeling, non-fluorescent DCFH-DA dye that easily penetrates into the cells gets hydrolyzed by intracellular esterase to DCFH, and DCFH traps inside the cells and gets oxidized by H_2O_2 . As shown in Fig. 2B, fluorescence emitted by DCF following ROS-mediated oxidation of DCFH was measured every 30 min up to 3 h incubation. Treatment with COS and G-COS reduced the DCF fluorescence intensity, resulting the scavenging activity increased against intracellular ROS in a dose- and time-dependently. G-COS were able to scavenge radicals significantly throughout the incubation time at all tested concentration.

In this research, DNA oxidation was carried out by combining effect of 200 μM Fe (II) and 2 mM H_2O_2 on the integrity of genomic DNA isolated from SW1353 cells. The inhibitory activity on DNA oxidative damage was subjected by DNA electrophoresis in the presence or absence of COS and G-COS. After 10 min of reaction, almost all DNA was damaged in the control group treated only with Fe(II)- H_2O_2 (Fig. 3A). However, G-COS exerted a protective effect on radical-mediated DNA damage in a clear dose-dependent manner. Furthermore, G-COS inhibited more than 90% DNA damage at 100 $\mu g/ml$ based on the intensity of DNA bands. In contrast, only about 20% DNA damage was inhibited by COS at 100 $\mu g/ml$.

As shown in Fig. 3B, the protein carbonyl groups formation was increased when SW1353 cells were exposed to hydroxyl radicals. When the cells in the reaction mixture were treated with varying concentrations of G-COS and COS, the protein carbonyl groups formation was clearly decreased compared to $\cdot OH$ alone-treated control group. Through the protein carbonyl groups content, the results show that G-COS inhibited about 80% of the formation of protein carbonyl groups in SW1353 cells at 100 $\mu g/ml$ concentration. In addition, G-COS inhibited oxidation of membrane protein that was significantly higher than that of COS at all the tested concentrations.

First, a sensitive fluorescence probe (DPPP) was used to measure the lipid hydroperoxide level of SW1353 cells produced by strong carbon-centered radical generating agent (AAPH). DPPP molecules are successfully penetrated into the cell membranes and hydroperoxides (oxidation products of lipids) preferably react to DPPP to produce DPPP-oxide fluorescence. DPPP itself is not fluorescent, but DPPP-oxide is fluorescent with high fluorescence [10]. After 6 h of incubation with AAPH, the DPPP-oxide fluorescent intensity increased more than threefold due to carbon-centered radical-mediated membrane lipid peroxidation (Fig. 3C). The results show that an increase in DPPP-oxide fluorescence was inhibited by the treatment of G-COS. At 100 $\mu g/ml$, G-COS could inhibit membrane lipid peroxidation around 62%. Accordingly, G-COS could inhibit membrane lipid peroxidation dose-dependently. In contrast, a comparatively low reduction in fluorescent intensity was observed in the presence of COS about 50% at 100 $\mu g/ml$. In addition, the most frequently used method to determine membrane lipid peroxidation is the TBARS method. The results confirmed that G-COS could decrease TBARS in the cells in a similar manner with DPPP-oxide fluorescence result (Fig. 3D). Furthermore, G-COS had higher antioxidant activity compared to COS at all concentrations. The antioxidant activity of G-COS was about 80% at the highest concentration (100 $\mu g/ml$) compared with $\cdot OH$ alone-treated control group. The results of this study demonstrate that G-COS could suppress cellular lipid peroxidation through scavenging ROS because of the improvement of proton transfer by the galloyl group.

Effect of G-COS on antioxidant enzymes

A large number of studies have focused on the pathogenetic significance of oxidative stress in osteoarthritis, which has been associated with increases in signs of oxidative stress and lower levels of the body's natural antioxidants such as SOD and GSH with many diseases. SOD is one

of the major antioxidant enzymes because it reduces the damaging reactions of superoxide. Thus, it protects cells from the toxicity of superoxide. GSH plays an important role in regulating the intracellular redox status. The increase in GSH level protects cells against death either by removing free radicals or by conjugating with toxicants.

The intracellular free radical scavenging effects of G-COS were assessed through the property of an antioxidant enzyme, the mRNA and protein expression levels of antioxidant enzymes (SOD and GSH) were determined by RT-PCR and Western blot analysis in SW1353 cells. As shown in Fig. 4A and Fig. 4B, all the mRNA and protein expression levels of antioxidant enzymes were up-regulated with the treatment of G-COS in a dose-dependent manner. The results indicate that G-COS could be effective scavenger against radicals by increasing the expression levels of antioxidant enzymes in SW1353 cells.

Expression and nuclear translocation of NF- κ B in the presence of G-COS

NF- κ B plays a crucial role in the development and progression of arthritis *in vivo*. The link between joint cartilage destruction during inflammation and NF- κ B was studied essentially from the inhibition of NF- κ B activation by cellular antioxidants. Our results show that G-COS are capable of decreasing activation of NF- κ B especially in a medium induced with reactive oxygen species. A clear increase of NF- κ B (p50 and p65) protein levels was generated with the stimulation of H₂O₂ in SW1353 cells. Compared to H₂O₂ alone-treated group, both p50 and p65 protein expression levels were dose-dependently reduced in plasma proteins by G-COS treatment (Fig. 5A). Furthermore, G-COS showed a significant decrease of NF- κ B translocation from cytoplasm to nucleus when nuclear extracts were tested for both p50 and p65 levels (Fig. 5B). These data suggest that G-COS inhibit the NF- κ B expression and nucleus translocation in H₂O₂-stimulated SW1353 cells.

ACKNOWLEDGEMENTS

This research was supported by a grant from Marine Bioprocess Research Center of the Marine Biotechnology Program funded by the Ministry of Land, Transport and Maritime, Republic of Korea.

REFERENCES

- [1] Henrotin, Y., Kurz, B., and Aigner, T. (2005) Oxygen and Reactive Oxygen Species in Cartilage Degradation: Friends or Foes? *Osteoarthr. Cartilage*, 13, 643-54.
- [2] Seven, A., Guzel, S., Aslan, M., and Hamuryudan, V. (2008) Lipid, Protein, DNA Oxidation and Antioxidant Status in Rheumatoid Arthritis. *Clin. Biochem.*, 41, 538-43.
- [3] Roman-Blas, J. A., and Jimenez, S. A. (2006) NF- κ B as A Potential Therapeutic Target in Osteoarthritis and Rheumatoid Arthritis. *Osteoarthr. Cartilage*, 14, 839-48.
- [4] Jeon, Y. J., and Kim, S. K. (2000) Production of Chitooligosaccharides using Ultrafiltration Membrane Reactor and Their Antibacterial Activity. *Carbohydr. Polym.*, 41, 133-41.
- [5] Park, P. J., Je, J. Y., and Kim, S. K. (2003) Free Radical Scavenging Activity of Chitooligosaccharides by Electron Spin Resonance Spectrometry. *J. Agric. Food Chem.*, 51, 4624-27.
- [6] Yen, G. C., Duh, P. D., and Tsai, H. L. (2002) Antioxidant and Pro-Oxidant Properties of Ascorbic Acid and Gallic Acid. *Food Chem.*, 79, 307-13.

- [7] Alvarez-Parrilla, E., Rosa, L. A., Amarowicz, R., and Shahidi, F. (2011) Antioxidant Activity of Fresh and Processed Jalapeno and Serrano Peppers. *J. Agric. Food Chem.*, 59, 163-73.
- [8] Hiramoto, K., Johkoh, H., Sako, K. I., and Kikugawa, K. (1993) DNA Breaking Activity of the Carbon-Centered Radical Generated from 2,2'-Azobis(2-Amidinopropane) Hydrochloride (AAPH). *Free Radic. Res. Com.*, 19, 323-32.
- [9] Hansen, M. B., Nielsen, S. E., and Berg, K. (1989) Re-Examination and Further Development of A Precise and Rapid Dye Method for Measuring Cell Growth/Cell Kill. *J. Immunol. Methods*, 119, 203-10.
- [10] Takahashi, M., Shibata, M., and Niki, E. (2001) Cytotoxic Effect of Formaldehyde with Free Radicals Via Increment of Cellular Reactive Oxygen Species. *Free Radical Bio. Med.*, 31, 164-74.
- [11] Kim, J. A., Kong, C. S., Seo, Y. W., and Kim, S. K. (2010) *Sargassum Thunbergii* Extract Inhibits MMP-2 And -9 Expressions Related With ROS Scavenging in HT1080 Cells. *Food Chem.*, 120, 418-25.
- [12] Sambrook, J., and Russell, D. (2001) *Molecular Cloning A Laboratory Manual*. Cold Spring Harbor Laboratory Press, New York, 84-87.
- [13] Veerman, E. C. I., Nazmi, K., Hof, W. A. T., Bolscher, J. G. M., Hertog, A. L. D., and Amerongen, A. V. N. (2004) Reactive Oxygen Species Play No Role in the Candidacidal Activity of the Salivary Antimicrobial Peptide Histatin 5. *Biochem. J.*, 381, 447-52.
- [14] Mendis, E., Kim, M. M., Rajapakse, N., and Kim, S. K. (2008) Sulfated Glucosamine Inhibits Oxidation of Biomolecules in Cells Via A Mechanism Involving Intracellular Free Radical Scavenging. *Eur. J. Pharmacol.*, 579, 74-85.

THE STUDY OF MECHANISM OF CHITIN AND CHITOSAN HYDROLYSIS

Vitaly Yu. Novikov

*Knipovich Polar Research Institute of Marine Fisheries and Oceanography (PINRO), Murmansk, Russia
E-mail: nowit@pinro.ru*

INTRODUCTION

The study of chitin and chitosan chemical hydrolysis is interesting at perfection of production methods of chitinous materials and for a further refinement of chemical transformation mechanisms of natural polysaccharides.

There are two basic reactions during chitin's hydrolysis: the cleavage of the glycosidic linkages leading to destruction, and splitting of the amide linkages leading to deacetylation.

Acid hydrolysis is the most studied process of chemical transformation of chitin at which there is almost equivalent cleavage of glycosidic and amide linkages. Acid hydrolysis is applied to production of chitin oligosaccharides and monomers, therefore the basic attention of researchers is given to polymer chain destruction.

Alkaline hydrolysis is studied less in details. The main quantity of publications is devoted alkaline deacetylation which is used for chitosan production. Destruction is investigated a little. First, it explained by difficulty of hydrolysates identification: monosugars in alkaline condition destruct with high speed. Secondly, a speed of alkaline cleavage of glycosidic linkages is very low that makes difficulties for its studying.

Stopping of deacetylation reaction during alkaline treatment represents the greatest interest at studying of kinetics of chitin deacetylation. For an explanation of this experimental fact, some explanations are offered. The presence of crystal and amorphous regions in chitin is the most recognized one [1].

In the present report I would like to generalize some experimental data on chitin and chitosan hydrolysis in acid and alkaline conditions for the purpose of development of mathematical modeling.

MATERIALS and METHODS

Chitin and chitosan were prepared in laboratory on known method [2] from shell waste of Kamchatka crab *Paralithodes camtschaticus*. The prepared chitin contained less than 0.1 % of mineral substances and lipids, about 0.3 % of protein.

Chitosan was prepared by treating of chitin in 50 % NaOH at 100 °C within 1 h. The chemical hydrolysis of chitin and chitosan was carried out in thermostatically controlled glass flask at constant agitating. A hydrolysis in a nitrogen atmosphere made in sealed ampoules.

For reprecipitation of samples in NOH the chitin was dissolved in alkali as it is presented in article [3]. A chitin solution in 10 % NaOH was filtrated through filter Shota in vacuum. Then chitin was precipitated by neutralization of solution by 10 % HCl to pH 6.5. Chitin was reprecipitated also after dissolution in cold concentrated HCl. A solution was filtrated through filter Shota in vacuum. Chitin was precipitated by addition of excess of cold distilled water. Chitosan was reprecipitated from solution in 0.1 N HCl by neutralization to pH 7.5. All precipitates were separated by centrifuging and washed out by distilled water. The wet reprecipitated chitin and chitosan were prepared. A part of wet precipitates were dried at 60 °C for production of dry samples.

Degree of deacetylation (*DD*) of chitosan was defined by potentiometric titration of chitosan solution in 0,1 M HCl [4] and by IR-spectroscopy [5]. Infra-red absorption spectra of chitosan in KBr tablets were recorded on the spectrophotometer IR-420 (Shimadzu, Japan) over the range from 4000 to 400 cm^{-1} .

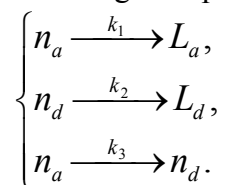
Molecular weight (*MW*) was defined by viscosimetry (for chitosan) [6] and by HPLC of carboxymethylchitin [7]. In case of the former the samples were deacetylated to *DD* about 80 %. Then its were N-acetylated completely with acetic anhydride and finally carboxymethylated with monochloroacetic acid in an alkaline condition.

Degree of crystallinity (χ_{cp}) was determined by the techniques offered in works [8, 9]. Researches of structural properties of chitin and chitosan samples were made in Tananaev Institute of Chemistry and Technology of Rare Elements and Mineral Raw Materials of the Kola Science Centre of RAS on diffractometer DRON-2 by the X-ray phase analysis on radiation $\text{CuK}\alpha$ with use of the Ni-filter in angle range $2\theta = 6-36^\circ$. Initial wet samples and dry samples in petrolatum oil suspension put on sapphire base, have been used for measurements [10]. Phase identification was made according to tables YCPDS and the publication [11].

RESULTS and DISCUSSION

The influence of different acids on kinetics of chitin destruction was studied at research of acid hydrolysis. By working out of mathematical model of acid degradation the following initial positions were used: during acid hydrolysis both glycosidic, and amide linkages cleavage, the glycosidic linkages near to acetylated amino group at C2 atom, decompose with greater speed, at the expense of anchimeric assistance of acetyl group.

The mathematical model including three reactions has been developed and used for an estimation of reaction's rate constants at its fitting to experimental kinetic curves.



where n_a – quantity of linkages at C1 atom of acetylated unit, n_d – quantity of ones of deacetylated unit, L_a and L_d – quantity of split linkages near to acetylated and deacetylated units, respectively, k_1 and k_2 – rate constants of glycosidic linkage cleavage, k_3 – rate constant of amide linkage cleavage.

The system of the differential equations of destruction process looked like:

$$\left\{ \begin{array}{l} dn_a(t)/dt = -(k_1 + k_2) \times n_a(t), \\ dn_d(t)/dt = k_3 \times n_a(t) - k_2 \times n_d(t), \\ dL(t)/dt = k_1 \times n_a(t) + k_2 \times n_d(t). \end{array} \right.$$

where $L = L_a + L_d$ – total quantity of split glycosidic linkage.

Unlike work [12] we modeled kinetics of change of chitin molecular weight. The constants counted on model fitted to experimental data are resulted in table 1. Cleavage of glycosidic linkage as assume, submits to the mechanism of nucleophilic substitution S_N1 catalyzed by acid [13]. Apparently from table 1, rate constants of hydrolysis of both glycosidic linkages increase with growth of degree of ionization of acids among $\text{CH}_3\text{COOH} < \text{H}_3\text{PO}_4 < \text{HCl} < \text{H}_2\text{SO}_4 < \text{HClO}_4$. This dependence confirms passing of glycosidic linkage hydrolysis on mechanism S_N1 at which reaction rate rises with increase in polarity of solvent.

Table 1. pK_a and rate constants ($\times 10^3 \text{ min}^{-1}$) of acid chitin hydrolysis, (initial *DD* 12.0 %)

Acid	CH ₃ COOH	H ₃ PO ₄	H ₂ SO ₄	HCl	HClO ₄
pK_a	4.7	2.12	− 5.6	− 6.7	− 8.95
k_1	16.35	35.00	82.9	71.9	140.00
k_1	0.31	0.61	2.05	0.61	4.80
k_3	86.1	140.00	16.0	13.76	38.05

On the other hand, the anions of studied acids place on decrease of their nucleophilicity in the following row: $\text{PO}_4^{-3} > \text{CH}_3\text{COO}^- > \text{SO}_4^{-2} \sim \text{Cl}^- \sim \text{ClO}_4^-$. Independence of rate constants k_1 and k_1 from nucleophilicity also confirms probability of mechanism S_N1 . The rate constant of amide linkage cleavage also estimated from hydrolysis model (see table 1). The calculated values k_3 correlated with nucleophilicity of acid anions among $\text{H}_2\text{SO}_4 < \text{HCl} < \text{HClO}_4 < \text{CH}_3\text{COOH} < \text{H}_3\text{PO}_4$. This data, apparently, has confirmed mechanism S_N2 for the deacetylation reaction, offered in [13].

Chitin alkaline degradation was studied in deaerated solutions.

It is now precisely enough positioned that in an alkaline condition polysaccharides participate in reactions of depolymerization, hydrolytic and oxidation decomposition and stabilization of reactive functional groups. Under normal conditions alkaline degradation of polysaccharides is insignificant. At elevated temperature the great number of transformations occurs. Most important of them: depolymerization (single step removal of monomer units) from the reducing end of a molecule (so-called reaction of "peeling"); rearrangement of a reducing endgroup and formation of group, resistant to against "peeling" ("a chemical stopping") [14, 15]; destruction (randomly cleavage of glycosidic linkages in chain). In chitin the eliminating of acetyl groups (deacetylation) also occurs. Peeling and hydrolysis reactions mainly lead to loss of polysaccharides and decrease of polymer chain length [14].

Results of long alkaline hydrolysis of chitin have shown that within 1-2 days from the hydrolysis beginning the section of sweeping decrease of *MW* which then is replaced by destruction with smaller speed (figure 1) [7] is observed.

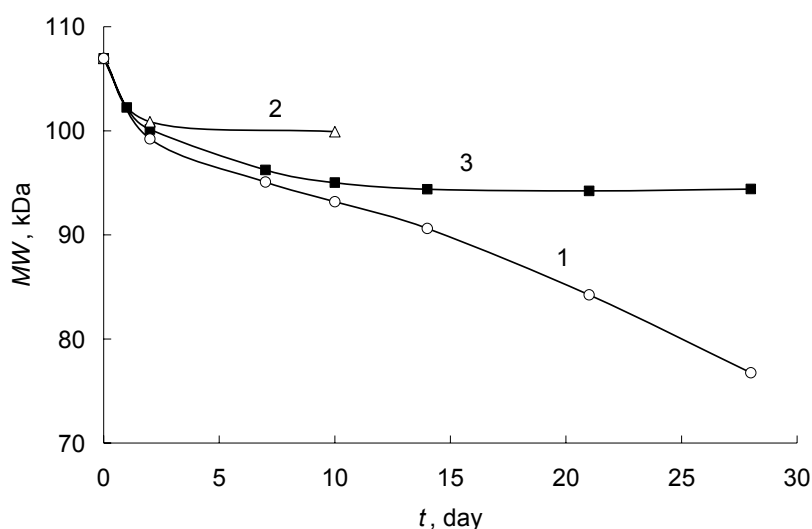


Figure 1. Kinetic curves of chitin degradation in deaerated solutions. Temperature 98 °C: 50 % NaOH (1); 10 % NaOH (2) and H₂O (3).

The reaction rate on the second section increases with increase in concentration of alkali (fig. 1, curves 1 and 2). This data allows to assume the existence of "peeling" process in the first

days of hydrolysis [16, 17]. The mechanism of chitosan "peeling", apparently, is analogous to that of cellulose [18].

It is interesting to note that in water decomposition rate with other things being equal comes nearer to that in 50 % NaOH. But in water the destruction mechanism, apparently, matches to acid hydrolysis. The plateau on the kinetic curve is called by the deacetylation, leading to stabilization of polymer's glycosidic linkages.

Thus, at chitosan deacetylation the decomposition rate of polymer chain is very small in comparison with speed of cleavage of amide linkages. The basic contribution to decrease of MW to the first tens hours of alkali treatment will be brought in by depolymerization from the reducing end. Casual cleavage of internal glycosidic linkages, as well as follows from its chemical properties, can be observed considerably after several days of hydrolysis. In actual practice of chitin deacetylation the appreciable contribution to destruction are yielded by oxidation decomposition by molecular oxygen of air which has been shown by us in water and various organic solvents (acetone, tetrahydrofuran, acetonitrile) in which the hydrolysis cannot have a place [7].

For an estimation of the contribution of supermolecular structure of chitin in reaction of deacetylation we have studied influence of initial chitin DD on kinetics and crystallinity of samples. It is known that at increase of DD crystalline structure of chitin is destroyed, an amorphicity is increased, and then crystalline structure of chitosan [1, 19] is formed. If this fact occurs, with growth of initial chitin DD and quantity of amorphous region the reaction rate and depth of deacetylation should increase. In view of such change, it is necessary to expect that the kinetics of deacetylation of chitin/chitosan samples with various DD will differ.

In the previous works [20, 21] the alkaline deacetylation of chitin and chitosan with various initial DD has been investigated. Normalization of kinetic curves to $DD = 0$ has shown that the kinetics of chitin and chitosan deacetylation does not depend from initial DD . This result that calls into question the influence of crystallinity on reaction kinetics.

We have made more correct experiment, using samples of chitin with measured degree of crystallinity (Table 1 [11]).

Table 2. Crystallinity of chitin and chitosan samples

Sample	$\chi_{kp}, \%$	
	dry	wet
Chitin initial	61.1	-
reprecipitated from NaOH	55.5	8.8
reprecipitated from HCl	60.7	8.5
Chitosan initial	35.8	-
reprecipitated from HCl	37.5	3.8

The data in figure 2 show that deacetylation rate of initial chitin samples (dry (1) and wet (2)) is higher than reprecipitated ones (dry (3) and wet (4)).

Maximum DD ($t > 40$ min) of dry samples appears above, than at wet. The least rate of deacetylation and DD were observed at the wet reprecipitated chitin (the curve 4) with the least crystallinity ($\chi_{kp} = 3.8 \%$). Apparently, the hydration of polysaccharide molecules occurs in water. In alkali solution the additional solvation of molecules with hydroxyls-ions occurs.

In an alkaline condition the hydrolysis of amide linkages begins with nucleophilic attack by OH-ions on carbonyl carbon of acetamide groups. The solvent sheath complicates this nucleophilic attack that leads to decrease in rate and depth of deacetylation.

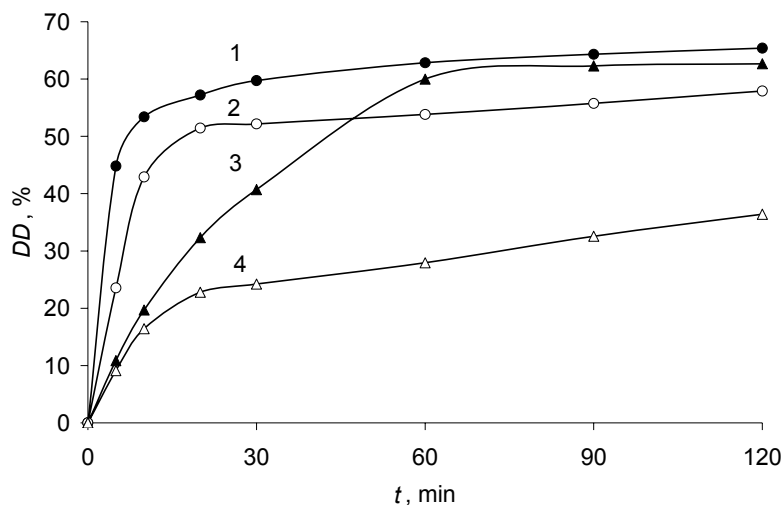


Figure 2. Kinetic curves of chitin deacetylation in 50 % NaOH, 100 °C:
initial dry (1), initial wet (2), dry reprecipitated from HCl (3), and wet reprecipitated from HCl (4) samples.

In wet initial chitin only a part of chitin molecules are solvated that leads to decrease of deacetylation rate and limiting *DD* (curves 1 and 2). Decreasing deacetylation rate on the first section (0-30 min) of kinetic curve of reprecipitated dry chitin (the curve 3) in comparison with dry and wet initial chitin (curves 1 and 2) probable are explained by close packing of polysaccharide molecules after recrystallization. In the initial samples prepared by consecutive removal of protein and inorganic salts from crab shell the chitin is more porous. In the wet reprecipitated chitin almost all molecules are completely solvated and also are follow-up solvated by hydroxyls-ions at treating by alkali (the curve 4).

CONCLUSIONS

Thus, our data has confirmed that with increase in degree of ionization the rate of glycosidic linkage cleavage increases and does not depend univocal from nucleophilicity of acid anion, that is a reaction can be supported by mechanism S_N1 .

The investigation of alkaline of chitin allows to assume that degree of crystallinity makes considerably smaller impact on deacetylation rate. Formation of a solvate (hydrated) shell round polysaccharide macromolecules interferes with nucleophilic attack by hydroxyls-ions and the main influence on reaction stopping makes.

Apparently, we have received additional acknowledging to a hypothesis of passing of two parallel reactions - deacetylation and formation of low-active intermediate which is destroyed at washing [21].

REFERENCES

- [1] Kurita, K., Sannan, T. and Iwakura, Y. (1977) Studies on chitin, 4. Evidence for formation of block and random copolymers of N-acetyl-D-glucosamine and D-glucosamine by hetero- and homogeneous hydrolysis. *Makromol. Chem.*, 178 (12), 3197-202.
- [2] No, H. K. and Meyers, S. P. (1997) Preparation of chitin and chitosan. In *Chitin Handbook* (R. R. A. Muzzarelli and M. G. Peter, ed.) pp. 475-89, Crottamare. Italy: Atec Edizioni, European Chitin Society.

- [3] Sannan, T., Kurita, K. and Iwakura Y. (1975) Studies on chitin. 1. Solubility change by alkaline treatment and film casting. Makromol. Chem. Short Commun., 176 (4), 1191-5.
- [4] Nud'ga, L. A., Plisko, E. A. and Danilov S. N. (1973) N-Alkylation of chitosan. Zhurnal Obshchei Khimii [(Russ. J. Gen. Chem.)], 43 (12), 2756-60.
- [5] Wang, T., Turhan, M. and Gunasekaran, S. (2004) Selected properties of pH-sensitive, biodegradable chitosan-poly(vinyl alcohol) hydrogel. Polym. Int., 53, 911-8.
- [6] Pavlov, G. M. and Selyunin, S. G. (1986) High-speed sedimentation, molecular mass and conformational parameters of certain soluble derivatives of chitin. Polym. Sci. U.S.S.R., 29 (8), 1925-30.
- [7] Chebotok, E. N., Novikov, V. Yu. and Konovalova, I. N. (2006) Depolymerization of chitin and chitosan in the course of base deacetylation. Russ. J. Appl. Chem., 79 (7), pp. 1162-6.
- [8] Rabek, J. F. (1980) Experimental Methods in Polymer Chemistry. Physical Principles and Applications. Chichester, New York, et al.: A Wiley-Interscience Publication. John Wiley and Sons. 861 p.
- [9] Gorbacheva, I. N., Ovchinnikov, Yu. K., et al. (1988) An X-ray study of the structure of chitosan. Polym. Sci. U.S.S.R., 30 (12), 2694-8.
- [10] Chebotok, E. N., Novikov, V. Yu. and Konovalova, I. N. (2007) Kinetics of base deacetylation of chitin and chitosan as influenced by their crystallinity. Russ. J. Appl. Chem., 80 (10), 1753-8.
- [11] Paralikar, K. M. and Balasubramanya R. H. (1984) Electron diffraction study of alpha-chitin. J. Polym. Sci. Part C: Polym. Lett., 22 (10), 543-6.
- [12] Einbu, A. and Varum K. M. (2008) Characterization of chitin and its hydrolysis to GlcNAc and GlcN. Biomacromol., 9 (7), 1870-5.
- [13] Varum, K. M., Ottoy, M. H. and Smidsrod O. (2001) Acid hydrolysis of chitosans. Carbohydr. Polym., 46 (1), 89-98.
- [14] Fengel D. and Wegener G. (1984) Wood (Chemistry, Ultrastructure, Reactions). Berlin, New York: Walter de Gruyter. xiii, 613 p.
- [15] Pavasars, I., Hagberg, J., et al. (2003) Alkaline degradation of cellulose: mechanisms and kinetics. J. Polym. Environ., 11 (2), 39-47.
- [16] Focher, B., Beltrame, P. L., et al. (1990) Alkaline N-deacetylation of chitin enhanced by flash treatments. Reaction kinetics and structure modifications. Carbohydr. Polym., 12 (4), 405-18.
- [17] Yang, B. Y., Ding, Q. and Montgomery, R. (2010) Heterogeneous components of chitosans. Biomacromol., 11 (11), 3167-71.
- [18] BeMiller, J. N. and Whistler, R. L. (1962) Alkaline degradation of amino sugars. J. Org. Chem., 27 (4), 1161-64.
- [19] Focher, B., Naggi, A., et al. (1992) Chitosans from *Euphausia superba*. 2: Characterization of solid state structure. Carbohydr. Polym., 18 (1), 43-9.
- [20] Novikov, V. Yu., Orlova, T. A. and Voronina, I. E. (1990) Kinetics of chitin and chitosan deacetylation reaction. News of Institutes of Higher Education. Food Technol., 5, 64-7.
- [21] Novikov, V. Yu. (2003) Chemical hydrolysis of chitin and chitosan. Proc. of the VIIth Int. Conf. "Modern Perspectives in Chitin and Chitosan Studies", 38-42. Moscow: VNIRO Publ.

THE PROPERTIES OF CHITOSAN GELS CONTAINING DIFLUCORTOLONE VALERATE LOADED NANOPARTICLES

Ipek Ozcan, Taner Senyigit, Mine Ozyazici, Ozgen Ozer*

Ege University, Faculty of Pharmacy, Department of Pharmaceutical Technology, Bornova, Izmir-Turkey.

*E-mail address: ozgen.ozer@ege.edu.tr

INTRODUCTION

Topical glucocorticoids (TG) are highly effective drugs widely used in dermatology for the treatment of inflammatory diseases. However, severe adverse effects associated with long-term TG application limit their use. Over the years, research has focused on strategies to optimize potency of TG while minimizing adverse effects [1]. Diflucortolone valerate (DFV) is one of the potent glucocorticosteroid according to the corticosteroid classification system released by British National Formulary [2]. Chitosan is a cationic polysaccharide with many interesting biopharmaceutical properties, such as biocompatibility, biodegradability, bioadhesion and penetration enhancer properties [3,4].

The aim of this study was to prepare and characterize difluocortolone valerate loaded lecithin/chitosan nanoparticles. In order to have a semisolid consistency, the nanoparticulate system was incorporated into a chitosan gel with different ratios. Characterization included rheological and textural properties measurements were also performed to assess the applicability of the chitosan gel to the skin surface.

MATERIALS and METHODS

Materials

DFV was a kind gift from Roche, Turkey. Lecithin (Lipoid S45) and chitosan (MW 140 KDa) were purchased from Lipoid AG (Ludwigshafen, Germany) and Primex (Haugesund, Norway), respectively. Medium molecular weight chitosan (MW 190–310 kDa, deacetylation degree 75–85%) was obtained from Sigma, USA. All other chemicals were of analytical grade.

Preparation and Characterization of Nanoparticles

Lecithin/chitosan nanoparticles were prepared according to the method previously reported by Sonvico et al [5], by direct injection of soybean lecithin alcoholic solution into chitosan/water solution.

Briefly, an ethanolic solution of lecithin 2.5% (w/v) containing DFV and 2% w/v of isopropyl myristate (IPM) was prepared. Nanoparticles were obtained by rapidly injecting of the lecithin ethanolic solution through a glass pipette (internal diameter 0.75 mm, injection rate 40 ml/min) under mechanic stirring (Ultraturrax TP 18/10-10N, IKA Werke, Germany), into a chitosan solution obtained by diluting with distilled water 0.5 ml of 1 % (w/v) chitosan solution in 0.275 N HCl. In the colloidal suspension, lecithin/chitosan was present in ratio 20:1 (w/w) and the DFV content was 0.1 % w/v.

The average particle size and size polydispersity of the nanoparticles were determined by the dynamic laser light scattering method (Nanosizer Coulter N4 Plus[®]) (Malvern Instruments, UK). The zeta potential of nanoparticles was measured in aqueous dispersion with a Zetasizer 4 (Malvern Instruments, UK) at 25 °C.

Preparation and Characterization of Chitosan Gels

A blank chitosan gel in water was prepared by dissolving 2 g of chitosan in 100 ml of acetic acid 1.5 % w/v water solution.

The colloidal suspension obtained at the end of DFV-loaded nanoparticles preparation process was incorporated in blank chitosan gel in three different ratios (1:9, 1:3, and 1:1).

The pH and the viscosity values of blank and DFV loaded chitosan gels were measured with pH-meter and digital rotational viscosimeter (DV III, Brookfield, USA), respectively. For viscosity measurements, the spindle (number 29) was rotated at 25 rpm. Viscosity of formulations was measured at $25 \pm 1^\circ\text{C}$. All analysis was replicated at least six times.

Mechanical Properties of Chitosan Gels

Evaluation of mechanical properties of the formulations was performed using a Stable Micro System Texture Analyser in texture profile analysis (TPA) mode. From the resultant force-time plot, mechanical parameters such as hardness, adhesiveness, cohesiveness, compressibility and elasticity were defined. All analysis was performed at least in triplicate.

RESULTS and DISCUSSION

Lecithin/chitosan nanoparticles with and without DFV were characterized in terms of size, zeta potential and size distribution. Table 1 shows the characteristics of nanoparticle formulations.

Table 1. Physicochemical properties of nanoparticles

Formulations	Particle Size (nm)	Zeta Potential (mV)	Polydispersity Index (PI)
Blank nanoparticles	213.4 ± 12	35.3 ± 3.2	0.190 ± 0.03
DFV loaded nanoparticles	204.2 ± 10	41.4 ± 1.6	0.149 ± 0.02

The colloidal particles produced were characterized by size near 210 nm and high positive surface charge, attributed to the presence of chitosan chains on the particle surface. In this study, the size distribution resulted to be narrow, considered the calculated polydispersity index of nanoparticle dispersion was below 0.2.

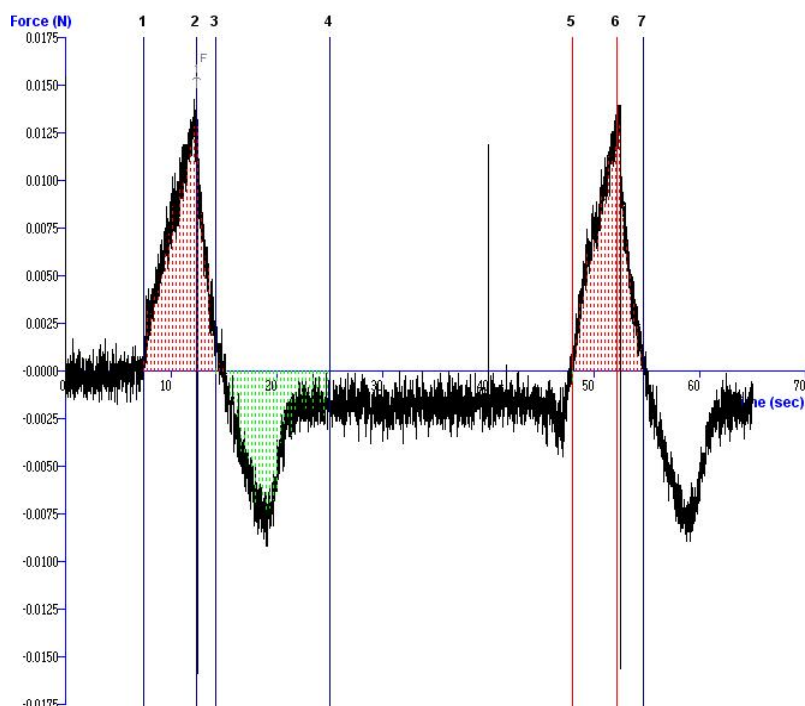
DFV nanoparticle colloidal suspension was incorporated in aqueous chitosan gels for a more convenient topical use. The gel was selected as topical dosage form since it could maintain on the skin the preparation designed for treating local inflammatory event, reducing the drug transdermal permeation. The pH and viscosity values of formulation prepared at 1:9 ratio were found as 4.8 and 13100 ± 0.42 cps, respectively.

Mechanical Properties of Chitosan Gels

Mechanical properties of gels for topical delivery are important for the maximum benefit of the patient from the formulation. TPA defines the mechanical parameters in terms of hardness, adhesiveness, cohesiveness, compressibility and elasticity. The TPA graph and calculated mechanical properties of drug free and BMV loaded nanoparticle: chitosan gels are presented in Table 2 and Figure 1, respectively.

Table 2. Mechanical properties of formulations

Formulation	Ratio	Hardness (N)±SD	Compressibility (N mm) ± SD	Adhesiveness (N mm) ± SD	Cohesiveness ± SD	Elasticity ± SD
Chitosan gel		0.012±0.001	0.026±0.004	0.018±0.001	0.926±0.052	0.814±0.078
BMV loaded	1:1	0.009±0.001	0.021±0.002	0.010±0.002	0.910±0.014	0.962±0.052
nanoparticle:	1:3	0.010±0.001	0.023±0.003	0.012±0.002	0.857±0.021	0.916±0.028
Chitosan gel	1:9	0.012±0.001	0.028±0.004	0.016±0.001	0.894±0.042	0.882±0.039

**Figure 1. TPA graph of drug free chitosan gel.**

Hardness is defined as the maximum peak force during the first compression cycle. The hardness of chitosan gels, which determines the ease of application on the skin, was between 0.009-0.012 N, acceptable for topical gel application and in accordance with previous studies [6]. The hardness and compressibility of the gels were raised when the viscosity of gel formulations increased. The highest compressibility (0.028±0.004 N.mm) was obtained with 1:9 ratio. Adhesiveness is the work required to overcome the attractive forces between the surface of the sample and the surface of the probe and it is related to bioadhesion. In this study, the adhesiveness of gel decrement was affected by added nanoparticle ratio.

TPA also provides information about cohesiveness. Cohesiveness describes the ratio of the area under the force-time curve produced on the second compression cycle to that produced on the first compression cycle. The high value of cohesiveness provides full structural recovery following gel application [7]. All gel formulations were showed a enough high cohesiveness

value (>0.856 N.mm), which is suitable for topical application. Elasticity is the rate at which the deformed sample returns to its undeformed condition after the removal of the deforming force. According to the elasticity results, it can be assumed that chitosan gels had an acceptable elasticity value.

From the results of TPA experiments, it can be concluded that chitosan gels (include or exclude nanoparticles) has suitable mechanical properties for topical administration.

On the basis of above observations, chitosan gels loaded with lecithin/chitosan nanoparticles could be successfully prepared with good physical characteristics for topical use. The formulation prepared with 1:9 ratio provided the best physical properties regarding applicability to the skin. These nanoparticle-in-gel formulations will be used for further studies to increase accumulating capacity for inducing epidermal targeting and to improve the risk-benefit ratio of topically applied DFV.

ACKNOWLEDGEMENTS

This work was supported by The Scientific and Technological Research Council of Turkey (Project number: 109S433).

REFERENCES

- [1] Brazzini, B., Pimpinelli, N. (2002) New and Established Topical Corticosteroids in Dermatology. *Am. J. Clin. Dermatol.*, 3(1), 47-58.
- [2] British National Formulary. (2004) London: British Medical Association and the Royal Pharmaceutical Society of Great Britain.
- [3] Hejazi, R., Amiji, M. (2003) Chitosan Based Gastrointestinal Delivery Systems *J. Control. Release*, 89, 151-165.
- [4] Senel, S., McClure, S.J. (2004) Potential applications of chitosan in veterinary medicine. *Adv. Drug. Deliv. Rev.*, 56, 1467-1480.
- [5] Sonvico, F., Cagnani, A., Rossi, A. et al. (2006) Formation of self-organized nanoparticles by lecithin/chitosan ionic interaction. *Int. J. Pharm.*, 324, 67-73.
- [6] Bruschi, M.L., Jones, D.S., Panzeri, H., et al. (1997) Semisolid systems containing propolis for the treatment of periodontal disease: in vitro release kinetics, syringeability, rheological, textural, and mucoadhesive properties. *J. Pharm. Sci.*, 96, 2074-2089.
- [7] Jones, D.S., Woolfson, A.D., Brown, A.F. (1997) Textural, viscoelastic and mucoadhesive properties of pharmaceutical gels composed of cellulose polymers. *Int. J. Pharm.*, 151, 223-233.

STUDIES ON GAMMA IRRADIATION EFFECTS ON CHITOSAN MICROPARTICLES

Fırat Sakar¹, Suna Erdogan¹, A. Yekta Ozer^{1*}, Sevdâ Senel², Seyda Colak³

¹*Faculty of Pharmacy, Department of Radiopharmacy, 06100 Sıhhiye,*

²*Faculty of Pharmacy, Department of Pharmaceutical Technology, 06100 Sıhhiye,*

³*Faculty of Engineering, Department of Physics Engineering, Beytepe, Hacettepe University, Ankara-Turkey*

**E-mail: ayozer@hacettepe.edu.tr*

INTRODUCTION

Chitosan is obtained from the alkaline deacetylation of chitin, which is a glucose-based, unbranched polysaccharide widely available in nature. Chitosan exhibits a variety of physicochemical and biological properties resulting in numerous applications in different fields and it is widely used in the drug delivery systems.

Pharmaceutical products intended for parenteral administration have to be sterilized. γ -irradiation seems to be a suitable sterilization technique for drug delivery systems. However, gamma irradiation might also affect the performance of these systems for example polymers resulting crosslinking. Therefore, the influence of γ -irradiation on the characteristics of polymeric microspheres should be investigated carefully [1, 2].

In this study, chitosan microparticles prepared by different types of chitosan such as chitosan (medium MW), glutamate and chloride and effect of gamma irradiation on these microparticles were evaluated by determining the change of size, surface morphology, thermal behavior and EPR thermograms.

MATERIALS and METHODS

Three types of chitosan were employed as Chitosan (medium MW) (MW=109-310 kDa) (Sigma, USA), Chitosan glutamate (MW=350 kDa) (Protosan UP G214) (Novamatrix, Norway) and Chitosan chloride (MW=150-400 kDa) (Protosan UPC 213) (Novamatrix, Norway). The degree of deacetylation of these chitosan types were 75-80%, > 90 % and 75-90 %, respectively. All other chemicals were of analytical grade and used as received.

Preparation of Chitosan Microparticles: 0.5 g chitosan was dispersed in %1 (v/v) aqueous lactic acid solution and then 4 ml glutaraldehyde (1 %) solution was added for cross-linking. This chitosan solution was stirred for 2 h using magnetic stirrer. Thus, chitosan solution was then spray-dried to obtain empty chitosan microparticles. Spray-drying was performed using a Buchi Mini Spray Dryer B290 (Switzerland) with a standard nozzle (0.7 mm) [3]. Spray-drying conditions such as inlet and outlet temperature, aspirator rate, pump rate and compressed spray air flow were set at 140 °C, 67 °C, 85%, 10% and 40-50 psi, respectively.

For the chitosan microparticles made of chitosan glutamate and chloride, the same preparation method was employed by dissolving in distilled water instead of lactic acid solution. The atomizing air pressure was 60 kPa. Atomization occurred by the force of the compressed air, disrupting the liquid into small droplets, when the liquid was fed to the nozzle with peristaltic pump. The hot air and the droplets were blown together into a chamber. The solvent in the

droplets was evaporated and discharged out through an exhaust tube. This dry product was collected in a collection bottle, afterwards.

Gamma-Irradiation of Chitosan Microparticles: Empty chitosan microparticles were placed in vials, sealed under vacuum and gamma irradiated at ambient temperature at the dose rate of 10, 25 and 40 kGy by using ^{60}Co (0.79 kGy.h^{-1}) as the radiation source (Turkish Atomic Energy Agency, Gamma Irradiation Facility, Ankara).

Characterization of Chitosan Microparticles: Three types of chitosan (medium MW, glutamate and chloride) microparticles were characterized for their mean particle size, surface morphology (SEM images), electron paramagnetic resonance (EPR) spectroscopy and differential scanning calorimetry (DSC) behavior before and after irradiation [4, 5].

Mean Particle Size: Mean particle size was analyzed by dispersing the empty microparticles (irradiated and non-irradiated) in an aqueous solution of Tween 80 (0.1 %). Ultrasonication was employed for 1 min in order to prevent the microparticle aggregation during the particle size measurements. Dynamic Light Scattering (DSL) determinations were carried out by using Malvern Multisizer (Model 2000).

Surface Morphology: Scanning Electron Microscopy (SEM) technique was employed (Fei Quanta 400F Field Emission SEM, Germany) in order to determine the surface morphology and topography. For SEM micrographs, three types of chitosan microparticles were fixed on a brass stub using double-sided adhesive tape and then were made electrically conductive by coating in vacuum with a thin layer of gold, for $0.3 \mu\text{s}$, at 20 kV and 20 mm WD.

EPR Analysis: EPR determinations of irradiated and non-irradiated samples were carried out at room temperature. Chitosan microparticles were transferred into sealed quartz tubes of about 4mm internal diameter and recorded using a EPR spectrophotometer (Bruker EMX 113X-Band EPR) equipped with cylindrical cavity (ER-4119HS) resonator containing a standard sample (DPPH). Signal intensities were calculated from first derivative spectra of the absorption peak plotted against magnetic field and compared with that obtained for the standard sample under the same spectrometer operating conditions. The spectrometer operating conditions adopted during the experiments were; central field: 350 MT, sweep width: 1000 mT, microwave frequency: 9-852 GHz, microwave power: 1mW, modulation frequency: 100 kHz, modulation amplitude: 0.1 mT, receiver gain: 5.02×10^4 , sweep time: 83.89 s, time constant: 20.48 s.

Thermal Analysis: DSC thermograms were obtained by using a Universal V4.5A. TA Instruments, differential scanning calorimeter with a thermal analyzer. Irradiated and non-irradiated chitosan microparticle samples were weighted exactly and were sealed in aluminium pans and heated in an inert atmosphere. An empty pan was taken as reference. The equipment was calibrated with an indium sample. Chitosan microparticles were scanned at $10^\circ\text{C.min}^{-1}$ from -25 to 300°C .

RESULTS AND DISCUSSION

Surface morphology was affected from irradiation for chitosan microparticles. After gamma irradiation, the microparticles exhibited relatively smoother surface due to the disruption of the edges of polymeric wrinkles by gamma irradiation.

Figure 1 shows the scanning electron photomicrographs of gamma irradiated and non-irradiated chitosan microparticles. Gamma irradiation induced the surface morphology and surface smoothness was induced. The change in topology could be observed with 50.000X magnification of SEM.

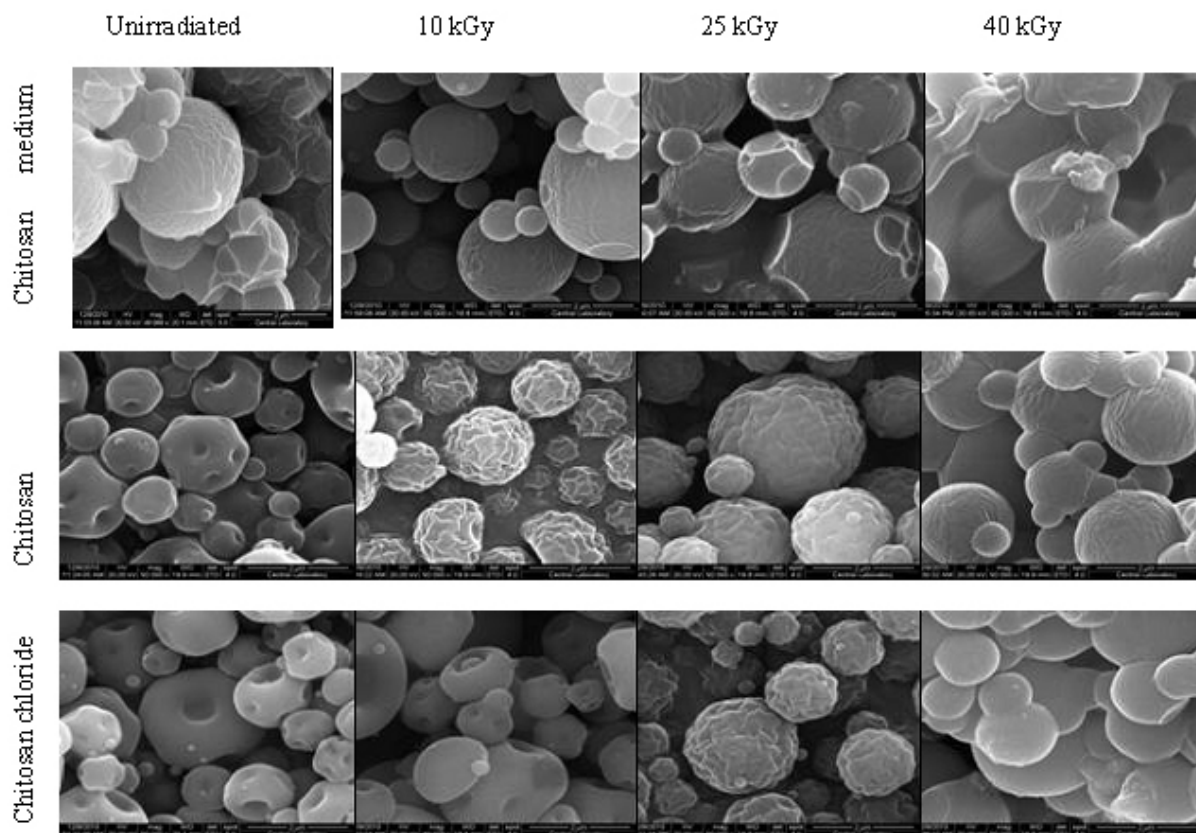


Figure 1: Scanning photomicrographs of different chitosan microparticles.

For chitosan microparticles; there was a slight difference in SEM photomicrographs of non-irradiated and irradiated at different dose rates. With the high gamma rates, the morphologic modifications increased.

For chitosan glutamate microparticles; there were sunken on the surface for unirradiated ones. But surface smoothness increased with the high doses of irradiation.

For chitosan chloride microparticles; the same observation with chitosan glutamate microparticles were obtained for the chloride microparticles. Surface smoothness increased with the increasing irradiation doses.

Particle size decreased considerably for the gamma-irradiated chitosan microparticles prepared by chitosan medium MW and chitosan glutamate. But, irradiation did not affect the mean particle size for the chitosan chloride made microparticles. The decrease in particle size was significant for the high doses of irradiation (like 25 and 40 kGy than 10 kGy) for chitosan glutamate and chitosan medium MW particles. Such phenomenon could be due to the considerable shrinkage of microparticles depending on irradiation. During irradiation at high doses, ionizing radiation induces some structural modifications of polysaccharides such as chitin/chitosan and their water-soluble derivatives in aqueous solution. Such irradiated polymers can be crosslinked and can adopt more ordered and more stable conformations. As a result, the particle size of these different type of chitosan microparticles containing polysaccharides also may undergo alterations as a result of possible crosslinking reactions [6].

The **EPR spectra** recorded for non-irradiated solid chitosan (medium MW) samples gave very low EPR signal which can be hardly distinguishable from noise. The spectroscopic splitting factors g and the peak-to-peak width for the solid chitosan (medium MW) microparticles were about $g = 2.0073$ and $\Delta H_{pp} = 0.14$ mT, respectively.

Dose-response curves of these samples were also investigated and it was found that they gave the varying of I_{pp} ($=I_1 + I_2$) which is normalized to the mass of the sample with the absorbed dose. This curve can also give an idea about the radical yield of the gamma irradiated chitosan (medium MW) sample. From dose-response curve, it can be concluded that the irradiated chitosan (medium MW) sample was not very much affected by gamma irradiation dose and the radiolytical intermediates produced after irradiation is only 30 % greater for the 10 kGy gamma irradiated sample than that of other samples irradiated at 25 kGy and 40 kGy doses (Figure 2).

The EPR spectra recorded for non-irradiated solid chitosan glutamate samples gave very low EPR signal intensity which is hardly distinguishable from the noise. The spectroscopic splitting factors g and the peak-to-peak width for the solid chitosan glutamate microparticles were about $g = 2.0073$ and $\Delta H_{pp} = 0.11$ mT, respectively.

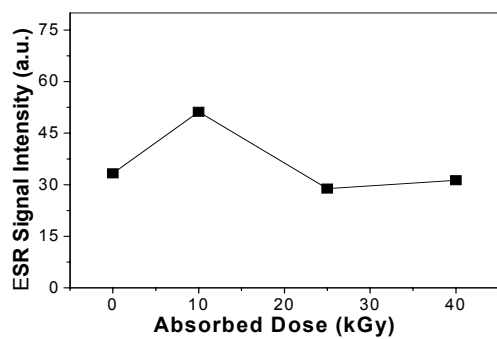
Dose-response curve of irradiated chitosan glutamate sample gave the change of I_{pp} ($=I_1 + I_2$) which is normalized to the mass of the sample versus the absorbed dose. This curve can also give a good approximation about the amount of radical yield of the gamma irradiated samples. Depending on the dose-response curve results, it can be concluded that the irradiated chitosan glutamate sample was mostly affected by 25 kGy irradiation dose and radiolytical intermediates produced by irradiation decreased sharply after this critical dose value (Figure 2).

The EPR spectra recorded for non-irradiated solid chitosan chloride samples gave very low EPR signal intensity, hardly distinguishable from the noise. The spectroscopic splitting factors g and the peak-to-peak width for the solid chitosan glutamate microparticles were about $g = 2.0071$ and $\Delta H_{pp} = 0.18$ mT, respectively.

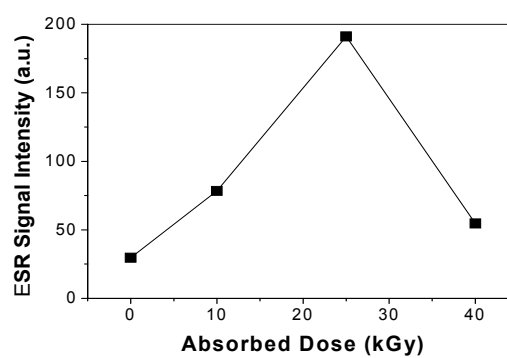
Dose-response curve of irradiated chitosan chloride sample gave the change of I_{pp} ($=I_1 + I_2$) that was normalized to the mass of the sample with the absorbed dose. This curve is also an indication of the amount of radical yield of the irradiated samples. As it can easily be seen from the dose-response curve, the irradiated chitosan chloride sample was the mostly affected by gamma irradiation at the critical irradiation dose of 25 kGy and radiolytical intermediates produced by irradiation decreased sharply after this dose value (Figure 2).

Besides, no change in the spectrum shape was obtained for the 3 types of chitosan samples irradiated at different doses (as it can be seen from the recorded EPR spectra) indicating that the type of radicals produced upon irradiation are independent from the absorbed dose.

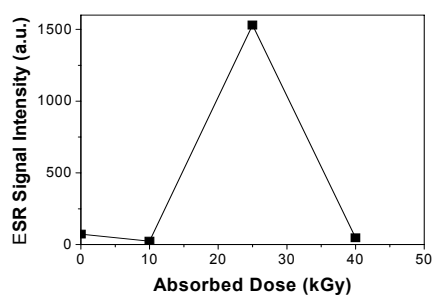
In general, EPR analysis is a crucial evaluation test for gamma irradiated samples. According to the abovementioned EPR analysis data, it was concluded that the gamma irradiation affected different type of chitosan microparticles but, this effect was slight and the radicals produced upon irradiation quenched in a short time.



(a)

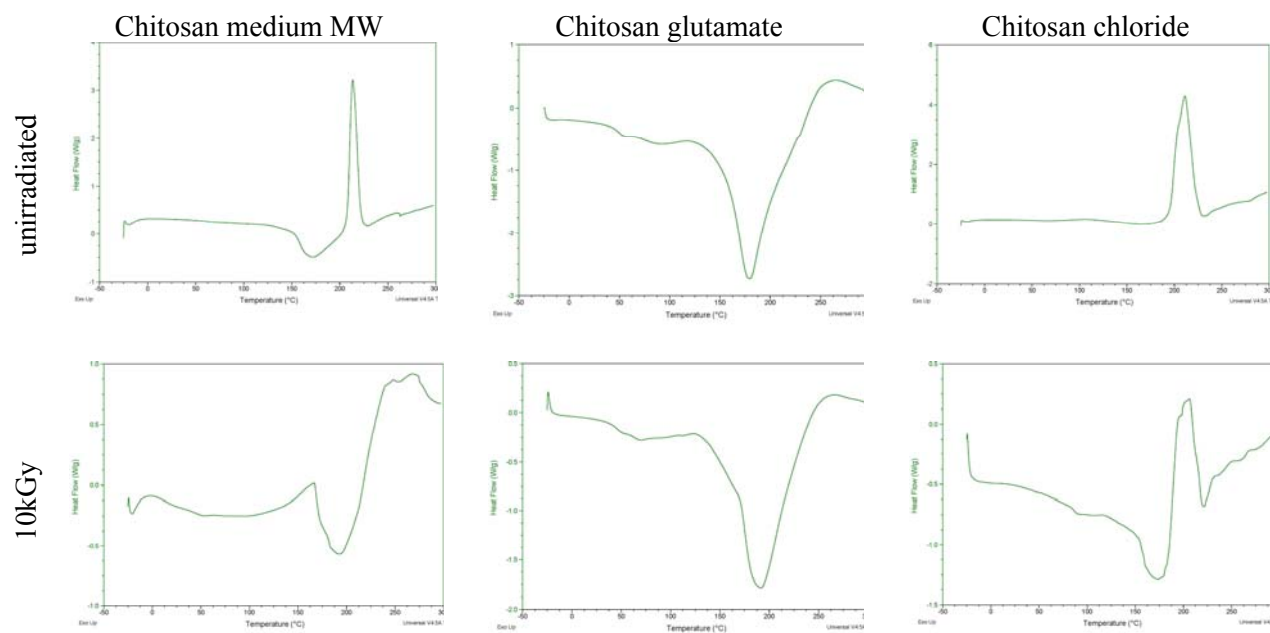


(b)



(c)

Figure 2: Dose-response curve of chitosan (medium MW) (a), chitosan glutamate (b) and chitosan chloride (c) microparticles



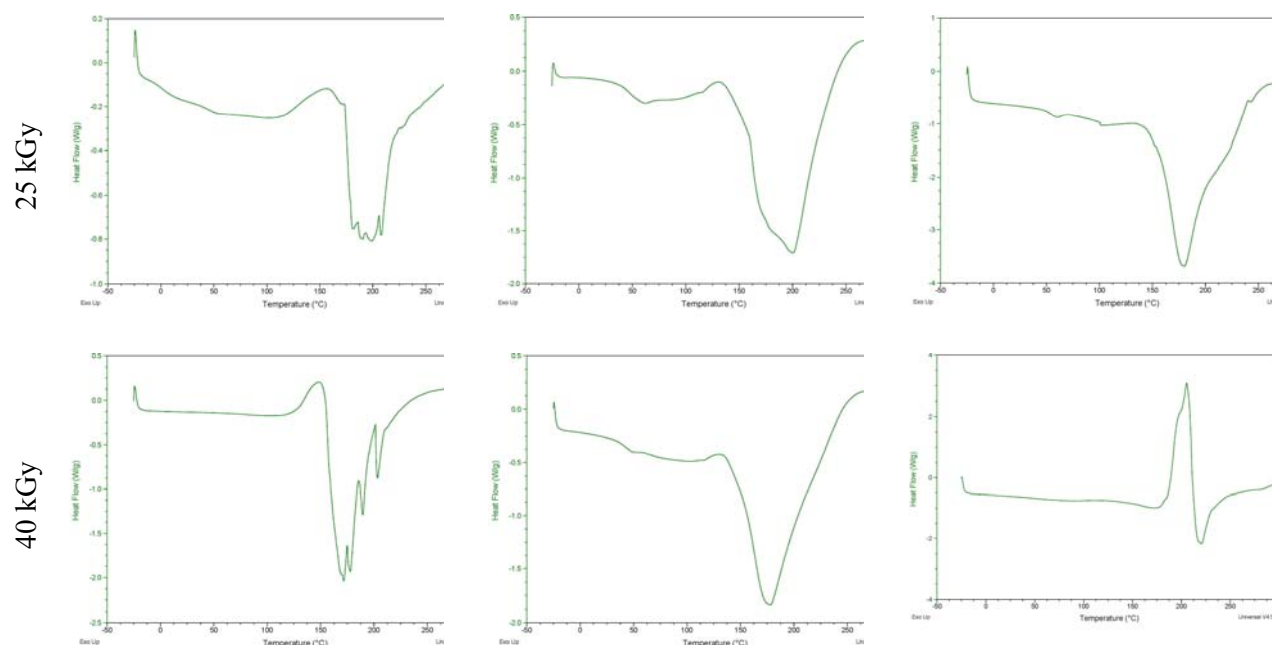


Figure 3: DSC thermograms of different types of chitosan microparticles before and after irradiation.

DSC thermograms of irradiated and non-irradiated different type of chitosan microparticles have been showed in Figure 3. The thermograms of different chitosan microparticles irradiated at 25 kGy were almost the same (about 200 °C). No peaks indicative for other transitions were observed in irradiated microparticles. So, gamma radiation at the standart dose of 25 kGy does not alter the matrix composition. But, for the higher irradiation doses, transition peaks were observed for chitosan chloride microparticles showing the alteration. Among the others, chitosan glutamate microparticles were the most resistant systems against gamma-irradiation.

ACKNOWLEDGEMENT

The authors wish to thank Abdi İbrahim Drug Company (Turkey), İbrahim Ethem Ulagay-Menarini Drug Company (Turkey) and Deva Drug Company (Turkey) for their valuable technical support for this research. The authors acknowledge Yelda Zencir, Hacettepe University, Faculty of Engineering, Department of Food Engineering for their valuable help for DSC studies.

REFERENCES

- [1] Erdogan, S., Ozer, A.Y., Ekizoglu, M., Ozalp, M., Colak, S., Korkmaz, M. (2006) Gamma irradiation of liposomal phospholipids. *FABAD J Pharm Sci.*, 31, 182-190.
- [2] Turker, S., Ozer, A.Y., Kılıc, E., Ozalp, M., Colak, S., Korkmaz, M. Gamma irradiated liposome/noisome and lipogelosome/niogelosome formulations for the treatment of rheumatoid arthritis (submitted).
- [3] He, P., Davis, S.S., Illum, L. (1999) Chitosan microspheres prepared by spray drying. *Int. J. Pharm.*, 187, 53-65.
- [4] Choi, W.S., Ahn, K.J., Lee, D.W., Byun, M.W., Park, H.J. (2002) Preparation of chitosan oligomers by irradiation. *Polym. Deg. Stab.*, 78, 533-38.
- [5] Montanari, L., Costantini, M., Signoretti, E.C., Valvo, L., Santucci, M., Bartolomei, M., Fattibene, P., Onori, S., Faucitano, A., Conti, B., Genta, I. (1998) Gamma irradiation effects on poly(DL-lactide-co-glycolide) microspheres. *J. Control. Release*, 56(1-3), 219-29.
- [6] Desai, K.G., Park H.J. (2006) Study of gamma irradiation effects on chitosan microparticles, *Drug Delivery*, 13, 39-50.

POLYSACCHARIDE ANALYSIS BY REVERSED-PHASE HPLC

Mariya N. Portsel¹, Vitaly Yu. Novikov^{2*} and Irina N. Konovalova¹

¹*Murmansk State Technical University*

²*Knipovich Polar Research Institute of Marine Fisheries and Oceanography (PINRO),
Murmansk, Russia*

**E-mail: nowit@pinro.ru*

INTRODUCTION

Chondroitin sulfate (CS) is a major component of connective tissue and is partially responsible for providing the flexibility of these tissues. CS is a sulfated glycosaminoglycan. Its macromolecules consist of alternating monomer units of glucuronic acid and N-acetyl-galactosamine, sulfated in the 4 or 6 position. Oral administration of CS may help treat symptoms of osteoarthritis, and dietary supplements containing CS that claim to promote healthy joints are readily available. Predominant sources of CS raw materials are bovine trachea, porcine skin and rib cartilage, and shark cartilage. Marine aquatic organisms are interesting as a raw material for preparing of such polysaccharides as chitin and chondroitin sulfate.

CS with low molecular weight is produced by different methods of acid hydrolysis and used for the manufacture of drugs. Therefore, an important practical and theoretical task is to study physical and chemical mechanism of acid hydrolysis of CS to oligomers and monomers, their subsequent identification and quantitative relationships between them. Quantitative analysis of CS in raw materials and food additives containing CS is an extremely challenging task due to the wide range of molecular weight of CS, its poor UV absorption, and strongly ionic nature. Other related GAGs may be present as impurities or fillers in the formulations of CS, and thus any analytical method, aiming at the quantification of CS must be selective for CS in the presence of other GAGs. Reaction with carbazole [1, 2], titration with cetyl pyridinium chloride [3], and size exclusion chromatography [4] are used for the analysis of CS, however, these methods can not distinguish between CS and other GAGs, which may be part of nutritional supplements and other products.

MATERIALS and METHODS

The preparations CS from cartilages of salmon *Salmo salar* and chitin (CN) from shell of shrimp *Pandalus borealis*, prepared on known methods [5, 6] was used in the investigation. The hydrolysis of CS and CN preparations was made as follows. Sample of CS (CN) was placed in a flask with a glass stopper and hydrochloric acid was added (1 ml of acid per 0.01 g of a sample). The flask densely closed by a glass stopper was heated on a water bath with stirring, evaporated acid was reverted in a flask by means of reflux condenser. Samples of hydrolysate (1 ml) was collected at regular time intervals. The hydrolysate was dried under vacuum for hydrochloric acid removal. For the further analyses dry hydrolysate was dissolved in distilled water.

The quantitative content of glucuronic acid was determined by Dishe's method. For this purpose 5 ml of 1 % sodium tetraborate solution in concentrated sulfuric acid was added carefully in a test tube with 1 ml of hydrolysate solution and mixed with water cooling. Further the mixture was heated on a water bath (90 °C) for 10 minutes, and then it was cooled in running water. 0,2 ml of carbazole solution (0,125 % w/v, absolute ethanol) were added in a test tube. The solution

was mixed and again heated up on a water bath (90 °C, 15 minutes), then it was cooled to room temperature. The standards for calibration and blank solution were prepared in the same way. Further absorption spectrums of solutions were recorded against a blank solution on 400-700 nm on spectrophotometer Shimadzu UV-3101PC. Relative absorption was calculated on three points; concentration of glucuronic acid was determined on a calibrating curve. Galactosamine and glucosamine can then be separated and quantified by reversed-phase chromatography with precolumn derivatization with fluorescence detection [7,8]. HPLC method for quantitative analysis of CS by the content of D-galactosamine in acid hydrolysates was used [9]. This method is applicable to qualitative analysis of other polysaccharides, such as CN and hyaluronic acid by the content of D-glucosamine.

5 ml of 1 % NaBH₄ solution in water were added to 4 ml of hydrolysate. D-Glucosamine and D-galactosamine in hydrolysate turned in glucosaminitol and galactosaminitol, accordingly. The mix was stood at room temperature not less than 3 hours. After that the reaction was stopped by adding of 1 ml of acetic acid (2 mole/l).

Reagent for modification of the reduced hydrolysate (OPA) was prepared as follows: 25 mg orthophthalic aldehyde were dissolved in 1 ml of methanol, then 5,6 ml of saturated solution of sodium tetraborate and 25 µl β-mercaptoethanol were added. 0,4 ml of OPA reagent were added to 0,2 ml of hydrolysate and were shaken up 1 minute. Further 1 ml of potassium phosphate solution of (2,72 g per 50 ml of water) were added to a mix. The prepared solution at once was seated in the chromatograph autosampler.

The HPLC apparatus was Shimadzu LC system, consisting of a degasser, a binary pump, an autosampler, a temperature regulated column compartment, a UV-VIS variable wavelength detector, and fluorescence flow cell. Chromatographic column C-12, size 4.6 × 250 mm was heated to 35 ° C. The composition of buffer A: 0.05 M NaH₂PO₄ in 30% ethanol. Buffer B consists of ethanol/water/tetrahydrofuran in the ratio of volume fractions 70:30:0,6. Flow rate was 0.8 ml/min.

RESULTS and DISCUSSION

CS preparation used in our research, contained impurities of protein, therefore amino acids were liberated during acid hydrolysis. As a result the peaks of amino acids overlapped on peak of D-galactosamine derivative at chromatographic fractionation of CS hydrolysate. Therefore such eluent gradient was selected, which have allowed to separate amino acid peaks and peak of OPA-derivatived galactosaminitol. On chromatograms of CN hydrolysate peaks of amino acids were not detected that testifies to absence of protein pollution of investigated CN. Chromatograms of hydrolysate CS and CN are resulted in figure 1.

During acid hydrolysis of CS glycosidic links of macromolecule are destroyed. N-acetylglactosamine is desulfated during hydrolysis, and remains in a solution, glucuronic acid, unstable in acidic medium, is destroyed. With increasing time of hydrolysis, N-acetylglucosamine is destroyed also under the influence of hydrochloric acid. Kinetics of D-galactosamine formation from CS and kinetics of glucuronic acid destruction was studied.

Hydrolysis of CN in acid medium is accompanied by formation of D-glucosamine, chitin monomer. The kinetics of D-glucosamine formation during hydrolysis was studied, and a specific reaction rate was defined.

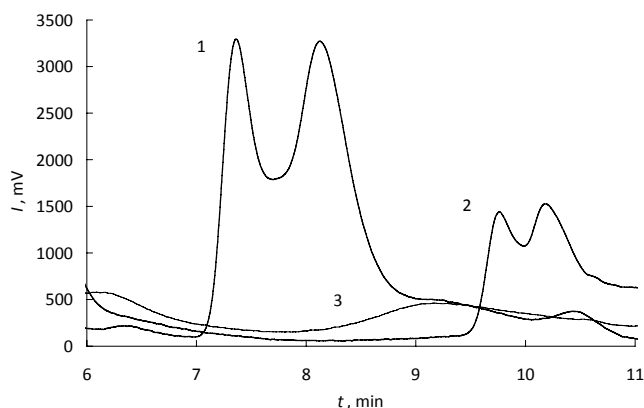


Figure1. Chromatograms of hydrolysates.

Hydrolysate of chitin (1), hydrolysates of chondroitin sulfate (2) and mixture of amino acids (3).

It is known that for reactions in solution (e.g. hydrolysis of organic compounds in the presence of strong mineral acids as catalysts), the true second-order reaction was reduced by a significant excess of a reagent whose concentration is virtually unchanged during the reaction. As a result, the reaction order of this is equal to the first order of the reactants. Under experimental conditions, the ratio of acid: chondroitin sulfate (chitin) was 100:1.

According to the kinetic law of mass action rate of the elementary step of the reaction is proportional to the concentration of the participating agents.

First order kinetic equation was used to calculate the rate constants for the chondroitin sulfate (chitin) hydrolysis with formation of galactosamine (glucosamine). Equation : $b(t) = A_0 \cdot (1 - e^{-k_1 t})$, where t - time; b - concentration of galactosamine (glucosamine), A_0 - initial concentration of chondroitin sulfate (chitin); k_1 - the reaction rate constant. Since the rise of the concentration of glucuronic acid was not fixed, only its decomposition was studied: $c(t) = C_0 \cdot e^{-k_2 t}$, where t - time, c - concentration of glucuronic acid, C_0 - initial concentration of glucuronic acid; k_2 - reaction rate constant. Knowing the initial concentration of glucuronic acid in sample, the initial concentration of CS in the sample can be calculated. For the mathematical analysis of these transformations and the calculation of reaction rate constants software Microsoft Excel and Maple 12 was used. Figures 2 and 3 show the kinetic curves of chondroitin sulfate hydrolysis, in Figure 4 - kinetic curve of chitin hydrolysis.

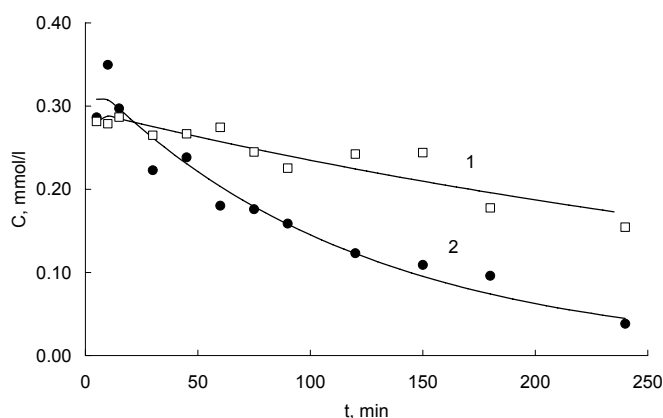


Fig. 2 - The concentration of glucuronic acid during acid hydrolysis of chondroitin sulfate. Solid line - model, markers - the experimental values. HCl concentration: 1. - 4 mol/l; 2. - 6 mol/l.

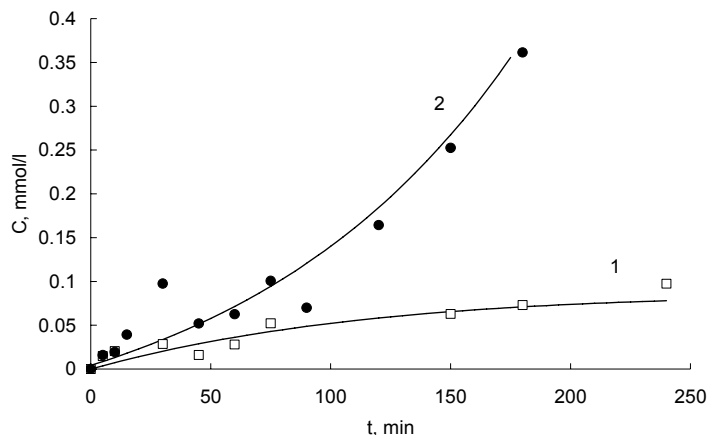


Fig. 3 – The concentration of galactosamine during acid hydrolysis of chondroitin sulfate. Solid line - model, markers - the experimental values. HCl concentration: 1. - 4 mol/l; 2. – 6 mol/l.

Figures 2 - 4 show that the calculated curves of galactosamine (glucosamine) formation almost coincide with experimental ones. Calculated rate constants for the corresponding reactions k_1 and calculated initial concentrations of chondroitin sulfate (chitin) are shown in Table 1.

Table 1. Rate constants of polysaccharide hydrolysis reactions (k_1). A_0 – initial concentration of polysaccharide sample

Polysaccharide	$k_1 \times 10^4, \text{c}^{-1}$		$A_0, \text{mmol/l}$	
	4 N HCl	6 N HCl	calculated	experimental
Chitin	7.5-8.1	-	10.9-11.2	12.0
Chondroitin sulfate	4.6-5.2	5.9-7.1	1.16-1.33	1.0

Thus, the mathematical model, presenting process of CS and CN hydrolysis, can be applied for calculation of concentration of CS and CN in an initial sample of substance.

Rate constants of glucuronic acid destruction in CS were calculated (Table 2).

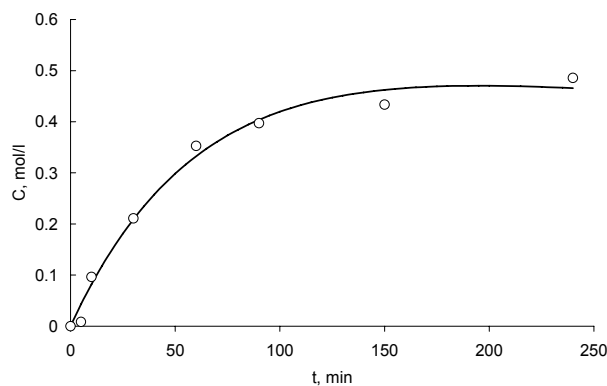


Fig. 4 - The concentration of glucosamine during acid hydrolysis of chitin. Solid line - model, markers - the experimental values. The concentration of HCl is 4 mol/l.

Table 2. Rate constants of glucuronic acid destruction reaction (k_2), C_0 – initial concentration of glucuronic acid

C_{HCl}	$k_2 \times 10^3, c^{-1}$	$C_0, \text{mmol/l}$	
		calculated	experimental
4 N	2.2-2.4	0.291-0.293	0.5
6 N	8.4-9.1	0.325-0.331	0.5

Calculated concentration of glucuronic acid in sample is slightly underrated. Therefore to calculate CS concentration in investigated preparations it is better to use the mathematical model, where data of D-galactosamine formation is applied.

ACKNOWLEDGEMENTS

The work was supported by the Federal Target Program «The scientific and scientific-pedagogical personnel of Innovative Russia», State Contract No. P744

REFERENCES

- [1] Jo, J.-H., Do, J.-R., et al. (2005) Optimization of shark (*Squatina oculata*) cartilage hydrolysis for the preparation of chondroitin sulfate. Food Sci. Biotechnol., 14 (5), 651-5.
- [2] Dische, Z. (1947) A new specific color reaction of hexuronic acids. J. Biol. Chem., 167(1), 189-98.
- [3] Liang, Z., Bonneville, C., et al. (2002) Development and validation of a photometric titration method for the quantitation of sodium chondroitin sulfate (bovine) in Cosequin DS chewable tablet. J. Pharm. Biomed. Anal., 28(2), 245-9.
- [4] Way, W. K., Gibson, K. G. and Breite, A. G. (2000) Determination of chondroitin sulfate in nutritional supplements by liquid chromatography. J. Liq. Chromatogr. Relat. Technol., 23(18), 2851-60.
- [5] Takai, M., Kono, H. (2003) Salmon-origin chondroitin sulfate. Pat. US 20030162744, Int. Cl. A61K 031/737, C08B 037/00.
- [6] No, H. K. and Meyers, S. P. (1997) Preparation of chitin and chitosan. In Chitin Handbook (R. R. A. Muzzarelli and M. G. Peter, ed.) pp. 475-89, Crottamare. Italy: Atec Edizioni, European Chitin Society.
- [7] Du, J. and Eddington, N. (2002) Determination of the chondroitin sulfate disaccharides in dog and horse plasma by HPLC using chondroitinase digestion, precolumn derivatization, and fluorescence detection. Anal. Biochem., 306(2), 252-8.
- [8] Plaas, A. H., Hascall, V. C. and Midura R. J. (1996) Ion exchange HPLC microanalysis of chondroitin sulfate: quantitative derivatization of chondroitin lyase digestion products with 2-aminopyridine. Glycobiology, 6(8), 823-9.
- [9] Studelska, D. R. (2006) Quantification of glycosaminoglycans by reversed-phase HPLC separation of fluorescent isoindole derivatives. Glycobiology, 16 (1), 65-72.

CHITOOOLIGOSACCHARIDES INHIBITS LIPOPOLYSACCHARIDES-INDUCED INOS AND COX-2 EXPRESSION IN BV2 MICROGLIA

Pangestuti Ratih¹, Soon-Sun Bak², Se-Kwon Kim^{1,2*}

¹Marine Biochemistry Laboratory, Department of Chemistry, Pukyong National University, South Korea

²Marine Bioprocess Research Center, Pukyong National University, Busan 608-737, South Korea

*E-mail address: sknkim@pknu.ac.kr

INTRODUCTION

Microglia are the resident immune cells in the central nervous system (CNS), they enter the system from the blood circulation early in an organism's development and serve a role of immune surveillance [1]. Ramified or resting microglia constitute 5-20% of glial populations in the CNS [2]. Recent study demonstrates that activation of microglia and the resulting production of pro-inflammatory and neurotoxic factors is sufficient to induce neurodegeneration in rat model [3]. Once chronically activated, microglia will release a variety of potentially neurotoxic compounds and pro-inflammatory mediators. The mediators include nitric oxide (NO), prostaglandin E₂ (PGE₂), pro-inflammatory cytokines such as tumor necrosis factor- α (TNF- α), interleukin-6 (IL-6), and interleukin-1 β (IL-1 β) and reactive oxygen species (ROS). Moreover, activation of microglia and excessive amounts of pro-inflammatory mediators released by microglia have been observed during the pathogenesis of Parkinson's disease (PD), Alzheimer's disease (AD), multiple sclerosis (MS), AIDS dementia complex, as well as post neuronal death in cerebral stroke and traumatic brain injury [3-4]. Thus, mechanism to regulate microglia activation may have important therapeutic potential for the treatment of neurodegenerative diseases. For this reason, a great interest has been developed by scientists for the screening and evaluation of the potential candidate neuroprotective agents which are able to attenuate microglial inflammatory responses.

Chitooligosaccharides (COS), depolymerized products of chitosan, has received considerable attention as bioactive material due to their biocompatible, biodegradable, non-toxic and non-allergenic natures. In the past few decades, COS have been of interest due to their potential applications in a broad range of fields including food; cosmetics; medicine; and agriculture. Furthermore, several studies have provided insight into neuroprotective effect of COS such as suppressing effect on β -amyloid formation [5-6]; acetylcholinesterase inhibitory activity [7-8]; antioxidant [6] and apoptosis inhibitors [9-10]. Furthermore, COS has been reported to modulate inflammatory responses in amyloid- β peptide (A β) peptides and IL-1 β -induced human astrocytes cells [11]. Astrocytes and microglia, two types of glial cells in the mammalian brain are involved in inflammation-mediated neurodegeneration [12]. Nevertheless, no study has been performed regarding modulation of inflammatory response by COS in microglia cells.

This study was undertaken to examine the pharmacological and biological effects of COS with four different molecular weight ranges (<1 kDa, 1-3 kDa, 3-5 kDa and 5-10 kDa) on the expression of inducible nitric oxide synthase (iNOS) and cyclooxygenase-2 (COX-2) and also the production of NO and PGE₂ in BV2 microglia stimulated with LPS.

MATERIALS and METHODS

Materials

COS were kindly donated by Kitto Life Co. (Seoul, Korea). Cell culture medium [Dulbecco's Modified Eagle's Medium (DMEM)], penicillin/streptomycin, Fetal Bovine Serum (FBS) and the other materials required for culturing cells were purchased from Gibco BRL, Life Technologies (Grand Island, US). LPS from *Escherichia coli* 026:B6, Griess reagent, 3-(4,5-dimethyl-thiazol-2-yl)-2,5-diphenyltetrazolium bromide (MTT) were purchased from Sigma (St. Louis, US). TRIzol[®] RNA extraction was provided by Invitrogen Ltd. (Paisley, UK). RT-PCR reagents were purchased from Promega (Madison, US). Specific antibodies used for western blot analysis were purchased from Santa Cruz Biotechnology Inc. (Santa Cruz, US) and Amersham Pharmacia Biosciences (Piscataway, US); other chemical and reagents used in this study were of analytical grade.

Assessment of cell viability

The murine BV2 microglia was a kind gift of Prof. Il Whan Choi (Inje University, Korea). Cell viability was determined by MTT reduction assay as described by Hansen *et al.* [13]. In brief, cells were seeded into 96-well plates and incubated for 24 h in the presence of different sample concentration, then 100 μ l of MTT (0.5 mg/ml final concentration) was added and incubated for another 4 h. The dimethylsulphoxide (DMSO) were then added and the absorbance was measured at 540 nm by using enzyme-linked immunosorbent assay (ELISA) microplate reader (Tecan Autria GmbH).

NO and PGE₂ production assay

The inhibitory effects of COS on the production of pro-inflammatory cytokines were determined by an ELISA. NO were determined according to the Griess reagent assay. The conditioned medium analyzed as per the manufacturer's instruction with Quantikine mouse PGE₂ Immunoassay (R&D Systems Inc, Minneapolis, USA)

Semiquantitative Reverse Transcription Polymerase Chain Reaction (RT-PCR)

Total RNA was extracted from BV2 cells treated with LPS in the presence or absence of COS using TRIzol[®] reagent, as reported in the manufacturer's manual. Equal amount of RNA (2 μ g) was used for each cDNA synthesis reaction. Single stranded cDNA was amplified by PCR with specific primers for iNOS, COX-2, glyceraldehyde 3-phosphate dehydrogenase (GAPDH).

Western blot analysis

Standard procedures were used for western blotting, where BV2 cells treated with COS followed by LPS treatment (1 μ g/ml) for 24 h were lysed in RIPA buffer. Western blots were visualized using a LAS3000[®] Luminescent image analyzer and protein expression was quantified by Multi gauge V3.0 software (Fujifilm Life Science, Tokyo, Japan).

RESULTS and DISCUSSION

Initially, to investigate the cytotoxic effect of COS, BV2 microglia were cultured with four different molecular weight ranges of COS from 10 to 500 μ g/ml concentrations. As presented in Figure 1, four different molecular weights COS exerted no significant ($p < 0.05$) toxic effect on BV2 microglia under tested concentrations after 24 hours treatment. According to those results, 500 μ g/ml concentration of COS was selected for further analysis in this study.

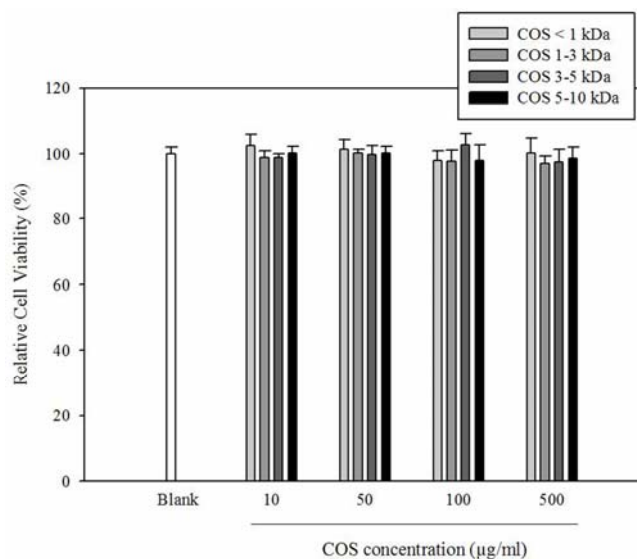


Figure 1. Effects of COS on the viability of BV2 microglia

Furthermore, we determined the effect of COS on NO and PGE₂ production in LPS-stimulated BV2 microglia. As shown in Figure 2, COS were shown to be able to inhibit NO and PGE₂ production. Stimulation with LPS markedly induced the production of NO and PGE₂ compared to non-stimulated one. The attenuation of NO and PGE₂ releases varied between COS <1 kDa, COS 1-3 kDa, COS 3-5 kDa and COS 5-10 kDa. COS <1 kDa appear to be the most effective in suppressing the NO and PGE₂ levels compared to COS 1-3 kDa, COS 3-5 kDa and COS 5-10 kDa. Among inflammatory mediators release by microglia, NO and PGE₂, the product of iNOS and COX-2 respectively, are the main cytotoxic mediators participating in the innate response in mammals [14-15]. NO derived from microglia has been implicated in the damage of myelin-producing oligodendrocytes in demyelinating disorders like multiple sclerosis and neuronal death during neuronal degenerating conditions [16]. Additionally, PGE₂ has been found to be elevated in the brain of early AD [12]. Thus, agents that inhibit the production of these inflammatory mediators have been previously considered as potential candidates for the treatment of neurodegenerative diseases. The results of this study demonstrated that COS inhibited NO and PGE₂ production. Notably, the inhibitory effects of COS on the LPS-induced productions of NO and PGE₂ in BV2 microglia were not due to the cytotoxicity of COS, as assessed by MTT assay.

In order to determine whether COS inhibitory effect on NO and PGE₂ level was associated with decreased of iNOS and COX-2 expressions in BV2 microglia, we studied the ability of four different molecular weights of COS at 500 µg/ml concentrations to affect the mRNA transcription and protein expression level of iNOS and COX-2. As shown in PCR and western blot result (Figure 3), LPS treatment significantly increased the expression of iNOS and COX-2. However, the expression was markedly attenuated in BV2 microglia pre treated with COS. A clear difference was observed between activities of four different molecular weight ranges of COS and COS with low molecular weight (<1 kDa) down regulate iNOS and COX-2 more effectively than other COS tested in this study.

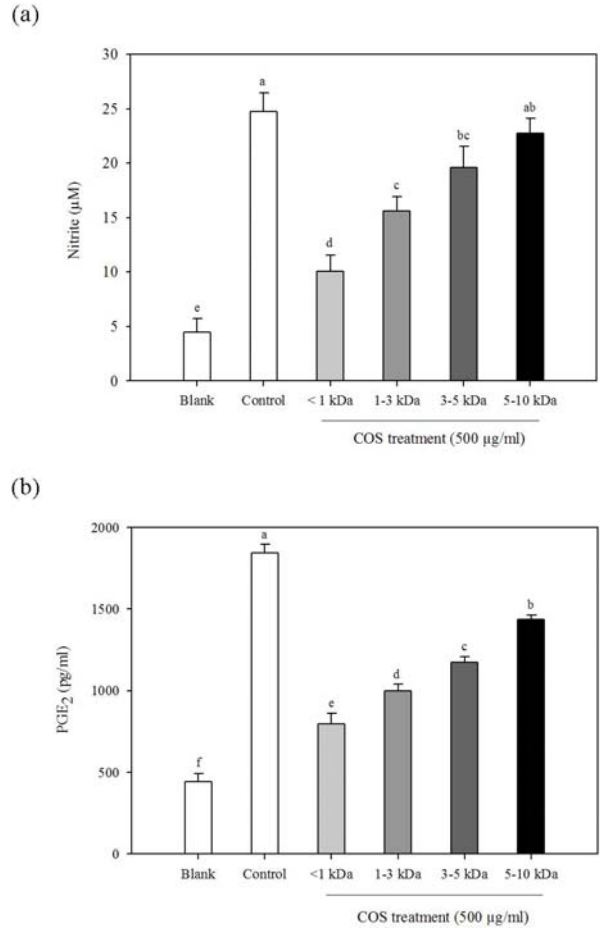


Figure 2. Effects of COS on LPS-induced NO (a) and PGE₂ (b) production in BV2 microglia. ^{a-f} Symbolize that the different letters in each sample are significantly different ($p < 0.05$) by Duncan's multiple range test

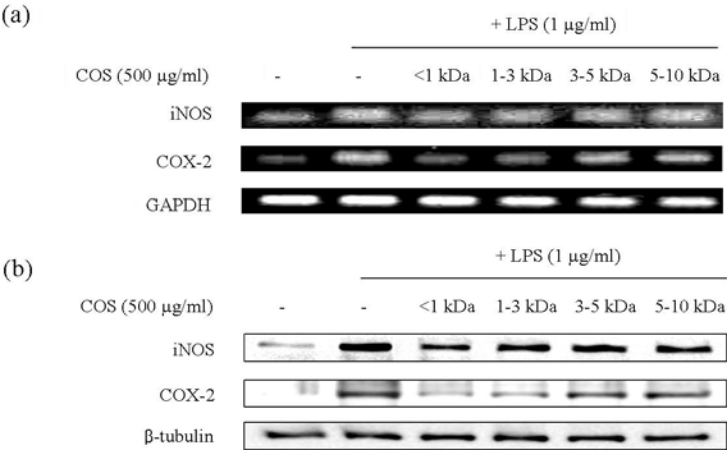


Figure 3. Effects of COS on LPS-induced iNOS and COX-2 gene (a) and protein (b) expression in BV2 microglia.

In all assays performed in this study, COS <1 kDa possess the highest inhibitory effects on pro-inflammatory generation, followed by COS 1-3 kDa, COS 3-5 kDa and COS 5-10 kDa,

respectively. Importantly, it remains unknown why <1 kDa was the most effective molecular weight for COS activity. However, we suggested that the different molecular weight ranges of COS might lead to variable absorption, which corresponds to the different inhibitory effects in BV2 microglial responses. In addition, several natural antioxidants have been shown to directly inhibit the expression of cytokines, iNOS and COX-2, and thus reduce inflammation. The suppressive effects of these antioxidant compounds on the production of the associated inflammatory mediators are strongly associated with their ability to scavenge ROS. In our previous study, we found that lower molecular weight COS possess stronger ROS scavenging activity compared to high molecular weight COS. The rationale for this is, low molecular weight of COS may incorporate into the cells more efficiently and donate proton effectively compared to higher molecular weight one. Thus, may correlate to the high anti-inflammatory activity of low molecular weight COS observed in this study.

Collectively, the findings in this study suggest that COS exhibit anti-inflammatory activity which is dependent on its ability to regulate the iNOS and COX-2 in LPS-stimulated BV2 microglia. COS may ultimately prove useful in the treatment of inflammatory diseases and beneficial characteristics for the treatment of neurodegenerative disease which accompanied with microglial activation. Furthermore, future studies are expected to confirm the anti-inflammatory effects of COS in a representative animal model.

ACKNOWLEDGEMENTS

This research was supported by a grant from Marine Bioprocess Research Center of the Marine Biotechnology Program funded by the Ministry of Land, Transport and Maritime, Republic of Korea.

REFERENCES

- [1] Allen, N. and Barres, B. (2009) Neuroscience: glia—more than just brain glue. *Nature*, 457, 675-677.
- [2] Kim, S. and de Vellis, J. (2005) Microglia in health and disease. *J. Neurosci. Res.*, 81, 302-313.
- [3] Liu, B. I. N., Gao, H.M., Wang, J.Y., Jeohn, G.-H., Cooper, C. L. and Hong, J.S. (2002) Role of Nitric Oxide in Inflammation-Mediated Neurodegeneration. *Ann. NY Acad. Sci.*, 962, 318-331.
- [4] Lull, M. E. and Block, M. L. (2010) Microglial Activation and Chronic Neurodegeneration. *Neurotherapeutics*, 7, 354-365.
- [5] Byun, H., Kim, Y., Park, P., Lin, X. and Kim, S. (2005) Chitooligosaccharides as a novel [beta]-secretase inhibitor. *Carbohydr. Polym.*, 61, 198-202.
- [6] Khodagholi, F., Eftekharzadeh, B., Maghsoudi, N. and Rezaei, P. (2010) Chitosan prevents oxidative stress-induced amyloid formation and cytotoxicity in NT2 neurons: involvement of transcription factors Nrf2 and NF- κ B. *Mol. Cell. Biochem.*, 337, 39-51.
- [7] Lee, S., Park, J., Kim, S., Ahn, C. and Je, J. (2009) Chitooligosaccharides suppress the level of protein expression and acetylcholinesterase activity induced by A [beta] 25-35 in PC12 cells. *Bioorg. Medicinal Chem. Lett.*, 19, 860-862.
- [8] Yoon, N., Ngo, D. and Kim, S. (2009) Acetylcholinesterase inhibitory activity of novel chitooligosaccharide derivatives. *Carbohydr. Polym.*, 78, 869-872.
- [9] Koo, H., Jeong, H., Hong, S., Choi, J., An, N. and Kim, H. (2002) High molecular weight water-soluble chitosan protects against apoptosis induced by serum starvation in human astrocytes* 1. *J. Nutr. Biochem.*, 13, (4), 245-249.
- [10] Zhou, S., Yang, Y., Gu, X., Ding, F., Chitooligosaccharides protect cultured hippocampal neurons against glutamate-induced neurotoxicity. *Neurosci. Lett.*, 444, 270-274.

- [11] Kim, M.S., Sung, M.J., Seo, S.B., Yoo, S.J., Lim, W.K. and Kim, H.M. (2002) Water-soluble chitosan inhibits the production of pro-inflammatory cytokine in human astrocytoma cells activated by amyloid [beta] peptide and interleukin-1[beta]. *Neurosci. Lett.*, 321, 105-109.
- [12] Blasko, I., Stampfer-Kountchev, M., Robatscher, P., Veerhuis, R., Eikelenboom, P. and Grubeck-Loebenstein, B. (2004) How chronic inflammation can affect the brain and support the development of Alzheimer's disease in old age: the role of microglia and astrocytes. *Aging Cell*, 3, 169-176.
- [13] Hansen, M., Nielsen, S. and Berg, K. (1989) Re-examination and further development of a precise and rapid dye method for measuring cell growth/cell kill. *J. Immunol. Methods*, 119, 203-210.
- [14] Vane, J. and Botting, R. (1995) New insights into the mode of action of anti-inflammatory drugs. *Inflamm. Res.*, 44, 1-10.
- [15] Boscá, L., Zeini, M., Través, P. and Hortelano, S. (2005) Nitric oxide and cell viability in inflammatory cells: a role for NO in macrophage function and fate. *Toxicol.*, 208, 249-258.
- [16] Pahan, K., Sheikh, F., Namboodiri, A. and Singh, I. (1997) Lovastatin and phenylacetate inhibit the induction of nitric oxide synthase and cytokines in rat primary astrocytes, microglia, and macrophages. *J. Clin. Invest.*, 100, 2671-2679.

NANOMATERIALS BASED ON CITOSAN BOMBYX MORI

S.Sh. Rashidova^{*}, R.Yu. Milusheva, S.M. Yugay

Institute of Polymer Chemistry and Physics, Academy of Sciences of Uzbekistan, Tashkent

^{}E-mail: carbon@uzsci.net, milur@rambler.ru*

INTRODUCTION

Features of the structure of polysaccharides, in particular chitosan (CHS), stipulate the possibility of wide application of this polymer in the food industry, medicine, agriculture and biotechnology. Receiving of nanoparticles (NP) and the creation of nanostructures based on CHS can significantly improve the efficiency of polymer materials in modern technology. The advisability of developing scientific research in the area of chitosan *Bombyx mori* in Uzbekistan is determined by the presence of raw source - waste of silk production, which annual amount is 10-15 thousand tons.

MATERIALS and METHODS

Calculation of parameters for prediction of the compatibility of polymer-polymer systems based on natural polysaccharides chitin and chitosan with synthetic polymers carried out by the method of Hildebrand and using Small and Hoy tables. Creating a model of atomic structure of biopolymer molecules was conducted with using of the program HyperChem.

For the formation of the NP on the basis of natural and synthetic polymers in the transition of process solution - solid phase was used cast film method for making samples from polymer aqueous solutions and their mixtures of different concentrations at different component ratio

For the study of the objects was used a complex physical and chemical methods: infrared spectroscopy, X-ray diffraction, sorption studies were carried out on a high vacuum apparatus with mercury seal and Mack Ben quartz balance. Optical and electron microscopy studies were performed on the SEM-200 (scanned) electron microscope, TEM-100 (Ukraine) and LEO 912 (Germany) (transmission). For the ultrasonic treatment was used an ultrasonic disperser UZDN-2M - 22 kHz

The degree of substitution at carboxymethylation and sulfation was determined by using conductometer EC 215 (NANNA Instruments, Germany).

RESULTS and DISCUSSION

Studies have performed as with the theoretical aspects of identifying the mechanisms of formation of nanoparticles and nanostructures in polymers, studying their characteristics and properties, so using them in medicine and agriculture

The calculation of solubility parameters of chitosan with synthetic polymers (PVA, PVP, PVCL, PEO) was conducted. Negative values of the energy density interaction and the Flory-Huggins parameter indicate strong interacting of heterogeneous macromolecular in mixtures of CHS-PVA and CHS-PEO (tab.1). Macromolecules of chitin and chitosan contain a numerous of atoms (tens of thousands). Therefore, to study their interactions were used fragments of molecules (clusters). Assembling the fragments of macromolecules was carried out in a software package Hyperchem.

This program allows to simulate the electronic and atomic structure of complex molecular and crystalline systems of various sizes up to the nanoscale. As models of chitin and chitosan macromolecules were used fragments, consisting of three glycosidic residues - combined by β -1,4-glucosidic bonds with three molecules of 2-amino-2-deoxy- β -D-glucopyranose. Using the program Chem 3D Ultra, and HyperChem were calculated optimum geometric parameters (bond lengths, valent and torsion angles) and the total energy of the molecules. Equilibrium geometry was performed by molecular dynamics method with minimizing the total energy relatively to the internuclear distances.

Table 1 Parameters of the interaction of systems of CHS- PEO, CHS- PVA

System	χ_{12}	Density of Interaction energy	Δg_x
CHS- PVA	-0,348	-3,2	$< 0 >$ 0
CHS- PEO	-0,13	-0,8	-

Hydrodynamic studies of chitosan were conducted. For samples of CHS with various molecular mass (MM) obtaining, chitosan was subjected to degradation at the presence of persulfate potassium (PP). MM CHS was adjusted by varying the concentration of the PP and the reaction time. The values of $[\eta]$ and M_η of chitosan samples are given in Table 2. Assuming that the length of the elementary unit of polymer $\lambda \approx 0,51$ nm, the contour length (L) and the number of segments (N) of chitosan in solutions were calculated by using expressions:

$$L \approx M_\eta \lambda / M_0 \approx P \lambda$$

$$N \approx L / \lambda$$

where $M_0 \approx 161$ molecular mass of elementary unit, P - degree of polymerization

Table 2. Molecular characteristics of chitosan samples

Sample №	$[\eta]$, dl/g	M_η	P	L, nm	N
CHS (1)	2,15	110000	683	345	17
CHS (2)	1,95	98000	608	310	15
CHS (3)	1,44	68000	422	210	11
CHS (4)	1,07	46000	298	150	8

The peculiarities of the transition of chitosan samples with different L (or N) in the anisotropic state at the deformative action in the shear flow were generated on the device "Reotest-2. Experiments were carried out for 3% solutions of chitosan prepared in a 2% solution CH_3COOH -water.

It was revealed that for chitosan samples $L \approx 400$ nm ($N \approx 20$) и $L \approx 665$ nm ($N \approx 35$) value of efficient viscosity $\ln \eta_{\text{eff}}$ intensively decreases with increasing of rate gradient γ up to 80 s^{-1} , then remains practically constant. This is due to the transition of macromolecules in the anisotropic state as a result of deformation-orientational ordering at the shear field. In the case of chitosan $L \approx 120$ nm, where $N < 13$, the macromolecules being thermodynamically prone to transition into the liquid crystalline (LC) state and is easily oriented without much deformation on the direction of flow. As a result, $\ln \eta_{\text{eff}}$ decreases more quickly at $\gamma < 80 \text{ s}^{-1}$. Further $\ln \eta_{\text{eff}}$ dynamically growing up to $\gamma < 140 \text{ s}^{-1}$, and then stabilized. Growth of $\ln \eta_{\text{eff}}$ is due to the

increased friction between the oriented chitosan molecules without deformation. Stabilization $\ln\eta_{\text{eff}}$ in area $\gamma > 140 \text{ s}^{-1}$, as in the case of other samples of chitosan, associated with the deformation of the orientational ordering of chains in the flow. When the forward and reverse measurement of viscosity occurs the hysteresis effects observed, which clearly defined at small γ for samples $N < 13$, i.e. for nanostructured chitosan. The presence of hysteresis indicates the presence of chitosan molecules in the anisotropic state, as well as the feature of the anisotropic properties of molecules, due to the difference between chains with different nanostructures.

Grafted of vinylcaprolactam copolymers on CHS by reaction of radical initiation were synthesized. Depending of synthesis conditions can be obtained as branched polymers so copolymers of three-dimensional structure.

Thus, at high concentrations of PP in system the obtained samples have three-dimensional structure caused by high concentration of active centers in the chains of macromolecules and their subsequent recombination.

Polymer blends of chitosan with N-vinylcaprolactam (VCL) having nanostructured morphology were obtained. During the formation of nanoparticles and nanostructures at the two-component systems based on the thermodynamically incompatible polymers CHS and PVCL stabilization problem was solved by formation of nanostructured compositions based on PVCL with low MM, as well as the using of grafted copolymers as stabilizers of nanostructures in polymer blends.

For the first time the chemical modification of synthesized water-soluble chitosan derivatives *Bombyx mori*: sulfate-SCHS, ascorbate-ACHS, and carboxymethylchitosan-CMCHS. **Sulfation of chitosan samples** of *Bombyx mori* was carried out in chlorosulfonic acid at varying reaction conditions; temperature and reaction time contribute to the regulation of sulfur content, the degree of substitution, and solubility product (Table 3).

Table 3. Parameters of the sulfation reaction of chitosan *Bombyx mori*

Samples	The reaction conditions		N, %	S, %	γ_s	O _s	N _s	O _s /N _s	P, %
	T, °C	t, min							
CHS	120	120	7,36	-	-	-	-	-	95*
SCHS-1	50	60	4,39	9,76	0,68	7,16	6,26	1,14	80
SCHS-2	60	45	4,08	9,55	0,66	7,21	6,31	1,14	75
SCHS-3	80	60	4,30	11,91	0,90	6,63	5,80	1,14	95

* - in 2% aqueous solution of CH₃COOH

As can be seen from the table, raising the temperature to 80°C (sample SCHS-3) helps to increase the sulfur content and degree of substitution of sulfogroup at chitosan, as well as its solubility (P). Reducing the time sulfation (45 min) for sample SCHS-2, despite the fact that the temperature is much higher (60°C) than in the synthesis of SCHS-1 (50°C), leads to a decrease in the values of parameters S, γ_s and P

Quantitative characteristics and substitution of sulfogroups at chitosan was evaluated by conductometric titration assay. It was shown that the substitution of sulfogroups occurs by both by NH₂-groups, and by the OH-groups of chitosan molecules.

Degree of substitution of sulfogroups (γ_s) calculated by the formula:

$$\gamma_S \approx 168,4\omega_S / (3200 - 81\omega_S)$$

The distribution of sulfogroups between the carboxyl and amino groups were assessed by the ratio upon O_S and N_S substitution, calculated using the following formulas:

$$O_S \approx 100m_S / (168,4 + 81\gamma_S) \quad \text{и} \quad N_S \approx 100m_N / (168,4 + 81\gamma_S)$$

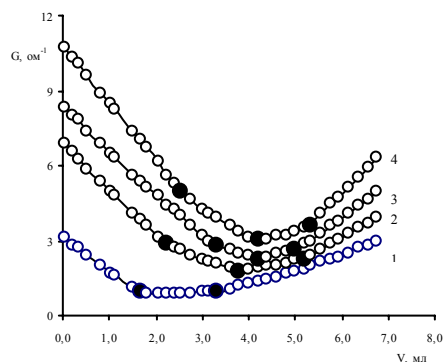


Fig. 1. Curves of conductometric titration of sample solutions: 1-CHS, 2 - SCHS-1, 3 - SCHS-2, 4 -SCHS-3

Assessment of distribution of sulfogroups by the hydroxyl and amino groups was showed that the content of SO_3H -groups for all samples of CHS obtained by varying the reaction conditions is to 1.14 times greater for OH-groups. This confirms the assumption that the sulfation of chitosan molecules is carried out not only by the NH_2 -groups, but also by OH-groups at C-3 and C-6.

Carboxymethylation reaction carried out by reaction of O-alkylation of alcoholate groups, leading to the adduct formation, preferably substituted by hydroxyl group at C-6 (CH_2OH) elementary link of the chain.

It was revealed that depending on temperature and reaction time can be obtained samples carboxymethylchitosan with varying degrees of substitution (DS) of carboxymethyl groups and the solubility in water. Reducing the reaction time of carboxymethylation reduces DS in the synthesized samples.

Assessment of the degree of substitution CMCHS carried out using nuclear magnetic resonance (NMR) spectroscopy and conductometric titration

A linear reduction of T_1 relaxation time with increasing content CH_2COONa at CMCHS groups was found. γ dependence of T_1 can be described by the following expression $\gamma = a \times T_1$, where the function slope $a = 70$. On the basis of this expression was defined degree of substitution of the samples CMCHS by the multiplication $a \times T_1$, using the value of T_1 , as measured by impulse NMR spectroscopy.

Fig. Figure 2 shows a comparative graph of curves of conductometric titration of the samples CHS (a) and CMCHS (b)

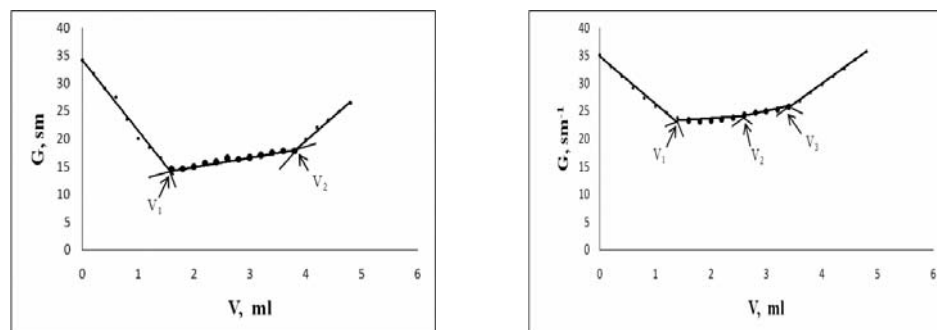
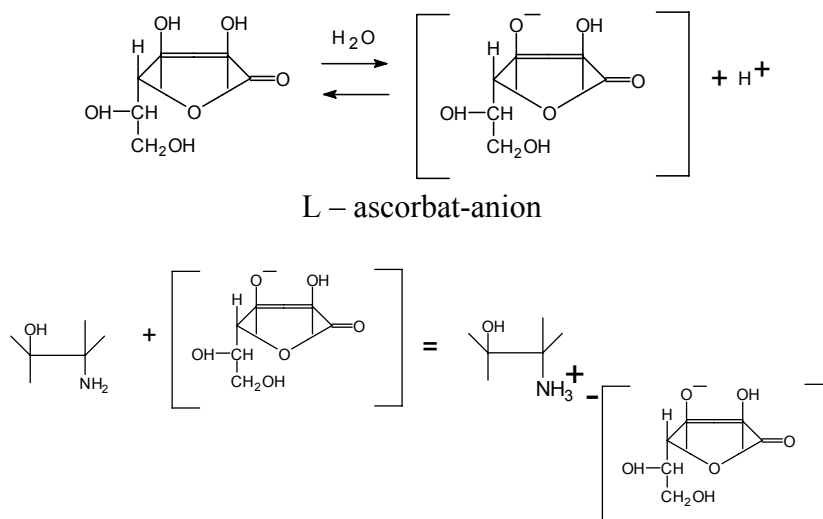


Figure 2 . Curves of conductometric titration of the samples CHS (a) and CMCHS (b)

Depending on the reaction conditions the degree of substitution CMCH was 0,56-0,88

Synthesis of chitosan ascorbate was performed by methods of direct and reverse potentiometric titration with alkali solutions of chitosan with the addition of ascorbic acid and yield of up to 53%.



The structure of synthesized ascorbate CHS was proved by IR- and NMR- spectroscopy (Fig. 3)

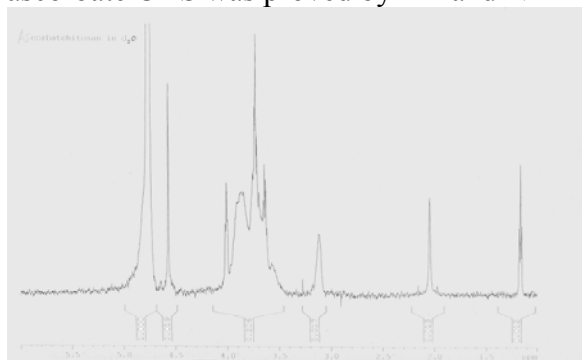


Figure 3. NMR spectrum ACHS

Receiving of nanostructure forms of chitosan ascorbate was carried out with help of the choice of precipitants, the initial concentration of polymer solution and ultrasonic dispersion. Electron microscopic studies have shown (see Figure 4) that for all samples, regardless to the concentration of the solution of ascorbate chitosan, the formation of nanostructures with particle sizes from 4 to 20 nm is observed. It could be seen that a more homogeneous structure by the

distribution and size is generated from a solution with $C \approx 0,1\%$ of ACHS. It was revealed that lower concentrations of initial solution ACHS ($C < 0,5\%$), lead to the formation of smaller-sized nanoparticles, what apparently associated with a decrease of viscosity solution and, consequently, easier the formation of nanostructures.



Figure 4. TEM images of nanostructured ACHS

The method of chemical precipitation of metals from salts solutions under the action of a reducing agent, is one of the priority directions of nanosized particles receiving. Such reactions are redox interaction with the formation of a zero-valent metal. By this method from solution of chitosan *Bombyx mori* were synthesized nanosized metal particles of cobalt. At the selected conditions CHS acts simultaneously as a reductant metal and as nanostabilized matrix formed metal NPs. Varying the synthesis conditions were derived metal complexes of CHS *Bombyx mori*, with cobalt content 2-7%. Electron microscopic studies revealed nanoparticles of different sizes from 50 to 500 nm (Fig. 5).

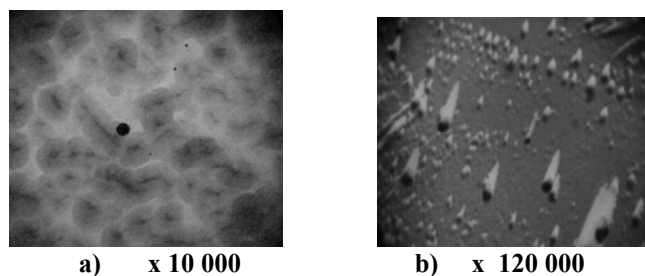


Figure 5. Electron micrographs of the polymer metal complexes on the base of CHS and Co

For a sample polymer metal complexes CHS-Co - Fig.5 a typical nanoparticle (NP) inherent the spherical shape of 17 to 40 nm. Micrograph of a higher resolution allows to see that for the most particles even with seemingly spherical form was observes morphology the core - shell consisting of a metal-core, which has nanorod form with a width of 8 nm and a length of $16 \div 40$ nm.

Researches on the development and application of the method electrospinning for polymer nanofibers are developed. The principal features of this method to obtain chitosan-based nanofibers were identified.

Synthesized chitosan *Bombyx mori* derivatives (so called preparation - UZHITAN) are used as protectants with stimulating effect in agriculture. Synthesized polymetallo complexes and water-soluble chitosan derivatives *Bombyx mori* find applications as an alternative to imported medical preparations with antibacterial, reparative and anticoagulant properties.

BILAYER ALGINATE/CHITOSAN-SPOTTED FILM FORMATION BY PHASE SEPARATION PROCESS OF CHITOSAN-CITRATE EMULSION FROM ALGINATE/CHITOSAN SUSPENSION

Anyarat Watthanaphanit¹, Hiroshi Tamura², and Ratana Rujiravanit^{1, 3*}

¹*The Petroleum and Petrochemical College, Chulalongkorn University, Bangkok, Thailand*

²*Faculty of Chemistry, Materials and Bioengineering, Kansai University, Osaka 564-8680, Japan*

³*Center for Petroleum, Petrochemicals, and Advanced Materials, Chulalongkorn University, Bangkok 10330, Thailand*

**E-mail address: Ratana.r@chula.ac.th*

INTRODUCTION

Bioactive dressings for enhancing wound healing have been continuously developed for years. Constituents and design of a dressing depends on type, severity, and position of the wound. Generally, the aims of wound care treatment are focused on promoting recovery, preventing further harm caused by the spread of infection, and avoiding scar formation. Therefore, an ideal wound dressing should maintain a moist environment at the wound-dressing interface, prevent secondary infections, and be biocompatible and non-allergenic [1].

Alginate, an anionic biopolymer, is extensively used in wound healing application and well known in literature as well as in a commercial point of view. Algisite[®] (Smith & Nephew, Inc.), Kaltostat[®] (Convac Tec), SeaSorb[®] (Coloplast Sween Corp.), and Tegagen[™] (3M Health Care) are examples of alginate-based wound dressings commercially available nowadays [2]. Alginate offers many advantages over traditional cotton and gauze dressings because of its gel forming ability that makes alginate be able to provide a moist environment to a wound, leading granulation and reepithelialization of tissues. The gel type dressing can absorb excess wound exudate, relieve pain, and help in removing the dressing without much trauma. In addition, alginate based dressings have been demonstrated to prevent bleeding of wound blood, activate macrophages within the chronic wound bed, and generate a pro-inflammatory signal. All of these properties lead the alginate dressings to initiate a resolving of wound inflammation [3]. Normally, no single dressing is appropriate for all wound types and all stages of wound healing since the process of the healing is a set of coordinated responses to tissue injury. Like alginate, the lack of antimicrobial activity is its weakness.

Chitosan is a natural antimicrobial agent known to be effective against a wide range of microorganisms [4]. Combination of alginate and chitosan can compliment each other in the properties of the final products. However, because of the opposite charges between alginate and chitosan, a direct mixing of the two polymers would readily coagulate or form gels. The gel formation leads to unfeasibility in the preparation of a miscible doped solution which is a major problem of the fabrication of alginate/chitosan hybridized materials. Previously, chitosan in the form of an emulsion has been reported as a means to incorporate a high content of chitosan into an alginate aqueous solution [5]. The key of the method is the complexation of chitosan with citric acid to form chitosan-citrate complex (CcC) which exhibits non-polar character. The CcC can readily penetrate into the core of the SDS/olive oil (primary o/w emulsion) micelles. Consequently, when the chitosan-citrate emulsion (CcE) is mixed with the alginate aqueous solution, under the optimal condition, *stable* alginate/chitosan suspensions are obtained.

Schematic drawing represents the concept of the proposed method is shown in Figure 1. The obtained suspension was used as a dope suspension for wet spinning. By this means, the wet-spun hybridized fibers exhibited spotty features both inside and on the fiber surface. These spots are attributed to the presence of the emulsified chitosan–citrate complex particles [5].

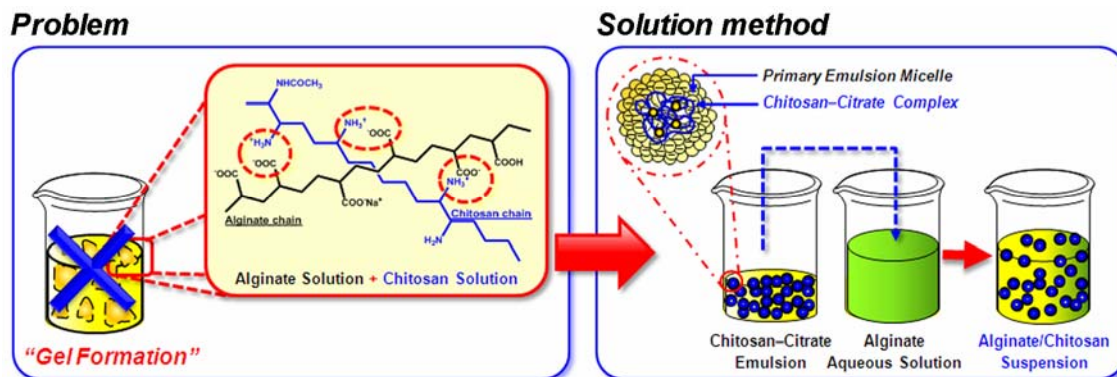


Figure 1 Schematic drawing represents concept of proposed method to solve problems associated with the formation of gels due to ionic complexation between alginate and chitosan reported by Watthanaphanit et al. [5].

In the present study, *unstable* alginate/chitosan suspensions were prepared in order to fabricate bilayer alginate/chitosan-spotted films. The concept of the bilayer film formation is to find the optimal condition, in which, the oily phase containing chitosan was allowed to be separated from the alginate aqueous phase. Figure 2 shows schematic drawing represents the concept of the bilayer alginate/chitosan-spotted film formation and design functions of the bilayer film. Normally, phase separation can occur when the inclusion of the CcC into the SDS/olive oil micelles is complete and viscosity of the alginate solution is suitable. However, the CcC inclusion is highly dependent on composition of the pure components. In this study, the effect of concentration of the olive oil used for preparing the CcE was investigated. Stability of the alginate/chitosan suspensions prepared by using different ratios of chitosan in the chitosan solution to the volume of the primary emulsion was observed by adding Amido Black 10B aqueous solution into the alginate/chitosan suspensions before leaving them standing at room temperature for 3 days.

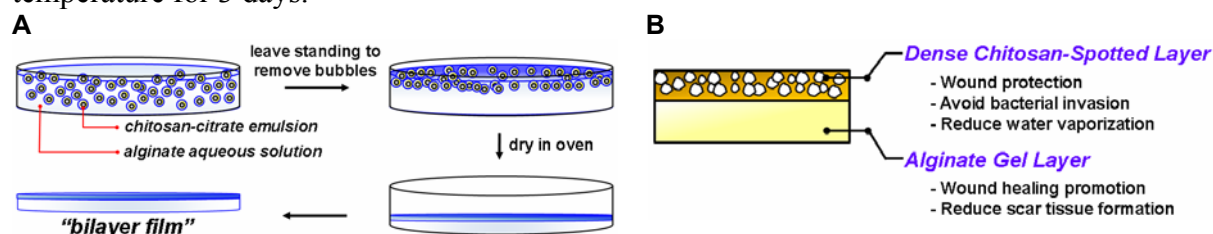


Figure 2 Schematic drawing represents (A) concept of bilayer alginate/chitosan-spotted film formation and (B) designed functions of the bilayer film.

MATERIALS and METHODS

Materials:

Chitosan flakes from crab shells ($M_w = 40000$ Da) was kindly provided by Fujibo Co., Ltd. (Japan). Sodium alginate, olive oil, sodium dodecylsulfate (SDS; 95.0% purity), anhydrous citric

acid (98.0% purity), calcium chloride dihydrate ($\text{CaCl}_2 \cdot 2\text{H}_2\text{O}$), Amido Black 10B, sodium hydroxide pellet (NaOH ; 96.0% purity), acetic acid (99.9% purity), and methanol (MeOH ; 99.7% purity) were purchased from Wako Pure Chemical Industries Co., Ltd. (Osaka, Japan).

Methods:

Preparation of Chitosan Gel and Chitosan–Citrate Emulsion

Chitosan gel and chitosan emulsion were prepared by the method described by Watthanaphanit et al. [5]. To prepare the chitosan gel, chitosan flakes (10 g) were first suspended in 1000 mL of distilled water under vigorous stirring (13200 rpm for 20 s). Subsequently, 20 mL of acetic acid was added into the chitosan aqueous suspension under vigorous stirring (13200 rpm for 60 s) to obtain a chitosan aqueous solution. NaOH 10% aqueous solution was then added under vigorous stirring (13200 rpm for 1 min) to adjust the pH of the chitosan aqueous solution to 10–12. When the pH of the solution reached 10–12, a clear chitosan gel was formed. The gel was further dialyzed in distilled water at room temperature to remove the residual NaOH until the neutral pH was obtained. After that, the chitosan gel was separated from the aqueous medium by centrifugation at 10000 rpm. The obtained chitosan gel was kept in a refrigerator prior to further use.

For chitosan emulsion, two kinds of solutions were separately prepared: (1) *chitosan solution* was prepared by adding citric acid powder into the chitosan gel (the weight ratio of the chitosan gel in its dry state to citric acid was 1:1) under vigorous stirring until the chitosan gel dissolved completely; (2) *o/w emulsion*, referred to as the “*primary emulsion*”, was prepared by homogenizing olive oil and 1 %w/v SDS aqueous solution under vigorous stirring (10600 rpm for 2 min). The volume ratio of the olive oil to the SDS solution was 6:4. The primary emulsion was then added dropwise into the chitosan solution under vigorous stirring to obtain the suspension which is hereafter referred to as “chitosan–citrate emulsion” (CcE).

In order to investigate effect of the primary emulsion content on the size of chitosan particles in the chitosan–citrate emulsion, ratios of chitosan in the chitosan solution to the volume of the primary emulsion were varied to be (a) 1 g/5 mL, (b) 1 g/10 mL, (c) 1 g/20 mL, and (d) 1 g/40 mL.

Preparation of Alginate/Chitosan Suspension and Bilayer Alginate/Chitosan-Spotted Film

The suspension for preparing the alginate/chitosan-spotted films were prepared by adding the chitosan–citrate emulsion dropwise into the 2 %w/v alginate aqueous solution under vigorous stirring (13200 rpm for 20 min). The volumetric ratio of the chitosan–citrate emulsion to the alginate solution was fixed to obtain the suspensions with the weight ratio of chitosan to alginate as 10 %w/w. Prior to film formation, the alginate/chitosan suspensions (with different conditions of chitosan–citrate emulsions) were characterized for the appearance and the size of emulsified chitosan particles using an Olympus BX50 optical microscope. The diameters of individual emulsified chitosan–citrate complex particles were determined from representative microscopic images, from which ca. 50 particles were measured for their width and length using SemAfore 4.0 image-analytical software. Stability of the suspensions was observed by adding Amido Black 10B aqueous solution into the suspensions before leaving them standing at room temperature for 3 days. Phase separation phenomenon was then visually observed. Alginate/chitosan-spotted films were produced by a solvent casting technique. The suspensions (40 mL) were poured on a plastic Petri dish of 20 cm×15 cm and left to stand until the trapped air bubbles were removed before drying in an oven at 50 °C. Subsequently, the dried films were immersed into a 5 %w/v CaCl_2 aqueous solution to permit cross-linking for 24 h. Next, they were washed with methanol and finally dried at room temperature.

Characterization of Films

In order to confirm the formation of bilayer films, staining of the films was achieved by immersing the dried films in 0.01 %w/v Amido Black 10B aqueous solution for 8 h and repeatedly rinsed with distilled water to remove the excess dye on the film surface. The stained films were then observed for their top and bottom surface morphology under an Olympus BX50 optical microscope.

RESULTS and DISCUSSION

Stability of the Alginate/Chitosan Suspension with Different Conditions of Chitosan–Citrate Emulsions

Stability of the alginate/chitosan suspension was determined by investigating the location of chitosan after the suspension was stained with Amido Black 10B dye and left standing at room temperature for 3 days. The cationic, protonated amino groups of chitosan can form a complex with the anionic sulfate group of the anionic dye. Therefore, blue area represents a location of chitosan. Figure 3A shows representative photographic images of 10 %w/w alginate/chitosan suspension with different ratios of chitosan in the chitosan solution to the volume of the primary emulsion.

Evidently, phase separation of the CcE from the alginate/chitosan suspension was complete at a condition of 1 g of chitosan/40 mL of primary emulsion. The result revealed complete inclusion of the CcC in the primary emulsion at this condition. Possible fundamental character of the constituents presented in each corresponding parts are shown in Figure 3B.

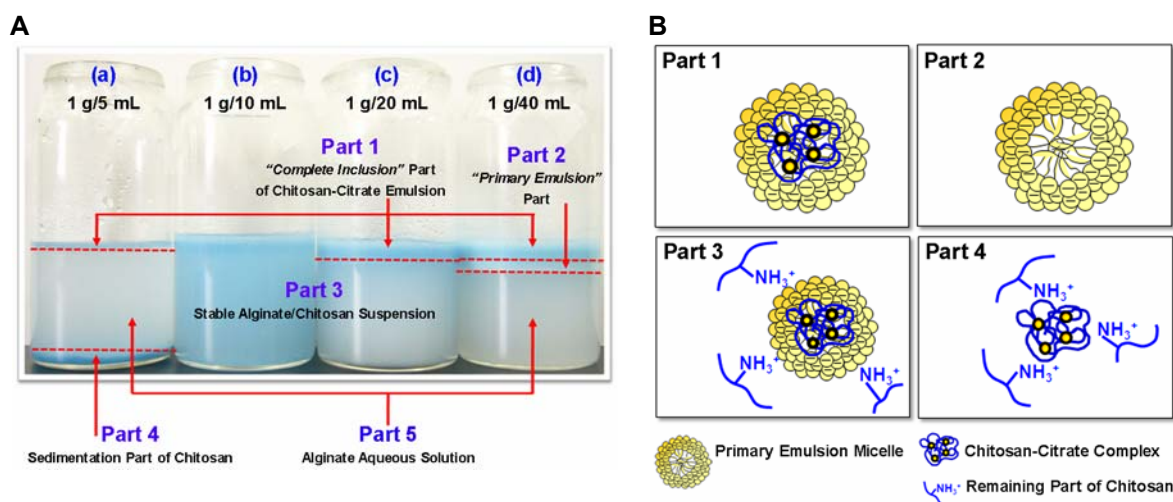


Figure 3 (A) Photographic images of 10 %w/w alginate/chitosan suspension with the ratio of chitosan in the chitosan solution to the volume of the primary emulsion of (a) 1 g/5 mL, (b) 1 g/10 mL, (c) 1 g/20 mL, and (d) 1 g/40 mL. The images were taken after mixing the suspension with Amido Black 10B dye solution and left standing for 3 days. (B) Schematic drawing of possible fundamental character of the constituents presented in the corresponding part of the alginate/chitosan suspension.

Surface Morphology of the Films

Similar to the result shown in Figure 3A, staining of the alginate/chitosan-spotted films with Amido Black 10B is a potent tool for examining the appearance of the emulsified chitosan–citrate particles within the obtained films. Photographic images in Figure 4 confirm the formation of the bilayer films when the ratio of chitosan in the chitosan solution to the volume of the

primary emulsion of 1 g/20 mL was applied. Figure 5 shows representative microscopic images of 10 %w/w alginate/chitosan-spotted films with different ratios of chitosan in the chitosan solution to the volume of the primary emulsion. Spotty features are attributed to the presence of emulsified chitosan–citrate particles. It is obvious that the phase separation to form the bilayer film could be achieved at a condition of 1 g of chitosan/40 mL of primary emulsion. The result might be explained by the complete inclusion of the CcC in the primary emulsion as described above.

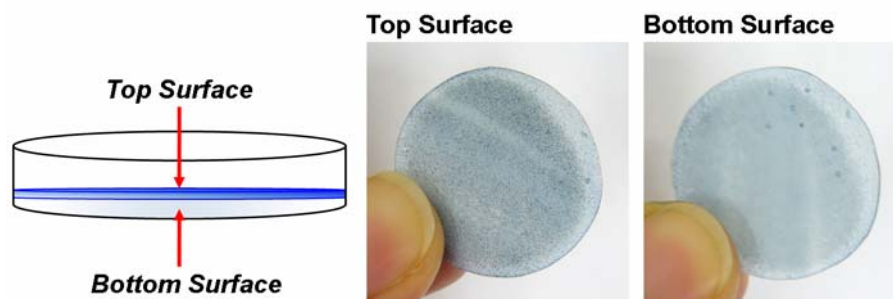
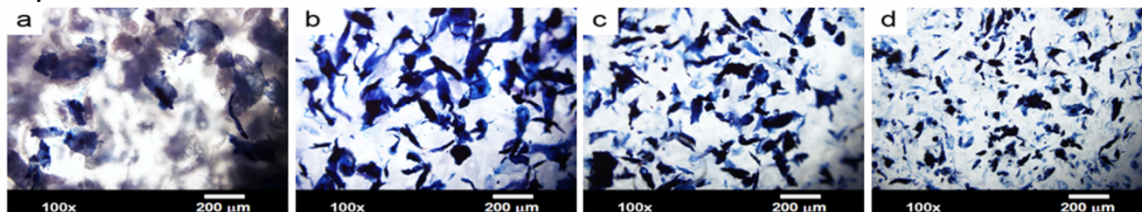


Figure 4. Photographic images of 10 %w/w alginate/chitosan-spotted films (dry state) with the ratio of chitosan in the chitosan solution to the volume of the primary emulsion of 1 g/20 mL showing the top and the bottom part of film after the film was stained with 0.01 %w/v Amido Black 10B aqueous solution.

Top Surface



Bottom Surface

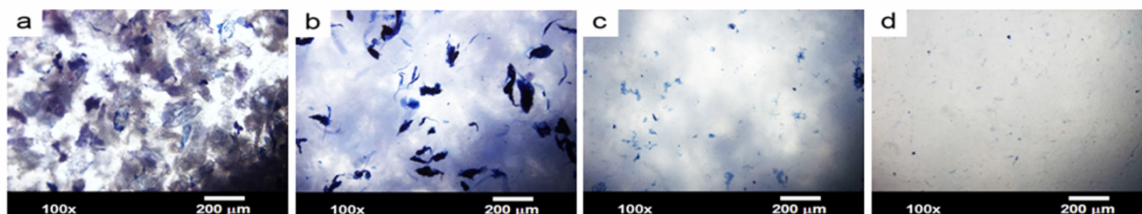


Figure 5. Microscopic images of 10 %w/w alginate/chitosan-spotted films with the ratio of chitosan in the chitosan solution to the volume of the primary emulsion of (a) 1 g/5 mL, (b) 1 g/10 mL, (c) 1 g/20 mL, and (d) 1 g/40 mL, after they was stained with 0.01 %w/v Amido Black 10B aqueous solution.

Size of Emulsified Chitosan–Citrate Particles Distributed in the Films

Average widths and lengths of the emulsified chitosan particles of each condition are shown in Figure 6. As shown in Figure 6, the increasing amount of the primary emulsion caused the decreasing of dimensions of the spots. The width of spots was decreased from ca. 60 μm for the condition of 1 g/5 mL to ca. 20 μm for the condition of 1 g/40 mL. The length of spots was decreased from ca. 140 μm for the condition of 1 g/5 mL to ca. 60 μm for the condition of 1 g/40 mL. In addition, apart from the occurrence of the smaller spot size, spot shape became rounder and tend to exist mostly on the top layer of the films. The decreasing of the spot size might be due to the increase in the number of the o/w micelles when the primary emulsion content was

increased. Therefore the higher amount of CcC could be incorporated into the micelles. The oily phase containing complete inclusion of the CcC could separate from the alginate aqueous phase during film forming process. Finally, the alginate/chitosan-spotted films having bilayer structure could be fabricated.

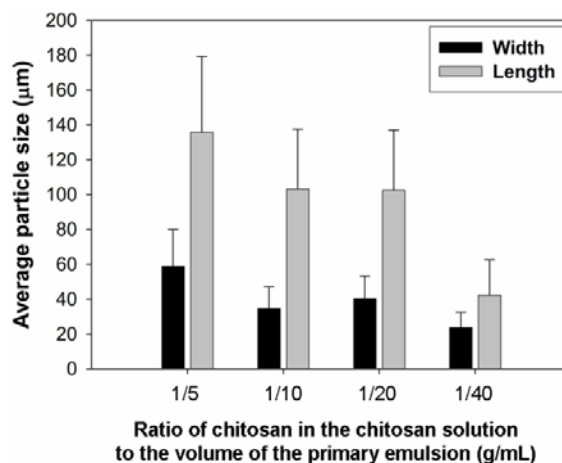


Figure 6. Average particle sizes of chitosan–citrate emulsion particles in 10 %w/w chitosan–spotted alginate films with the ratio of chitosan in the chitosan solution to the volume of the primary emulsion of 1 g/5 mL, 1 g/10 mL, 1 g/20 mL, and 1 g/40 mL.

ACKNOWLEDGEMENTS

The first author would like to acknowledge the Ratchadapisek Somphot Endowment Fund, Chulalongkorn University, for granting her post-doctoral fellowship. Financial supports from the Development and Promotion of Science and Technology Talents Project (DPST, Thailand) and Japan Society for the Promotion of Science (JSPS) are gratefully acknowledged.

REFERENCES

- [1] Lloyd, L.L., Kennedy, J.F., Methacanon, P., Paterson, M., and Knill, C.J. (1998) Carbohydrate polymers as wound management aids. *Carbohydrate Polymers*, 37(3), 315–322.
- [2] Paul, W., and Sharma, C. (2004) Chitosan and alginate wound dressings: A short review. *Trends in Biomaterials & Artificial Organs*, 18(1), 18–23.
- [3] Thomas, A., Harding, K.G., and Moore, K. (2000) Alginates from wound dressings activate human macrophages to secrete tumour necrosis factor- α . *Biomaterials*, 21(17), 1797–1802.
- [4] Chung, Y.C., Su, Y.P., Chen, C.C., Jia, G., Wang, H.L., Wu, J. C.G., and Lin, J.G. (2004) Relationship between antibacterial activity of chitosan and surface characteristics of cell wall. *Acta Pharmacologica Sinica*, 25(7), 932–936.
- [5] Watthanaphanit, A., Supaphol, P., Furuike, T., Tokura, S., Tamura, H., and Rujiravanit, R. (2009) Novel chitosan–spotted alginate fibers from wet-spinning of alginate solutions containing emulsified chitosan–citrate complex and their characterization. *Biomacromolecules*, 10, 320–327.

PREPARATION OF β -CHITIN POROUS STRUCTURE COMBINING SOLVENT EXCHANGE INDUCED PHASE SEPARATION AND SUPERCRITICAL DRYING PROCESS

P. Ratanajaiaroen^{1*}, M. Ohshima¹

¹*Chemical Engineering Department, Kyoto University, Katsura Campus, Nishikyo-ku, Kyoto, Japan*

**E-mail address: fai@cheme.kyoto-u.ac.jp; oshima@cheme.kyoto-u.ac.jp*

INTRODUCTION

Recently, much attention has been paid to preparation of highly porous biomaterials due to their potential applications not only in biotechnological fields such as tissue engineering and drug delivery systems but also in cleaning technologies such as dyes and heavy metal ions removals. Chitin is an aminopolysaccharide derived from various fungi, the shells of insects and crustacean shell waste. It is composed of $\beta(1\rightarrow4)$ linked 2-acetamido-2-deoxy- β -D-glucose units (or *N*-acetylglucosamine) forming a long and linear polymer chain. Because of the presence of the acetamide group, which is similar to the amide linkage of protein in living tissues, chitin is biocompatible and safe for human applications [1]. According to many studies, chitin was found to enhance and accelerate wound healing [2]. It also promoted cell attachment and the spreading of both normal human keratinocytes and fibroblasts [3]. Moreover, chitin can be degraded by lysozyme and it can subsequently generate harmless products when presented in human body [4]. However, limited utilization of chitin has been reported due to the formation of strong inter- and intra-molecular hydrogen bonds in chitin, which are difficult to be broken.

Several processing techniques such as water-soluble [5], water-insoluble particles leaching [6], and lyophilization [7-8] have been performed and developed to obtain porous chitin matrices. Nevertheless, there is also some limitations even in the porous chitin. These limitations come from the fact that the proposed preparation schemes were mostly time-consuming and provided the porous chitin with low interconnectivity and entrapment of organic solvents inside the polymeric network.

Supercritical fluid technology is an alternative environmentally friendly technique that overcomes these limitations. However, there is a limited compatibility of supercritical carbon dioxide (sc-CO₂) with water at the ordinary temperature and pressure used in sc-CO₂ processing. Therefore, a water/organic solvent substitution step was added to the process [9-11].

In this study, sc-CO₂ drying technique was employed to increase the interconnectivity and porosity of porous chitin material. By combining solvent-exchange induced phase separation and sc-CO₂ drying processes, the highly porous structured β -chitin was successfully prepared. Morphology observations and nitrogen adsorption measurement were performed to evaluate the cell morphology and surface area of the obtained porous chitin. The change in crystalline structures of β -chitin after the fabrication and sc-CO₂ drying process was also detected by the X-ray diffraction method.

MATERIALS and METHODS

Materials

Formic acid (98.0%) and the other chemicals used in this study were also purchased from Wako Chemical Co. (Japan). All chemicals were of analytical reagent grade and were used without further purification. Distilled water was taken from the deionizer (Autostill WG240,

Yamato Scientific Co., Ltd, Tokyo, Japan). β -chitin was derived from squid pens which were purified according to the following procedure.

Experimental

Purification of squid pens

Firstly, decalcification was conducted by immersing squid pen flakes in 1 M hydrochloric acid (HCl) for 2 days. The squid pen flakes were then separated and treated in a deproteinization process where the flakes were immersed in 4% (w/v) sodium hydroxide (NaOH) solution for 24 h. Then, the mixture was heated on a hot plate at 80°C for 4 h in order to obtain pure β -chitin flakes. Finally, the treated chitin flakes were washed with water and dried in an oven at 60°C for 24 h.

Preparation of β -chitin gel

A known amount of β -chitin flakes was suspended in formic acid (98%). The suspension was then frozen at -20°C and kept overnight. After freeze-thawed at room temperature, chitin-formic acid solution with 1wt % chitin concentration was obtained. After pouring the chitin solution into a PP plastic-mold, distilled water was poured directly onto the chitin solution. The volume ration of chitin solution to distilled water was set to 1/2, which was enough for the solvent-exchange to induce a phase separation and the gel formation. β -chitin gel was then neutralized with 1M NaOH, soaked and washed several times with distilled water until pH became neutral. Finally, β -chitin gel was immersed in a bath of 2-propanol for a few days via exchanging fresh 2-propanol several times to allow the water/organic solvent substitution.

Sc-CO₂ gel drying

After soaked with 2-propanol, β -chitin gel was loaded into a cup-shaped aluminium foil and put in a high-pressure vessel. The vessel was pressurized with CO₂ to 10MPa while keeping the temperature at 40 °C, in which CO₂ became supercritical state. The sc-CO₂ drying were conducted for 6 h. During sc CO₂ drying, the pressure was controlled by intermittent purging with continuous CO₂ feeding. After drying, the pressure was then released gradually to preventing the sample from foaming.

Morphology observation

The cell morphology of sc-CO₂ dried samples was examined by scanning electron microscopy (Tiny-SEM 1540 and SEM JEOL, JSM-6340FS). The samples were coated with gold-palladium *in vacuo* prior to the SEM observation. Transmittance electron microscopy observation (TEM) was also performed (TEM JEOL, JEM-1010). The Sc-CO₂ dried samples were dispersed in ethanol and pour on a Cu grid before vacuum drying and TEM observation.

Nitrogen adsorption measurement

Nitrogen adsorption measurement with liquid nitrogen was performed by a BELSORP-mini II-KS (BEL Japan, Inc.). The attached analysis software was used to calculate Brunauer-Emmet-Teller (BET) surface area.

X-ray diffraction (XRD)

XRD patterns of the chitin samples were collected on a Rigaku X-ray generator (RINT 2000) operated at 40 kV, 20 mA and 2 θ range 5-40° with Ni-filtered Cu K α radiation.

RESULTS and DISCUSSION

Morphology observation

β -chitin gel was successfully fabricated by the solvent-exchange-induced phase separation. After replacing water and soaking in 2-propanol (Figure 1a), sc-CO₂ drying was performed

according to the aforementioned procedure. After drying the gel (Figure 1b), the surface and cross-section morphologies were observed. The results were shown in Figures 2a and b. It was found that chitin particles were formed throughout the whole sample. Relating to Figure 2a and b, Figure 2c shows the agglomeration of the chitin particles together with the fibrils arrangement on the particles surface. Moreover, the nano-fibril network was observed inside the particles as shown in TEM images (Figures 3a and b). These TEM images indicated the formation of highly porous structure via sc-CO₂ dry was achieved. Silva et al. [12] reported that a porous formation and nanofiber meshwork were obtained in thier chitin by the solvent extraction and sc-CO₂ drying treatments. However, in their studies, α -chitin was used and dissolved in ionic liquids. Furthermore, the specific surface area of their porous chitin was in the range from 108 to 145 m² g⁻¹ and no particles formation was observed. On the other hand, our porous chitin was prepared from β -chitin without using ionic liquids. The average pore diameter was about 18 nm and the specific surface area is about 403.88 m² g⁻¹ as detailed in the next section.

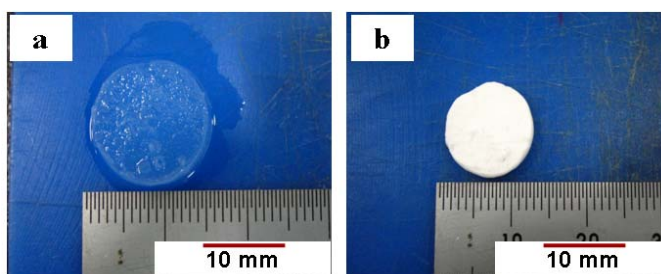


Figure 1. (a) β -chitin gel soaked with 2-propanol before and (b) after Sc-CO₂ drying

Porous structure characteristics

The porous structure of the resulting porous chitin was analyzed by nitrogen (N₂) adsorption at liquid nitrogen temperature. Figure 4a shows the N₂ adsorption-desorption isotherms of our porous chitin. The adsorption-desorption isotherms were categorized into the type IV by the IUPAC classification [13]. This type of isotherm indicates the mesoporous structure with pores 2-50 nm in diameter. Figure 4b shows the pore size distribution, ranging from 5-25nm. The average pore diameter was found to be 17.77 nm, which corresponds to the void space in the nano-fibril network. In addition, the obtained porous chitin exhibits the high BET surface area, up to 403.88 m² g⁻¹. This is due to the presence of fibril network struture, where the fibril width is about 6.95 nm (assuming density of β -chitin, 1.425 g cm⁻³). However, this is different in size from those observed by SEM. This could be explained by a loose coagulation of the fibrils arrangement [14]. As a result, the surface is accessible to N₂ adsorption and provides the high surface area.

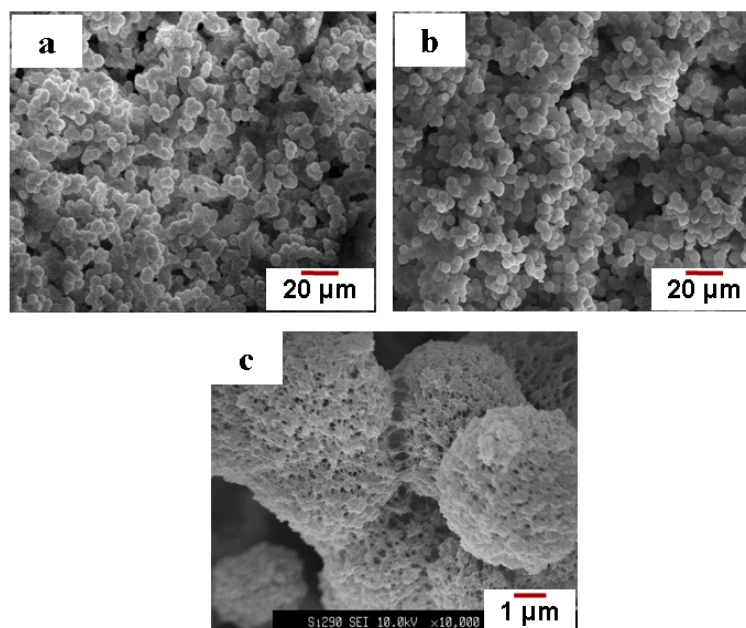


Figure 2. (a) surface, (b) cross-section morphology of β -chitin gel after Sc-CO₂ drying, and (c) agglomerated β -chitin particles

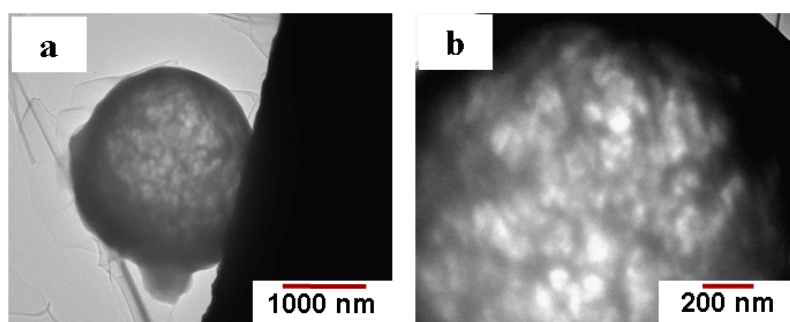


Figure 3. (a) and (b) nano-fibrillar network inside the β -chitin particle

XRD crystallinity

The crystalline structure of chitin has been reported in several papers[15-17]. As shown in Figure 5a, our original β -chitin (chitin flake) exhibits the diffraction peaks at (010) and (100), which correspond to the inter and intra-planar crystalline structure[17]. Comparing the XRD patterns between the original β -chitin flake and the resulting porous chitin, a decrease in crystallinity of the inter (010) and intra-planar (100) crystalline structure was detected at the porous chitin. It could be considered that a de-crystallization of β -chitin occurred when the chitin flakes were dissolved in formic acid. Furthermore, the peak (010) was shifted to a wide angle, which indicated a shrinkage of the inter-planar (010) crystalline structure. The shifted interplanar distance from original was calculated by Bragg equation. The resulting Δd (010) was about 0.73 Å. This indicates a conversion of β -chitin to α -chitin crystalline structure at the gel formation and drying steps [17-19].

CONCLUSION

In this study, the highly porous β -chitin was successfully prepared by combining solvent-exchange-induced phase separation and sc-CO_2 drying processes. The obtained porous structure exhibits high surface area and high porosity with mesopores and the nano-fibrillar network. This structure is considered as an ideal for various applications such as drug delivery systems, dye, and heavy-metal ions removal in cleaning technologies.

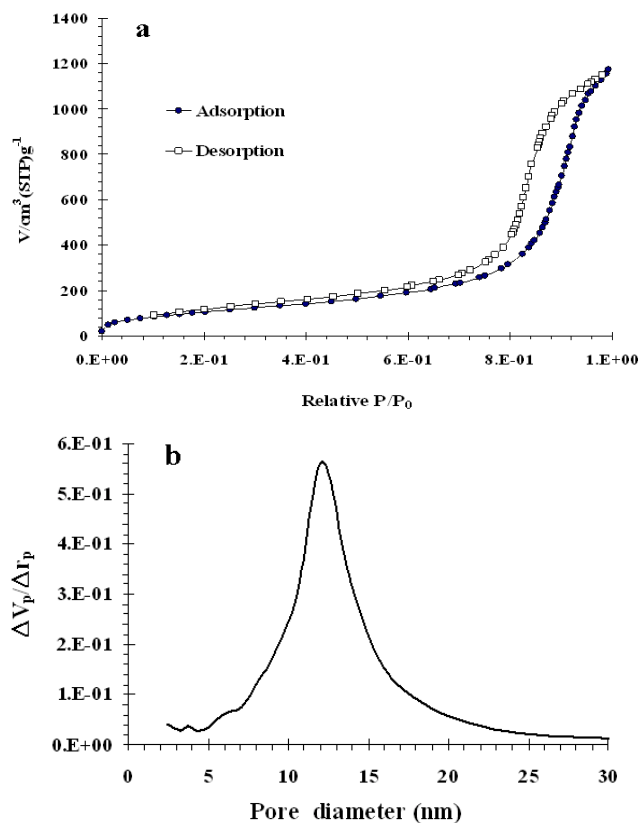


Figure 4. (a) nitrogen adsorption-desorption isotherms and (b) porous size distribution of β -chitin after Sc-CO_2 drying

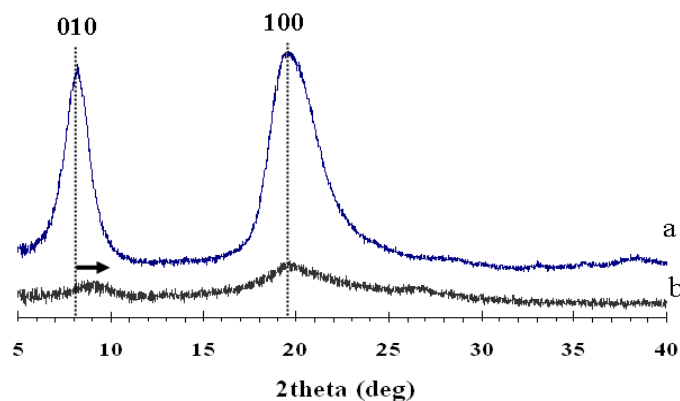


Figure 5. XRD patterns of (a) β -chitin flakes and (b) β -chitin porous structure after Sc-CO_2 drying. Arrow indicates the shifted interplanar from original peak

REFERENCES

- [1] Muzzarelli, R. A. A. (1997) Human enzymatic activities related to the therapeutic administration of chitin derivatives. *Cellular and Molecular Life Sciences (CMLS)*, 53, 131-140.
- [2] Minagawa, T., Okamura Y., Shigemasa Y., Minami, S., Okamoto Y. (2007) Effects of molecular weight and deacetylation degree of chitin/chitosan on wound healing. *Carbohydrate Polymers*, 67, 640-644.
- [3] Noh, H.K., Lee, S.W., Kim, J.M., Oh, J.E., Kim, K.H., Chung, C.P., Choi, S.C., Park, W.H., Min, B.M. (2006) Electrospinning of chitin nanofibers: Degradation behavior and cellular response to normal human keratinocytes and fibroblasts. *Biomaterials*, 27, 3934-3944.
- [4] Kurita, K., Kaji, Y., Mori, T., Nishiyama, Y. (2000) Enzymatic degradation of α -chitin: susceptibility and the influence of deacetylation. *Carbohydrate Polymers*, 42, 19-21.
- [5] Lee, S.B., Kim, Y.H., Chong, M.S., Lee, Y.M. (2004) Preparation and characteristics of hybrid scaffolds composed of α -chitin and collagen. *Biomaterials*, 25, 2309-2317.
- [6] Tsiotsis, C., Tsivintzelis, I., Papadopoulou, L., Panayiotou, C. (2009) A novel method for producing tissue engineering scaffolds from chitin, chitin-hydroxyapatite, and cellulose. *Materials Science and Engineering C*, 29, 159-164.
- [7] Chow, K.S., Khor, E., Wan A.C.A. (2001) Porous chitin matrices for tissue engineering: Fabrication and *in vitro* cytotoxic assessment. *Journal of Polymer Research*, 8(1), 27-35.
- [8] Maeda, Y., Jayakumar, R., Nagahama, H., Furuike, T., Tamura, H. (2008) Synthetic, characterization and bioactivity studies of novel α -chitin scaffold for tissue-engineering application. *International Journal of Biological Macromolecules*, 42, 463-467.
- [9] Cardea, S., Pisanti, P., Reverchon, E. (2010) Generation of chitosan nanoporous structures for tissue engineering applications using a supercritical fluid assisted process. *J. of Supercritical Fluids*, 54, 290-295.
- [10] Reverchon, E., Cardea, S., Rapuano, C. (2008) A new supercritical fluid-based process to produce scaffolds for tissue replacement. *J. Supercrit. Fluids*, 45, 356-364.
- [11] Reverchon, E., Pisanti, P., Cardea, S. (2009) Nanostructured PLLA-hydroxyapatite scaffolds produced by a supercritical assisted technique. *Ind. Eng. Chem. Res.*, 48, 5310-5316.
- [12] Silva, S.S., Duarte, A.R.C., Carvalho, A.P., Mano, J.F., Reis, R.L. (2011) Green processing of porous chitin structures for biomedical applications combining ionic liquids and supercritical fluid technology. *Acta Biomaterialia*, 7, 1166-1172.
- [13] Sing, K.S.W. (1989) The Use of Gas Adsorption for the Characterization of Porous Solids. *Colloids and Surfaces*, 38, 113-124.
- [14] Jin, H., Nishiyama, Y., Wada, M., Kuga, S. (2004) Nanofibrillar cellulose aerogels. *Colloids and Surfaces A: Physicochem. Eng. Aspects*, 240, 63-67.
- [15] Gardner, K.H., Blackwell, J. (1975) Refinement of the structure of α -chitin. *Biopolymers*, 14, 1581-1593.
- [16] Cardenas, G., Cabrera, G., Taboada, E., Miranda, S. (2004) Chitin characterization by SEM, FTIR, XRD, and ^{13}C cross polarization/mass angle spinning NMR. *J Appl Polym Sci*, 93, 1876-85.
- [17] Nagahama, H., Higuchi, T., Jayakumar, R., Furuike, T., Tamura, H. (2008) XRD studies of α -chitin from squid pen with calcium solvent. *International Journal of Biological Macromolecules*, 45, 309-313.
- [18] Saito, Y., Putaux, J.-L., Okano, T., Gaill, F., Chanzy, H. (1997) Structural Aspects of the Swelling of α Chitin in HCl and its Conversion into β Chitin. *Macromolecules*, 30, 3867-3873.
- [19] Saito, Y., Okano, T., Gaill, F., Chanzy, H., Putaux, J.-L. (2000) Structural data on the intracrystalline swelling of α -chitin. *International Journal of Biological Macromolecules*, 28, 81-88.

CHITOSAN NANOPARTICLES CONTAINING siRNA TARGETING VEGF for ANTI-ANGIOGENIC GENE THERAPY

Emine ŞALVA^{1,2*}, Suna ÖZBAŞ-TURAN¹, Jülide AKBUĞA^{1*}

¹ Marmara University, Faculty of Pharmacy, Department of Pharmaceutical Biotechnology

² Marmara University, Vocational Health School, Pathology Laboratory, İstanbul, Turkey

*E-mail address: esalva@marmara.edu.tr and jakbuga@marmara.edu.tr

INTRODUCTION

Solid tumor growth, persistence and metastases are dependent on angiogenesis, relying on the generation of new blood vessels to maintain proliferation, survival and dissemination of the malignant cells. Although numerous growth factors have been identified as potentially positive angiogenic factors, vascular endothelial growth factor (VEGF) is the major regulator of tumor associated angiogenesis in carcinoma by acting with trans membrane receptor tyrosine kinase receptors, VEGFR-1 (flt-1), VEGFR-2 (KDR/flk-1) and NRP-1. VEGF and its receptors have been implicated in the angiogenesis that occurs in many solid tumors including breast, colon cancers, hepatoma, bladder, gastric and prostate cancers. Several strategies have been developed for targeting the VEGF pathway as part of anticancer therapy. RNAi-mediated silencing of oncogenic regulators that play major roles in tumor transformation, growth and metastasis has been considered a promising strategy for cancer therapy [1-3].

RNAi (RNA interference) is already a valuable and well-used research tool in the analysis of molecular mechanisms for many diseases including cancer. RNAi, which is mediated by small interfering RNA (siRNA) has been developed to achieve suppression of specific gene expression in mammalian cells. Recently, this silencing mechanism has been widely used to knockdown cancer-associated genes, holding great promise in the field of cancer therapy [4-6]. However, the delivery of siRNAs in cancer gene therapy strategies may be limited by their degradation in blood and extracellular fluids. Therefore, the efficiency of carrier system or delivery is an important subject in this technology. To date, a number of gene delivery systems have been developed including viral –based vector and non-viral-based vector. Viral vectors are more powerful vehicles for gene transfer than non-viral vector, but their applications are limited due to safety issues. Non viral vectors have been successfully used for gene delivery [7-8]. Among these, chitosan has been considered to be a good gene carrier since it is known as a biodegradable, biocompatible and low toxic biopolymer with high cationic potential. Chitosan nanoparticles have been used for drug delivery due to their high stability and are easily taken up into cells by endocytosis [1-3]. Thus, the development of siRNA loaded nanoparticle approaches to achieve RNAi in mammalian cells should overcome obstacles of delivery [9-16].

The aims of this study are to evaluate siRNA-loaded (VEGF-A, VEGFR-1, VEGFR-2, NRP-1) chitosan nanoparticles for cellular uptake and RNAi effects using human breast cancer cells in vitro.

MATERIALS AND METHODS

Materials

Chitosan (75 kDa and 75-85% degree of deacetylation) and tripolyphosphate (TPP) were purchased from Sigma (St Louis, MO, USA). Dulbecco's modified Eagle's medium (DMEM), fetal bovine serum (FBS), Trypsin-EDTA and penicillin-streptomycin were purchased from

Gibco BRL (Rockville, MD, USA). siRNA-VEGF-A, siRNA-VEGFR1, siRNA-VEGFR2 and siRNA-NRP1 (Dharmacon, Lafayette, CO, USA), ELISA kit for VEGF were used (Invitrogen, Camarillo, CA, USA). A thorough analysis by BLAST was performed on all siRNA sequences used in this study to demonstrate that these sequences have no homology to other genes. All the other chemicals were of cell culture and molecular biology grade.

Preparation of siRNA Loaded Chitosan Nanoparticles

Ionotropic gelation method of Calvo et al. [17] was used for the nanospheres preparation. Chitosan was dissolved in acetate buffer (0.1 M tris acetate/0.1 M acetic acid, pH 5.4) to form of 0.25% (w/v) chitosan solution. TPP aqueous solution (0.25%, w/v) containing siRNA (20 µg/µl) was dropped into the aqueous acidic solution of chitosan in the equal volume under constant stirring at room temperature. The nanoparticle suspension was gently stirred for 30 min at room temperature for gelation. Formed nanoparticles were separated by centrifugation at 12,000xg at 10 min (Eppendorf 5810 R, Germany). The supernatant was discarded and particles were washed with double distilled water. Freeze-dried (Leybold-Lyovac, Germany) nanoparticles were stored at 4°C until using. The supernatant was spectrophotometrically analyzed at 260 and 280 nm by for siRNA content. Encapsulation efficiency was calculated measuring the difference between the total amount of siRNA added in the preparation medium and the amount of non-entrapped siRNA remaining in the aqueous supernatant after processing.

Characterization of Chitosan-siRNA Nanoparticles

Mean particle diameter (Z-average) and zeta potential (surface charge) of nanoparticles were determined using Malvern 3000 HS_A (Malvern, UK). The measurements were made at 25 °C in triplicate. For both of the measurements, nanoparticles were suspended in 10mM acetate buffer at pH 5.5 and in phosphate buffered saline (PBS) at pH 7.4. The morphological examination of nanoparticles were made by Scanning Electron Microscopy (SEM, Jeol, JSM 5200, Japan).

siRNA Stability Assay

Stability of siVEGF-loaded chitosan nanoparticles against enzyme and serum was analyzed. For stability study, nanoparticles containing 10 µg siVEGF were reacted with 20 ng/ml RNase A or 10% FBS at 37°C. Reaction was carried out at 37°C and aliquots were taken at different intervals. For the inhibition of reaction 0.5 M EDTA was used. The integrity of siRNA was examined using the agarose electrophoresis [11].

In vitro release studies

siVEGF release was determined by incubating the nanoparticles (20µg siVEGF) in PBS at 37°C ± 0.5°C. At appropriate time intervals, samples were centrifuged and the supernatant was replaced with fresh medium and the amount of siRNA released in the supernatant was measured spectrophotometrically (Biospec UV 1601-Shimadzu, Japan) at 260 nm.

In Vitro Transfection

MCF-7 and MDA-MB435 breast cancer cell lines were from American Type Culture Collection (ATCC, Rockville, MD) and used for transient transfection experiments. The cell lines were maintained in Dulbecco's Minimum Essential Medium (DMEM) media supplemented with 10% FBS and antibiotics at 37°C under 5% CO₂ incubator. Cells were plated in 24-well plate at a cell density of 5.0x10⁴ cells/well and incubated overnight. Transfections were performed on cells that were approximately 70% confluent. siRNA-loaded nanoparticles (0.1µg siVEGF for each well) were added to in 24-well plates and incubated for 1-6 days post-transfection. The cells were washed twice with ice cold PBS and lysed in 100µl of lysis buffer by freezing and thawing

(incubation at -20°C for 30 min in a deep-freezer and then 37°C for 30 min). Cell debris was removed by centrifugation at 12.000 g. The supernatant was removed [12, 14].

The Determination of VEGF Amount

ELISA for VEGF was performed in the supernatant of the cell culture suspension, according to manufacturer's instructions (Biosource, California). VEGF protein was analyzed using solid phase sandwich ELISA. Absorbance was determined by spectrophotometric reading at 450 nm. All the experiments were repeated thrice and the standard deviation (\pm) was calculated [11].

RESULTS AND DISCUSSION

In this study, nanoparticles were prepared for VEGF inhibition based RNA interference method and *in vitro* silencing effect of complexes were studied in different breast cancer cell lines. Selection of cell line in *in vitro* silencing study is important.

The Control with Gel Retardation Assay of Nanoparticles

The complete binding of siVEGF for chitosan-TPP nanoparticles was showed by gel retardation assay (Fig. 1).



Fig. 1. Binding efficiency of siRNA to the chitosan associated with TPP nanoparticles. Lane 1. Free siRNA, lane 2-3. siRNA loaded chitosan nanoparticles

Morphology, Size, Zeta Potential and Encapsulation Efficiency of Test Nanoparticles

SEM was used to examine the morphology of test nanoparticles prepared (Fig.2). As shown, nanoparticles were spherical in shape with relatively homogenous size distribution. Encapsulation efficiency was obtained as measured by spectrophotometry for all the entrapped siRNA chitosan-TPP nanoparticles. The siRNA encapsulation ranged from 86.7 ± 0.84 to $95.98 \pm 0.50\%$. The sizes of nanoparticles ranged from 246 ± 10.07 nm to 270 ± 14.12 nm. Zeta potential values of nanoparticles changed between 17.09 ± 0.71 – 41.45 ± 0.43 mV in pH 5.5 and between $+27.5 \pm 1.2$ mV and 30.05 ± 0.40 mV in pH 7.4.

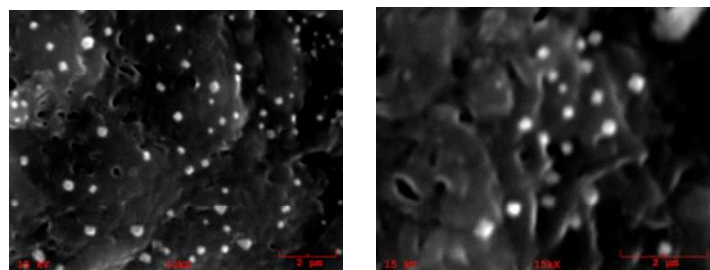


Fig. 2. SEM photograph of siRNA loaded chitosan nanoparticles

In Vitro Release Study of Nanoparticles

Release of siVEGF from nanoparticles were observed during 30 days that siRNA release completed (Fig. 3). Burst effect on siRNA release profile was not seen in the first day. 50% of siRNA released from NPs within the first 13 days.

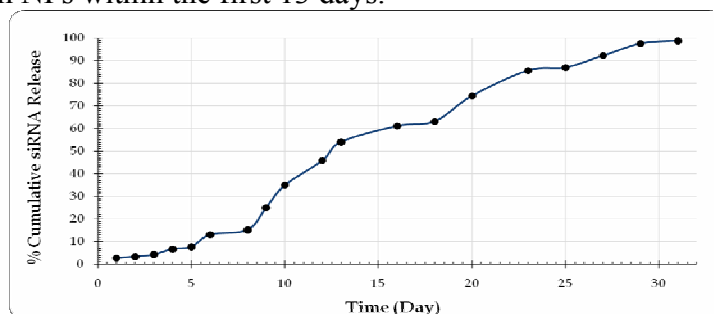


Fig.3. In vitro release study

Stability of siRNA in serum and enzyme

In order to test the protection of siRNA by chitosan nanoparticles from serum enzymes attacks such as nucleases and RNases, serum stability assay was performed. As seen in Figures 4a and 4b, the chitosan nanoparticles efficiently protected the siRNA from degradation.

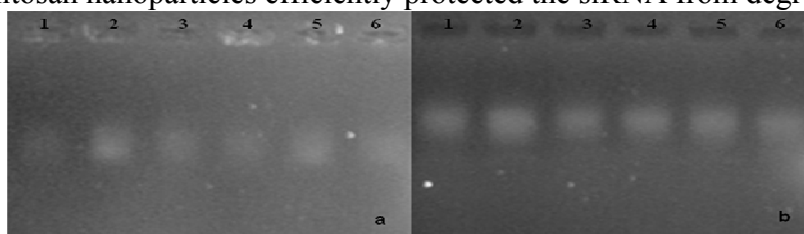


Fig. 4. Enzyme and serum stability of nanoparticles. Lanes 1-6: 1, 2, 4, 24, 48 and 72 hours

In Vitro Transfection and VEGF Inhibition Studies

For in vitro transfection study, two breast cancer cell lines were tested; MDA-MB435 and MCF-7. To investigate whether nanoparticles were capable of introducing the cell, FITC-siVEGF loaded chitosan nanoparticles transfection and distribution were followed by fluorescence microscopy. The intensity of fluorescence of the cell within 24-72 hrs after transfection showed the cellular uptake of the nanoparticles (Fig.5).

In vitro VEGF concentrations in the cells found are given in Fig.6. The highest gene inhibition was measured in MDA-MB-435. In vitro silencing effect of nanoparticles in the cells as follows MDA-MB435 > MCF-7. In this study, chitosan, a new gene delivery system contributed to the breast cancer cells, therapeutic effect of VEGF-siRNA.

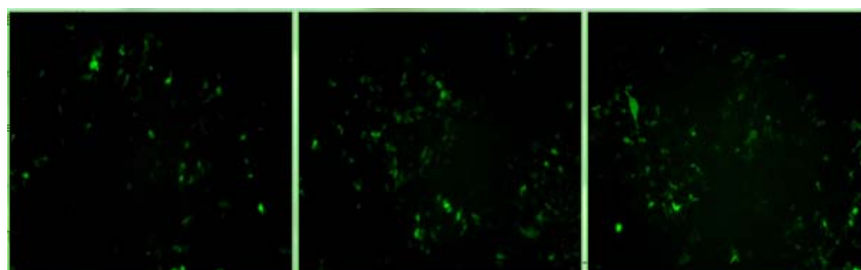


Fig. 5. MDA-MB-435 cell line transfected with FITC-siRNA loaded chitosan nanoparticles (24-72 h).

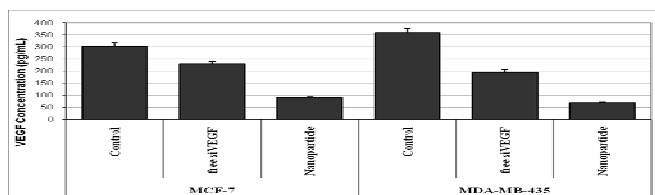


Fig.6. Inhibition of VEGF production with siVEGF loaded chitosan nanoparticles.

ACKNOWLEDGEMENTS

This study was supported by Marmara University Scientific Research Projects Association (SAG-DKR-290906-0185) and Turkish Association For Cancer Research and Control (Terry Fox Cancer Foundation).

REFERENCES

- [1] Bai, Y., Deng, H., Yang, Y., Zhao, X. et.al. (2009) VEGF-targeted short hairpin RNA inhibits intraperitoneal ovarian cancer growth in nude mice. *Oncology, Clin Trans Res.* 77, 385-394.
- [2] Kim, S.H., Jeong, J.H., Lee, S.H., et al. (2008) Local and systemic delivery of VEGF siRNA using PEC micelles for effective treatment of cancer. *J Cont Rel.* 129, 107-116.
- [3] Matsumoto, G., Kushibiki, T., Kinoshita, Y., et al. (2006) Cationized gelatin delivery of a plasmid DNA expressing small interference RNA for VEGF inhibits murine squamous cell carcinoma. *Cancer Sci.* 97, 313-321.
- [4] Ilbashir, S.M., Harborth, J.et.al. (2001) Duplexes of 21-nucleotide RNAs Mediate RNA interference in cultured mammalian cells. *Nature*, 411, 494-98.
- [5] Hannon, G.J., (2002) RNA interference. *Nature*, 418, 244-51.
- [6] Leung, R.K.M., Whittaker, P.A, (2005) RNA interference:from gene silencing to gene-specific therapeutics. *Pharmacology&Therapeutics*, 107, 222-39.
- [7] Zhang, S., Zhao, B., Jiang, H., Wang, B.A, (2007) Cationic lipids and polymers mediated vectors for delivery siRNA. *J. Cont. Rel.* 123, 1-10.
- [8] Schiffelers, R.M., Ansari, A., Xu, J., et.al. (2004) Cancer siRNA therapy by tumor selective delivery with ligand-targeted sterically stabilized nanoparticle. *Nucleic Acids Res.* 32, e149.
- [9] Kim, T., Jiang, H., (2007) Chemical modification of chitosan as a gene carrier in vitro and in vivo. *Prog. Polym.Sci.* 32, 726-53.
- [10] Akbuğa, J. (2007) Chitosan for nucleic acid delivery. *Advances in Chitin Science.* Vol X 179-85
- [11] Şalva, E., Akbuğa, J. (2010) In vitro silencing effect of chitosan nanoplexes containing siRNA expressing vector targeting VEGF in breast cancer cell lines. *Die Pharmazie* 65(12), 896-903.
- [12] Şalva, E., Akbuğa, J. (2009) Comparison of silencing effect of chitosan/psiRNA complexes in different cell lines. *Advances in Chitin Science.* Vol XI, 203-208.
- [13] Şalva, E., Kabasakal, L., Eren, F., Çakalağaoğlu, F., Özkan, N., Akbuğa, J. (2010) Chitosan/Short Hairpain RNA Complexes for Vascular Endothelial Growth Factor Suppression Invasive Breast Carcinoma. *Oligonucleotides.* 20 (4), 183-190.
- [14] Şalva, E., Özbaş-Turan, S., Akbuğa, J. (2010) Chitosan nanoparticles containing shRNA targeting VEGF as cancer therapeutic. *Human Gene Therapy*, 21(10), 1412.
- [15] Liu, X., Howard, K., et.al. (2007) The influence of polymeric properties on chitosan/siRNA nanoparticle formulation and gene silencing. *Biomaterials*, 28,1565-71.
- [16] Kim W.J., Chang C.W., Lee W, Kim S.W., (2007) Efficient siRNA delivery using water soluble lipopolymer for anti-angiogenic gene therapy. *J.Cont.Rel.* 118:3,357-63.
- [17] Fernandez-Urrusuno R., Calvo P., Remunan-Lopez C., Vila Jato J.L. (1999) Chitosan nanoparticles: A new vehicle for increasing the nasal absorption of peptides. *Proc. Int. Symp. Control. Rel. Bioact. Mater.*, 26: 353-354.

THE CORRELATION STUDY OF CHITIN AND ACIDIC MAMMALIAN CHITINASE IN ALLERGIC ASTHMA

Hui-San Chen^{1#}; Chao-Lin Liu^{3#}; Horng-Heng Juang²; Ching-Jen Yang^{1,3}; Chia-Jen Wu², Yu-Ting Huang^{1,3}; Chia-Rui Shen^{1,2*}

¹Department of Medical Biotechnology and Laboratory Science, ²Graduate Institute of Biomedical Sciences, Chang Gung University, Kweishan 333, Taiwan

³Department of Chemical Engineering and Graduate School of Biochemical Engineering, MingChi University of Technology, New Taipei City 243, Taiwan

*E-mail address: crshen@mail.cgu.edu.tw

INTRODUCTION

The prevalence and severity of allergic diseases such as asthma has increased dramatically during the past decade. In fact, WHO has recognized asthma with major public health concern. Chronic airway inflammation with pathological immune response is the hallmark of asthma. The key feature of asthma is the production of allergen-specific IgE, resulting in immediate-type hypersensitivity reactions followed by the development of late-phase responses such as eosinophil recruitment, mucus production, and airway hyperresponsiveness (AHR). Eosinophilic inflammation driven by helper T cell type 2 (Th2) cytokines is deemed to play a crucial role in the pathogenesis of asthma [1].

Chitin, a polymerized sugar and the fundamental component of the exoskeletons of invertebrates, is emerging as a potentially crucial and previously under-appreciated environmental factor in asthma [2]. In fact, the major allergens are mites and cockroaches, and chitin is their abundant component. Indeed, a recent report has shown that chitin was detected in home dust samples and chitin concentrations correlate with dust mite antigen, indicating the potential relationship between chitin exposure and asthma development or severity [3]. Chitinases comprise a group of related enzymes remarkably well-preserved across mammalian species, including humans [4]. Growing evidence suggests that an increased expression of acidic mammalian chitinase (AMCase) may play a role in the pathogenesis of asthma. It has been reported that acidic mammalian chitinase (AMCase) is hyper-expressed in the lung of patients with asthma and in animal models of asthma [4-8]. Such induction of AMCase was found not only in lung epithelial cells but also in alveolar macrophages in ovalbumin (OVA)-stimulated mice [5, 8]. Also, AMCase has been hypothesized to associate with Th2-mediated inflammation through an IL-13-dependent mechanism [5, 9-12], due to the significant hyper-expression of AMCase in IL-13-transgenic mice. In contrast, IL-13-null mice failed to express AMCase even in the exposure of an allergen challenge [5], indicating an IL-13-dependent pathway. However, although the inhibition of AMCase activity with specific antibodies showed to reduce the inflammatory response in BALF and lung tissues, it appeared that such reduction of AMCase activity did not lead to consequent changes in IL-4 and IL-13 expression. In our laboratory, we adapted RNAi technology to further knock down AMCase expression, which led to the significant reduction of allergic responses [9]. Importantly, we found that downregulation of AMCase expression was accompanied by suppression of IL-13 in BALF cells. Although lung IL-13 was not entirely suppressed by down-regulation of AMCase activity, the existence of other molecular pathways controlling AMCase expression can be estimated.

In the current study, we attempt to correlate the exposure of chitin, the allergic mediators and the expression of AMCase. We have demonstrated the elicited expression of AMCase in the

lung tissues not only from ovalbumin induced allergic asthma mouse model but also Der P2 induced allergic asthma mice. Also, the mouse AMCase promoter was cloned and constructed as a reporter vector. The effects of chitin, its derivatives as well as allergic mediated molecules were evaluated on the AMCase expression in the lung cells.

MATERIALS AND METHODS

Cell culture MLE-12, 3T3 and RAW cell lines were cultured and maintained in Dulbecco's modified Eagle's medium (DMEM) containing 5% fetal bovine serum (FBS) with 5% CO₂ in humidified air at 37°.

Asthmatic animal induction protocol. Animal studies were approved by the Institutional Animal Care and Use Committee of Chang Gung University (Taoyuan, Taiwan). Pathogen-free wild-type female BALB/cByJNarl mice from the National Laboratory Animal Center (Taipei, Taiwan) were used. Mice were 6–8 weeks old at the beginning of the experiment. Mice were injected intraperitoneally with chicken OVA or Der P2 (20 µg) complexed to alum or with normal saline alone. The process was repeated 3 days later. Thirteen days after the first immunization, animals were reinjected intraperitoneally with OVA or Der P2. Moreover, mice received by inhalation either an aerosol of OVA or Der P2 (2%, w/v) in normal saline or normal saline solution alone. Mice were thereafter challenged four times with allergens on days 16, 20, 23, and 27. Mice were sacrificed on day 28.

Real-time PCR Expression of AMCase, humanized Renilla green fluorescent protein (hrGFP), and actin was analyzed by real-time PCR, using a LightCycler PCR system (Roche, Indianapolis, IN). Actin 300 (forward primer, 5-GAAACTACATTCAAT TCCATC-3; reverse primer, 5-CTAGAAGCACTTGCGGT GCAC-3) was used as a housekeeping gene. The reaction parameters for actin 300 and hrGFP amplification (forward primer, 5-ATGGTGAGCAAGCAGATCCTG-3; reverse primer, 5-GGTGCGCTCGTACACGAAGCC-30) were as follows: initial denaturation at 95° for 10 min, followed by 35 cycles at 95° for 10 sec, 508C for 10 sec, and 72° for 10 sec.

AMCase was amplified using the following primers: forward, 50-TGGACACACCTTCATCCTGA-30; and reverse, 50-AACA AGCCCTGCTTGACAAT-30. After initial denaturation at 95 ° for 10 min, 45 cycles were performed at 95° for 10 sec, 50 ° for 10 sec, and 72 ° for 10 sec.

Western blot analysis Cell and tissue samples for AMCase analysis were prepared with lysis buffer. After separation by sodium dodecyl sulfate–polyacrylamide gel electrophoresis (SDS–PAGE), the samples were identified by incubation with rabbit antimouse AMCase antibodies and developed with an enhanced chemiluminescence (ECL) detection kit (GE Healthcare Life Sciences, Piscataway, NJ). A monoclonal antibody against β-actin was used as control.

Mouse AMCase Reporter vector construction and transient gene expression assay The reporter vector contains the specific mouse AMCase promoter cloned by PCR and then ligated into pGL3-Basic vector (Promega Bioscience) after digestion with Kpn I and Hind III. Cells were transiently transfected using Tubofect transfection reagent as described elsewhere. Briefly, cells were plated onto 6-well plates at 1×10^5 cells/well and transfected with 3 µl/well of Tubofect transfection reagent with 3 µg/well of reporter vector. The luciferase reporter vector transfected cells were treated with different concentrations of camptothecin in RPMI 1640 medium with 10% FCS for an additional 24 hr. Each treatment was repeated four times and each experiment was repeated at least three times. Cell lysate (100 µl) was used for the luciferase assay with a luciferase assay kit and the luciferase activity was measured in relative light units using a LumiCount Luminometer (Packard BioScience, Meriden, CT).

Statistical analysis Results are presented as means \pm SEM. Data were analyzed by nonparametric Mann–Whitney U test. A two-tailed pvalue less than 0.05 was considered statistically significant.

RESULTS AND DISCUSSION

Levels of AMCase in the lungs of OVA- or Der P2- sensitized mice

To investigate whether elevated levels of AMCase expression were specifically located in the airways of OVA- or Der P2-sensitized mice, we harvested and analyzed the lung tissues 24hr after the last allergen challenge. It can be seen from Figure 1A that the elicited levels of AMCase expression were found in the lungs of Der P2- sensitized mice as compared to those of normal controls. Notably, 17- and 5-fold increases in AMCase mRNA level were found in the lung tissues of both OVA- or Der P2-sensitized mice (Figure 2B), respectively. Additionally, there were no major differences in AMCase expression in peritoneal cells from sensitized animals compared with control mice treated with normal saline (data not shown). Similar findings were obtained when examining AMCase protein levels using western blot analysis (data not shown). Hence, the hyperexpression of AMCase was confined chiefly to the airways.

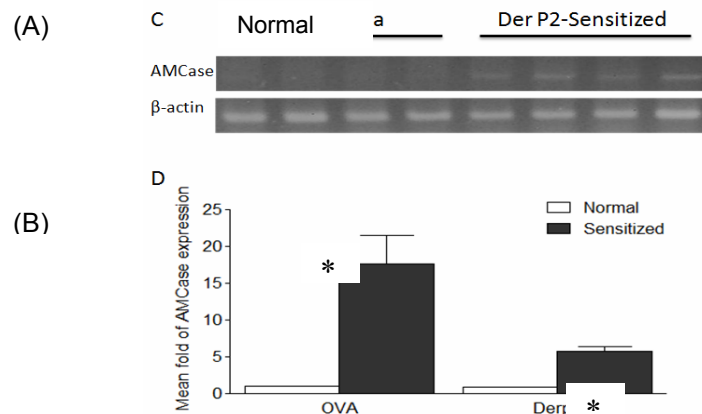


Figure 1 AMCase expression level after mouse sensitized by ovalbumin and Der-P2. Cell samples from lung tissues were harvested from normal saline controls, OVA and Der-P2 sensitized mice, and their AMCase expression was quantified via (A) RT-PCR, (B) real-time PCR (* $p < 0.05$, nonparametric Mann–Whitney test).

AMCase reporter vector construction and AMCase expression

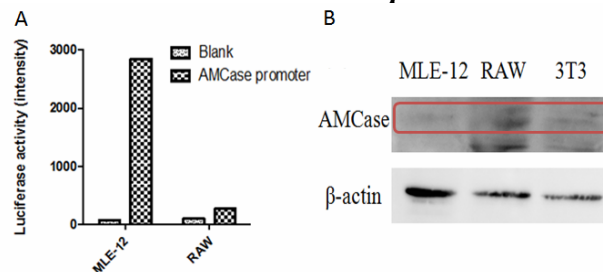


Figure 2. The expression of AMCase. (A) The reporter vector containing the AMCase promoter and encoding luciferase was transfected to MLE (mouse lung epithelial)-12 and RAW macrophage cells, and the luciferase activity was measured after 48 hours of transfection. (B) The protein levels of AMCase in MLE-12, RAW and 3T3 fibroblast cells were analyzed by Western blot.

The specific mouse AMCase promoter was cloned by PCR accordingly, and the reporter vector pGL3 was constructed containing the AMCase promoter and encoding luciferase. The AMCase expression in the cells can be therefore evaluated by measuring the luciferase activity in the cells transiently transfected with the reporter vector. Figure 2A shows that significant higher

levels of AMCase expression in the mouse lung epithelium MLE-12 cells, in contrast to the RAW macrophages. Such expression profiles were confirmed by Western blot analysis using anti-AMCase antibody for specific detection (Figure 2B). Indeed, the expression of AMCase in most cell lines appeared to be really low, not only detected using Western blot but also real-time PCR assays. To confirm the results demonstrated by reporter luciferase assays, we have further utilized nested RT-PCR and obtained the similar findings (data not shown).

The effects of chitin on AMCase expression

To correlate the exposure of chitin and the expression of AMCase and evaluate if such correlation contributes to the development of allergic asthma, we have identified the effects of chitin, its derivatives as well as allergic mediated molecules on the AMCase expression in the lung cells. Results were summarized in Figure 3. The levels of AMCase expression were presented by the luciferase activity and shown in relative light units. It can be seen from Figure 3A that a relative low level of AMCase was expressed in MLE-12 cells, whereas the adding of chitin induced the expression of AMCase. Following the higher doses of chitin challenge, the expression levels of AMCase increased. Similar patterns were found in the addition of a chitin derivative, oligo-chitin (Fig 3B). In this study, we have also utilized PMA as a positive control to stimulate the AMCase expression (Fig 3C).

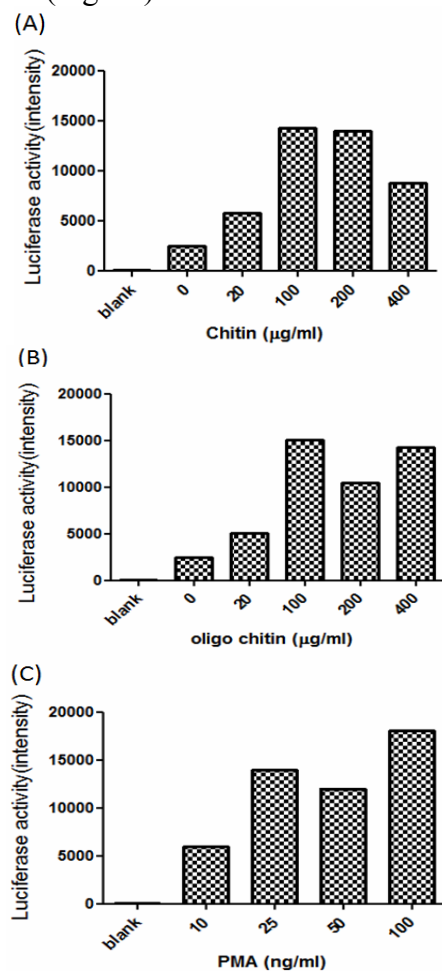


Figure 3. The effect of chitin derivatives on the expression of AMCase in MLE-12 cells. The plasmid construct containing the AMCase promoter and encoding luciferase was transfected to MLE-12 and RAW cells, and the luciferase activity was measured after 48 hours of incubation. At 24 hours post-transfection, different doses of (A) chitin (B) oligo chitin (C) PMA were added to the cultures.

In this study, we have demonstrated that AMCase were both increased in the lung tissues of the mice, which were primed and sensitized with ovalbumin or Der-P2. In particular, AMCase was highly expressed in ovalbumin-sensitized mice. Although Western blot analysis showed that AMCase was expressed in a pretty low level in MLE-12 cells. However, using the more sensitive promoter assay, we showed that AMCase indeed expressed in a relatively high level in MLE-12 cell line, but not in RAW cells. Also, here we revealed that chitin derivatives were able to stimulate the expression of AMCase. Although there are still studies ongoing, the obtaining results would provide pieces of evidence to a more detail molecular understanding of AMCase, and further contribute to allergic disease mechanisms.

ACKNOWLEDGEMENTS

HSC and CLL contributed equally. This study was financially supported by the grants of Nation Science Council 98-2320-B-182-014-MY3 and Chang Gung Memorial Hospital/ Chang Gung University BMRP440 to CRS.

REFERENCES

- [20] Passalacqua, G., and Ciprandi, G. (2008) Allergy and the lung. *Clin. Exp. Immunol.* 153(Suppl. 1), 12–16.
- [21] Thomas, W.R. Hales, B.J., Smith, W. (2010) House dust mite allergens in asthma and allergy. *Trends in Molecular Medicine*, 16(7), 321–328.
- [22] Blanc, P.D., Dyken, S., Locksley, R., Quinlan, P.J., Balmes, J.R., Iribarren, C., Katz, P. P., Yelin, E.H., Trupin, L. and Eisner, M.D. (2010) Chitin detection in home dust sampling. *Am. J. Respir. Crit. Care Med.*, 181: A4668.
- [23] Boot, R.G., Blommaert, E.F., Swart, E., Ghauharali-Van Der Vlugt, K., Bijl, N., Moe, C., Place, A., and Aerts, J.M. (2001) Identification of a novel acidic mammalian chitinase distinct from chitotriosidase. *J. Biol. Chem.*, 276, 6770–6778.
- [24] Zhu, Z., Zheng, T., Homer, R.J., Kim, Y.K., Chen, N.Y., Cohn, L., Hamid, Q., and Elias, J.A. (2004) Acidic mammalian chitinase in asthmatic Th2 inflammation and IL-13 pathway activation. *Science*, 304, 1678–1682.
- [25] Bierbaum, S., Nickel, R., Koch, A., Lau, S., Deichmann, K.A., Wahn, U., Superti-Furga, A., and Heinzmann, A. (2005) Polymorphisms and haplotypes of acid mammalian chitinase are associated with bronchial asthma. *Am. J. Respir. Crit. Care Med.*, 172, 1505–1509.
- [26] Chupp, G.L., Lee, C.G., Jarjour, N., Shim, Y.M., Holm, C.T., He, S., Dziura, J.D., Reed, J., Coyle, A.J., Kiener, P., Cullen, M., Grandsaigne, M., Dombret, M.C., Aubier, M., Pretolani, M., and Elias, J.A. (2007). *N. Engl. J. Med.*, 357, 2016–2027.
- [27] Yang, C.J., Liu, Y.K., Liu, C. L., Shen, C.N., Kuo, M.L., Su, C.C., Tseng, C.P., Yen, T.C., and Shen, C.R. (2009) Inhibition of Acidic Mammalian Chitinase by RNA Interference Suppresses OVA-Sensitized Allergic Asthma. *Hum. Gene Ther.*, 20, 1597–1606.
- [28] Ramanathan, M., Lee, W.K., and Lane, A.P. (2006) Increased expression of acidic mammalian chitinase in chronic rhinosinusitis with nasal polyps. *Am. J. Rhinol.*, 20, 330–335.
- [29] Kawada, M., Hachiya, Y., Arihiro, A., and Mizoguchi, E. (2007) Role of mammalian chitinases in inflammatory conditions. *Keio J. Med.*, 56, 21–27.
- [30] Bucolo, C., Musumeci, M., Maltese, A., Drago, F., and Musumeci, S. (2008) Effect of chitinase inhibitors on endotoxin induced uveitis in rabbits. *Pharmacol. Res.*, 57, 247–252.
- [31] Musumeci, M., Bellin, M., Maltese, A., Aragona, P., Bucolo, C., and Musumeci, S. (2008) Chitinase levels in the tears of subjects with ocular allergies. *Cornea*, 27, 168–173.

CARBOXYMETHYL CHITIN STRUCTURE, SPECTRAL AND STRENGTH CHARACTERISTICS OF IT'S FILMS

L.N. Shirokova^{1*}, A.S. Petrosyan¹, V.A. Alexandrova¹, G.A. Vihoreva²

¹ *A.V. Topchiev Institute of Petrochemical Synthesis RAS, Moscow, Russia*

² *A.N. Kosygin Moscow Textile State University, Moscow, Russia*

**E-mail address: shirokova@ips.ac.ru*

INTRODUCTION

Chitin or poly(β (1-4)-N-acetyl-D-glucosamine) is one of the most abundant polysaccharides found in nature. It is well known that chitin cannot be dissolved in common solvents. This obviously limits practical utilization of this material. Additionally, the N-deacetylated derivative of chitin – chitosan, can be dissolved in aqueous solutions only with a pH<6.5. Carboxymethyl derivative of chitin is water-soluble in a wide pH interval and exhibits low toxicity, biodegradability, sorption capacity, ability to form films and hydrogels [1-3]. Due to such unique combination of properties carboxymethyl chitin (CMC) found wide application in various areas of biology and medicine: controlled drug delivery systems, biosensors, bone repairing, wound healing and etc [4,5]. For chemical CMC modification, in particular, polymer-similar transformations it is necessary to realize CMC polyelectrolyte macromolecules behavior at different pH media during such modifications.

Taking into account this consideration, various forms of 6-O-carboxymethyl chitin have been obtained: acidic form (CMC-H), salt form (CMC-Na) and mixed form with equal (50%) share of CMC-H and CMC-Na links in CMC chain. Structure and properties of these CMC forms and films on their basis were investigated.

MATERIALS and METHODS

Materials

Chitin was purchased from UAB “Bioprogress”, Russia. All other chemicals (sodium alkali, monochloroacetic acid, isopropanol) were analytical grade and used without further purification.

Methods

A water soluble chitin derivative – 6-O-carboxymethyl chitin with MW 8.0×10^4 and carboxymethylation degree of 1.0 was prepared from chitin in salt form (CMC-Na) as described in [6]. Average molecular weight of carboxymethylated chitins was measured with sedimentation on a *MOM 3180 analytical ultracentrifuge* (“**MOM** Hungarian Optical Works”, Hungary) using a rotor speed of 5000 rpm and equipped with *Philpot–Svenson refractometric optical system*.

A glass column filled with KU-2-8 cationit exchanger (full static exchange capacity was not less than 1.8 mg-equiv./cm³, grain size – 0.315-1.25 mm) was used to obtain CMC-H. The required amount of CMC-Na polymer (pH 7.5) was passed through ion-exchange column at a rate of 20 drops/min. Eluate was collected at pH=3.

All samples were investigated with a Fourier transform infrared spectroscopy (IFS/66V FTIR-spectrometer, “Bruker Optics”, Germany) via the film and ATR (freeze-dried samples) methods in the range 4000-400 cm⁻¹.

TGA/DSC1 derivatograph (“Mettler Toledo Ltd”, Switzerland) was used to evaluate the thermal properties of CMC samples (about 8 mg) under Ar atmosphere at a heating rate of 10°C min⁻¹ from 30 to 550°C.

Carboxymethyl chitin films were prepared from 2% (w/w) CMC water solutions poured onto Petri dishes and left for 24 h for the solvent to evaporate. Films of 50–60 μm were used in this investigation.

Evaluation of mechanical properties of carboxymethyl chitin films was performed on Instron 1121 tension tester ("Instron Ltd.", U.K.).

RESULTS and DISCUSSION

Structural formulas of 6-O-carboxymethyl chitin in acid form (CMC-H), salt form (CMC-Na) and mixed form with equal (50%) share of CMC-H and CMC-Na links in CMC chain is shown in Fig. 1. The ^{13}C NMR studies by G. A. Vihoreva et al. confirmed that substitution for the $-\text{CH}_2\text{COONa}$ group in CMC-Na occurs predominantly at the oxygen atom at C6 carbon (95%) [5].

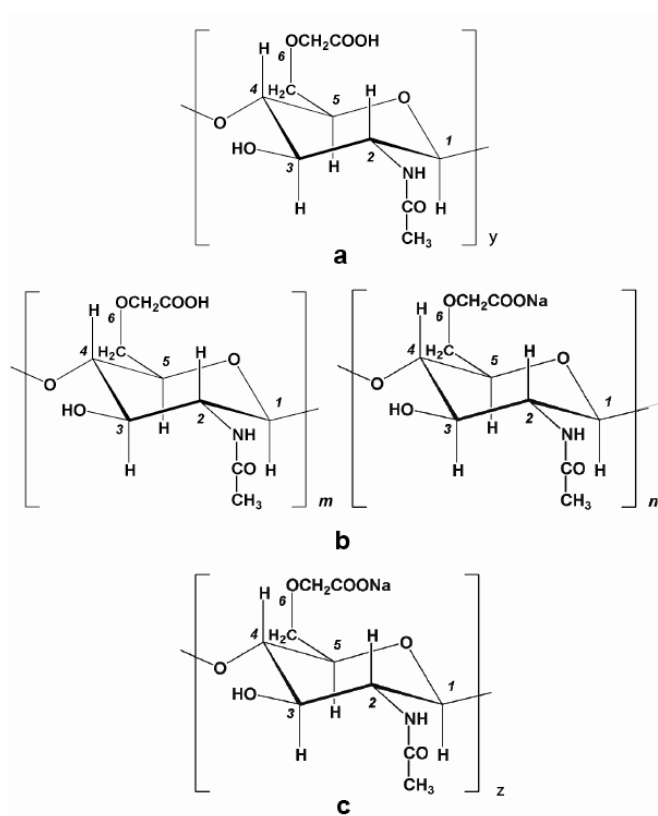


Figure 1. Structural formulas of 6-O-carboxymethyl chitin in acid form (CMC-H) – a, salt form (CMC-Na) – c and mixed form with equal (50%) share of CMC-H and CMC-Na links in CMC chain – b ($n=m$)

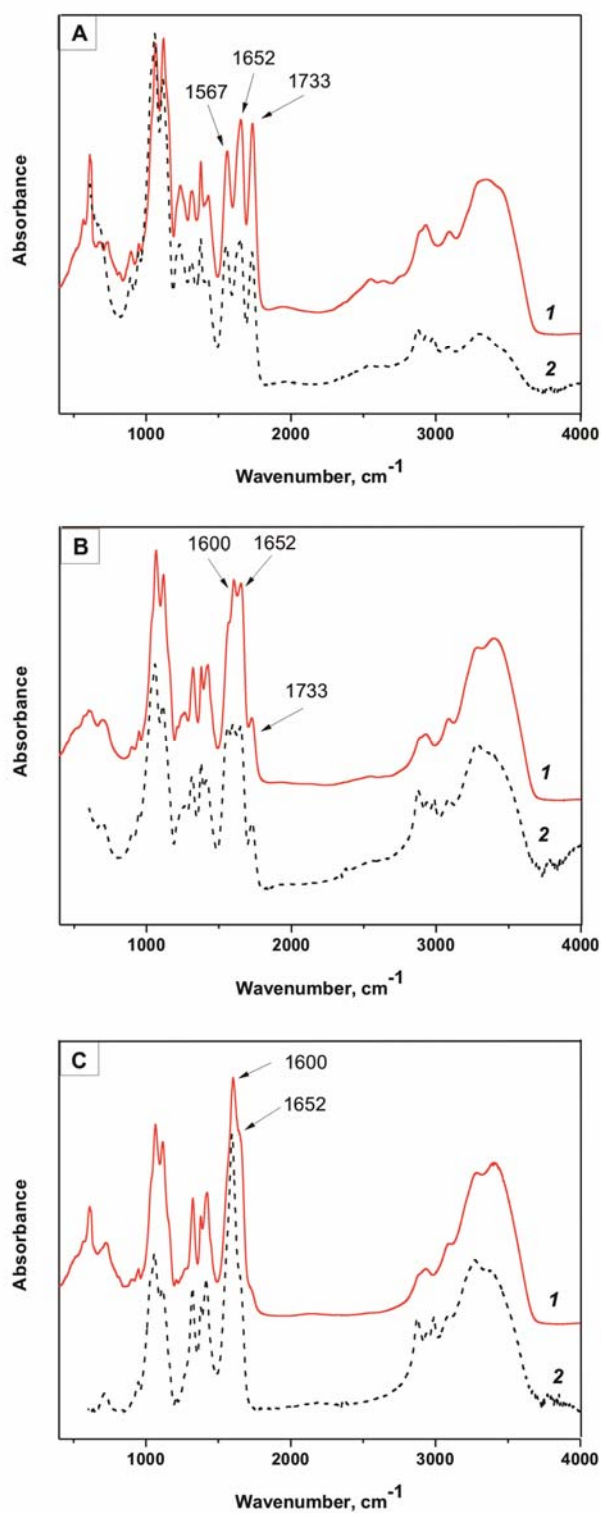


Figure 2. FTIR-spectra of CMC-H form (a), salt CMC-Na form (c) and mixed form with equal (50%) share of CMC-H and CMC-Na links in CMC chain (b) in film form (1) and in freeze-dried samples (2)

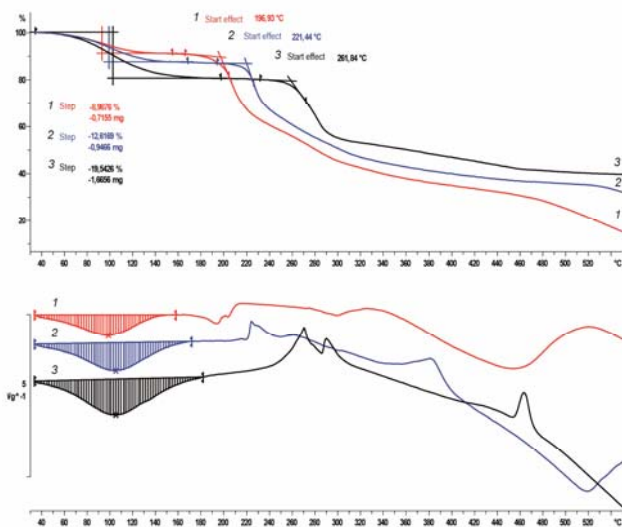


Figure 3. TGA and DTA thermograms of CMC-H form (1), salt CMC-Na form (3) and mixed form with equal (50%) share of CMC-H and CMC-Na links in CMC chain (2) in freeze-dried samples

FTIR-spectra of CMC-H form (a), salt CMC-Na form (c) and mixed form with equal (50%) share of CMC-H and CMC-Na links in CMC chain (b) as in film form (1), and so freeze-dried samples (2) are shown in Fig. 2.

The absorption bands with the maximum at 1733 and 1567 cm^{-1} in FTIR spectra of CMC-H confirmed the presence of C=O bond in the carboxyl groups and carboxylate-ions, correspondingly [7-9]. In

contrast to that, intensity of characteristic absorption peak at 1563 cm^{-1} (C=O in the carboxylate-ion) of mixed form is significantly reduced; at the same time in CMC-Na FTIR data the spectral characteristics of such band are absent.

The absorbance band with maximum at 1733 cm^{-1} and 1567 cm^{-1} related to C=O band (in carboxyl group and carboxylate anion, correspondingly) confirmed the presence of protonated –COOH and deprotonated –COO⁻ forms of carboxyl groups in the structure of CMC-H form [7,8]. The band intensity of carboxyl group at 1733 cm^{-1} in the mixed form of CMC is weaker than that for CMC-H form. At the same time the new absorption band at 1600 cm^{-1} related to carboxylate anion with counter ion Na⁺ appeared. The intensity of this absorption band in CMC-Na form was higher than that for mixed CMC form. Note, that intensity of band at 1733 cm^{-1} carboxyl group in CMC mixed form has fallen sharply and appears only as a shoulder to band at 1652 cm^{-1} (acetamide group).

Polysaccharides usually have a strong affinity for water and in the solid state these macromolecules may have a disordered structure which can be easily hydrated [11]. As it is known, the hydration properties of chitin-chitosan row polymers depend on the primary and supra molecular structure [10]. Fig. 3 shows thermogravimetry (TGA) and differential scanning calorimetry (DSC) data of CMC forms under Ar atmosphere between 30-550°C. From the DSC data it is observed that thermal transformations of CMC forms took place in three stages. The first stage (up to 140-150°C) was related to evaporation of water present in the freeze-dried samples of CMC forms. The second stage when samples were heated higher 170°C was an exothermic peak, which was connected with CMC decomposition (deacetylation, decarboxylation and others). The third weight loss stage at 335°C and higher was related to carbonization of the samples due to glycosidic and other bands cleavage in CMC macromolecules. These results are in agreement with [11].

Comparative study using TGA showed that CMC hygroscopicity is significantly depend on CMC form. It is know, that incorporation of carboxyl groups into a polysaccharide side chain resulted in an elevation of polymer water sorption ability. Besides hydrogen bonding (characterizing all CMC forms) for a salt polymer form an ion-dipole interaction is inherent in the type of electrostatic salvation. So, the most hygroscopic CMC-Na is able to absorb 20% mass. of water at room temperature, at the same time this value for CMC-H was 9% mass. and for mixed

form – 13% mass. Onset temperature of decomposition of CMC acid form CMC-H was 197°C, for mixed form – 221°C and for CMC-Na – 262°C. Apparently, the presence of free carboxyl groups in acid form CMC-H promotes such reactions as decarboxylation, formation of anhydride bonds and etc., accompanying the thermal transformations of the polymer.

Analysis of data on the mechanical strength investigation of CMC films showed that index of elastic modulus for CMC-H films was higher than for CMC-Na films. Such difference is possibly due to an additional intermacromolecular hydrogen bonds formation in CMC-H as compared to CMC-Na form.

CONCLUSIONS

So, CMC properties essentially depend on CMC polymer forms: CMC-Na, CMC-H and mixed form. The increase in share of CMC-Na links in polymer chain led to an elevation of CMC hygroscopicity. Note, that because of hydrogen bonding system formation CMC-H form films is more strength than CMC-Na films.

ACKNOWLEDGEMENTS

We are grateful to G. N. Bondarenko and **G. A. Shandryuk** for FTIR and TGA/DSC investigations, respectively.

REFERENCES

- [1] Tokura, S.; Nishimura, S.; Sakairi, N.; Nishi, N. (1996) Biological activities of biodegradable polysaccharide. *Macromol. Symp.*, 101, 389–96.
- [2] Sandford, P. A. (1989) In *Chitin and chitosan*. (G. Sjak-Braek, T. Anthonsen, P. A. Sandford, ed.) pp. 51–69, London, U.K.: Elsevier Applied Science.
- [3] Zhao, L.; Mitomo, H.; Nagasawa, N.; Yoshii F.; Kume T. (2003) Radiation synthesis and characteristic of the hydrogels based on carboxymethylated chitin derivatives. *Carbohydr. Polym.*, 51, 2, 169–175.
- [4] Tokura, S.; Miura, Y.; Johmen, M.; Nishi, N.; Nishimura, S. I. (1994) Induction of drug specific antibody and the controlled release of drug by 6-O-carboxymethyl-chitin. *J. Control. Release*, 28, 1–3, 235–241.
- [5] Tokura, S.; Tamura H. (2001) O-carboxymethyl-chitin concentration in granulocytes during bone repair. *Biomacromolecules*, 2, 2, 417–421.
- [6] Vihoreva, G. A.; Gladyshev, D. Yu.; Bazy, M. R.; Barkov, V. V.; Gal'braikh, L. S. (1992) Influence of activating additives on the structure and reactivity of chitin and chitosan, and synthesis of their carboxymethylated derivatives. *Cellul. Chem. Technol.*, 26, 6, 663–674.
- [7] Pretsch, E.; Buhlmann, F. and Affolter, C. (2000) *Structure Determination of Organic Compounds: Tables of Spectral Data*. Springer, Heidelberg.
- [8] Schmidt W. H. (2005) *Optical Spectroscopy in Chemistry and Life Sciences: An Introduction*. Wiley-VCH Verlag GmbH, 384 p.
- [9] Muramatsu, K.; Masuda, S.; Yoshihara, Y.; Fujisawa, A. (2003) In vitro degradation behavior of freeze-dried carboxymethyl-chitin spongers processed by vacuum-heating and gamma irradiation. *Polym. Degrad. Stab.* 81, 327–332.
- [10] Phillips, G. O.; Takigami, S.; Takigami, M. (1996) *Food Hydrocolloids*, 10, 11–19.
- [11] Liu, H., Du, Y., Yang, J. & Zhu, H. (2004). Structural characterization and antimicrobial activity of chitosan/betaine derivative complex. *Carbohydr. Polym.*, 55, 291–297.

THE STUDY OF SOLUBILITY OF COMMERCIAL CHITOSANS WITH DIFFERENT FRACTIONAL COMPOSITION

A.N. Sonina*, G.A. Vikhoreva, L.S. Galbraikh

A.N. Kosygin Moscow State Textile University

**E-mail address: nastyasonina@mail.ru*

INTRODUCTION

The diversity of chitosan-based goods and fields of their use is constantly increasing, as well as the number of sources of initial materials and manufacturers. For this reason, it becomes necessary to characterize the polymer structure more exhaustively, including characteristics of its chemical and physical heterogeneity, and to regulate it in some cases. When cellulose, a natural polymer with the structure close to that of chitosan, is being processed into strong threads, there is a stage where the low-molecular-mass hemi-fraction with a different structure and solubility is washed out of commercial cellulose [1]. In the case of chitosans with low degree of deacetylation, such stage and characterization of the fractional composition are even more desirable. For example, if we want to optimize the conditions of chitosan solution processing into a nanofibrous material using dieless electrical spinning, the degree of deacetylation and the pattern of chitin and chitosan fragment alteration (determining both the surface properties and the bulk ones, such as solubility, structure, rheology, and conductivity) may be among the factors that determine the success of the electrospinning process as well [2].

Chitosan in the form of a polybase is insoluble in water owing to low basicity of amino groups in the polymer and high strength of intermolecular bonds, especially in ordered and crystalline regions of chitosan. Water-soluble substances are chitosan oligomers, as well as partially reacylated chitosan, an unusual kind of copolymer containing approximately equal amounts of alternating chitosan and chitin units. It is also known that titration of dilute water-acid solutions of the polymer, especially low-molecular-weight and low deacetylated specimens, does not cause precipitation of the polymer and the system remains homogeneous virtually up to neutral and alkaline pH [3, 4].

MATERIALS and METHODS

This study concerns the solubility of commercial chitosan specimens with different size of particles (<0.3, ~ 1, and 1-2 mm), molecular masses (190, 340, and 750 kDa) and degrees of deacetylation (0.86, 0.70 and 0.82, respectively) in water and low-concentration (0.1–1.0%) acetic acid solutions at different hydromodules. We used chitosans with amorphous-crystal structure without any step of purification or precipitation. The solubility was calculated according to the data of gravimetric analysis, and the pH value of the mixture was recorded at the end of dissolution. Molecular masses were determined with a viscometer Ubbelode with capillary diameter 0.56 mm using 0.2 M sodium acetate solution in 2% acetic acid to dissolve chitosan and the following equation $[\eta] = 1.38 \times 10^{-4} M^{0.85}$ [5] to calculate the M_{η} value. Degree of substitution for amino groups and degree ionization of its (α) were calculated on the

potentiometric titration data. The potentiometric titration was performed on a PHM 82 pH meter (Radiometer, Denmark) using a combined electrode GK2321C.

RESULTS AND DISCUSSION

The results of solubility determination in water at 5–50°C showed that this value does not exceed 1.5% for chitosans Ch-190 and Ch-340¹. A certain increase in the amount of the eluted component at increasing temperature, just as was assumed, is due to its more complete extraction from broken crystallites. Identification of water-soluble fraction by IR spectroscopy showed that the spectra of the initial and washed specimens (curves 1 and 2 in Fig. 1) are virtually identical, and spectrum 4 of the water-soluble fraction differs, above all, by lesser intensity and lower resolution in the range of pyranose cycle absorption (900–1100 cm⁻¹); this fact indicates presence of admixtures, change in the environment of C–O–C bonds, and low molecular mass of this fraction. Secondly, this spectrum is distinguished by configuration of bands in the 1300–1650 cm⁻¹ range, which is characteristic of ionized carboxyl and amino groups. The presence of the salt form of chitosan in the product, after deacetylation in the alkaline medium and washing with water as the final stages of production, may be due to its formation during neutralization of the alkaline reaction mixture for facilitation of chitosan washing.

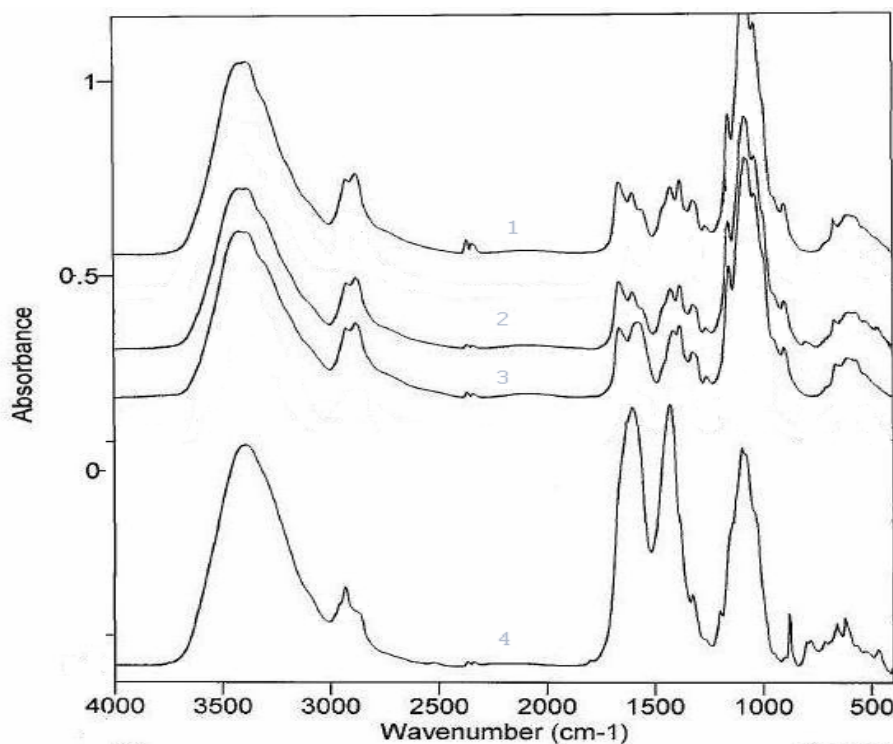


Figure 1 - IR-spectra initial (1) and washed out by water (2) chitosan Ch-190 and fractions: water-soluble (4) and insoluble in 0, 1 % acetic acid (3)

¹ The number in the designation of chitosan corresponds to its molecular weight in kDa.

According to the data of Fig. 2, the yield of soluble fractions increases with increasing acetic acid concentration and hydromodulus as molar parity acid/ NH_2 and a share protonated thus raises.

The visually observable complete solubility of commercial chitosans with deacetylation degree 0.70–0.86 takes place at acetic acid : chitosan molar ratio at least 1.0-1.3, which ensures $\text{pH} < 5.0$ and amino group ionization degree ~ 0.9 (Figs. 3, 4).

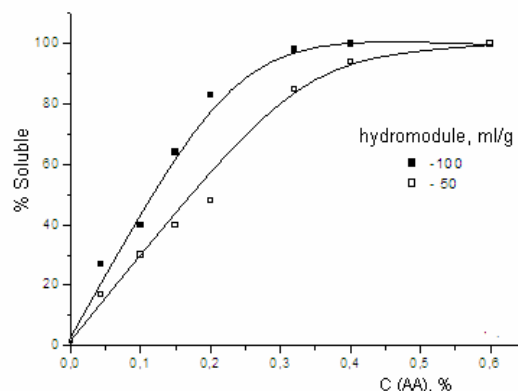


Figure 2 - Dependence of solubility Ch-190 on concentration of acetic acid at the hydromodule 50 (1) and 100 (2)

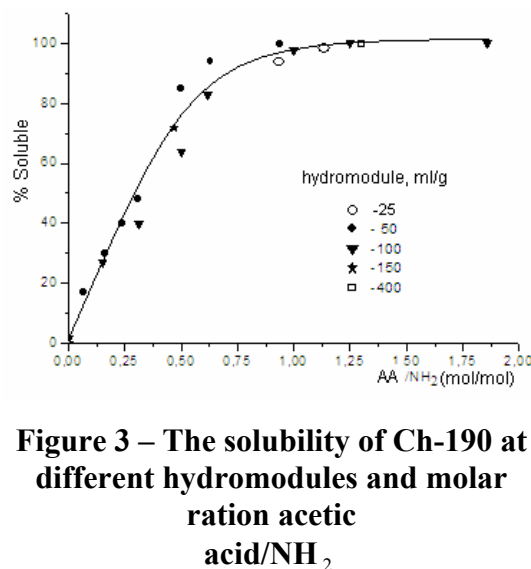


Figure 3 – The solubility of Ch-190 at different hydromodules and molar ration acetic acid/ NH_2

It is natural that the solubility decreases with increasing molecular mass (Fig.5); however, it is unexpected that the solubility increases as the deacetylation degree decreases within the studied range. Note that the deacetylation degree and molecular mass of fractions that are soluble at a low acid : chitosan ratio and low total degree of amino group protonation (0.2-0.25) turned out to be lower than the deacetylation degree and molecular mass of the initial product. This, combined with the higher solubility of less deacetylated Ch-340 and the literature data on water solubility of partially reacetylated chitosan, confirms the conclusion that the solubility of the polymer in neutral media significantly depends on the ratio of acetyl and amino groups in its macromolecules and on the nature of their distribution.

The fraction that was not dissolved in 0.1% acetic acid was not completely dissolved in excess of 0.1 M HCl either. Separation of this fraction by centrifuging showed that, for example, the content of the fraction that is insoluble in excess of strong acid is $\sim 2\%$ in Ch-190 and its degree of deacetylation is very low, below 0.02; i.e., it is virtually chitin. Nevertheless, virtually 100% solubility of Ch-190 in 0.4% acetic acid is attained at 1.3-fold molar amount of the acid. The apparent reason for this fact is more uniform distribution of the aforementioned chitin fraction in the initial polymer than in the product after removal of highly deacetylated fragments.

Estimation of solubility in the experiment on polymer precipitation from the acetic acid solution yields higher values of this parameter (curve 3 in Fig. 4); this fact is due to more equilibrium course of the process in contrast to direct dissolution of the semicrystalline polymer. On the contrary, fractions obtained by deposition from solution at a relatively high total degree of amino group protonation have the highest molecular mass.

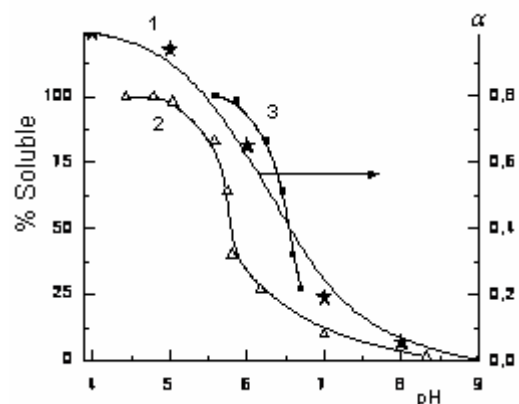


Figure 4 - Influence pH on α (1) and an exit of soluble fractions Ch-190 in the conditions of fractional dissolution (2) and sedimentation (3)

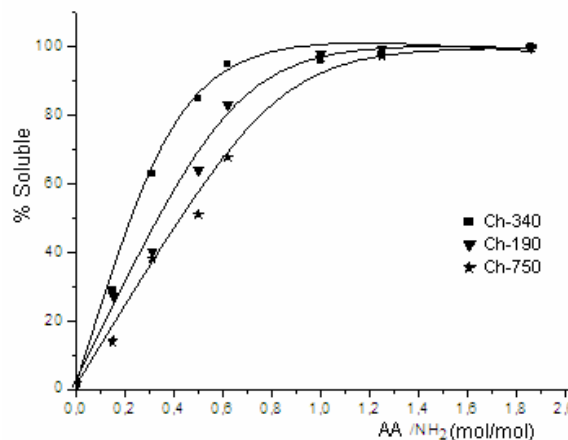


Figure 5 - Solubility of chitosans with different MM and DD

Thus, these results confirm that it is possible to estimate the heterogeneity of polymer structure and obtain polymer fractions that are water-soluble and especially suitable for a number of biomedical applications.

REFERENCES

- [1] Rogovin, Z.A. (1972) Chemistry of cellulose. Chemistry. Moscow.
- [2] Jayakumar, R., Prabakaran, M., Nair, S.V. (2010) Novel chitin and chitosan nanofibers in biomedical applications. *Biotechnology Advances*, 28, 142–150.
- [3] Varum, K.M., Ottoy, M.H., Smidsrod, O. (1994) Water-solubility of partially N-acetylated chitosans as a function of pH: effect of chemical composition and depolymerisation *Carbohydrate Polymers*, 25, 65-70.
- [4] Aiba, S. (1989) Studies on chitosan: 2. Solution stability and reactivity of partially N-acetylated chitosan derivatives in aqueous media *International Journal of Biological Macromolecular*, 11, 4, 249-252.
- [5] Gamzazade, A.I., Shlimak, V.M., Sklyar, A.M. (1985) Investigation of the hydrodynamic properties of chitosan solutions. *Acta Polym.*, 36, 8, 420-424.

OBTAINING OF CHITIN AND CHITOSAN IN THE COMPREHENSIVE TREATMENT PROCESS OF SHELL CONTAINING WASTES OF CRUSTACEANS

N.G. Strokov*, A.V. Podkorytova

*Russian Federal Research Institute of Fisheries and Oceanography
(FGUP "VNIRO"), 17 V.Krasnoselskaya, Moscow, 107140, Russia*

**E-mail: chitosan@vniro.ru*

INTRODUCTION

Currently, great attention is paid to the creation of modern and highly effective comprehensive technologies for processing of raw materials, including aquatic bioresources, for obtaining biologically active substances. The shell containing wastes of crustaceans (SCWC) (shrimps and crabs of different species, Antarctic krill, etc.) are easy to approach raw materials for the creation and implementation of such technologies. Economic effectiveness of SCWC treatment is very low as the wastes are used only as forage products and often dumped overboard or cast off. However, in addition to chitin, the SCWC includes biologically active substances such as carotenoids, lipids, fat-soluble vitamins (A and D), proteins, enzymes and minerals necessary for normal functioning of human organism being valuable components for biologically active food additives.

The standard technology for producing chitin and chitosan from waste of crustaceans involves sequential separation of protein and mineral component of the shell by treating the raw material with alkali and acid reagents, forming a large amount of runoff, which must be collected later and sent to the neutralization, clearance, regeneration [1]. In addition, remain underutilized fat, protein and mineral components of raw materials, which lose their biological activity during the transformation in to unstructured salt forms.

We have developed comprehensive and environmentally friendly technology for production of chitin and chitosan from shell containing raw materials. The technology is based on the use of supercritical carbon dioxide extraction, biotechnological and chemical processes. The comprehensive approach to shell containing wastes treatment is based on obtaining several biologically active products in one technological cycle: carotenoid-lipid complex (CLC), protein hydrolyzate and chitosan, as well as on their subsequent purposeful use.

In this regard, the obtaining process of chitin involves degreasing and bleaching of raw materials, SCWC low-fat enzymolysis followed by removal of the remaining nitrogen and minerals in a single treatment of chitin precipitate with sodium hydroxide and double treatment with hydrochloric acid. For further chitosan obtaining treatment of chitin with highly concentrated alkali is rational.

MATERIALS and METHODS

The shell containing wastes of tiger shrimp *Penaeus monodon* which had been sublimationally dried with temperature 35 degrees below zero, pressure about 0.250, and moisture less than 2%, were used as a raw for getting biologically active substances. Supercritical carbon

dioxide extraction of carotenoid-lipid complex was carried out in industrial mounting KOERS 2 under the pressure of 350 atm., at temperature of 70 °C for 120 min.

The content of carotenoid astaxanthin in the CLC was determined by using spectrophotometrical method on the spectrophotometer APEL PD-303S (Japan), based on carotenoids have maximum level of absorption in the ultraviolet spectrum. The length of a wave, corresponding to a maximum of absorption, is defined by the nature of a carotenoid and properties of solvent. A solution of astaxanthin in chloroform has a maximum of absorption at the length of wave of 490 nanometers.

The content of astaxanthin C (mg of astaxanthin per 100 g of sample) was determined by the formula:

$$C = \frac{D \cdot V \cdot 100}{250 \cdot m},$$

D - optical density of a solution of lipids in chloroform at length of a wave of 490 nanometers;

V - volume of a binary mix, ml;

m - weight of a hinge plate of a crude fabric, g;

250 – average specific factor of absorption of carotenoids ml·sm·mg⁻¹.

RESULTS and DISCUSSION

Shell containing wastes of tiger shrimp was 46.0% and they contain 15.5% of protein, lipids 2.9%, minerals 8.7% and 2.5% chitin.

Mainly organic solvents are used to extract the fat-soluble active substances of various kinds of raw materials. However, in recent years more efficient and environmentally friendly extracting substances are used, specifically carbon dioxide in the supercritical state [2, 3].

Discoloration of shell containing wastes and extraction of carotenoid-lipid complex was carried out using supercritical carbon dioxide extraction. The moisture content in raw materials should not exceed 3-5%. It is found that if moisture in SCWC is above 5% a significant increase in acid number of CLC happens. It indicates a deep hydrolytic decay of CLC under action of water which contributes forming of carbonic acid while carbon dioxide extraction.

Carotenoid-lipid complex is obtained by supercritical carbon dioxide extraction it has good organoleptic characteristics - an oily bright red liquid its smell is peculiar to shrimp fat, with no signs of oxidation. Its high-quality characteristics are: acid and peroxide number is 24.09 mg KOH/g fat and 0.93 mmol O₂/kg. In addition, the carotenoid-lipid complex has a high biological value due to content of carotenoids - astaxanthin, which has antioxidant activity, its content is 14.2 mg/100 g. It is characterized by a high content of polyunsaturated fatty acids, up to 67.0%, including essential acids up to 40.0%.

Yield of astaxanthin is 6.65% while carotenoid-lipid complex supercritical carbon dioxide extraction of SCWC. It is significantly higher yield of CLC than organic solvents extraction method – 3.3%. CLC extracted from SCWC can be a source of polyunsaturated fatty acids and essential fatty acids and used as a component of dietary supplements.

After bleaching and degreasing SCWC ground up to the average particle size of 3-4 mm, thus increasing the active surface of the raw materials, which is good for biotechnological and chemical processes.

Enzymatic hydrolysis is the most appropriate way that allows to keep all the essential and nonessential amino acids, vitamins, carbohydrates, macro-and micronutrients. With that said, the first stage of deproteinization is performed by enzymatic hydrolysis of the enzyme preparations:

Protosubtilin G20H. Its proprieties are: activity 150 units/mg at pH 7.0-7.5 and a temperature of 52 °C. Papain 2% solution (activity of 800-900 units/mg) at pH 6.0-7.0 and a temperature of 50-70 °C. Hydrolysis effectiveness of shell containing wastes from tiger shrimps was determined by the accumulation of free amino nitrogen in hydrolyzates and it was found that the best enzyme for the protosubtilin hydrolysis concentration is 0.5% of suspension mass during 4 hours. Hydrolysis by 2% papain solution continues for 4 hours at enzyme concentration 0.4% of suspension mass, which is more appropriate.

Established that shrimps degree of transition of protein in the liquid phase reaches 66.7% during the enzymatic hydrolysis of shell containing wastes from tiger shrimps as using protosubtilin or papain.

After filtering and fractionation of liquid enzymatic hydrolyzates were subjected to freeze-drying, and chitin containing sediment was sent to demineralization.

Partial removal of proteins under the influence of enzyme preparations can not only shorten the duration of subsequent chemical deproteinization and as a consequence, the entire production cycle, but also to have a product of full value consisting of 70-75% protein, which composition is represented by a complete set of essential and nonessential amino acids.

Minerals were removed from the chitin containing sediment by processing it with a weak solution of hydrochloric acid (HCl 4.0%) for 4-6 hours with a temperature of 85 °C and constant stirring, of the reaction mass. Bath module was 1:6. After the end of demineralization the obtained chitin containing sediment was washed until the pH of the wash water equaled 6.0-6.5.

The second stage of deproteinization was performing with 4.0% solution of sodium hydroxide for 2 hours at a temperature of 20-24 °C with constant stirring of the reaction mass. Bath module was 1:6. After deproteinization reaction mixture was filtered and washed with water to pH 6.0-6.5.

The yield of chitin was 16.2% by weight of fat-free shell containing wastes. Chitin can be used as a standalone product, or managed for chitosan obtaining.

Deacetylation of chitin was carried out in 50.0% solution of sodium hydroxide during 3 hours with a temperature of 100-120 °C. Value of chitin in alkali solution equals 1:20. After the deacetylation reaction mass was filtered and washed with water until neutral, dried at a temperature of 55-60 °C. The yield of chitosan was 87-95% of the weight of dry chitin.

One of the most important indicators of the quality of chitosan is the degree of deacetylation which was 90-98%. The solubility of chitosan in 1% solution of acetic acid is 99.9%, mineral content is 0.3-0.5%.

All products obtained from shell containing wastes of tiger shrimps (CLC, enzymatic hydrolyzates and chitosan) comply with Sanitary standards 2.3.1078-01 on the results of microbiological studies, as well as the content of toxicants and can be used as a food product, microbiological media and components of dietary supplements.

Thus the technology of chitin and chitosan is developed (Figure 1), which allows comprehensive approach, without waste, environment friendly, recycling of underutilized raw materials - shell containing wastes of crustaceans, and obtaining of several biologically active products in one production cycle:

- **the carotenoid-lipid complex** is characterized by a high content of unsaturated fatty acids (up to 60%), including ω -3 and ω -6 acids, it also contains carotenoid - astaxanthin showing a pronounced antioxidant activity. It can be used for creating therapeutic and prophylactic preparations with a wide range of pharmacological properties, cosmetic products, and flavors for food industry.

- **enzymatic hydrolyzate** consists of protein with the extent of 70-75%, its composition being represented by a complete set of essential and nonessential amino acids; it is used for feed and food industries, as well as for microbiological studies aimed at preparing culture media used for microorganisms identification;

- **chitosan** offers a wide range of molecular weights and deacetylation degree by 90-98% and possesses wound healing, antibacterial and sorption properties.

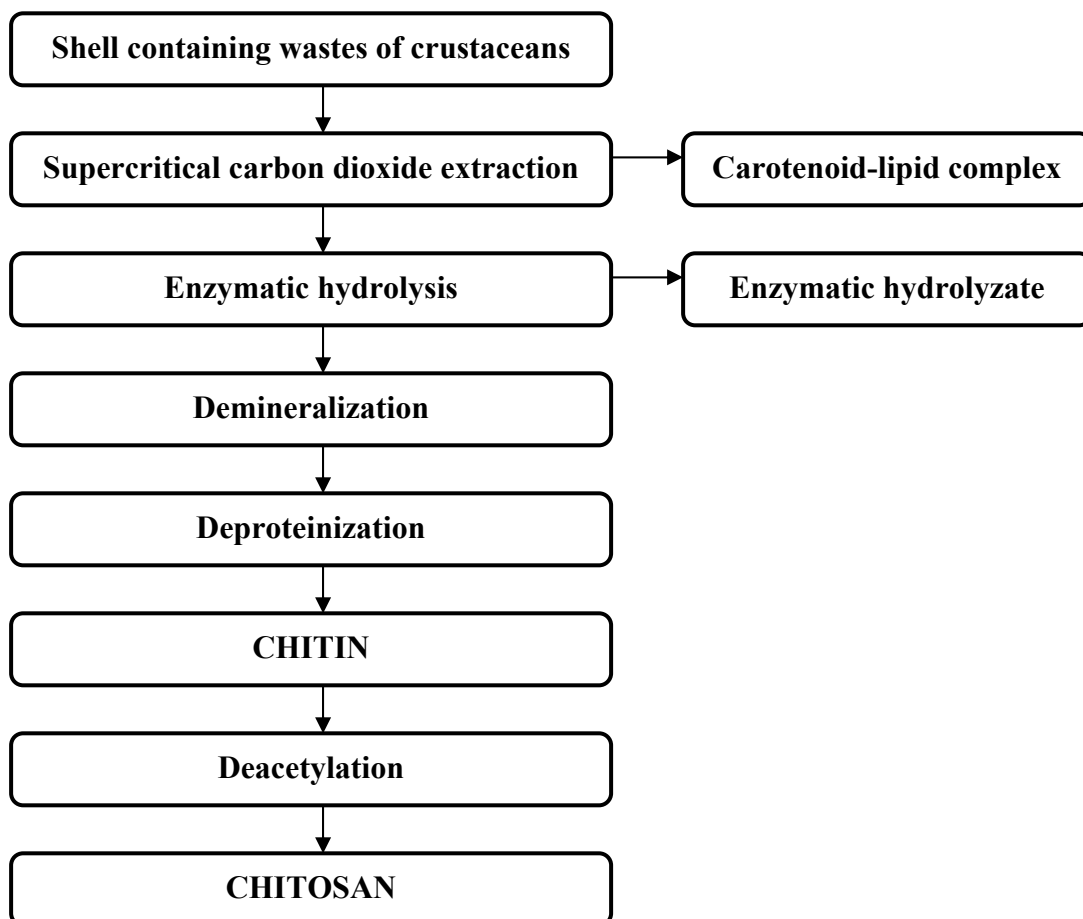


Figure 1. The flow sheet of complex processing SCWC

REFERENCES

- [1] Muzzarelli R.A.A. (1997) Chitin Handbook. European chitin society.
- [2] Heidi Brogle (1982) CO₂ as a solvent: its properties and applications in Chemistry and Industry pp. 21 – 23.
- [3] McHugh M.A., Krukonis V.J. (1986) Supercritical fluid extraction: principles and practice.

CHITIN OLIGOSACCHARIDES ATTENUATED TRANSFORMING GROWTH FACTOR BETA 1-INDUCED PULMONARY FIBROSIS THROUGH HUMAN ALVEOLAR EPITHELIAL CELLS TRANSFORMATION

Quang Van Ta¹, Chang-Suk Kong², Se-Kwon Kim^{1,2*}

¹*Department of Chemistry, Pukyong National University, Busan 608-737, Republic of Korea*

²*Marine Bioprocess Research Center, Pukyong National University, Busan 608-737, Republic of Korea*

**E-mail address: sknkim@pknu.ac.kr*

INTRODUCTION

Idiopathic pulmonary fibrosis (IPF) is a progressive and lethal disease. Current treatments for IPF show poor efficiency and do not prevent disease progression or reduce the high mortality rates [1]. It is now well recognized from that a number of growth factors and cytokines, such as transforming growth factor-beta 1 (TGF- β 1), interleukin-1 beta (IL-1 β), tumor necrosis factor-alpha (TNF- α), are able to induce fibrogenesis through inducing epithelial cells transformation. Among them, TGF- β 1 has an important role in regulation of pulmonary inflammation and fibrosis. Furthermore, TGF- β 1 treatment induces alveolar epithelial cells transition to mesenchymal cells with a myofibroblast-like phenotype [2, 3]. Chitin and its derivatives have important biological properties such as angiotensin-I converting enzyme (ACE-I) inhibition, matrix metalloproteinases (MMPs) enzyme inhibition [4, 5], myoperoxidase inhibition [6], acetylcholinesterase inhibition [7], anti-cancer [8], anti-allergy [9]. Chitin oligosaccharides or N-acetyl chito-oligosaccharides (NA-COSs) are hydrolyzed products of chitin and until now, there are no reports on their activities against fibrosis on cellular systems. Therefore, in this study, we investigated the inhibitory effect of NA-COSs on TGF- β 1-induced fibrosis through promoting human epithelial cells transformation. Our results demonstrated that NA-COSs inhibit TGF- β 1 induced changes in human alveolar epithelial cells included E-cadherin, α -SMA, MMP-2 and collagen type I protein expression. These results suggested that NA-COSs have potential benefit in prevention of TGF- β 1 induced lung fibrosis.

MATERIALS and METHODS

Cytotoxicity level of A549 cells was measured using MTT assay. Cells were seeded at a density of 3×10^3 cells per well onto 96-well plate. After overnight attachment, cells were maintained in serum-free DMEM containing 0.25% bovine serum albumin (BSA) for 24 h. On the next day, new serum-free media was replaced and cells were incubated with different concentration of NA-COSs. After 48 h incubation, MTT assay were performed. The data are expressed as means from at least three independent experiments and $p < 0.05$ was considered significant.

After 48 h incubation with TGF- β 1, cells were used for immunocytochemistry staining. Cells were then incubated with anti E-cadherin, anti fibronectin, anti α -tubulin, and anti α -SMA antibodies. Expression of proteins were detected by incubating with goat anti mouse Alexa 545 and donkey anti goat Alexa 488. Cells nuclei were visualized by staining with 1 μ g/ml (w/v) Hoescht-33258 dye.

Total proteins were collected and western blot was performed as previously described [5] with specific anti-E-cadherin, anti- α -tubulin, anti- β -tubulin, anti-collagen type I, and anti- α -SMA antibodies.

Results are shown as mean \pm SD. The comparison of different groups was carried out using two-tailed unpaired Student's *t*-test and differences at or under to $p < 0.05$ were considered statistically significant and reported as in legends.

RESULTS and DISCUSSION

The result showed that, NA-COSs have no cytotoxicity effect on A549 cells even at 1000 μ g/ml of concentration of NA-COSs (Fig. 1). At high concentration of NA-COSs, A549 cells showed no reduction in cell viability.

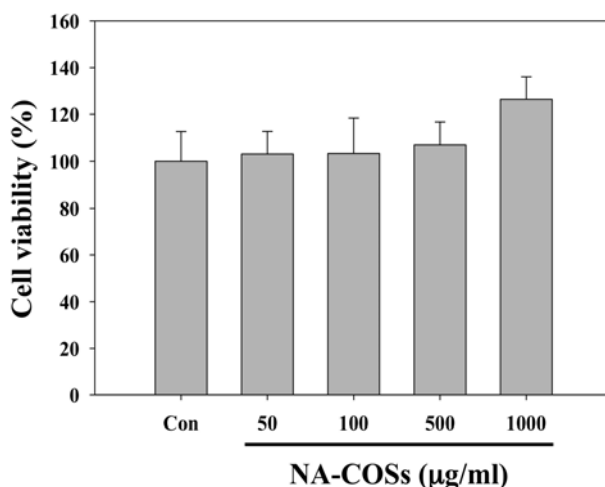


Figure 1. Effect of NA-COSs on viability of human alveolar epithelial cells (A549)

In the presence of 2.5 ng/ml TGF- β 1, the morphology of A549 cells changed from the classical cobblestone appearance of alveolar epithelial cells to predominantly elongated fibroblast-like cells (Fig. 2). At 500 μ g/ml concentration of NA-COSs, A549 cells showed no change in cell morphology. In addition, pre-treatment with NA-COSs did not affect cells morphology in the presence of TGF- β 1. This result suggested that NA-COSs may have prevention effect on TGF- β 1-induced change in cell morphology.

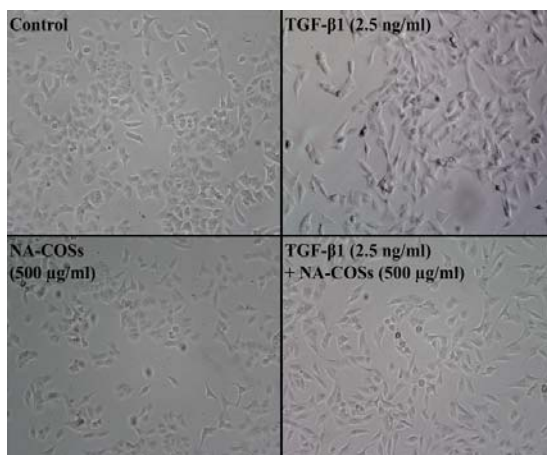


Figure 2. Effect of NA-COSs on TGF- β 1-induced change in alveolar epithelial cells (A549) morphology

The immunocytochemistry staining figures and western blot data showed that A549 cells decreased expression of E-cadherin after 48 h incubation. However, NA-COSs did not show affect on E-cadherin expression in A549 cells. At 500 $\mu\text{g/ml}$ concentration of NA-COSs, A549 cells increased expression E-cadherin which was suppressed by TGF- β 1-induced transformation (Fig. 3). In addition, TGF- β 1-induced transformation resulted in increase expression of fibronectin which is the marker of mesenchymal cells. Pre-treatment with 500 $\mu\text{g/ml}$ concentration of NA-COSs attenuated the expression of fibronectin in A549 in presence of TGF- β 1 (Fig. 3A).

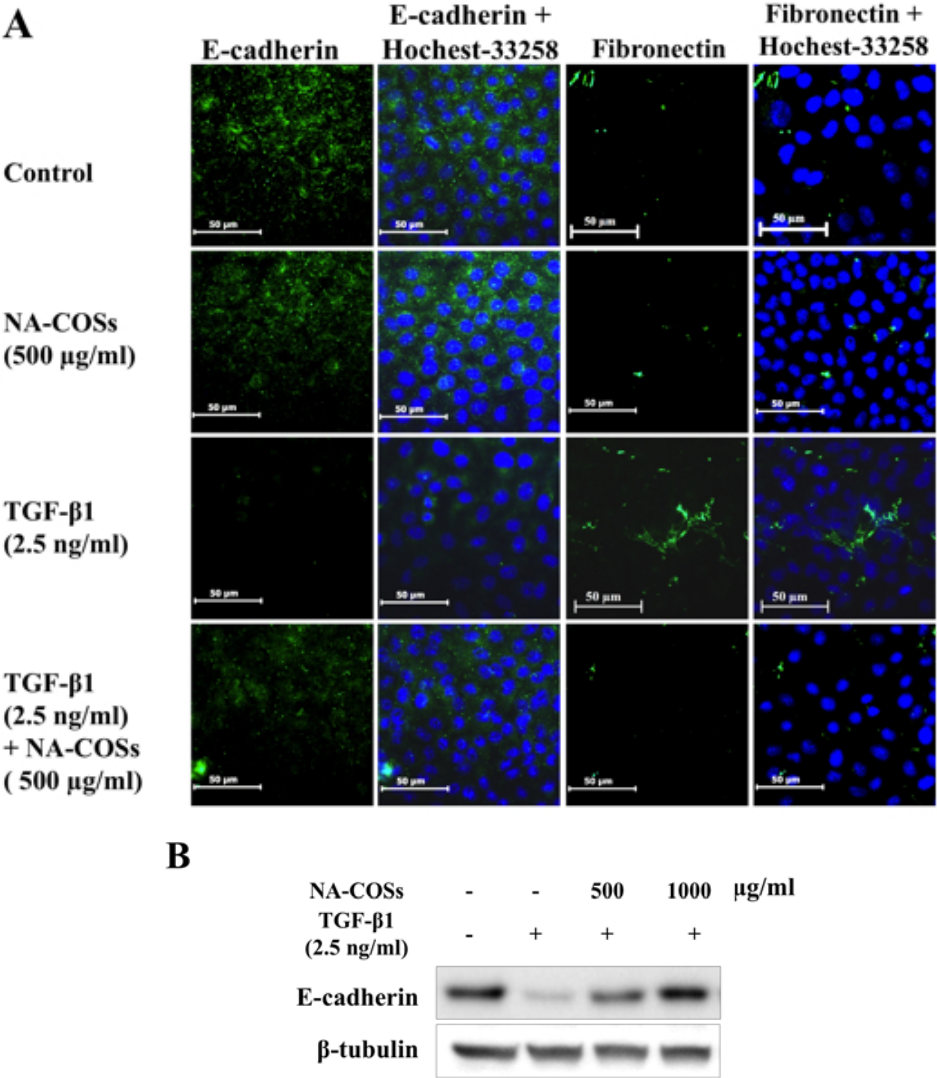


Figure 3. Effect of NA-COSs on TGF- β 1-induced changes in E-cadherin and fibronectin protein expression.

In our study, A549 cells increased expression of α -SMA after treatment with TGF- β 1 for 48 h but did not increase in NA-COSs treated group (Fig. 4A). However, pre-treatment with NA-COSs showed decrease of α -SMA in the presence of TGF- β 1 dose dependent manner (Fig. 4B). In addition, we observed that the increase of acetylated α -tubulin after treatment with TGF- β 1. Immunocytochemistry and western blot data have shown that acetylated α -tubulin increased in TGF- β 1 treated group but did not increase in control and NA-COSs treated groups (Fig. 4A).

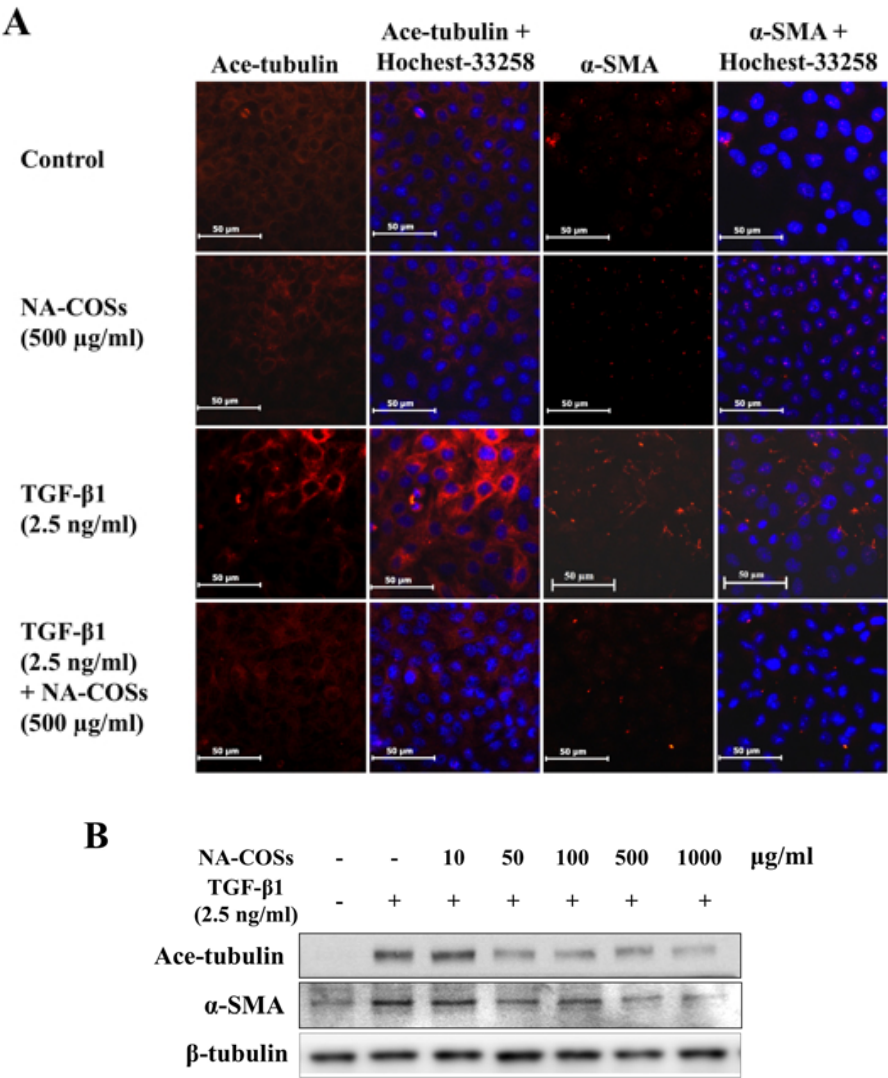


Figure 4. Effect of NA-COSs on TGF-β1-induced change in α -tubulin acetylation and α -SMA protein expression

In the presence of 2.5 ng/ml TGF- β 1, collagen type I and MMP-2 proteins induced expression compare with control group. However, collagen type I and MMP-2 protein level has down-regulated in pre-treatment NA-COSs groups (Fig. 5).

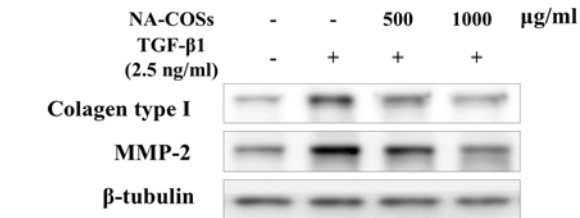


Figure 5. Effect of NA-COSs on TGF-β1-induced changes in collagen type I and MMP-2 protein expression.

The present research showed that NA-COSs can prevent down-regulation of E-cadherin in TGF-β1-induced cells. In addition, they also prevent up-regulation of fibroblast markers, such as fibronectin and α -SMA. Furthermore, NA-COSs can decrease expression of mobility proteins, such as actylated α -tubulin, collagen type I, and MMP-2. Base on these results, it has shown that NA-COSs can attenuat TGF-β1-induced alveolar epithelial cell transformation. We suggest that NA-COSs can be used as agents which can prevent fibrosis induce by TGF-β1 in cellular

systems. Moreover, NA-COSs have beneficial applications in future not only in cellular fibrosis but also in cellular metastasis.

ACKNOWLEDGEMENTS

The authors acknowledge Marine Bioprocess Research Center of Marine Bio 21 Project, funded by the Ministry of Land, Transport and Maritime Affairs, Republic of Korea.

REFERENCES

- [1] Tan, X. H., Dagher, H., Hutton, C. A., Bourke, J. E. (2010) Effects of PPAR γ Ligands On TGF- β 1-Induced Epithelial-Mesenchymal Transition In Alveolar Epithelial Cells. *Respir Res.*, 11, 21
- [2] Kasai, H. Allen, J. T., Mason, R. M., Kamimura, T., Zhang, Z. (2005) TGF- β 1 Induces Human Alveolar Epithelial To Mesenchymal Cell Transition (EMT). *Respir Res.*, 6:56
- [3] Câmara, J., Jarai, G. (2010) Epithelial-Mesenchymal Transition In Primary Human Bronchial Epithelial Cells Is Smad-Dependent And Enhanced By Fibronectin And TNF- α . *Fibrogenesis & Tissue Repair*, 3, 2
- [4] Kim, M. M., Kim, S. K. (2006) Chitooligosaccharides Inhibit Activation And Expression Of Matrix Metalloproteinase-2 In Human Dermal Fibroblasts. *FEBS Letters*, 580, 2661-2666.
- [5] Ta, V. Q., Kim, M. M., Kim, S. K. (2006) Inhibitory Effect Of Chitooligosaccharides On Matrix Metalloproteinase-9 In Human Fibrosarcoma Cells (HT1080). *Mar Biotechnol*, 8, 593-599.
- [6] Ngo, D. N., Qian, Z. J., Je, J. Y., Kim, M. M., Kim, S. K. (2008) Aminoethyl Chitooligosaccharides Inhibit The Activity Of Angiotensin Converting Enzyme. *Process Biochemistry*, 43, 119-123.
- [7] Yoon, N. Y., Ngo, D. N., Kim, S. K. (2009) Acetylcholinesterase Inhibitory Activity Of Novel Chitooligosaccharide Derivatives. *Carbohydr Polym*, 78, 869-872.
- [8] Kim, S. K., Ngo, D. N., Rajapakse, N. (2006) Therapeutic Prospective Of Chitin, Chitosan And Their Derivatives. *Journal of Chitin and Chitosan*, 11, 1-10.
- [9] Vo, T. S., Kong, C. S., Kim, S. K. (2011) Inhibitory Effects Of Chitooligosaccharides On Degranulation And Cytokine Generation In Rat Basophilic Leukemia RBL-2H3 Cells. *Carbohydr Polym*, 84, 649-655.

ANTIBACTERIAL ACTIVITY OF OLIGOCHITOSAN AGAINST METHICILLIN-RESISTANT STAPHYLOCOCCUS AUREUS (MRSA): MOLECULAR WEIGHT AND pH EFFECTS

Sergey Kulikov¹, Evgeniya Bezrodnykh², Ruslan Khairullin¹, Yulia Philippova³, Sergey Lopatin⁴, Igor Yamskov², Vladimir Tikhonov^{2*}

¹ Kazan Scientific Research Institute of Epidemiology and Microbiology, Kazan, Russia.

² A.N. Nesmeyanov Institute of Organoelement Compounds, Russian Academy of Sciences, Moscow, Russia.

³ Kazan Federal University, Kazan, Russia.

⁴ Centre "Bioengineering", Russian Academy of Sciences, Moscow, Russia.

*E-mail address: tikhon@ineos.ac.ru

INTRODUCTION

The analysis of indoor-air bacteria shows that mostly collected in hospitals, public buildings, and aircraft cabins is Gram-positive *Staphylococcus aureus* that can cause a wide variety of diseases in humans and animals through either toxin production or penetration. Patients with a compromised immune system are often at risk of developing infections. These infections are more of a threat to the patients because *S. aureus* is becoming more and more resistant to many commonly used antibiotics including penicillin, amoxicillin, tetracycline, erythromycin, linezolid, vancomycin, and methicillin [1]. Increased problems with human allergy have been also observed in the patients receiving antibiotic agents for treatment. As a result, benefits and safety of many biocides are the subjects of debates among regulators specializing in medicine, food, cosmetics, environmental sciences, and toxicology. Therefore, there is a need for non-toxic new biocides that could be topically active against broad spectrum of the invasive and noninvasive human pathogens and could reduce the level of administration of classic antibiotics.

Chitosan produced by a partial or complete deacetylation of chitin represents a collective name for a group of polysaccharides consisting of glucosamine and N-acetylglucosamine or glucosamine only. Oligochitosan may be considered as a chitosan having much lower molecular weight (MW) and viscosity than the parent chitosan or, in other words, as a mixture of lowest and highest chitooligosaccharides. Oligochitosan can be produced by depolymerization of a high molecular weight (HMW) chitosan. Numerous investigations of antimicrobial activity of chitosan and oligochitosan against many bacteria, filamentous fungi and yeasts have been published so far, and nowadays it is commonly accepted that antimicrobial activity of chitosan depends on its MW and degree of deacetylation (DD) and experimental conditions but controversial evidences for a correlation between biocidal activity and MW of chitosan have been found.

In our opinion, the controversial results concerning biocidal activity and its correlation with MW of chitosan have been found mainly because so far most investigators either have used only few chitosan samples, and molecular weight distribution/polydispersity haven't taken into account. That is, some of the biological effects reported for chitosan may be caused by the presence of lowest and highest chitooligosaccharides in chitosan. This means that every sample before investigating also must be characterized by its polydispersity ($MW/MN = PI$). The controversy may be also caused by the presence of by-products and variation in the chemical structure of end-units and acetyl-group distribution along polysaccharide chain of oligochitosans due to the differences in methods used for hydrolysis of HMW chitosan.

In this paper, we describe the preparation of well-characterized oligochitosan samples varying in MW and having narrow polydispersity as well as their bactericidal activities against methicillin-resistant *S. aureus* focusing on the MW-activity relationship at different pH values in order to evaluate the potential of oligochitosan as a possible alternative to the application of classic antibiotics and chemical biocides. However, we totally realize that it can't be the only remedy in all cases.

MATERIALS and METHODS

Preparation of oligochitosan: low molecular weight (LMW) chitosan (M_v 70 kDa, DD 80 mol.%) used for preparation oligochitosan samples was purchased from ALDRICH. LMW chitosan was dissolved in hydrochloric acid, and the solution heated at 70°C. Oligochitosan hydrochloride was precipitated with ethanol (1:3 v/v) and dried in vacuum over solid sodium hydroxide. Oligochitosan stock solutions were filtrated through a 0.22 μ m pore-size syringe filter (Millipore, Swinnex) and stored at 4°C until usage.

Molecular weight and polydispersity: The weight-average (M_w) and number-average (M_n) molecular weights and polydispersity indexes ($PI=M_w/M_n$) of oligochitosan samples were determined by SEC-HPLC method described in [2]. Monodispersed dextrans (M_w 1080, 4440, 9890, 43500, 66700, 123600, and 196300 Da (SIGMA) were used as calibration standards.

Degree of deacetylation (DD, mol. %) was determined by 1H -NMR method [3].

Bacterial strains and antibacterial test condition: The strain of methicillin-resistant *S. aureus* ATCC 35591 used in the studies was obtained from State Research Institute for Standardization and Control of Medical Biological Preparations (Moscow, Russia). The bacterial strain subcultured fortnightly was maintained on the plates with the standard B-medium (1% tryptone, 0.5% yeast extract, 0.5% NaCl, 0.1% K_2HPO_4 , 0.1% glucose, 12 g/liter agar) at 4°C and used as a starting inoculum culture. Bacteria stock solution (30ml) was prepared by the use of 5% (v/v) inoculum.

Minimal inhibition concentration (MIC) of oligochitosan samples were determined by a broth microdilution assay in accordance with modified method described in [4]. Briefly, a set of 2-fold serially diluted oligochitosan solutions in 0,1M TES-MES buffers (pH values are shown in Table 2) were prepared in a sterile 96-well polystyrene microplate. The microplate containing oligochitosan solution (100 μ l each) and bacterial cells in amount of 2×10^5 CFU per ml was incubated at 37°C for 48 h. Growth of the tested microorganism was monitored at 590 nm every 6 h for 48 h by an ELISA reader (Biolog, Hayward, CA). The MIC was defined as the lowest concentration of oligochitosan required for complete inhibition of bacterial growth at the described conditions. All experiments were carried out in triplicate.

RESULTS and DISCUSSION

Oligochitosan preparation and characterization

There are several chemical methods for deep depolymerization of chitosan including acidic and enzymatic depolymerization as well as by means of nitrous acid (sodium nitrite), periodic acid (sodium periodate), and hydrogen peroxide. In order to prepare a set of oligochitosan samples differing in molecular weights we chose the most investigated method which has been used for depolymerization of LMW chitosan, namely the depolymerization of chitosan by hydrochloric acid. This method was chosen since a) it doesn't require the usage neither of an expensive purified form of chitosanolytic enzyme nor a cheaper complex of chitosanolytic enzymes whose usage requires separation of oligochitosan from foreign matters [5-7]; b) its impact on the chemical structure of chitosan is minimal in comparison with the method that uses

hydrogen peroxide [8, 9]; c) the product doesn't have reactive aldehyde end-groups capable of producing of Schiff-bases and other by-products which are formed during depolymerization of chitosan by means of nitrous acid (sodium nitrite) or periodic acid (sodium periodate) [10-12].

The method of chitosan depolymerization in hydrochloric acid solution is highly specific, and the cleavage between two conjunct N-acetylglucosamine units and between N-acetylglucosamine-glucosamine units mainly occurs [13, 14].

The process of chitosan depolymerization was carried out in 6M HCl at 70 °C for 1÷6 h and led to the cleavage of glycosidic bonds and formation of oligochitosan of much lower MW depending on the duration of chitosan hydrolysis. After acidic hydrolysis, oligochitosan samples were analyzed by SEC-HPLC method to determine their MW and PI. Partial deacetylation was also observed, so that the degrees of deacetylation of oligochitosans obtained after the acidic hydrolysis (Table 1) were much higher (DD 94÷99 mol. %) than that of the parent chitosan in accordance with previously published data [15], except for sample 7 (DD 78 mol.%). No significant differences in FTIR spectra between oligochitosan samples were observed except for sample 7 (DP 32) where the increased intensity of C=O (amide I) stretching band at 1615 cm⁻¹ occurred (data not shown).

As a result, twelve oligochitosan samples having MW in the range of 0.73÷19.99 kDa and a low polydispersity were obtained (Table 1). These samples were used in the experiments with *S. aureus*.

Table 1. Characteristics of oligochitosan samples

Sample number	M _w ±0.03 kDa	PI±0.08	DP*	DD±1 (mol. %)
1	0.73	1.41	4	95
2	1.52	1.39	8	93
3	2.09	1.40	12	97
4	2.28	1.34	13	97
5	3.58	2.71	20	95
6	4.22	1.38	24	97
7	5.52	1.92	32	78
8	8.30	1.50	49	99
9	9.68	1.44	56	97
10	12.76	1.39	74	95
11	15.05	1.61	87	94
12	19.99	1.66	116	98

*- average degree of polymerization was calculated in accordance with DD values

Antibacterial activity of oligochitosan towards S. aureus

From the practical point of view, oligochitosan has several advantages over chitosan: a) oligochitosan solution has a very low viscosity; b) oligochitosan is more compatible with surfactants, stabilizers and emulsifiers, sugars, 40% ethanol, salt, glycerin, organic acids and colorants so that its application has no undesirable impact on the physicochemical properties of consumer goods; c) application of oligochitosan in pharmaceutical, textile, cosmetic and food products does not interfere with the current technologies used.

The published data concerning the biocidal activity of oligochitosan against *S. aureus* contain the controversial results on the relationship between MW and activity of oligochitosan as well as chitosan, and these data are as controversial as the data for other bacteria tested. Thus, HMW chitosans (M_w 28÷1671 kDa) were found to be more active ($MIC \geq 800 \mu\text{g/ml}$) in comparison with oligochitosans having M_w 1÷22 kDa (DD values were not shown) [16]. Ultramicroscopic studies revealed that, chitooligosaccharides ($MW < 3$ kDa, DD not shown) were less active than HMW chitosan (MW 628 kDa, DD 80-85%) towards *S. aureus* whereas the opposite was true for *E. coli* [17]. Among chitooligosaccharides ($MW < 5$ kDa; DD 80-85%) and HMW chitosans (MW 107÷628 kDa, DD 80-85%), the first ones exhibited the lowest activity. The MIC varied from 1000 $\mu\text{g/ml}$ in the case of HMW chitosan to 2300 $\mu\text{g/ml}$ in the case of chitooligosaccharides [19]. Low molecular weight chitosan with the viscosity-average molecular weight ranged from 5 kDa to 27 kDa (DD 85%) showed a low activity ($MIC \geq 1000 \mu\text{g/ml}$) towards *S. aureus* [19]. The absence of the statistically reliable differences was found between three separate fractions of chitooligosaccharides MW 10÷5, 5÷1 and < 1 kDa (DD not shown). All these fractions had MIC 600 $\mu\text{g/ml}$ for *S. aureus* [20]. The controversial data on the activity of a series of the well-defined chitosan samples (M_w 1.4÷400 kDa, DD 85-88%) against *S. aureus* was found in [21] where it was shown that chitosan activity increased in the row $17 > 2.8 > 1.4$ kDa and reduced in the row $78 > 17 > 48 > 130 > 400$ kDa while half-N-acetylated chitosan and chitooligomers had no significant antimicrobial activity. No activity at all was found for enzymatically produced oligochitosan samples with $MW < 8$ kDa, MW 10.1 kDa and MW 12.0 kDa although some samples with MW 11÷15 were active and had MIC 400÷1600 $\mu\text{g/ml}$. Despite that in the agreement with the earlier found DD-activity relationship, antibacterial effect of active oligochitosan samples was higher in the case of samples with DD 92% than that of samples having DD 80% [22]. And only once it was demonstrated that MW of chitosan did not influence antibacterial activity of chitosan against *S. aureus* at all [23].

As reviewed above, in most cases oligochitosan samples were not characterized by PI and DD values, and only few oligochitosan samples were used in many of earlier studies. Therefore, there is a lack of data on biocidal activity of oligochitosans against *S. aureus*, and the basic question which we ought to clarify first of all is what molecular weight does oligochitosan has to have in order to possess the highest biocidal activity against *S. aureus* at neutral pH values?

As seen in Table 2, oligochitosans markedly inhibit the growth of *S. aureus*, while the activity is affected by pH. Oligochitosan samples 1 and 2 with lowest molecular weights (DP 4 and 8) exhibit the lowest activity in pH ranged from 5.5 to 8.00. Their MIC values are found to be not less than 1000 $\mu\text{g/ml}$. Samples 5÷12 (DP 20÷116) demonstrate the highest activity at pH values which are very close to neutral ones (pH 6.00÷6.75). The activity reduces with increase in pH since partial deprotonation of amino-groups of oligochitosan at basic pH lead to decrease in its bactericidal activity. Only samples 5÷7 (DP 20÷32) possess moderate activity at neutral and basic pH 7.00÷7.75. Nevertheless, the activity of samples 5÷12 (DP 20÷116) is higher at pH 6.5 than that at pH 5.5 in contradiction to the data published in [24]. These results indicate that oligochitosan samples 5÷12 can be used even at neutral pH.

Table 2. MICs ($\mu\text{g/ml}$) of oligochitosan samples at different pH

pH	DP									
	4	8	12	20	24	32	56	74	87	116
5.50	≥ 100 0	≥ 100 0	416	83	104	125	31	31	31	31
5.75	≥ 100 0	≥ 100 0	250	83	83	104	31	31	31	31
6.00	≥ 100 0	≥ 100 0	250	62	62	62	26	26	26	26
6.25	≥ 100 0	≥ 100 0	250	52	52	62	15	13	13	13
6.50	≥ 100 0	≥ 100 0	416	52	52	62	8	8	8	8
6.75	≥ 100 0	≥ 100 0	500	83	62	104	8	8	8	8
7.00	≥ 100 0	≥ 100 0	833	166	104	125	250	250	250	250
7.25	≥ 100 0	≥ 100 0	≥ 100 0	250	208	250	500	500	500	500
7.50	≥ 100 0	≥ 100 0	≥ 100 0	500	500	500	≥ 100 0	≥ 100 0	≥ 100 0	≥ 100 0
7.75	≥ 100 0	≥ 100 0	≥ 100 0	833	833	833	≥ 100 0	≥ 100 0	≥ 100 0	≥ 100 0
8.00	≥ 100 0	≥ 100 0	≥ 100 0	≥ 100 0	≥ 100 0	≥ 100 0	≥ 100 0	≥ 100 0	≥ 100 0	≥ 100 0

REFERENCES

- [1] Donadio, S., Maffioli, S., Monciardini, P., Sosio, M., Jabes, D. (2010) Antibiotic discovery in the twenty-first century: current trends and future perspectives. *J. Antibiotics*, 63, 423-430.
- [2] Lopatin, S.A., Derbeneva, M.S., Kulikov, S.N., Varlamov, V.P., Shpigun, O.A. (2009) Fractionation of chitosan by ultrafiltration. *J. Anal.Chem.*, 64, 648-51.
- [3] Hirai, A., Odani, H., Nakajima, A. (1991) Determination of degree of deacetylation of chitosan by ^1H NMR spectroscopy. *Polym. Bull.*, 26, 87-94.
- [4] Raafat, D., Barga, K., Haas, A., Sahl, H.G. (2008) Insight into the mode of action of chitosan as an antibacterial compound. *Appl. Env. Microbiol.*, 74, 3764–3773.
- [5] Kim, S.K., Rajapakse, N. (2005) Enzymatic production and biological activities of chitosan oligosaccharides (COS): A review. *Carbohydrate Polymers*, 62, 357-368.
- [6] Ilyina, A.V., Tikhonov, V.E., Albulov, A.I., Varlamov, V.P. (2000) Enzymatic preparation of acid-free-water soluble chitosan. *Process Biochemistry*, 35, 563-568.

- [7] Aam, B.B., Heggset, E.B., Norberg, A.L., Sørli, M., Vårum, K.M., Eijssink, V.G.H. (2010) Production of chitooligosaccharides and their potential application in medicine. *Mar. Drugs*, 8, 1482-1517.
- [8] Tian F., Liu Y., Hu, K., Zhao B. (2004) Study of the depolymerization behavior of chitosan by hydrogen peroxide. *Carbohydrate Polymers*, 57, 31-37.
- [9] Qin, C.Q., Du, Y.M., Xiao, L. (2002) Effect of hydrogen peroxide treatment on the molecular weight and structure of chitosan. *Polym. Degrad. Stab.*, 76, 21-218.
- [10] Allan, G.G., Peyron, M. (1995) Molecular weight manipulation of chitosan II: prediction and control of extent of depolymerization by nitrous acid. *Carbohydr. Res.*, 277, 273-282.
- [11] Tømmeraas, K., Vårum, K.W., Christensen, B.E., Smidsø, O. (2007) Preparation and characterization of oligosaccharides produced by nitrous acid depolymerization of chitosan. *Carbohydr. Res.*, 333, 137-144.
- [12] Vold, I.M.N., Christensen, B.E. (2005) Periodate oxidation of chitosans with different chemical compositions. *Carbohydr. Res.*, 340, 679-684.
- [13] Einbu, A., Grasdalen, H., Vårum, K.W. (2007) Kinetics of hydrolysis of chitin/chitosan oligomers in concentrated hydrochloric acid. *Carbohydr. Res.*, 342, 1055-1062.
- [14] Einbu, A., Vårum, K.W. (2007) Depolymerization and de-N-acetylation of chitin oligomers in hydrochloric acid. *Biomacromolecules*, 8, 309-314.
- [15] Vårum, K.W., Ottøy, M.H., Smidsø, O. (2001) Acid hydrolysis of chitosan. *Carbohydrate Polymers*, 46, 89-98.
- [16] No, H.K., Park, N.Y., Lee, S. H., Meyers, S.P. (2002) Antibacterial activity of chitosans and chitosan oligomers with different molecular weight. *Int. J. Food Microbiol.*, 74, 65-72.
- [17] Eaton, P., Fernandes, J.C., Pereira, E., Pintado, M.E., Malcata, F.X. (2008) Atomic force microscopy study of the antimicrobial effects of chitosans on *Escherichia coli* and *Staphylococcus aureus*. *Ultramicroscopy*, 108, 1128-1134].
- [18] Fernandes, J.C., Tavaría, F.K., Soares, J.C., Ramos, Ó.S., Monteiro, M.J. (2008) Antimicrobial effects of chitosans and chitooligosaccharides, upon *Staphylococcus aureus* and *Escherichia coli*, in food model systems. *Food Microbiol.*, 25, 922-928.
- [19] Gerasimenko, D.V., Avdienko, I.D., Bannikova, G.E., Zueva, O.Yu., Varlamov, V.P. (2004) Antibacterial effects of water-soluble low-molecular-weight chitosans on different microorganisms. *Applied Biochemistry and Microbiology*, 40, 253-257.
- [20] Jeon, Y.J., Park, P.J., Kim, S.K. (2001) Antimicrobial effect of chitooligosaccharides produced by bioreactor. *Carbohydrate Polymers*, 44, 71-76.
- [21] Qin, C., Li, H., Xiao, Q., Liu, Y. Zhu, J. Du, Y. (2006) Water-solubility of chitosan and its antimicrobial activity. *Carbohydrate Polymers*, 63, 367-374.
- [22] Lin, S.B., Lin, Y.C., Chen, H.H. (2009) Low molecular weight chitosan prepared with the aid of cellulose, lysozyme and chitinase: Characterization and antibacterial activity. *Food Chemistry*, 116, 47-53.
- [23] Han, Y., Jeon, D. (2004) Antibacterial activity of chitosan against *Staphylococcus aureus* – The effect of water-solubility, degree of deacetylation and molecular weight of chitosan on antimicrobial activity. *J. Korean Soc. Cloth. Text.*, 28, 807-818.
- [24] Wang, G.H. (1992) Inhibition and inactivation of five species of food-born pathogens by chitosan. *J. Food Prot.*, 55, 916-919.

EFFECT OF PREPARATION CONDITIONS ON PHYSIOCHEMICAL PROPERTIES AND PHYTIC ACID ADSORPTION OF CHITOSAN/TRIPOLYPHOSPHATE/GENIPIN CO-CROSSLINKED BEADS

Min-Lang Tsai*, Chin-Yo Yang

Department of Food Science, National Taiwan Ocean University, 2 Pei-Ning Road, Keelung 20224, Taiwan, R.O.C.

*E-mail: tml@mail.ntou.edu.tw

INTRODUCTION

Chitosan (Figure 1A) is a high molecular weight polysaccharide and is composed of glucosamine and *N*-acetyl-glucosamine. It is a widely distributed biopolymer due to its ready availability, with cationic polyelectrolyte in acid solution, and, due to its non-toxicity and biodegradability. Chitosan is considered to be both a versatile and an environmentally friendly raw material. It can be applied in food processing, agriculture, biomedicine, biochemistry, wastewater treatment, paper, textiles, cosmetics, nanoparticles, hydrogel, liquid crystals, membranes and microcapsules [1]. To stabilize chitosan gel under acidic conditions or during enzymatic degradation, the amino group has to be crosslinked. Tripolyphosphate (TPP) (Figure 1B) is non-toxic and phosphatic polyanion which can interact with chitosan via electrostatic forces to form ionic crosslinked networks [2]. Genipin (Figure 1C) is an aglucone of geniposide extracted from *Gardenia jasminoides*. Genipin, a natural cross-linker, is obtained from geniposide via enzymatic hydrolysis. Genipin is considered an ideal biomedical material due to it is 10,000 times less toxic than glutaraldehyde [3].

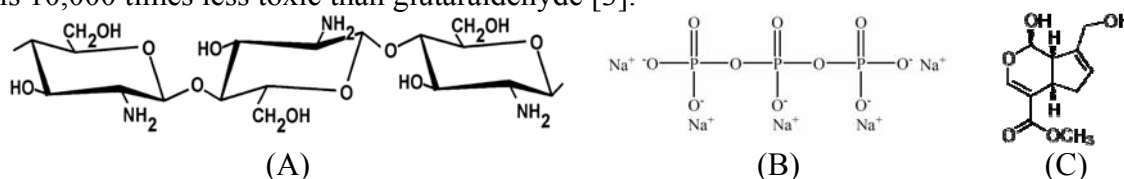


Figure 1. The structure of (A) chitosan, (B) tripolyphosphate, and (C) genipin.

Phytic acid is found in abundance in cereals, beans, nuts, oilseeds, tubers, pollen, spores, and organic soil [4]. Phytate is the major storage form of phosphorous in plants; up to 80 % of phosphorous is found in the seeds [5]. Phytic acid, which is anions, is often considered an anti-nutrient due to its ionization behavior and ability to chelate with multivalent cations such as Zn^{2+} , Ca^{2+} , and Fe^{3+} thus preventing mineral absorption [6]. Phytic acid has antioxidant and anticancer effects and can lower blood cholesterol and lipids. In recent, both *in vivo* and *in vitro* experiments have demonstrated inhibitive and therapeutic effects of the dephosphorylation of phytic acid on colorectal cancer, colon cancer, and **rectal carcinoma** [7].

Chitosan is considered an adsorbent due to its amino and hydroxyl groups and is used to adsorb phenolic compounds, proteins, peptides, dyes, and metal ions [8-10]. This study examined the physiochemical properties of chitosan beads and conducted phytic acid adsorption experiments under different pH values employing tripolyphosphate (TPP)/genipin co-crosslinked chitosan beads. In future research, we expect to selectively adsorb phytic acid in soybean whey using the co-crosslinked chitosan beads.

MATERIALS and METHODS

Materials

The preparation method of chitosan was as described by Tsai et al. [11]. The degree of deacetylation (DD) and molecular weight (MW) of chitosan was determined with FTIR [12] and size exclusion high-performance liquid chromatography [13] respectively. In this study, DD and MW of chitosan was 80% and 900 kDa, respectively. Acetic acid was purchased from Merck (Darmstadt, Germany). Sodium triphosphate (TPP), sodium hydroxide, and sodium acetate anhydrous were purchased from Sigma-Aldrich (St. Louis, MO, USA). Genipin was purchased from Challenge Bioproducts (Taichung, Taiwan).

Preparation of non-crosslinked chitosan beads

Chitosan (1 g) was dissolved in 100 ml 0.5 % acetic acid solution and the solution was vibrated at 600 rpm for 24 h to prepare the chitosan solution. The chitosan solution was applied through a 25 G x 1" syringe needle mounted by the syringe pump at a controlled flow rate of 0.42 ml/min to 1 N NaOH (15% ethanol) to produce chitosan beads of 1.8 mm in diameter. The chitosan beads were washed until neutral and stored at 4°C [14].

Preparation of TPP/genipin co-crosslinked chitosan beads

Chitosan (1 g) was dissolved in 300 ml 0.5 % acetic acid solution and the solution was vibrated at 600 rpm for 24 h to prepare the chitosan solution. TPP was dissolved in deionized water to prepare 0.01 M TPP solutions. The TPP solutions were adjusted from pH 9 to 7, 5, 3, and 1, respectively. Genipin was added to TPP solutions with different pH values to prepare 0.01 M TPP/0.01 M genipin solution, respectively. The chitosan solution was applied through a 25 G x 1" syringe needle mounted by the syringe pump at a controlled flow rate of 0.42 ml/min to TPP/genipin solutions and stored for 24 h to achieve crosslinking of the chitosan beads. After crosslinking, the solidified beads were stirred for two days in ultrapure water (Millipore) to remove residual TPP and genipin, then stored at 4°C [2].

Determination of degree of crosslinking of chitosan beads

The degree of crosslinking of chitosan beads was determined by ninhydrin (NHN) assay which can determine the percentage of free amino groups in crosslinked chitosan beads [15]. The ninhydrin solution was prepared as follows: Solution A: 1.05 g citric acid, 10 ml (1 M) NaOH, and 0.04 g $\text{SnCl}_2 \cdot 2\text{H}_2\text{O}$ were mixed, then deionized water added until 25 ml; Solution B: 1 g ninhydrin was dissolved in 25 ml ethylene glycol monomethyl ether. Solutions A and B were mixed and vibrated for 45 min and then stored in a dark bottle. The chitosan beads were lyophilized for 6h and then weighted. Lyophilized beads (5.0 mg) were placed into a 1.5 ml Eppendorf tube and then 0.5 ml ninhydrin solution was added. The solution was heated for 20 min at 100°C and then cooled to room temperature. The mixture was vibrated and centrifuged at 4500 rpm for 5 min at 25°C. Then, the absorbance at 570 nm was measured with an ELYSA reader. The concentration of free amino groups was proportional to the absorbance. With D-glucosamine as a standard, a calibration curve was established and calculated the concentration of the free amino groups of samples. Every sample was tested three times. The calculation equation for degree of crosslink was as follows:

$$\text{Degree of crosslink (\%)} = \frac{A - B}{A} \times 100, \text{ where } A \text{ is the mole of free amino groups of non-}$$

crosslinked chitosan beads, and B is the mole of free amino groups of co-crosslinked chitosan beads.

Determination of gel strength and rigidity of chitosan beads

The gel strength and rigidity of the chitosan beads was determined with a texture analyzer (TA-XT2, Haslemere, England). The needle probe moved at 1.0 mm/sec to perform penetration testing. Every sample was tested five times to obtain the average. The unit of breaking force, deformation at break, gel strength, and rigidity was expressed as g, mm, g x mm, and g/mm, respectively.

Adsorption of phytic acid of chitosan beads

Chitosan beads were dipped in blank solutions at different pH values (1, 3, 5, 7, and 9) for 4 h. The beads were then taken out and drained. Chitosan beads (30 mg) were added into phytic acid solutions at pH 1, 3, 5, 7, and 9 ($C_0 = 200 \mu\text{g/ml}$, $V = 10 \text{ ml}$). After the adsorption experiment at 25°C for 24 h, the concentration of the phytic acid (C) was tested to determine the adsorption of phytic acid. Adsorption rate (%) = $(1 - C/C_0) \times 100$.

RESULTS and DISCUSSION

Figure 2A shows a photograph of a non-crosslinked chitosan bead (NB). Figure 2B-2D show photographs of chitosan beads co-crosslinked with TPP/genipin at pH 1, 3, 5, 7, and 9 after 5, 12, and 24 h. The result showed that the crosslinking solutions are transparent. The degree of crosslinking of chitosan beads increased as the crosslinking time increased; thus, the color changes were more obvious. The results were similar to those of Yuan et al. [16]. In addition, the color of the bead was influenced by the pH values. The NB, CB1 and CB3 (The chitosan beads co-crosslinked TPP/genipin under pH 3 solution) were whiter. With the increase in pH values of solutions, the color of the beads changed from light green (pH 5) to dark green (pH 7) to deep green (pH 9) indicating different crosslinking degree for different pH values. According to this phenomenon, Mi et al. [2] explained that TPP will ionize and form a five valence anion in water. In acidic solutions, the phosphate groups interacted with the amino groups of chitosan to form ionic crosslinked networks. In addition, the carbonyl group of genipin will bind the amino groups of chitosan in neutral or alkaline solution; or the O in the chemical structure of genipin will be replaced by the N in the amino groups of chitosan, which is a covalent bond with greater strength.

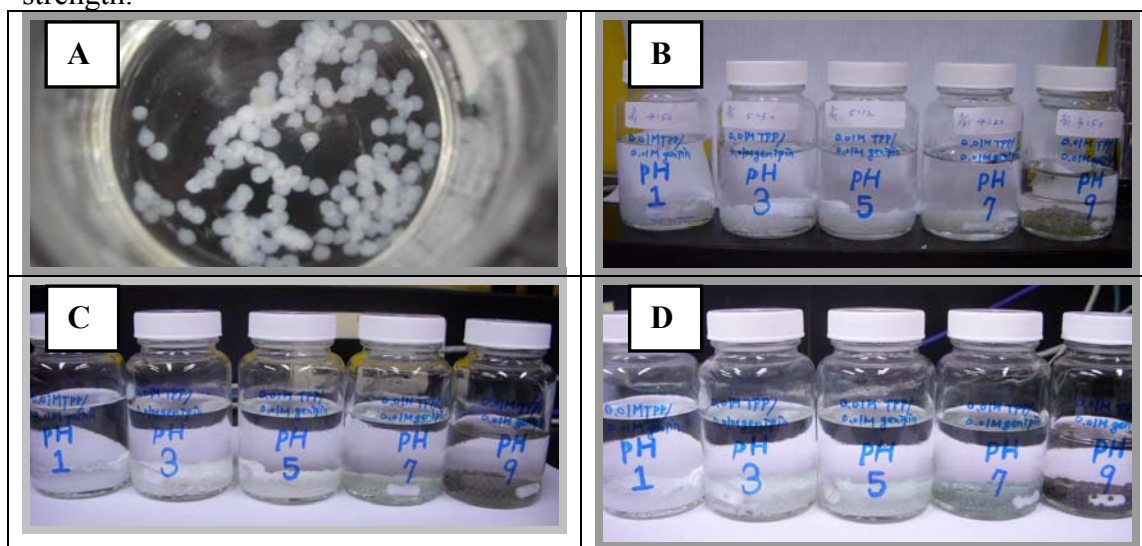


Fig. 2. (A) Photograph of non-crosslinked chitosan beads. Photograph of the chitosan beads crosslinked with TPP/genipin at different pH conditions after (B) 5 h, (C) 12 h, (D) 24 h.

Table 1 shows the size, degree of crosslinking, and gel strength of chitosan/TPP/genipin co-crosslinked beads prepared using different pH solutions. Table 1 shows that the size of the bead

was between 2.40 mm and 1.94 mm; the size decreased as the pH values increased. The smallest size of the non-crosslinked chitosan bead (NB) was 1.76 mm (prepared at pH 12.0). The amino groups of chitosan chain were protonated in acidic solutions so the conformation was extended; thus, the size of beads was larger. In neutral and alkaline solutions, the chitosan chain was electrically neutral so the conformation was contracted. The covalent bonds produced by the crosslinking of genipin also contributed to the contracted conformation; thus, the size of the bead was smaller. The results corresponded to those of Kamiński et al. [17] where the genipin crosslinked chitosan microsphere was swollen when dipped into solutions at pH values below 6.5 and contracted when the solutions were at pH values higher than 6.5.

According to Table 1, the degree of crosslinking of the co-crosslinked chitosan bead was between 59.22%-81.20%. The degree of crosslinking decreased as the pH value of the solutions increased. The results were similar to those of Mi et al. [2]. At lower pH values, chitosan failed to react with genipin due to the cations on chitosan chain and only performed ionic crosslinking with TPP (physical interaction). So, in lower pH solution causing the chitosan bead has the higher degree of crosslinking. However, at pH values higher than 6.5, the crosslinking degree of the chemical reaction between chitosan and genipin was not high due to require more energy. Further, the ionic crosslinking between TPP and chitosan was low. These led to lower degree of crosslinking of chitosan bead. The results corresponded to those for gel strength. Under acidic conditions (pH 2, 3, and 5), the gel strength of chitosan beads was weaker due to the physical interaction. Under neutral and alkaline conditions, the gel strength of chitosan beads was superior due to more chemical crosslinking.

Table 1. The degree of crosslinking, size, and gel strength of chitosan/TPP/genipin beads prepared in different pH solutions

Solution	Size (mm)	Crosslinking degree (%)	Gel strength (g·mm)
pH 1	2.40 ± 0.16 ^d	81.20 ± 3.51 ^d	0.04 ± 0.00 ^a
pH 3	2.22 ± 0.13 ^c	76.65 ± 2.90 ^c	0.23 ± 0.11 ^a
pH 5	2.02 ± 0.04 ^b	74.64 ± 0.45 ^c	0.49 ± 0.13 ^a
pH 7	2.00 ± 0.12 ^b	65.29 ± 1.28 ^b	7.08 ± 1.81 ^c
pH 9	1.94 ± 0.11 ^b	59.22 ± 1.38 ^a	4.39 ± 0.79 ^b
NB*	1.76 ± 0.09 ^a	0.00	0.04 ± 0.02 ^a

* NB expressed non-crosslinked chitosan beads. Values are mean ± S.D. (n = 3). Different letters (^{a-d}) in the same column indicate significant differences ($p < 0.05$) between samples.

Table 2. The phytic acid adsorption (%) of chitosan bead (30 mg) adsorbed in different pH of solution at 24 h.

Type	pH 1	pH 3	pH 5	pH 7	pH 9
NB*	10.1 ^{cd}	22.7 ^a	16.9 ^b	12.3 ^c	7.9 ^d
CB1	15.4 ^a	14.1 ^a	10.8 ^b	9.7 ^b	8.2 ^c
CB3	17.0 ^a	14.4 ^b	8.9 ^c	9.8 ^c	10.5 ^c
CB5	14.4 ^a	12.7 ^b	7.0 ^c	5.2 ^d	4.1 ^e
CB7	18.4 ^a	17.4 ^a	6.9 ^b	5.4 ^c	5.2 ^c
CB9	19.2 ^a	17.4 ^b	12.9 ^c	9.5 ^d	5.7 ^e

* NB expressed non-crosslinked chitosan beads. CB1 expressed chitosan bead co-crosslinked TPP/genipin under pH 1 solution. The rest may be deduced by analogy. Different letters (^{a-d}) in the same row indicate significant differences ($p < 0.05$) between samples.

Table 2 indicated that the phytic acid adsorption behavior of chitosan beads prepared under different co-crosslinking conditions was investigated at different pH values. The initial concentration of phytic acid was 200 µg/ml. The results showed the NB demonstrated favorable adsorption capabilities that adsorbed 22.7% and 16.9% of phytic acid, respectively under acidic

conditions (pH 3 and 5) for 24 h. However, the adsorption results below pH 1 were not satisfactory (10.1%) due to the intolerance of NB to strong acid. The acid dissolution of the structure of the chitosan bead led to decrease in adsorption amount. In neutral and alkaline solutions, the adsorption of phytic acid was 12.3% and 7.9%, respectively.

Table 2 also shows that the adsorption amount of TPP/genipin co-crosslinked chitosan beads (CB1, CB3, CB5, CB7, and CB9) for phytic acid decreased as the pH values increased. This trend may be related to the degree of protonation. When the degree of protonation increased (more cations), the adsorption capability for phytic acid (anions) was stronger. In addition, at low pH values (pH 1 and 3), compared with other CBs, CB7 and CB9 had favorable adsorption capability for phytic acid due to lower crosslinking degree of chitosan beads (Table 1). At pH 1 and 3, the CB7 and CB9 displayed greater adsorption capabilities for phytic acid due to more free amino groups in the lower crosslinking degree of beads. At pH 3, 5, and 9, the all beads demonstrated poorer adsorption capabilities due to low protonation degree of the chitosan chain.

ACKNOWLEDGEMENTS

The authors wish to express their appreciation for the financial support from National Science Council, ROC (NSC 97-2313-B-019-007-MY3).

REFERENCES

- [1] Rinaudo, M. (2006) Prog. Polym. Sci., 31, 603-632.
- [2] Mi, F. L., Sung, H. W., Shyu, S. S., Su, C. C. and Peng, C. K. (2003) Polymer, 24, 6521-6530.
- [3] Sung, H. W., Huang, R. N., Huang, L. L. H. and Tsai, C. C. (1999) J. Biomat. Sci. Polym. Ed., 10, 63-78.
- [4] Febles, C. I., Arias, A., Hardisson, A., Rodríguez-Alvarez, C. and Sierra, A. (2002) J. Cereal Sci., 36, 19-23.
- [5] Lopez, H. W., Leenhardt, F., Coudray, C. and Remesy, C. (2002) Int. J. Food Sci. Tech., 37, 727-739.
- [6] Wodzinski, R. J. and Ullah, A. H. (1996) Adv. Appl. Microbiol., 42, 263-302.
- [7] Dost, K. and Tokul, O. (2006) Anal. Chim. Acta, 558, 22-27.
- [8] Babel, S. and Kurniawan, T. A. (2003) J. Hazard. Mater., 97, 219-243.
- [9] Bailey, S. E., Olin, T. J., Brica, R. M. and Adrin, D. D. (1999) Water Res., 33, 2469-2479.
- [10] Crini, G. (2005) Prog. Polym. Sci., 30, 38-70.
- [11] Tsai, M. L., Chang, H. W., Yu, H. C., Lin, Y. S. and Tsai, Y. D. (2011) Carbohydr. Polym., (accepted).
- [12] Baxter, A., Dillon, M. and Anthony, K. D. (1992) Int. J. Biol. Macromol., 14, 166-169.
- [13] Tsaih, M. L. and Chen, R. H. (1999) J. Appl. Polym. Sci., 71, 1905-1913.
- [14] Shu, X. Z. and Zhu, K. J. (2002) Int. J. Pharm., 201, 51-58.
- [15] Mi, F. L., Tan, Y. C., Liang, H. C., Huang, R. N. and Sung, H. W. (2001) J. Biomat. Sci. Polym. Ed., 12(8), 835-850.
- [16] Yuan, Y., Chesnutt, B. M., Utturkar, G., Haggard W. O., Yang, Y., Ong, J. L. and Bumgardner, J. D. (2007) Carbohydr. Polym., 68, 561-567.
- [17] Kamiński, K., Zazakowny, K., Szczubialka, K. and Nowakowska, M. (2008) Biomacromolecules, 9, 3127-3132.

THERMOPHYSICAL AND MECHANICAL PROPERTIES OF POLY(CHITOSAN-B-LACTIDE)

**N.E. Tsverova, A.E. Mochalova,
A.G. Morozov, I.L. Phedushkin, A.V. Markin, A.S. Koryagin, L.A. Smirnova**

Nizhny Novgorod State University. NI Lobachevsky

E-mail: smirnova_la@mail.ru

At the present time it is actual to synthesize biocompatible and biodegradable polymeric materials. The production of such materials and their employment will help to resolve several issues the most important of which is relating to environmental issues, as well as problems of production of medical devices functionality. [1-4]

In the first case is to obtain non-toxic biodegradable polymers for packaging products, tableware, polymer films. There is an acute question of obtaining biodegradable, biocompatible polymeric materials and composites for implants. Now implants for bone tissue regeneration based on biopolymers and hydroxyapatite are received abroad [7].

Perspective direction at creation biodegradable and biocompatible polymer functionality is using of synthetic polyesters - polylactide, polyglycolide and natural polysaccharides.

Polylactide and polyglycolide is nontoxic and allowed for use in medicine. They use for making absorbable surgical threads brand Dexon, manufactured in the USA - copolymers containing 10-12% of lactide and 90-88% glycolide [5,6]. Polyglycolide and products of its biodegradation don't cause the characteristic tissue reaction and effect on biochemical parameters of urine and blood.

Representative of a class of natural polysaccharides - chitosan has unique properties: high reactivity and sorption capacity, hypoallergenic, non-toxic, it is biodegradable and biocompatible [3]. Chitosan should be modified for using it in the manufacture of implants, because it is fragile polymer [1,3].

The purpose of our research is investigating thermophysical properties blend compositions of chitosan and polylactide homopolymers with different ratios of components and the poly(chitosan-b-lactide). We used the following reagents:- chitosan with molecular weight $1,2 \times 10^5$ and the degree of deacetylation 0,8 - 0,82- polylactide with a molecular weight 6×10^4 .

Block copolymers were obtained by mechanical action on solutions of homopolymers of chitosan and polylactide. The formation of block copolymer was proved by infrared spectroscopy. In the spectrum of the block copolymer, previously abluted of homopolymers, there is a characteristic peak corresponding to the absorption frequency of carbonyl group (1757.9 cm^{-1}), (fig 1).

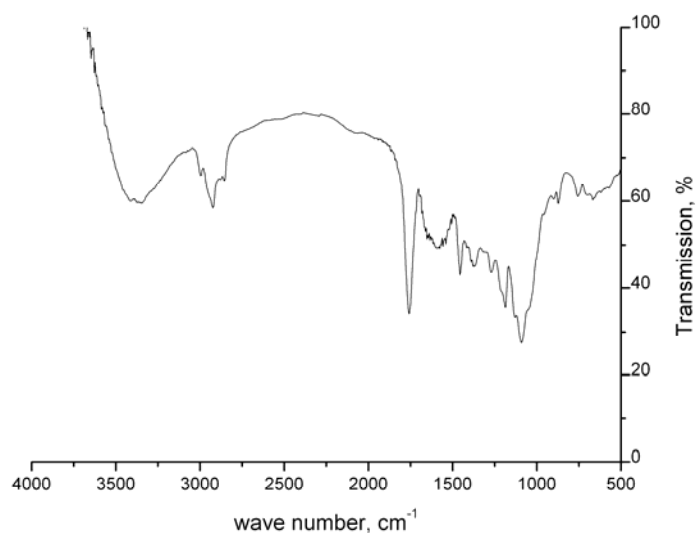


Fig 1. Fourier transform infrared spectrum of poly(chitosan-b-lactide).

It should be noted when the blend compositions of chitosan and polylactide were obtained then interpolymer complex formed and precipitated. That's why we used poly(chitosan-b-lactide) as a compatible base for homogeneity of components in solution. It was allowed to prevent of agglomeration of components and get homogeneous films.

The physico-mechanical and thermophysical properties of obtained samples were investigated. Physico-mechanical properties of films of poly(chitosan-b-lactide) are higher than that of the original polysaccharide homopolymers and blends of chitosan and polylactide. An increase of elongation of the films of block copolymer by factor of 3 with a slight increase in tensile strength in comparison with initial polysaccharide was observed (table 1.).

Table 1. Tensile strength and elongation of the film block copolymer of chitosan with lactide.

Composition	σ , MPa	ε , %
chitosan	30,9	2,6
poly(chitosan-b-lactide)	36,0	8,0

Thermophysical behavior of poly(chitosan-b-lactide) was investigated by DSC and TG - analysis's in the temperature range 20⁰ C - 400⁰ C..It's determined that the sample of poly(chitosan-b-lactide) has two temperatures of devitrification: $T^0_{g,1} = 53 \pm 1^0$ C , $T^0_{g,2} = 145 \pm 1^0$ C (Fig .2).

According to the TG- analysis we determined relatively high stability of poly(chitosan-b-lactide) , namely, the thermal destruction begins at 230⁰ C and a maximum allocation of products of thermal decomposition is observed at 275⁰ C.

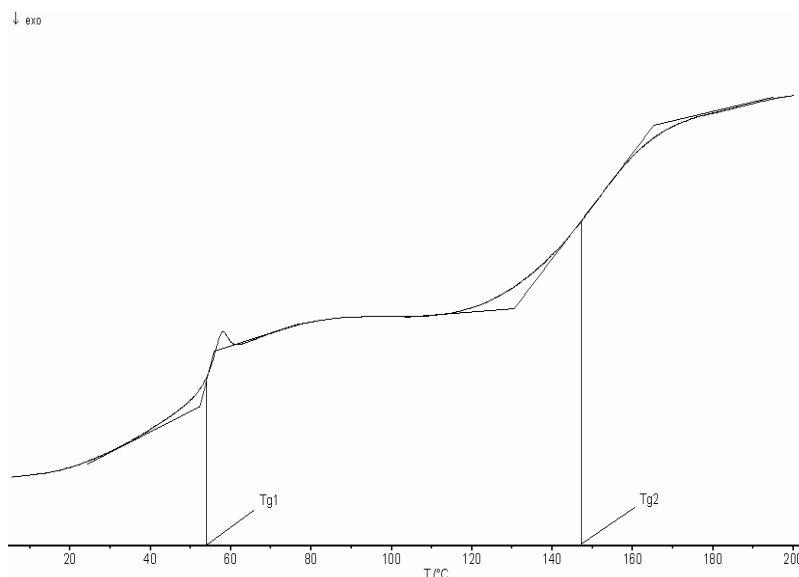


Fig 2 . DSC – curve of poly(chitosan-b-lactide).

The rods of poly(chitosan-b-lactide) were obtained by 2 cm long and 0.5 cm wide and studied their biodegradation in vivo in experimental animals. Laboratory mice have been put the rods - implants and were sewn under the skin into the cuts between the shoulder blades. Length of experience was 3 weeks. It was found that the implant is completely resorbed under the skin of mice with no signs of inflammation.

Thus it can be suggested that the implant is promising for use as a matrix for building tissue. Further research may be directed to study the influence of increase bone tissue at bone fractures.

REFERENCES

- [1] Jalal Zohuriaan-Mehr, M. (2003) Advances in Chitin and Chitosan Modification through Graft Copolymerization: A Comprehensive Review. Iranian Polymer Journal, 14(3), 235-265.
- [2] Kolybaba, M., Tabil, L.G. S., Panigrahi, W.J., Crerar, T., Powell, B. Wang. Biodegradable Polymers: Past, Present, and Future. Paper Number: RRV03-0007.
- [3] An ASAE Meeting Presentation Skryabin K.G, Vikhoreva G.A, Varlamov V.P. (2002) Chitin and chitosan. Production properties and usage. Moscow: Nauka.
- [4] Galbraikh L.S. (2001) Chitin and chitosan: structure, properties, application. Soros Educational Journal, 1, 51-56.
- [5] Kuz'mina, N.L., Biber, B.L., Abakumova, G.L., Barshadskaya, E.N. (1989) Problems of formulation and usage of surgical suture thread. Survey. info. Ser. Chemical fiber industry. - M.: NIITEKHIM, - 78 p.
- [6] Dauner, M., Planck, H. (2001) Progress in fibers for human implants. Proceedings of International Conference "Fibres and Textiles for the Future", Tampere University of Technology, 147 - 158.
- [7] Pielichowska, K. and Blazewicz, S. (2010) Bioactive Polymer/Hydroxyapatite (Nano)composites for Bone Tissue Regeneration. /Advances in polymer science. Biopolymers, 232.

PHYSICO-CHEMICAL PROPERTIES OF SALTS OF CHITOSAN WITH BENZOIC ACID

V.F. Uryash^{1*}, E.A. Fedoseeva², N.Yu. Kokurina¹, V.B. Fedoseev³, A.V. Uryash⁴

¹*Research Institute of Chemistry, Nizhny Novgorod State University, Nizhny Novgorod, Russia*

²*R.E. Alekseev Nizhny Novgorod State Technical University, Nizhny Novgorod, Russia*

³*Nizhny Novgorod State University, Nizhny Novgorod, Russia*

⁴*Mount Sinai Medical Center, Department of Research, Miami Beach, Florida, USA*

**E-mail: ltch@ichem.unn.ru*

INTRODUCTION

Transformation of chitosan into the salt form allows to receive its aqueous solutions that essentially expands scope of this valuable natural polymer. However, the physico-chemical properties of these compounds are not studied until now. Therefore, it was defined the temperatures of physical transitions of the salt of chitosan (ChTS) and benzoic acid (BA) by the method of differential thermal analysis (DTA) in the range of $-190-400^{\circ}\text{C}$.

MATERIALS AND METHODS

Benzoate of chitosan was obtained by induced dissolution of equimolar (per link of glucosamine) amounts of both components in distilled water. It was used the crab chitosan with $M_n=1.36 \cdot 10^5$ and the degree of deacetylation (DD) of 82%. BA was used by chemically pure grade. Films were cast on a glass surface and were dried to the constant weight at room temperature (No.1) and 65°C (No.2).

By differential thermal analysis studied the physical and chemical properties of polymer compositions. The design of the device and the experimental technique are described in [1]. Quartz served as a reference. The charges of the specimen and the reference were 0.2–0.3 g. The specimen temperature and the temperature difference between the specimen and the reference were measured with a chromel-copel thermocouple with an error of 0.5 degrees. The thermocouple was calibrated using a reference platinum resistance sensor and reference substances within the entire temperature range. The experiment was carried out in the helium atmosphere. The heating rate in the experiments was 5 degrees/min. A deviation from linearity did not exceed 1%. Initially the sample was cooled at the rate of $\sim 20 \text{ K/min}$ from room temperature to -190°C .

RESULTS AND DISCUSSION

During the initial heating it was observed endothermic peak of evaporation of sorbed water at $t_{\text{vap}}(\text{H}_2\text{O}) = 136^{\circ}\text{C}$ for the initial air-dry chitosan (Figs. 1, curves 1; Table 1). After evacuation of the sample the content of water is determined as 8.7 mass%. On the thermogram for the dehydrated chitosan it was manifested several relaxation transitions of endothermal nature (β - and two devitrification), similar to those observed in the studied previously polysaccharides [2–8]. The destruction of chitosan proceeds into two stages (Figs. 1, curves 3; Table 1), releasing energy in the form of heat ($t_{\text{dest1}} = 306^{\circ}\text{C}$ and $t_{\text{dest2}}=327^{\circ}\text{C}$).

Table 1

Averaged temperature of the physical transitions in the chitosan and its salts with benzoic acid

<i>Sample</i>	m, г	H ₂ O, mass%	t _{vap} (H ₂ O), °C	t _γ , °C	t _β , °C	t _{g1} , °C	t _{g2} , °C	t _{tr.} , °C	t _{dest1} , °C	t _{dest2} , °C	Δm up to dry, mass%
Crab chitosan (initial) MM=1.36 10 ⁵ D DD=82%	0.2727	8.7	136	---	61.5	97.5	133	279 (endo)	306 (exo)	327 (exo)	48
Crab chitosan (washed from BA) No.3	0.2642	9.5	126	---	34	80	122	230 (endo)	279 (exo)	---	43
ChTS+BA (dried slowly) No.1	0.1793	7.3	125.5	---	45	76	115	---	181 (exo)	222.5 (endo)	37
ChTS+BA (dried at t=65 ⁰ C) No.2	0.3986	7.0	149.5	-30	36	92	133	---	193 (exo)	228 (endo)	24

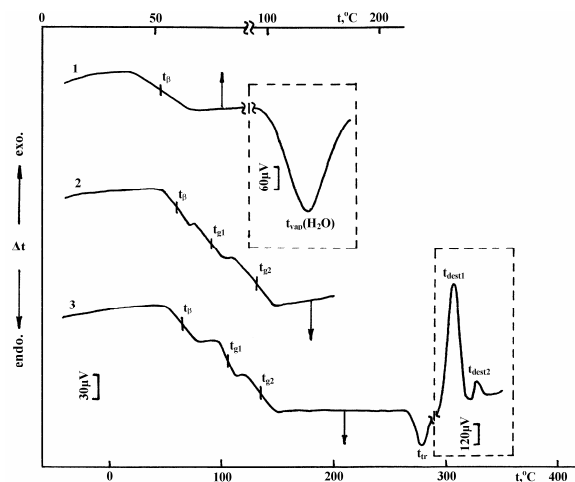


Figure 1. Thermograms of crab chitosan obtained at three repeated heating cycles:
(1) the first, (2) the second, (3) the third

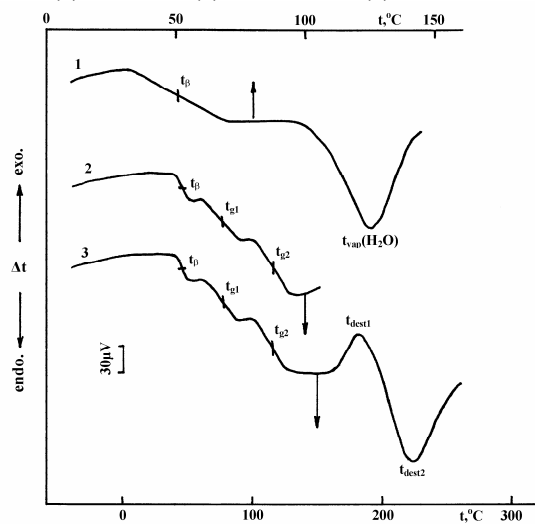


Figure 2. Thermograms of sample No.1 obtained at three repeated heating cycles:
(1) the first, (2) the second, (3) the third

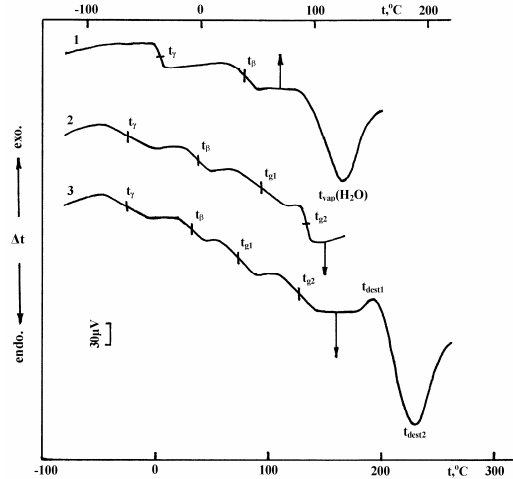


Figure 3. Thermograms of sample No.2 obtained at three repeated heating cycles:
(1) the first, (2) the second, (3) the third

After regenerating of the chitosan by removing the BA (sample No.3) from the films the junction temperatures were dropped (Table 1). 9.5 mass% adsorbed H₂O were contained in the film of regenerated chitosan. Its destruction proceeded into one stage at 279°C. This indicates that after removal of BA from the chitosan film its structure becomes less ordered.

In the films prepared from the salt forms of chitosan, the water content was 7.0-7.3 mass%. The temperature of drying of the films influenced on the temperature of evaporation of sorbed water and relaxation transitions. $t_{\text{vap}}(\text{H}_2\text{O}) = 149.5^\circ\text{C}$ for the sample No.2, and 125.5°C for the sample No.1. The glass transition temperature ($t_{\text{g1}} = 76^\circ\text{C}$ at No.1 and 92°C at No.2; $t_{\text{g2}} = 115^\circ\text{C}$ at No.1 and 133°C at No.2) also rose. The nature of the process of degradation of chitosan benzoate changes with comparing to the initial polysaccharide.

REFERENCES

- [1] Uryash, V.F., Mochalov, A.N., Pokrovsky, V.A. (1978). Device of the differential thermal analysis. *Thermodynamics of Organic Compounds: Intercollege Bull., Gorky Univ. Publ.*, 7, 88-92.
- [2] Uryash, V.F., Rabinovich, I.B., Mochalov, A. N., Khlyustova, T.B. (1985). Thermal and calorimetric analysis of cellulose, its derivatives and mixtures with plasticizers. *Thermochim. Acta*, 93, 409-12.
- [3] Uryash, V.F., et al. (2010). Physical–chemical properties of natural polymers – potential carriers and delivery systems of biologically active substances for human applications. In *Physical Organic Chemistry: New Developments* (K.T. Burley, ed.) pp.183-265, Nova Sci. Publ., Inc.
- [4] Uryash, V.F., et al. (2005). Thermodynamic characteristics of pectin of different etherification degree in the 6-330 K range. *Zh. Fiz. Khim.*, 79, 1383-89
- [5] Uryash, V.F. (2002). Thermodynamics of chitin and chitosan. In *Chitin and Chitosan. Fabrication, Properties, and Application* (K.G. Skryabin, G.A. Vikhoreva, V.P. Varlamov, eds.) pp.119-29, Nauka.
- [6] Uryash, V.F., et al. (2004). Thermodynamic characteristics of amylase, amylopectin and starch within the 6—320 K range. *Zhurn. Fiz. Khimii*, 78, 796-804.
- [7] Uryash, V.F., Karyakin, N.V., Gruzdeva, A.E. (2001). Optimization of the production process of biologically active substances based on calorimetric data, *Perspektivnye Materialy*, 6, 61-9
- [8] Uryash, V.F., Larina, V.N., Kokurina, N.Yu., Novoselova, N.V. (2010). The thermochemical characteristics of cellulose and its mixtures with water. *Zh. Fiz. Khim.*, 84, 1023-29.

INTERACTION OF RADIONUCLIDES WITH SORBENTS BASED ON CHITOSAN HYDROGEL

**I.E. Veleshko¹, V.V. Nikonorov², A.N. Veleshko¹, E.V. Rumyantseva¹,
N.R. Kildeeva², L.S. Gal'braikh²**

¹*NIC «Kurchatov institute», Moscow, Russia*

²*Kosygin Moscow State University Moscow, Moscow, Russia*

**E-mail address: acaesar@bk.ru*

INTRODUCTION

Presently working out of the technological industrial schemes providing minimization of industrial wastes is one of the most important problems. For that problems solution utilization of chitosan may be perspective. But there are limited data concerning radionuclides adsorption on chitosan in literature sources.

As industrial product chitosan manufactures in flakes and powders with different particle sizes. Use of these products is definitely difficult and adsorption processes have diffusive limitation in surface layer of adsorbent. It is well known that adsorption efficiency increases in samples of chitosan with amorphous structure. Crosslinking of chitosan by glutaric aldehyde (GA) that easily reacts with amino groups leads to formation of a continuous grid of the gel with additional durability. Carrying out gel formation at negative temperatures allows achieve stabilization of porous structure and reception of super macroporous hydrogels with grid of connected cavities. Due to hydrophylic property and high porous structure such hydrogels are capable to keep a significant amount of solutions with a various chemical compound and provide high kinetic and dynamic characteristics of adsorbents [1].

For radionuclides recovery the adsorption methods are very useful. Processes of adsorption of U, Eu and Pu on chitosan have been investigated in [2, 3]. Unfortunately, chitosan has a little effective for Sr removing. Carrying out functionalization of crosslinking chitosan increases adsorption capacity and selectivity for various types of elements retaining material durability. The literature analysis has been shown that actinides (An), lanthanides (Ln) and Sr show the selectivity to the sorbents with phosphatic groups.

Adsorption laws of U, Pu, Am, Eu recovery on crosslinking by GA chitosan hydrogel (CCTS) and U, Pu, Am, Eu, Sr recovery on additional crosslinking by pyridoxal 5'-phosphate chitosan hydrogel (CCTS-PLP) have been shown in this paper.

MATERIALS and METHODS

CCTS and CCTS-PLP were manufactured by biopolymers cryochemistry laboratory (A.N.Nesmeyanov Institute of Organoelement Compounds Russian Academy of Sciences). Molecular weight of polymers and desacetylation were 470 kDa and 0.85 correspondingly. In our study we used chemically pure and ultrapure grade chemicals, and the radionuclides ²³³U, ²³⁹Pu, ²⁴¹Am, ¹⁵²Eu и ⁹⁰Sr. γ -Spectrometric measurements were performed on an AMA-03F+ device equipped with an IGC-12 γ -ray detector (IGT, USA), and the α - and β -radiometric measurements, on a Quantulus 1220 spectrometer using standard potassium-free cells and OptiPhase HiSafe III liquid scintillator.

Adsorption properties of CCTS and CCTS-PLP have been studied in dynamic and kinetic experiments and in model solutions with different chemical composition. Radionuclides ²³³U,

^{152}Eu , ^{90}Sr have been used as radiotracer for weight amount of these elements. Their specific activity was 10^6 Bq/l.

By γ -ray spectrometry and α - and β -ray radiometry, we determined the radionuclide content in the initial solution and in samples taken from the mother liquor in the course of the experiment. Distribution coefficients were determined by formula:

$$K_d = (C_0 - C) \cdot V / (C \cdot m) = (A_0 - A) \cdot V / (A \cdot m), \quad (1)$$

where C_0 and A_0 are the initial concentration ($\text{mg} \cdot \text{ml}^{-1}$) and initial radionuclides activity ($\text{counts} \cdot \text{min}^{-1}$), respectively; C and A are the corresponding equilibrium quantities; V , solution volume, ml; and m , weight of dry CCTS and CCTS-PLP sorbents, g.

For investigation of solid samples infrared spectroscopy method has been applied. Spectra have been obtained by using Fourier transform infrared spectrometer (FTIR) WQF-510 Rayleigh in range of wave lengths $4000\text{--}400 \text{ cm}^{-1}$ and at indoor temperature. To spectra processing MainFTOS program has been used.

RESULTS and DISCUSSION

In fig 1. dependences of K_d ^{233}U , ^{249}Pu , ^{241}Am , from pH in solutions on CCTS-PLP have been presented. Adsorption curves of ^{233}U , ^{249}Pu , ^{152}Eu passed through a maximum and K_d ^{241}Am stabilization observed at $\text{pH} > 6$. Maximum K_d for the elements are $1.8 \cdot 10^4$, $4.1 \cdot 10^3$, $4.9 \cdot 10^3$ и $1.4 \cdot 10^4 \text{ ml/g}$ correspondingly. CCTS has been less effective then CCTS-PLP. For it obtained K_d for the elements were $^{233}\text{U} - 7.6 \cdot 10^3$, $^{249}\text{Pu} - 5.3 \cdot 10^2$, $^{241}\text{Am} - 6.2 \cdot 10^3$ и $^{152}\text{Eu} - 2.1 \cdot 10^2 \text{ ml/g}$ at pH 5,3,6,4 correspondingly. Unlike An from Ln, K_d dependence for ^{90}Sr from pH has step character. Distribution coefficients $^{90}\text{Sr}^{2+}$ have linearly increase intervals at pH 2-4 and 6-8, and constant values at pH 4-6 and 8-9.5. Maximum K_d was found at $\text{pH} = 8$ (10^3 ml/g). Chemical forms of investigated elements in a solution can cause such distinctions. On the other hand, efficiency of elements interaction with CCTS and CCTS-PLP has been defined by a physical and chemical condition of sorbents, owing to their protonation. Besides it, presence of phosphatic groups in CCTS-PLP leads to growth adsorption ability of the modified sorbent.

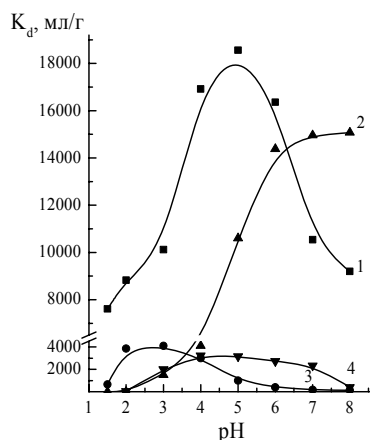


Fig 1. pH dependence K_d for $^{233}\text{UO}_2^{2+}$ (1), $^{239}\text{Pu}^{4+}$ (2), $^{241}\text{Am}^{3+}$ (3) и $^{152}\text{Eu}^{3+}$ (4) on CCTS-PLP from $[\text{NaNO}_3] = 5 \text{ g/l}$. $V/m=1000$,

$$[^{233}\text{UO}_2^{2+}] - 4 \cdot 10^{-6}; [^{239}\text{Pu}^{4+}] - 1.2 \cdot 10^{-6}; [^{241}\text{Am}^{3+}] - 1.7 \cdot 10^{-9}; [^{152}\text{Eu}^{3+}] - 10^{-4} \text{ mol/l}.$$

Kinetic curves of $^{233}\text{UO}_2^{2+}$ and $^{152}\text{Eu}^{3+}$ adsorption on CCTS and CCTS-PLP, $^{239}\text{Pu}^{4+}$ and $^{241}\text{Am}^{3+}$ on CCTS-PLP and $^{90}\text{Sr}^{2+}$ on CCTS-PLP have been presented on fig. 2 (a, b). Adsorption

balance for $^{233}\text{UO}_2^{2+}$ on CCTS and CCTS-PLP reached for 15-20 minutes, for $^{152}\text{Eu}^{3+}$ on CCTS – 20 minutes, and on CCTS-PLP for 60 minutes. But CCTS is not so efficient for these elements. The calculated values of static exchange capacity (SEC) have not been exceeded $2.9 \cdot 10^{-3}$ mmol/g (60 min). The use of CCTS-PLP led to increase SEC to $5.6 \cdot 10^{-2}$. Kinetic equilibrium has been established for $^{239}\text{Pu}^{4+}$ and $^{241}\text{Am}^{3+}$ on CCTS-PLP for 40-60 minutes. For $^{90}\text{Sr}^{2+}$ on CCTS-PLP (fig. 2b) kinetic balance has been established for 10-15 minutes.

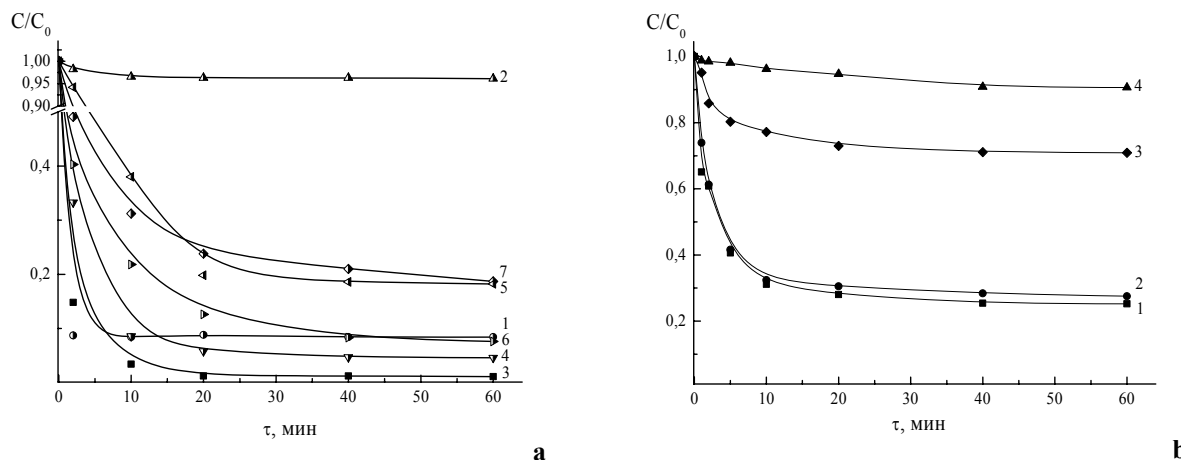


Fig.2 Kinetic of radionuclides adsorption on CCTS and CCTS-PLP:

- (a) $^{233}\text{UO}_2^{2+}$ (1) and $^{152}\text{Eu}^{3+}$ (2) adsorption on CCTS and $^{233}\text{UO}_2^{2+}$ (3, 4), $^{239}\text{Pu}^{4+}$ (5), $^{241}\text{Am}^{3+}$ (6), $^{152}\text{Eu}^{3+}$ (7) on CCTS-PLP, pH for $^{233}\text{UO}_2^{2+}$ - 5, $^{241}\text{Am}^{3+}$ - 8, $^{239}\text{Pu}^{4+}$ - 3, $^{152}\text{Eu}^{3+}$ - 4. $V/m = 1000$, $[^{233}\text{UO}_2^{2+}]$ - $1,4 - 1.3 \cdot 10^{-3}$ - $4.2 \cdot 10^{-6}$; $[^{239}\text{Pu}^{4+}]$ - $5 - 1.2 \cdot 10^{-6}$; $[^{241}\text{Am}^{3+}]$ - $6 - 10^{-6}$; $[^{152}\text{Eu}^{3+}]$ - $2,7 - 10^{-4}$ mol/l;
 (b) $^{90}\text{Sr}^{2+}$ adsorption on CCTS-PLP pH 9.5; $V/m=1000$; $[\text{Sr}(\text{NO}_3)_2]$, mol/l: 1 - $5.6 \cdot 10^{-4}$, 2 - $1.4 \cdot 10^{-3}$, 3 - $2.8 \cdot 10^{-2}$, 4 - $2.8 \cdot 10^{-1}$.

For initial parts of kinetic curves speeds of chemical reactions (v_{CR}) have been calculated for all investigated elements (table 1).

Table 1. Values of v_{CR} , diffusion (D), Biot numbers in adsorption processes of U, Pu, Am, Eu on CCTS and U, Pu, Am, Eu, Sr on CCTS-PLP in aqueous solution 5 g/l NaNO_3

Sorbent type	Elements	C_{int} , mol/l	K_d , ml/g	v_{CR} mol/(l·s)	D, m^2/s	Bi
CCTS	^{233}U	$1.3 \cdot 10^{-3}$	$1.0 \cdot 10^3$	10^{-5}	$2.1 \cdot 10^{-8}$	1.1
	^{152}Eu	10^{-4}	$2 \cdot 10^2$	$1.3 \cdot 10^{-8}$	$1.4 \cdot 10^{-8}$	5
CCTS-PLP	^{233}U	$4.2 \cdot 10^{-6}$	$1.8 \cdot 10^4$	$2.2 \cdot 10^{-7}$	$7.8 \cdot 10^{-9}$	3
		$1.3 \cdot 10^{-3}$	$1.1 \cdot 10^4$	$2 \cdot 10^{-5}$	$4.5 \cdot 10^{-8}$	0.9
	^{239}Pu	$1.8 \cdot 10^{-6}$	$4.1 \cdot 10^3$	$3 \cdot 10^{-8}$	$3.3 \cdot 10^{-9}$	2.5
	^{241}Am	$3.2 \cdot 10^{-8}$	$1.4 \cdot 10^4$	$2 \cdot 10^{-7}$	$6.5 \cdot 10^{-9}$	3.5
	^{152}Eu	10^{-4}	$4.9 \cdot 10^3$	$3.9 \cdot 10^{-7}$	$1.2 \cdot 10^{-8}$	8
	^{90}Sr	$4.4 \cdot 10^{-4}$	$2.7 \cdot 10^3$	$2.6 \cdot 10^{-6}$	$1.4 \cdot 10^{-8}$	6

Comparison of speed values has been shown that v_{CR} on CCTS-PLP higher then on CCTS for $^{233}\text{UO}_2^{2+}$ in 2 times, and $^{152}\text{Eu}^{3+}$ - 10. By kinetic curves (fig. 2 a, b) diffusion coefficients and Biot numbers have been calculated. It is known that at values $\text{Bi} < 0.1$ chemical processes proceed

in external diffusive, and at values $Bi > 30$ – intradiffusive area. In table 1, values of Biot numbers for $^{233}\text{UO}_2^{2+}$ and $^{152}\text{Eu}^{3+}$ for adsorption on CCTS were 1.1 and 5 correspondingly, and for adsorption on CCTS-PLP for all investigated elements were in an interval of values from 0.9 to 8. Based on that it has been concluded the adsorption mechanism for all investigated radionuclides is compound and consists of external diffusive and intradiffusive processes in different ratio. But main stage is external diffusive.

Adsorption isotherms of $^{233}\text{UO}_2^{2+}$ and $^{152}\text{Eu}^{3+}$ (a) and $^{90}\text{Sr}^{2+}$ on CCTS and CCTS-PLP have been shown in fig.3. Experimental SEC values on CCTS were for U – 4.2 and Eu – 0.036, and on CCTS-PLP for U – 4.6, Eu – 0.47 and Sr – 30.3 mmol/g. Based on SEC full static exchange capacity (FSEC) has been calculated. For processing the results Langmuir equation has been used. Values of SEC and FSEC for $^{233}\text{UO}_2^{2+}$ adsorption on CCTS and CCTS-PLP have been 4.8 и 5.3 for $^{152}\text{Eu}^{3+}$ – 0.05 and 0.51 mmol/g. Increase of FSEC in case of CCTS-PLP can be explained by presence of phosphatic groups $\equiv\text{R}=\text{O}$ with high electronic donor properties in the sorbent. FSEC value for $^{90}\text{Sr}^{2+}$ adsorption on CCTS-PLP was 39.8 mmol/g. High values of experimentally received and calculated FSEC apparently can be connected with the difficult mechanism of interaction $^{90}\text{Sr}^{2+}$ with CCTS-PLP in alkaline environment.

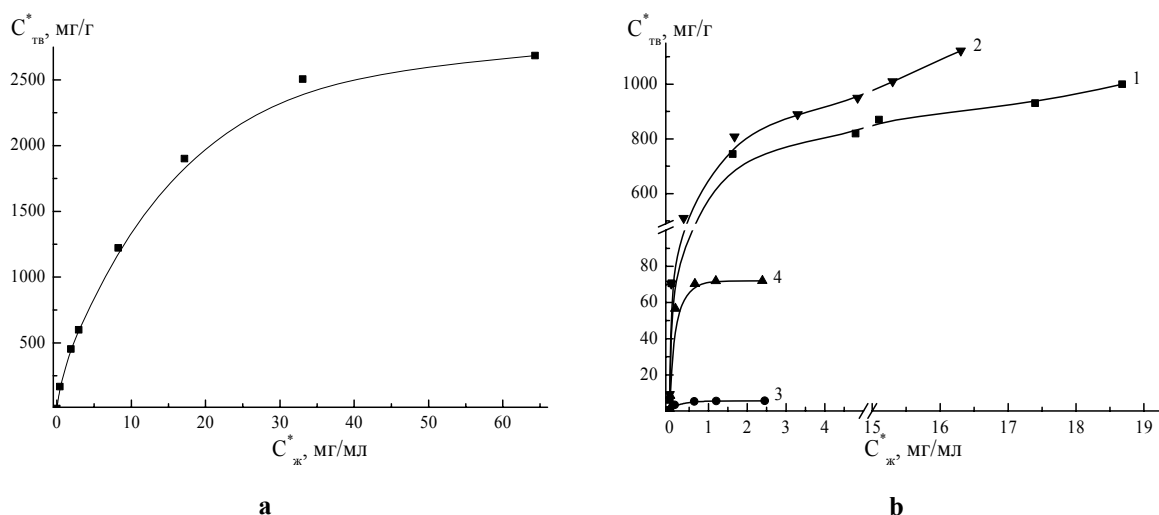


Fig.3 Isotherms of adsorption radionuclides on CCTS and CCTS-PLP ($T = 298 \text{ K}$, $V/m = 1000$):

(a) $^{233}\text{UO}_2^{2+}$ and $^{152}\text{Eu}^{3+}$ adsorption on CCTS (1, 3) and CCTS-PLP (2, 4) in solutions UO_2SO_4 ($\text{pH}=5$) and $\text{Eu}(\text{NO}_3)_3$ ($\text{pH}=4$); (b) $^{90}\text{Sr}^{2+}$ on CCTS-PLP in solution $\text{Sr}(\text{NO}_3)_2$, $\text{pH } 9.5$.

In the conditions of adsorbent saturation according to isotherms structures of complexes PLP/Me have been defined. It was established that PLP formed with UO_2^{2+} 1:1.1 complexes and with Eu^{3+} – 1:1.3.

For definition of fields of practical CCTS and CCTS-PLP use investigations of radionuclides adsorption from solutions with various salts compounds have been conducted in a wide range of concentration. It was shown that presence of salts reduced efficiency of UO_2^{2+} and $^{90}\text{Sr}^{2+}$ adsorption. Nevertheless in solutions with concentration of salts 10 g/l K_d remain near 10^3 ml/g .

For the solutions modeling a liquid radioactive waste with the low maintenance of salts (5 g/l NaNO_3), method of adsorption clearings from An and Sr on filtering columns with CCTS-

PLP has been tested. U, Pu and Am have been quantitatively allocated after 300 columnar volumes, and Sr after 200 columnar volumes. The sorbent flow-rate was less than 1 г/л. Change of pH values corresponding to the maximum K_d for the elements allowed to realize carrying out of process of fractional extraction of radionuclides from solutions on columns.

ACKNOWLEDGEMENTS

The study was financially supported by the Federal Special Program “Science and science-educational staffs in innovation Russia 2009-2013” (project no. 16.740.11.0059).

REFERENCES

- [1] Meade, S.J., Miller, A.G., Gerrard, J.A. (2003) The role of dicarbonyl compounds in non-enzymatic crosslinking: a structure–activity study. *Bioorganic & Medicinal Chemistry*, 11, 853-62.
- [2] Bhatnagar, A., Sillanpää, M. (2009) Application of chitin- and chitosan-derivatives for the detoxification of water and wastewater. *Advances in Colloid and Interface Science*, 152, 26-38.36.
- [3] Myasoedova, G.V., Nikashina, V.A. (2006) Adsorption methods for radionuclides recovery from water media. *Russian Chemical Journal*, L, 55-63.

BEHAVIOUR OF RADIONUCLIDES IN FLOCCULATION PROCESSES ON CHITOSANS OF VARIOUS MOLECULAR WEIGHTS

I.E. Veleshko*, A.N. Veleshko, E.V. Rummyantseva

Russian Research Centre Kurchatov Institute, Moscow, Russia

**E-mail address: veleshko@irtm.kiae.ru*

INTRODUCTION

Operation of nuclear fuel cycle enterprises frequently involves removal of wastes containing radioactive substances into the environment. The presently existing approaches to spent nuclear fuel (SNF) management lead to the presence of the nuclear fuel components (U, Pu), transuranium elements (TUE) Np, Am, Cm, and others, their fission products including Cs, Sr, and lanthanides (Ln), and also ^{63}Ni , ^{60}Co , and ^{54}Mn formed in structural materials of nuclear installations in repositories and fuel rod cooling basins. Also, some of these radionuclides are major components of solutions that are low-level liquid radioactive wastes (LLW). Despite active efforts made to localize radioactive substances, they still get into the environment, including the World Ocean.

The chemistry of the majority of radioactive elements, especially actinides (An), is very complex. In solutions, U, Np, Pu, and Am can exist in various oxidation states. Depending on pH and the presence of complexing agents, An exist in the ionic form, undergo hydrolysis with the formation of colloidal and pseudocolloidal particles, and form strong coordination compounds [1-3].

The presence of inorganic salts in high concentrations considerably complicates the use of ion-exchange, sorption, and extraction processes for localization of radioactive elements both in the course of treatment of process solutions and in environmental monitoring of natural waters. Therefore, in practice solutions are often subjected to preliminary clarification with preconcentration of radionuclides on precipitates of a small volume. The flocculants and coagulants commonly used are $\text{Fe}(\text{OH})_3$, $\text{Al}(\text{OH})_3$, LaF_3 , etc. [4]. In environmental monitoring of sea areas, coprecipitation is also used for preconcentration of An, including Pu. $\text{Fe}(\text{OH})_3$ is the most effective and the most commonly used for this purpose [5, 6].

It is known, that chitosans and their derivatives are used as flocculants in wastewater treatment to remove heavy metals, dyes, and surfactants. The advantages of ashless organic coprecipitants over inorganic coprecipitants were outlined in [7]. It was shown that the degree of coprecipitation from 0.01 M HNO_3 solutions on HMWC with MW = 1500 kDa and LMWC with MW = 5 kDa reached 95-99% for Pu and 85-90% for ^{60}Co and ^{54}Mn , whereas for ^{90}Sr and ^{137}Cs it was as low as 50 and 30%, respectively. It was found that, for all the examined radionuclides, the degree of coprecipitation was independent of the degree of deacetylation (DD) characterizing the content of free amino groups in chitosan, and also of MW. There are no data on the behavior of other radionuclides in the course of flocculation on chitosans in the literature.

The results of investigation in the behavior of radionuclides in the course of coprecipitation on chitosans from multicomponent solutions are given in this paper.

MATERIALS and METHODS

In our study we used samples of HMWC (MW 700 kDa, DD 85%) and LMWC (MW 5 kDa) of crab origin, submitted by the Bioinzheneriya Center of the Russian Academy of Sciences. The investigation of the solubility of chitosans showed that HMWC and LMWC were insoluble in distilled water but readily soluble at $\text{pH} < 3$. The solubility of chitosans in acid solutions was in the range 8-10 and 10-15 $\text{g}\cdot\text{l}^{-1}$ for HMWC and LMWC, respectively. An increase in pH of the solution to 6 for LMWC and 8 for HMWC caused formation of a voluminous white precipitate. In both cases, the residual concentration of chitosan in the mother liquor was 0.45 $\text{g}\cdot\text{l}^{-1}$. In seawater at pH 8.5, the solubility of HMWC and LMWC decreased to 0.045 $\text{g}\cdot\text{l}^{-1}$.

In our study we used chemically pure and ultrapure grade chemicals, Barents Sea water, and the radionuclides ^{233}U , ^{239}Pu , ^{241}Am , ^{152}Eu , ^{90}Sr , ^{90}Y , and ^{60}Co .

γ -Spectrometric measurements were performed on an AMA-03F+ device equipped with an IGC-12 γ -ray detector (IGT, USA), and the α - and β -radiometric measurements, on a Quantulus 1220 spectrometer using standard potassium-free cells and HiSafe 3 liquid scintillator.

Experiments on coprecipitation of radionuclides from solutions of various chemical compositions were performed as follows. Radionuclides were added to a model solution or Barents Sea water. The volume activity of the resulting solutions was $(2-5) \times 10^3 \text{ Bq}\cdot\text{l}^{-1}$. Then a definite amount of a freshly prepared 10 $\text{g}\cdot\text{l}^{-1}$ aqueous solution of HMWC or LMWC was added. In so doing, a voluminous white precipitate formed. The suspension was shaken for the required time, with pH monitoring with a Hanna 8314 pH meter. At definite intervals, 1-ml samples were taken from the mother liquor. Before sampling, the solid and liquid phases were separated by centrifugation.

By γ -ray spectrometry and α - and β -ray radiometry, we determined the radionuclide content in the initial solution and in samples taken from the mother liquor in the course of the experiment.

The degree of coprecipitation α (%) of radionuclides on chitosan from solution was calculated by the formula:

$$\alpha = [(A_0 - A_t) / A_0] \times 100,$$

where A_0 and A_t are the initial radionuclide content in solution and that after precipitation at a definite time, respectively.

RESULTS and DISCUSSION

Figures 1a and 1b show data on the coprecipitation of ^{233}U , ^{239}Pu , ^{241}Am , ^{152}Eu , ^{90}Sr , ^{90}Y , and ^{60}Co in relation to the HMWC and LMWC concentration in solution. As can be seen, with both kinds of chitosan α of all the examined radionuclides, except ^{60}Co and ^{90}Sr , reached virtually maximal values at chitosan concentration in solutions of 1 $\text{g}\cdot\text{l}^{-1}$. With HMWC, α was 80% for ^{152}Eu and ^{90}Y , 99% for ^{233}U and Am, and 85% for ^{239}Pu (Fig. 1a). In contrast to Am, ^{152}Eu , and ^{90}Y , the degree of coprecipitation α of ^{60}Co monotonically increased with an increase in the chitosan concentration in solution and at $[\text{HMWC}] = 5 \text{ g}\cdot\text{l}^{-1}$ reached 40%. For ^{90}Sr in the entire examined range of chitosan concentrations, α did not exceed 3%.

In the experiments with LMWC (Fig. 1 b), the α values for Am, ^{152}Eu , and ^{90}Y differed insignificantly (92-99%). For ^{60}Co and ^{90}Sr , range of chitosan concentrations from 0 to 1 $\text{g}\cdot\text{l}^{-1}$. Further increase in the LMWC amount had virtually no effect on α of ^{90}Sr , but monotonically increased it for ^{60}Co . The resulting values of α at $[\text{LMWC}] = 5 \text{ g}\cdot\text{l}^{-1}$ were 40 and 60% for ^{90}Sr and

^{60}Co , respectively. Comparison of the results showed that coprecipitation of all the examined elements was more efficient on LMWC than on HMWC. To assess the possibility of using chitosans in practice as flocculants, we performed experiments on coprecipitation of radionuclides from various salt solutions in a wide concentration range. The results obtained for the effect of Na_2SO_4 , NaCl , Na_2CO_3 , NaNO_3 , and Na_3PO_4 concentrations on the coprecipitation of $^{233}\text{UO}_2^{2+}$ on HMWC showed that the efficiency of the coprecipitation decreases in the order $\text{Na}_2\text{SO}_4 > \text{NaCl} > \text{Na}_2\text{CO}_3 > \text{NaNO}_3 > \text{Na}_3\text{PO}_4$.

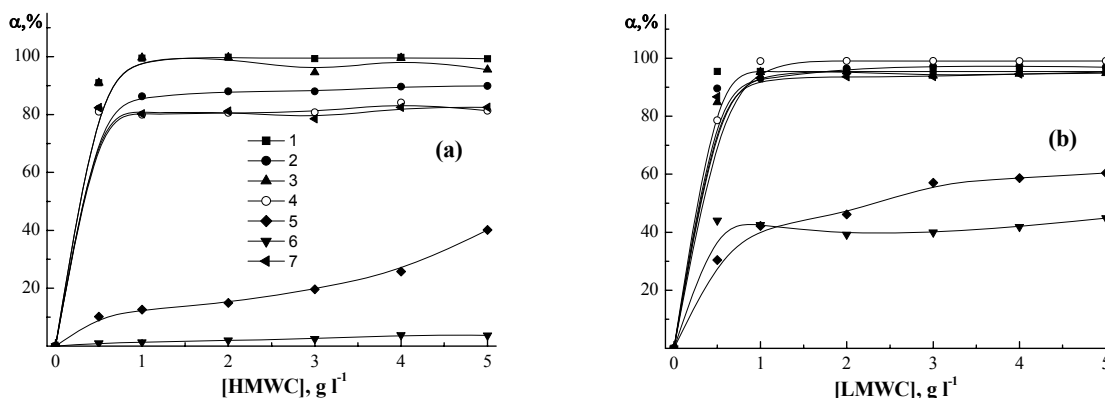


Fig. 1 Degree of coprecipitation α of (1) ^{233}U , (2) ^{239}Pu , (3) ^{241}Am , (4) ^{152}Eu , (5) ^{90}Sr , (6) ^{90}Y , and (7) ^{60}Co with (a) HMWC and (b) LMWC as a function of the chitosan concentration in 5 g l^{-1} NaNO_3 solution, pH 9.5.

In contrast to $^{233}\text{UO}_2^{2+}$ the presence of salts had virtually no effect on α of ^{241}Am and ^{239}Pu . In NaNO_3 solutions, α of ^{241}Am and ^{239}Pu was 99%, and in Na_2SO_4 and NaCl solutions, 95%. For ^{152}Eu , a complex pattern was observed. With an increase in the salt concentration in solution, α first increased and reached a maximum (95%) at a Na_2SO_4 or NaCl concentration of 10 g l^{-1} . With NaNO_3 , the highest α (88%) was observed at a salt concentration of 30 g l^{-1} . Further increase in the concentration of salts in solution led to a decrease in α of ^{152}Eu . Nevertheless, in the entire examined concentration range ($0\text{--}100 \text{ g l}^{-1}$), α remained no less than 80%. In contrast to ^{241}Am and ^{152}Eu , ^{60}Co did not noticeably coprecipitate with HMWC. The α value obtained for ^{60}Co from NaNO_3 solutions did not exceed 7%.

Table 1 shows data on the effect of salt concentrations on the degree of coprecipitation of various radionuclides with LMWC.

As can be seen, the degree of coprecipitation α of $^{233}\text{UO}_2^{2+}$ in solutions of all the examined salts differed insignificantly and was in the range 47–66%. For Pu and Am, and also for ^{152}Eu , α in all the solutions exceeded 90% irrespective of the kind of the salt. In contrast to HMWC, ^{60}Co coprecipitated with LMWC to 25–35% from NaCl and Na_2SO_4 solutions and to 41% from NaNO_3 solutions.

The data we obtained on the coprecipitation of Pu and U with LMWC in salt solutions allowed us to consider the possibility of using LMWC for Pu preconcentration from seawater with simultaneous separation of Pu from U. The use of LMWC forming a voluminous precipitate at pH 6 excluded the possibility of simultaneous coprecipitation of Ca^{2+} and Mg^{2+} ions present in seawater in macroconcentrations (0.39 and 1.23 g l^{-1} , respectively).

With the aim to develop the procedure, we examined how the LMWC concentration varied in the range $0\text{--}1 \text{ g l}^{-1}$ affects the degree of coprecipitation α of Pu and U from Barents Sea water. It was determined, that at $[\text{LMWC}] = 0.2 \text{ g l}^{-1}$, α of Pu was 92%, in the range $0.2\text{--}0.7 \text{ g l}^{-1}$ it

increased insignificantly (95%), and further increase in the chitosan concentration did not noticeably affect the efficiency of the Pu coprecipitation. In contrast to Pu, the degree of coprecipitation α of U monotonically increased in the entire examined range of LMWC concentrations. Therefore, studies were performed at $[LMWC] = 0.2 \text{ g}\cdot\text{l}^{-1}$ when the difference in the α values for U and Pu was maximal.

Table 1. Effect of inorganic salts on the degree of coprecipitation α of An, ^{152}Eu , and ^{60}Co with LMWC from salt solutions ($[LMWC] = 1 \text{ g}\cdot\text{l}^{-1}$, pH 9.5)

Salt	C, $\text{g}\cdot\text{l}^{-1}$	α , %				
		^{233}U	^{239}Pu	^{241}Am	^{152}Eu	^{60}Co
NaNO_3	10	47	85	97	90	41
NaCl	10	51	97	96	96	26
	20	-	-	-	-	24
	40	-	-	-	-	35
Na_2SO_4	10	49	94	94	93	25
	20	-	-	-	-	27
	40	-	-	-	-	24
Na_2CO_3	10	51	-	-	-	-
Na_3PO_4	10	66	-	-	-	-

The results obtained for the kinetics of Pu and U coprecipitation from Barents Sea water showed, that the kinetic equilibrium on LMWC was attained within 20-30 min for both elements.

Based on the results we obtained, a procedure was developed for seawater analysis for the total Pu content. The procedure was tested in expeditions in the Kara and Barents Seas. To perform the analysis, seawater samples were taken from a definite depth. The sample volume was 100 l. A 2-l portion of a $10 \text{ g}\cdot\text{l}^{-1}$ LMWC solution (pH 3) was added to the sample. To coprecipitate Pu with LMWC, the solution was alkalized to pH 6 by adding an ammonia solution with vigorous stirring. The chitosan precipitate formed, after settling (12 h) and solution decantation, was filtered off and dried at 95°C in air. Then the LMWC containing Pu and U was subjected to wet combustion in a mixture of H_2O_2 and concentrated HNO_3 , taken in 1:5 volume ratio. The small mineral residue was dissolved in 20 ml of 7 M HNO_3 . Radiochemical separation of Pu and U was performed by extraction with trioc- tylamine (TOA), followed by reductive stripping with a hydroxylamine hydrochloride solution. The dry residue after the evaporation was dissolved in 5 ml of 7 M HNO_3 . From the resulting solution, a target for α -ray spectrometry was prepared. The experiments showed that the chemical yield of Pu from seawater samples with the suggested procedure was as high as 84%, in contrast to the traditionally used procedures [5, 6] with $\text{Fe}(\text{OH})_3$ as coprecipitant (Pu yield 43%). The specific activity of Pu in samples of near-bottom seawater in gulfs of the Novaya Zemlya archipelago was $(150-170) \pm 20 \text{ mBq}\cdot\text{m}^{-3}$.

ACKNOWLEDGEMENTS

The study was financially supported by the Russian Foundation for Basic Research (project no. 06-04-08291-ofi).

REFERENCES

- [1] Nazarenko, V.N., Antonovich, V.P., and Nevskaya, E.M. (1979) *Gidroliz ionov metallov v razbavlennykh rastvorakh* (Hydrolysis of Metal Ions in Dilute Solutions). Moscow – Atomizdat.
- [2] Moskvina, A.I. (1975) *Koordinatsionnaya khimiya aktinoidov* (Coordination Chemistry of Actinides). Moscow – Atomizdat.
- [3] Sapozhnikov, Yu.A., Aliev, R.A., and Kalmykov, S.N. (2006) *Radioaktivnost' okruzhayushchei sredy* (Environmental Radioactivity). Moscow – Binom.
- [4] Rovnyi, S.I., Sokhina, L.P., and Goncharuk, L.V. (2006) Coprecipitation of neptunium(IV) and plutonium(IV) with hydrolyzed iron(III) in carbonate solutions *Radiochemistry*, 48, 431–34.
- [5] Pavlotskaya, F.I., Zh. (1997) Basic principles of radiochemical analysis of environmental samples and methods for determining strontium and transuranic radionuclides. *Anal. Chem.*, 52, 126–43.
- [6] Goryachenkova, T.A., Emel'yanov, V.V., Kazinskaya, I.E., et al. (2000) Plutonium Content in Water and Bottom Sediments of the Kara Sea. *Radiokhimiya*, 42, 264–67.
- [7] Kosyakov, V.N., Veleshko, I.E., Yakovlev, N.G., et al. (2003) Water-Soluble Chitosans as Flocculants for Deactivation of Liquid Radioactive Wastes. *Radiochemistry*, 45, 366–69.

ENHANCEMENT OF OSTEOBLAST CELL GROWTH BY AMYLOPECTIN ADDITION IN CHITOSAN/NATURAL HYDROXYAPATITE SCAFFOLD FOR BONE TISSUE ENGINEERING

Jayachandran Venkatesan¹, Se-Kwon Kim^{1,2*}

¹Department of Chemistry, Pukyong National University, Busan 608-737, Republic of Korea

²Marine Bioprocess Research Center, Pukyong National University, Busan 608-737, Republic of Korea

*E-mail address: sknkim@pknu.ac.kr; venkatjchem@gmail.com

INTRODUCTION

Over the last two decades, there is a growing interest in the field of artificial organ material preparation, transplantation, surgical reconstruction and the use of artificial prostheses to treat the loss or failure of an organ or tissue [1]. Autograft and allograft are considered ultimate for bone grafting procedure providing osteoconductive and osteoinductive growth factors. However, limitations in donor site, additional surgery, disease transmission and expenditure pose a need to develop alternatives to autografts and allografts[2].

Recently some tricomponent systems have been developed with improved cell proliferation on the composite scaffolds as compared to single component system. Several researchers have addressed the use of tricomponent system for bone tissue engineering including Chitosan/Hydroxyapatite system with other materials [3-5]. In this manuscript, we have proposed the use of amylopectin as another component in the tricomponent system to improve the scaffold properties for bone tissue engineering.

MATERIALS AND METHODS

Low molecular weight (~310 KDa) chitosan powder was purchased from Kitto life Co. Ltd., South Korea. Hydroxyapatite was isolated from *Thunnus obesus* bone. Amylopectin was purchased from Sigma. Human osteosarcoma (MG-63) cell line was obtained from American Type Culture Collection (Manassas, VA, USA). All other chemicals used were of analytical grade purchased from Sigma-Aldrich Corp. (St. Louis, MO, USA).

Isolation of HAp from *Thunnus obesus* bone

HAp was isolated from the bone of tuna (*Thunnus Obesus*), as described previously [6].

Scaffolds preparation

2.5 g of low molecular weight chitosan was dissolved in 250 ml of 2% acetic acid solution. The solution was stirred overnight on a mechanical stirrer (RW 20.n Labortechnik) and sonicated for 1 h to remove any air bubble for chitosan scaffold.

2.5 g of the isolated Tuna bone HAp was suspended in 50 ml of water and carefully transferred into the chitosan solution with the help of dropper for make Chitosan/HAp scaffold.

2.5 g of the isolated Tuna bone HAp was suspended in 50 ml of water and carefully transferred into the chitosan solution with the help of dropper. The solution was mechanically stirred for 24 h to disperse the HAp particles in the polymer matrix in a homogeneous manner. Simultaneously, 2.5 g of amylopectin was slowly added to the stirring chitosan-HAp solution and the mixture was stirred overnight for preparation of chitosan/HAp/Amylopectin scaffold.

These solutions were transferred to small petri dish (35 x 10 mm) with 5 to 6 g of solution/dish to freeze at -80 °C for 5 h and finally lyophilized in freeze dryer to form scaffolds. These scaffolds were immersed in 10% NaOH solution for 1 d and then washed with excess

amount of water till the pH became neutral. All the neutralized scaffolds were then lyophilized once again to make them ready for experimentation.

General Characterization

Thermal gravimetric analysis was achieved by the use of Pyris 7 TGA analyzers, Perkin Elmer Inc., USA with scan range from 50 to 900 °C at constant heating rate of 10 °C min⁻¹ with continuous nitrogen flow. The stretching frequencies of samples were examined by Fourier Transform Infrared Spectroscopy, Perkin Elmer (USA) and spectrum GX spectrometer within the range of 400 to 4000 cm⁻¹. The phase and crystallinity were evaluated using X-ray diffractometer (PHILIPS X'Pert-MPD diffractometer, Netherland) and Cu-K α radiation 1.5405 Å over a range of 5 to 80° angle, step size 0.02, scan speed 4°/min with 40 kV current and 30 mA voltage. Morphology and porosity of scaffolds were obtained by scanning electron microscopy. Cell proliferation was checked with MTT assay method.

RESULTS and DISCUSSION

Material selection and scaffold preparation

In this study, we have used three raw materials i.e. Chitosan, HAp and Amylopectin which can mimic all the qualities of extracellular matrix of bone such as biocompatibility, biodegradability and bioactivity. Chitosan, HAp and Amylopectin were used in this experiment in equal proportion to prepare Chitosan/HAp/Amylopectin scaffold. HAp and Chitosan were obtained from the processed wastes of Tuna bone and Crab shell, which is useful in decreasing the magnitude of environmental pollution. The prepared scaffolds are shown in the Figure.1.

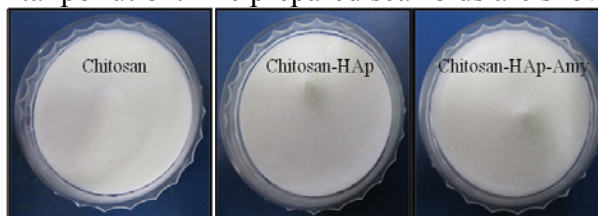


Figure .1. Digital camera images of scaffolds

Porosity measurement

The total porosity was estimated using liquid displacement method; porosity of Chitosan scaffold was much higher (94.86%) as compared to Chitosan/HAp (92.77%) and Chitosan/HAp/Amylopectin (89.54%) scaffolds. In Chitosan/HAp scaffold, some chemical interaction may occur between the NH₂ group of Chitosan and OH group of HAp which decreases the porosity.

Water uptake and retention abilities

The water uptake and water retention ability of Chitosan scaffold was higher when compared to Chitosan/HAp and Chitosan/HAp/Amylopectin scaffolds. As evident from the results, addition of HAp and Amylopectin to pure Chitosan leads to a decrease in the degree of water absorption. Furthermore, the water retention ability of Chitosan/HAp and Chitosan/HAp/Amylopectin scaffolds were comparable with slight difference but were much less when compared to the pure Chitosan scaffold.

Stretching frequency of scaffolds

In order to illustrate intermolecular interactions between components in the scaffolds, FTIR spectrum was obtained (Figure. 2). From the IR spectra of HAp, the spectrum showed the characteristic absorption bands of natural HAp reported. Briefly, a large number of bands appeared in the HAp spectra (3571, 1459, 1415, 1089, 962, 633 and 571 cm⁻¹) that were similar to HAp reference spectrum close to reported data [6]. For Chitosan scaffold, the spectrum

showed the typical characteristic absorption bands of Chitosan as reported earlier ; Chitosan exhibits characteristic bands around 3440 cm^{-1} corresponding to the stretching vibration of N–H with combination to -OH stretching vibration, while 1647 cm^{-1} and 1606 cm^{-1} are the characteristic peaks of amide I and amide II, respectively. The sharp peaks at 1409 cm^{-1} are assigned to the $-\text{CH}_3$ symmetrical deformation mode and 1074 cm^{-1} and 1031 cm^{-1} correspond to the C–O stretching vibrations ($\nu(\text{C}-\text{O}-\text{C})$). FT-IR spectrum of composite Chitosan/HAp and Chitosan/HAp/Amylopectin scaffolds contain characteristic peaks of all the raw materials like Chitosan, HAp and Amylopectin.

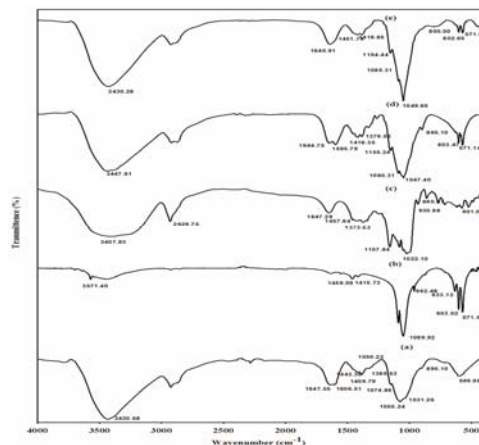


Fig.2. Infra red spectroscopy images of (a) Chitosan (b) Hydroxyapatite (c) Amylopectin (d) chitosan/HAp scaffold, (e) Chitosan/HAp/Amylopectin.

X-ray diffraction studies

Phase and crystallinity of the composite scaffolds were observed with X-Ray diffraction analysis. The diffraction patterns of Chitosan, natural HAp, Amylopectin, Chitosan/HAp and Chitosan/HAp/Amylopectin have been shown in Figure. 3. In Chitosan scaffold, three main peaks were observed at 10.5° , 20.0° (maximum intensity) and 22.5° , respectively; corresponding to characteristic peaks of Chitosan. This peak angle (20.0°) was found in Chitosan/HAp composite scaffold, whereas, this peak was not observed in Chitosan/HAp/Amylopectin scaffold. In Chitosan/HAp/Amylopectin composite scaffold, diffraction peaks were observed at 25.4° and 31.4° which revealed the presence of HAp.

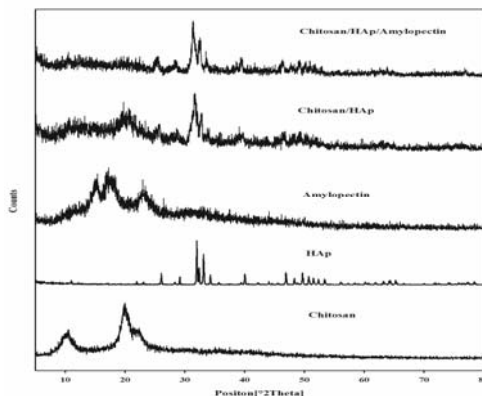


Fig.3. XRD spectrums of Chitosan, HAp, Amylopectin, Chitosan/HAp scaffold and Chitosan/HAp/Amylopectin.

Optical microscopy analysis

The dispersion of HAp particles and amylopectin in the chitosan matrix was also observed by Optical Microscopy as shown in Figure. 4. The optical microscopic image of Chitosan clearly

indicated improper pore structure whereas addition of HAp and Amylopectin polymer matrix improved the porosity. The optical microscopy images of Chitosan/HAp/Amylopectin shows the well-dispersed status of Amylopectin in the matrix with slight aggregation. This indicated that the Amylopectin is uniformly distributed within the chitosan matrix.

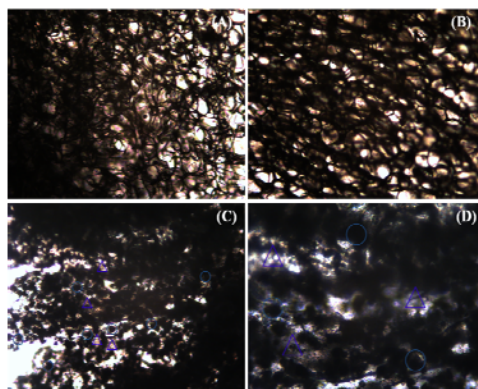


Fig.4. Optical microscopic images of (a) chitosan scaffold (b) Chitosan/HAp scaffold (c) Chitosan/HAp/Amylopectin scaffold and (d) dispersion of HAp and amylopectin particles in chitosan matrix

Morphology studies of the scaffolds

The SEM images depicted that the composite scaffolds were three dimensional, with almost equal porous structure and with good interconnectivity. According to the SEM images, HAp and Amylopectin particles were seen uniformly dispersed in the Chitosan (Figure. 5 (b and c)). Interconnected porosity structure were found in all the three type of scaffolds. This might be the basis of the flexible behavior of Chitosan scaffold.

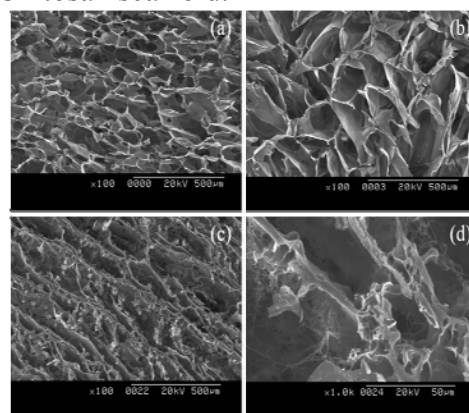


Fig.5. Scanning Electron microscopic images : (a) Chitosan scaffold, (b) Chitosan/HAp scaffold (c) Chitosan/HAp/Amylopectin scaffold and (d) high magnification image of Chitosan/HAp/Amylopectin scaffold

Cell proliferation assay

The cell proliferation of respective scaffolds were investigated through MTT assay. The results are shown in Figure. 6. The scaffolds showed no cytotoxicity on MG-63 cell line. Osteoblast like cells, MG-63 exhibited superior cell proliferation on the highly interconnected porous composite Chitosan/HAp/Amylopectin scaffold as compared to the chitosan scaffold.

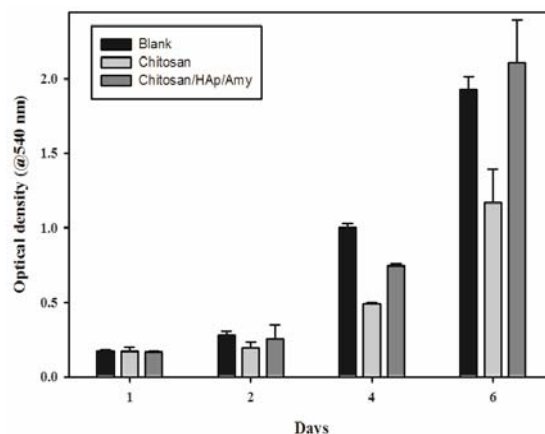


Fig.6. Cell proliferation of MG-63 cells on scaffolds as a function of days, measured by MTT assay which represents active mitochondrial activity of living cells. Optical density was significantly higher on the composite scaffold on day 6 compared to pure Chitosan scaffold.

ACKNOWLEDGEMENTS

This work was supported by a grant from Marine Bioprocess Research Centre of the Marine Bio 21 Center funded by the Ministry of Land, Transport and Maritime, Republic of Korea.

REFERENCES

- [1] Langer, R. and Vacanti, J. (1993) Tissue engineering. *Science.*, 260(5110), 920-926.
- [2] Giannoudis, P. Dinopoulos, H. and Tsiridis, E. (2005) Bone substitutes: an update. *Injury.*, 36(3S), 20-27.
- [3] Thein-Han, W. and Misra, R.D.K (2009) Biomimetic chitosan–nanohydroxyapatite composite scaffolds for bone tissue engineering. *Acta Biomater.*, 5(4), 1182-1197.
- [4] Venkatesan, J., & Kim, S.-K. (2010) Chitosan Composites for Bone Tissue Engineering-An Overview. *Mar. Drugs.*, 8(8), 2252-2266.
- [5] Venkatesan, J. Qian, Z.J. Ryu, B. Ashok Kumar, N. and Kim, S.-K. (2011) Preparation and characterization of carbon nanotube-grafted-chitosan-natural hydroxyapatite composite for bone tissue engineering. *Carbohydr. Polym.*, 83(2), 569-577.
- [6] Venkatesan, J. and Kim, S. K. (2010) Effect of Temperature on Isolation and Characterization of Hydroxyapatite from Tuna (*Thunnus obesus*) Bone. *Materials.*, 3(10), 4761-4772.

NOVEL ANALYTICAL APPLICATIONS OF CHITOSAN

L.I. Malinina, P.V. Rodionov, I.A. Veselova, T.N. Shekhovtsova

Moscow State University

**E-mail address: limalinina@mal.ru*

INTRODUCTION

Chitosan is known to be a good absorbent for many organic compounds; in particular, a large number of studies have been devoted to the chemosorption of quinones on chitosan due to the practical importance of this process, e.g. synthesis of new polymers and purification of wastewaters from phenolic compounds after their oxidation. The most extensive studies on the subject were carried out by Paine et al [1], Muzarrel et al [2] and some other groups. It has been supposed that this process proceeds as Michaelis addition [3]. However, despite a variety of possible applications of this process to our best knowledge we were the first researchers to propose the application of such reaction for the purposes of analytical chemistry.

The aim of this material is to present the data of a cycle of studies carried out by the authors devoted to utilizing chitosan both as an analytical reagent and enzyme immobilization matrix in the same system. Such advantageous combination provided the creation of a simple and reliable analytical device for laboratory and in-field analysis which can operate in aqueous or mixed media and determine some phenolic compounds.

MATERIALS and METHODS

Reagents and chemicals. Horseradish peroxidase, mushroom tyrosinase, laccase, low molecular weight chitosan, hydroquinone, pyrocatechol, quercetin, rutin, esculetin, and imidazole were purchased from Sigma, 2-(N-morpholino)ethanesulfonic acid (MES) monohydrate was produced by Fluka, whereas hydrogen peroxide and components of phosphate buffer solution were obtained from Merck. All chemicals were used without any further purification.

Apparatus. Deionized water with specific electroconductivity 18.2 MOhm/cm was prepared employing Millipore Simplicity. All absorption measurements were carried out using Shimadzu UVmini1240 UV-vis spectrophotometer. pH meter was supplied by Mettler Toledo. Atomic force microscopy (AFM) image was obtained using NT-MTD scanning probe microscope.

Construction of the biosensor and the measurement procedure. Chitosan solution (1%, w/v) was prepared by dissolving 0.4 g of chitosan powder in 40 mL of acetic acid (0.5%, v/v). The viscous chitosan solution was stirred overnight at the room temperature. A homogeneous stock solution of a enzyme/chitosan mixture was prepared from the required amount of 1% (w/v) chitosan and enzyme solutions. The formulation was changed according to the certain experiment. The stock solution was pipetted onto a glass slide and spread over a clean glass slide (14×38 mm) and left to air-dry. The obtained biosensor slides were kept at 4°C before use.

To carry out the analysis, a glass slide, covered with the chitosan/enzyme film as discussed above, was immersed into a container with the selected buffer solution (and, in some cases, organic solvent) and required concentrations of hydrogen peroxide (if necessary) and the analyte (or the sample). After having been exposed to the reaction mixture and left to stay overnight, the slide was air-dried and its absorption spectrum was registered in the range from 200 to 700 nm. The buffer solution, its pH and concentration, the volume of the reaction mixture, as well as

analyte and hydrogen peroxide (when peroxidase was used) concentrations were varied according to a certain experiment as indicated below. The analytical signal was the absorption of the film after the analysis procedure minus the absorption of the film itself at 345 nm (in the case of hydroquinone, esculetin, pyrocatechol) or 280-300 nm (quercetin, rutin).

RESULTS AND DISCUSSION

The performance of the proposed analytical system is based on the following subsequent reactions:

- i. enzymatic oxidation of the phenolic compound into a quinonic product;
- ii. interaction of the formed quinonic product with amino groups of chitosan yielding a strongly light absorbing adduct (this process was thoroughly investigated by Payne *et al* [1, 3]).

Since chitosan is an excellent film-forming agent and its films are transparent and almost do not absorb light, UV-vis spectroscopy in absorbance mode was chosen to measure the response of the biosensor and transparent glass slides were selected as the support for the sensitive biolayer. A simple procedure described above was developed for obtaining uniform and transparent films of chitosan/enzyme complex on a glass slide. The signal was measured as described in the experimental section. Such construction of the biosensor allowed dealing with non-transparent or non-homogeneous solutions since there was no need to register the absorption of the solution itself. We chose a number of phenolic compounds for these studies including model compounds of a simple structure (hydroquinone, resorcinol, pyrogallol, pyrocatechol and others) and a number of biologically active phenolic compounds containing similar fragments (quercetin, esculetin, rutin). Such row helped to understand the principles of the selectivity and study the influence of organic polar solvent on the considered analytical system.

In order to control the selectivity and sensitivity of the proposed device, we studied the influence of the enzyme, component concentration, composition of the reaction media and influence of polar solvents.

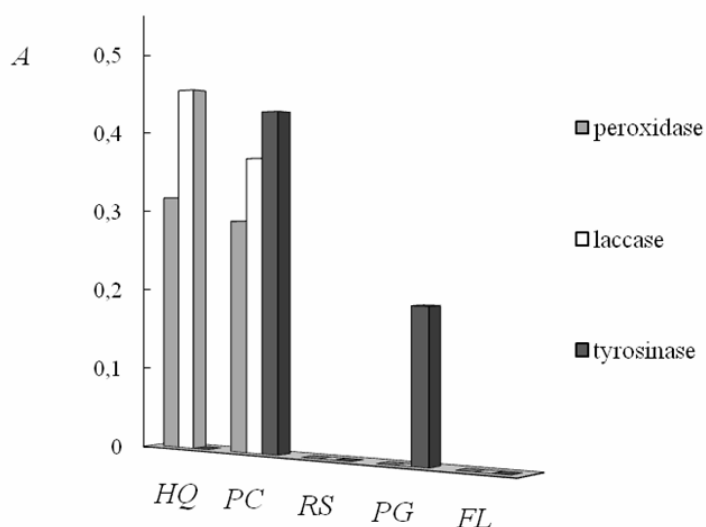


Fig. 1. Comparison of the response of the films including different enzymes towards 50 μM solutions of similar phenolic compounds (HQ – hydroquinone, PC – pyrocatechol, RS – resorcinol, PG – pyrogallol, FL – phloroglucinol).

Enzymes. Horseradish peroxidase, mushroom tyrosinase, and laccase were used as catalysts, all the three enzymes being known to catalyze oxidation of phenolic compounds. However, since

they have different selectivity (e.g. tyrosinase does not catalyze the oxidation of *p*-substituted phenols) and activity, their was significant difference in the selectivity and sensitivity of the sensors on their base as well (see Fig. 1). Horseradish peroxidase and mushroom tyrosinase appeared to be the most promising catalysts and therefore were used in the further experiments: horseradish peroxidase has appeared to be the best enzyme for the sensitive determination of phenolic compounds while mushroom tyrosine provided selective determination of *ortho*-substituted phenolic compounds.

Medium design. Since both enzyme and chitosan are polyelectrolytes and their state depends on pH and ionic strength of the medium, we studied the influence of these parameters on the sensor operation.

The response of the chitosan/peroxidase biosensor appeared not to depend on ionic strength of the phosphate buffer solution in the range from 1.25 to 5 M (phosphate buffer solution was chosen for this study as it is a widely used medium for enzymatic oxidation of phenolic compounds. At the same time, in the case of phenolic compounds of simple structure (hydroquinone and pyrocatechin), pH appeared to have a similar dramatic effect on the response regardless of the catalyst employed. It is interesting to note that maximum response of the biosensor in the pH range from 5.0 to 8.0 corresponds to pH 6.5, which is close to the reported $pK_a \sim 6.3 - 6.4$ of chitosan [2].

To study whether such high efficiency of the biosensor at this pH was due to some special interaction of chitosan and enzyme, some further investigation was performed by the example of chitosan/peroxidase film. The biosensor slides were soaked in phosphate buffer solution at pH of 6.0, 6.5 or 7.0 for some time and then their response was studied using fresh buffer solution for the reaction. As the obtained data evidenced, the response decreased along with the increase of the soak time at pH of 6.0 and 7.0. However, the response of the biosensor did not change after soaking the biosensor in the buffer solution with pH 6.5 for as long as 2 hours. Consequently, unlike pH 6.0 and 7.0, at pH 6.5 the interaction of the biomolecules is strong enough to hold them nearby (thus preventing the enzyme leaching from the film) and their space separation in a solution, at least to the extent, which could be significant for the response of the biosensor. Therefore, the particularly high response at pH 6.5 might be due to the especially strong noncovalent attraction of peroxidase and chitosan under these conditions: the first – enzymatic – reaction takes place near the surface of the biosensor and, as a result, space availability of the resultant quinone is high, thus providing its efficient interaction with chitosan. Besides, pH 6.5 lays within the range of the maximal activity of HRP.

The type of the buffer solution was found to be extremely important for the performance of the biosensor. The following organic and inorganic buffer systems were tested in terms of the biosensor response towards hydroquinone at pH 6.5: phosphate, phosphate-citric, MES (2-(*N*-morpholino)ethanesulfonic acid – KOH), glycine, imidazole buffer solutions. The response in organic buffer solutions appeared to be extremely low, moreover, the film turned muddy (the muddiness of the film was evaluated as its absorbance at 700 nm, where no reaction product absorption is observed) and uneven, probably, because of the precipitation of the components of the buffer solution on the film surface. Besides, the response of the biosensor was maximal in phosphate buffer solution. For those reasons, the latter was used for further experiments.

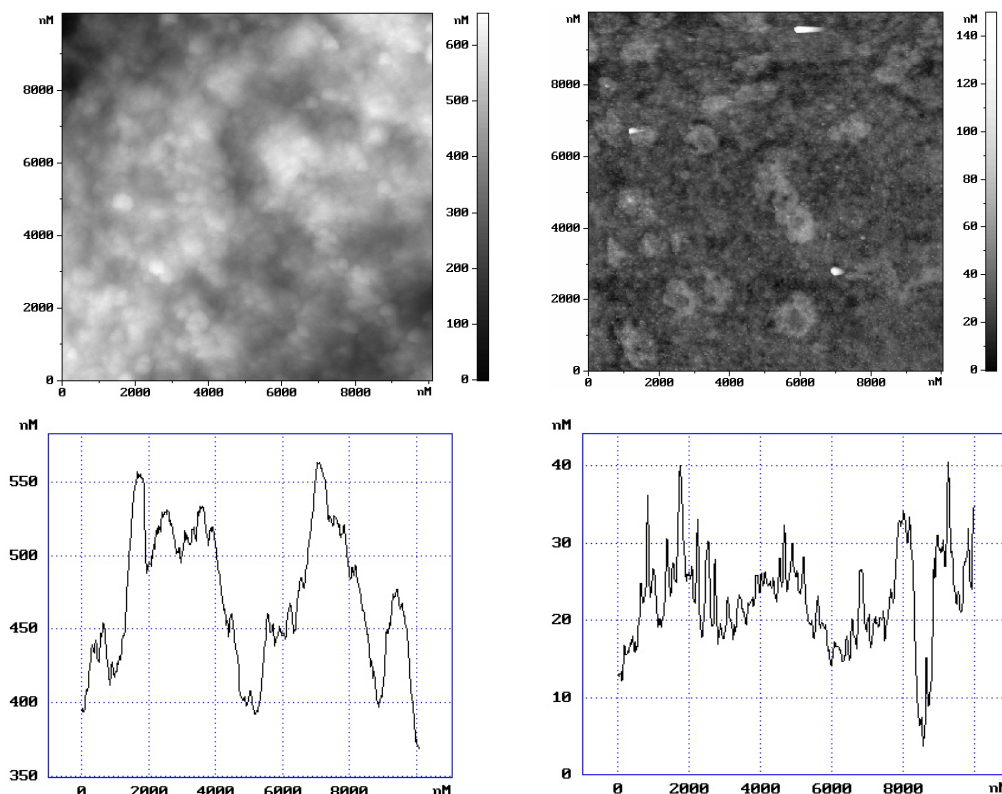


Fig. 2. AFM images and surface profiles of the chitosan/oxidase films kept in aqueous medium (0.05 M phosphate buffer solution, pH 6.5) (on the left) and in DMSO-aqueous medium (0.05 M phosphate buffer solution, pH 6.5, DMSO) (on the right).

Another interesting approach involves the **application of mixed media** for carrying out the reaction. It appeared that the introduction of small concentrations of polar solvent dimethyl sulfoxide (DMSO) increases the signal of the sensor both in the cases of water-soluble and water-insoluble analytes. Varying the concentration of the solvent demonstrated that the best signals are obtained with 10 vol.% of DMSO. Probably, such effect is associated with the second stage – the reaction between quinines and chitosan – since enzymes are known to decrease their activity in the presence of organic solvents. However, this effect provides the opportunity of determining poorly soluble compounds or samples without significant dilution of the extracts in organic solvents. Moreover, the films chitosan/oxidase appeared to have more even and uniform surface according to the results of atomic force microscopy (see Fig. 2): the fluctuations in the film height are significantly less in the case of films kept in mixed media. The image is color coded, with brighter features being greater in height. The film was also studied using optical microscopy and, as a result, its thickness was estimated to be about 5 microns.

Optimization of biosensor performance. The following parameters of the system were varied in order to achieve the best analytical signals: amounts of horseradish peroxidase and chitosan, hydrogen peroxidase concentration (which was adjusted for each analyte), sample volume and presence/absence of agitation.

On the investigation of the effect of the chitosan/oxidase complex content on the response of the biosensor the latter was found to grow linearly with the growth of the amount of the complex stock solution, used for creating the biolayer. Considering the linearity of this dependence, this increase should be attributed only to the growth of the film thickness (corresponding to l value in the Buger-Lambert-Beer law), while the amount of the absorbed

quinone seems not to depend on chitosan content, which always is in a great excess to hydroquinone under the investigated conditions. Change of the enzyme content at the constant amount of chitosan appeared not to affect the response in the range of peroxidase concentration in the system from 0.11 to 5.5 U/mL, implying that at peroxidase activity larger than 0.11 U/mL the response is limited by the adduct formation, not the enzymatic oxidation of the analyte.

The optimum concentration of hydrogen peroxide (which is required for the catalytic oxidation) was found to be 1 mM in the case of hydroquinone and pyrocatechol and 0.5 mM in the case of quercetin, rutin and esculetin, since such concentration provided the maximal response of the biosensor. The growth of the response along with the increase of the sample volume (the concentration of the analyte being constant) studied by the example of hydroquinone evidences that chitosan film concentrates the quinonic oxidation product due to chemisorption. However, a large volume of the reaction mixture causes diffusion difficulties. Stirring the reacting mixture with a magnetic stirrer, placed inside the cuvette, somewhat increased the signal but significantly complicated the analysis procedure and therefore was not used further.

Chemosorption isotherm of hydroquinone, pyrocatechol, quercetin, esculetin and rutin by the film is satisfactorily approximated by a hyperbole, which is typical for sorption processes, first of all, for the ones obeying Langmuir law. However, in the regions of small concentrations these dependences are close to linear and thus can be used as a calibration curve for the determination of the indicated analytes.

Analytical performance of the optical biosensor

Under the chosen conditions (chitosan content 2 mg, the enzyme content 0.05 nmol, 0.05 M phosphate buffer solution, pH 6.5, reaction mixture volume 5 mL, hydrogen peroxide concentration 1 mM or 0.5 mM depending on the analyte), the analytes can be determined with the characteristics indicated in the table.

Table. Analytical characteristics and application of the biosensor on the basis of chitosan/peroxidase film for the determination of phenolic compounds

Analyte	Linear range, μM^*	Detection limit, μM	Sensitivity, M^{-1}	Organic solvent	Real sample
Hydroquinone	20-200	3	6.8×10^3	-	Skin-bleaching ointment
Catechol	20-250	7	3.2×10^3	-	-
Quercetin	10-150	3	12.5×10^3	10% DMSO	Pharmaceutical preparation for injections
Rutin	10-150	10	3.9×10^3	10% DMSO	Food supplement
Esculetin	10-200	10	3.6×10^3	10% DMSO	-

*In all cases RSD of the results of the determination did not exceed 8%.

In addition to the instrumental registration of the response, the latter can be also evaluated visually, since the intensity of the biolayer depends on the initial concentration of the analyte. An example of such color scale is provided in Fig. 3.

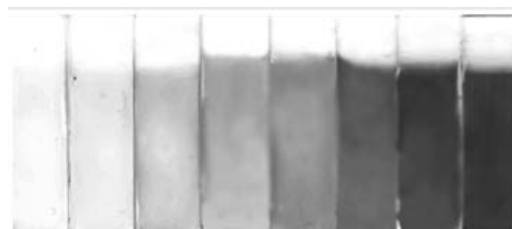


Fig. 3. Color scale for visual determination of hydroquinone (20, 40, 100, 150, 200, 400, 600, 1000 μM)

The combination of the two reactions provides the opportunities to eliminate the influence of non-phenolic (except for quinones) interfering substances which can be present in the tested sample: the products of enzymatic oxidation of phenolic compounds (quinones) are the only compounds in the system that undergo chemical interaction with chitosan and thereby incorporate into the film, the absorbance of which is used as the signal. Concerning the selectivity of the system towards phenolic compounds of similar structure, we have shown that even if the tested solution contains hydroquinone, resorcinol, pyrogallol, phloroglucinol, and catechol, only the latter compound makes a contribution to the response of the sensor, which has statistically significant difference from the blank experiment. As for the pair rutin/quercetin, the sensor exhibits different sensitivity towards rutin as compared with quercetin which might be due to a larger size of its molecule although the responses towards quercetin and rutin appeared to be additive. For this reason the biosensor can be used for the determination of quercetin or rutin when only one of them is present in the sample or in cases when rutin content is lower as compared with quercetin content.

The fabricated biosensor shows excellent stability (it was investigated using 100 μM of hydroquinone) and thus can be stored for at least a month before use (the biosensor, stored for 30 days at 4°C, provides $98 \pm 8\%$ ($n=4$, $P=0.95$) of the response provided by a new biosensor). Moreover, the indicating adduct appeared to be also very stable, and its absorption did not change when storing the biosensor at least for 6 weeks after the analysis procedure. Thus, a unique feature of the developed biosensor is the possibility to determine the hydroquinone preliminary in 'out-of-lab' mode using a colour scale (red-brown colour of varying intensity) and then to measure the response spectrophotometrically (at 345 nm) when it is necessary and convenient for the user.

Another notable feature of the developed biosensor is that the analytical signal is measured as the absorbance of the biosensor slide itself. As a result, emulsions and solutions, which are not transparent, can be analyzed without preliminary treatment. In case if any particles of the sample (e.g., ointment) are left on the surface of the slide, the film can be carefully washed with water. No risk of the analyte leaching from the film exists since it is bound covalently to chitosan. Moreover, in the case of the proposed optical biosensor the values of absorbance for the concentrations of the analyte 20 – 200 μM are in the range 0.4 – 1.6, and therefore, its use does not require employing expensive highly sensitive and precise equipment.

The biosensor was tested in the analysis of some pharmaceuticals, herbal materials and dietary supplements (see the Table).

Conclusion. The novel approach combining the reactivity and film-forming properties of chitosan allowed creating a simple and reliable device for the determination of phenolic compounds of different structure in real samples of various nature.

ACKNOWLEDGEMENTS

The authors thank Russian Foundation for Basic Research (project 09-03-00-823-a) and Russian Federation Ministry of Education and Science (contract P868) for financial support of this investigation.

REFERENCES

- [1] Payne, G. F., M. V. Chaubal, and T. A. Barbari (1996). Enzyme-catalyzed polymer modification: reaction of phenolic compounds with chitosan films. *Polymer*, 37, 4643–48.
- [2] Ravi Kumar, M. N. V., R. A. A. Muzzarelli, C. Muzzarelli, H. Sashiwa, and A. J. Domb (2004). Chitosan Chemistry and Pharmaceutical Perspectives. *Chem. Rev.*, 104, 6017–84.
- [3] Kumar G., J. F. Bristow, P. J. Smith, and G. F. Payne (2000). Enzymatic gelation of the natural polymer chitosan. *Polymer*, 41, 2157–68.

PRODUCTION AND PROPERTIES OF CHITOSAN-CONTAINING FIBERS

S.A. Uspenskiy, A.N. Sonina, G.A. Vikhoreva*, L.S. Galbraikh

A.N. Kosygin Moscow State Textile University

**E-mail: vikhorevag@mail.ru*

INTRODUCTION

The production of filaments and yarns is a promising direction in the use of chitin and chitosan. In particular, the finely dispersed fibrous form of chitosan sorbents makes it possible to attain the best hydrodynamic and kinetic characteristics of sorption and regeneration processes. Considering that the layers most actively participating in the sorption processes are the surface layers, it is appropriate to produce filaments and yarns with the “core-chitosan coat” structure. Solvents commonly used in processing of chitosan for production of various items are aqueous solutions of monobasic acids (primarily acetic acid), aqueous solutions of lithium salts, and solutions of lithium chloride in organic solvents. For economic and environmental reasons, the use of dilute acetic acid solutions is the most desirable. However, since it is impossible to make highly concentrated fluid acetic acid solutions of the polymer, research on dry (thermal) spinning of filaments and yarns is lacking, just as their production.

The aim of this study was to optimize the conditions of producing chitosan-containing filaments with the coat–core structure, which can be of interest as sorbents and surgical threads.

MATERIALS and METHODS

We used rayon and nylon-6 zero-twist yarns and chitosans with deacetylation degree 0.88 ± 0.02 and molecular mass 60 (Ch-60) and 190 kDa (Ch-190). The chitosan solutions were prepared via preliminary swelling in water, dissolution in acetic acid at molar ratio of acid: chitosan 2.2, and subsequent dilution with ethanol, water–ethanol mixture, or water for attaining the required polymer concentration (1–8 wt %) and ethanol content (10–40 wt %). In comparative experiments viscosity of the solutions were measured at a fixed value of shear stress (σ) or velocity gradient (j) 3 s^{-1} , after conditioning for 24–30 hours. Rheological curves of solution were measured with a Rheotest-2 rotary viscometer. Viscosity of solvents was measured in capillary viscometer with a known constant for the calculation of dynamic viscosity. Intrinsic viscosity of chitosan solutions was determined at 25°C in the viscometer Ubbelode with capillary diameter 0.56 mm. To identify the effect of ethanol on the thermodynamic quality of solvent, and, consequently, the conformation and the degree of macromolecules association, the ionic strength was created by minimal amount of sodium acetate (0.04 mol/l) that subsided polyelectrolyte swelling. The concentration of acetic acid and the initial concentration of chitosan solution are 0.4%. The optical density (D) of 1% solutions was determined on a spectrophotometer UNICO 1200/1201 in the wavelength range (λ) at 350 - 900 nm with intervals of 40 nm. The calculation of solution's turbidity (τ), number (N) and radius (r) of scattering particles carried in the range 420 - 600 nm, where the difference of optical density of chitosan solutions with and without alcohol is the most significant according to formulas [1]:

$$\tau = 2,3D_{cp} / l \quad N = 1,26 \cdot 10^{17} \tau / \lambda_{cp}^2 \alpha^2 k \quad r = \lambda_{cp} \alpha / 2 \cdot 3,14n_0$$

where l is длина кюветы см, α and k - characteristic constants of light scattering, n_0 - refractive index of the solvent.

RESULTS and DISCUSSION

Earlier it has been shown that even slight (10%) reduction of the molecular mass of chitosan during standing in acetic acid solutions results in a significant (40–50%) decrease in its dynamic viscosity [2]. Therefore, it was proposed to introduce the stage of “maturation” into the technological process of chitosan solution processing into ready products: the spinning solution was to be left to stand for 20–30 h in order to facilitate the subsequent stages of filtering, deaeration and spinning itself without impairing the strength properties of the resultant products.

Since acetic acid solutions have a high boiling point (above 100°C), it would be appropriate to introduce a more volatile component, such as ethanol, for faster solidification of chitosan films and coats. The choice of ethanol was due to its good compatibility with the water and acetic acid, its nontoxicity and shown earlier its influence on porous structure chitosan films [3]. Ethanol is a precipitant for chitosan; therefore, the thermodynamic quality of the mixed solvent was evaluated using viscometric measurements. It was also necessary to study the effect of ethanol on chitosan solutions because, according to our and literature data, addition of ethanol affects the strength of acetic acid and the viscosity of its solutions.

The monotonic decrease in the intrinsic viscosity and the increase in Huggins constants within the studied range of alcohol : water ratios (curves 1 and 2 in Fig. 1, respectively) confirm the conclusion that the thermodynamic quality of the alcohol-containing solvent deteriorates. The data on the initial dynamic viscosity of 1–8% polymer solutions (Fig. 2) – in particular, the fact that the higher the alcohol and chitosan content in them, the more significant the increase in this value upon addition of alcohol – also agree with known concepts of the effect of solvent quality on the properties of solutions.

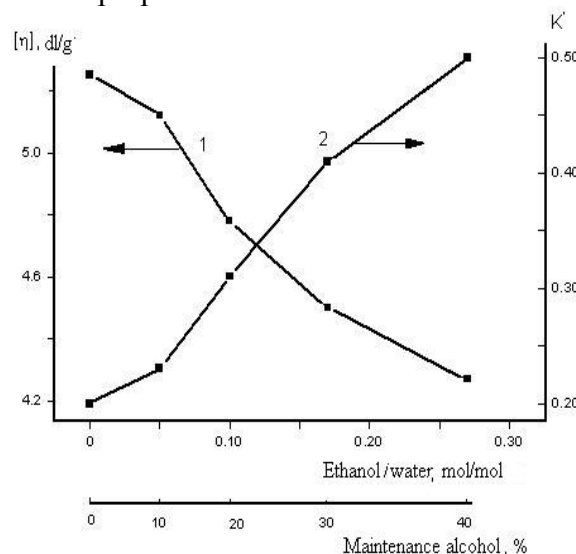


Figure 1- Influence of the solvent composition on the intrinsic viscosity (1) and Huggins constant (2)

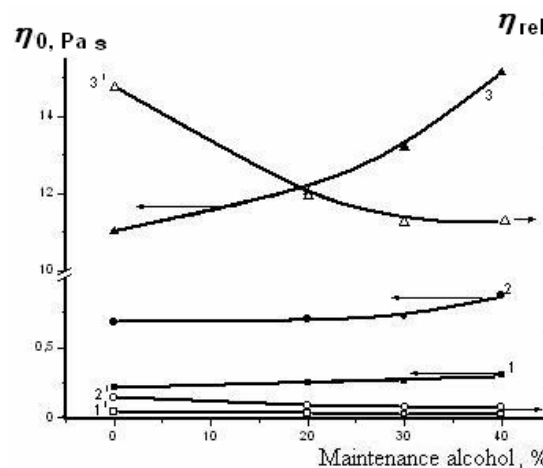


Figure 2 - Dependence of viscosity (1-3) and the relative viscosity (1'-3') of chitosan Ch-190 solutions 1 (1,1'), 3 (2,2') и 8% (3,3') on the ethanol content

Meanwhile, if we evaluate the effect of alcohol on the relative viscosity of solutions (curves 1'-3' in Fig. 2), which reflects the contribution of the polymer to the total viscosity, we see that it

decreases with addition of alcohol, since the dynamic viscosity of the water–ethanol–acetic acid three-component solvent increases by a factor of more than 2 (from 1.0 to 2.4 mPa s) as the ethanol content increases to 40%. Hence, the increase in the viscosity of ethanol-containing chitosan solutions may be also due to properties of the solvent itself, whose structural associates in concentrated polymer solutions form macroscopic clusters, which significantly raise the initial viscosity of the system.

When ethanol was added, one could visually observe lesser turbidity and higher homogeneity of concentrated (6–8%) chitosan solutions; for 1% solutions, this effect was confirmed by calculations (curve 1 in Fig. 3). Calculations also showed that addition of ethanol leads to a significant decrease in the number of scattering particles (curve 2) with a certain increase in their average size (curve 3), which can be explained by additional dissolution of the smallest gel particles, so that the average detectable size of scattering particles increases.

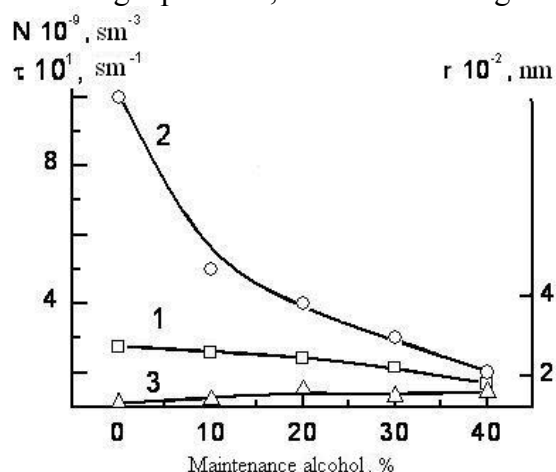


Figure 3 - Dependence of turbidity of 1% solutions of Ch-190 (1), numbers (2) and particle size (3) on the maintenance of ethanol

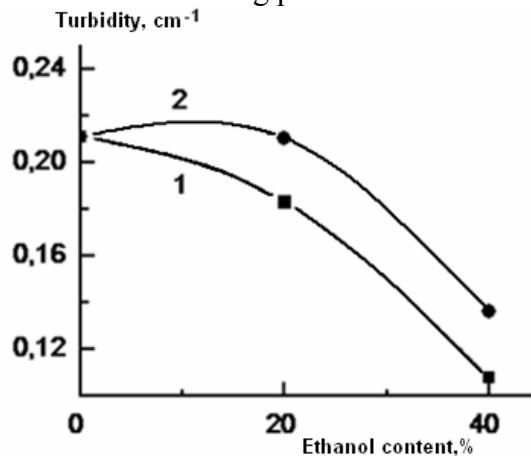


Figure 4 - Influence of ethanol content on turbidity of 1% chitosan Ch-190 solutions prepared by subsequent dilution with ethanol (1), and also by direct dissolution of polymer in alcohol-containing solvents (2)

Additional dissolution of associates (fluid micro- and nanocrystals) takes place owing to heating of the mixture due to the energy released in the exothermal process of ethanol–water interaction. This explanation is confirmed by higher turbidity of chitosan solutions prepared by direct dissolution of the polymer in alcohol-containing solvents (see Fig. 4) and also by brief reversible reduction of the system viscosity upon addition of the next portion of ethanol, which is visually observed as an increase in the stirrer rotation rate, much more significant than its increase due to system dilution with the same amount of water. It is not excluded also, that ethanol plays a role of an acceptor of H-bonds.

As is shown (see Fig. 5), the presence of 40% ethanol in the spinning solutions of chitosan results in approximately twofold increase in the solidification rate of films or yarn coats. In turn, for this reason it becomes possible to use either a lower temperature or a lesser height of the quench duct, or to increase the spinning rate and the stability of chitosan-coated yarn production. The high rate of coat solidification from the alcohol-containing chitosan solution ensures not only homogeneity of the coat but also its higher content on the yarn, since chitosan will not adhere to the yarn guide appliances.

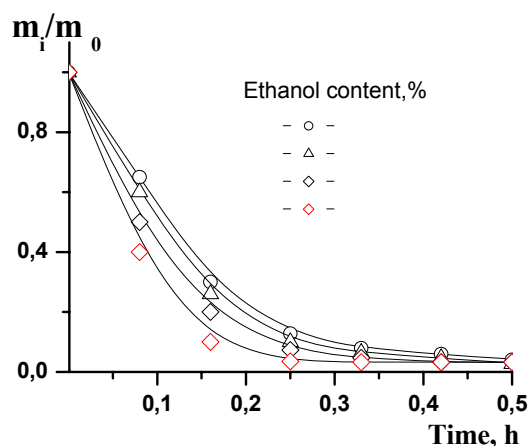


Figure 5 - Solidification rate curves of 8% Ch-190 solutions at 60°C and forming films with thickness 30 μm

Thus, our examination shows that up to 40% ethanol may be introduced into spinning solutions of chitosan, since it does not lead to phase separation in the solution or significant increase in its initial viscosity and does not affect the viscosity of 8% solutions at the shear velocity gradient above 10 s^{-1} , that is, at even minor mechanical action, such as during stirring and transportation of solutions. Adding ethanol into the spinning solution, just as varying the polymer concentration and the diameter of the die, one can control the thickness of the applied chitosan coat. One could expect that the presence of ethanol and the fast evaporation of the solvent would lead to formation of films with

a porous structure. As is seen in photographs, chitosan forms a structurally uniform nonporous and virtually defect-free coat, where, on the whole, modified yarns with a high (no less than 15%) content of chitosan have a core-coat structure. The chitosan coat makes a zero-twist rayon yarn look like a monofilament, whereas a yarn with a low ($\sim 1\%$) content of chitosan (see Fig. 6) is rather impregnated with it, because it was produced using a less concentrated low-viscosity polymer solution, which penetrates into the interfilament space as well, although chitosan forms a film on the yarn surface even in this case.

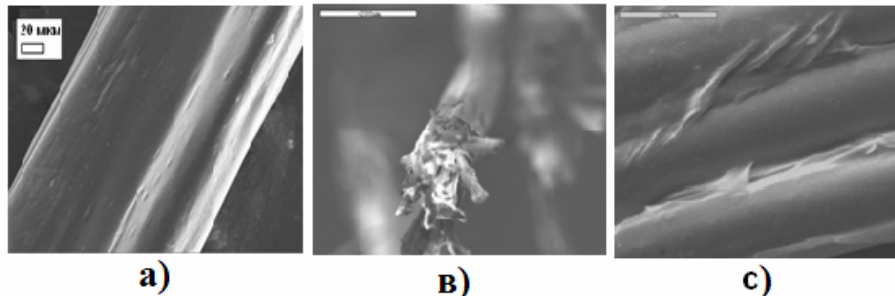


Figure 6 - Microphotos of thread with a chitosan cover 50 (a), 15 (b) and 1-2 % (c) put from ethanol containing solutions

Films formed from alcohol-free and alcohol-containing solutions of low-molecular-mass chitosan Ch-60 at room temperature have a well-organized porous structure, which could be advantageous for the kinetics of the sorption process; however, films solidified at 100°C do not preserve the porous structure. Evidently, relaxation processes of structurization under these conditions take place at a rate that is comparable to the solvent evaporation rate, not leading to phase separation in the system. At the same time, solidification of solutions of higher-molecular-mass chitosans Ch-190 under the same conditions does not lead to formation of films with a porous structure, and introduction of ethanol, according to electron microscopic findings, has virtually no effect on the film structure. However, according to the data of atomic force microscopy, the surface of films formed from ethanol-containing solutions (Fig. 7 d–7f) is more homogeneous in comparison with films formed from alcohol-free solutions (Fig. 7a–7c), which is

especially clearly seen in 3D images, where the scale at the ordinate axis characterizes the surface roughness.

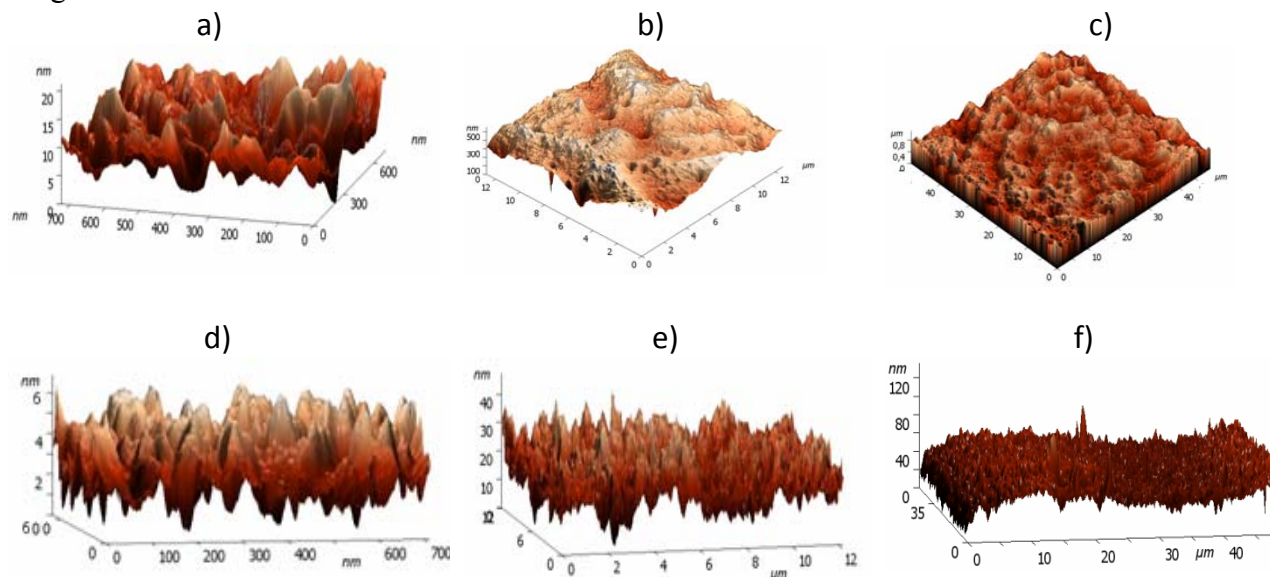


Figure 7 - Images of a surface of the chitoan films formed from ethanol free (a-c) and ethanolcontaining solutions (d -f)

Introduction of ethanol into the spinning solution of low-molecular-mass chitosan leads to deterioration of its strength properties, evidently owing to changes in the closed porosity; at the same time, introduction of ethanol for high-molecular-mass chitosans does not lead to deterioration of their strain–strength properties (see Table). The stress–strain curves of high-molecular-mass chitosan are characterized by transition into forced rubberlike state with formation of a neck, whereas it is absent from low-molecular-mass chitosan, which is characterized by brittleness.

Table – The influence of ethanol content on strain–strength properties of chitosan films

Chitosan	Ethanol content, %	Strain, %	E, GPa	Strength, MPa \pm 1
Ch-60	0	2 \pm 1,0	3,35	54
	20	1 \pm 0,2	2,86	29
	40	1 \pm 0,2	3,07	29
Ch-190	0	10 \pm 2,0	4,09	91
	20	12 \pm 4,0	4,25	90
	40	10 \pm 2,0	4,16	87

It is natural that the linear density and absolute strength of yarns change in parallel with the content of the chitosan coat, whereas the dependence of relative breaking strength (P_0) is opposite. The slight increase in P_0 at coat content about 2-5% is explained by the fact that this amount of applied chitosan does not yet form a coat but instead impregnates the initial zero-twist rayon yarn and increases the mutual adhesion of separate monofilaments.

The sorption capacity of the fibrous chitosan sorbent was studied in relation to copper ions in order to compare the model experiments with other sorbents. As is seen from the kinetic

sorption curves, fibrous chitosan sorbents have better kinetic characteristics of sorption and high equilibrium sorption capacity (per unit amount of chitosan) than granulated ones. Considering that the surface layers take the most active part in the sorption process, it seemed interesting to optimize the content of chitosan on the yarns.

Results of this study showed that the optimum content of chitosan is $30 \pm 5\%$, which corresponds to coat thickness 10–12 μm . Such a thin coat ensures high rate of the sorption process and sufficiently high equilibrium sorbent capacity.

Determination of strength and linear density of the fibrous chitosan sorbent under the conditions of activation and regeneration showed a slight decrease in chitosan content on the yarns during activation and its invariable content at regeneration, remaining at the level that is sufficient for practical use in sorption.

ACKNOWLEDGMENTS

This work was supported by the Ministries of Education and Science of the Russian Federation (the contract № 16.740.11.0059). The authors are thankful to Dr. A. Albulov and Dr. A. Chernyshenko for chitosan samples.

REFERENCES

- [1] Klenin, V.I., Shchyogolev, S.Y., Lavrushin, V.I. (1977) Characteristic features of light scattering of dispersed systems. Ed. Dr. S. Ya Frenkel. Saratov: Izd. Saratov University.
- [2] Mironov, A.V., Vikhoreva, G.A., Uspenskiy, S.A., Kildeeva, N.R. (2007) Reasons for unstable viscous properties of chitosan solutions in acetic acid. Polymer Science, Ser. B, 49, 1–2, 15-17.
- [3] Nud'ga, L. (1992) Chitin- and chitosan-base biomaterials. Mater. 3-th All-Union Conf. on Chitin and Chitosan. Moscow: VNIRO., 40-44.

PROTECTIVE EFFECT OF N-ACETYL CHITOOLIGOSACCHARIDES AGAINST MICROGLIA-MEDIATED NEUROINFLAMMATION

Thanh-Sang Vo¹ and Se-Kwon Kim^{1,2*}

¹ Department of Chemistry, Pukyong National University, Busan 608-737, Republic of Korea

² Marine Bioprocess Research Center, Pukyong National University, Busan 608-737, Republic of Korea

*E-mail address: sknkim@pknu.ac.kr

INTRODUCTION

Microglia, a specialized form of macrophage residing in the central nervous system, are believed to be the major cell type responsible for inflammation-mediated neurotoxicity. The activation of microglia leads to the production and release of numerous proinflammatory and neurotoxic mediators, such as TNF- α , PGE₂, IL-1, IL-6, and NO [1]. Moreover, microglia activation can provoke a complex array of intracellular signaling pathways involving mitogen-activated protein kinases (MAPKs) and nuclear factor (NF)- κ B-mediated gene expression [2]. Therefore, the modulation of microglia activation is an effective therapeutic approach against neurodegenerative diseases.

Chitin and its derivatives have been of interest in the past few decades due to biological potentials for a wide range of applications such as in food, cosmetics, and biomedicine [3]. Among them, N-acetyl chitoooligosaccharides have been known as therapeutic agents against oxidant, microbe, and tumor [4–6]. However, the anti-inflammatory activity of NA-COS remains to be evaluated. Therefore, we were interested in examining the anti-inflammatory mechanisms of NA-COS on BV-2 microglia under LPS-stimulation.

MATERIALS and METHODS

Materials

Enzyme immunoassay reagents for cytokine assays were purchased from R&D Systems (Minneapolis, MN, USA). LPS from *Escherichia coli* 026:B6, nuclear and cytoplasmic extraction reagent, and Griess reagent were purchased from Sigma (St. Louis, MO, USA). Specific antibodies used for western blot analysis were purchased from Santa Cruz Biotechnology Inc. (Santa Cruz, CA) and Amersham Pharmacia Biosciences (Piscataway, NJ).

NO production assay. NO level in the culture supernatant was measured by the Griess reaction as described earlier [7]. In brief, BV-2 cells were stimulated for 24 h with LPS (1 μ g/ml, final concentration) in the presence or absence of various concentrations of NA-COS. Aliquots (50 μ l) of the supernatants were incubated with 50 μ l of Griess reagent for 15 min. This was followed by measurement of absorbance values at 540 nm using a microplate reader (Tecan Austria GmbH). The nitrite concentrations were calculated with reference to a standard curve of sodium nitrite generated by known concentrations.

Enzyme-linked immunosorbent assay (ELISA). For immunoassays, BV-2 cells were treated with different concentrations of NA-COS before stimulated with LPS (1 μ g/ml, final concentration) for 24 h. The supernatant was collected, and production of PGE₂, IL-1 β , IL-6, and TNF- α was quantified by sandwich immunoassays following the protocol of R&D systems.

Western blot analysis. Western blotting was used for detection of protein expression. Cells were washed three times with PBS and lysed in RIPA lysis buffer (NP-40, Sigma–Aldrich, USA). Equal amounts of protein were separated on 10% SDS-PAGE, transferred onto a nitrocellulose membrane, and then blocked in TBS-T buffer (20 mM Tris, pH 7.6, 0.1% Tween 20) containing 5% (w/v) bovine serum albumin. After incubation with the appropriate primary antibody, the

membranes were incubated for 1 h at room temperature with a secondary antibody conjugated to horseradish peroxidase. Following three washes in Tris-buffered saline-Tween (TBS-T), immunoreactive bands were visualized using the electrochemiluminescence (ECL) detection system. In a parallel experiment, nuclear protein was prepared using nuclear extraction reagents according to the manufacturer's protocol.

Reverse transcriptase-polymerase chain reaction (RT-PCR)

RT-PCR was used to analyze the mRNA expression of cytokine. Total RNA was isolated using the TRIzol reagent (Invitrogen, Paisley, UK). Total RNA from the cells was reverse-transcribed using M-MLV reverse transcriptase to produce cDNA. RT-generated cDNAs encoding TNF- α , IL-1 β , IL-6, and glyceraldehyde 3-phosphate dehydrogenase (GAPDH) were amplified by PCR using selective primers. Primer sequences used in this study were as follows: for TNF- α , forward 5'-ATG-AGC-ACA-GAA-AGC-ATG-ATC-3' and reverse 5'-TAC-AGG-CTT-GTC-ACT-CGA-ATT-3'; for IL-1 β , forward 5'-ATG-GCA-ACT-GTT-CCT-GAA-CTC-AAC-T-3' and reverse 5'-TTT-CCT-TTC-TTA-GAT-ATG-GAC-AGG-AC-3'; for IL-6, forward 5'-AGT-TGC-CTT-CTT-GGG-ACT-GA-3' and reverse 5'-CAG-AAT-TGC-CAT-TGC-ACA-AC-3'; for GAPDH, forward 5'-TGA-AGG-TCG-GTG-TGA-ACG-GAT-TTG-GC-3' and reverse 5'-CAT-GTA-GGC-CAT-GAG-GTC-CAC-CAC-3'. Following amplification, portions of the PCR reactions were electrophoresed on an agarose gel.

RESULTS and DISCUSSION

NO and PGE₂ play an important role in neurodegeneration and their pathogenesis [8, 9]. Therefore, these two proinflammatory mediators have been considered as therapeutic targets to reduce the progression of neurodegenerative disorders. Interestingly, NA-COS has shown to inhibit LPS-induced NO and PGE₂ production in a concentration-dependent manner in BV-2 microglia (Figure 1). Therefore, NA-COS are regarded as protective agents against neurodegeneration via reducing NO and PGE₂ production.

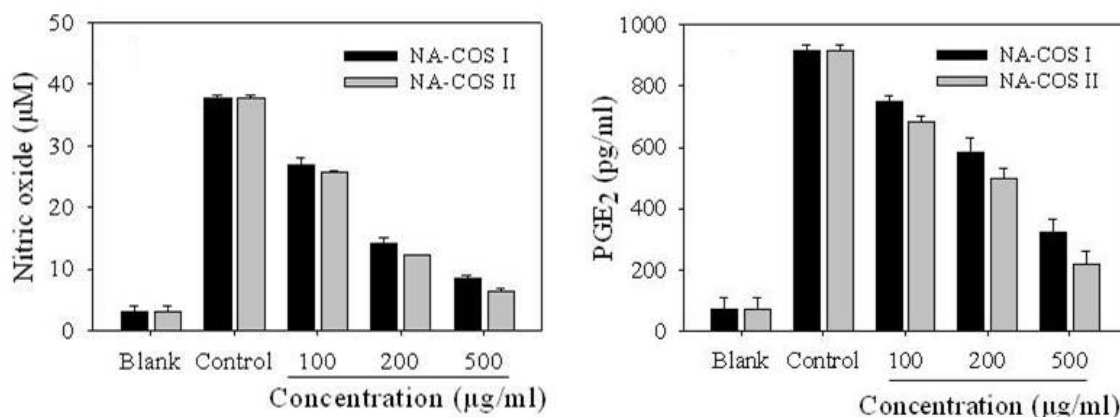


Figure 1. Effects of NA-COS on NO and PGE₂ production in LPS-stimulated BV-2 microglia. The cells were treated with the indicated concentration of NA-COS (100, 200, or 500 μg/ml) before LPS (1 μg/ml) treatment for 24 h. Amount of NO was measured using the Griess reaction. The PGE₂ concentration was measured using a commercial ELISA kit. Each determination was made in triplicate, and the data are expressed as means \pm SD. $p < 0.05$ is significantly different value compared to the control group. NA-COS I and NA-COS II are N-acetyl chitooligosaccharides of molecular weight ranges of below 1 kDa and 1–3 kDa, respectively. Blank: –NA-COS–LPS; Control: –NA-COS+LPS.

Moreover, neuroinflammatory response is also characterized via the production of cytokines such as TNF- α , IL-1 β , and IL-6. Several studies have also reported a key role for proinflammatory cytokine overproduction as a potential driving force for pathology progression

in acute neurodegenerative disorders [10, 11]. Consequently, the inhibition of cytokine production or function is a significant mechanism in alleviation of neuronal injury or death in neurodegenerative diseases. Here, we have found that NA-COS induced a dose-dependent suppression on the production and mRNA expression of TNF- α , IL-1 β , and IL-6 in LPS-stimulated BV-2 microglia (Figure 2). According to these observations, NA-COS emerge as a promising therapeutic candidate to inhibit the LPS-induced microglia activation in the CNS. However, the mechanism underlying the inhibitory effects of NA-COS on inflammatory responses in LPS-induced BV-2 cells remains to be elucidated.

The transcription factor NF- κ B plays a central role in the induction of proinflammatory gene expression, and is considered as a promising target for the treatment of inflammatory diseases [12]. Thus, the blockade of NF- κ B transcriptional activity can inhibit the expression and production of proinflammatory mediators. Noticeably, NA-COS prevented the cytoplasmic degradation of I κ B- α and nuclear translocation of p50/65 proteins in LPS-activated BV-2 microglia (Figure 3). These findings imply that the inhibitory effects of NA-COS on the production of inflammatory mediators are mediated, at least in part, via the inactivation of the NF- κ B signaling pathway.

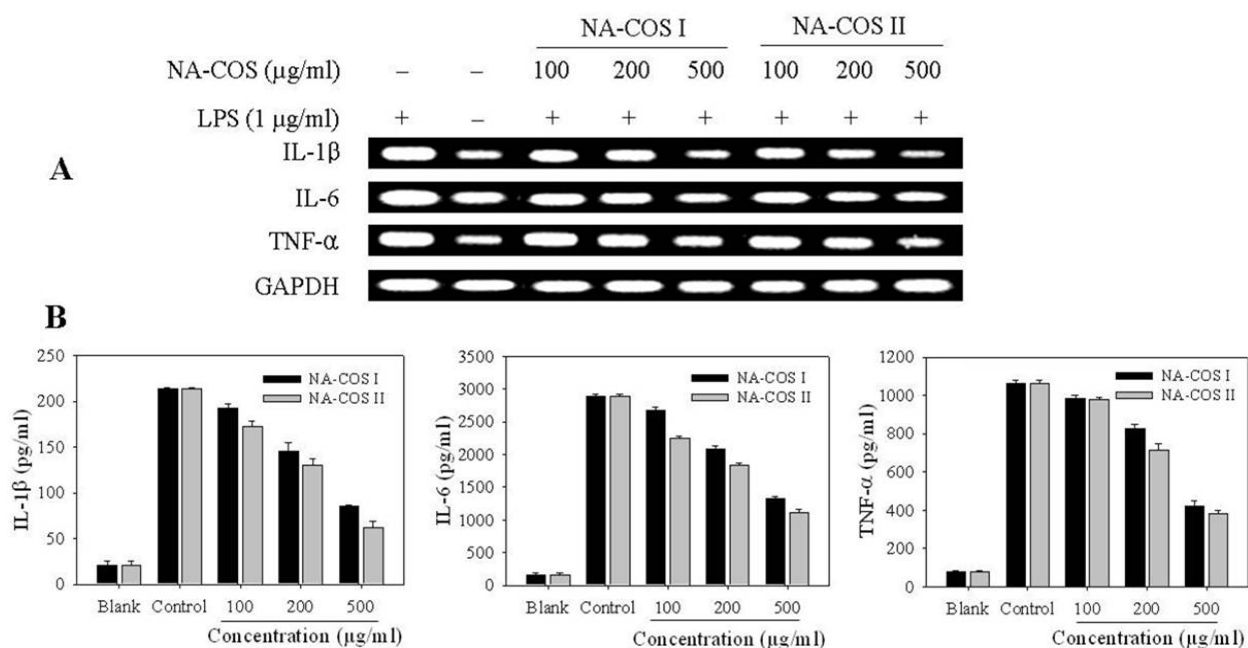


Figure 2. Effects of NA-COS on the expression (A) and production (B) of proinflammatory cytokines in LPS-activated BV-2 microglia. The cells were incubated with various concentrations of NA-COS in the presence or absence of LPS (1 μ g/ml) for 24 h. After incubation of LPS, total mRNAs were isolated using the TRIzol reagent, and the mRNA level of IL-1 β , IL-6, and TNF- α was determined by RT-PCR. GAPDH was measured as an internal control (A). Extracellular levels of IL-1 β , IL-6, and TNF- α were quantified using ELISA assay kits (B). Each determination was made in triplicate, and the data are expressed as means \pm SD. $p < 0.05$ is significantly different value compared to the control group. Blank: -NA-COS-LPS; Control: -NA-COS+LPS.

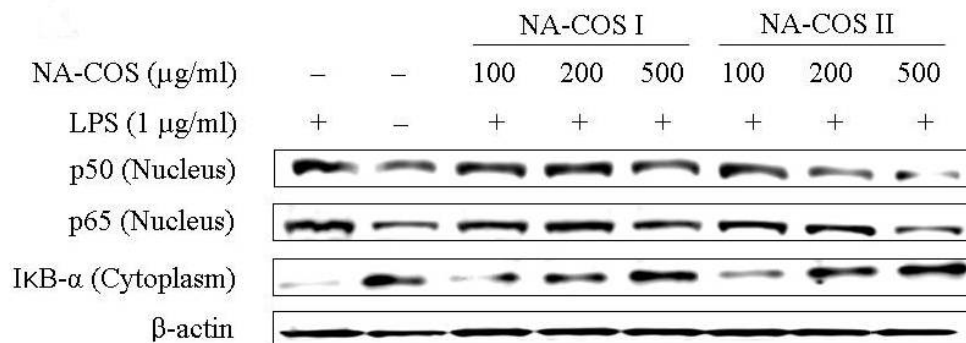


Figure 3. Effects of NA-COS on NF- κ B activation in LPS-stimulated BV-2 microglia. The cells were pre-incubated with the indicated doses of NA-COS prior to LPS treatment for 1 h. (A) Cytosolic and nuclear protein extracts were prepared by commercial kit from sigma (MO, USA). The p50 and p65 subunits of NF- κ B in nuclear protein extract and level of I κ B- α in the cytosolic protein extract were determined by a Western blot analysis. The β -actin was used as an internal control.

Substantially, various intracellular signaling pathways are involved in the modulation of NF- κ B activity and inflammatory mediator expression. The MAPKs include ERK, p38 kinase, and JNK subgroups which are responsible for most cellular responses to cytokines and external stress signals, and crucial for regulation of the production of inflammatory mediators [13]. Thus, we investigated the effect of NA-COS on the LPS-induced phosphorylation of MAPKs in BV-2 microglia. The present study indicates that NA-COS are potent inhibitors of ERK, p38 and JNK phosphorylation (Figure 4). These results suggest that MAPKs are involved in the inhibitory effect of NA-COS on proinflammatory mediator expression and NF- κ B activation.

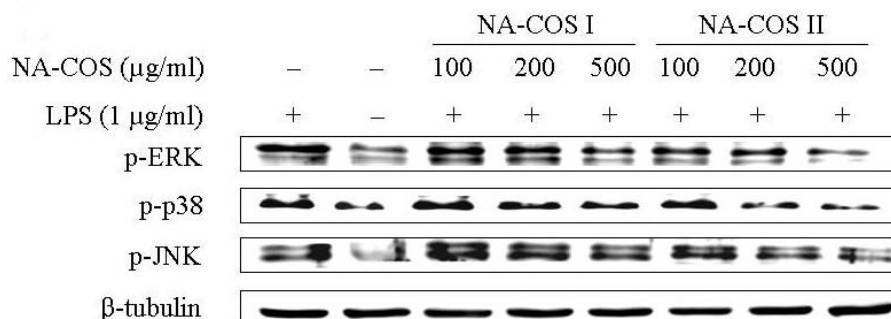


Figure 4. Effects of NA-COS on MAPKs activation in LPS-stimulated BV-2 microglia. The cells were pre-incubated with the indicated doses of NA-COS prior to LPS treatment for 1 h. Total cell lysates obtained after the LPS stimulation were subjected to Western blotting to assess the phosphorylation level of ERK, p38, and JNK protein. β -tubulin was detected to confirm the equal loading of the samples. The phosphorylation of ERK, p38, and JNK were abbreviated by p-ERK, p-p38, and p-JNK, respectively.

In conclusion, NA-COS exhibit an anti-inflammatory activity that is dependent on its ability to regulate the production of proinflammatory mediators via the attenuation of NF- κ B activation and MAPKs phosphorylation in LPS-stimulated BV-2 microglia. These results support that NA-COS could be a potential therapeutic candidate for neurodegenerative diseases caused by microglia activation. However, future studies are needed to confirm the neuroprotective property of NA-COS in an animal-mediated neuroinflammatory model.

ACKNOWLEDGEMENTS

This research was supported by a grant from the Marine Bioprocess Research Center of the Marine Biotechnology Program funded by the Ministry of Land, Transport and Maritime, Republic of Korea.

REFERENCES

- [1] Liu, B. and Hong, J. S. (2003) Role Of Microglia in Inflammation-Mediated Neurodegenerative Diseases: Mechanisms and Strategies for Therapeutic Intervention. *J. Pharmacol. Exp. Ther.*, 304, 1–7.
- [2] Trudler, D., Farfara, D. and Frenkel, D. (2010) Toll-Like Receptors Expression and Signaling in Glia Cells in Neuro-amyloidogenic Diseases: Towards Future Therapeutic Application. *Mediators Inflamm.*, 2010, pii: 497987.
- [3] Park, B. K. and Kim, M. M. (2010) Applications of Chitin and its Derivatives in Biological Medicine. *Int. J. Mol. Sci.*, 11, 5152–64.
- [4] Ngo, D. N., Lee, S. H. and Kim, M. M. et al. (2009) Production of Chitin Oligosaccharides with Different Molecular Weights and Their Antioxidant Effect in RAW 264.7 Cells. *J. Funct. Foods*, 1, 188–98.
- [5] Ngo, D. N., Kim, M. M. and Kim, S. K. (2008) Chitin Oligosaccharides Inhibit Oxidative Stress in Live Cells. *Carbohydr. Polym.*, 74, 228–34.
- [6] Wang, S. L., Lin, H. T. and Liang, T. W. et al. (2008) Reclamation of Chitinous Materials by Bromelain for The Preparation of Antitumor and Antifungal Materials. *Bioresource Technol.*, 99, 4386–93.
- [7] Verdon, C., Burton, B. and Prior, R. (1995) Sample Pre-treatment with Nitrate Reductase and Glucose-6-Phosphate Dehydrogenase Quantitatively Reduces Nitrate While Avoiding Interference by NADP⁺ When The Griess Reaction Is Used to Assay for Nitrate. *Anal. Biochem.*, 224, 502–8.
- [8] Liu, B., Gao, H. M. and Wang, J. Y. et al. (2002) Role of Nitric Oxide in Inflammation-Mediated Neurodegeneration. *Ann. N.Y. Acad. Sci.*, 962, 318–31.
- [9] Cimino, P. J., Keene, C. D. and Breyer, R. M. et al. (2008) Therapeutic Targets in Prostaglandin E₂ Signaling for Neurologic Disease. *Curr. Med. Chem.*, 15, 1863–9.
- [10] Mrak, R. E. and Griffin, W. S. (2005) Glia and Their Cytokines in Progression of Neurodegeneration. *Neurobiol. Aging*, 26, 349–54.
- [11] Van Eldik, L. J., Thompson, W. L. and Ralay Ranaivo, H. et al. (2007) Glia Proinflammatory Cytokine Upregulation as a Therapeutic Target for Neurodegenerative Diseases: Function-based and Target-based Discovery Approaches. *Int. Rev. Neurobiol.*, 82, 277–96.
- [12] Barnes, P. J. and Karin, M. (1997) Nuclear Factor-KappaB: a Pivotal Transcription Factor in Chronic Inflammatory Diseases. *N. Engl. J. Med.*, 336, 1066–71.
- [13] Karunakaran, S. and Ravindranath, V. (2009) Activation of P38 MAPK in The Substantia Nigra Leads to Nuclear Translocation of NF-KappaB in MPTP-treated Mice: Implication in Parkinson's Disease. *J. Neurochem.*, 109, 1791–9.

EFFECT OF CHITOSAN AND N- CARBOXIMETHYL CHITOSAN ON THE GROWTH AND SOLUBLE PROTEINS OF PEA (*PISUM SATIVUM* L) ROOTS

Yakovleva V.G.^{1*}, Tarchevsky I.A.¹, Levov A.N.², Egorova A.M.¹

¹*Kazan Institute of Biochemistry and Biophysics of Kazan Science Centre of RAS, Kazan*

²*Centre bioengineering RAS, Moscow*

**E-mail address: yakovleva@mail.knc.ru*

INTRODUCTION

A well-known feedback between resistance and growth rate occurs when plants are treated with elicitors of pathogen resistance. Among the elicitors are chitosans, oligosaccharide products of the chitin degradation with different molecular weight. The ratio of the residues of chitin and chitosan determines the strength of the immune response. Chemical modification of chitosans also affects their activity [1], and may enable the creation of antipathogenic preparations. Chitosans not only elicit resistance of plants, but also can suppress their growth. This property applies to the yeast extract containing chitoooligosaccharides, and elicitor-induced production of phytoalexins which play a defense role against pathogen invasion is being associated with a notable growth suppression [2]. This thesis is confirmed by certain antagonism between oligosaccharide elicitors and auxins (in other words, between the processes of immunity induction and the processes of plant growth) [3].

Induction of immunity under the influence of elicitors or change of the activity of the growth processes under the action of phytohormones involves changes of proteomes in various organs of plants. It was shown that oligosaccharide products of chitin degradation were able to bring about changes in proteomes of plants [4, 5].

The aim of the work presented here was to study how these elicitors effect the growth and root proteome of pea. Peas were chosen because their roots can easily be measured, and their proteomes was previously analyzed by us during the investigation of the effect of salicylic acid - a key factor in systemic immunity on plants [6, 7].

MATERIALS and METHODS

Pea (*Pisum sativum* L., cv. Tan) seedlings were grown under white fluorescent light with a 16-h light cycle ($250 \mu\text{M m}^{-2} \text{s}^{-1}$) at 25°C in Hoagland-Arnon liquid medium and were used for experimentation on the 8th day following germination. In the experiments on the effect of chitosan or N-carboximethyl chitosan (N-CMC) on the growth of pea seedlings primary and lateral roots we used 3 and 8 day-old plants. Pea seedlings roots were placed in solutions of effectors for 5 days. Seedlings in liquid medium without effectors were the control.

The linear oligosaccharide chitosan with MW 3,5 kDa and the degree of deacetylation (DD) 0,85 was obtained in our experiment by the enzymatic hydrolysis of the high molecular chitosan 700 kDa and DD 0,85 under the action of carbohydrases preparation Celloveridin [8]. The degree of deacetylation was determined by conductometric titration, middling-viscosity M.r. was calculated according to the Mark-Hauvink equation. The linear oligosaccharide N-CMC composed of 2-carboxymethylamido-2-deoxy-D-glucopyranose with the degree of substitution 0,37 was obtained [9] from chitosan with MW 58 kDa and DD 0,85 (Fig.1). The degree of N-CMC substitution was determined with the help of NMR spectroscopy.

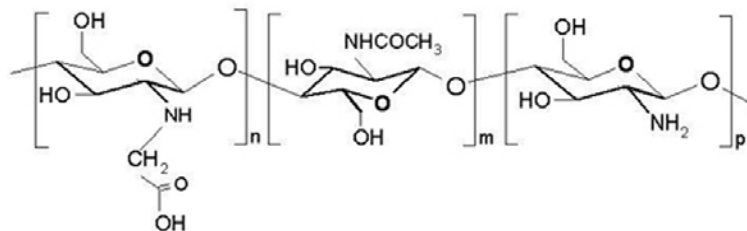


Figure 1. Formula of N-CMC

The extraction of soluble protein was performed in 0.025 M Tris-HCl pH 8.3 buffer containing 2 mM EDTA, 100 mM DTT and 1% protease inhibitors cocktail (Sigma, USA) at 4°C. The homogenates were centrifuged at 16000 g for 10 min at 4°C. The supernatant contained soluble proteins precipitated by the ice cold solution 20% TCA/acetone (10% final concentration), the samples were left in the refrigerator -20°C for 1 hour. Then the samples were centrifuged (16000 g, 10 min) and washed three times in the ice-cold acetone. Protein pellets were dissolved in buffer (6 M urea, 2 M thiourea, 2% CHAPS, 2% Triton X-100, 50 mM DTT and 0.5% Bio-Lyte (Bio-Rad)).

2D-electrophoresis was conducted using the 17 cm strips with the immobilized linear gradient pH 4-7. Each protein sample (400 µg) was adjusted to isoelectric focusing (IEF) buffer (6 M urea, 2 M thiourea, 2% CHAPS, 2% Triton X-100, 50 mM DTT, 0.5% Bio-Lyte and bromophenol blue). IEF was performed during 12 hours. After IEF the strips were incubated with equilibration buffer. The protein separation according to the molecular mass was carried out in 12.5% PAGE. Gels were stained with Coomassie brilliant blue G-250. Images were analyzed using Phoretix 2D advanced software (Nonlinear Dynamics). Three independent gels were analyzed and the significance of changes in the protein spots was assessed using the Student *t* test at $p \leq 0.05$. Only spots that displayed reproducible >1.5 fold change were used for further identification. Trypsin-digested peptides were extracted according to a previously described protocol [7]. Sample solution (0.5 µl) and 2.5 dihydroxybenzoic acid (10 mg×ml⁻¹ in 20 % acetonitrile in water with 0.5 % TFA), were mixed on a target and the obtained mixture was dried on the air. Mass-spectra were obtained on the tandem MALDI-TOF-TOF mass spectrometer Ultraflex II BRUKER (Germany) supplied with UF laser (ND). Mass-spectra were obtained in the mode of positive ions with the use of reflectron. Accuracy of the measured mass of fragments was 1Da.

RESULTS and DISCUSSION

N-CMC treatment of 3 day-old pea seedlings with 2 cm primary roots increased of both primary and lateral roots length compared with the control and roots treated with chitosan (Fig. 2). In 8 day-old seedlings, N-CMC caused strong branching of the lateral roots that was not observed in the control and in roots treated with chitosan. There were no significant differences between the growth of roots of control plants and treated with chitosan.

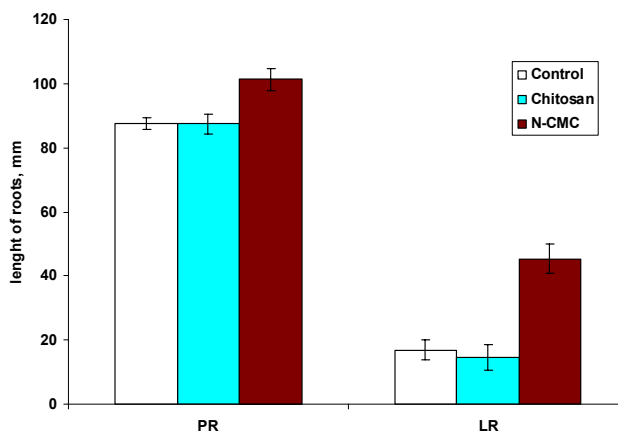


Figure 2. Effect of N-CMC on the growth of primary (PR) and lateral (LR). 3 day old pea seedlings was treated by 70 μ g/ml N-CMC for 5 days. Values represent means \pm SE (n=16) and statistical differences are indicated by $p \leq 0.01$

The fundamental difference in root growth reaction to chitosan and N-CMC allowed us to assume that these elicitors would cause a significant difference in proteomes changes. N-CMC-induced branching of lateral roots is similar to the activation of auxin growth function. The reason for this may be a certain chemical similarity in the structure of heteroauxin and N-carboxymethyl radical forming a part of N-CMC (Fig. 1). It is possible that N-CMC as auxin stimulation of the development of root system and the formation of lateral roots in different plants is mediated by NO accumulation [10]. Most probably N-CMC in our experiments, like auxin, is able to induce NO formation and as a result branching of pea lateral roots.

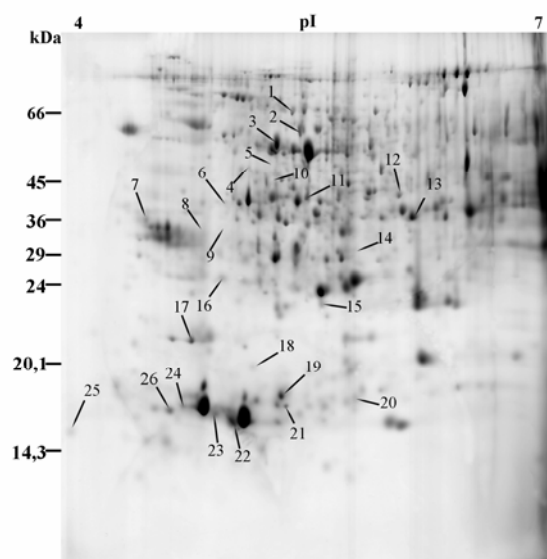
Proteins from pea roots were separated by two-dimensional polyacrylamide gel electrophoresis, and 600 proteins were detected by Coomassie brilliant blue staining. Both chitosan and N-CMC caused considerable changes in the protein pattern of pea roots. Compared to the control, both chitosan and N-CMC increased the content of 12 proteins (spots 7, 11, 12, 15, 18, 19, 20, 21, 23, 24, 25, 26), induced the new expression of protein 10 and decrease the level of expression of 4 proteins (spots 1, 2, 3 and 17), Fig 3 A, B. Only chitosan induced the synthesis of 3 new proteins (spots 6, 8, 9) not observed in roots of the control and increased the expression of 2 proteins (spots 16, 22), Fig.3B. N-CMC induced the expression of 3 new proteins (spots 4, 5 and especially 14) and down regulated the expression of 1 protein (spot 13), Fig. 3B.

We identified some of the proteins induced by both chitosan and N-CMC (Table) by "peptide fingerprinting" and MS/MS spectra. Among these are glutamine synthetase root isozyme A (spot 12), β -subunit B of elongation translation factor I (spot 7), highly similar to auxin-induced protein (aldo-keto reductase family) (spot 10), ABR17, belonging to the family PR-10 protein (spot 18), ABA-responsive protein (spot 22), calmodulin (spot 25), and pathogenesis-related protein PR10 (spot 26). Some of these proteins (spots 18, 22, 26) are defense proteins increasing the plant's resistance to pathogens and abiotic stressors.

Only chitosan induced synthesis of isoflavone reductase (spot 9), 1-aminocyclopropane-1-carboxylate oxidase (ACC oxidase, spot 6), a 14-3-3-like protein (spot 8) and glutathione-S-transferase (spot 16).

Some proteins induced only by N-CMC were identified (Table): actin (spot 5), adenosine kinase 1 (spot 4) and cytosol L-ascorbate peroxidase (spot 14). Special attention must be given to the fact that N-CMC significantly increases the expression of ABA- responsive protein ABR17 (family PR-10 protein) comparing to the control and chitosan.

A



The increase of actin content can be connected with an intensive branching of the pea lateral roots under the influence of N-CMC and with the cytoskeleton formation in the dividing primordial meristematic cells. N-CMC-induced branching of lateral roots is similar to the activation of auxin growth function. The reason for this may be a certain chemical similarity in the structure of heteroauxin and N-carboximethyl radical forming a part of N-CMC.

The differences in chitosan-induced and N-CMC-induced changes of proteomes are quite explicable since the chitin and chitosan residues are present in both chitosans but in addition to

B

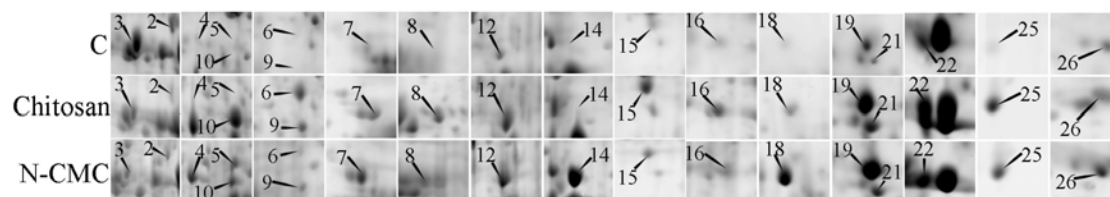


Figure 3. 2-DE of pea roots soluble proteins. A- control; B- proteins, differentially expressed under the action of chitosan and N-CMC

them N-CMC contains the N-carboxymethyl residues (Fig 1).

It could be predicted that there will be more induced proteins in the N-CMC proteome than the chitosan proteome. Indeed, in the N-CMC proteome unlike the chitosan and control proteomes proteins 4, 5 and 14 appeared, and there was an increase in the expression of proteins 7, 18, 20 and 23, and a decrease expression of protein 22. Proteins 6, 8, 9 were induced only by chitosan elicitor not expressed in N-CMC proteomes.

The proteome analysis showed that both chitosan and N-carboxymethyl chitosan can induce the expression of the same proteins that may be classified as defense proteins, and could thereby increase the resistance of plants to the pathogens and abiotic stressors. At the same time N-CMC induced a considerable increase of the content of some proteins (actin, ADK 1) being of importance for the auxin type activation of growth processes. As mentioned above the similarity of N-CMC and IAA action on branching of lateral roots can be explained by the fact that in N-CMC there is a structural element similar to that of IAA. N-CMC competitively inhibits synthesis of some chitosan-induced defense proteins.

Table. Identified soluble pea root proteins differentially expressed under the action of chitosan and N-carboximethyl chitosan

No spot ¹	NCBI accession no ²	Protein name ³	Th. MM/pI ⁴	Matched peptides/ Sequence ⁵	Score ⁶	Spot intensity ratio ⁷	
						Chit/ control	N- CMC/ control
4	gi 15232763	Adenosine kinase 1 [<i>Arabidopsis thaliana</i>]	37.8/5.29	7	104	ND	A
5	gi 1666228	Actin [<i>Pisum sativum</i>]	41.6/5.31	10	85	ND	A
6	gi 398997	ACC oxidase (1-aminocyclopropane-1-carboxylate oxidase) [<i>Pisum sativum</i>]	36.0/5.06	18	170	A	ND
7	gi 38232568	Translational elongation factor 1 subunit B beta [<i>Pisum sativum</i>]	25.3/4.41	ATEAEDD DDDDVDL FGEETEEE KK	241	+12,70	+14,0
8	gi 4850247	14-3-3 – like protein [<i>Pisum sativum</i>]	29.3/4.82	12	93	A	ND
9	gi 1708427	Isoflavone reductase [<i>Pisum sativum</i>]	35.4/5.39	19	244	A	ND
10	gi 2462750	Highly similar to auxin-induced protein (aldo-keto reductase family) [<i>Arabidopsis thaliana</i>]	41.9/5.34	IQNLNQNI GALSVK	232	A	A
12	gi 121333	Glutamine synthetase root isozyme A [Pisum sativum]	39.3/6.13	9	154	+3,4	+4,7
14	gi 1351963	L-ascorbate peroxidase, cytosolic (PsAPx 01) [<i>Pisum sativum</i>]	27.2/5.52	11	147	ND	A
16	gi 37051105	Glutathione-S-transferase [<i>Pisum sativum</i>]	26.7/5.0	8	118	+3,2	+1,0
18	gi 1703042	ABR17 (family PR-10 protein) [<i>Pisum sativum</i>]	16.6/5.07	9	137	+4,6	+39,9
22	gi 20631	ABA-responsive protein [<i>Pisum sativum</i>]	16.6/5.07	7	97	+2,2	-0,6
25	gi 166655	Calmodulin3 [<i>Arabidopsis thaliana</i>]	16.15/4.1	7	100	+19,6	+19,0
26	gi 1513162	Pathogenesis-related protein PR10 [<i>Pisum fulvum</i>]	16.7/4.94	SIEIVEGN GGAGTIK	471	+1,9	+1,7

Note¹ – spot numbers on the image;² – accession protein in NCBI database;³ – identified proteins;⁴ – MW/pI – MW/pI – molecular weight of protein (kDa) and pI value from database;⁵ – number of peptides/peptide fragment;⁶ – corresponds to the score retrieved by the MASCOT program. Protein scores greater than 66 are significant (p<0,05);⁷ – Expression level “+” increase or “-” decrease of proteins ; A – appear; ND - not detectable

ACKNOWLEDGEMENTS

This Work Was Supported in Part by Grant of the President of Russian Federation for State Support of Leading Scientific Schools 6992.2010.4.

REFERENCES

- [1] Rabea, E.I., Badawy, M.E.I., Rogge, T.M., Stevens, C.V., et al. (2005) Insecticidal and Fungicidal Activity of New Synthesized Chitosan Derivatives. *Pest. Manag. Sci.*, 61, 951–960
- [2] Chen, H., Chen, F. (2000) Effect of Yeast Elicitor on the Secondary Metabolism of Ti-transformed *Salvia Miltiorrhiza* Cell Suspension Cultures. *Plant. Cell Rep.*, 19, 710–717.
- [3] McDougall, G.J., Fry, S.C. (1989) Structure Activity Relationships for Xyloglucan Oligosaccharides with Antiauxin Activity. *Plant Physiol.*, 89, 883-887.
- [4] Chivasa, S., Hamilton, J.M., Pringle, R.S., Ndimba, B.K., et al. (2006) Proteomic analysis of differentially expressed proteins in fungal elicitor-treated Arabidopsis cell cultures. *J. Exp. Bot.*, 57, 1553-1562
- [5] Ferri, M., Tassoni, A., Franceschetti, M., Righetti, L., et al. (2009) Chitosan Treatment Induces Changes of Protein Expression Profile and Stilbene Distribution in *VitisVvinifera* Cell Suspension. *Proteomics*, 9, 610-624.
- [6] Tarchevsky, I.A., Yakovleva, V.G., Egorova, A.M. (2008) Proteomic Analysis of Changes in Pea Roots Caused by the Apoptosis-Inducing Concentration of Salicylic Acid. *Doklady Biochem. Biophys.*, 422, 274-278.
- [7] Tarchevsky, I.A., Yakovleva, V.G., Egorova, A.M. (2010) Proteomic Analysis of Salicylate-Induced Proteins of Pea (*Pisum Sativum* L.) Leaves. *Biochemistry*, 75, 590-597.
- [8] Il'ina, A.V., Tkacheva, I.V., Varlamov, V.P. (2002) Depolymerization of High-Molecular-Weight Chitosan by the Enzyme Preparation Celloviridine G20x. *Prikl Biokhim Mikrobiol.*, 38, 132-135.
- [9] Muzzarelli, R.A.A., Tanfani, F., Emanuelli, M., S. Mariotti, M. (1982) N-Carboxybenzyl Chitosans. Novel Chelating Polyampholytes. *Carbohydrate Polymers*, 2, 145-157.
- [10] Gouvea, C.M.C.P., Souza, J.F., Magalhaes, C.F.N., Martins, I.S. (1997) NO-releasing Substances than Induce Growth Elongation in Maize Root Segments. *Plant Growth Regul.*, 21, 183-187.

CHARACTERIZATION OF A NEW HYDROGEN SULFIDE INDICATOR

E.T. KATO JR.¹, C.M.P. Yoshida² and T.T. Franco^{1*}¹ School of Chemical Engineering –State of University of Campinas, UNICAMP,
CEP13083-852, Campinas – SP, Brazil.² Federal University of São Paulo-UNIFESP, Department of Exact and Earth Science, Av. Prof.
Arthur Riedel, 275, CEP 09972-270, Diadema – SP, Brazil.

*E-mail: franco@feq.unicamp.br

The environmental concern over the use of synthetic materials on packaging industry influence the value of research projects on alternative packaging materials. A new, biodegradable, fast, simple manufacturing and colorimetric indicator of hydrogen sulfide gas (H₂S) was developed combining chitosan as tridimensional biopolymer matrix and a non toxic colorimetric indicator. The H₂S indicator system can be applied in different industries, as petrochemical, paper mills, food, etc. Chitosan is the very abundant natural biopolymer derived from chitin, which is discarded at tons by the fishing industry. Hydrogen sulfide (H₂S) is a flammable and colorless gas with a sweetish taste and characteristic odor of rotten eggs that can be poisonous at high concentrations. Card paper sheets were coated with chitosan suspension (2.0%, w/w) and colorimetric indicator (0.25%, w/w) using a manual applicator. Mechanical and water absorption (Cobb Test) properties of the H₂S indicator system were studied. Young's modulus, fracture strain, stretching, traction resistance and resistance to bending were assessed. The Young's modulus, fracture strain and traction resistance of the H₂S indicator system were comparable to a non-coated card paper. The resistance to bending on cross direction increased 10 %, increased 8% on machine direction and water absorption significantly increases 86% when compared with a non-coated card paper. The results of mechanical tests showed that the colorimetric indicator system had the main characteristics very similar to coated card paper.

Keywords: Chitosan, hydrogen sulfide, colorimetric, biodegradable and indicator**1. INTRODUCTION**

The environmental concern from consumers forced an increased demand to replace synthetic packaging for renewable derived polymers and cellulose based packaging applications is permanently increased. They are biodegradable and safe for the environment, although present lower water and gas barrier^[1].

Chitosan is a polysaccharide derived from chitin by removing the acetyl groups with alkali.^[2] Chitosan is an excellent film-forming linear polymer with a backbone consisting of β -(1-4)- 2-acetamido-2-deoxy-D-glucose (*N*-acetyl glucosamine - GlcNAc) residues and glucosamine residues (GlcN), which is characterized by the degree of acetylation (DA) and average molecular weight (MW), among other properties, *e.g.* degree of polymerization^[3]. Chitosan has a low toxicity and is biodegradable. Also, depending on its molecular structure, size and concentration, may inhibit the growth of fungi, bacteria and yeasts^[4]. The association of chitosan to paper provides specific functionalities and maintains the environment-friendly characteristic of the material. Chitosan associated with cellulose have been studied as additive on paper production and paper surface treatment by decades. Reis et al.^[5] studied the effects of chitosan coating on Kraft paper, according to the authors the application of chitosan coating (3.5 g.m⁻², wet basis) on Kraft paper sheets provides a significantly lower WVPR (by *ca* 43%) and water absorption

capacity (by *ca* 35%) as compared to uncoated Kraft paper. The association of chitosan to paper increases the mechanical resistance and improves the color retention of the cardpaper^{[6][7][8]}. The printability increases with the chitosan addition^[9], possible due to the reduction of water absorptiveness.

A hydrogen sulfide (H₂S) indicator system was characterized in this study. This system detects and indicates the presence of hydrogen sulfide (H₂S). This indicator system has wide application, since applications in control of leaks in the petrochemical industry communicating the presence of H₂S in case of leaks in the line of recovery in critical points (joints, valves, connections, etc.), even in quality control of food products informing the consumer a potential microbiological changes in the product during transportation and storage, indicating the state of product freshness.

The aim of this work was to investigate the tensile properties and water absorption of the H₂S indicator system.

2. MATERIALS and METHODS

2.1. MATERIALS

Commercial chitosan used in this study was provided by Primex (Island), obtained from the exoskeleton of coldwater shrimps with a DA of 18 % and a molecular weight, MW, of 2.38×10^5 g mol⁻¹ (dn/dc of 0.135 mL.g⁻¹) and polydispersivity of 2.89. Glacial acetic acid (Synth – Brazil), iron(II) sulphate heptahydrate (Sigma – Germany; 99 +%), ferrous sulphide (Synth – Brazil; 25 %), sodium carbonate (Synth – Brazil, 99 +%) and card paper (Triplex TP 250) (250 g m⁻², Suzano Papel e Celulose, Brazil) were also used.

2.2. MÉTODS

2.2.1 PRECONDITIONING

The H₂S indicator system and uncoated card paper sheets were preconditioned at 23 ± 1 °C and $50 \pm 2\%$ relative humidity before analysis, in accordance with the ASTM D685^[10] standard method.

2.2.2. MECHANICAL CHARACTERIZATION

2.2.2.1. STIFFNESS EVALUATION

The stiffness of the indicator system containing ferrous sulphate (FeSO₄) as colorimetric indicator of H₂S was measured in accordance with the ASTM D5342^[11] standard method. The samples, of dimensions 38.1 ± 0.3 mm by 70 ± 1 mm, in both directions: machine direction (MD) and cross-machine direction (CMD) were pre-conditioned in desiccators containing silica for 72 hours at room temperature ($25^\circ \pm 2^\circ$ C) and analyzed with the stiffness instrument, RI- 5000, manufactured by Regmed - Brazil.

2.2.2.2. TENSILE PROPERTIES

The tensile properties (mean force, elongation, tensile energy absorption, tensile strength, breaking length and tensile index) of H₂S indicator system were measured in accordance with the ASTM D828^[12] standard method. The samples, of dimensions 15 mm by 210 ± 1 mm, machine direction (MD) and cross-machine direction (CMD) were pre-conditioned in desiccators containing silica for 72 hours at room temperature ($25^\circ \pm 2^\circ$ C) and analyzed with an automatic dynamometer, DI-21, manufactured by Regmed - Brazil.

2.2.3. WATER ABSORPTION (COBB TEST)

Water absorption capacity was determined in accordance with standard T441om-90.^[13] The weight gain was measured using Mettler AE 163 analytical scales. The results are expressed in g.m⁻². The samples of dimensions, 125 mm x 125 mm, were pre-conditioned in desiccators containing silica for 72 hours at room temperature (25 ± 2 ° C). They were individually weighed

on an analytical balance, fixed on Cobb equipment (Regmed, Brazil) for analysis of water absorptiveness. A volume of 100 mL of distilled water was put in contact with the area bounded by the ring of the device (internal diameter of 11.28 ± 0.02 cm corresponding to an area of approximately 100 cm^2) for 120 s. Excess water was then quickly removed and sample was again weighed to calculate the water absorptiveness. There were at least 10 replicates per experiment.

2.2.4. STATISTICAL ANALYSES

Statistical analyses were carried out with the Statistic version 5.0 program (Statisc Inc., USA). Differences between the means were detected using a multiple comparison Tukey test.

3. RESULTS AND DISCUSSIONS

Card paper sheets (250 g.m^{-2}) were used to prepare H_2S indicator system and their surfaces were coated with chitosan suspension. The concentration of chitosan was 3.0 % w/w and concentration of indicator was 1.50 % w/w in coating suspension. The H_2S indicator system presents a slightly continuous and homogeneous yellow color.

3.1. MECHANICAL CHARACTERIZATION

Mechanical characterization is an important property of packaging materials that measures the ability of the studied packaging to resist the process of production.

3.1.1. STIFFNESS EVALUATION

The values obtained for both directions of the paper (MD and CMD) of stiffness are averages of ten (10) measures (Table 1).

Table 1. Stiffness (g.cm) comparison between H_2S indicator system and uncoated card paper.

Sample	CD				CMD			
	R	L	Bending moment (g.cm)	Bending moment (mN.m)	R	L	Bending moment (g.cm)	Bending moment (mN.m)
Uncoated Card paper	60 ± 3.12^a	84.5 ± 2.85^b	72.25 ± 2.19^d	7.09 ± 0.21^f	135 ± 4.32^a	172 ± 3.39^c	153.33 ± 3.30^e	15 ± 0.34^g
H_2S indicator system	65 ± 8.88^a	94 ± 6.70^c	79.48 ± 2.79^e	7.80 ± 0.30^g	140 ± 7.19^b	187 ± 6.43^d	163.44 ± 4.89^f	16.18 ± 0.29^h

a-h: different letters in the same column are statistically different with 95% of confidence. Tukey's test $p < 0,05$.

The bending moment in the CMD of H_2S indicator system showed an increase from 72.25 to 79.48 g.cm, on direction MD showed a increase from 153.33 to 163.44 g.cm, when compared with the uncoated card paper. According to Rhim and Kim^[14] the stiffness of card paper increased with a PLA coating, Samyn et al.^[15] reported that card paper coated with styrene maleic anhydride (SMA) had stiffness similar to uncoated card paper and Reis et al^[5] reported that Kraft paper coated with chitosan emulsion film presented lower stiffness than uncoated Kraft paper.

3.1.2. TENSILE PROPERTIES

The results of tensile properties (force, elongation, tensile energy absorption, tensile strength, breaking length and tensile index) showed in Table 2 are averages of ten (10) measures.

Table 2. Mechanical properties comparison between H_2S indicator system and uncoated card paper.

Sample	Mean force (N)	Elongation (%)	Tensile energy absorption (J.m^{-2})	Tensile strength (kN.m^{-1})	Breaking length (km)	Tensile index (kN.m.kg^{-1})
Intelligent sensor (MD)	$244,53 \pm 4,37$	3,69	368,21	16,30	6,65	2,65
Uncoated card paper (MD)	$236,31 \pm 7,47$	3,55	342,75	15,75	6,43	2,66
Intelligent sensor (CMD)	$135,82 \pm 2,85$	7,04	446,38	9,22	3,76	0,79
Uncoated card paper (CMD)	$138,25 \pm 3,65$	7,11	440,78	9,05	3,69	0,76

The mechanical properties remained almost unchanged, according to Bordenave et al.^[16] this system was modified by the introduction of chitosan, but the cellulose fibers network still drive the mechanical behavior of the materials, i.e. the amount of chitosan was not enough to disturb the interactions between the potentially negatively charged cellulose fibers.

In agreement with Samyn et al.^[15] and Kibirkštis & Kabelkaitė^[17] the mean force in MD is higher compared to CMD due to anisotropy of the paper. Reis et al.^[5] reported that the mechanical properties of chitosan coated kraft paper remained almost unchanged with a 13.3 % reduction in the elongation of CMD.

3.2. WATER ABSORPTION (COBB TEST)

The water absorption was determined for the H₂S indicator system and uncoated card paper (Table 3). According to Reis et al.^[5] in cellulosic materials, water absorption depends on the type of cellulose and the coating material. The water absorptiveness provides information about the quantity of water absorbed by the card paper, in grams per square meter, when in direct contact with water.

Table 3. Water absorptiveness comparison between H₂S indicator system and uncoated card paper.

Sample	Absorption (g/m ²)
Intelligent sensor	100,75±3,10
Uncoated card paper	54,09±20,37

The water absorptiveness was increased with the biopolymer coating in the H₂S indicator system when compared with the uncoated card paper, the same was observed by Rhim, Lee & Hong^[18], this effect is due to hydrophilicity of the chitosan. Reis et al.^[5] reported a reduction in water absorption by up to 35% even using chitosan as coating.

CONCLUSIONS

Coating of chitosan suspension to the H₂S indicator system lead to an increase in stiffness compared with the uncoated card paper. The tensile properties did not change when compared to uncoated card paper, i.e. the cellulose fibers network still drive the mechanical behavior of the materials. The water absorptiveness increased almost 100% compared to uncoated card paper it was associated with the hydrophilicity of the polymer matrix. The impact of the humidity on the H₂S sensibility response should therefore be studied.

ACKNOWLEDGEMENTS

This work was financially supported by FAPESP, CNPq and CAPES. The authors thank Primex for providing chitosan.

REFERENCES

- [1] [Gällstedt, M.; Hedenqvist, M.S. PACKAGING-RELATED MECHANICAL AND BARRIER PROPERTIES OF PULP-FIBER-CHITOSAN SHEETS. Carbohydrate Polymers 63: 46–53, 2006.
- [2] Peter, M.G. CHITIN AND CHITOSAN FROM FUNGI, in: A. Steinbüchel (Ed.), Biopolymers, Vol. 6: Polysaccharides II, Weinheim: Wiley-VCH, 2002, pp. 123 - 157 (ISBN 3-527-30227-1).

- [3] Muzzarelli R.A.A. CHITOSAN-BASED DIETARY FOODS, *Carbohydr. Polym.*, 29: 306-316, 1996.
- [4] Tikhonov V.E, Stepnova EA, Babak VG, Yamskov IA, Palma-Guerrero J, Jansson H-B, Lopez-Llorca LV, Salinas J, Gerasimenko DV, Avdienko ID and Varlamov VP, BACTERICIDAL AND ANTIFUNGAL ACTIVITIES OF A LOW MOLECULAR WEIGHT CHITOSAN AND ITS N-2(3)-(DODEC-2-ENYL)SUCCINOYL/-DERIVATIVES. *Carbohydrate Polymers*. Vol. 64. Pp. 66-72, 2006.
- [5] Reis, A.B.; Yoshida, C.M.P.; Reis, A.P.C. and Franco, T.T. APPLICATION OF CHITOSAN EMULSION AS A COATING ON KRAFT PAPER. (wileyonlinelibrary.com) DOI 10.1002/pi.3023. Society of Chemical Industry, 2011.
- [6] Allan,G.G.,Carroll, J. P.,Hirabayashi,Y.,Muvundamina,M.,&Winterown, J. G. CHITOSAN-COATED FIBERS ADVANCES IN CHITIN AND CHITOSAN, *Proceedings of international conference, fourth*, pp. 765–76, 1989.
- [7] Makino, Y., & Hirata, T. MODIFIED ATMOSPHERE PACKAGING OF FRESH PRODUCE WITH A BIODEGRADABLE LAMINATE OF CHITOSAN–CELLULOSE AND POLYCAPROLACTONE. *Postharvest Biology and Technology*, 10, 247–254, 1997.
- [8] Struszczyk, H. & Kivekäs, O. (1990). MICROCRYSTALLINE CHITOSAN - SOME AREAS OF APPLICATION. *British Polymer Journal*, 23, 261–265. *Technologies*, v.6, n.4, p.459-464, 2005.
- [9] Thomson, G. MAKING BETTER PAPER WITH SHRIMPS. *Pulp and Paper International*, 26, 33, 1985.
- [10] ASTM, STANDARD PRACTICE FOR CONDITIONING PAPER AND PAPER PRODUCTS FOR TESTING *Annual Book of ASTM Standards*. American Society for Testing and Materials, Atlanta, D685, 1993.
- [11] ASTM. RESISTANCE TO BENDING OF PAPER AND PAPERBOARD (TABER-TYPE TESTER IN BASIC CONFIGURATION). *Annual Book of ASTM Standards*. American Society for Testing and Materials, Atlanta, D5342, 1993.
- [12] ASTM. TENSILE PROPERTIES OF PAPER AND PAPERBOARD USING CONSTANT-RATE-OF-ELONGATION APPARATUS. *Annual Book of ASTM Standards*. American Society for Testing and Materials, Atlanta, D828, 1997.
- [13] TAPPI TEST METHODS. Technical Association of the Pulp and Paper Industry, Atlanta, GA, 1994.
- [14] Rhim, J.-W. and Kim, J.-H. PROPERTIES OF POLY(LACTIDE)-COATED PAPERBOARD FOR THE USE OF 1-WAY PAPER CUP. *Journal of Food Science—Vol. 74*, Nr. 2, 2009.
- [15] Samyn, P.; Deconinck, M.; Schoukens, G.; Stanssens, D.; Vonck, L. and Abbeele, H. V. MODIFICATIONS OF PAPER AND PAPERBOARD SURFACES WITH A NANOSTRUCTURED POLYMER COATING. *Progress in Organic Coating*. 69, p. 442-454, 2010.
- [16] Bordenave, N. Grelier, S. Pichavant, F. and Coma V. WATER AND MOISTURE SUSCEPTIBILITY OF CHITOSAN AND PAPER-BASED MATERIALS: STRUCTURE–PROPERTY RELATIONSHIPS. *J. Agric. Food Chem.* 55, p. 9479–9488, 2007.
- [17] Kibirkštis, E.; Kabelkaitė, A. RESEARCH OF PAPER/PAPERBOARD MECHANICAL CHARACTERISTICS. *Mechanika*. Nr.3(59), p. 34-41, 2006.
- [18] Rhim, J.W.; Lee J.H. and Hong, S.I. WATER RESISTANCE AND MECHANICAL PROPERTIES OF BIOPOLYMER (ALGINATE AND SOY PROTEIN) COATED PAPERBOARDS. *LebensmWiss Technol*. 39: p.806–13, 2006.

PROPERTIES AND CDNA CLONING OF THE STOMACH CHITINASE FROM COMMON MACKEREL *SCOMBER JAPONICUS*

Masahiro MATSUMIYA*, Mana IKEDA, Keiko HUTAMI, Sonomi TANAKA, Miyuki ARIMOTO, Shinya ITO, and Kouji MIYAUCH

Department of Marine Science and Resources, College of Bioresource Sciences, Nihon University, Fujisawa, Kanagawa 252-0880, JAPAN

**E-mail address: matsumiya@brs.nihon-u.ac.jp*

INTRODUCTION

Chitinases (EC 3.2.1.14) are enzymes that randomly hydrolyze the β -1, 4 glycosidic bonds of chitin and produce *N*-acetylchitooligosaccharides (GlcNAc)_n. Chitinases are widely distributed in nature and serve important biological functions in activities such as nutrient intake, morphological change, defense, and attack [1]. Fish stomach chitinases have the physiological function of degrading chitinous substances ingested as food. Chitinases are essential enzymes for the enzymatic production of (GlcNAc)_n and GlcNAc, which are gradually proving to have a variety of physiological roles [2, 3]. Consequently, research on chitinases in various organisms will not only clarify these physiological roles but will also be of use in the production of (GlcNAc)_n and GlcNAc.

Fish stomach chitinases have been purified from the stomachs of several fish, and their properties have been clarified [4-9]. These reports suggest that the number of isozymes and substrate specificity of fish stomach chitinases differ depending on species of fish, in connection with their feeding habits [4]. Common mackerel *Scomber japonicus* lives in seawater (ca. 0.5 M NaCl) and takes a crustacean as food. The stomach of fish produces chitinase to chemically disrupt the chitinous envelope of crustacean in the existence of seawater. Therefore, properties and structure of the stomach chitinase from seawater fish is interesting.

In this study, therefore, we tried to clarify the enzymatic properties and clone the cDNA of the stomach chitinase from common mackerel *Scomber japonicus* in order to study its potential as a (GlcNAc)_n producing enzyme.

MATERIALS and METHODS

Chemicals. *N*-acetylchitooligosaccharides ((GlcNAc)_n, n=2-6) and pNp-(GlcNAc)₂ were purchased from Seikagaku Kogyo (Tokyo, Japan). Shrimp shell chitin (α -chitin, chitin EX) was from Funacoshi (Tokyo, Japan), and crab shell chitin (α -chitin) was from Tokyo Kasei (Tokyo, Japan). Squid pen chitin (β -chitin) was a generous gift from Kyowa Tecnos (Chiba, Japan). Microalgae chitin (β -chitin) and silkworm cuticle chitin (α -chitin) were generously supplied by Dr. K.J. Kramer and Dr. A Haga, respectively. All other reagents were of the highest grade commercially available.

Enzymes. The common mackerel *Scomber japonicus* stomach chitinase (SjChi, 47kDa by MALDI-TOF-MS) was purified by the method of Matsumiya *et al.* [9]. Microbe *Streptomyces griseus* chitinase was purchased from Sigma-Aldrich (St. Louis, Mo, USA).

Assay of chitinase activity. When using pNp-(GlcNAc)₂ as a substrate, enzyme activity was measured by the method of Ohtakara [10]. Released *p*-nitrophenol was measured at 420 nm. When using 0.5% colloidal chitin or, α - or β -chitin, enzyme activity was measured by the method of Ohtakara [10]. Reducing sugars produced were measured by the Schales' reagent.

Protein measurement. Protein concentration was measured by the method of Bradford [11] using bovine serum albumin as the standard protein.

HPLC analysis of the hydrolysis products of (GlcNAc)_n (n = 2–6) by chitinase. The hydrolysis products of (GlcNAc)_n (n = 2–6) produced by SjChi and their anomer formation ratios were analyzed by the method of Koga *et al.* [12]. Namely, 5 μ l of enzyme solution and 25 μ l of 0.22 mM (GlcNAc)_n were added to 25 μ l of 0.1 M sodium acetate buffer (pH 4.0) and incubated at 25 °C for 10 min. The reaction was stopped by cooling to 0 °C in an ice bath, and the reactant solution was analyzed by HPLC using a TSK-GEL Amide-80 column (4.6 mm x 250 mm). (GlcNAc)_n was eluted with 70% acetonitrile at a flow rate of 0.8 ml/min, and absorbency was detected at 210 nm.

Amino acid sequence analysis. The N-terminal amino acid sequence of SjChi was analyzed using a protein sequencer (PE Applied Biosystems 447/120A, Foster City, CA).

cDNA cloning. Total RNA was isolated from the common mackerel stomach by use of Isogen (Nippon Gene, Toyama, Japan). First-strand cDNA synthesis was performed on 2 μ g of total RNA by using Reverse Transcriptase M-MLV (RNase H free) (Takara Bio, Shiga, Japan) with oligo(dT). The cDNA was cloned by the rapid amplification cDNA ends (RACE) method using the primers, which were designed on the basis of the N-terminal amino acid sequence of SjChi, consensus region among vertebrate chitinases, and sequenced. The amplified cDNA fragment was subcloned into plasmid. The plasmid containing the cDNA encoding SjChi was used to transform JM109 competent cells and was subjected to sequence analysis.

RESULTS and DISCUSSION

HPLC analysis of cleavage patterns and anomeric forms of products in the hydrolytic reaction of (GlcNAc)_n (n = 2–6) by SjChi. By the method of Koga *et al.*, we investigated the cleavage pattern of a short soluble substrate (GlcNAc)_n due to SjChi and the product's anomeric form. Fig. 1 shows the results of analysis by HPLC of products in the hydrolytic reaction of (GlcNAc)₆ by SjChi as an instance. Table 1 shows the substrate specificity of SjChi toward (GlcNAc)_n (n = 2–6). SjChi showed almost no hydrolytic activity toward (GlcNAc)_{2,3}, but it hydrolyzed (GlcNAc)₄₋₆ and produced (GlcNAc)₂₋₄ with increased β -anomers, in the same way as family 18 chitinases. The enzyme hydrolyzed (GlcNAc)_n to produce two molecules of (GlcNAc)₂, and it hydrolyzed (GlcNAc)₅ to produce (GlcNAc)₂ (64.3%) and (GlcNAc)₃ (35.7%). Furthermore, it hydrolyzed (GlcNAc)₆ to produce two molecules of (GlcNAc)₃ (5.4%) and (GlcNAc)₂ + (GlcNAc)₄ (94.6%, n = 2 >> 4). From these results, it was thought that this enzyme is an endo-type chitinase, and that it hydrolyzes the 2nd to 4th glycosidic links from the non reducing end of (GlcNAc)_n same as that of silver croaker chitinase [9].

Substrate specificities of SjChi for crystalline chitin. To investigate the hydrolyzing activity of SjChi toward crystalline chitin, chitinase activities was measured using several substrates, including crab shell chitin, shrimp shell chitin, and silkworm cuticle chitin as crystalline α -chitin, and squid pen chitin and micro algae chitin as a crystalline β -chitin, and colloidal chitin as a non-crystalline chitin. As shown in Fig. 2, SjChi hydrolyzed all the crystallin chitins which investigated this study and showed higher activity toward β -chitin and colloidal chitin than α -chitin. Among the α -chitins, shrimp shell and crab shell α -chitins were degraded more efficiently than silkworm cuticle α -chitin.

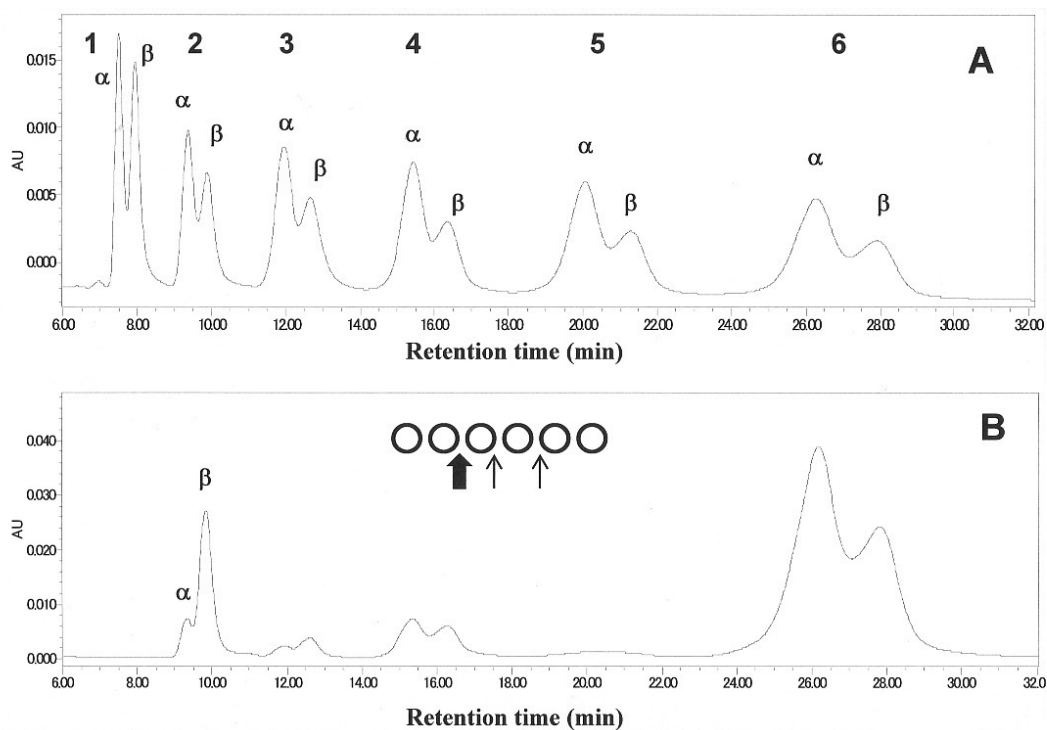


Fig. 1. HPLC analysis of the hydrolysis products of (GlcNAc)₆ by SjChi.
 A, (GlcNAc)_n (n = 1–6) as standard; B, (GlcNAc)₆ hydrolysis products by SjChi.

Table 1 Reaction pattern and cleavage patterns of (GlcNAc)_n (n = 2–6) by SjChi

Substrate	Reaction pattern	Activity (U/mg)	Cleavage patterns
G2	ND	ND	ND
G3	III → I + II	trace	○ ○ ○ ↑100%
G4	IV → II + II	65.9	○ ○ ○ ○ ○ ↑100%
G5	VI → II + IV	114	○ ○ ○ ○ ○ ○ ↑ ↑ 64.3% 35.7%
G6	VI → II + IV → III + III	-	○ ○ ○ ○ ○ ○ ○ ○ ↑ 94.6% ↑ ○ ○ ○ ○ ○ ○ ○ ○ ↑5.4%

ND, Not detected. G, GlcNAc.

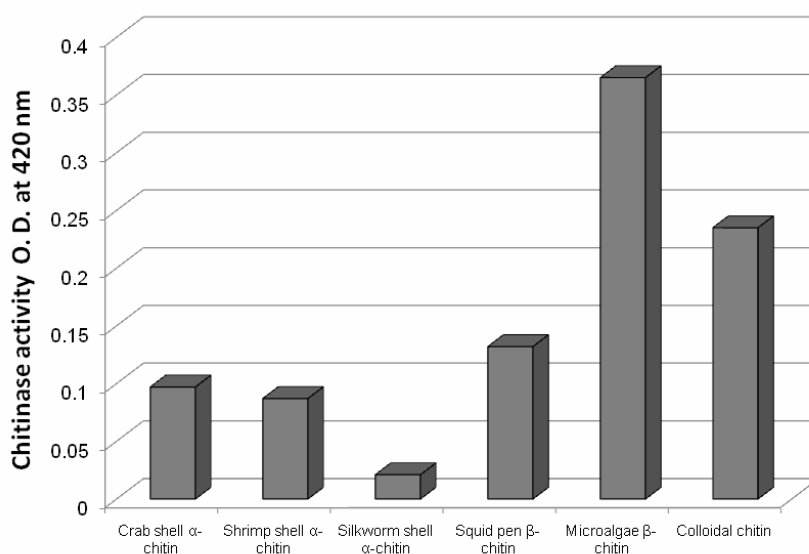


Fig. 2. Substrate specificity of SjChi toward crystalline chitin.

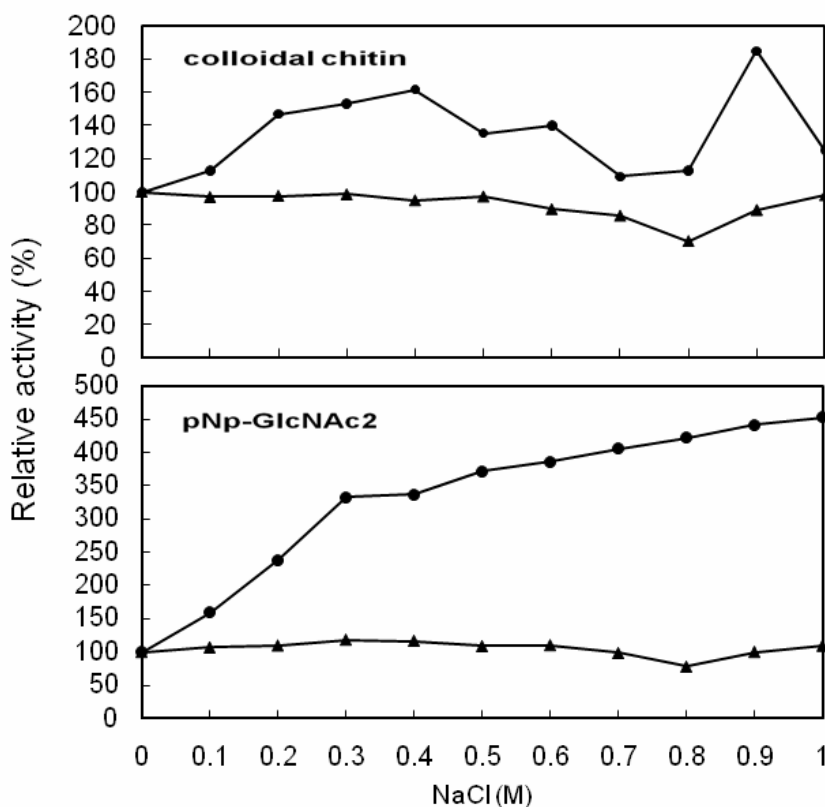


Fig. 3. Effect of NaCl on SjChi (●) and *Streptomyces griseus* chitinase (▲) activities toward colloidal chitin and pNp-(GlcNAc)₂. Chitinase activity was measured by using colloidal chitin and pNp-(GlcNAc)₂ as substrates, and adding NaCl to the reactant solution so that the final concentration was 0 to 1 M. For comparison, the effect of NaCl was similarly measured using the chitinase of *Streptomyces griseus*.

Effect of NaCl on SjChi activity. Common mackerel lives in seawater (ca. 0.5 M NaCl) and takes a crustacean as food. The stomach of fish produces chitinase to chemically disrupt the chitinous envelope of crustacean in the existence of seawater. Therefore, we investigated the effect of NaCl on chitinase activity. As shown in Fig. 3, when using colloidal chitin as a substrate, the chitinase was activated, showing 136% activity with the presence of 0.5 M NaCl. However, the rate of activation decreased with the addition of 0.7-0.8 M NaCl, showing about 110%. When using pNp-(GlcNAc)₂ as a substrate, chitinase activity was activated, dependent on concentration, by the presence of NaCl, and 372% of the relative activity was observed with the presence of 0.5 M NaCl. This value was higher than that of silver croaker chitinase, 230% of the relative activity [9]. In the *S. griseus* chitinase studied for comparison, no activation was observed in activity measurement of either substrate with the addition of NaCl, and activity was inhibited with the presence of 0.8 M NaCl. The properties of SjChi coincide well with the feeding habit and digesting condition of common mackerel. Furthermore, SjChi has high potential as a (GlcNAc)_n producing enzyme in the presence of NaCl.

cDNA cloning of common mackerel chitinase. One clone was successfully obtained from common mackerel stomach by 5' and 3' RACE amplifications. The cDNA contained a 1422bp open reading frame with a coding potential for a 474 amino-acid peptide. The deduced amino-acid sequences of the chitinase revealed a typical vertebrate chitinase structure containing a signal peptide, a catalytic domain (GH family 18), a linker region, and a C-terminal chitin binding domain. The N-terminal amino acid sequences of SjChi that was purified enzyme from the stomach of common mackerel, Y I L S X Y F T N W A Q Y R P G A G K Y L P T N I D P X L, was detected at the deduced amino-acid sequences of the catalytic domain. The deduced amino acid sequences of the obtained cDNA showed 85% and 83% identity with *Pennahia argentata* stomach chitinase 1 (AB605774.1) and *Paralichthys olivaceus* stomach chitinase 1 [13], respectively.

ACKNOWLEDGEMENTS

We express our deepest gratitude to Dr. Atsunobu Haga of the National Institute of Agrobiological Sciences and Dr. Karl J. Kramer of Kansas State University for providing silkworm cuticle chitin and microalgae chitin, respectively. This work was partially supported by Grant-in-Aid for Scientific Research(C) (no. 215802) and College of Bioresource science, Nihon-University Grant.

REFERENCES

- [19] Gooday, G.W. (1999) Aggressive and defensive roles for chitinases. Chitin and Chitinases (P. Jolles, and R.A.A. Muzzarelli eds.) pp. 157–169, Birkhauser Publishing, Basel.
- [20] Matsumiya, M. (2004) Enzymatic production of N-acetyl-D-glucosamine using crude enzyme from the liver of squids. Food Sci. Technol. Res., 10, 296–299.
- [21] Wang, Z. Zheng, L. Yang, S. Niu, R. Chu, E. Lin, X. (2007) N-Acetylchitooligosaccharide is a potent angiogenic inhibitor both in vivo and in vitro. Biochem. Biophys. Res. Commun., 357, 26–31.
- [22] Matsumiya, M. Arakane, Y. Haga, A. Muthukrishnan, S. Kramer, K.J. (2006) Substrate specificity of chitinases from two species of fish, Greenling, *Hexagrammos otakii*, and common mackerel, *Scomber japonicus*, and the insect, Tobacco hornworm, *Manduca sexta*. Biosci. Biotechnol. Biochem., 70, 971–979.

- [23] Molinari, L.M. Pedroso, R.B. Scoaris, D.O. Ueda-Nakamura, T. Nakamura, C.V. Dias Filho, B.P. (2007) Identification and partial characterization of a chitinase from Nile tilapia, *Oreochromis niloticus*. *Comp. Biochem. Physiol. B*, 146, 81–87.
- [24] Kono, M. Matsui, T. Shimizu, C. (1987) Purification and some properties of chitinase from the stomach of red sea bream *Pagrus major*. *Nippon Suisan Gakkaishi*, 53, 131–136.
- [25] Kono, M. Matsui, T. Shimizu, C. Koga, D. (1990) Purification and some properties of chitinase from the stomach of Japanese eel, *Anguilla japonica*. *Agric. Biol. Chem.*, 54, 973–978.
- [26] Matsumiya, M. Mochizuki, A. (1995) Purification and characterization of chitinase from the stomach of common mackerel *Scomber japonicas*. *Bull. Coll. Agric. Vet. Med. Nihon Univ.*, 52, 131–136.
- [27] Ikeda, M. Miyauchi, K. Mochizuki, A. Matsumiya, M. (2009) Purification and characterization of chitinase from the stomach of silver croaker *Pennahia argentatus*. *Protein Expr. Purif.*, 65, 214–222.
- [28] Ohtakara, A. (1988) Chitinase and β -N-acetylhexosaminidase from *Pycnoporus cinnabarinus*, *Method in Enzymology* (W.A. Wood, S.T. Kellogg eds.) pp. 462–470, Academic Press, New York.
- [29] Bradford, M. (1976) A rapid and sensitive method for the quantitation of microgram quantities of protein utilizing the principle of protein–dye binding. *Anal. Biochem.*, 72, 248–254.
- [30] Koga, D. Yoshioka, T. Arakane, Y. (1998) HPLC analysis of anomeric formation and cleavage pattern by chitinolytic enzyme. *Biosci. Biotechnol. Biochem.*, 62, 1643–1646.
- [31] Kurokawa, T. Uji, S. Suzuki, T. (2004) Molecular cloning of multiple chitinase genes in Japanese flounder, *Paralichthys olivaceus*. *Comp. Biochem. Physiol. B*. 138, 255–264.

MACROPOROUS CHITOSAN FOAMS OBTAINED IN OIL-IN-WATER (O/W) HIGHLY CONCENTRATED EMULSIONS

Jonathan Miras*, Susana Vilchez, Conxita Solans, Jordi Esquena

*Institute for Advanced Chemistry of Catalonia (IQAC), CSIC
Jordi Girona, 18-26, 08034, Barcelona, Spain*

**E-mail: jonathan.miras@iqac.csic.es*

INTRODUCTION

Highly concentrated emulsions or high internal phase emulsions (HIPEs) are characterized by a dispersed phase volume exceeding 0.74, the maximum packing fraction of monodispersed and undistorted spherical droplets [1, 2]. Porous foams or polyHIPEs (polymerised High Internal Phase Emulsions) can be produced through a highly concentrated emulsion templating synthesis by polymerizing or crosslinking in the continuous phase of the emulsion, followed by dispersed phase (emulsion droplets) removal [3, 4]. PolyHIPEs combine highly porous structure, low bulk density, high permeability and high surface area. In addition, polyHIPEs can absorb relatively large amounts of liquids. These polyHIPEs would be interesting for immobilization of enzymes, fuel cell and battery applications [5], as selective membranes, supports for catalysts [6], templates for the preparation of other materials [7], etc. Moreover, biodegradable polyHIPEs would be applied for tissue engineering scaffold applications [8].

The present work describes the development of a new method to synthesize chitosan porous materials using oil-in-water (O/W) highly concentrated emulsions as templates [9] by covalently crosslinking with a natural reagent, genipin (Figure 1). Genipin is extracted from gardenia fruits (*Gardenia jasminoides* Ellis). Nowadays, genipin is a crosslinker widely used. It is about 5000-10000 times less cytotoxic than glutaraldehyde [10]. The main application of genipin is as crosslinker of polymers [11, 12] such as cartilage substitutes, manufacture of drug carriers for controlled release or encapsulation of biological products and medication of wounds. The droplet size of emulsions used as template was determined by laser diffraction. The morphology of chitosan foams was characterized by scanning electron microscopy (SEM). Also, nitrogen sorption and Helium pycnometry were used to determine the porosity. Macroporous materials, with specific surface around 25 m²/g and low density, < 0.1 g/mL, were obtained.

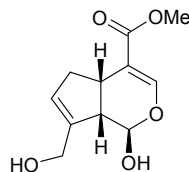


Figure 1. Molecule of genipin

MATERIALS AND METHODS

Materials

Nonionic surfactant Synperonic A7 (C₁₃₋₁₅EO₇) with HLB of 12.2 (Uniqema). Chitosan medium molecular weight (Sigma-Aldrich) with deacetylation degree of 85% and molecular weight of 300 kDa. Decane (Fluka) with 98% purity. Genipin (Challenge Bioproducts Co.) with an average molecular weight of 226 g/mol.

Preparation of solutions

Chitosan solution was prepared by dissolving 2%wt in 1% (v/v) acetic acid. This solution was shaken overnight by magnetic agitation to ensure complete dissolution. Genipin was dissolved in phosphate buffer at pH 7.4 with a concentration of 1%wt.

Preparation of highly concentrated emulsions

Oil-in-water highly concentrated emulsions were prepared (Table 1) by dropwise addition of decane to the mixture Synperonic A7/acetic acid (Emulsion 1) or Synperonic A7/Chitosan solution (Emulsions 2 and 3) at 25°C with mechanical stirring at 700 rpm. Finally, water (Emulsion 1), phosphate buffer (Emulsion 2) or genipin solution (Emulsion 3) were added while the emulsion was stirred.

TABLE 1. Composition (wt%) of highly concentrated emulsions

Emulsion	Surfactant	Aqueous phase	Oil phase
1	2% Synperonic A7	9% acetic acid (1%wt) 9% water	80% decane
2	2% Synperonic A7	9% chitosan solution (2%wt) 9% phosphate buffer	80% decane
3	2% Synperonic A7	9% Chitosan solution (2%wt) 9% Genipin solution (1%wt)	80% decane

Optical microscopy

Highly concentrated emulsions were observed with a Reichert Polyvar 2 microscope and images were processed using the IM5000 software, both supplied by Leica (Germany).

Particle size measurements

Droplet size distribution and droplet size average of highly concentrated emulsions were determined by laser diffraction with a Mastersizer 2000 instrument (Malvern Instruments Co.) equipped with a Hydro 2000G dispersion unit. Laser diffraction measurements were performed by dilution of highly concentrated emulsions with Synperonic A7 solution at the critical micelle concentration.

Preparation of macroporous foams (polyHIPEs) made of chitosan

Highly concentrated emulsions were kept in a water bath for three days at 40°C for crosslinking reaction. Then, chitosan polyHIPEs were cleaned by Soxhlet extraction with ethanol and water for 12 hours, respectively. Finally, polyHIPEs were dried in a freeze dryer to remove residual water.

Crosslinking percentage of polyHIPEs

The crosslinking percentage of chitosan polyHIPE (Equation 1) was calculated by Soxhlet extraction for 48h using a 5%wt acetic acid solution as extracting solvent [13].

$$\text{Crosslinking percentage (\%)} = \left(1 - \frac{w}{w_0}\right) \times 100 \quad \text{Equation 1}$$

where w_0 and w are the weights before and after Soxhlet extraction, respectively.

Scanning electron microscopy (SEM)

The porous structure of freeze-dried polyHIPEs was characterized using a scanning electron microscope (Hitachi 4100). Samples were coated by gold sputtering.

Helium pycnometry. Matrix or skeleton density of macroporous foams was determined using a Helium pycnometer Micromeritics Accupyc 1330. The average density was calculated by means of the measurement of four replicas.

Nitrogen sorption isotherms

The specific surface area of chitosan polyHIPEs was determined using a Micromeritics Tristar 3000 porosimeter by the application of Brunauer-Emmett-Teller method (BET) [14]. Adsorption and desorption isotherms were carried out at 77K. Samples were outgassed at 55°C for six hours and weighed before sorption analysis.

RESULTS AND DISCUSSION

The systems chitosan solution/water/Synperonic A7/decane (Emulsion 1) and chitosan solution/phosphate buffer/Synperonic A7/decane (Emulsion 2) were studied by laser diffraction at 40°C to determine the stability and droplet size distribution of highly concentrated emulsion, as a function of time from 0h to 72h (Figure 2). Moreover, the influence of chitosan was studied in the stability and droplet size of emulsions. Then, the chitosan solution/genipin solution/Synperonic A7/decane system (Emulsion 3) was characterized by laser diffraction to determine the droplet size distribution and average droplet size at zero time (Figure 2A). This study cannot be performed as a function of time because crosslinking reaction takes place during measurements.

The incorporation of chitosan in the highly concentrated emulsion produces a decrease in the average droplet size, as observed in Figure 2. At $t=0$ h, all three emulsions showed a monomodal distribution but emulsions 2 and 3 (Figure 2A) showed a decrease of size, from $\sim 6 \mu\text{m}$ to $\sim 2 \mu\text{m}$, because of chitosan addition. Emulsions were stable for a period of time of 24 h at 40°C. After 72h, emulsions 1 and 2 showed a bimodal droplet size distribution (Figure 2B).

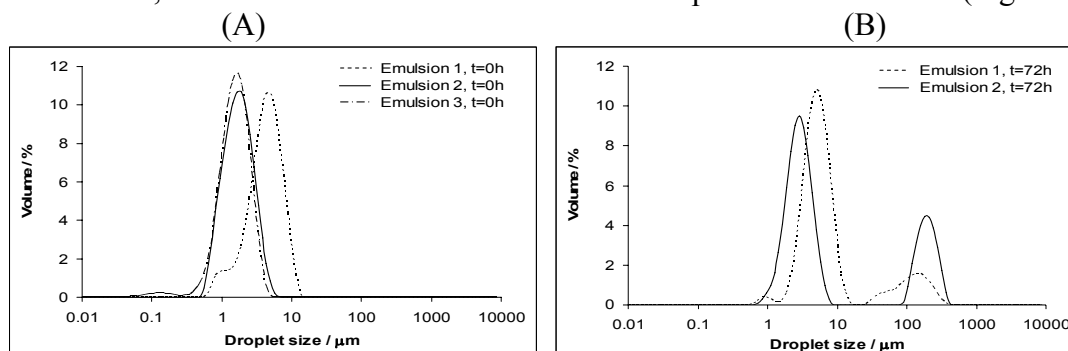


Figure 2. Droplet size distribution of: (A) Emulsions 1, 2 and 3 after preparation; (B) Emulsions 1 and 2 72 h hereafter

This bimodal size distribution was attributed to emulsion instability. It was confirmed by optical microscopy. An example is shown in Figure 3, referred to emulsion 2, comparing at zero time and 72 hours later. For better imaging, the emulsions were diluted, as described in the experimental section, prior to observations.

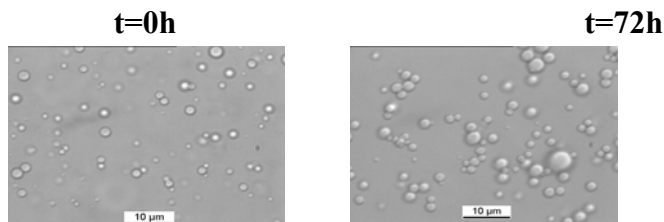


Figure 3. Optical microscopy images of emulsions obtained from highly concentrated emulsion in the system chitosan solution/phosphate buffer/Synperonic A7/decane at 40°C as a function of time, 0h and 72h. The emulsions were diluted just before observations

A chitosan porous foam (polyHIPE) crosslinked with genipin has been obtained using a highly concentrated emulsion as template. Optical micrograph of the structure of the highly concentrated emulsion is shown in Figure 4. The droplets have a polyhedral shape, typical structure of highly concentrated emulsions, with an average droplet diameter below 5 μm .

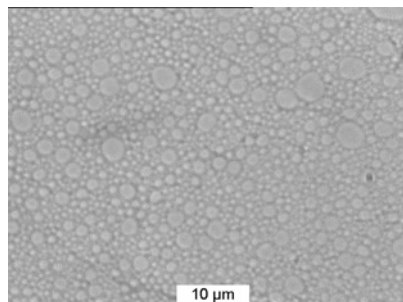


Figure 4. Optical micrograph of the highly concentrated emulsion at $t=0\text{h}$ in the system Synperonic A7/genipin solution/chitosan solution/decane

After keeping the emulsion for three days at 40°C a dark bluish and elastic monolith was obtained. A colour change was observed from the white original emulsions to the final blue monolith. The colour change is due to the oxygen radical-induced polymerization of genipin in the presence of air [15].

Chitosan polyHIPE was obtained after removal of surfactant, decane and water by ethanol and water Soxhlet extraction and freeze-drying. The crosslinking percentage of the final material was determined by acetic acid Soxhlet extraction, obtaining a value of 91%. Moreover, the skeleton density was determined by Helium pycnometry. An average density value of 1.578 g/cm^3 was obtained with a standard deviation of 0.016 g/cm^3 .

The morphology of the chitosan polyHIPE was characterized by SEM. As shown in Figure 5, this material has a uniform macroporous and open-cell structure with a diameter of the pores smaller than $0.5\text{ }\mu\text{m}$. The difference between the pore diameter of the material and the diameter of the drops of the highly concentrated emulsion ($1.75\text{ }\mu\text{m}$) could be due to shrinking during washing and drying.

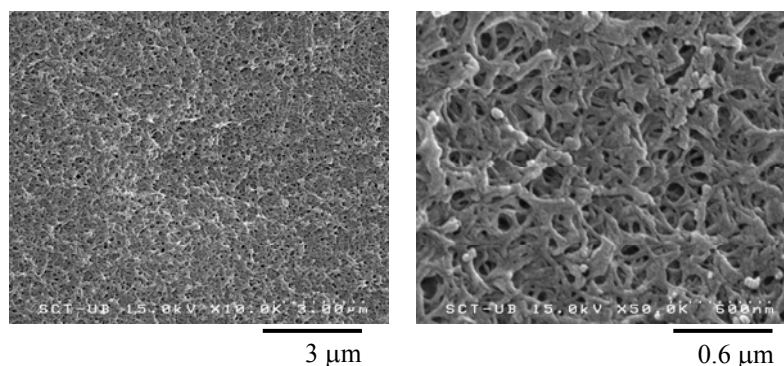


Figure 5. SEM micrographs of chitosan polyHIPEs at two different magnifications

Nitrogen sorption isotherms were also performed to determine the specific surface area of chitosan polyHIPEs. The observation of a hysteresis loop at relative pressures (p/p_0) in the range of 0.60 and 0.98 indicates the presence of macropores (Figure 6).

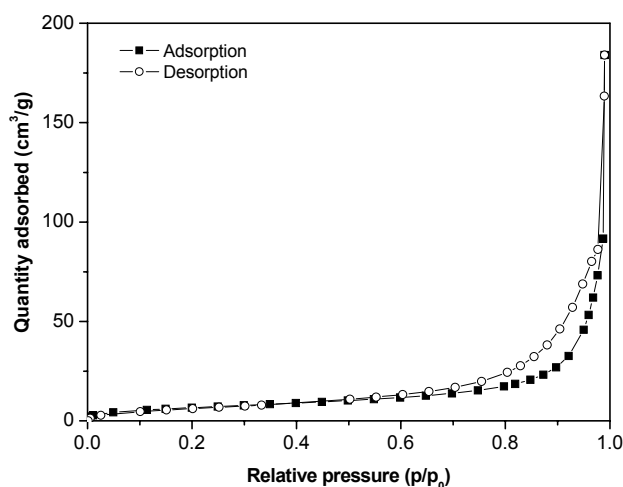


Figure 6. Nitrogen sorption isotherms of chitosan polyHIPE

The specific surface area, calculated by fitting the BET equation to the adsorption curve, for relative pressures between 0.05 and 0.3, was 25.2 m²/g. This low value confirms the macroporosity of the chitosan polyHIPE.

CONCLUSIONS

Chitosan polyHIPEs were successfully obtained using oil-in-water (O/W) highly concentrated emulsions as templates via chitosan crosslinking with genipin. This material has a uniform macroporous structure with a diameter below 0.5 μm. Macroporous chitosan polyHIPEs, with specific surface area of 25.2 m²/g, were obtained. Chitosan polyHIPE is a suitable candidate in pH-responsive drug delivery systems due to chitosan is a non-toxic and biocompatible polymer. Other applications of this material could be as absorbent by its swelling capacity due to the presence of macropores.

ACKNOWLEDGEMENTS

The authors greatly acknowledge the Spanish Ministry of Science and Innovation (CTQ2008-06892-C03-01 project) for the financial support.

REFERENCES

- [1] Lissant, K. J. (1966). The geometry of high-internal-phase-ratio emulsions. *J. Col. Int. Sci.*, 22, 462-68.
- [2] Princen, H. M. (1979). Highly concentrated emulsions. I. Cylindrical systems. *J. Colloid. Interf. Sci.*, 71 (1), 55-66.
- [3] Solans, C., Esquena, J., Azemar, N. (2003). Highly concentrated (gel) emulsions, versatile reaction media. *Cur. Op. Col. Interf. Sci.*, 8 (2), 156-163.
- [4] Esquena, J., Solans, C. (2006). Highly concentrated emulsions as templates for solid foams, in: *Emulsions and emulsion stability*. Ed. J. Sjöblom, Francis & Taylor (Surfactant Science Series).
- [5] Gross, A.F., Nowak, A.P. (2010). Hierarchical carbon foams with independently tunable mesopore and macropore size distributions. *Langmuir*, 26 (13), 11378-83.
- [6] Ungureanu, S., Laurent, G., Deleuze, H. et al. (2010). Syntheses and characterization of

- new organically grafted silica foams. *Col. Interf. Surf. A*, 360 (1-3), 85-93.
- [7] [Lépine, O., Birot, M., Deleuze, H. (2009). Preparation of a Poly(furfuryl alcohol)-Coated Highly Porous Polystyrene Matrix. *Macromol. Mat. Eng.*, 294, 599-604.
- [8] Lumelsky, Y., Lalush-Michael, I., Levenberg, S., Silverstein, M.S. (2009). A degradable, porous, emulsion-templated polyacrylate. *J. Pol. Sci., Part A: Pol. Chem.*, 47 (24), 7043-53.
- [9] Esquena, J., Solans, C., Vílchez, S., Erra, P., Miras, J. (2010). Materiales poliméricos macroporosos y meso/macroporosos obtenidos em emulsiones concentradas y altamente concentradas. Spanish patent P200930038,
- [10] Nishi, C., Nakajima, N., Ikada, Y. (1995). In vitro evaluation of cytotoxicity of diepoxy compounds used for biomaterial modification. *J. Biomed. Mat. Res.*, 29 (7), 829-34.
- [11] Muzzarelli, R.A.A. (2009). Genipin-crosslinked chitosan hydrogels as biomedical and pharmaceutical aids. *Carbohydr. Pol.*, 77, 1-9.
- [12] Vílchez, S., Samitier, V., Porras, M., Esquena, J., Erra, P. (2009). Chitosan hydrogels covalently crosslinked with a natural reagent, *Tens. Surf. Deterg.*, 46, 13-7.
- [13] Chao, A.C., Yu, S.H., Chuang, G.S. (2006). Using NaCl particles as porogen to prepare a highly adsorbent chitosan membranes. *J. Memb. Sci.*, 280 (1-2), 163-74.
- [14] Brunauer, S., Emmett, P.H., Teller, E. (1938). Adsorption of gases in multimolecular layers, *J. Amer. Ch. Soc.*, 60 (2), 1723-32.
- [15] Butler, M.F., Ng, Y.F., Pudney, P.D.A. (2003). Mechanism and kinetics of the crosslinking reaction between biopolymers containing primary amine groups and genipin. *J. Pol. Sci., Part A: Pol. Chem.*, 41 (24), 3941-53.

SYNTHESIS OF ORGANOSOLUBLE CHITOSAN DERIVATIVES WITH POLYPHENOLIC SIDE CHAINS

Minoru Morimoto¹, Takayuki Tono², Yasuhiro Iri², Yoshitaka Taruno², Yoshihiro Shigemasa², Shinsuke Ifuku², Hiroyuki Saimoto^{2*}

¹Research Center for Bioscience and Technology, Tottori University, Koyama,
Tottori 680-8550, Japan

²Department of Chemistry and Biotechnology, Graduate School of Engineering,
Tottori University, Koyama, Tottori 8552, Japan

*E-mail address: saimoto@chem.tottori-u.ac.jp

INTRODUCTION

Chitin and chitosan have attracted increasing attention as functional substrates for use in agricultural, food, medicinal and industrial fields. Although chitosan shows unique chemical properties because of the presence of an active amino group, chitosan itself is not soluble in common organic solvents and neutral water. Introduction of carbohydrate branches into chitin and chitosans gives branched polysaccharide analogs, which show good water solubility and new chemical and biological functions [1–4]. As an application of the regioselective phenolic coupling reaction [5,6], a one-pot synthesis of chitosan derivatives with polyphenolic side chains was developed in this research. These derivatives showed improved solubility in some organic solvents. The UV absorption properties and self-aggregation behavior of these chitosan derivatives were also investigated in this study.

MATERIALS and METHODS

Materials

The following chitosans were supplied by Koyo Chemical Co. Ltd. (Osaka, Japan):

1 (L0221-20FD, degree of deacetylation (DDA) 90%, *M_w* 5 kDa, *M_n* 2 kDa, hydrochloride); **2** (SC12181, DDA 80%, *M_w* 9 kD, *M_n* 2 kD, hydrochloride). Phenolic compounds and other reagents were purchased from Wako Pure Chemical Industries, Ltd. (Osaka, Japan) and used as received. Chitosan derivatives **8** and **10** were prepared according to the reported procedure [7].

N-(2,6-Dihydroxy-3-methoxycarbonylphenyl)methylation of chitosan (typical procedure)

To an aqueous solution (50 ml) of chitosan hydrochloride **2** (1.29 g, 5.0 mmol as amino group) was added an aqueous formaldehyde solution (37wt%, 405 mg, 5.0 mmol as HCHO). After stirring at 65°C for 1 h, a methanol solution (50 mL) of methyl 2,4-dihydroxybenzoate (**3**) (841 mg, 5.0 mmol) was added to the reaction mixture. The whole solution was stirred at 65°C for 24 h. After cooling, the reaction mixture was poured into acetone (1000 mL), giving a precipitate that was separated by centrifugation. The precipitate was dissolved in water (40 mL), and lyophilized to give chitosan derivative **4** (1.27 g, degree of substitution (DS) 0.2, 87% yield). The DS was calculated from the ratio of N% to C%, which was estimated by elemental analysis. ¹H NMR (D₂O) δ 2.09 (*N*-Ac), 3.0–3.1 (C(2)-H of GlcN unit), 3.5–4.1 (C(3), C(4), C(5), C(6)-H of chitosan chain, C(2)-H of GlcNAc unit, COOCH₃, and Ar-CH₂N), 4.6–4.9 (C(1)-H of chitosan chain), 6.57 (d, *J*=7.3 Hz, C(5)-H of benzene ring), 7.84 (d, *J*=7.3 Hz, C(4)-H of benzene ring); IR (KBr) 3100–3600, 1668, 1622, 1439, 1281, 1070 cm⁻¹.

N-(3-(2-Hydroxyethoxycarbonyl)-2,6-dihydroxyphenyl)methylated chitosan (**6**)

^1H NMR (D_2O) δ 2.06 (*N*-Ac), 3.1–3.3 (C(2)-H of GlcN unit), 3.5–4.1 (C(3), C(4), C(5), C(6)-H of chitosan chain, C(2)-H of GlcNAc unit, $\text{OCH}_2\text{CH}_2\text{O}$, and $\text{Ar-CH}_2\text{N}$), 4.4–4.9 (C(1)-H of chitosan chain), 6.63 (d, $J=9.0$ Hz, C(5)-H of benzene ring), 7.96 (d, $J=9.0$ Hz, C(4)-H of benzene ring); IR (KBr) 3100–3600, 1655, 1624, 1452, 1278, 1069 cm^{-1} .

Evaluation of solubility and UV protective properties

A sample (10 mg mL^{-1}) was soaked in each solvent at 20–25 $^\circ\text{C}$. After 24 h, the solubility was evaluated using the mass of recovered sample (mg) from soluble and insoluble fractions.

To determine the UV absorption property, a methanol solution of **8b** was coated on a PET film (Lumirror, thickness 0.21 mm, Toray Industries Inc., Tokyo, Japan) and dried. The concentration of the 3-benzoyl-2,6-dihydroxyphenyl group in **8b** was addusted to $0.47 \mu\text{mol/cm}^2$.

Evaluation of self-aggregation behavior

Fluorescence spectra of aqueous solution of 8-anilinonaphthalene-1-sulfonic acid ($1.2 \times 10^{-6} \text{ mol L}^{-1}$, λ_{ex} 350 nm) was measured in the presence of each sample (**2**, **3**, **4d**, **8a**, **9**, **10**; 0–0.9 mg mL^{-1}).

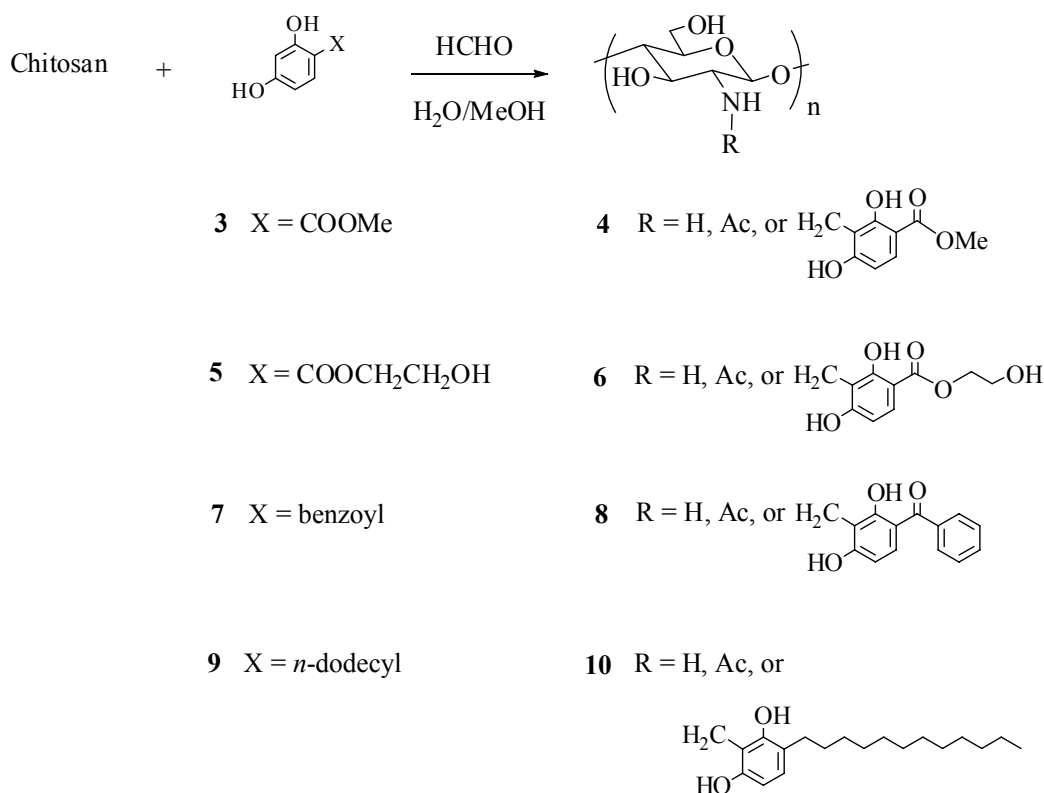


Figure 1. Synthesis of chitosan derivatives.

RESULTS and DISCUSSION

Treatment of chitosan with formaldehyde and methyl 2,4-dihydroxybenzoate (**3**) in aqueous methanol gave *N*-(2,6-dihydroxy-(3-methoxycarbonyl)phenyl)methylated chitosan **4** in a one pot synthesis (Figure 1).

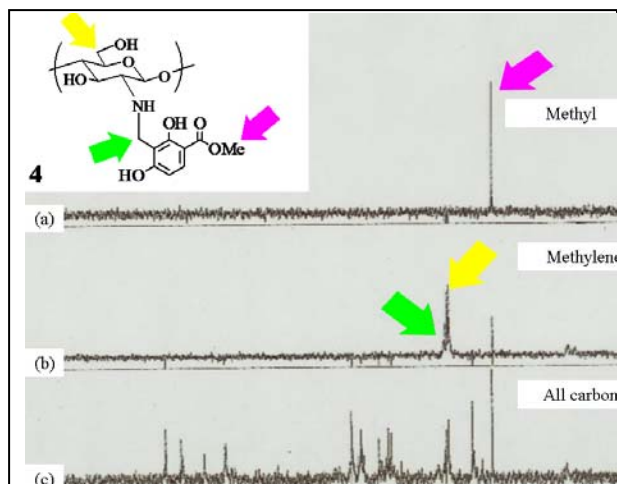


Figure 2. ^{13}C NMR analysis of **4** in D_2O . (a) Methyl carbons (DEPT), (b) methylene carbons (DEPT), and (c) all carbons.

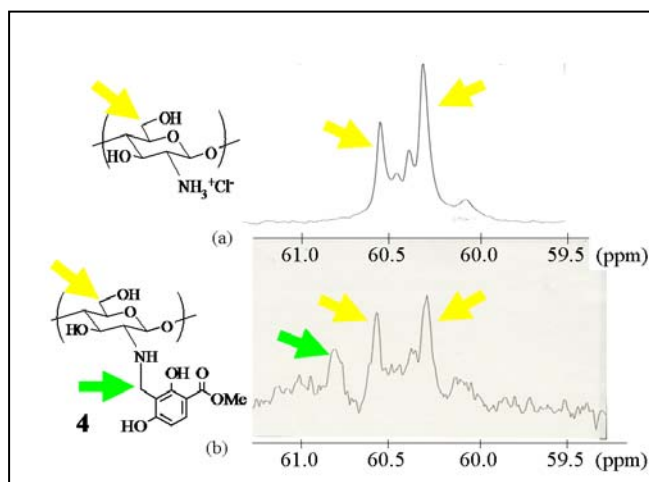


Figure 3. ^{13}C NMR (DEPT) analysis of methylene carbons. (a) Chitosan **2**, (b) product **4**.

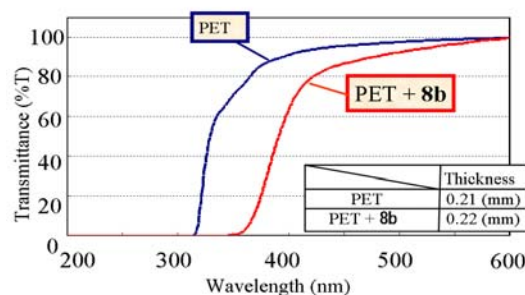
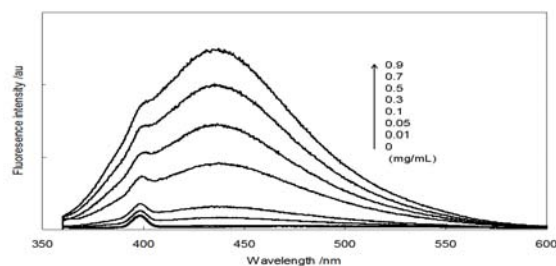
We have previously reported regioselective reactions of phenolic substrates in protic media [5,6], and in this research, regioselective C-C bond formation was accomplished at the C(3) position of methyl 2,4-dihydroxybenzoate (**3**) to give **4**. Although the ^1H NMR analysis of the product **4** showed two doublet signals corresponding to the aromatic protons with an *ortho*-coupling constant $J=7-9$ Hz, signals corresponding to the methyl ester and $\text{Ar-CH}_2\text{N}$ of **4** overlapped signals corresponding to the chitosan chain in the ^1H NMR analysis. Therefore, ^{13}C NMR analysis was performed to confirm the correspondence of the signal to the methyl ester and $\text{Ar-CH}_2\text{N}$ of **4**. Among all of the signals for **4** shown in Figure 2 (c), ^{13}C NMR analysis in DEPT mode show selected signals corresponding to the methyl ester carbons (52 ppm) and methylene carbons (59–61 ppm) (Figure 2 (a) and (b)). Figure 3 shows magnified spectra of the methylene carbon area. Compared with the C(6) methylene carbon signals of the starting chitosan shown in Figure 3 (a), a new methylene carbon signal (60.8 ppm) appeared in the ^{13}C NMR spectrum of **4** (Figure 3 (b)). Formation of a new link between the amino group of the chitosan and the aromatic ring of **3** was confirmed by this new signal.

Table 1. One-pot Synthesis of Chitosan Derivatives

Entry	Chitosan (mmol as -NH ₂)	HCHO (equiv)	Phenol (equiv)	Product (yield/%)	DS	Solubility (mg/ml) in MeOCH ₂ CH ₂ OH
1	1 (5.0)	(1)	3 (1)	4a (91)	0.1	4.9
2	1 (5.0)	(2)	3 (2)	4b (83)	0.3	7.2
3	1 (5.0)	(3)	3 (3)	4c (87)	0.7	10
4	2 (5.0)	(1)	3 (1)	4d (87)	0.2	2.3
5	2 (5.0)	(3)	3 (3)	4e (76)	0.5	6.4
6	2 (5.0)	(1)	5 (1)	6a (99)	0.2	3.2
7	2 (5.0)	(3)	5 (3)	6b (94)	0.6	7.3
8	2 (5.0)	(1)	7 (1)	8a (95)	0.1	5.4
9	2 (5.0)	(3)	7 (3)	8b (96)	0.4	6.6
10	2 (5.0)	(1)	9 (1)	10 (95)	0.03	-

As shown in Table 1, chitosan derivatives **6**, **8**, and **10** were obtained from phenolic compounds **5**, **7**, and **9**, respectively. Entries 1–5 in Table 1 show that the DS increased with an increase in the amount of added formaldehyde and **3**. Because the solubility of chitosans **1** and **2** in 2-methoxyethanol was low (ca. 1 mg/mL), the new derivatives **4a–4e** exhibited improved solubility in organic solvent. Although chitosan derivatives **6** and **8** exhibited the similar improved solubility in 2-methoxyethanol, chitosan derivative **10** with hydrophobic long alkyl chain was sparingly soluble in 2-methoxyethanol.

Figure 4 shows the UV absorption properties of the PET film coated with compound **8**. PET film coated with the chitosan derivative **8b** reduced transmittance of UV-A (315–400 nm), while the PET film absorbs UV-B and -C.

**Figure 4.** UV absorption properties of PET film coated with compound **8**.**Figure 5.** Fluorescence spectra of ANS in water as a function of concentration of **4**.
[**4d**]: 0–0.9 mg/mL; [ANS]: 1.2 × 10^{−6} mol/L; λ_{ex}: 350 nm.

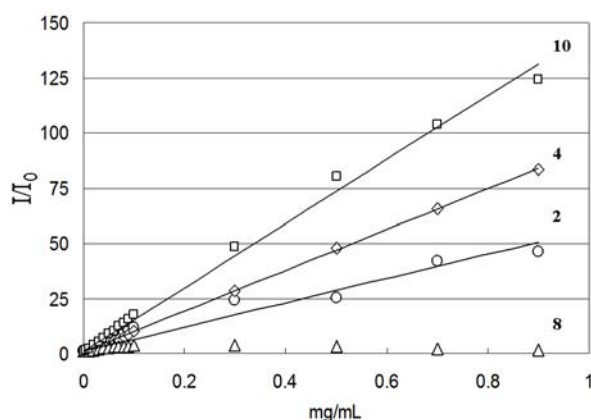


Figure 6. Plot of fluorescence intensity ratio (I/I_0) for ANS versus concentration of the samples.

I and I_0 are fluorescence intensity at peak top in the presence and absence of the samples [2, 4d, 8a, or 10]: 0–0.9 mg/mL; [ANS]: 1.2×10^{-6} mol/L; λ_{ex} : 350 nm.

Polysaccharides bearing hydrophobic side chains such as aromatic or alkyl groups are known to form the self-aggregate by hydrophobic interactions between the side chains. 1-Anilino-8-naphthalenesulfonate (ANS) is a well-known fluorescence probe to evaluate microscopic polarity. Fluorescence intensity of ANS in water is usually weak. When ANS was incorporated to the hydrophobic environments like micelle or membranes, the fluorescence intensity is markedly enhanced. Fluorescence intensity of ANS in water was increased with an increase in the concentration of chitosan samples (2, 4, and 10).

Typical spectral change was shown in Figure 5. No increase in fluorescence intensity was observed in the case of the benzoyl derivative 8 and 2,4-dihydroxybenzophenone (7) which is the side chain model of 8 (data, not shown). This result suggests the side chain made up by benzophenone structure behaves as a fluorescence quencher. As shown in Figure 6, relative fluorescence intensities at the peak top (I/I_0) were plotted as a function of concentration of samples (2, 4, 8, and 10) and a linear correlation was yielded except for 8. In the cases of the side chain models (3 and 9), however, the relative fluorescence intensities at the peak top (I/I_0) remained nearly zero. These results suggested the chitosan derivatives such as 4 and 10 formed the hydrophobic core effectively by the intramolecular and intermolecular aggregation between the polysaccharides chains. Hydrophobicity of the core would be depended on the hydrophobicity of the side chains (dodecylphenyl > methoxycarbonylphenyl).

ACKNOWLEDGEMENTS

This work was supported in part by Grants-in-Aid for Scientific Research (C) (Grant No. 22550197).

REFERENCES

- [1] Hashimoto, M., Morimoto, M., Saimoto, H., Shigemasa, Y., and Sato, T. (2006) Lactosylated chitosan for DNA delivery into hepatocytes: the effect of lactosylation on the physicochemical properties and intracellular trafficking of pDNA/chitosan

- complexes. *Bioconjug. Chem.*, 17, 309–316.
- [2] Hashimoto, M., Morimoto, M., Saimoto, H., Shigemasa, Y., Yanagie, H., Eriguchi, M., and Sato, T. (2006) Gene transfer by DNA/mannosylated chitosan complexes into mouse peritoneal macrophages. *Biotechnol. Lett.*, 28, 815–821.
- [3] Li, X., Tsushima, Y., Morimoto, M., Saimoto, H., Okamoto, Y., Minami, S., and Shigemasa, Y. (2000) Biological activity of chitosan-sugar hybrids: specific interaction with lectin. *Polym. Adv. Technol.*, 11, 176–179.
- [4] Morimoto, M., Nakao, M., Ishibashi, N., Shigemasa, Y., Ifuku, S., and Saimoto, H. (2011) Synthesis of novel chitosan with chitosan side chains. *Carbohydr. Polym.*, 84, 727–731.
- [5] Saimoto, H., Yoshida, K., Murakami, T., Morimoto, M., Sashiwa, H., and Shigemasa Y., (1996) Effect of calcium reagents on aldol reactions of phenolic enolates with aldehydes in alcohol. *J. Org. Chem.*, 61, 6768–6769.
- [6] Omura, Y., Taruno, Y., Irida, Y., Morimoto, M., Saimoto, H., and Shigemasa, Y. (2001) Regioselective Mannich reaction of phenolic compounds and its application to the synthesis of new chitosan derivatives. *Tetrahedron Lett.*, 42, 7273–7275.
- [7] Saimoto, H., Morimoto, M., Hakone, Y., Tanaka, Y., Irida, Y., Taruno, Y., Shigemasa, Y., and Ifuku, S., (2009) Synthesis of new chitosan derivatives by a regioselective Mannich reaction. *Advances in Chitin Science*, Vol.XI, pp.457–462.

SURFACE MODIFICATION OF POLYAMIDE FABRICS WITH CHITOSAN HYDROGELS CROSSLINKED WITH GENIPIN

S. Vilchez*, A.M. Manich, J. Miras, R. Molina, P. Erra, J. Esquena

Institute for Advanced Chemistry of Catalonia, IQAC-CSIC

Jordi Girona 18-26. 08034 Barcelona, Spain.

**E-mail address: susana.vilchez@iqac.csic.es*

INTRODUCTION

Nowadays, for the development of the textile industry textile materials with high added-value are required. There are different approaches to provide new or improved functionalities to textiles. Most of them are based on surface incorporation of a very thin layer of products with high added-value. The incorporation of hydrogels on textile surface is an interesting strategy to confer new properties to the fabrics, which is considered an easy way to efficiently obtain modified surface textiles. Among hydrogels, those sensitive to external stimuli are of great interest for functional finishing of textiles since they undergo reversible volume changes in response to a small variation in external stimuli such as pH, temperature, ionic strength, magnetic field and ultraviolet light [1, 2]. In recent years, considerable research attention has been focused on this kind of hydrogels [3]. Hydrogels are often crosslinked to give stability to the structure. Among other reagents, glutaraldehyde, formaldehyde and tripolyphosphate have been widely used to crosslink chitosan. However, they present some toxicity problems which can be solved by using genipin, a naturally crosslinking reagent used in herbal medicine and in the fabrication of food dyes.

In this work, chitosan hydrogels crosslinked with genipin have been incorporated onto the surface of polyamide fabrics by the padding technique. The successful hydrogel incorporation was confirmed by cryo-scanning electron microscopy (cryo-SEM) and X-ray photoelectronic spectroscopy (XPS). The water absorption ability of the coated fabrics was studied through thermogravimetric dynamic vapour sorption (TG-DVS), which showed higher moisture content of fabrics compared to uncoated. The porous structure of the fabrics was also studied by thermoporosimetry, which allows the study of pore structures of materials in the presence of water.

MATERIALS and METHODS

Materials

Chitosan medium molecular weight and degree of deacetylation of 85% was obtained from Sigma-Aldrich (Steinheim, Germany). Genipin with an average molecular weight of 226 g/mol, was from Challenge Bioproducts Co. (Taichung, Taiwan). All other reagents and solvents used were of reagent grade. Polyamide fabrics with 86.21 m²/g weight was supplied by AITEX.

Synthesis of genipin crosslinked chitosan hydrogels

Chitosan hydrogels crosslinked with genipin were prepared as described in a previous work [4]. Briefly, chitosan solution was freshly prepared by dissolving 1% w/w in distilled water containing of acetic acid (1% v/v) with continuous stirring for 24 h. Genipin solutions were prepared at 0.05% w/w by dissolving genipin in phosphate buffer pH 7.4. The reaction of chitosan and genipin occurred at room temperature after mixing both solutions at a ratio of 1:1 (w/w).

Hydrogel application on polyamide fabric

Chitosan hydrogel crosslinked with genipin were applied on polyamide fabrics by the padding technique. Fabrics were immersed in pre-hydrogel solution and through squeeze rolls with an HVF laboratory padder (Mathis, Switzerland) at a padding speed of 3 m/min and a squeeze roll pressure of 3 bar, and left to dry at room temperature. With the aim to increase hydrogel presence on fabric surface, the full process was repeated two times after conditioning the samples at 22°C and 50% relative humidity (RH). Plasma pre-treatment and ultraviolet post-treatment were also performed in order to know the influence on hydrogel coating. Plasma pre-treatment generates new chemical groups on the polyamide fabric that could improve chitosan hydrogel adhesion. It was carried out at 280 Pa and 30 W for 120 seconds on each side of the fabric before its immersion in the pre-hydrogel solution. The ultraviolet post-treatment was carried out for 3 h with a light bulb (125 W, Iwasaki Electric H125-BL) with a maximum emission wavelength of 366 nm after pre-hydrogel solution application.

Characterization methods

The surface morphology of polyamide fabrics was determined by cryo-scanning electron microscopy (cryo-SEM) using a Jeol JSM-840 microscope with a cryo-chamber. Swollen fabrics with distilled water were frozen and sputter-coated with gold before observation by cryo-SEM analysis.

X-ray photoelectronic spectroscopy (XPS) analysis was performed using a spectrometer PHI model 5500 Multitechnique System, in order to verify the chitosan hydrogel presence on polyamide fabrics. The samples were irradiated with an X-ray source operating at 350 W. Survey scans were taken in the range of 0-1100 eV, with pass energy of 187.85 eV. High resolution scans were obtained on the C_{1s}, O_{1s}, N_{1s} photoelectron peaks, with pass energy of 23.5 eV. Elemental chemical composition has been estimated after a linear background subtraction from the area of the different photo-emission peaks, modified by their corresponding sensitivity factors [5].

The water absorption ability was evaluated by dynamic vapour sorption (DVS). Adsorption/desorption isotherms, from 5 to 95% relative humidity (RH) at 25°C, were determined with a Q5000 SA (TA Instruments). Samples were previously conditioned at 0% RH for 2 hours at 25°C. The adsorption isotherms of water was determined by increasing relative humidity from 5% to 95%.

Thermogravimetric assays were performed with a DSC III Setaram instrument with hastelloy pans of 1 mL. The sample was first cooled at -20 °C for 1 hour, temperature low enough to freeze free and confined liquid. Then, the sample was heated up slowly at 0.2 °C/min from -20°C to 4°C. From these DSC results the energy absorbed at each temperature can be calculated and it can be transformed into water volume inside the pores.

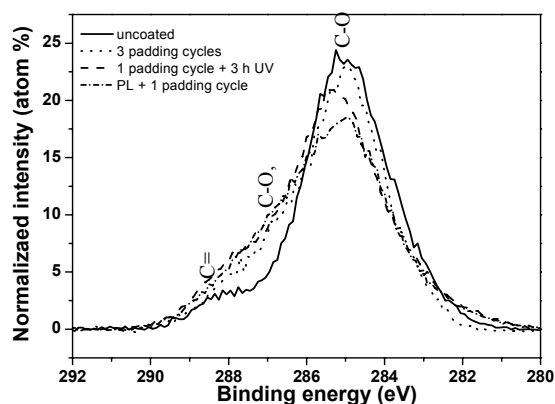
RESULTS and DISCUSSION

The presence of the hydrogel on polyamide fabrics was analyzed by XPS because the thickness of the coating was too thin to be detected by infrared spectroscopy. The results of elemental composition and atomic ratio of polyamide fabrics are presented in Table 1. As it can be seen, the hydrogel coating is confirmed by XPS since the coated fabrics show higher oxygen percentage and O/N ratio closer to 4, the theoretical ratio to chitosan, compared to uncoated fabric.

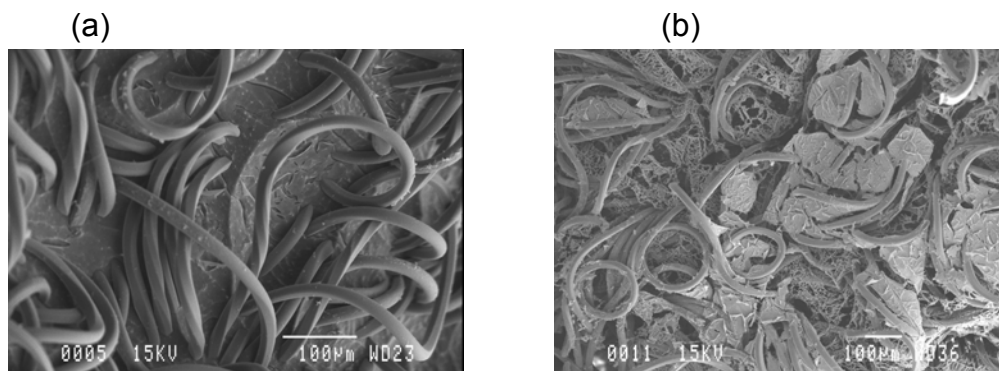
Table 1: Elemental composition in mole percent and atomic ratios determined by XPS for uncoated fabric and fabric coated with chitosan hydrogel.

Polyamide fabrics	C	O	N	C/N	C/O	O/N
Uncoated	70.9	15.6	6.5	10.9	4.6	2.4
3 padding cycles	69.3	21.0	6.2	11.3	3.3	3.4
1 padding cycle+3h UV	69.6	22.1	8.3	8.4	3.2	2.7
Plasma+1 padding cycle	73.6	17.9	8.5	8.4	3.2	2.7

Moreover, the high-resolution spectra of C_{1s} photoelectron peaks shows the increase of the signal corresponding to hydroxyl groups (C-O, binding energy 286.7) which is attributed to chitosan hydrogel coating (Figure 1).

**Figure 1: High-resolution spectra of C_{1s} photoelectron peaks for the uncoated and fabric coated with hydrogel**

By means of cryo-SEM technique chitosan hydrogel presence on polyamide fabrics was evidenced. As it can be seen in Figure 2, when uncoated fabrics were previously immersed in water, a film of frozen water can be observed between fibres. However, a porous network structure can be seen in fabrics coated with hydrogel, which could correspond to swollen hydrogel.

**Figure 2: Uncoated fabric (a) and fabric coated with 3 padding cycles (b) both fabrics were previously immersed in water.**

The comfort of textiles is determined in a great extent by the ability of the fabrics to absorb water. However, some fabrics, among them polyamide, exhibit low moisture absorbance, which negatively influence on the comfort sensation of garments. By coating the fabrics with chitosan hydrogel, the water sorption increases as shown in Figure 3. This sorption behaviour can influence positively on the comfort and wear properties of the garments.

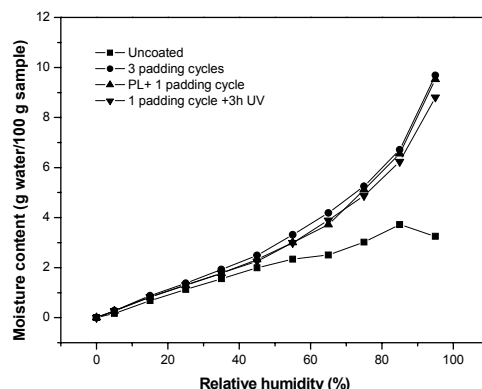


Figure 3: Moisture content of fabrics coated with chitosan hydrogel for different treatments.

Water desorption isotherms were used to estimate the monolayer capacity (X_m) the constants related to bonding energy for primary (C) and secondary (K) sorbed layers and the maximum water sorption capacity at 100% of relative humidity (X_1) of uncoated fabric and fabric coated with chitosan hydrogel. Table 2 shows the different parameters obtained by applying Guggenheim, Andersen and de Boer (GAB) equation [6]. Evaluation of all these results shows that the monolayer capacity (X_m) of the uncoated fabric is higher than in the fabrics with the hydrogel coating. However, the constant K, which is the measure of free enthalpy of the sorbate molecules in the pure liquid and the layers above the monolayer, is higher in the samples with the chitosan hydrogel. This means that water affinity in the monolayer of uncoated fabric is higher than in the fabrics with the hydrogel coating. However, samples with hydrogel coating show better water affinity in the secondary sorbed layers due to chitosan hydrogel presence resulting in a higher capacity of water adsorption at higher relative humidities.

Table 2: Monolayer capacity X_m , maximum water sorption capacity at 100% RH X_1 , C and K constants of GAB fits using the desorption values and determination coefficient R^2 .

	X_m	X_1	C	K	R^2
Uncoated	2.74	7.78	3.36	0.69	0.9995
3 padding cycles	2.42	11.82	4.42	0.80	0.9996
Plasma+ 1 padding cycle	2.35	11.92	4.56	0.81	0.9993
1 padding cycle+3h UV	2.41	10.68	4.18	0.79	0.9996

An important parameter that should be considered is the porosity because textile materials can be used as a suitable support to drug delivery. There are different techniques to study the porosity, among them; thermoporosimetry that allows the study of pore structure of materials in the liquid state. This is an appropriate method to measure the porosity of hydrogels, since the original porous structure can be preserved.

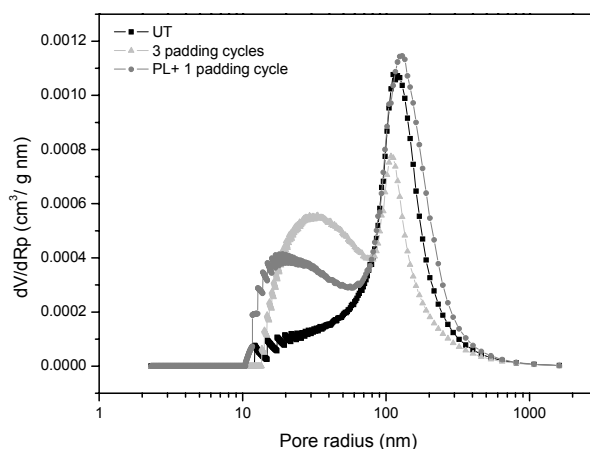


Figure 4: Pore size distribution of uncoated fabric and fabric coated with chitosan hydrogel with three padding cycles and with plasma and hydrogel with one padding cycle.

Figure 4 shows the pore radius distribution of uncoated polyamide fabrics and fabrics coated with chitosan hydrogel. The uncoated fabric has a pore radius distribution the maximum of which is around 100 nm. When hydrogel is applied, pore distributions with maximum around 20 and 30 nm can be observed which correspond to the hydrogel coating.

ACKNOWLEDGEMENTS

The authors acknowledge financial support from Spanish Ministry of Science and Innovation under project CTQ2008-06892-C03-01. The authors also acknowledge financial support from *Instituto Tecnológico Textil (AITEX)*.

REFERENCES

- [1] Liu, B., Hu, Y., (2005) The application of temperature-sensitive hydrogels to textiles: A review of Chinese and Japanes investigations, *Fibres & Textiles in Eastern Europe*, 13, 45-49
- [2] Crespy, D., Rossi, M.R., (2007) Temperature-responsive polymers with LCST in the physiological range and their applications in textiles, *Polymer International*, 56, 1461-68
- [3] Qiu, Y., Park, K. (2001) Environment-sensitive hydrogels for drug delivery, *Adv. Drug. Delivery Rev* 53 (3), 321-39
- [4] Vilchez, S., Samitier, V., Porras, M., Esquena, J., Erra, P., (2009) Chitosan hydrogels covalently crosslinked with a natural reagent, *Tens. Surf. Deterg.*, 46, 13-17
- [5] Wagner, C. D., Davis, L.E., Zeller, H. V., Taylor, J. A., Raymond, R. H., Gale, L. H., (1981) Empirical atomic sensitivity factors for quantitative analysis by electron spectroscopy for chemical analysis, *Surf. Interf. Anal.* 1981, 3, 211-25.
- [6] Timmermann, E.O., (2003) Multilayer sorption parameters: BET or GAB values?, *Colloids and Surfaces A: Physicochem. Eng. Aspects*, 220, 235-60.

BIOLOGICAL AND COSMETIC EFFECTS OF CHITIN NANOFIBER

**Saburo Minami^{1*}, Keisuke Tani¹, Tomohiro Osaki¹, Tomohiro Imagawa¹,
Takeshi Tsuka¹, Yoshiharu Okamoto¹, Atsushi Kagoshima², Shinsuke Ifuku³, and Hiroyuki
Saimoto³**

¹ *Department of Veterinary Clinical Medicine, School of Veterinary Medicine, Tottori University*

² *Shallbe Co., Ltd*

³ *Graduate School of Engineering, Tottori University*

**E-mail address: minami@muses.tottori-u.ac.jp*

INTRODUCTION

It was a difficult to obtain α -chitin nanofiber because of its water insolubility compare to acid water soluble chitosan. However, Ifuku *et al.* had succeeded to get chitin nanofiber from wet chitin powder extracted from crab and shrimp shells by simple grinding treatment in 2009 [1]. In 2010, they had succeeded in getting nanofiber from dried crab shell powder under acidic condition [2] and also developed the methodology of getting nanofiber under neutral condition from prawn shell in 2011 [3]. The chitin nanofibers obtained were highly uniform and width of nanofiber was approximately 10-20 nm. They also reported X-ray diffraction profiles of the chitin nanofibers obtained, the four diffraction peaks of chitin nanofibers which corresponded to 020, 110, 120, and 130 planes respectively are typical crystal patterns of α -chitin [2]. They also succeeded to make chitosan coated chitin-nanofibers (CCCN) by deacetylation of a commercially available chitin powder in 20% NaOH solution. Degree of deacetylation of nanofibers obtained was 10.6% and X-ray diffraction profiles maintained typical crystal patterns of α -chitin [2].

Three percent of the chitin nanofiber and CCCN dispersions are too viscous like a paste, and the 1 % dispersions show a gel form, so handling is easy to smear it to a skin. A field of chitin application will be become wide and variety by fibrillation of chitin bundle. For application of the nanofibers, Ifuku *et al.* [2] made optically transparent nanocomposites using the chitin nanofibers with acrylic resin. However, application of the chitin nanofibers is not known yet, especially in biological fields.

We attempt to use the chitin nanofibers and CCCN to skin for detecting biological effects in epidermis and dermis using hairless mouse (HR-1) and also determine cosmetic effects on human skin.

MATERIALS and METHODS

The chitin nanofiber and CCCN dispersions, chitin suspension and chitosan solution were prepared in acetic acid solutions (AcOH) under pH 3 and pH 6. AcOH-under pH 3 and pH 6 were also prepared for control. Each sample was smeared to the dorsal skin of HR-1 using a glass lot. After single application of each sample, skin was taken at 4 and 8 hrs, and histological observation of the skin was performed. In the histological observation (Hematoxylin-Eosin stain), thickness of epidermis and density of collagen fiber network in dermis were estimated by image analysis, and elastic fiber (Elastica van Gieson stain) appearance was also observed.

In human cosmetic application, a skin lotion without substances for moisture effects, such as hyaluronic acid, glycerin etc. was prepared for the control lotion. CCCN was added to the control lotion. Final concentration of CCCN was 6%. Ten female volunteers aged in 30 to 50 years old were used as a skin moisture monitor. Skin moisture content was measured by a skin moisture

checker (MY-808S, Scalar Co.Ltd., Tokyo) before and after application (at 1, 4 and 8 hours) under air conditioning room (23 degree of C, humidity does not controlled). After using the two types lotions for 7 days, a questionnaire for user's feelings (sense of use, sense of skin moisture, sense of skin firm and elasticity, makeup sitting, sense of skin quality, and total evaluation) were performed in 50 female volunteers age in 30 to 50 years old, by double blind method.

RESULTS and DISCUSSION

Effects of nanofiber on the murine skin: the thickness of epithelium significantly increased in the CCCN group than the control group at 4 hours after application (Fig. 1). The density of collagen fiber network also significantly increased in the nanofiber group than the control group at 4 hours after application. At 8 hours after application, the density of collagen fiber network significantly increased than the control and AcOH groups (Fig. 2). The elastic fiber appearance seemed to increase in the nanofiber group (Fig. 3).

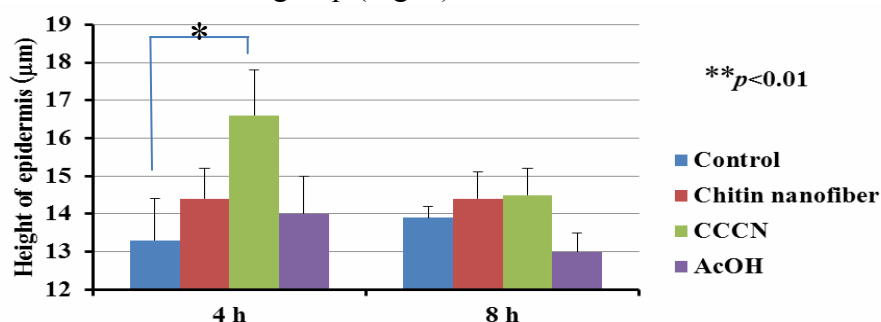


Fig. 1. The height of epidermis after application of each sample

Effects of nanofiber on the human skin: The skin moisture content was significantly maintained in the nanofiber group than the control group at 1, 4, and 8 hours (Fig. 4).

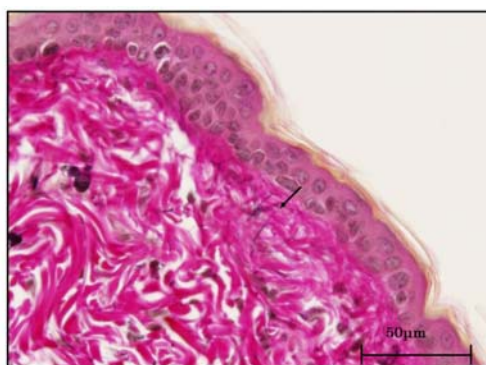


Fig.3. Increasing of elastic fibers beneath the epidermis in the chitin nanofiber applied mouse (Elastica van Gieson stain)

Results of the skin moisture content were shown in Fig.4. The skin moisture content was decreasing with time dependently, however, the skin moisture contents of CCCN lotion group is significantly maintained compared to the control at each time.

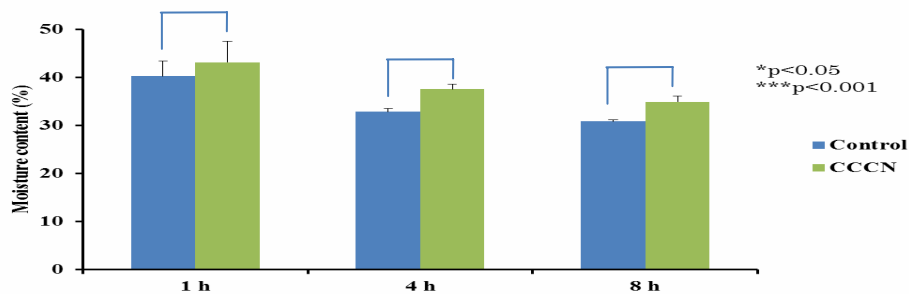


Fig. 4. Skin moisture content (%) at each hour after application of CCCN lotion

The results of the questionnaire showed good or excellent feeling after using the CCCN contain lotion. The results of total evaluation was shown in Fig. 5. In the control, the sum of terrible, bad or common answered persons were 45, but in the nanofiber were only 4. On the other hand, the sum of the good and excellent answered persons were 5 in the control, however in the nanofiber were 46. There is significant difference between them ($\chi^2=67.3$, $p<0.01$).

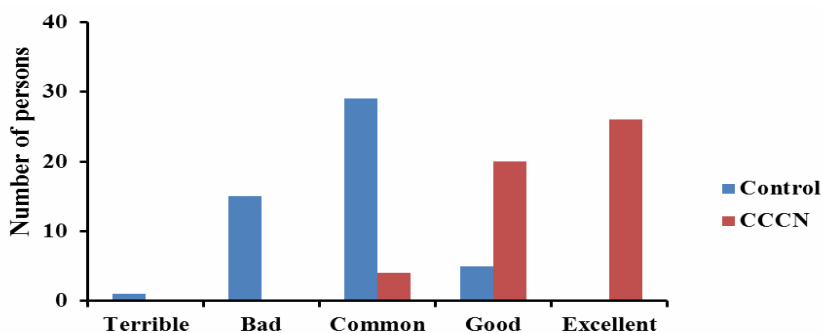


Fig. 5. The results of total evaluation

By ageing, decreasing of a thickness of skin epithelium and a collagen density were reported. A splitting of collagen fiber induced decreasing of skin mechanical strength and cellular dysfunction of epidermis. In the present experiment, pH3 samples, especially in acetic acid samples caused splitting of collagen fibers. In UV exposure to skin, collagen fiber splitting is well known side effect caused by reactive oxygen species (ROS)[4]. Oxidation by ROS induces inflammatory mediators such as matrix metalloproteinases (MMPs). MMPs degradate collagen, elastine and other proteins, so over up-regulation of MMPs is main endogenous factor of skin ageing[5]. Acetic acid also caused collagen splitting, however chitin nanofiber or CCCN prevent collagen splitting, and induces usefull response as collagen fiber regeneration and elastic fiber regeneration. In human experiment, CCCN content lotion causes good moisture preserve in the skin. These results showed chitin nanofiber or CCCN has anti-ageing effects on skin and are usefull materials for cosmetics.

REFERENCES

- [1] Ifuku, S., Nogi, M., Yoshioka, M., Morimoto, M., Saimoto, H. and Yano, H. (2009) Preparation of chitin nano-fibers with a uniform width as α -chitin from crab shells. *Biomacromolecules*, 10, 1584-1588.

- [2] Ifuku, S., Nogi, M., Yoshioka, M., Morimoto, M., Yano, H. and Saimoto, H. (2010) Fibrillation of dried chitin into 10-20 nm nanofibers by simple grinding method under acidic conditions. *Carbohydr. Polym.*, 81, 134-139
- [3] Ifuku, S., Nogi, M., Abe, K., Yoshioka, M., Morimoto, M., Saimoto, H., Yano, H. (2011) Simple preparation method of chitin nanofibers with a uniform width of 10-20 nm from prawn shell under neutral conditions. *Carbohydr. Polym.*, 84, 762-764
- [4] Vicentini, F.T., Fonseca, Y.M., Pitol, D.L., Iyomasa, M.M., Bentley, M.V., Fonseca, M.J. (2010) Evaluation of protective effect of a water-in-oil microemulsion incorporating quercetin against uvb-induced damage in hairless mice skin. *J. Pharm. Pharm. Sci*, 13, 274-285
- [5] Fisher, G.J., Quan, T., Purohit, T., Shao, Y., Cho, M.K., He, T., Varani, J., Kang, S., Voorhees, J.J. (2009) Collagen fragmentation promotes oxidative stress and elevates matrix metalloproteinase-1 in fibroblasts in aged human skin. *Am. J. Pathol.*, 174, 101-114

EVALUATION OF THE EROSION CHARACTERISTICS OF COLON TARGETED TABLETS PREPARED WITH PECTIN AND CHITOSAN

Mine Özyazıcı*, Zeynep Ay Senyigit

Ege University, Faculty of Pharmacy, Department of Pharmaceutical Technology, 35100, Bornova, Izmir, Turkey

**E-mail address: mine.ozyazici@ege.edu.tr*

INTRODUCTION

In recent years, colon-specific delivery systems have gained importance for the treatment of colon diseases like inflammatory bowel diseases, Crohn's disease, infectious diseases and colon cancer. Prodrugs, coating with pH-sensitive polymers, time-dependent delivery systems, pressure controlled delivery systems, systems formulated with colonic bacterial degradable polymers are main approaches for colon targeting. The use of carriers that are degraded exclusively by colonic bacteria is one of the approaches for colon-specific drug delivery. The various carriers being evaluated for colon specific drug delivery based on the colonic bacterial action are polysaccharide based carrier systems such as pectin, guar gum, xanthan gum, chitosan, amylase [1].

Ornidazole (1-(2-hydroxy-3-chloropropyl)-2-methyl-5-nitroimidazole) is a 5-nitroimidazole derivate drug, widely used for the treatment of a variety of clinical conditions including intestinal amoebiasis, anaerobic infections, trichomoniasis and Crohn's disease. It is more effective against amebiasis than metronidazole, which is the most commonly used nitroimidazole derivative in therapy. Ornidazole is rapidly absorbed from stomach and small intestine. Therefore, most of the drug may enter into systemic circulation when administrated in conventional tablet dosage form and unwanted side effects can be seen. Crohn's disease is a chronic disorder that causes inflammation of the digestive or gastrointestinal tract. It most commonly affects the end of the small intestine (ileum) and the beginning of the large intestine (colon). The inflammation can cause pain and make the intestines empty frequently, resulting in diarrhea. Ornidazole is an effective and safe drug for the treatment of active Crohn's disease [2].

The aim of this study is to evaluate the erosion characteristics of compression coated tablets of ornidazole prepared with biodegradable pectin and chitosan.

MATERIALS AND METHODS

Materials

Ornidazole was a kind gift from Abdi İbrahim İlaç San. ve Tic. A. Ş. (Turkey). Pectin was donated by Wyeth İlaçları A. Ş. (Turkey). Chitosan was gifted from A&E Connock (England). Pectinex 3XL was a gift from Novo Nordisk (Switzerland). All other solvents and reagents were of analytical grade.

Preparation of tablets

Preparation of core tablets

For the preparation of core tablets, ornidazole was dry mixed with PVP and granulated with water. Wet granules were sieved through 1 mm and dried overnight at room temperature. Tablets containing 200 mg ornidazole were compressed with 10 mm flat faced punches using a hydraulic hand press tablet machine (Perkin-Elmer) with a pressure to 5.0 tons for 10 seconds.

Preparation of compression coated tablets

Core tablets of ornidazole were compression coated with 400 mg mixture of pectin and chitosan in varying proportions. Half of this coating material was placed in the 13 mm die cavity of the flat faced punches. The core tablet was carefully positioned in the centre of the die cavity and was filled with the other half of the coating material. The coating material was compressed around the core at an applied force of 5.0 tons for 10 seconds [3]. Compositions of compression coat are given in Table 1.

Table 1. Composition of coat formulation

Code	Composition of compression coat	
F1	80% Pectin	20% Chitosan
F2	60% Pectin	40% Chitosan

Erosion testing

Tablets were then tested in vitro to determine their erosion patterns. Formulations were first tested in pH 1.2 hydrochloric acid buffer for 2 h and then continued with pH 6.8 phosphate buffer for 3 h. At the end of 5 hours 1% pectinolytic enzyme was added to the medium and test continued for 24 hours. The erosion testing was performed using paddle method according to USP 24 with 50 rpm paddle speed and 900 mL medium was maintained at 37°C. The tablets were removed from medium at the corresponding time points and then dried in an oven at 45°C for 24 h and erosion was determined gravimetrically [4]. This erosion testing was also performed without pectinolytic enzymes to determine the effect of enzyme to tablet erosion.

RESULTS and DISCUSSION

The results of erosion testing showed that, firstly a surrounding gel layer formed around the tablets. Then, gel layer thickness increased and original tablet shape disappeared while spherical shape was formed. Finally, the spherical system was slowly dissolved/eroded with pectinolytic enzymes. Figure 1 and 2 shows the remaining amount of tablet mass with or without pectinolytic enzymes.

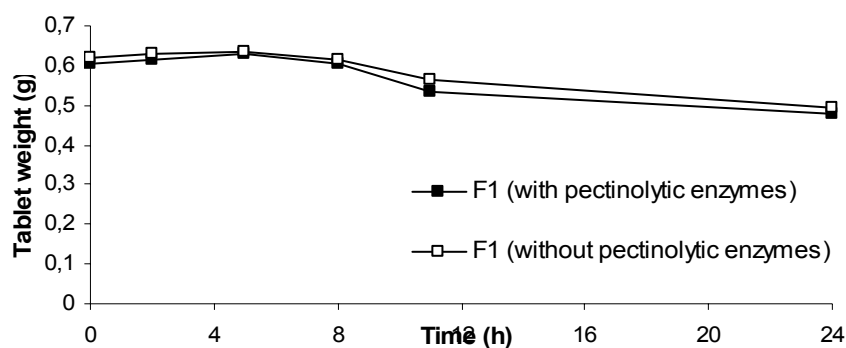


Figure 1: Erosion profiles of F1 in buffer system

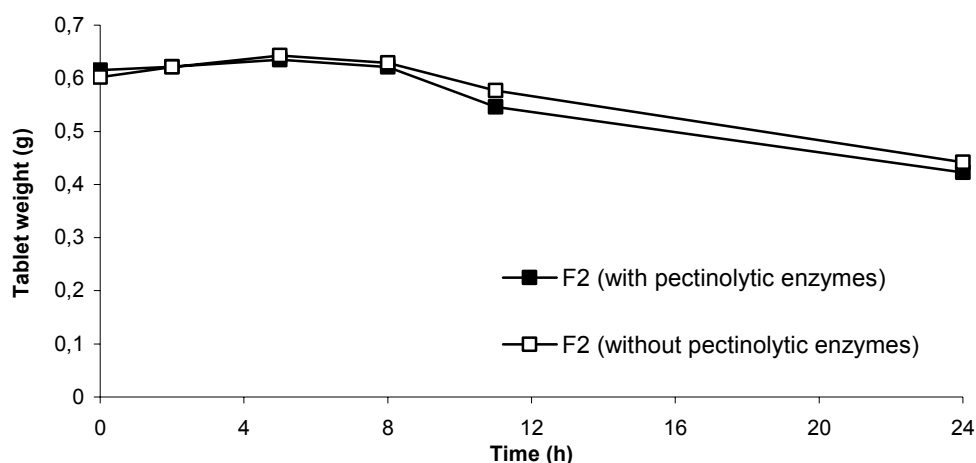


Figure 2: Erosion profiles of F1 in buffer system

CONCLUSION

The results showed that, chitosan and pectin are potential polymers for colon-specific drug delivery systems because chitosan-pectin coat is capable of protecting the drug being released in the stomach and small intestine.

REFERENCES:

- [1] Ashford, M. (1993). An evaluation of pectin as a carrier for drug targeting to the colon. *J. Control. Release*, 26, 213–220.
- [2] Krishnaiah, Y.S.R. (2003). In vivo evaluation of guar gum-based colon-targeted drug delivery systems of ornidazole in healthy human volunteers. *J. Drug Target.*, 11, 109-115.
- [3] Turkoglu, M. (2002). In vitro evaluation of pectin-HPMC compression coated 5-aminosalicylic acid tablets for colonic delivery. *Eur. J. Pharm. Biopharm.* 53, 65-73.
- [4] Turkoğlu, M. (1999). Pectin-hydroxypropylmethylcellulose drug delivery system for colon targeting. *Pharm. Ind.*, 61, 662-665.

Authors Index

A

Abdel-Mohsen A.M. 3
 Abramchuk S. 36
 Ahn Byul-Nim 24
 AKBUĞA Jülide 248
 Akopova T.A. 155
 Albulov A.I. 8, 175
 Alexandrova V.A. 10, 258
 Almeida Érika V.R. 96
 Aly A.S. 3
 Arimoto Miyuki 338
 Asqarov B. 16
 Avramenko V. 48
 Azimov J.T. 20, 170

B

Bak Soon-Sun 24, 224
 Baklagina Yu.G. 42
 Bannikova G.E. 76
 Batyrbekov A.A. 180
 Benavente M. 29, 106
 Bernard Fr. 185
 Bezrodnykh E. 36, 276
 Blagodatskikh I. 36
 Blinova M.I. 42
 Bochek A.M. 42
 Bratskaya S. 48
 Buhantsev O.V. 8

C

Campana-Filho Sérgio P. 54, 90, 96
 Chen Hui-San 253
 Chernyshenko A.O. 155
 Cverova N.E. 126

D

David L. 54
 Delezuk Jorge Augusto de Moura 54
 Desbrieres J. 59
 Dolgopyatova N..V. 67
 Draczyński Z. 71
 Drozd N.N. 76

E

Egorova A.M. 327
 Ehrenfeld F. 59
 Eom Tae-Kil 82, 86
 Erra P. 356
 Esquena J. 344, 356

F

Fedoseev V.B. 290
 Fedoseeva E.A. 290
 Firat Sakar 213
 Franco T.T. 102, 114, 333
 Frederico F.R. 102
 Frolova M.A. 8

G

Galbraikh L.S. 155, 263, 294, 316
 Garcia I. 106
 García-López M. 165
 Gofman I.V. 42
 Gómez-Mariño R. 165
 González-Sotelo C. 165
 Gueddari Nour Eddine El 185

H

Heppe A. 111
 Honorato T.L. 102, 114
 Hrdina R. 3
 Huang Yu-Ting 253
 Hutami Keiko 338

I

Ikeda Mana 338
 Il'ina A.V. 76
 Inoyatova F.H. 180
 Ito Shinya 338

J

Juang Horng-Heng 253
 Juang Ruey-Shin 121

K

Kalashnikov I.N. 126
 Kato E.T. JR. 333
 Karadeniz F. 144, 149
 Karagozlu M.Z. 144, 149
 Kawada T. 131
 Khairullin R. 276
 Kildeeva N.R. 138, 294
 Kim Jung-Ae 24
 Kim Se-Kwon 24, 82, 86, 144, 149, 197, 224, 271,
 Kokurina N.Yu. 126, 290
 Kong Chang-Suk 24, 144, 149, 271
 Konovalova I.N. 219
 Koryagin A.S. 287
 Kukhareva L.V. 42
 Kulikov S. 36, 276

L

Larina V.N. 126
 Lesnyakova L.V. 155
 Levov A.N. 76, 327
 Lim Biing-Cheng 160
 Lin Kai-Ming 160
 Lin Tsung-Han 121
 Liu Chao-Lin 121, 160, 253
 Lopatin S.A. 276
 Lozinsky V.I. 138
 Lucas Jean-Michel 54

M

Makarov V.A. 76
 Malinina L.I. 309
 Manich A.M. 356
 Marasulov M. 170
 Marcasuzaa P. 59
 Mariano M.S. 96
 Markin A.V. 287
 Martínez J. 29
 Maslova G.V. 175
 Matsumiya Masahiro 338
 Mikhailov G.M. 175
 Mikhailov S.N. 138
 Milusheva R.Yu. 16, 20, 170, 180, 230
 Miras J. 344, 356
 Mironenko A. 48
 Miyauch K. 338
 Mochalova A.E. 126, 287
 Moerschbacher B.M. 114, 185
 Molina R. 356
 Moreno L. 29, 106
 Morozov A.G. 287
 Mucha M. 192

N

Nemtsev S.V. 175
 Nepomnyashchiy A. 48
 Ngo Dai-Hung 197
 Nikonorov V.V. 294
 Novikov V.Yu. 67, 203, 219
 Nudga L.A. 42, 175

O

Ohshima M. 242
 Oksengendler B.L. 16, 20, 170
 Özbas-Turan S. 248
 Ozcan I. 209
 Ozer O. 209
 Ozer Yekta 213

Ozyazici M. 209, 365

P

Panarin E.F. 42
 Pangestuti R. 24
 Pérez-Martín R.I. 165
 Perminov P.A. 138
 Petrosyan A.S. 10, 258
 Petrova V.A. 42
 Phedushkin I.L. 287
 Philippova Yu. 276
 Pinaev G.P. 42
 Podkorytova A.V. 267
 Portsel M.N. 219
 Putintsev N.M. 67

R

Ramos-Ariza P. 165
 Rashidova S.Sh. 16, 20, 170, 180, 230
 Ratanajajaroen P. 242
 Ratih P. 224
 Reynaud S. 59
 Rodionov P.V. 309
 Rodrigues S. 114
 Rujiravanit R. 236
 Rumyantseva E.V. 294, 299
 Ryu BoMi 197

S

Saburo Minami 361
 Saimoto H. 350
 ŞALVA E. 248
 Samujlenko A.J. 8
 Samusenko I.A. 42
 Savchik E.Iu. 76
 Senyigit T. 209
 Sergeev A. 48
 Sevda Senel 213
 Seyda Colak 213
 Shekhovtsova T.N. 309
 Shen Chia-Rui 253
 Shinkarev S.M. 8
 Shirokova L.N. 10, 258
 Simanenkova L.M. 138
 Smirnov V.F. 126
 Smirnova L.A. 126, 287
 Smirnova O.N. 126
 Solans Conxita 344
 Sonina A.N. 263, 316
 Spichkina O.G. 42
 Strokova N.G. 267
 Suna Erdogan 213

T

Ta Quang Van 271
Tamura Hiroshi 236
Tanaka Sonomi 338
Tarchevsky I.A.
Tikhonov V. 36, 276
Tolstakov A.S. 76
Trombotto Stéphane 54
Tsai Min-Lang 282
Tsverova N.E. 287
Turaeva N.N. 16, 20, 170
Tylman Michał 192

U

Uryash A.V. 290
Uryash V.F. 126, 290
Uspenskiy S.A. 316

V

Varlamov V.P. 76
Veiga Sara C.P. 90
Veleshko A.N. 294, 299
Veleshko I.E. 138, 294, 299
Venkatesan J. 304
Veselova I.A. 309
Vieites-Fernández J.M. 165
Vikhoreva G.A. 76, 155, 258, 263, 316
Vílchez Susana 344, 356
Vladimirov L.V. 138
Vo Thanh-Sang 322
Voznesenskiy S. 48

W

Watthanaphanit A. 236
Wu Chia-Jen 253
Wunder A. 111

Y

Yakovleva V.G. 327
Yamakov Igor 36, 276
Yang Ching-Jen 253
Yang Chin-Yo 282
Yoneda Y. 131
Yoshida C.M.P. 333
Yudintseva N.M. 42
Yugay S.M. 230

Z

Zelenetsky A.N. 155